United Nations
Educational, Scientific and
Cultural Organization

Intergovernmental
Oceanographic
Commission

Technical Series 115

Oceanographic and biological features in the Canary Current Large Marine Ecosystem

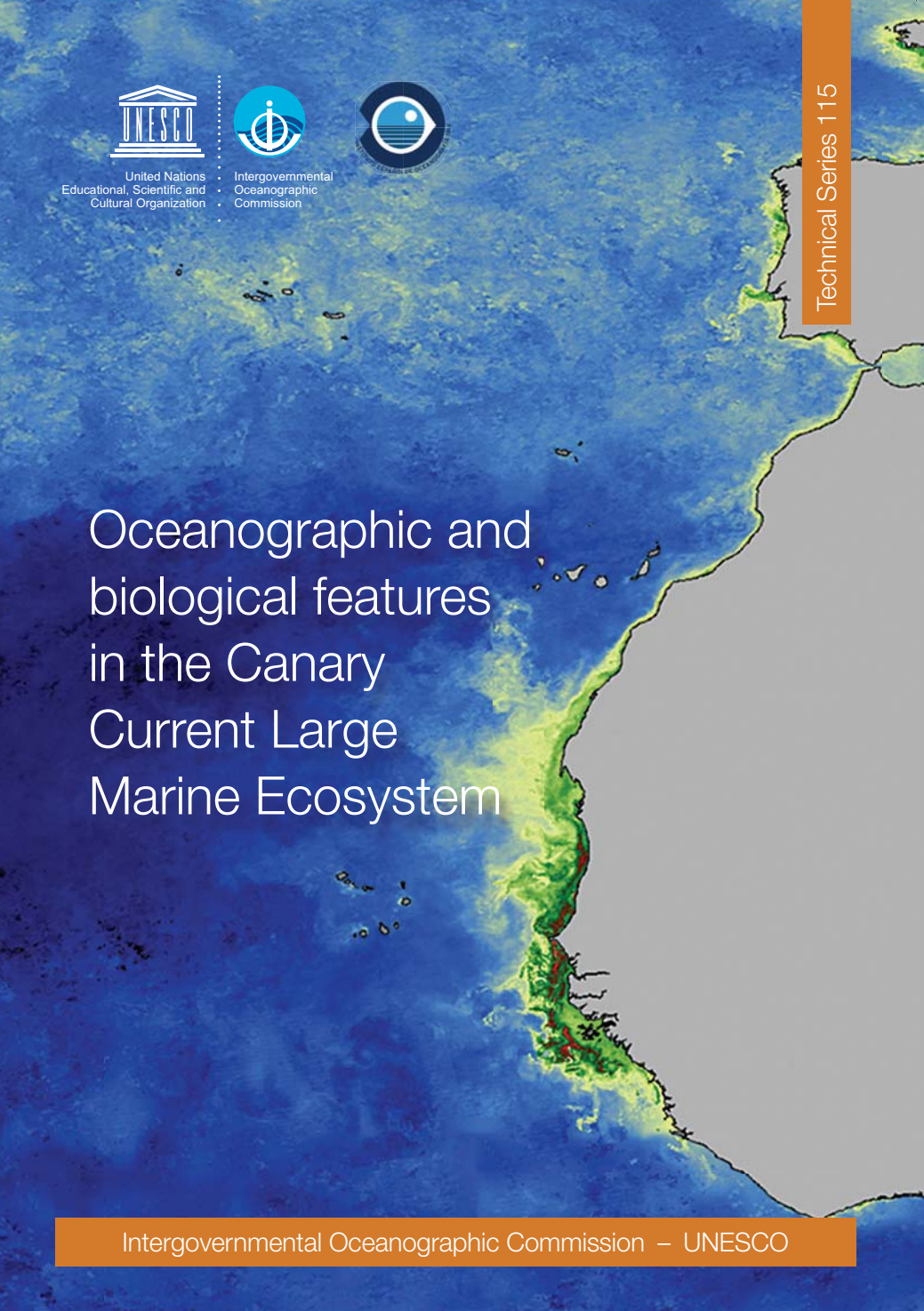

Intergovernmental Oceanographic Commission – UNESCO

Intergovernmental Oceanographic Commission of UNESCO (IOC-UNESCO)

United Nations Educational, Scientific and Cultural Organization · Intergovernmental Oceanographic Commission

UNESCO's Intergovernmental Oceanographic Commission (IOC), established in 1960, promotes international cooperation and coordinates programmes in marine research, services, observation systems, hazard mitigation, and capacity development in order to understand and effectively manage the resources of the ocean and coastal areas. By applying this knowledge, the Commission aims to improve the governance, management, institutional capacity, and decision-making processes of its 147 Member States with respect to marine resources and climate variability and to foster sustainable development of the marine environment, in particular in developing countries. The Commission responds, as a competent international organisation, to the requirements deriving from the United Nations Convention on the Law of the Sea (UNCLOS), the United Nations Conference on Environment and Development (UNCED), and other international instruments relevant to marine scientific research, related services and capacity-building.

Instituto Español de Oceanografía (IEO)

The Spanish Institute of Oceanography (IEO), founded in 1914, is a public research body attached to the Ministry of Economy and Competitiveness. The IEO is dedicated to marine science research, especially in relation to scientific knowledge of the ocean, sustainable marine living resources and fisheries, aquaculture and the marine environment. The IEO is committed to addressing the challenges facing the ocean for the benefit of society and is also an advisory institution on oceanographic research, ocean health and conservation and fish stock management for the Spanish government. The IEO networks with the Spanish scientific community, as well as partner organizations in many countries; it also fosters a long-standing commitment to international cooperation with developing countries aimed to ensure the sustainable use of marine resources and the oceanographic research. The IEO represents Spain in most intergovernmental science and technology forums related to the ocean and its resources such as the Intergovernmental Oceanographic Commission of UNESCO (IOC-UNESCO), the International Council for the Exploration of the Sea (ICES), the Mediterranean Science Commission (CIESM), and the Committee for the Eastern Central Atlantic Fisheries (CECAF) among others.

Spanish Agency for International Development Cooperation (AECID)

GOBIERNO DE ESPAÑA · cooperación española

AECID, the Spanish Agency for International Cooperation for Development, is a public entity under the Ministry of Foreign Affairs and Cooperation, in charge of the coordination of the Spanish policy on international cooperation for development, aimed to the reduction of poverty and the achievement of sustainable human development. Since its foundation in 1988, the Agency has established international alliances and strengthened Spain's relations with other countries and multilateral institutions such as the United Nations agencies. This work has contributed to the recognition of Spain as a reliable partner in the field of international cooperation, promotion of equitable and sustainable societies and respect for human dignity. It is also an AECID primary objective to promote and encourage the presence of Spanish experts in international organizations devoted to international cooperation such as UNESCO and other agencies in the United Nations.

Cover photo: Phytoplanktonic blooms along the coast of Northwest Africa and Iberian Peninsula, as seen from the concentration of chlorophyll-a, in March 2013, deduced from the data of the MODIS sensor. Numerous mesoscale features such as fronts and filaments can be observed. Image by Hervé Demarcq, IRD

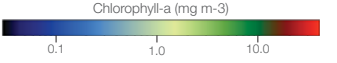

Intergovernmental Oceanographic Commission

Technical Series 115

Oceanographic and biological features in the Canary Current Large Marine Ecosystem

Editors:
Luis Valdés
Itahisa Déniz-González

United Nations
Educational, Scientific and
Cultural Organization

Intergovernmental
Oceanographic
Commission

With the support of the Spanish Agency for International Development Cooperation (AECID)

GOBIERNO DE ESPAÑA

cooperación española

UNESCO 2015

Disclaimer

The designations employed and the presentation of the material in this publication do not imply the expression of any opinion whatsoever on the part of the Secretariats of UNESCO and IOC concerning the legal status of any country or territory, or its authorities, or concerning the delimitation of the frontiers of any country or territory.

The authors are responsible for the choice and the presentation of the facts contained in this publication and for the opinions expressed therein, which are not necessarily those of UNESCO and do not commit the Organization.

For bibliographic purposes, this document should be cited as: Valdés, L.[1] and Déniz-González, I.[1] (eds). 2015. *Oceanographic and biological features in the Canary Current Large Marine Ecosystem*. IOC-UNESCO, Paris. IOC Technical Series, No. 115: 383 pp.

[1] Intergovernmental Oceanographic Commission of UNESCO (IOC-UNESCO), Paris, France

The publication *Oceanographic and biological features in the Canary Current Large Marine Ecosystem* is also available online at:

http://www.unesco.org/new/en/ioc/ts115

(IOC/2015/TS/115)

LIST OF CONTENTS

page

ACKNOWLEDGEMENTS 5

EXECUTIVE SUMMARY 7

1. INTRODUCTION 19

2. OCEAN GEOMORPHOLOGY AND GEOLOGICAL MATERIALS 23

2.1. MAIN GEOMORPHOLOGIC FEATURES IN THE CANARY CURRENT LARGE MARINE ECOSYSTEM 23

2.2. OCEANIC INTRAPLATE VOLCANIC ISLANDS AND SEAMOUNTS IN THE CANARY CURRENT LARGE MARINE ECOSYSTEM 39

2.3. SAHARAN DUST INPUTS TO THE NORTHEAST ATLANTIC 53

3. HYDROGRAPHIC STRUCTURE AND OCEAN CIRCULATION 63

3.1. REGIONAL WEATHER DYNAMICS AND FORCING IN TROPICAL AND SUBTROPICAL NORTHWEST AFRICA 63

3.2. WATER MASSES IN THE CANARY CURRENT LARGE MARINE ECOSYSTEM 73

3.3. EASTERN BOUNDARY CURRENTS OFF NORTH-WEST AFRICA 81

3.4. COASTAL UPWELLING OFF NORTH-WEST AFRICA 93

3.5. CANARY ISLANDS EDDIES AND COASTAL UPWELLING FILAMENTS OFF NORTH-WEST AFRICA 105

3.6. WAVES AND TIDES IN THE CANARY CURRENT LARGE MARINE ECOSYSTEM 115

4. BIOGEOCHEMICAL CHARACTERISTICS OF THE MARINE ECOSYSTEM 133

4.1. INORGANIC NUTRIENTS AND DISSOLVED OXYGEN IN THE CANARY CURRENT LARGE MARINE ECOSYSTEM 133

4.2. INORGANIC CARBON, PH AND ALKALINITY IN THE CANARY CURRENT LARGE MARINE ECOSYSTEM 143

4.3. ORGANIC MATTER DYNAMICS IN THE CANARY CURRENT 151

4.4. PHYTOPLANKTON AND PRIMARY PRODUCTIVITY OFF NORTHWEST AFRICA 161

4.5. HARMFUL ALGAL BLOOM EVENTS IN THE CANARY CURRENT LARGE MARINE ECOSYSTEM 175

4.6. ZOOPLANKTON IN THE CANARY CURRENT LARGE MARINE ECOSYSTEM 183

5. LIFE IN THE SEA 197

5.1. PELAGIC FISH STOCKS AND THEIR RESPONSE TO FISHERIES AND ENVIRONMENTAL VARIATION IN THE CANARY CURRENT LARGE MARINE ECOSYSTEM 197

5.2. DEMERSAL FISH IN THE CANARY CURRENT LARGE MARINE ECOSYSTEM 215

5.3. THE BENTHOS OF NORTHWEST AFRICA 231

5.4. CEPHALOPODS IN THE CANARY CURRENT LARGE MARINE ECOSYSTEM 245

page

5.5. BIODIVERSITY AND BIOGEOGRAPHY OF DECAPOD CRUSTACEANS IN THE CANARY CURRENT LARGE MARINE ECOSYSTEM 257

5.6. SEA TURTLES OFF NORTHWEST AFRICA 273

5.7. BIODIVERSITY OF CETACEANS IN COASTAL WATERS OF NORTHWEST AFRICA: NEW INSIGHTS THROUGH PLATFORM-OF-OPPORTUNITY VISUAL SURVEYING IN 2011-2013 283

6. INTERANNUAL, INTERDECADAL AND LONG-TERM VARIABILITY 299

6.1. OPEN OCEAN TEMPERATURE AND SALINITY TRENDS IN THE CANARY CURRENT LARGE MARINE ECOSYSTEM 299

6.2. SEA LEVEL VARIABILITY AND TRENDS IN THE CANARY CURRENT LARGE MARINE ECOSYSTEM 309

6.3. RECENT CHANGES AND TRENDS OF THE UPWELLING INTENSITY IN THE CANARY CURRENT LARGE MARINE ECOSYSTEM 321

6.4. TRENDS IN PHYTOPLANKTON AND PRIMARY PRODUCTIVITY OFF NORTHWEST AFRICA 331

6.5. OCEAN ACIDIFICATION IN THE CANARY CURRENT LARGE MARINE ECOSYSTEM 343

BIBLIOGRAPHY 351

LIST OF ACRONYMS 379

ACKNOWLEDGEMENTS

The elaboration of this publication about the "Oceanographic and Biological features in the Canary Current Large Marine Ecosystem" (CCLME) would not be possible without the generous financial support of a donor. The Spanish Agency for International Development Cooperation (AECID) has funded the project *Enhancing oceanography capacities on Western Africa countries*, in which framework this document was envisioned. The AECID interest in the IOC objectives and its support over the past two years, have been really encouraging.

This comprehensive characterization of the CCLME was accomplished thanks to the dedication of 54 scientists contributing to this volume. These experts have reviewed the scientific information available and the Marine Science built in the CCLME during decades. In addition, they have kindly shared their own knowledge, gained during years of hard work in high level scientific research. We would like to warmly thank all the lead authors and co-authors for their commitment and very professional work in the elaboration of this publication.

We also recognize the generous involvement of the organizations where our contributors work. By alphabetical order, these organisations are:

African Union Interafrican Bureau for Animal Resources (AU-IBAR), Kenya
Centre de Recherche Scientifique de Conakry-Rogbane (CERESCOR), Guinea
Centre National des Sciences Halieutiques de Boussoura (CNSHB), Guinea
Consejo Superior de Investigaciones Científicas (CSIC), Spain
Conservação do Ambiente e o Desenvolvimento Sustentável (BIOS.CV), Cabo Verde
Conservation and Research of West African Aquatic Mammals (COREWAM)
DDECOMAR, Mauritania
Fisheries Research-Department of Agriculture, Forestry and Fisheries (DAFF), South Africa
Institut de recherche pour le développement (IRD), France
Institut fondamental de l'Afrique Noire (IFAN)-Université Cheikh Anta Diop (UCAD), Senegal
Institut Mauritanien de Recherches Océanographiques et des Pêches (IMROP), Mauritania
Institut National de Recherche Halieutique (INRH), Morocco
Instituto Español de Oceanografía (IEO), Spain
Instituto Geográfico Nacional (IGN), Spain
Instituto Mediterráneo de Estudios Avanzados (IMEDEA), Spain
Instituto Nacional de Meteorologia e Geofísica (INMG), Cabo Verde
Intergovernmental Oceanographic Commission (IOC)-UNESCO, France
John Abbott College, Canada
Ministry of Economic Affairs, the Netherlands
Observatorio Ambiental de Granadilla (OAG), Spain
Peruvian Centre for Cetacean Research, Peru
Puertos del Estado-Ministerio de Fomento, Spain
University of Cape Town (UCT), South Africa
University of Las Palmas de Gran Canaria (ULPGC), Spain
University of Vigo (UVIGO), Spain

Illustrations are a key part of the publication. We acknowledge the authors for the elaboration of new material specifically designed to be published in this book. We would like to thank in particular Hervé

Demarcq for the elaboration *ad hoc* of the cover figure and Luis Miguel Agudo Bravo for the elaboration of homogenised cartographies for different articles in this publication, such as the map in the Introduction.

Besides, we got the permission to reproduce photos taken by different scientists from different institutions and it must be also highlighted the compromise of different publishers that allowed us to reproduce free of charge figures published in journals and books of which they are responsible. By alphabetical order, these publishers are: Academic Press, American Meteorological Society, Institut de Ciències del Mar-Consejo Superior de Investigaciones Científicas, Csiro Publishing, Gobierno de Canarias, Eurosurveillance, John Wiley & Sons Limited, Nature Publishing Group, NOAA's National Marine Fisheries Service, Norwegian Geological Society, Springer and Taylor & Francis.

A dedicated Workshop on "Oceanographic and Biological features and trends in the Canary Current Large Marine Ecosystem" was organised under the frame of the project. It was held in Casa África (Las Palmas de Gran Canaria, Spain) from 27 to 29 January 2015. Casa África is a Consortium among the Ministerio de Asuntos Exteriores y Cooperación–AECID (Spain); the Canary Islands Government (Spain); and the City Council of Las Palmas de Gran Canaria (Spain). We would like to thank Casa África staff for their hospitality, dedication and generous support.

We, as editors, would like to express our sincere gratitude to the 18 contributors participating in the Workshop. They reviewed, improved and enriched the manuscripts with very good comments and provided valuable input and good advice in an enthusiastic and motivating atmosphere.

Our partner in this project, the Instituto Español de Oceanografía (IEO), has been instrumental for the success of all the activities planned in the project, and fundamental in the elaboration of this publication. An active and fruitful collaboration has been established with 12 IEO experts, who have shared their expertise and the know-how gained by the IEO during decades of international cooperation programs with African countries.

We also thank our colleagues at the IOC-UNESCO Secretariat; who were instrumental for the successful development of the project.

EXECUTIVE SUMMARY

The Canary Current Large Marine Ecosystem (CCLME) is one of the 4 major upwelling systems in the world. 54 marine scientists from 25 institutions have worked in a collaborative manner to make a complete characterization of the CCLME. The result is a detailed description of: (i) the ocean geomorphology and geological materials; (ii) the hydrographic structure and the ocean circulation; (iii) the biogeochemical characteristics of the marine ecosystem; (iv) the life in the sea; (v) and the interannual, interdecadal and long-term variability.

Here we present a summary of the oceanographic and biological features of the CCLME, based in reviews of the scientific knowledge built over decades of research in the area, combined with new data shared by the authors of each of the articles. The main conclusions of this global analysis are presented below, followed by the challenges for scientific research and management goals in the CCLME, which can be used to guide new scientific projects in the region.

Ocean Geomorphology and Geological Materials

- The CCLME shelf is the typical, in width and composition, of the passive continental margins. In general, the continental shelf has a mean width between 40–50 km, with exceptions like Bank D´Arguin (widest) or Dakar (narrowest).
- Geomorphological variations are the result of the sedimentary contributions associated to river basins. This river basins influence the genesis and the presence of the canyons in the platform and slope. These canyons are the main geomorphological features in the region. The sedimentary rocks have a maximum age of 200 Ma. It is important to remark the presence of a coral reef with more than 400 km of length in the shallowest Mauritania slope.
- Although tectonic processes occur throughout the entire CCLME, they do not have a great influence.
- The Canary Islands and the Cape Verde Islands Volcanic Provinces, placed within the CCLME, show sets of volcanic islands and seamounts related to magma-driven processes over tens of millions of years at the Canary and Cape Verdean hotspots. Continuous volcanism in both provinces has been reported for the last 142 Ma (Upper Cretaceous) on the Canaries and the last 26 Ma (Oligocene) on Cape Verde Islands, with contemporary volcanism in both archipelagos and on different islands and seamounts.
- Islands and seamounts of CCLME appear with complex or simple morphologies, dome-shaped to irregular relieves, and total heights ranging 4000-8000 m from the bottom to island highest peak (Teide-Pico Viejo, Tenerife Island), but less than 3500 m on seamounts. The geomorphological studies in the intraplate volcanic islands confirm the presence of the island platform developed in the older islands, not observed in the younger islands. Gravitational slides and canyons have been detected in all the islands.
- Seamounts are also biodiversity hotspots, where slopes modify the circulation regimen of both deep and shallow currents, and thus changing the biogeochemical constituents of seawater.
- Other geomorphologies have been found in the CCLME, such as: (i) gravitational process like debris flows; (ii) salt domes; (iii) pockmarcks.
- Atmospheric dust deposition is an important source of essential and limiting nutrients and metals to the ocean affecting the oceanic carbon uptake, phytoplankton growth and productivity.

NEW CHALLENGES:

- *The zones containing salt domes as prominent as those constituting intrusions in the sedimentary sequence are areas of great interest for the exploration of fossil hydrocarbons and are currently being explored by a number of oil companies.*
- *There is a lack of detailed geomorphological and sedimentary information on the more southerly zone of the CCLME (Cape Verde archipelago, and the waters of Gambia, Guinea-Bissau and Guinea). It is recommended that geophysical and geological campaigns should in future be undertaken in this area.*
- *In geological terms, there is an increasing interest in the understanding of the origin, nature and evolution of the constituent materials of the seamounts, as well as in investigating potential mineral resources. New geological data from: (i) igneous rocks, (ii) sedimentary rocks and (iii) sediments; are needed for those seamounts not studied yet. Those data reflect altogether the volcanic origin and the underwater evolution of these edifices.*
- *Economic interests surface on seamounts due to related geo-resources (e.g. phosphorites, methane hydrates, ferromanganese crusts and nodules) and bio-resources (e.g. fisheries).*
- *In both scientific and economic terms, interdisciplinary studies of the undersea mountains open up a wide range of opportunities for new international research projects in the future.*
- *Dust deposition measurements are very scarce in the CCLME. More observations of the variability of nutrient deposition are needed for a better understanding of the ocean biogeochemistry and to be able to evaluate quantitatively the dust impact on the ocean productivity. Long-term measurements are strongly required to validate the models in the region.*
- *Human activities may be increasing atmospheric dust in the region as a consequence of the land use and climate change, which produce changes in precipitation. An ever-growing demand of water resources for croplands, urban use and grazing might produce an increase of anthropogenic emissions associated with ephemeral water bodies. The projections for regions, such as sub-Saharan Africa, which are known highly active sources today, are uncertain and need to be prospected.*

Hydrographic Structure and Ocean Circulation

- From south to north, climate in this region ranges from equatorial, tropical wet and dry, tropical monsoon, semi-arid to desert.
- The Azores subtropical high causes a surface north-east continental airmass with maintained subsidence and stability, and the West African monsoon circulation flow are the major systems that influence the weather in the region. The continental airmass is very dry and gets even drier while moving across the Sahara Desert. Some local and regional systems are associated to the synoptic variability of the mid-level African easterly jet, that is generated in response to the inverse latitudinal surface temperature gradient during northern hemisphere spring. In altitude, the prevailing strong sub-tropical westerly jet is characterized by convergence into the low pressure areas and divergence in the anticyclonic surface flow.
- The humid summer monsoon, which determines transition between stable and unstable conditions, is the most important system, since it is the principal source of precipitation distribution associated to large scale convective events and synoptic wave perturbations. During summer, with baroclinic and barotropic gradient increase, the winds become easterlies.
- Atmospheric systems like the subtropical moving highs, the tropical plumes and the Saharan air layer, are also important regional forcing mechanisms.

- In the CCLME water masses of very different origin converge. The upper levels, between 100 dbar and 700 dbar, are occupied by North Atlantic Central Waters and South Atlantic Central Waters that feed the rich wind driven upwelling ecosystem. The Antarctic Intermediate Water and the warmer and saltier Mediterranean Water occupy the intermediate layer, between 700 dbar and 1500 dbar. The North Atlantic Deep Water, formed in the Labrador Sea, occupies the layers deeper than 1500 dbar.
- The Cape Verde Frontal Zone separates the clockwise motion of the eastern boundary currents in the anticyclonic subtropical gyre from the predominant anticlockwise motions within the northeastern tropical gyre. The frontal system is the site of substantial along-slope flow convergence and offshore transport – the subtropical Canary and Canary Upwelling Currents meet the tropical Mauritania and Cape Verde Current, originating the North Equatorial Current.
- The northeasterly winds along Northwest Africa cause offshore surface water transport which leads to the upwelling of subsurface denser waters, producing a coastal front typically about 200 m deep. The front gives rise to a southward coastal jet which feeds from the interior ocean, hence becoming the easternmost Canary Upwelling Current, and provides high spatial and temporal coherence among all latitudes along Northwest Africa.
- Between the front and the continental slope, the relatively homogeneous upwelled waters become the site of the Poleward Undercurrent. Typically centred at depths of about 300-400 m but often reaching the sea surface, the Poleward Undercurrent flows from Cape Verde, through the Cape Verde front and all the way to the Gulf of Cadiz.
- Both the southward Canary Upwelling Current and the northward Poleward Undercurrent constitute the true skeleton of the CCLME.
- The upwelling filaments may play a central role in the biogeochemical fluxes balances of the CCLME. The CCLME is also source of mesoscale eddies induced by the Canary Islands. These eddies are not present in other Eastern Boundary Upwelling Systems, and may have a great impact on the modulation and distribution of physical and biogeochemical properties, both locally and regionally. Those eddies build up the Canary Eddy Corridor.
- There is a decrease of mean significant wave heights southwards, with most common values between 1 m and 3 m and mean direction varying from West in the Gulf of Cadiz, to North and Northwest as we move southwards and in the Morocco coast respectively and Northeast finally in the Canary Islands. Maximum recorded significant wave heights vary from 6.6 m in Cádiz buoy to 5.7 m and 5.2 m in Las Palmas and Tenerife buoys respectively. The position of the buoys may reveal only local wave regime (useful just for local applications).
- The tide is mainly semidiurnal in the whole region and dominates significantly the sea level record – the meteorological component accounts only for the 5% of sea level variability in the Eastern Canary Islands. Tides range between 1.5 m and 3.5 m.
- The tidal waves propagate from South to North as a Kelvin wave, with maximum amplitudes near the coast.

<u>NEW CHALLENGES</u>:

- *Interactions between the continental surface-wind circulation systems over tropical and sub-tropical Northwest Africa and the surrounding ocean basin remains as a challenge in the CCLME research.*
- *There are many uncertainties in the biogeochemical fluxes balances of the CCLME that must be solved. In this regard an effort is needed on conducting high resolution surveys, on implementing coupled physical-biological modelling and on monitoring the mesoscale structures.*

- *The connection between the subtropical and tropical gyres, including the subtropical cell and the system of zonal tropical jets, has not yet been characterized.*
- *The spatial and temporal variability of the Canary Upwelling Current and Poleward Undercurrent remain as topics of open research. In particular, the behavior of the Poleward Undercurrent as it crosses the Cape Verde frontal system, the Canary Archipelago and the Gulf of Cadiz is yet to be elucidated.*
- *There is a lack of proper understanding of the processes that lead to the generation of eddies both at the coastal upwelling and Cape Verde fronts. The relevance of eddies, lateral intrusions and vertical mixing on both the intensity of cross-frontal exchange and the mean circulation fields are yet to be identified.*
- *It remains to properly assess the origin, extent and relevance of the large (late-fall and early-winter) current reversal that has been observed to recurrently take place south and east of the Canary Islands.*
- *The role of the Canary Eddy Corridor on enhancing the ocean productivity in the region and on modulating the large scale circulation and hence climate variability through deep mixing needs to be assessed.*
- *The installation and maintenance of permanent stations are very important for waves and tides characterization. This is very important for local, national and international applications (i.e. early warning systems) as well as for scientific studies.*
- *There is a lack of buoys and tide gauges in the CCLME south of the Canary Islands and the mainland African coast. But it is also important to share the existent data on tidal constants and sea level data from the hydrographic offices in the African countries.*
- *It is important to establish more tide gauges to obtain a detailed knowledge of the local variations of the tide and to feed high resolution tidal models.*
- *Hindcasts of waves by means of wave models and high resolution tidal models should be extended also to cover the whole region, for a real understanding of the spatial variability of the waves and tides in this area.*

Biogeochemical Characteristics of the Marine Ecosystem

- Inorganic nutrients increase with depth as a result of the remineralization of organic matter. In the CCLME there is also a marked latitudinal gradient, with the Cape Verde Frontal Zone separating relatively nutrient-poor and oxygen-rich subtropical waters from the nutrient-rich and oxygen-poor tropical waters.
- Coastal upwelling brings the subsurface waters towards the sea surface, hence raising the nutrient levels along a latitudinal coastal band off Northwest Africa; this represents a lateral source of nutrients to both gyres, especially to the nutrient-poor subtropical one.
- In the southernmost portion of our domain, within the tropical waters, the oxygen minimum zone of the North Atlantic Ocean develops. In this region, high primary production and slow ventilation of the subsurface waters lead to enhanced remineralization and low oxygen levels.
- The Inorganic carbon content and the acidity of the seawaters in the Canary region present significant changes at least over the upper 1000 m during the last fifteen years. The Eastern North Atlantic Ocean at the Canary Island region is increasing its storage capacity for excess carbon dioxide (CO_2) by 0.85 mol m^{-2} yr^{-1}. Models predict different CO_2 responses to upwelling intensification along the Canary Upwelling Ecosystem.

- The Canary Current upwelling system, one of the most productive coastal systems worldwide, is characterized by a combination of areas of permanent and very seasonal primary productivity. This variability is mostly driven by two factors: the strength of the upwelling-favourable wind, maximum in the Saharian region, and the nutritive quality of the upwelling waters, much higher South of Cape Blanc. Consequently, maximum summer productivity is observed in the central part of the system (20°N-25°N) and seasonally south of Cape Blanc (20°N) from February to May. Maximum levels of primary productivity between 5 g of Carbon m^{-2} d^{-1} and 10 g of Carbon m^{-2} d^{-1} are observed in these regions.
- The satellite observation allows the precise quantification of the offshore extent of the productive influence of the upwelling, moderate in Morocco up to 25°N and very pronounced from 10°N to 23°N.
- Consecutive to the intense seasonal variability, the planktonic diversity is much higher in the southern part of the system, although not precisely quantified. An adequate knowledge of this diversity and its functional structure is therefore lacking.
- Knowledge of Harmful Algal Blooms species and their impacts in the major eastern boundary upwelling systems is disparate between systems and is least studied off Northwest Africa. Nevertheless the few documented studies of Harmful Algal Blooms within this region indicate a similar diversity to that recorded in other upwelling systems, and include those species responsible for Paralytic shellfish poisoning, Diarrhetic shellfish poisoning, Amnesic shellfish poisoning and azaspiracid poisoning. Also present off Northwest Africa, but generally absent from the other major upwelling systems, are those species responsible for the Ciguatera fish poisoning and microcystin-producing cyanobacterial blooms. Their presence is afforded by the subtropical habitat provided by the island archipelagos found within the CCLME.
- Copepod species in the CCLME accounted for 60–95% of the zooplankton abundance and makes the bulk of the mesozooplankton biomass.
- Two main groups of copepod species can be identified in the CCLME representing biogeographical and ecological characteristics. One group is characterized by tropical and subtropical species, related to a sub region with a low influence of the upwelling nutrient enriched waters (Cape Verde, Canary Islands and Cape Blanc); and a second group encompasses subtropical and luso-boreal species identified along the Northwest Africa coast (Cape Spartel-Cape Blanc) which is submitted to a strong seasonality of upwelling and coastal nutrient rich waters.
- Zooplankton production and its seasonality vary with latitude, as a result of the seasonality of upwelling, its regime and strength, with the highest values in the Southern part (from Conakry to Cape Blanc) and the lowest values in the Canary Island archipelago and North Moroccan coast (from Cape Bedouzza to Cape Spartel) throughout the annual cycle. A succession from small to medium and large calanoids and gelatinous organisms from the upwelled waters to the ocean is the rule and this pattern is coupled with a switch of the feeding mode of the zooplankters. A phytoplankton-based diet was observed in the inshore upwelling zone whereas a microzooplankton based diet was observed offshore under more oligotrophic conditions.
- Mesoscale activity in the CCLME, mostly cyclonic and anticyclonic eddies and filaments, has an important influence in key biological processes. The interaction between filaments and eddies promote a net transport of organic matter to the open ocean with consequences in fluxes and also in the distribution of phyto- zooplankton and fish larvae which are advected to open ocean waters.

NEW CHALLENGES:

- *The relevance of the distributions of inorganic nutrients and dissolved oxygen to the trophic chain in the CCLME is unquestionable. Nevertheless, an improved understanding of the physical and biogeochemical processes, and their interactions, is still necessary for predicting how anthropogenic climate change may affect the CCLME future evolution.*
- *Experimental data should be gathered in order to sustain model results in CO_2 responses to upwelling intensification along the CCLME.*
- *The Canary Upwelling Ecosystem is mostly known from its physical components as well as from its important specific fisheries, but a much more detailed knowledge of its first trophic level is necessary in order to understand how its environmental, ecological and human aspects interact. Modeling, either biogeochemical or ecosystemic is part of the solution but it will not allow alone a full understanding of the Canary Current upwelling system – and therefore its responsible management – unless essential missing data are collected on species diversity and their ecological meaning. The recent international initiatives as Ocean Biographic Information System (OBIS) will greatly help in gathering essential data – sometimes old – on this diversity, essential to understand what the presently observed variability and trends really mean in term of ecosystem equilibrium in order to preserve it for the benefit of humanity.*
- *It is intended that the brief review on Harmful Algal Blooms will provide the foundation and stimulus for further studies of the ecology and dynamics of Harmful Algal Blooms, of their toxins, and of the public health and socioeconomic impacts of Harmful Algal Blooms within this region.*
- *More studies are needed to verify that the patterns observed in zooplankton composition and distribution 30-35 years ago are still valid and that climate change and variability of upwelling strength is neither altering the cycles nor the productivity of the CCLME.*
- *Also the plankton physiology deserves future work as these organisms live longer than any other plankton and are the food of diel vertical migrants (large zooplankton and micronekton), which also transport carbon from the ocean upper layers to the deep-sea through active flux. This mechanism should shed light about the fate of the huge productivity of upwelling areas.*

Life in the Sea

- Among the pelagic fish species in West Africa, the small pelagic such as sardinella, sardine and horse mackerel are very important for food security in the region. Most pelagic species are migratory, and hence the stocks of these fish are shared by several coastal states. The stocks of small pelagic exhibit large natural variations because the recruitment and migration of these species is strongly influenced by hydrographic variations.
- Research on small pelagic fish has been hampered so far by the lack of reliable age readings, consistent catch per effort series, and acoustic surveys. As a result, stock assessments and management advice have not been very precise. Moreover, there is no international management system yet in place for the conservation of small pelagic fish in West Africa.
- Information on benthos biodiversity is scarce in the CCLME and inventories of marine fauna are only currently available for Morocco and the Canary Islands. Although a latitudinal biodiversity pattern is not observed for the epibenthos across the CCLME, highest diversity values are recorded in Western Sahara, being also higher on the shelf and upper slope than in deep waters. Epibenthic communities maintain a similar structure throughout the CCLME, despite the differences in their

specific composition. Suspension-feeder assemblages, previously recorded in the entire upwelling area, do not seem to play an important role in the current epibenthic communities.

- In addition to decapods (the most important group in terms of abundance and biomass), also molluscs, echinoderms, sponges, cnidarians and polychaetes are important benthic representatives. Echinoderms, mainly holothuroids, are clearly dominant in deep waters.
- An important faunistic change between tropical and temperate biota has been reported at Cape Blanc latitude.
- Although tropical coral reefs have not been reported in Northwest Africa, vulnerable ecosystems, like the giant cold-water coral reef, canyon systems, seamounts and grounds of sponges and gorgonians, already exist in deep waters of the continental slope.
- The CCLME cephalopods show high abundances and biomasses, which are also highly diverse. This marine ecosystem presents 139 cephalopods species, many of them having a worldwide distribution.
- Species of the families Ommastrephidae, Loliginidae, Octopodidae and Sepiidae represent the main cephalopod resources with high commercial value, which explains why in this region we can find one of the largest cephalopod fisheries in the Eastern Atlantic. These cephalopods represent a mixture between tropical, temperate and cold water species.
- Coastal cephalopods are dominated by sepiids, loliginids and shallow waters octopuses, while oceanic cephalopods are largely dominated by ommastrephid and deep water octopuses' species.
- As it has been said before, decapods constitute the dominant benthic group in the CCLME. This crustacean group exhibits a great diversity, with a total number of 228 species registered, belonging to 54 families. Brachyura, with 87 different species, is the most diversified taxa, followed by Caridea and Anomura with 61 and 33 species, respectively. This high diversity in the CCLME area is favoured by the presence of typically temperate species in the northern area (Morocco-Western Sahara), subtropical-temperate species (from Morocco to Mauritania) and typically tropical species in the southern area (Guinea-Bissau–Guinea).
- When comparing one area to another, the decapod diversity in the most temperate and northern zone is higher than in the most tropical and southern zone, in part explained by the greater bathymetric range explored in the north. However, there are evidences of the exceptionally high diversity in Mauritania compared with other temperate zones, mainly explained by the special biogeographic and oceanographic special conditions in this area.
- Some decapod commercial species have been targeted by both artisanal and industrial fisheries for decades (i.e. *Parapenaeus longirostris, Penaeus notialis*, *Penaeus kerathurus*, *Aristeus varidens,* etc.). The exploitation of these resources has provided significant economic incomes to the coastal States. However, some stocks, as those of *P. longirostris* from Morocco and from Senegal-The Gambia, are considered overexploited. In addition, there is an indirect impact produced by the fishing pressure on benthic communities by disturbing their physical structures and habitats.
- Six of the seven existing sea turtle species inhabit the waters of the Canary Current. All turtle species in the CCLME are endangered and precise an urgent conservation plan.
- Marine mammal biodiversity remains incompletely documented off Northwest Africa, demonstrated by the 2011 discovery of a Southern Hemisphere breeding stock of *Megaptera novaeangliae* in 4 nations and another seven new range state records: *Grampus griseus* and *Stenella coeruleoalba* new for Atlantic Morocco; *Orcinus orca* and *Balaenoptera musculus* (The Gambia)*; Globicephala macrorhynchus* and *Stenella frontalis* (Guinea-Bissau) and *Stenella attenuata* (Guinea). A first sighting of *Stenella clymene* was recorded in Senegal, a rarely reported delphinid in the Canary Current. Recently the first record of Omura's whale *B. omurai* for the

Atlantic Ocean was encountered in southern Mauritania. In total at least 26 cetacean species have been confirmed from the study region, and others may follow.

NEW CHALLENGES

- *A better understanding of the effect of the hydrographic variations on the pelagic fish stocks is essential for improving stock assessments and management advice. Management has to be organised on an international basis, and it depends on reliable scientific assessments.*
- *Studies focused on the vulnerable marine ecosystems off Mauritania, as well as on the currently unknown benthic communities of deep-shelf and slope waters (Senegal, Guinea-Bissau, Guinea and Cape Verde), are strongly recommended in order to protect these deep-water areas threatened by the trawling fleets' displacement and oil and mineral resources exploitation.*
- *Benthic research in regional marine scientific institutes should be promoted and strengthened and be considered as a short-term priority line. The assessment of the main benthic taxa during scientific and commercial demersal surveys would improve the ecosystem approach to marine resources management and also help keep track of changes in benthic biodiversity over time.*
- *A better understanding on the cephalopods assemblages and ecologic interactions is essential to improve the comprehension of the cephalopods role in the CCLME. Cephalopods are an intermediate link in the food chains, acting as predators or preys in the ecosystem. In consequence, changes in their biomass can directly affect both other specific species and the entire ecosystem.*
- *Cephalopod resources in CCLME represent one of the most substantial fisheries in the Atlantic region. These resources must be managed under a sustainable point of view. This will be useful for a better stock assessment and management advice of the cephalopod resources in the area.*
- *Considering the significant role of decapods in the marine ecosystem, faunal monitoring programs on this and other benthic groups would allow following the status and trends of benthic communities in the CCLME. In this way, protection measures on those especially vulnerable benthic habitats could be recommended for their conservation.*
- *Fishing bycatch of sea turtles is an important threat in the area that should be monitored and significantly reduced in the next years. The most important sea turtle nesting beaches and feeding grounds should be included in marine and coastal protected areas.*
- *A long-term programme covering year-round survey effort, both ship- and shore-based, is required to better investigate the marine mammal biodiversity and biology off Northwest Africa, including their seasonality, migrations, habitat utilisation and abundance. Regional expertise in marine mammalogy must be further reinforced, and promoted as a postgraduate specialisation option among upcoming marine biologists.*
- *It is very important to protect stocks and habitats from the fishing pressure. Adopting the management measures recommended by the Fishery Committee for the Eastern Central Atlantic (CECAF) for the protection of overexploited stocks would ensure their sustainable exploitation. In addition, other management measures aiming to reduce the fishing impact on the ecosystem should be considered.*

Interannual, interdecadal and long-term variability

- The sea surface temperature in the CCLME for 32 years, in the period 1982-2013, shows a warming trend with a mean value of 0.28°C decade^{-1}.
- The warming trend shows significant changes linked to the different dynamical regimes that coexist in the CCLME region: (i) near the coast, in the area linked to the upwelling, between Cape Blanc and Cape Beddouza, the warming trend is not statistically different from zero; (ii) near the coast and in the oceanic waters under the influence of downwelling, between Cape Verde and Cape Blanc, the warming trend is higher (>0.5°C decade^{-1}), and statistically significant; (iii) in the oceanic regions, there is a statistically significant trend of 0.25°C decade^{-1}. This trend in oceanic SST is also observed in waters over the permanent thermocline (200-600 dbar) with a slight weaker statistically significant warming rate, up to 0.25°C decade^{-1}, which is density compensate with an increase in salinity of 0.02 decade^{-1}.
- Neither the intermediate waters nor the upper deep waters shows any statistically significant trend, however the deep waters (2600-3600 dbar) in the oceanic waters north of the Canary Islands, shows a warming rate of -0.01°C decade^{-1} and a freshening of -0.002 decade^{-1}.
- The larger sea level trends, both from tide gauges and altimetry, confirm the sea level rise for the last two decades, in comparison to the 20th century (IPCC, 2013).
- The dynamic of the coastal upwelling intensity can be described in the CCLME during the last 30 years, in terms of trend, interdecadal oscillation and high frequency.
- The long term trends from the global warming can now be estimated, although the seasonal aspects must be further investigated.
- The trends for all upwelling indices are not homogeneous (sometimes inverse) from North to South of the CCLME (hence the importance of splitting the CCLME into five areas). The spatial variability of these components of change is well pronounced and is a particular input from remote-sensing based studies.
- An empirical correction of MODIS (Moderate Resolution Imaging Spectroradiometer) chlorophyll-a data versus its SeaWiFS (Sea-viewing Wide Field-of-view Sensor) equivalent has made possible for the first time in the CCLME the computation of reliable linear trends directly related to the dynamic of the upwelling productivity from 1998 to 2014. After an important decrease of the planktonic biomass up to 2007 in the central and southern part of the system, the new 17-years time series shows a “back to normal” situation, characterized by relatively similar spatial patterns but lower trends. All sources of temporal variability and especially the interdecadal influences may have a strong impact on the computation of trends, which naturally decreases when considering longer time series, up to periods of 20 years or more.
- The CCLME is a region of active physical and biogeochemical processes with direct relevance to the global carbon cycle. Coastal upwelling systems experience natural ranges in surface seawater CO_2 concentrations and pH that are amongst the most extreme in the ocean. A lower ocean pH affects not only on the carbonate biochemistry, but also the chemistry of the compounds and elements present in seawater, mainly those relating to biological activity, such as nutrients and trace metals. pH in surface seawater at the Canary Islands region is decreasing at a rate of -0.0019 ± 0.0003 pH units since 1995.

NEW CHALLENGES:

- *It is necessary to understand the decadal variability in the sea surface temperature trends and its relation with the changes in the upper thermocline, and the atmospheric forcing.*
- *Analysis of high spatial resolution sea surface temperature should be done to contribute to the understanding of the causes of the different long term trends between dynamical regions in the CCLME.*
- *Sea surface temperature trends is not the only impact of global warming in the CCLME ecosystem, moreover, changes in the frequency of extreme sea surface temperature events may happen, and should be understood due its higher impact on the ecosystem.*
- *It is important to establish more sea level stations with long records south of the Canary Islands. At present, there are problems for a correct estimation of the trends in mean sea level; vertical local movements of the land or changes of reference may occur (i.e. accidents, malfunctions in the tide gauge, lack of adequate maintenance and data quality control and assessment).*
- *There is a need of regionalized sea level hindcasts for better understanding of sea level variability and trends (and their forcing mechanisms), not available for the CCLME.*
- *Evolution of extreme sea levels needs further research in order to understand its relation to the mean sea level trends.*
- *It is important to study the sea level anomaly maps from altimetry to obtain a real knowledge of the spatial pattern of sea level variability and trends, and their relation to meteorological and oceanographic features such as the North Atlantic Oscillation, the upwelling system, the main circulation patterns in the region, etc.*
- *Climate change can modify the upwelling dynamic and therefore its productivity. The global warming complexifies this natural dynamic. The combination of climate variability and fisheries impacts can change the functioning and biodiversity of the whole system, from the physic dynamics to all levels of marine life. Therefore, further investigation is needed to understand the climatic variability of the upwelling-favourable winds in the CCLME.*
- *The CCLME is a contrasted region in term of upwelling regimes and constitutes a unique upwelling system to study the interactions between the physical forcing at different time scales and some of its consequences in term of biological productivity and diversity, including decadal variability and long term trends consecutive to global warming.*
- *The systematic collection of time-series observations is required to improve predictions on future CO_2 uptake and the effects of ocean acidification on both the biogeochemical processes and the ecosystems.*

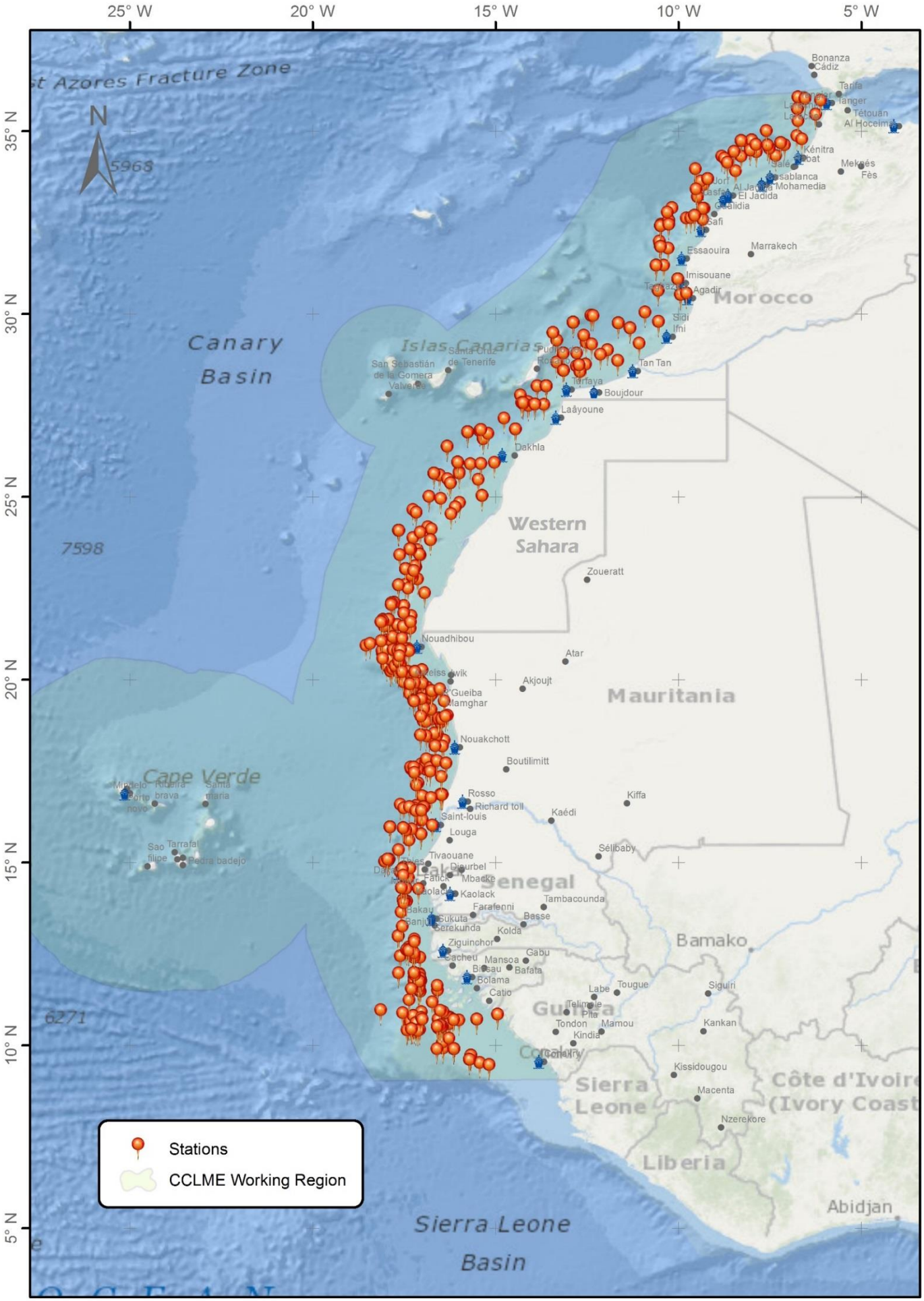
25° W
20° W
15° W
10° W
5° W
35° N
30° N
25° N
20° N
15° N
10° N
5° N
N
Azores Fracture Zone
5968
7598
6271
Canary Basin
Islas Canarias
Santa Cruz de Tenerife
San Sebastián de la Gomera
Valverde
Cape Verde
Morocco
Western Sahara
Mauritania
Senegal
Guinea
Sierra Leone
Liberia
Côte d'Ivoire (Ivory Coast)
Sierra Leone Basin
Bonanza
Cádiz
Tarifa
Tanger
Tétouan
Al Hoceima
Kénitra
Rabat
Meknès
Fès
Casablanca
Mohamedia
El Jadida
Safi
Essaouira
Marrakech
Imisouane
Agadir
Sidi Ifni
Tan Tan
Tarfaya
Boujdour
Laâyoune
Dakhla
Zoueratt
Nouadhibou
Atar
Akjoujt
Nouakchott
Boutilimitt
Rosso
Richard toll
Saint-louis
Louga
Kaédi
Kiffa
Sélibaby
Tivaouane
Diourbel
Mbacke
Kaolack
Tambacounda
Farafenni
Basse
Kolda
Ziguinchor
Cacheu
Mansoa
Gabu
Bissau
Bafata
Bolama
Catio
Bamako
Labe
Tougue
Siguiri
Telimele
Pita
Tondon
Mamou
Kindia
Kankan
Conakry
Kissidougou
Macenta
Nzerekore
Abidjan
Stations
CCLME Working Region

Geographical situation of the decapod specimens records from the CCLME deposited in the Collection of Decapod and Stomatopod Crustaceans of the Cádiz Oceanographic Centre - in Spanish *Colección de Crustáceos Decápodos y Estomatópodos del Centro Oceanográfico de Cádiz* (CCDE-IEOCD). For further information, see García-Isarch and Muñoz, 5.5 this volume. © 2013 Esri, DeLorme, NAVTEQ.

1. INTRODUCTION

Itahisa DÉNIZ-GONZÁLEZ and Luis VALDÉS

Intergovernmental Oceanographic Commission of UNESCO, France

The Canary Current Large Marine Ecosystem (CCLME) is an eastern boundary upwelling ecosystem (EBUE)[1], in fact one of the 4 major upwelling systems in the world. The CCLME extends from the Strait of Gibraltar (around 36°N 5°W) to Bissagos Islands in the South of Guinea-Bissau (around 11°N 16°W), embracing the coasts and Economic Exclusive Zones (EEZ) of Morocco, Western Sahara, Mauritania, Senegal, Gambia, Guinea-Bissau and Spain (Canary Islands). Also Cape Verde and Guinea are under the area of influence of the Canary Current, and therefore are considered as part of the CCLME in this publication (Fig. 1.1).

The coastline of the CCLME extends approximately 5000 km along the Northwest African coast (around 7600 km if the archipelagos coastline is included) and has an extension of 1,120,439 km^2. The continental shelf itself occupies 97,653 km^2. Although the archipelagos of Cabo Verde and Canary Islands are volcanic in origin, the CCLME only account for 0.2% of the world seamounts (Sea Around Us Project, 2015).

In the upwelling systems, deep cold and nutrients-rich waters reach the ocean surface sustaining high primary production during the upwelling season. On average the CCLME has a primary production of 1196 mgC m^{-2} d^{-1} (Sea Around Us Project, 2015), which means 8% of the primary production in the world ocean (Heileman and Tandstad, 2008). Mesoscale features, such as eddies and upwelling filaments, transport cold waters offshore, therefore enlarging the area of influence of the upwelled waters into the ocean. The main purpose of this volume is to review and present recent findings in the oceanographic features at large-scale (e.g. the main currents and the upwelling process) as well as at mesoscale (eddies, filaments) and relate the environmental variability with the biology, from plankton to marine mammals. Obviously the pelagic and demersal ecology of fish and macrobenthic organisms are treated in detail given the importance that they have for the economy of the region[2].

As indicated in the FAO report *The State of World Fisheries and Aquaculture* - SOFIA - (FAO, 2014a), Morocco is the major producer in terms of catches in the CCLME (and the 18th major producer in the world) with a total landed weight of 1,158,474 t in 2012, and the sector employees 870,000 fishermen only in this country. Also Morocco and Mauritania are the principal octopus exporters in the world.

The Fishery Committee for the Eastern Central Atlantic (CECAF) of the Food and Agriculture Organisation (FAO) promotes the sustainable utilization of the living marine resources within its area of competence by the proper management and development of the fisheries and fishing operations[3] and, therefore, it is in charge of the stocks management in the CCLME. The most important species in terms of landings in the Eastern Central Atlantic is sardine (*Sardina pilchardus*).

---

[1] In this publication, eastern boundary upwelling ecosystem (EBUE) and eastern boundary upwelling system (EBUS) are used interchangeably.

[2] In West African coastal countries, where fish has been a central element in local economies for many centuries, the proportion of animal protein that comes from fish is very high, e.g. 44% in Senegal and 49% in the Gambia (FAO, 2014a). It shall be taken into account that the total population in both countries in 2012 was 15,982,565

[3] Source: Regional Fishery Bodies summary descriptions. Fishery Committee for the Eastern Central Atlantic (CECAF). Fishery Governance Fact Sheets. In: FAO Fisheries and Aquaculture Department [online]. Rome. Updated 3 September 2013. http://www.fao.org/fishery/rfb/cecaf/en (accessed 13 April 2015)

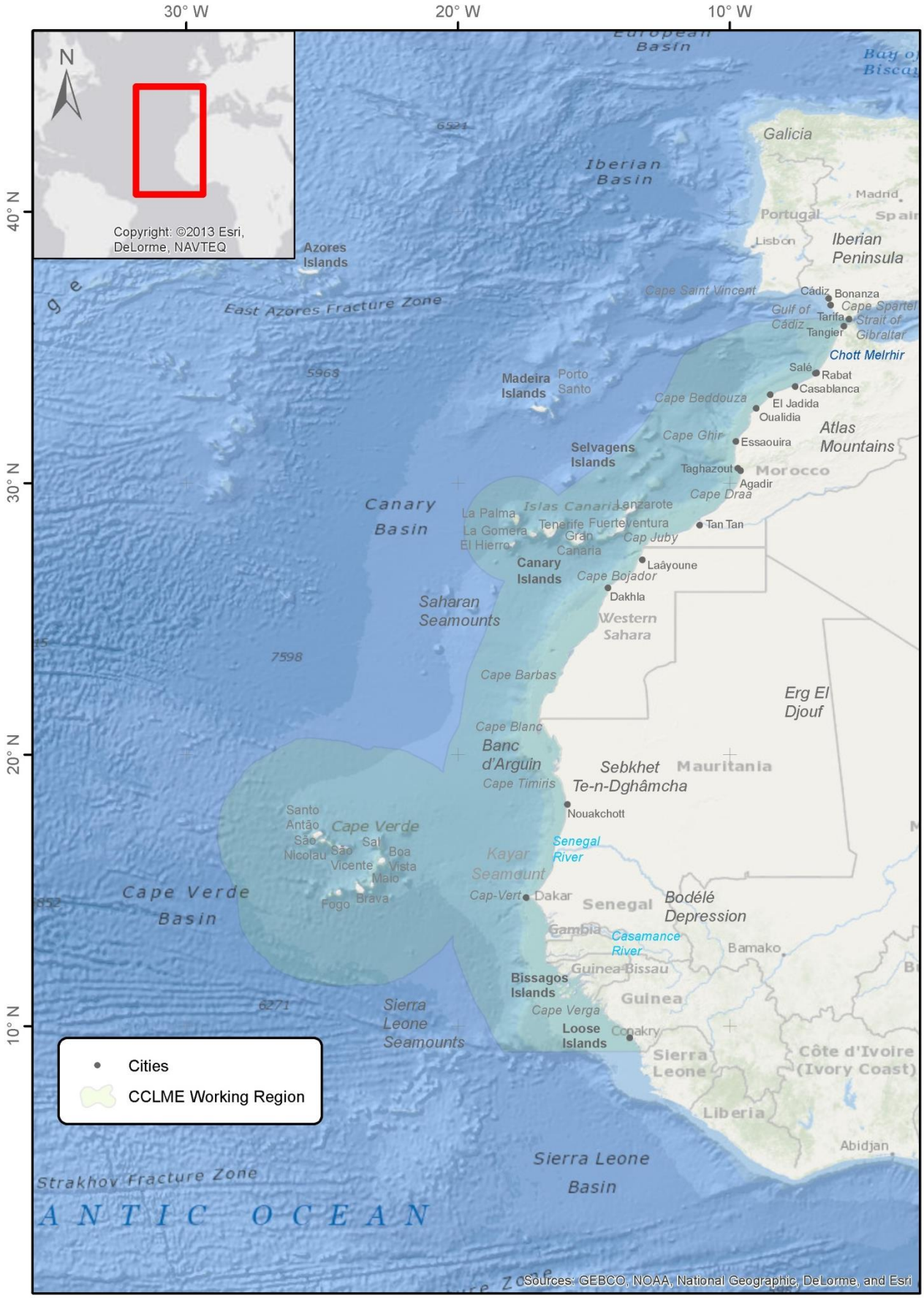

Figure 1.1. Area of study in the Northwest Africa, including the main geographical features cited in this volume.

The sardine stock in the area of Cape Bojador and southward to Senegal is considered underfished, but most of other pelagic stocks are considered either fully fished or overfished. In terms of invertebrates, the stocks of octopus (*Octopus vulgaris*) and cuttlefish (*Sepia* spp.) are the most commercially important, and both are overfished (FAO, 2014a).

The number of threatened fish species in the CCLME countries varies from 23 in Cape Verde to 67 in Guinea (Froese and Pauly, 2008). Meanwhile, the existence of Marine Protected Areas is very different among the countries and their creation has shown different trends over the last decades. While in Cape Verde, less of 0.001% of the territorial waters were protected in 2012, in Guinea-Bissau 45.85% of the territorial waters were protected in the same year[4]. The depletion of fisheries resources in coastal oceans is one symptom of mismanagement, which has to be addressed on the principles of an ecosystem-based approach such as proposed in the CCLME project[5] and in the EAF Nansen project[6].

The holistic concept of Large Marine Ecosystems (LMEs) encompasses large areas (on the order of 200,000 km^2 or greater) reaching from coastal areas to the EEZs, and the outer margins of the major current systems. Most of the ocean pollution and the coastal habitat alteration occur within the boundaries of the LMEs (Sherman, 2005). The LME Program promotes the ecosystem-based approach to support the assessment and management of marine resources and their environments. The approach uses indicators of ecosystem (i) productivity, (ii) fish and fisheries, (iii) pollution and ecosystem health, (iv) socioeconomics, and (v) governance (Sherman and Duda, 1999).

The total population in the CCLME countries and in the countries under the influence of the Canary Current was 65,443,762 people[7] in 2012 plus Western Sahara, with a population estimated in 567,315 people in 2010[8], and the Canary Islands, with a population of 2,104,815 people in 2014[9]. According to the data available, Morocco is the CCLME country with more scientists, with 28,089 scientists in headcounts in 2006, which means 910 researchers per million habitants. There are differences between countries, Senegal had 732 researchers per million in 2007, the Gambia had 30 researchers per million in 2005 and in Cape Verde 132 scientists per million[10] (UNESCO, 2010) [11]. This is in agreement to the % of the gross domestic product (GDP) dedicated by each of these countries to research and development[12]. Even if there are not disaggregated data, we can presume that a part of these researchers are dedicated to marine and natural sciences.

---

[4] Source: United Nations Environmental Program and the World Conservation Monitoring Centre, based on data from national authorities, national legislation and international agreements. Available at: World Data Bank, World development indicators database (last updated 12 March 2015). http://databank.worldbank.org/data/views/variableselection/selectvariables.aspx?source=world-development-indicators# (accessed 29 March 2015)

[5] Source: Canary Current LME Project. http://www.canarycurrent.org/en (accessed 11 January 2015)

[6] Source: EAF-Nansen Project. http://www.fao.org/in-action/eaf-nansen/en (accessed 16 April 2015)

[7] Sources: United Nations World Population Prospects. Available at: the World Bank website, http://data.worldbank.org/indicator/SP.POP.TOTL (accessed 9 February 2015)

[8] United Nations Department of Economic and Social Affairs, Population Division (2013). World Population Prospects: The 2012 Revision, DVD Edition. United Nations, New York. Available at: http://esa.un.org/wpp/Excel-Data/population.htm (accessed 9 February 2015)

[9] Source: Instituto Nacional de Estadística (INE, Spain) Website. www.ine.es (accessed 29 March 2015)

[10] Cape Verde data is expressed in Researchers in full-time equivalent (UNESCO, 2010)

[11] All the data exposed may be underestimated or partial

[12] Source United Nations Educational, Scientific, and Cultural Organization (UNESCO) Institute for Statistics. Available at: http://data.uis.unesco.org/Index.aspx?queryid=74 (accessed 18 April 2015)

As the result of all the scientific activities and the international cooperation programs carried out in the CCLME during decades, a lot of scientific surveys have been undertaken and there is abundant scientific literature in Marine Science. Research effort since 1975 and the data generated and available was compiled in the *Directory of Atmospheric, Hydrographic and Biological datasets for the Canary Current Large Marine Ecosystem* (Déniz-González et al., 2014) which identified a total of 425 datasets, 27 databases and 21 time-series sites in the area. This catalogue and the recovered data offer an exceptional opportunity for the researchers in the CCLME to study the dynamics and trends of a multiplicity of variables, and will enable them to explore different data sources and create their own baselines and climatologies under a spatial and temporal perspective.

The networking in the area has impulsed holistic review efforts that were published in Northwest Africa, for instance: (i) the book *Pêcheries ouest-africaines* (Cury and Roy, 1991) which describes the variability, instability and change of the fisheries in West Africa, relating the fisheries stocks fluctuations to the high natural spatial and temporal variability of the upwelling, but also the variability of the socioeconomic factors; (ii) the review about the CCLME in Arístegui et al. (2006), entitled *Oceanography and fisheries of the Canary Current/Iberian region of the Eastern North Atlantic (18a,E)*; and (iii) the review *Deep-sea ecosystems off Mauritania: Researching marine biodiversity and habitats in West African deep-water* (Ramos et al., submitted a), discussing in detail the biodiversity of one of the biggest CCLME countries.

The CCLME project has recently prepared a preliminary Transboundary Diagnostic Analysis (TDA) (FAO, 2014b), aiming to present the present state of knowledge in the CCLME (following the 5 indicators modules used in the LME Program listed above) and to point out its values, including an exhaustive diagnose to identify the environmental threats and stressors that will guide the priority intervention domains. The overexploitation of living marine resources, the degradation of biological diversity and habitats and the decline of the water quality are analyzed in depth.

All these reviews and reports were used in the current publication, *Oceanographic and biological features in the Canary Current Large Marine Ecosystem*, which attempts to update the scientific knowledge in the CCLME and is structured in the following sections: (i) the ocean geomorphology and geological materials; (ii) the hydrographic structure and the ocean circulation; (iii) the biogeochemical characteristics of the marine ecosystem; (iv) the life in the sea; (v) and the interannual/interdecadal and long-term variability. The main concepts are highlighted in the Executive Summary together with an indication of the gaps left in the up-to-date scientific research developed in the CCLME, evoking ideas on the topics in need of a deeper scientific research and management goals in the CCLME.

2. OCEAN GEOMORPHOLOGY AND GEOLOGICAL MATERIALS

2.1. MAIN GEOMORPHOLOGIC FEATURES IN THE CANARY CURRENT LARGE MARINE ECOSYSTEM

Luis M. AGUDO-BRAVO[1] and José MANGAS[2]

[1] Instituto Español de Oceanografía. Spain

[2] Instituto de Oceanografía y Cambio Global (IOCAG), Universidad de Las Palmas de Gran Canaria. Spain

2.1.1. INTRODUCTION

This work describes the main geomorphological features of the seabed on the Atlantic continental shelf of Northwest Africa (NWA) (region encompassing the Canary Current Large Marine Ecosystem - CCLME, Fig. 1.1). Knowledge of these geological shapes and the existing materials are fundamental for studying the biological habitats they comprise, particularly the benthonic and demersal ecosystems.

In general, geomorphological data on this region collected by universities and research centres is limited and sometimes inaccessible. This report is therefore based on research carried out by the Instituto Español de Oceanografía (IEO) in various oceanographic campaigns conducted in recent years together with scientific publications dealing with particular zones in this region. For this purpose, a review has been made of the geological data obtained in the seven multidisciplinary campaigns undertaken by the IEO throughout the continental margin of Morocco, Western Sahara and Mauritania between 2004 and 2010 (MAROC-04, MAROC-05, MAROC-06, MAURIT-0711, MAURIT-0811, MAURIT-0911 and MAURIT-1011 campaigns, Ramos et al., 2005a, 2010; Hernández-González et al., 2007, 2010). In these oceanographic campaigns, exploration of the seabed was carried out using multibeam echo sounders, high-profile seismic profiling and the direct collection of sediment samples and sedimentary rocks.

The passive continental margin of NWA marks the transition between the lithosphere of the African continent and the oceanic lithosphere generated in the Atlantic Ridge. Continental rift and ocean crust formation in this part of the East Atlantic took place over the course of 225 Ma. The substrate of this continental margin is therefore composed of Palaeozoic metamorphic rocks, the oldest sedimentary rocks are Triassic (sandstone, carbonate and salt deposits dating from some 200 Ma) and the ancient oceanic crust is Jurassic (some 180 Ma – Divins, 2003; Davison, 2005; Müller et al., 2008). As for the sedimentary rocks (carbonated and detrital), the oldest are of continental origin while the later ones are of marine origin from various depositional environments (coastal, shelf, slope and seabed). In slope and continental shelf zones, these sedimentary materials can all reach thickness of up to 10 km, while in seabed zones they are below 5 km (Divins, 2003). In this zone of NWA, various surveys have also been carried out in recent decades under the Deep Sea Drilling Project (DSDP) and Ocean Drilling Program (ODP), which have described the main geological features of the materials and morphologies of the continental margin (e.g. Uchupi et al., 1976; Von Rad and Ryan, 1979; Von Rad et al., 1982; Schmincke and Sumita, 1998). In addition, distensive tectonic structures have been cited throughout the region, most consisting of normal faults on an axis more or less parallel to the continental edge and structures perpendicular to the latter (Weaber et al., 1998; Tari et al., 2003; Davison, 2005; Davison and Daily, 2010). On the Morocco-Western Sahara-Canaries margin (Fúster Casas sedimentary trough), and on the Mauritania-Senegal-Guinea margin,

descriptions exist of numerous salt domes, pockmarks and faults associated with diapiric processes related to Triassic saline deposits that have fluidified and intruded into the stratigraphic column of the continental margin (Martínez del Olmo and Buitrago, 2002; Tari et al., 2003; Acosta et al., 2003a; Davison, 2005; Davison and Daily, 2010; Cuñarro et al., 2014). Finally, two volcanic archipelagos associated with hotspots and consisting of islands and numerous seamounts exist in ocean interplate areas of the CCLME (Schmincke and Sumita, 2010; Carracedo, 2011).

The main geomorphological features of the CCLME region are described below in a survey of four geographical areas selected on a north-south basis, namely Morocco-Western Sahara, Canary Islands, Mauritania, and Senegal–Guinea-Bissau–Guinea–Cape Verde Islands.

2.1.2. MOROCCO-WESTERN SAHARA

The continental margin of Morocco and Western Sahara extends from latitude 36° to 21°N and within longitudes 5.5° to 20°W. This northern sector of the CCLME was the site of the MAROC oceanographic campaigns (2004, 2005, 2006) carried out by the IEO. Bathymetric and geomorphological prospecting during these campaigns was undertaken using R/V *Vizconde de Eza*'s EM 300 multibeam echo sounder, which operates at a frequency of 30 Khz and provides data from 20 m to 5000 m, working at an average speed of 10 kn. Correction of the speed of sound in water was achieved by first developing sound velocity profiles using an SVPlus sensor produced by Applied Microsystems LTD in the area to be studied on a daily basis. Monitoring of the zones explored during the campaign, management of the unprocessed information and work planning with the multibeam echo sounder was achieved by designing a Geographical Information System (GIS).

On the continental margin of Morocco and Western Sahara, the average width of the continental shelf is some 40 km to 50 km, arriving at a minimum width of some 20 km opposite the Tamri National Park, to the north of Agadir. The head of the continental slope is situated at a depth of 200 m, and the foot is at 1500 – 2000 m in the North and 3000 m south of the latitude of the Canary Islands.

In geological terms, the Atlantic continental margin of Morocco and Western Sahara may be divided into three main zones, designated from North to South as:

(1) Margin corresponding to the olistrome (Gulf of Cadiz).
(2) Margin affected by turbidity phenomena.
(3) Margin dominated by the Agadir Canyon.

In addition, multibeam information obtained in the MAROC 04, 05 and 06 campaigns has made it possible to undertake more detailed zoning of this Atlantic margin of Morocco and Western Sahara and has made for a better understanding of the marine geomorphological features, as described below. The main geomorphological features identified (Figure 2.1.1) are:

(a) Strait of Gibraltar-Gulf of Cadiz domain.
(b) Gharb Basin domain, subdivided in two subdomains.
(c) Oum er Rabia domain.
(d) Tensift domain.
(e) High Atlas domain.
(f) Agadir Canyon domain.

(a) Strait of Gibraltar-Gulf of Cadiz (zone 1 in Figure 2.1.1):

This corresponds to the slope situated between the Gulf of Cadiz and the Gharb valley, a marine zone dominated by the allochtonous units fronting the flysch elements of the Campo de Gibraltar (Gibbons and Moreno, 2002). This domain has a very irregular, polygenetic geomorphology. The south-eastern part thus contains a series of narrow, deep-set channels, with isolated depressions some 20 m deep to 50 m deep, bounded by high structural elements, which serve to channel a large part of the deep currents exiting the Strait. These large geomorphological alignments are associated with displacement and overthrusting of the allochtonous units (Gibbons and Moreno, 2002).

Other morphologies occupying large areas in the zone are sediment waves and megarriples, resulting from strong currents proceeding from the Strait, and mud volcanoes up to 1 km in diameter, some of them collapsed. Certain of the mud volcanoes are surrounded by semi-circular depressions resulting from the collapse of escaped mud, which produces small runs.

These varied geomorphological features indicate the existence of a major dynamic (including at the present time) and produce very diverse environments and, in turn, generate a wide variety of habitats and biological zoning.

(b) Gharb Basin:

This domain is situated between the Gharb and Oum er Rabia rivers, and extends almost to Azemmour (zones 2 and 3 in Figure 2.1.1.). The terrestrial basin of the Gharb River continues into the sea but its bed has two zones with different geomorphologies, defined as the smooth-bed Gharb domain (b.1) and the Gharb domain with steps (b.2), which seem in reality to be landslide fronts and scars.

(b.1) Smooth-bedded Gharb subdomain (zone 2 in Figure 2.1.1):

It clearly continues the emerged basin of the Gharb, extending over the highest part, from the edge of the shelf to the middle slope in the north. It has fairly regular and flat beds with small waves that seem to indicate continuous sedimentation through constant currents that accumulate material throughout the shelf. Most of the sediments must derive from the emerged Gharb basin, to be reworked by the intermediate seabed currents, which produces fine terrigenous materials (fine sands and silts) or very fine (silts and clays).

(b.2) Ripple-bedded Gharb subdomain (zone 3 in Figure 2.1.1):

In this area, the width of the slope lessens and the gradient increases, with steps of from 50 m to 70 m at depths of between 1100 m and 1800 m. These steps have possibly been produced by debris slides, representing one of the various debris flows located in this margin, as evidenced by numerous turbidites. The morphology of this zone comprises alternating steps and cuvettes, elongated and sub-parallel to the gradient, which reveal a certain grain selection depending on whether the sediment is located in escarpment zones or cuvettes, although the beds are usually muddy.

(c) Oum er Rabia (zone 4 in Figure 2.1.1):

This domain has been called Oum er Rabia to reflect an appearance and distribution of materials indicating its association with the basin of this river, which flows into this zone. Here the margin is quite narrow, with fairly smooth and flat beds up to 1300 m deep. Beyond this depth the margin becomes steeper and is criss-crossed by well-defined channels. The notable geomorphological feature in this zone is the scar (trench),

sub-parallel to the coast, situated opposite El Jadida, at a distance of 800 m to 1700 m. This trench seems to be the start of a large-scale landslide in the area, so that its activity could have future repercussions on conditions in the domain.

The high zone of the margin in this domain has a flat and gently curving morphology, which could indicate, in the absence of seismic data, that in addition to the accumulation of sediments deriving from the coast, currents are redistributing the latter over the floodplain. In the middle and lower part of the slope, the uneven seabeds are more suited to the appearance of a wide variety of benthonic species or at least to their being better protected.

(d) Tensift (zone 5 in Figure 2.1.1):

In this domain the continental shelf is fairly wide and the slope relatively steep, being traversed by numerous channels. In the northern zone the channels are fairly narrow, with depths ranging from 30 m to 100 m, and with very steep sides. In the southern part the geomorphology seems to reveal the existence of various debris slide elements, crossed by broader channels than those in the north. Furthermore, the front part features small terraces, preceded by escarpment zones, which could indicate debris slide scars. In general, the sides north of all these channels are steeper gradient and taller.

With regard to the nature of the seabed sediments, the data obtained from the sets on the MAROC campaigns indicate that they are muddy in nature, although they are sandier towards the mouth of the Tensift River.

(e) High Atlas (zone 6 in Figure 2.1.1):

This domain is bounded by two small canyons and seems to constitute a large forestepping-type sedimentary unit, the results of inputs from the rivers flowing into the zone, which are the southern drainage exit of the Oum er Rabia basin, although the southern part below sea level reveals the continuity with the High Atlas chain.

The seabed seems smoother in the upper part while in the centre of the zone it appears rougher, which may be interpreted as an area containing thick detrital materials or corals.

In the northern part of this domain, on the middle and deep slope, there are gravitational landslide escarpments that may be thought to feed into the turbidite channels that extend into the deepest areas.

The sedimentary coverage, although it seems for the most part muddy, according to the samples gathered throughout the MAROC campaigns, contains a substantial sand fraction while the shallower and subhorizontal part of the domain gives way to gravel. In general, the sediments are thicker towards the river mouths and much finer in the southern part.

(f) Agadir Canyon (zone 7 in Figure 2.1.1):

This consists of a steep slope in the northern part of the canyon and some smoother areas in the southern part, although the seabeds are fairly even. It features deeply excavated channels, especially in the south, as well as a zone of done-shaped mounds, ringed by troughs, broadly similar in appearance to those found in the Strait of Gibraltar -Gulf of Cadiz domain.

Opposite the Sous River, the zone is also crossed by a series of channels reminiscent of the geomorphology found in the pro-delta areas, so that the zone in question could correspond to this type of deposit.

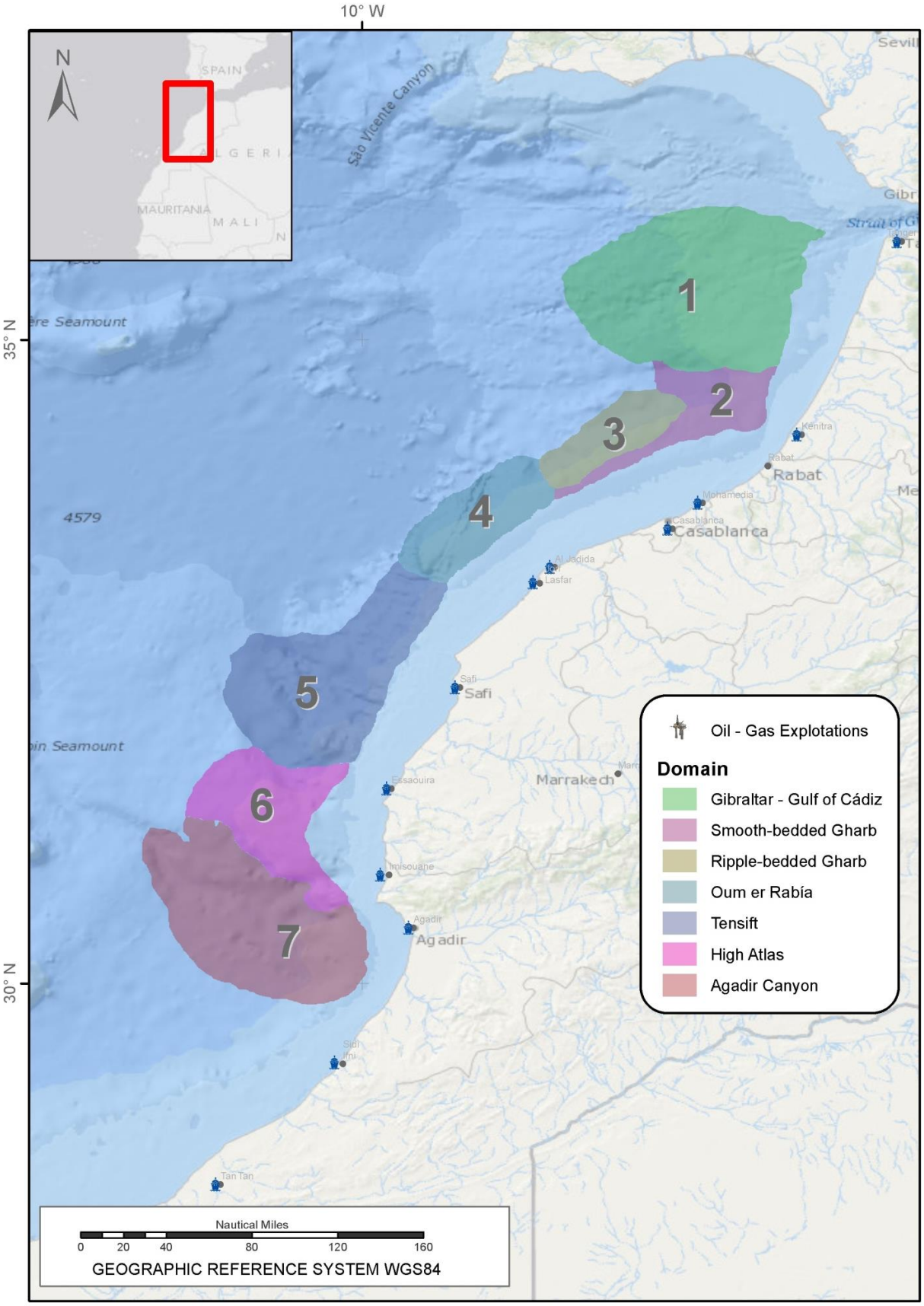

Figure 2.1.1. Map of the geomorphological domains in the Morocco-Western Sahara area.

2.1.3. CANARY ISLANDS

The Instituto Hidrográfico de la Marina (IHM) and the IEO have carried out four joint campaigns in the vicinity of the Canary Islands, between 1998 and 2001, on board R/V *Hespérides* and R/V *Vizconde de Eza*, under the project "Hydrographic Oceanographic Study of Spain's Exclusive Economic Zone (EEZ)", using the EM-12 and EM-1002 multibeam echo sounders.

Data collection and system operation took place uninterruptedly, on a 24-hour basis, the IHM and the IEO being jointly responsible for monitoring the information obtained.

Continuous seismic profiling was also carried out using the TOPAS parametric probe, as well as gravimetric profiling based on the Bel-Aerospace gravimeter, with data collection every 10 seconds, and magnetometric profiling using a Geométrics G-801 proton marine magnetometer, polarizing every 6 seconds and with an accuracy of 1 nT.

For its part, the IEO has collaborated in studies of the Spanish Exclusive Economic Zone, collaborating in four campaigns in the area of study, carrying out multibeam sonar cartography of the region (Fig. 2.1.2), high-resolution seismic profiling and direct sample collection (Clift and Acosta, 2005).

The result, partially available, is a detailed bathymetric cartography, as well as maps of gravimetric and magnetic anomalies (Clift and Acosta, 2005).

The Canary Islands is an archipelago of intraplate volcanic origin, located in the central part of the CCLME, very close to the North East of the African continental margin. The archipelago extends over more than 500 km and is formed by seven main islands. The islands emerge from an ocean floor whose depth increases towards the west, from some 1200 m to the west of Lanzarote and Fuerteventura, which are the easternmost islands, to 4000 m in the region of La Palma and El Hierro, which are the westernmost of the islands (see Mangas and Quevedo, 2.2 this book).

The most ancient islands, such as Fuerteventura, Lanzarote, Gran Canaria and La Gomera, have well-developed island shelves (Acosta et al., 2003b; Llanes et al., 2009; Cuñarro et al., 2014, Fig. 2.1.3). However, the more recent islands, such as Tenerife, La Palma and El Hierro, have no more than pronounced slopes extending from the coastal to the abyssal zones. The island slopes conceal underwater canyons, some of them connected to subaerial ravines. Escarpments have also been reported on the island aprons, some of them associated with large gravitational landslides or the head of underwater canyons (Fig. 2.1.3). Recent monogenetic strombolian volcanoes have also been described on the flanks of certain islands (Fig. 2.1.3).

The archipelago has a very long volcanic history which, with the exception of the more recent islands, La Palma and El Hierro, goes back 10 Ma or even 20 Ma. Some islands are characterized by distinct periods of volcanic activity, alternating with phases of rest and intense erosion, while others seem to have remained in almost continuous activity. The discontinuous character of volcanism complicates evaluation of the total volume of magma emitted and the rate of magmatic production.

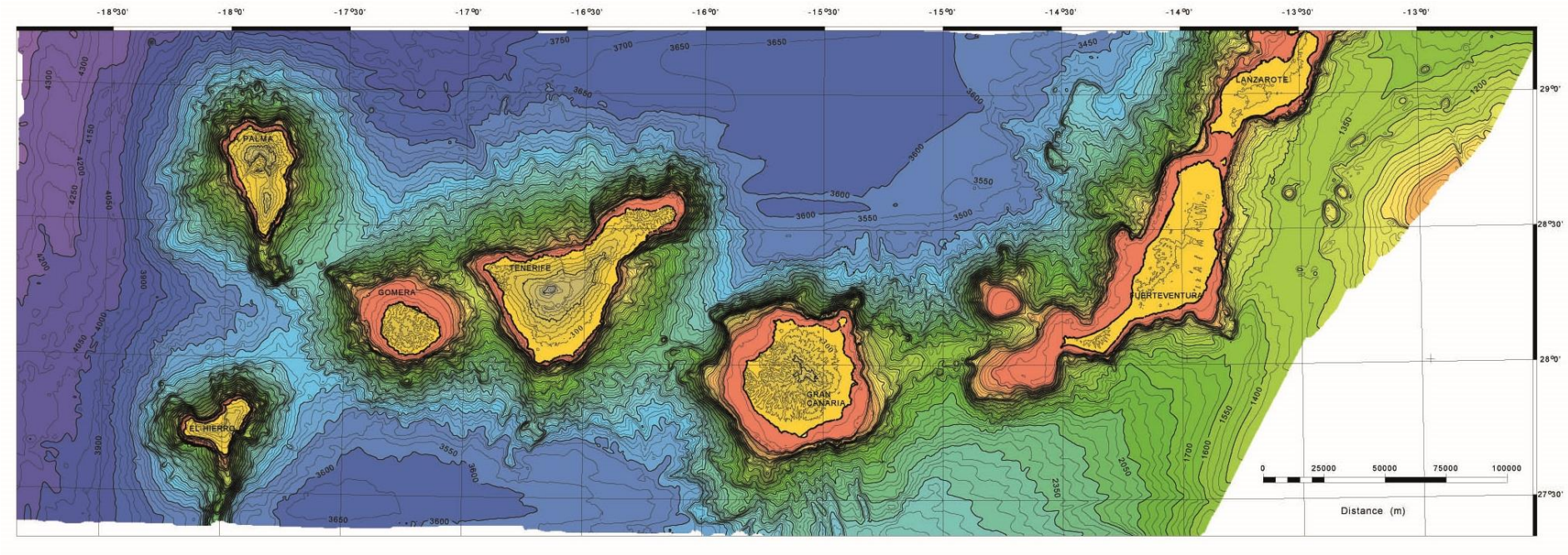

Figure 2.1.2. Bathymetric chart resulting from the cartography carried out during the EEZ campaigns (reproduced from Acosta et al., 2003b).

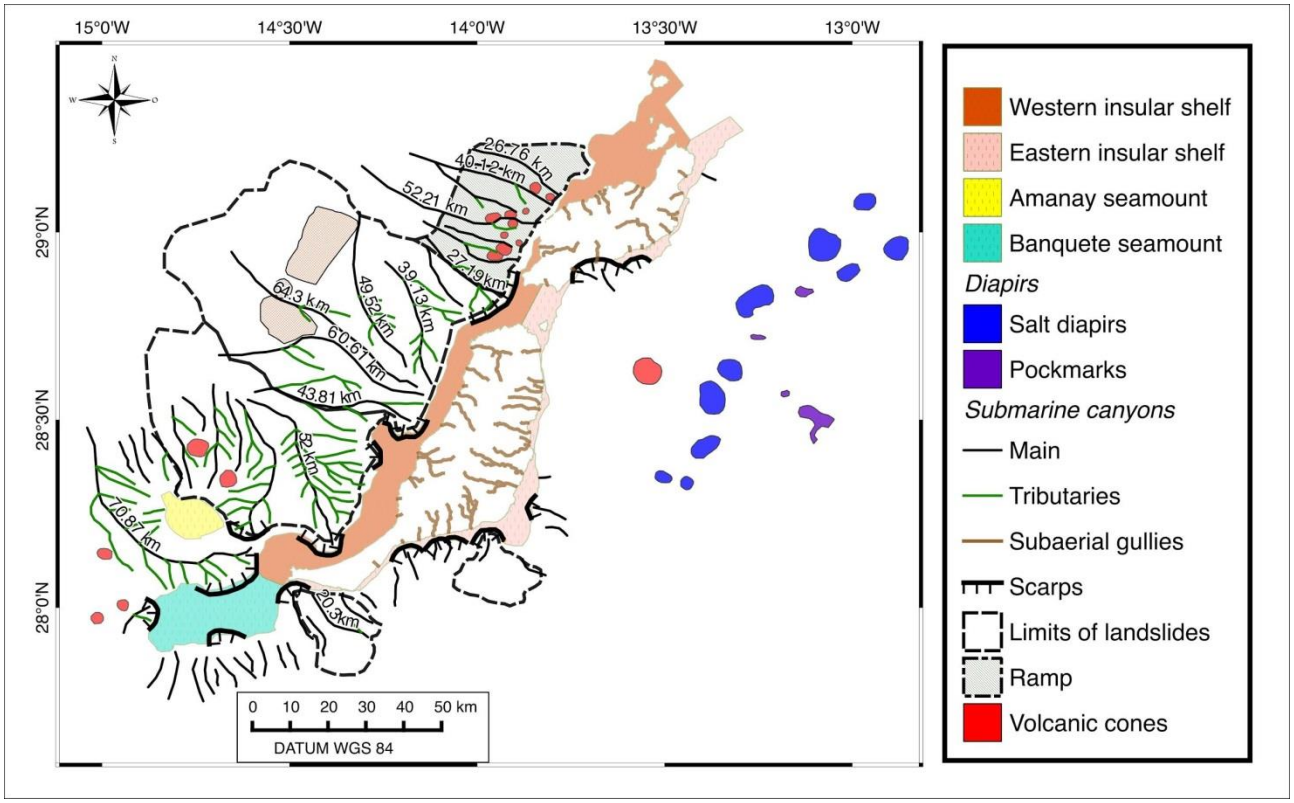

Figure 2.1.3. Geomorphological elements described on the seabed around the island edifices of Lanzarote and Fuerteventura (Canary Islands) (after Cuñarro et al., 2014).

However, Schmincke (1982) calculates the total volume for the islands of this archipelago at 20 x 103 km^3, including submarine and subaerial volcanic products and intrusive and sedimentary materials, while not taking into account material released by large landslides. The subaerial part of the islands is approximately 10% of the total volume of the island mass (Schmincke and Sumita, 2010).

Each island has a different geological history, having commenced its activity at different times and with its own particular duration and evolution. The relief and structure of the islands is characterized by four types of volcanic features: submarine volcanism, shield volcanoes, stratovolcanoes and areas with monogenetic strombolian volcanoes. The detailed evolution of volcanic activity, together with a general account of the evolution of magmatic activity over time, is described by Schmicke and Sumita (2010) and Carracedo (2011).

Oceanic islands throughout their geological history are subject to continuous erosive processes, constituting a major source of sediments that form great aprons several hundred metres in size on the flanks of islands. Among the erosive processes affecting the islands, major landslides and debris avalanches are the most significant volumetrically, since they have been frequent and have helped to dismantle the great volcanic edifices. In the Canaries, over the last 20 years, numerous research projects have focused on identifying and describing major gravitational landslides, in submerged and emerged zones alike. Compilations of the cartography of the landslides, the estimated age and volumes of each of them, the relations between them and comparisons with those of other archipelagos are to be found, for example, in the studies of Masson et al., 2002; Ancochea et al., 2004; Funck and Schmincke, 1998; Carracedo, 1999; Krastel et al., 2001; Acosta et al., 2003b; Cuñarro et al., 2014. In addition, four surveys carried out by the

ODP (Weaber et al., 1998) in the underwater aprons of Gran Canaria drilled down hundreds of metres and encountered volcanic-sedimentary slope facies materials (hemipelagic materials associated with debris flows from the continental margin, deposits of sandy-muddy turbidites, pyroclastic falls and volcano-sedimentary deposits of debris flows and island avalanches), these being genetically linked to the formation phases of the subaerial part of the island (Weaber et al., 1998). None of these surveys yielded submarine igneous materials (volcanic, subvolcanic and plutonic) from the island edifice.

Volcanic origin and heavy erosion characterize the marine zone of the island edifices, which have a narrow shelf and a steep slope, increasing over some 10-20 km from 80-100 m to 4000 m in the abyssal zone. The slopes of the island edifices are characterized by the presence of volcanic-sedimentary materials, consisting of lava stream fragments mixed with avalanche debris, block slides several kilometres in size (Schmincke and Sumita, 1998; Acosta et al., 2003b; Schmincke and Sumita, 2010; Cuñarro et al., 2014), as well as finer sediments on other parts of the slopes, which may be of polygenic origin (including detritus proceeding from the mouths of island ravines, coastal erosion, windborne material, debris flows and turbidites deriving from the continental margin).

Various debris flows, slides and turbidity currents have been identified in the Canary Islands zone, deriving from the African continental margin and extending to the abyssal zone outside the CCLME.

These sedimentary deposits consist of pelagic and volcanoclastic sediments, with very gentle gradients of less than 2° and volumes of hundreds of km^3, which have been termed the Sahara Slide and Canary Debris Flow, to the south and west of the archipelago, and the turbidity current that reaches to the Madeira abyssal plain to the north (Rothwell et al., 1992; Urgeles et al., 1997; Gee et al., 1999; Masson et al., 1998, 2006). These sedimentary deposits are thought to be the result of volcanic and seismic activity in the Canary Islands, together with gravitational landslide processes and eustatic movements in the continental margin throughout the Quaternary (Masson et al., 2006).

2.1.4. MAURITANIA

The Mauritanian margin extends from latitude 21° to 15.5° N and longitude 16° and 19°W approximately. It is one of the best known of all the CCLME thanks to the four ecosystem campaigns conducted by the IEO between 2007 and 2010 (Ramos et al., 2005a, 2010; Hernández-González et al., 2007, 2010). In addition to the Spanish campaigns, this review has used a number of published works in some zones (Antobrech and Krastel, 2006, 2007; Colman et al., 2005; Henrich et al., 2008, 2010; Krastel et al., 2006; Wien et al., 2007; Zühlsdorff et al., 2007).

The MAURIT oceanographic campaigns were carried out using geophysical equipment provided by R/V *Vizconde de Eza*, namely the EM 300 multibeam echo sounder (throughout the sampling zone) and continuous high-resolution TOPAS reflection seismics (from time to time). The EM 300 is a medium-range multibeam echo sounder that possesses great resolution and high data acquisition speed and is reliable and easy to use. It operates at a frequency of 30 kHz and provides complete scanning capacity for depths ranging from 10 m through shallow shelf depths, including some deep basins up to 5000 m. Using the TOPAS parametric survey, it is possible to obtain high-resolution profiles of the subsoil, which provides adequate knowledge of the geology and geomorphology.

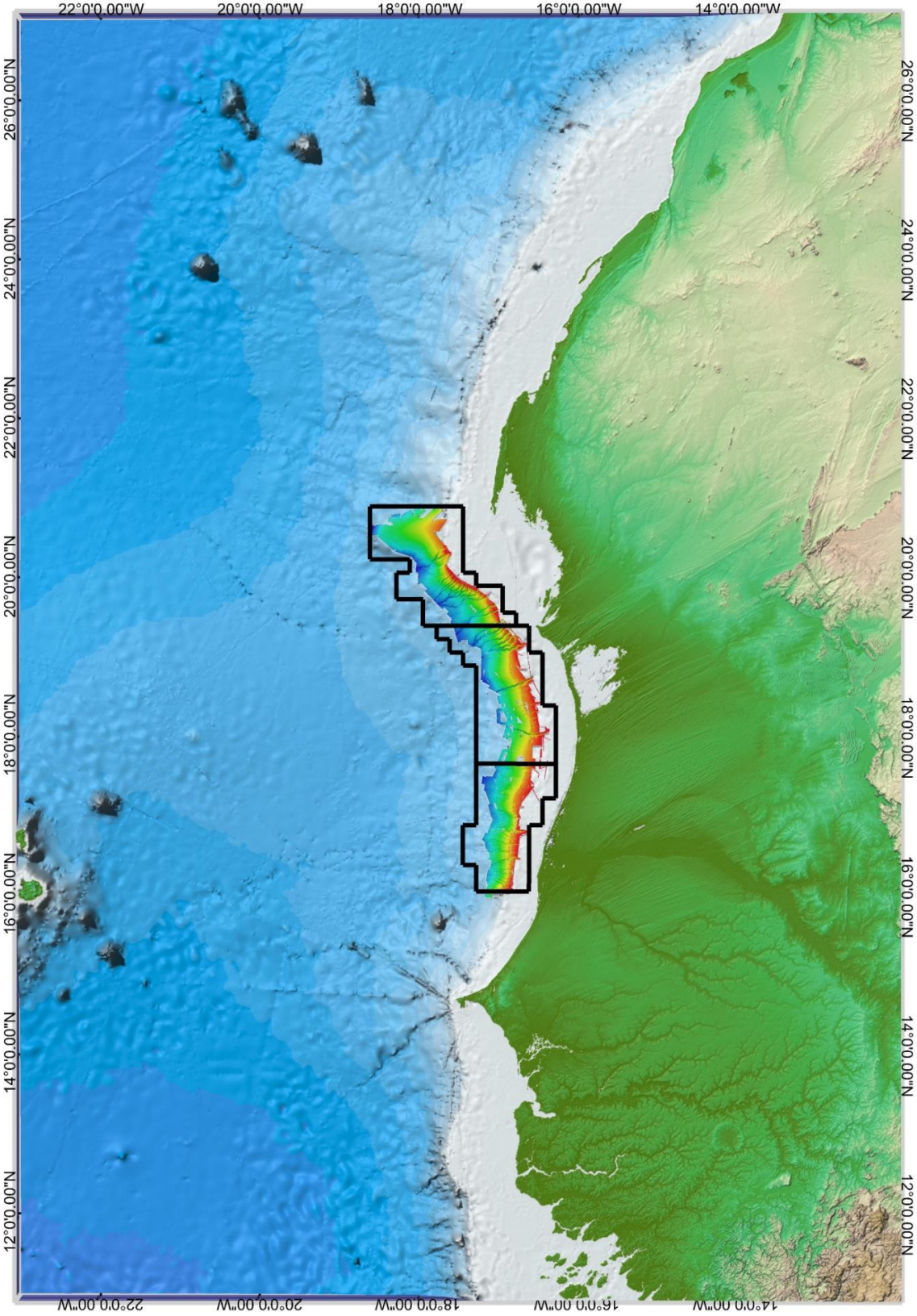

Figure 2.1.4. Chart of the studied area, involving satellite bathymetry (source Becker et al., 2009) and multibeam bathymetry, obtained during the MAURIT campaigns. The areas outlined in black correspond to the three sectors into which the area was divided for the thematic mapping exercise

Based on the oceanographic campaign data, the continental shelf on the Mauritanian margin has an average width of some 30-50 km, reaching a maximum width of some 140 km opposite the Arguin Bank. The head of the continental slope is situated at a depth of some 150-200 m and the foot at 2500 m.

The geomorphological features found in this part of the African continental margin (Figure 2.1.4.) are the result of a complex association of various geological processes. Notable among these are glacial processes that occurred during the last glaciation process, together with recent gravitational landslides linked to instabilities in the underwater slopes. The accumulation of a sizeable volume of sediments from the continental zones, transported by the existing and extinct rivers, can become unstable through seismic activity or the liberation of methane hydrates and can move downwards towards the deep ocean. In turn these landslides find themselves cut off by a system of underwater canyons that channel the existing sediment inputs, notably the Timiris and Kayar Canyons, which reach the deep ocean very close to the Cape Verde archipelago.

In accordance with the data collected by the IEO in the MAURIT campaigns (2007-2010), a distinction can be made between three different geomorphological domains corresponding to two major landslides, with their network of associated canyons, and a third geomorphological domain consisting of a large reef structure subparallel to the coast, which extends along the whole length of the Mauritanian margin. The main geomorphological features of these domains are described below.

(a) Cape Blanc-Timiris Canyon landslide domain

In this zone there is a clear enlargement of the shelf, which reaches 140 km compared with an average width of between 30 km and 50 km. This reflects the existence of the Arguin Bank, which occupies the inner and middle shelf, with depths of between 2 m and 15 m. On a single narrow strip of the outer shelf, the depths increase rapidly from 15 m to 150-200 m, which mark the edge of the continental shelf.

The northern part of the slope features two large groups of canyons, located opposite the Arguin Bank and Cape Timiris. These groups end by converging on two canyons at the foot of the slope which continue into the deep ocean.

(b) Mauritania-Kayar landslide domain

To the south of the previous domain, from almost the latitude of Nouakchot to Dakar, there is a large debris flow fed by aeolian materials from the Sahara Desert. This major landslide extends to the south of the Cape Verde Islands (Figure 2.1.5).

The Kayar Canyon crosses this landslide, veering south at Cape Verde until it reaches the Gambian abyssal plain.

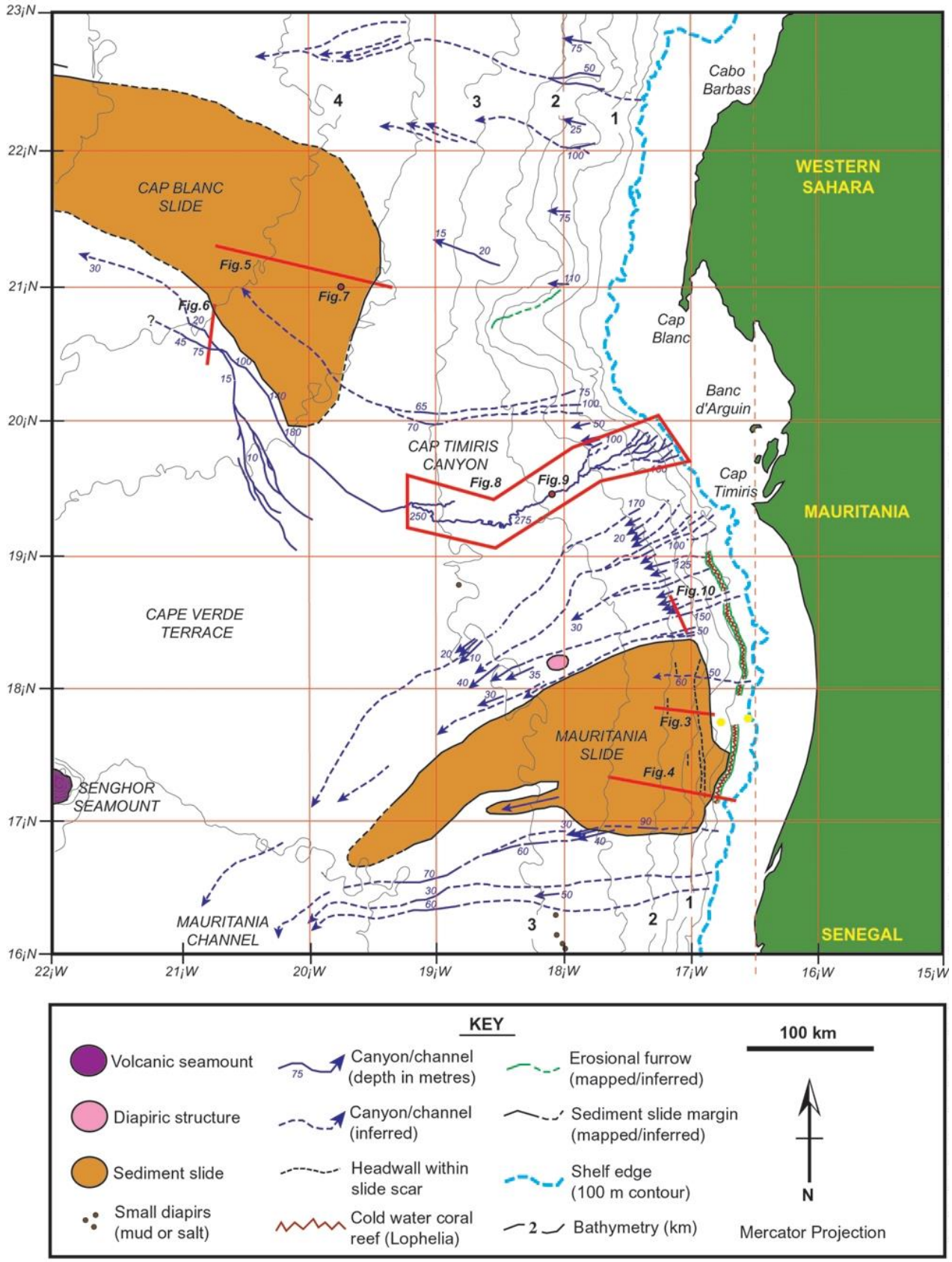

Figure 2.1.5. Localization of the Cabo Blanco, Mauritania and Timiris Canyon landslides (after Krastel et al., 2006)

(c) Coral reef domain

Between Cape Timiris and the Senegal River a positive structure has been observed, running parallel to the coast, which has been identified as a coral reef (Ramos et al., submitted b). The structure is located at a mean depth of some 100 m and is 405 km long and some 1700 wide (Fig. 2.1.5). It corresponds, according to the results of rock dredge samples, to a coral reef that appears bounded to the west and east by two channels some 50 m deep, parallel to the bioconstruction in question.

This reef is situated at an average depth of 500 m, the bathymetric limit of its crest remaining constant (around 450 m deep to 460 m deep) like that of its trenches (around 550 m).

The morphology identified shows various ramifications in an east-west direction, with very narrow crests (some 300 m to 600 m wide), despite the fact that canyons are present almost continuously throughout the stretch concerned. The reef is clearly dissected by the canyons, so that its genesis preceded the development of the latter. It has also been noted that in zones where it does not appear there are geomorphological features that point to the development of landslides on the flanks of the slopes (generally consisting of very fine mud), which must have covered the bioconstruction.

It would seem that the origin of the barrier corresponds to a period of colder and cleaner waters, characterized by a lower sea level. This barrier was affected subsequently by changes in the sea level and mud avalanches. The middle and lower slopes show signs of collapse and creeping, and on the upper slopes transitional landslips and forestepping deposits, which must have caused the demise of the corals through the development of turbidity currents that first silt up and then bury the reef. This activity seems to have been more marked in the north, a reduction of the erosive processes being observable in the south.

2.1.5. SENEGAL-GAMBIA-GUINEA BISSAU-GUINEA-CAPE VERDE ISLANDS

The southern part of the CCLME corresponds to the waters of Senegal, Gambia, Guinea-Bissau, Guinea and the Cape Verde Islands, from latitude 17.5° to 9°N and longitude 13.3° to 28.5°W approximately. The various geomorphological features are described below on the basis of existing publications (Jacobi and Hayes, 1982, 1984, 1992; Jarvis et al., 1980; Kidd et al., 1987).

The width of the shelf in this area varies between 10 km and 130 km, with an approximate surface area in this zone of 8700 km^2. Opposite Pointe des Almadies the edge of the continental shelf is situated at 5 km, increasing towards the south until it reaches 100 km at 12°45´N and 123 km opposite Guinea-Bissau. The head of the slope is at an average depth of 200 m, while the foot is situated at a depth of between 2500 m and 3000 m.

The Senegal basin is geologically related to that of Mauritania, and could be designated the Senegal-Mauritania basin, many of the geomorphological features being the same. This basin is the westernmost in the whole of West Africa and covers some 340,000 km^2. Its length from north to south is about 1000 km, with a maximum width of 560 km at the latitude of Dakar, its width decreasing towards the south, in the direction of Guinea, where it disappears.

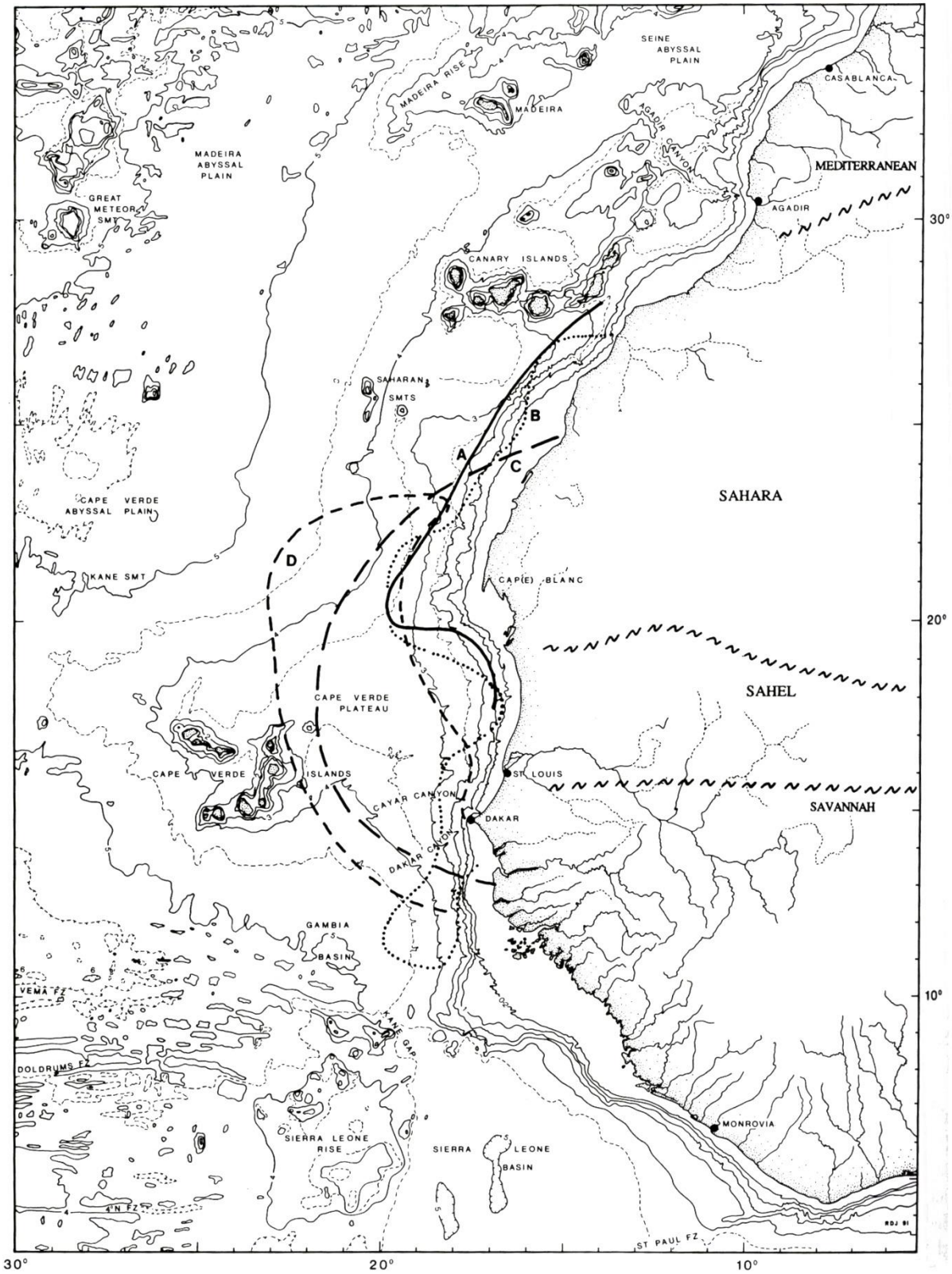

Figure 2.1.6. Chart with general bathymetric and morphological features of the NWA margin. The isobars represented by unbroken lines correspond to contours at an interval of 1000 m, and the dotted lines to contours at an interval of 500 m. The bathymetrics derive from data obtained from GEBCO. After Jacobi and Hayes (1992). © 1992 by Springer Science+Business Media New York. With permission of Springer Science+Business Media

The detailed cartography of this zone carried out by Jacobi and Hayes (1992, Figure 2.1.6) has highlighted numerous debris flow deposits, channels, turbidite deposits, sedimentary trenches and extensive areas with numerous sedimentary waves of diverse morphologies, which are produced by deep currents. Many of these debris flows and turbidites begin on the continental shelf, and their materials extend into the abyssal sea floor, beyond Cape Verde Islands. The direction of these sedimentary lobes is E-W and NE-SW.

From the tectonic standpoint, the Senegal-Mauritania basin is governed by a series of normal faults, in a north-south direction, which indicates that there is a generalized extension taking place in this region.

In general the deep seabed is fairly uniform, without major morphological features, apart from two sizeable underwater canyons, one to the north of Dakar, opposite Fossé de Kayar, and another opposite Dakar. More to the north, at 16°50'N and los 16°53'N, there are also two small canyons, on the border between the south of Mauritania and the north of Senegal, structurally related to the Senegal River, smaller than that described previously.

Mention should also be made of the existence, on the slope at 100 km to the north-west of Dakar, of three seamounts called Kayar, Petit Kayar and Petit Medina. Conical in shape and volcanic in origin, their crests in the case of the largest of them (Kayar Seamount) attain a depth of 184 m.

As regards the seabed of the Cape Verde archipelago, there are virtually no scientific publications on the submarine geomorphology of these island edifices. Reference should however be made to the studies carried out recently by Masson et al. (2008), analysing gravitational landslides on the slopes of the westernmost islands (Fogo, Santo Antão, São Vicente and São Nicolas), consisting of various ages debris avalanche deposits, debris flow deposits, escarpment landslides, turbidity canyons, underwater ravines and monogenic volcanic cones. In addition, there has been mapping, at the foot of these volcanic structures, of soundings of sediments transported by strong currents.

2.1.6. CONCLUSIONS AND RECOMMENDATIONS

The continental margin in CCLME is characterized by a large accumulation of sedimentary rocks and marine sediments attaining thickness of up to 10 km near the continent and under 5 km in the abyssal zones. This sedimentary sequence reveals the geological history of some 225 Ma (Triassic) in the Atlantic Ocean, this being the moment at which the continental fracture of Pangea occurred in this zone and the formation of the ocean crust on the ridge, beginning approximately 180 Ma ago (Jurassic). The current geomorphology of NWA is influenced by the erosive-sedimentary processes of coastal zones, continental shelf, slope and deep ocean, which occasionally reveal volcanic structures in the form of islands and intraplate seamounts, in both the Canaries and Cape Verde Islands zones.

The shelf zones in CCLME are typical of passive continental margins in subtropical median latitudes, in terms of both depth and incline and of the detrital sedimentary materials to be found there. Variations in geomorphological and material features are due to the presence of sedimentary inputs associated with active or fossil river basins, tectonic processes and morphologies having very little influence in this margin. In addition to these sedimentary inputs, the river basins have an impact on the genesis and presence of canyon systems on the continental shelf and, in turn, on their development on the slope, canyon systems being one of the main geomorphological features of slopes throughout the region.

Debris flow deposits are also very common in this margin, on both shelf and slope, and extend as far as the deep ocean zones, although part of them remains outside the area delimited by the CCLME.

At the same time, the deepest limits of the shelf serve as the head of turbidity systems found throughout the region, turbidite canyons with diverse orientations having been described together with related deposits of various dimensions.

There are also zones featuring numerous submarine salt domes at the foot of the continental slope and many of these diapirs appear as positive geomorphologies several kilometres long and hundreds of metres high. One of these diapir zones extends from Morocco to the Canary Islands (Fúster Casas trench), and the other from Mauritania to Guinea. These zones containing salt domes as prominent as those constituting intrusions in the sedimentary sequence are areas of great interest for the exploration of fossil hydrocarbons and are currently being explored by a number of oil companies. Mention should also be made of the existence of a fossil coral reef some 400 km in length, in the shallowest zone of the Mauritanian slope. There are also some isolated seamounts close to the shelf and slope, such as those to the north of Dakar (Kayar seamounts).

The morphological monotony of the abyssal plains is interrupted by the presence of large debris flow deposits and avalanche debris deriving from the subaerial and underwater flanks of the volcanic Canary and Cape Verde Islands. In addition, geomorphological studies confirm the existence of insular shelves in the oldest islands, together with submarine canyons and escarpments, associated with gravitational landslides. In the younger islands, there is no continental shelf although extensive scars of landslips and underwater canyons are to be found. Monogenic volcanic cones are also very common.

Finally, attention should be drawn to the lack of detailed geomorphological and sedimentary information on the more southerly zone of the CCLME (Cape Verde archipelago, and the waters of Gambia, Guinea-Bissau and Guinea). It is therefore recommended that geophysical and geological campaigns should in future be undertaken in this area.

Acknowledgements

This work was undertaken within the framework of the ECOAFRIK project and it is ECOAFRIK publication number 27. The authors wish to thank the IEO for supporting these biological and geological research projects. We should also like to offer our most sincere thanks to Dr Ana Ramos, head of the ECOAFRIK research project.

2.2. OCEANIC INTRAPLATE VOLCANIC ISLANDS AND SEAMOUNTS IN THE CANARY CURRENT LARGE MARINE ECOSYSTEM

José MANGAS[1], Luis Á. QUEVEDO-GONZÁLEZ[1] and Itahisa DÉNIZ-GONZÁLEZ[2]

[1] Instituto de Oceanografía y Cambio Global (IOCAG), Universidad de Las Palmas de Gran Canaria. Spain

[2] Intergovernmental Oceanographic Commission of UNESCO. France

2.2.1. INTRODUCTION

The Canary Current Large Marine Ecosystem (CCLME) involves part of the Atlantic-type (passive) African continental margin, a marine domain where sedimentary processes prevail in both coastal and oceanic environments. Indeed, external erosive agents and sediment-storing conditions appear in coastal areas, continental shelves (<200 m depth) and continental slopes linked to the abyssal plains with a depth range from 1000 m to 4000 m. Besides, sedimentary processes have occurred in the last 200 Ma (Lower Jurassic), once this central part of the Atlantic Ocean began to spread out. Thus, sedimentary rock layers and non-consolidated sediment layers reach together a thickness of 10 km width on this area (Divins, 2003). However, several areas exhibit geological anomalies due to magmatic processes (i.e. plutonic, sub-volcanic and volcanic) since 142 Ma ago (Lower Cretaceous), thus resulting in volcanic-originated intraplate archipelagos of both islands and seamounts (Van den Bogaard, 2013). A north-south sequence of such volcanic edifices, namely the archipelagos of Madeira Islands, Selvagens Islands, Canary Islands, Saharan Seamounts, Cape Verde Islands and Sierra Leone Seamounts, constitutes the Magmatic Belt of Western Africa (Fig. 1.1) (Schmincke and Sumita, 2010), placed over the continental rise and the abyssal plains at this passive margin. Nonetheless, the Canary Islands and surrounding seamounts, as well as the Cape Verde islands and nearest seamounts are just those included in the CCLME region (Fig. 1.1), alluding to the hereinafter called Canary Islands Volcanic Province (CIVP) (Fig. 2.2.1) and Cape Verde Islands Volcanic Province (CVIVP) (Fig. 2.2.2).

The Canary Islands archipelago is made up of 7 major islands and several islets placed in the vicinity of 28°N latitude. It extends over 500 km W of the easternmost one, Fuerteventura island, which is located 100 km off the African coastline at Cape Juby (Western Sahara) (Fig. 1.1). Considering the CIVP region, despite including approximately 100 seamounts, the largest ones were considered solely for this work (Tab. 2.2.1) (Fig. 2.2.1). CIVP seamounts expand over 700 km from Henry seamount (40 km SE of El Hierro island) to Anika seamount (300 km SE of Madeira Island). Besides, a major group of seamounts placed SW of El Hierro island, the Saharan Seamounts (e.g. Tropic, Endeavour, Bisabuelas), together with Essaouira seamount (290 km from Porto Santo, Madeira island) are geologically related to the CIVP (Van den Bogaard, 2013), even though placed out of reach of the CCLME limits. Also, seamount-rich Cape Verde archipelago extends over 500 km W of the easternmost island of Boa Vista, which is located 600 km away off Dakar (Senegal), comprising 10 islands and several islets too, and so, located around 16°N latitude (Fig. 2.2.2). In addition, there are three seamounts at 120 km to the north-west of Dakar, called Kayar, Petit Kayar and Petit Medina but they are independent to the Cape Verde archipelago (Fig. 1.1). Canary Islands and Cabo Verde archipelagos are part of the Macaronesian region, together with Madeira, Selvagens and Azores; even though the latter ones are found outside the CCLME region, as indeed is also the case for Sierra Leone Seamounts (Fig. 1.1).

In geological terms, the CIVP has been object of several studies (e.g. cartography, petrology, geochemistry, geomorphology, volcano-stratigraphy) for about two centuries (see review in Schmincke and Sumita, 2010; Carracedo, 2011), whereas the CVIVP studies began in the 20th century (Bebiano, 1932). In the 60-70 decades, research was leaded by Portuguese (Junta do Investigaçoes do Ultramar), North American and other European teams from several universities and research centres (see review in Anguita and Hernan, 2000; Madeira et al., 2010; Dyhr and Hom, 2010; Represas et al., 2012). Likewise, German research groups (Geldmacher et al., 2001, 2005, 2011; Van den Bogaard, 2013) and Spanish teams (Ancochea and Huertas, 2003; IEO, 2013a, 2013b; Quevedo-González et al., 2012, 2014) have also focused on geological characteristics of CIVP seamounts in the last 30 years. However, a research background of CVIVP seamounts is barely supported. On the other hand, the CCLME only includes 0.2% of the seamounts worldwide (Sea Around Us Project, 2015).

Hereby, this article reviews the geological knowledge of the Canary Islands and Cape Verde Islands volcanic provinces, so including the studied morphology of 28 seamounts in the CCLME region, together with some results obtained under the project LIFE+ INDEMARES (2009-2013), concerning the seamounts of Conception Bank, El Banquete and Amanay (Quevedo-González et al., 2012, 2014). In general, seamounts are submarine geological features showing a twofold interest, namely, scientific and economic (Staudigel and Clague, 2010). Seamounts are placed over oceanic intraplate geo-tectonic environments, and owe their origins to mantle-related igneous processes. Also, biogeochemical and hydrographical processes occur on these geological edifices. A variety of deep-water seamount-related ecosystems show enhanced biodiversity, and thus being worth to become protected areas. Economic interests surface due to related geo-resources (e.g. phosphorites, methane hydrates, ferromanganese crusts and nodules) (Hein et al., 2010) and bio-resources (e.g. fisheries). In both scientific and economic terms, interdisciplinary studies of these undersea mountains open up a wide range of opportunities for new international research projects in the future.

2.2.2. GEOLOGICAL SETTING

In regard to crustal characteristics, the CIVP and CVIVP are located over a thick, rigid and long-lived oceanic lithosphere, originated from the Mid-Atlantic Ridge and defined as a slow-spreading ridge (2.7 cm yr^{-1}) (Van den Bogaard, 2013). Canary Islands and seamounts from the CIVP emerge over a part of oceanic crust enclosed by the S1 (E of Lanzarote island) and the M21 (W of El Hierro island and E of Selvagens Islands and Essaouira seamount) magnetic anomalies. As a result, the oceanic crust involved is around 150-175 Ma old (Middle and Upper Jurassic) (Müller et al., 2008). Besides, the Moho discontinuity divides the oceanic crust and the upper mantle at 12 km depth under the western Canary Islands, while it is found at 22 km depth under the easternmost ones. Also, the oceanic lithosphere thickness is approx. 100 km for this area in the Atlantic Ocean (Bosshard and Macfarlane, 1979; Banda et al., 1981; Korhonen et al., 2007). Likewise, the oceanic crust under the Cape Verde Islands and seamounts (CVIVP) has an age of about 120-140 Ma (Lower Cretaceous), since they are enclosed within the M2 and M20 magnetic anomalies. On this case, Moho appears at 7 km depth throughout the entire region, while it is found at 22 km depth under volcanic edifices. Besides, oceanic lithosphere in the CVIVP region represents about 85 km in thickness (Ali et al., 2003; Pim et al., 2008; Represas et al., 2012).

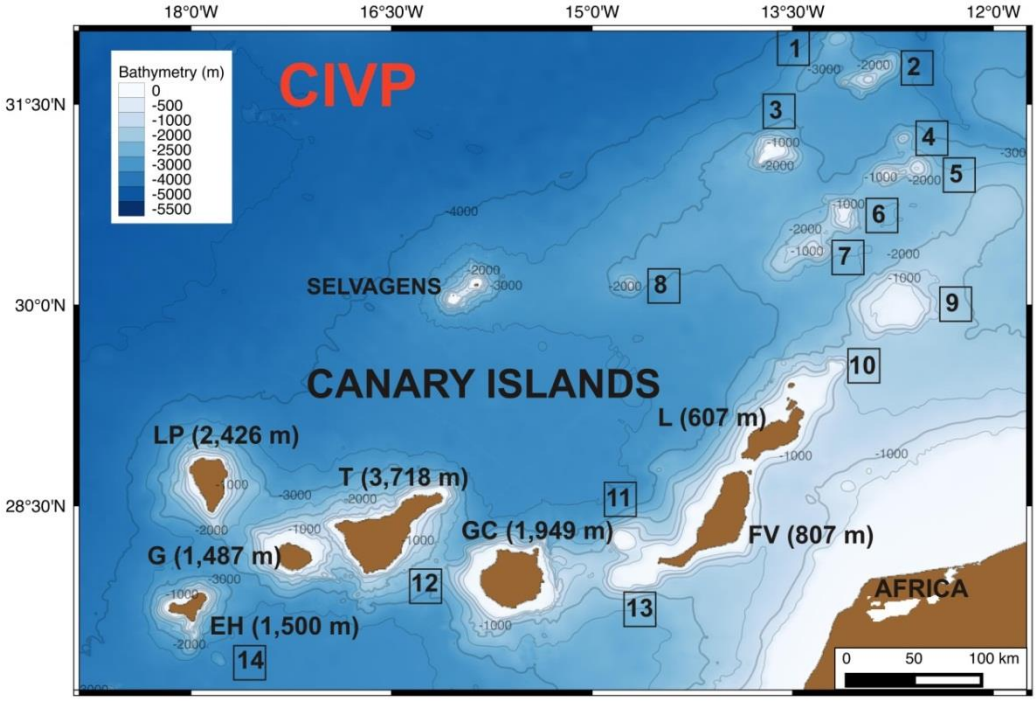

Figure 2.2.1. Bathymetry map showing the Canary Islands Volcanic Province (CIVP), located in the CCLME region. Labels in squares refer to each seamount (Tab. 2.2.1). Labels in brackets refer to the maximum height (m) for each island (modified from Becker et al., 2009). L: Lanzarote, FV: Fuerteventura, GC: Gran Canaria, T: Tenerife, G: Gomera, LP: La Palma, EH: El Hierro islands.

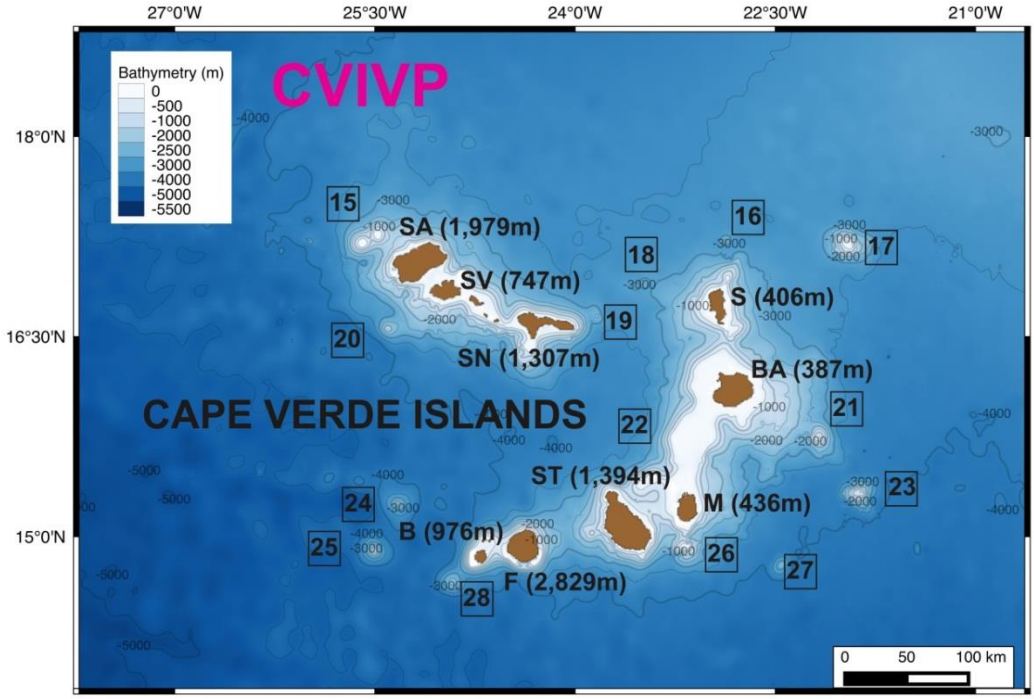

Figure 2.2.2. Bathymetry map showing the Cape Verde Islands Volcanic Province (CVIVP), located in the CCLME region. Labels in squares refer to each seamount (Tab. 2.2.1). Labels in brackets refer to the maximum height (m) for each island (modified from Becker et al., 2009). SA: Santo Antão, SV: São Vicente, SN: São Nicolau, S: Sal, BA: Boa Vista, M: Maio, ST: Santiago, F: Fogo, B: Brava islands.

Table 2.2.1. Morphometric characterization for seamounts in the CIVP-CVIVP regions (data used from GEBCO database - Becker et al., 2009 - and Google Earth). Seamounts types defined after Staudigel and Clague (2010): Sm (small seamount), M-s (mid-size seamount) and Sh (shallow seamount). Seamounts ages (Ma) after Van den Bogaard (2013).

#	Seamount	(approx. locations of unnamed seamounts)	Latitude (N)	Longitude (W)	Summit depth (m)	Basal depth (m)	Height (m)	Type	Shape / Align. / n-cones	Age (Ma)
Canary Islands Volcanic Province (CIVP)										
1	*(unnamed)*	NW Anika	32° 00′	13° 09′	2300	3700	1400	M-s	simple-truncated cone	
2	Anika		31° 43′	12° 52′	750	3400	2650	M-s	complex-extended / NE-SW	55
3	Dacia		31° 07′	13° 39′	45	3000	2955	Sh	complex-extended / NE-SW	47
4	*(unnamed)*	NE Dacia	31° 15′	12° 39′	1400	3200	1800	M-s	simple-truncated cone	
5	*(unnamed)*	E Dacia	30° 58′	12° 45′	350	2700	2350	Sh	complex-extended / ENE-WSW / 2	
6	Nico N		30° 39′	13° 06′	225	2500	2275	Sh	simple-truncated cone	
7	Nico S		30° 24′	13° 19′	400	2400	2000	Sh	complex-extended / NE-SW	
8	Last Minute		30° 08′	14° 42′	1200	3300	2100	M-s	simple-truncated cone	
9	Conception Bank		30° 00′	12° 43′	158	2500	2342	Sh	simple-truncated cone	18
10	*(unnamed)*	NE Lanzarote I.	29° 33′	13° 12′	145	1500	1355	Sh	simple-truncated cone	
11	Amanay		28° 14′	14° 44′	27	3400	3373	Sh	simple-truncated cone	15
12	El Hijo		28° 05′	16° 10′	2200	2800	600	Sm	simple-truncated cone	0.2
13	El Banquete		27° 59′	14° 40′	47	2200	2153	Sh	complex-extended / NE-SW	
14	Henry		27° 19′	17° 46′	3050	3800	750	Sm	simple-truncated cone	126
Cape Verde Islands Volcanic Province (CVIVP)										
15	Northwest		17° 14′	25° 31′	35	3500	3465	Sh	complex-extended / NE-SW / 2	
16	*(unnamed)*	NE Sal	17° 12′	22° 75′	1700	3250	1550	M-s	complex-extended / NE-SW	
17	Senghor		17° 10′	21° 55′	300	3300	3000	Sh	complex-extended / E-W	
18	*(unnamed)*	NW Sal	16° 53′	23° 30′	1300	3100	1800	M-s	simple-truncated cone	
19	*(unnamed)*	E São Nicolau	16° 38′	23° 50′	2400	3500	1100	M-s	simple-truncated cone	
20	*(unnamed)*	SW Santo Antão	16° 33′	25° 24′	1500	4000	2500	M-s	simple-truncated cone	
21	*(unnamed)*	SE Boa Vista	15° 44′	22° 10′	427	3300	2873	Sh	simple-truncated cone	
22	João Valente Bank		15° 43′	23° 00′	50	3500	3450	Sh	complex-extended / NE-SW	
23	Cape Verde		15° 19′	21° 51′	700	4000	3300	Sh	simple-truncated cone	
24	*(unnamed)*	NW Brava	15° 15′	21° 16′	2570	4200	1630	M-s	simple-truncated cone	
25	*(unnamed)*	W Brava	14° 53′	25° 29′	737	4500	3763	M-s	simple-truncated cone	
26	Sul do Maio		14° 55′	23° 10′	340	3600	3260	Sh	simple-truncated cone	
27	*(unnamed)*	SE Maio	14° 47′	22° 26′	2720	4100	1380	M-s	simple-truncated cone	
28	Cadamosto		14° 39′	24° 54′	1700	4200	2500	M-s	simple-truncated cone	

2.2.3 MANTLE PLUMES AND HOT SPOTS

A mantle-derived, plume-like model is adapted to the geological characteristics described in several studies for the CIVP-CVIVP regions consisting in fertile, anomalous mantle showing continuous volcanism over millions of years at oceanic intraplate zones, on specific areas called hotspots (Burke and Wilson, 1972; Duncan, 1984; Holik et al., 1991; Hoernle and Tilton, 1991; Hoernle and Schmincke, 1993a, b; Hoernle, 1998; Carracedo, 1994; Mata et al., 1998; Widom et al., 1999, Geldmacher and Hoernle, 2000; Gurenko et al., 2006). CIVP-CVIVP volcanism is caused by mantle-derived secondary plumes (in consonance with Courtillot et al., 2003). Seismic tomography conducted under the CIVP-CVIVP areas (e.g. Montelli et al., 2006; Zhao, 2007) indicates velocity anomalies for P and S waves within the lower mantle (from 2900 km depth, Gutenberg (G) discontinuity, to 660 km depth), and similarly, from the upper mantle to the oceanic lithosphere (from 660 km depth to 100 km depth). A stem-shaped plume from the lower mantle (from 2900 km depth) reaches the upper mantle (660 km depth) forming a bulb-shaped magma chamber of hundreds or thousands km^2. Thereafter, several small-sized secondary plumes appear within the upper mantle, leading to different hotspots with continuous volcanism. Besides, some authors have described mega-plumes from Cape Verde to Canary Islands, through Madeira Islands and NW of Africa, ending on the Iberian Peninsula, France and Germany, or even mega-plumes covering several archipelagos (Hoernle et al., 1995; Anguita and Hernan, 2000; Merle et al., 2006, 2009; Patriat and Labails, 2006). Further, other authors have described independent mantle plumes for each archipelago, where continental drift of the African oceanic plate allow the creation of islands and seamounts with an age progression from E to W on each volcanic province (e.g. Burke and Wilson, 1972; Schmincke, 1973; Hoernle and Tilton, 1991; Holik et al., 1991; Hoernle and Schmincke, 1993b; Carracedo et al., 1998; Geldmacher and Hoernle, 2000; Geldmacher et al., 2001, 2005; Barker et al., 2009; Madeira et al., 2010).

Likewise, the CIVP and CVIVP have been also related to both upper-mantle plume model and deep convection currents induced by thermal differences between a warmer asthenosphere and the relatively colder oceanic lithosphere, thus explaining recent and contemporary volcanism in the same archipelago, on islands placed at the furthest locations from each other (King and Ritsema, 2000). It has also been described a possible mantle plume, moving in space and time, responsible of volcanic edifices in different areas of the oceanic crust. For instance, the Saharan seamounts have formed in Jurassic and Cretaceous (<142 Ma); CIVP seamounts located NW during Cretaceous and Palaeocene (<70 Ma); and from Miocene to these days the Canary Islands and some seamounts (Fig. 1.1 and 2.2.1), with an age progression from the oldest basalts on Fuerteventura island and Lanzarote island (W) to the youngest island of El Hierro (E) aside from El Hierro Ridge (Van den Bogaard, 2013).

Hence, a scientific controversy about the existing deep mantle plume (lower and upper mantle) still remains for both volcanic provinces. However, researchers agree that these archipelagos are related to the activity of two independent oceanic intraplate hotspots. Indeed, they are considered isolated since the geochemical studies of radiogenic isotopes indicate several differences in isotopic relations of Nd, Pb and Hf elements. Nevertheless, these authors state that these hotspots indicate heterogeneous mantle sources related to mantle mixing processes of (i) old subducted oceanic crust (HIMU-type), (ii) depleted (DM-type) and (iii) enriched (EM-type) mantle in incompatible trace elements; either way, resulting magmas differ in ^{143}Nd:^{144}Nd; ^{206}Pb:^{204}Pb; ^{207}Pb:^{204}Pb and ^{176}Hf:^{177}Hf isotopic relationships (e.g. Hoernle and Tilton, 1991; Hoernle and Schmincke, 1993b; Mata et al., 1998; Gurenko et al., 2006, 2009; Martins et al., 2010; Geldmacher et al., 2011).

2.2.4. MAGMA CHAMBERS AND INTRAPLATE ISLANDS AND SEAMOUNTS FORMATION

From the asthenosphere, peridotitic, anomalous upper mantle, ranging 50-100 km depth, in the CIVP-CVIVP regions have suffered partial melting (about 10%), forming magma liquids with ultramafic-mafic compositions (primary magmas). These liquids have lower density than the solid residual peridotite, thus ascending until they reach rock layers with the same density, near Moho (between 7 km depth and 22 km depth in these provinces). Magma liquids stall as crustal intrusions, making up magma chambers, which are able to generate volcanic eruptions at the ocean bottom, forming islands and seamounts for hundreds of thousand years. As for instance, during the last eruption on El Hierro island in October 2011, about 22000 low-magnitude seismic events were detected, whose epicentres focussed between 10-25 km depth, covering an area of tens of km^2 (Martí et al., 2013; Rivera et al., 2013), thus reflecting where the magma chamber was located. In geochemical terms, igneous rocks appear in both provinces from sub-saturated alkaline magmas. Magma chambers containing magma liquids experience fractional crystallization, while decreasing its temperature and releasing volcanic materials to the upper layers. So, daughter magmas appear with ultramafic-mafic (e.g. basanites, nephelinites, trachybasalts) and intermediate-felsic (e.g. phonolites, trachytes, rhyolites) geochemical compositions, supporting effusive and explosive eruptions, respectively, and ultimately forming volcanic edifices of lava flows and pyroclastic flows.

Besides, these volcanic provinces respond to the intraplate oceanic islands formation model (Walker, 1990), which has been adapted for seamounts too (Staudigel and Clague, 2010). Also, several building stages for each particular island is possible (e.g. Gran Canaria island), as well as for each volcanic edifice, since one island might be formed by several edifices over time (e.g. Tenerife island is made up of 4 different edifices: Central, Teno, Anaga and Cañadas). Formation stages for volcanic islands are: (i) submarine and emerging stages (high eruption rates, ultramafic-mafic submarine flows and pillow lavas below 700 m depth; while pillow lavas and hyaloclastite flows above 700 m depth), (ii) subaerial shield-building stage (high eruption rates; mafic-intermediate subaerial flows; nephelinites, basanites, basalts, trachybasalts), (iii) declining stage (decreasing eruption rates; pyroclastic and lava flows; trachytes, phonolites and rhyolites of differentiated magmas), (iv) erosional stage (erosive and sedimentation phases); (v) rejuvenated stage (low-volume eruptions, ultramafic-mafic lava flows of a new magmatic chamber); (vi) atoll stage (erosion; sedimentation; gradual sinking and coral reef formation); and (vii) guyot stage (subsidence of the volcanic edifice).

In the case of seamounts, evolution phases are similarly defined: (i) small-sized mountains (submarine effusive lavas and mafic pillow lavas; volcanic edifice formation with less than 100 m height); (ii) medium-sized mountains (high-rate eruption of mafic lavas; edifice growth from 100 m height to 1000 m height); (iii) explosive shallow mountains (hyaloclastite flows, pillow lavas; less than 700 m depth); (iv) island stages (similar to those described for islands); and lastly, (v) submarine subduction stage (final collapse of undersea mountains beneath terrestrial subduction zones).

In both CIVP-CVIVP regions, volcanic materials of every formation stage have been studied. So, submarine-stage materials (referred to the basal complexes of the Canary Islands) crop out as magma-driven, uplifted blocks in CIVP (i.e. La Palma, La Gomera and Fuerteventura islands) and CVIVP (i.e. Sal, Maio and São Vicente islands). A basal complex is constituted of oceanic lithosphere materials (e.g. MORB-type volcanic rocks), submarine igneous rocks from the island edifices (i.e. volcanic, subvolcanic and plutonic), together with marine sedimentary rocks settled on the slopes. For instance, submarine igneous rocks crop out on Fuerteventura island, with an age between >70 Ma (Upper Cretaceous) and <33 Ma (Oligocene); and also La Palma island, aged 3-4 Ma (Pliocene). In regard to the CVIVP, on Sal island there are submarine rocks

dated about 26 Ma (Oligocene); whereas on Brava island, between 2-3 Ma (Plio-Quaternary) (e.g. Staudigel and Schmincke, 1984; Le Bas et al., 1986; Torres et al., 2002a; Gutiérrez et al., 2006). From shield-building and declining stages, geological samples have been studied on almost every island and a few seamounts of both provinces (see reviews in Schmincke and Sumita, 2010; Carracedo, 2011). Uplifted volcanic rocks of both shield-building stage and declining stage (e.g. Anika, Dacia, Last Minute, Conception Bank), and of rejuvenated stages (e.g. Dacia, Conception Bank, El Banquete and Amanay) serve as a case in point on seamounts too (Geldmacher et al., 2001, 2005, 2011; Van den Bogaard, 2013; Quevedo-González et al., 2014).

In addition, magma-driven processes of islands and seamounts can last millions of years, and so more one magma chamber can remain active in different zones of the volcanic provinces at the same time. As for instance, on Gran Canaria island, during the shield-building stage, effusive eruptions of ultramafic-mafic rocks released basalts and trachybasalts (14.5-14.1 Ma; 1000 km^3); later, a declining stage with explosive eruptions released trachy-phonolitic and trachy-rhyolitic materials (14.1-7.2 Ma; 1000 km^3); followed by erosional stage (7.2-5.3 Ma); and lastly by rejuvenated stage with erupted basanite-nephelinites, basalts, trachybasalts, trachytes and phonolites (5.3 Ma-1370 yr BP; 210 km^3) (Schmincke and Sumita, 2010). On the Oligocene (33-25 Ma), submarine eruptions also occurred in the vicinity of Lanzarote and Fuerteventura islands (CIVP), as well as near Sal island (CVIVP). Several island edifices were contemporary active in shield-building stages: from different edifices on the same island (i.e. Centro, Jandía and Norte edifices on Fuerteventura island; 23-16 Ma, Lower Miocene) and from different edifices (e.g. Lanzarote, Fuerteventura and Gran Canaria islands (CIVP); or Sal, Boa Vista and Maio islands (CVIVP); Lower Miocene, 15 Ma). Likewise, several islands have coexisted in declining stages (e.g. Gran Canaria and Maio islands) and meanwhile, other islands have been active in shield-building stages (e.g. Tenerife and La Gomera islands (CIVP); São Vicente and São Nicolau islands (CVIVP) (Upper Miocene, 9 Ma).

In general, the CIVP region remains active from the Lower Cretaceous (142 Ma) to these days, with volcanic edifices located over Jurassic oceanic crust (Van den Bogaard, 2013); whereas the CVIVP region show volcanism from the Oligocene (26 Ma), this time over Cretaceous oceanic crust (Geldmacher and Hoernle, 2000; Ancochea et al., 2010; Dyhr and Holm, 2010; Madeira et al., 2010). Moreover, Holocene and historic eruptions happened in both volcanic provinces. On the Canary Islands, the last eruption occurred as an undersea volcano off La Restinga, El Hierro Island, in 2011 (Martí et al., 2013; Rivera et al., 2013). Besides, the last subaerial eruption in the Cape Verde Islands was also historic and occurred on Fogo Island, in 2014 and 2015.

2.2.5. MORPHOMETRIC DESCRIPTION OF VOLCANIC SEAMOUNTS

Intraplate oceanic islands and seamounts of the CIVP-CVIVP are independent volcanic edifices, thus arising from abyssal plains at depths between 1000 m and 4000 m below sea level (Figs. 2.2.1, 2.2.2, 2.2.3), and thus, reaching top heights on Tenerife island (Teide-Pico Viejo; stratovolcano; 3817 m above sea level – a.s.l.) and on Fogo island (Pico do Fogo; stratovolcano; 2829 m a.s.l.). Further, there are some older islands in both archipelagos with a long-lived geological history, thus resulting in eroded islands and lower heights, as for instance, Lanzarote island (607 m a.s.l.) and Boa Vista island (387 m a.s.l.). Nonetheless, these volcanic islands are impressive edifices coming up from the ocean bottom, showing total heights between 4000 m and 8000 m, and so competing with the major continental mountains. In regard to islands topography, a high variability in both archipelagos is remarkable, due to different geological histories over

millions of years (see review in Ancochea et al., 2010; Dyrh and Holm, 2010; Madeira et al., 2010; Schmincke and Sumita, 2010; Carracedo, 2011).

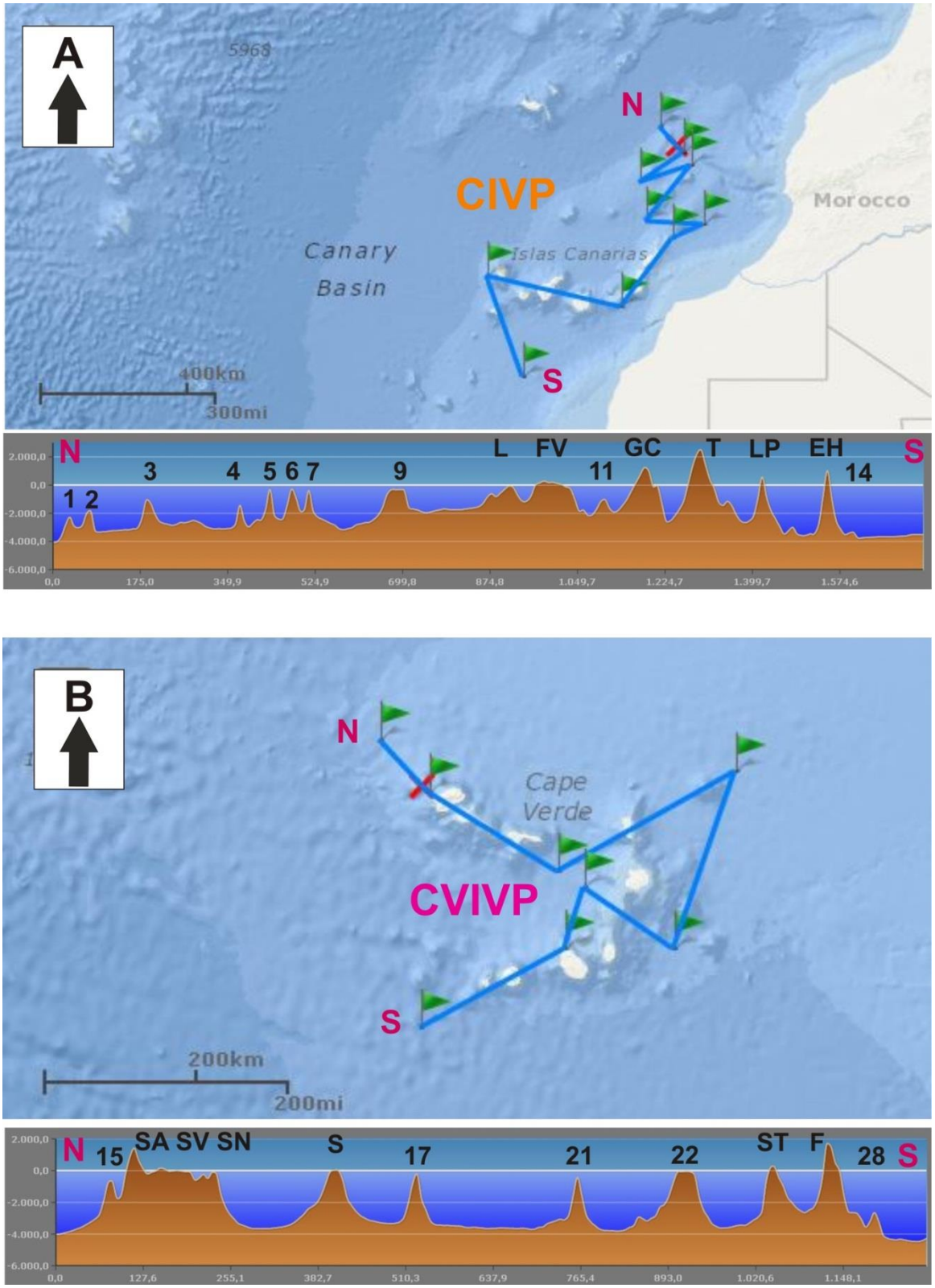

Figure 2.2.3. Bathymetric profiles on islands and seamounts of the CIVP (A) and CVIVP (B) (modified from Becker et al., 2009). Numbers refer to seamounts (see Tab. 2.2.1). Capital letters refer to island names (see Figs. 2.2.2 and 2.2.3)

From both CIVP and CVIVP areas, 28 seamounts were selected, in order to characterize their morphometric parameters and to classify them, in consonance to Staudigel and Clague (2010) (Tab. 2.2.1). In particular, a set of 14 seamounts were selected from each volcanic province. CIVP seamounts are placed between 27°N-32°N and 13°W-19°W (Figs. 2.2.1, 2.2.3A), whereas CVIVP seamounts are located between 14°N-17°N and 21°W-26°W (Figs. 2.2.2, 2.2.3B). Besides, 12 of the total selected seamounts are unnamed up to now, most of them from the CVIVP, since they have been poorly studied so far. On the remaining 16 seamounts some studies regarding cartography, petrology, geochemistry, geochronology and also geophysics have been conducted; but in general there is still a lack of knowledge of their geological history. Seamounts show varied shapes in a range from cone-shaped, rounded or elliptical-based mountains to more complex edifices, with elongated irregular bases, many of them aligned NE-SW direction (Tab. 2.2.1). These undersea volcanoes also exhibit significant different topographies, due to different geological histories.

According to Staudigel and Clague (2010) classification, only 2 of the total 28 seamounts analysed are defined as small seamounts (Sm) with a maximum height between 100 m and 1000 m (Tab. 2.2.1). On the one hand, the El Hijo seamount, with an age of 0.2 Ma (Van den Bogaard, 2013) is placed between Tenerife and Gran Canaria islands, and so standing presumably active as a young edifice with frequent seismicity on its surroundings. On the other hand, the Henry seamount, placed SW of El Hierro island, aged 126 Ma, is the oldest one known in the CCLME region. Secondly, there are 12 mid-size seamounts (M-s) with maximum heights over 1000 m, mostly rounded, dome-shaped mountains with an average height of 1987 m (CIVP) and 2028 m (CVIVP) (Tab. 2.2.1, Fig. 2.2.3). Instead, these long-lived and well-developed volcanic edifices remain poorly researched, as for instance, Anika seamount (55 Ma), having an elongated shape and NE-SW oriented, is characterized by shield-building rocks and may have reached the ocean surface becoming an emerged island on ancient periods (Geldmacher et al., 2001, 2005). Thirdly, there are 15 shallow seamounts (Sh) with summits above 700 m depth (8 in CIVP and 6 in CVIVP; Tab. 2.2.1; Figs. 2.2.3, 2.2.4). This class comprises volcanic edifices with important dimensions, since they show average heights of 2350 m (CIVP) and 3224 m (CVIVP). Further, several summits reach 175 m depth on the Canaries and 309 m depth on Cape Verde; mostly being flat-topped and dome-shaped mountains with minor slopes (Tab. 2.2.1; Figs. 2.2.3, 2.2.4), thus indicating they have lived a large geological history. In fact, the oldest shallow seamounts (18-47 Ma) (CIVP) may have been ancient islands, which suffered erosion and later subsidence to become seamounts. On sinking stages, they can be renamed as guyot, although this term usually refers to those having coral-reefs on the summits. In the CIVP, coral-reefs have not been described despite the presence of deep-sea, cold-water coral communities on the Canary seamounts (IEO, 2013a, 2013b). Also, shallow seamounts are commonly named, since they are placed on marine fishing areas: Dacia, Conception Bank, Amanay, El Banquete in the CIVP; and Senghor, João Valente, Cape Verde and Sul do Maio in the CVIVP. In regard to seamount heights, data values in Table 2.2.1 are approximated, since these volcanic edifices are partially covered by sedimentary rocks and recent marine sediments. Despite sedimentary layers can reach several kilometres, their thickness are not considered (Van den Bogaard, 2013).

In regard to the CCLME, seamounts geology has been hardly studied in the CIVP, whereas there are just a few research works in the CVIVP. Several oceanographic campaigns have been conducted for the last 30 years, including cartography, geomorphology, petrology, geochemistry, and to a lesser extent geophysical studies (e.g. Ancochea and Huertas, 2003; Geldmacher and Hoernle, 2000; Geldmacher et al., 2001, 2005; Dyhr and Holm, 2010, Represas et al., 2012; Van den Bogaard, 2013; Quevedo-González et al., 2014). In these campaigns, volcanic rocks and sediment samples were obtained together with detrital submarine sediments (Ancochea and Huertas, 2003; Geldmacher et al., 2001, 2005; Quevedo-González et al., 2012, 2014). Igneous rocks show a wide range composition from ultramafic rocks (i.e. nephelinites, basanites; Dacia and Amanay seamounts) and mafic rocks (i.e. alkaline basalts; at Conception Bank, El Banquete and

Amanay seamounts) to intermediate rocks (i.e. trachybasalts, phonolites, benmoreites; at Anika, Last Minute, Conception Bank, El Banquete and Amanay seamounts). These rocks belong to the shield-building stages, alkaline declining stage and rejuvenation stages, since rocks have shown different geochemical compositions with altered minerals and volcanic glass, as well as with non-altered minerals (Ancochea and Huertas, 2003; Geldmacher et al., 2001, 2005; Quevedo-González et al., 2014). Besides, sedimentary rocks studied are mainly bioclastic limestones, containing pelagic Foraminifera, among other bioclastic constituents, and together with individual minerals and rock fragments (Ancochea and Huertas, 2003; Quevedo-González et al., 2012, 2014).

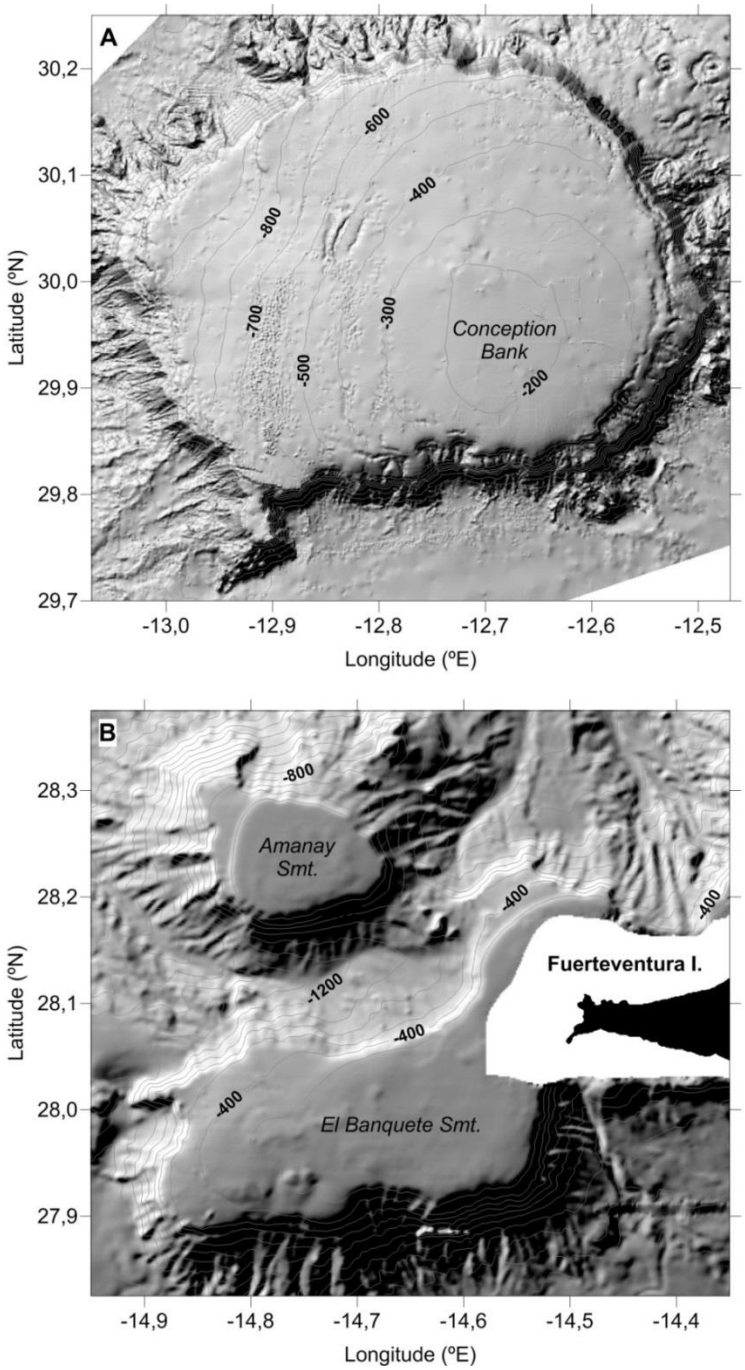

Figure 2.2.4. Bathymetry map showing the Canary seamounts: (A) Conception Bank (row 9; Tab. 2.2.1), (B) Amanay and El Banquete (rows 11 and 13; Tab. 2.2.1). Bathymetry data from the LIFE+ INDEMARES cruises (contour levels every 100 m (5A) and 200 m (5B)).

2.2.6. AMANAY, EL BANQUETE AND CONCEPTION BANK (CIVP)

The LIFE+ INDEMARES (2009-2013) Spanish national project, leaded by the Spanish Biodiversity Foundation, has allowed achieving a deeper knowledge of the biodiversity from several marine areas of the Spanish seas, and thus becoming included in the Natura 2000 network. Thus, selected marine areas on the Canary Islands focused research aims on three particular seamounts (Figs. 2.2.1, 2.2.3A, 2.2.4): Conception Bank (70 km NE of Lanzarote island), El Banquete and Amanay seamounts (20 km SW of Fuerteventura island). Hence, the Instituto Español de Oceanografía (IEO), as part of the project team, has leaded the oceanographic surveys collecting a wide variety of biological and geological samples (IEO, 2013a, 2013b). A geology research group, Geología Aplicada y Regional (GEOGAR), attached to the Instituto de Oceanografía y Cambio Global (IOCAG) and related to the Universidad de Las Palmas de Gran Canaria (ULPGC), has conducted a geological research collaboration in order to broadly characterize, for the first time, about 300 samples of igneous rocks (i.e. plutonic, subvolcanic and volcanic rocks), sedimentary rocks (e.g. limestones and ferromanganese crusts) and non-consolidated deep-sea sediments (Fig. 2.2.5).

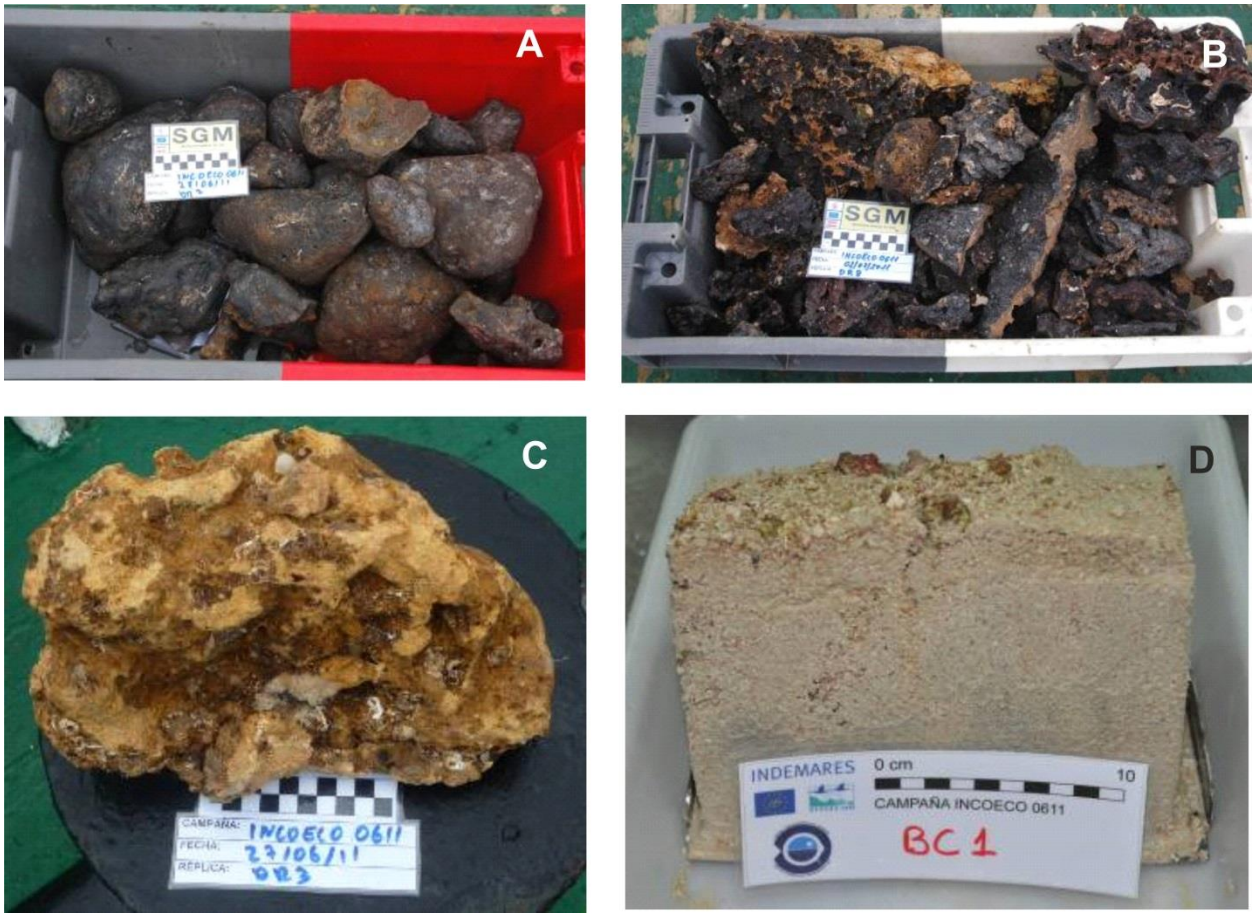

Figure 2.2.5. External features of samples dredged during the LIFE+ INDEMARES cruises at Conception Bank (INCOECO-0611): igneous rocks (A), ferromanganese crusts (B), carbonate limestones (C) and non-consolidated sediments (D).

Concerning the geological aims for this work, a multi-technical approach was used comprising several disciplines: sediments geo-characterization (i.e. grain-size, provenance, carbonate, organic matter, microscopy, mineralogy, petrography, geochemistry), and igneous rocks and sedimentary rocks geo-characterization (i.e. petrography, mineralogy, geochemistry). Hence, a number of methods was required

for these purposes (e.g. dry sieving, calcimetry, petrographic microscopy, scanning electron microscopy (SEM), inductively coupled plasma mass spectrometry (ICP-MS), electron microprobe analysis (EMPA), powder X-ray diffraction (XRD) procedures, Raman spectroscopy). Thereby, the foremost objective for this work is to characterize an evident geological diversity, through analysing textural, mineral and geochemical data, thus combining later these results to understand the origin, nature and evolution of the seamounts involved. In summary, here we show the main results of the most relevant findings for further discussion.

Firstly, a set of about 100 igneous rocks confirms a volcanic origin, so as expected, for Amanay, El Banquete and Conception Bank (Fig. 2.2.5A), and therefore, supporting an intraplate hotspot-driven volcanism, also responsible of the neighbouring islands and seamounts of the CIVP. Further, a petrography study and geochemical data show typical ocean island alkaline basalts series, comprising a wide range of plutonic, subvolcanic and volcanic (lava flows and pyroclastic flows) rock varieties (e.g. basalts, trachy-basalts and gabbros), and so characterized by the presence or absence of olivine, clinopyroxene, Ca-Na plagioclase, amphibole and Fe-Ti-oxides. Also, aegirine, Na-Ca plagioclase, sphene, apatite, biotite, among other minerals, appear in intermediate rocks (trachy-basalts). Further, volcanic and diabase-like rocks reveal a considerable geological alteration and mineral neo-formation due to seawater, as for instance, mineral alterations on rocks edges (e.g. mm-sized coatings of Fe-Mn-oxides), mineral replacements, but mostly mineral fillings in both vesicles and cracks (e.g. micritization, zeolitization, phosphatization).

Secondly, about 150 samples show a great diversity of sedimentary rocks, comprising mainly carbonated rocks and ferromanganese crusts, but also conglomerates and sandstones (Figs. 2.2.5B and 2.2.5C). Sedimentary rocks are reflecting both oceanic and geological processes: (i) carbonate rocks are mostly described by a variable fraction of bioclasts (mainly pelagic Foraminifera), apart from a varying degree of compaction and porosity (e.g. mudstone, packstone, grainstone) whereas cementing matrix is characterized by calcite minerals (i.e. micrite and sparite), in some samples phosphatized too; (ii) ferromanganese crusts appear typically as layers with botryoidal, isopachous, druzy textures (up to 3-4 cm in thickness), where mineralogical analysis indicates iron and manganese minerals (i.e. todorokite, goethite, hematite).

Thirdly, a set of 60 non-consolidated sediment samples was also taken into research (Fig. 2.2.5D). A mineral identification of significant amounts of (i) allochthonous quartz and dolomite; volcanic-related augite and plagioclase, as well as further calcium-magnesium minerals within the silty-clayey fraction, (ii) high levels of carbonate content (close to 90% on average), owing to high ratios of relative contents of bioclasts (up to more than 60% of pelagic Foraminifera) and finally, (iii) the low concentrations of Rare Earth Elements (by a few tens of parts per million - ppm) detected in selected samples, are some of the most relevant results concerning the deep-sea sediments of these Canary seamounts.

2.2.7. CONCLUSIONS AND FUTURE GOALS

The CIVP and the CVIVP are placed within the CCLME, showing sets of volcanic islands and seamounts related to magma-driven processes over tens of millions of years at the Canary and Cape Verde hotspots. These single hotspots are related to upper mantle-derived secondary plumes, and lastly, linked to lower mantle-derived plume, thus forming the whole Magmatic Belt off Western Africa. Continuous volcanism in both provinces has been reported for the last 142 Ma (Upper Cretaceous) on the Canaries and the last 26 Ma (Oligocene) on Cape Verde Islands to these days, with contemporary volcanism in both archipelagos and on different islands and seamounts. Also, the oldest ones constitute volcanic edifices formed in tens of

million years; whereas the youngest ones were formed within the last hundreds of thousand years up to a few million years. Indeed, these edifices have experienced different stages from submarine-subaerial volcanic to submarine inactive post-stages. A number of thousands of lava flows and pyroclastic flows were erupted and settled over Jurassic and Cretaceous oceanic crusts (CIVP: 175-155 Ma; CVIVP: 140-120 Ma), in order to form these edifices: volcanic materials with varied compositions (i.e. ultramafic to felsic rocks), volcano-sedimentary materials (i.e. limestones and other sedimentary rocks) and bioclast-rich, non-consolidated marine sediments.

Islands and seamounts appear with complex or simple morphologies, dome-shaped to irregular relieves, and total heights ranging 4000-8000 m from the bottom to island highest peaks, but less than 3500 m on seamounts. Besides, seamounts are partially covered by sedimentary rocks and deep sediment layers, sometimes reaching several kilometres. As a result, real heights remain underestimated. These geological undersea features are also biodiversity hotspots, where slopes modify the circulation regime of both deep and shallow currents, and thus changing the biochemical constituents of seawater. Thereafter, a set of several deep-water ecosystems is enhanced in both flora and fauna, also known as traditional fishing areas expected to become protected under preservation plans (IEO, 2013a, 2013b). In geological terms, there is also an increasing interest, in order to understand the origin, nature and evolution of the constituent materials from these submerged edifices, as well as to investigate potential mineral resources. For instance, the LIFE+ INDEMARES (2009-2013) project has studied Canary seamounts (i.e. Conception Bank, El Banquete and Amanay) and has provided new geological data from igneous rocks, sedimentary rocks and sediments; reflecting altogether the volcanic origin and the underwater evolution of these edifices. Hence, these geological features are undoubtedly a record of the bio-geo-physico-chemical processes occurred since both early and late submarine stages. Thereby, the resulting data from this work suggest new goals and chances for further studies, whether for geological purposes (e.g. combining with geophysical data), as well as for interdisciplinary proposals (e.g. statistical modelling of species distribution).

In the end, the geology background of the Canary and Cape Verde Islands appears quite supported by research works of the last decades; whereas a lack of research still remains concerning the neighbouring seamounts. Hereby, it is necessary to lead new oceanographic cruises in a medium term, in order to perform cartographic and geomorphologic studies, together with geophysical techniques to characterize deep-sea features on volcanic edifices and the underlying lithosphere. In this respect, the data collection of sediment and rock samples from the slopes is meaningful, since most of these edifices have never been studied before. Further studies remain waiting for more complete and detailed data on petrology, mineralogy, geochemistry, geochronology and volcano-stratigraphy, thus resulting in better understanding of the origin and evolution through time of these unknown seamounts in the CIVP and CVIVP. In addition, this research would help to know better about the nature of the lower and upper mantle in the CCLME region, since there is still a controversy in the scientific community, regarding the mantle-derived plume model beneath these hotspots.

Acknowledgements

This work is part of the national research project EC Life+ Project INDEMARES (2009-2013 - Code No. 110300900, www.indemares.es, accessed on 25 March 2015), including both INDEMARES-CONCEPCION and INDEMARES-FUERTEGC sub-projects. Hereby, the authors want to sincerely thank the Instituto Español de Oceanografía (IEO) for supporting these geological researches. Likewise, we thank L. M. Agudo (IEO, Madrid) and D. Cuñarro (IOCAG, Las Palmas de Gran Canaria) for their help in some figures on this paper.

2.3. SAHARAN DUST INPUTS TO THE NORTHEAST ATLANTIC

María Dolores GELADO-CABALLERO

Universidad de Las Palmas de Gran Canaria. Spain

2.3.1. INTRODUCTION

African dust inputs have important effects on the climate, marine biogeochemistry and human health. Atmospheric deposition is estimated to provide 450 Tg yr^{-1} of dust to the oceans (Jickells et al., 2005). Almost half of this estimated global dust input is provided by the arid regions of the Sahara and Sahel deserts resulting in a westward flow of material over the North Atlantic Ocean (Schütz et al., 1981; d'Almeida, 1986; Harrison et al., 2001). Mineral aerosols play an important role in the climate on account of their direct effect on the radiation budget and indirect relationship with cloud microphysical properties (Arimoto, 2001; Forster et al., 2007). Atmospheric dust deposition is an important source of essential and limiting nutrients and metals to the ocean (Measures et al., 1986; Duce et al., 1991; Baker et al., 2003; Mills et al., 2004; Jickells et al., 2005) affecting the oceanic carbon uptake, phytoplankton growth and productivity. Recent reports also suggest that dust inputs may promote nitrogen fixation (Mills et al., 2004; Duarte et al., 2006; Moore et al., 2009), by providing iron and other trace metals.

Intense African dust intrusion episodes have both social and economic repercussions on the areas that are subject to them, particularly affecting agriculture, air traffic with the reduced visibility (Criado and Dorta, 2003; Griffin and Kellogg, 2004), and human health, since the inhalation of dust can aggravate respiratory diseases or contribute to triggering epidemics (Julià-Serdà et al., 2005; Thomson et al., 2006)

Atmospheric deposition of mineral dust supplies nutrients such as iron and other trace metals to the oceans. However, there are only a few limited datasets of direct measurements of dry and wet deposition flux in oceanic regions obtained during cruises (Duarte et al., 2006; Baker et al., 2013) or from collection sites located on islands (e.g. López-García et al., 2013). In addition, sediment trap studies show contradictory results concerning the impact of the dust on biogenic particles flux. Dust can act as ballast to enhance downward sediment rates (Francois et al., 2002). Moreover, the results from sediment traps could be influenced by mesoscale processes and lateral transport (relevant in the Eastern Boundary Upwelling System) variable in time, which makes it difficult to interpret the observations in the sediment traps. Lithogenic flux studies using sediment trap material have been carried out in the Canary Current Large Marine Ecosystem (CCLME) region (e.g. Neuer et al., 2004; Ratmeyer et al., 1999) in an attempt to link the atmospheric dust input with mineral composition and biogeochemical processes in the water column. The mineral assemblage of aerosol dust and deep-sea sediments reveals different source origins (e.g. Caquineau et al., 1998). Brust and Waniek (2010) have observed that the minerals (quartz, smectite, illite and palygorskite) present in the flux of lithogenic particles in sediment traps refer to a mixture of sources in the North African regions, predominantly northwestern African areas (Mauritania, Western Sahara and Morocco), showing seasonal and interannual variations. Quartz, feldspar, smectite, kaolinite, illite and palygorskite (silicates); calcite, Mg-calcite and dolomite (carbonates); magnetite, hematite and pirolusite (oxides); halite and gypsum (evaporites) are some of the minerals observed in the lithogenic material (e.g. Goudie and Middleton, 2001; Menéndez et al., 2007; Kandler et al., 2007, 2011; Engelbrecht et al., 2014). The mineral dust component in Cape Verde and the Canary Islands is dominated by silicates, kaolinite being

the dominant clay mineral in the aerosol from Cape Verde in comparison with the higher illite concentrations found in the Canary Islands (Kandler et al., 2007, 2011).

2.3.2. DATA SOURCES AND METHODS

The first long-term dust observations were made in the North Atlantic in 1965 in Barbados and in 1972 in Miami (Prospero et al., 1995; Prospero, 1999). In the Canary Islands, two observation sites have carried out dust measurements since 1987 at Izaña (Tenerife) (Prospero and Lamb, 2003) and since 1996 at Pico de la Gorra (Gran Canaria) (Torres-Padrón et al., 2002). The first long-term dust measurements in Cape Verde were carried out between 1991 and 1994 (Chiapello et al., 1995, 1997). In general, there are almost no direct measurements of dust deposition flux in the ocean (i.e. using automatic deposition collectors), apart from data collected during cruises (e.g. Duarte et al., 2006 in the subtropical Northeast Atlantic region) and at island sampling sites (Gelado-Caballero et al., 2005; Menéndez et al., 2007; López-García et al., 2013, in Gran Canaria). However, it is also possible to calculate dry deposition fluxes indirectly from atmospheric aerosol concentrations and estimated particle deposition velocities (Baker et al., 2010).

Aerosol remote sensing data has also been a valuable tool for locating the major dust sources and determining the variability of aerosol distribution and transport pathways (Herman et al., 1997; Prospero et al., 2002; Mahowald et al., 2003; Torres et al., 2002b; Ginoux et al., 2012). Satellite data is used to detect sources, including small-scale structures ("hot spots") that could substantially contribute to global dust emissions (Koren et al., 2006; Schepanski et al., 2007). Sources associated with small-scale features such as "hydrologic" (ephemeral and inland water bodies) and "anthropogenic" sources associated with some form of land use (agriculture) are still uncertain. The estimates of dust optical depth using the Moderate Resolution Imaging Spectroradiometer (MODIS) Deep Blue algorithm have improved the detection of such dust sources. In addition, land-based remote sensing networks such as AERONET provide valuable information about Saharan dust outbreaks in the Northeast Atlantic region (NEA) region (Kaufman et al., 2005; Basart et al., 2009).

2.3.3. DUST OBSERVATIONS AND CLIMATOLOGY

2.3.3.1. Dust sources and emission

Mineral aerosols or desert dust are mainly soil particles suspended in the atmosphere by strong winds. Mineral aerosol production requires dry, non-vegetated and easily erodible soils (e.g. review by Mahowald et al., 2005). The major dust sources on a global scale are located in the arid regions of the Northern Hemisphere, extending from North Africa, the Middle East and Central and East Asia to China, grouped together as the "Dust belt" (Prospero and Lamb, 2003). The Sahara desert is considered by far the most active dust source in the world, although its contribution is confined to the Northern Hemisphere (Engelstaedter et al., 2006). Most of these dust sources are topographic depressions associated with deep alluvial deposits formed by intermittent flooding through the Pleistocene and Holocene (Prospero et al., 2002). Although many aspects of the global dust cycle are well known, the proportion in which different sources account for emissions is still uncertain on account of to the poor quantification of small-scale features (Table 2.3.1). Human interaction, especially attributable to intensive agriculture and deforestation, may account for 10%-50% of the total dust input. There is a wide range of estimates of the anthropogenic contribution to global dust emission: less than 10% (Tegen et al., 2004), 25% (Ginoux et al., 2012) or 50%

(Mahowald and Luo, 2003). For this reason, it would be necessary to establish the variations in anthropogenic dust sources because they are strongly dependent on climate variability.

Table 2.3.1. Estimates of mean annual dust emission for North Africa. The data compilation is based on the works of Goudie and Middleton (2001), Zender et al. (2004), Mahowald et al. (2005, 2010) and Huneeus et al. (2011) *The estimate is based on the sum of emissions from the individual source regions.

Reference	**Estimates for North Africa ($Tg\ yr^{-1}$)**
Jaenicke (1979)	260
Schutz et al. (1981)	260
D'Almeida (1986)	630-710
Marticorena and Bergamatti (1995)	586-665
Prospero (1996)	170
Swap et al. (1992)	130-460
Callot et al. (2000)	760
Ozer (2001)	1600
Luo et al. (2003)	1114*
Ginoux et al. (2004)	1430
Miller et al. (2004)	479-589
Kauffman et al. (2005)	240 ± 80
Mahowald et al. (2010)	1367
Huneeus et al. (2011)	800

According to the most recent work of Ginoux et al. (2012), North Africa accounts for 55% of global dust emissions with only 8% being anthropogenic, mostly from the Sahel. This is a larger source of dust of an anthropogenic nature than previously estimated (e.g. Prospero et al., 2002).There is a clear separation between the natural dust sources in the Sahara and the anthropogenic dust in the southern Sahel.

The natural dust sources in North Africa include the major depressions (Bodélé and Qattara); large basins with sand seas (Erg of Bilma, Erg el Djouf, Grand Erg, and Libyan Desert); ephemeral lakes (Sebkhet te-n-Dgâmcha, Chott el Djerid, and Chott Melrhir); lakes in the Tiris Zemmour region; and the Nile River Basin. All of them are considered mainly natural sources. There are additional origins associated with ephemeral lakes: Chott el Hodna and Chott ech Chergui in the Atlas Mountains. Other smaller anthropogenic sources can be identified in coastal Morocco and Western Sahara, Tunisia, Libya and Egypt. The Western and Central Sahara and, to a lesser extent, the Sahel, are the sources of mineral dust transported to the Canary and Cape Verde Islands.

2.3.3.2. Transport

The aerosols generated on the African continent are transported across the Atlantic over long distances, even reaching areas of the Caribbean, Central America and South America, especially in the summer months (Figure 2.3.1). This fact was already described in Darwin's writings aboard the *Beagle* expedition (Darwin, 1846). The transport mechanisms of African dust are well understood (Prospero, 1999; Goudie and Middleton, 2001). There are large seasonal and spatial variations in mineral dust concentration over the Atlantic Ocean, greatly affected by the seasonal latitudinal shift of the Intertropical Convergence Zone (ITCZ).

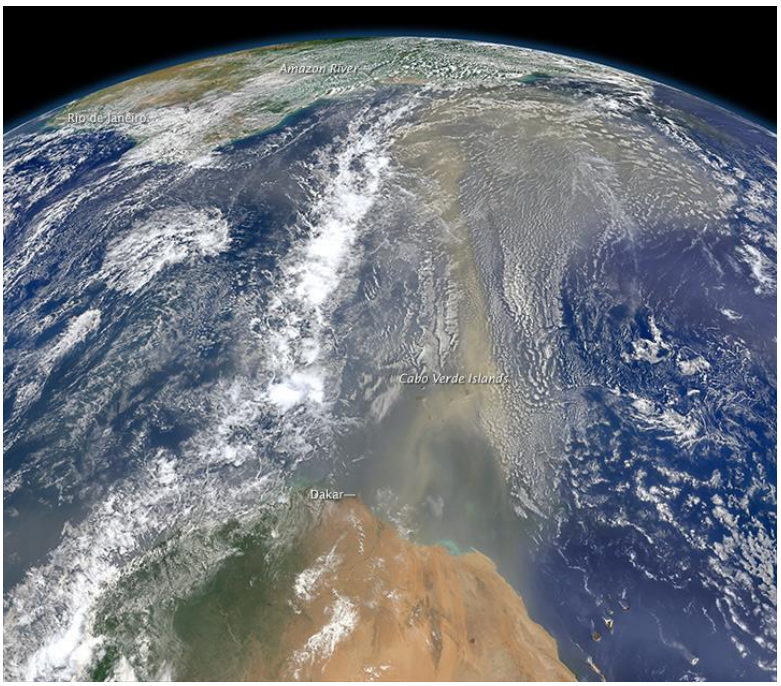

Figure 2.3.1. Dust heading west towards South America and the Gulf of Mexico on 25 June 2014. Visible Infrared Imaging Radiometer Suite (VIIRS) on Suomi NPP. NASA images by Norman Kuring, NASA's Ocean Color web.

During the summer, the ITCZ shifts northwards over the north-western part of the African continent (from approximately 5°N in winter to 19°N in summer), creating a thermal low over the surface of the African continent. This causes the North African high-pressure system to be located at higher altitude and consequently dust transport occurs high in the atmosphere within the so-called Saharan Air Layer (SAL). Dust transport is controlled by the African easterly jet and occurs between a height of 3 km and 6 km when the mineral dust layer is lifted above the Trade Wind Inversion layer (TWI) (Chiapello et al., 1995; Schepanski et al., 2009). The TWI restricts the vertical movements of mix between the Marine Boundary Layer (MBL) and the troposphere.

The MBL is limited by the base of the thermal inversion layer at altitudes that range between 500 m above sea level (a.s.l.) near the Azores High and 2000 m a.s.l. in the trade wind region close to the tropics. In subtropical regions, the upper limit of the marine boundary layer is usually bounded by the trade wind inversion layer. The TWI marks the boundary between the relatively cool and wet layer (MBL) and the relatively warm and dry layer located on the bottom of the free troposphere (Torres et al., 2001).

During winter, the ITCZ is located in its most southerly position and dust transport is controlled by high pressure systems located over the northern African continent. Mineral dust spreads over the NEA at relatively low altitudes, below 2 km height, and is injected mainly within the MBL (Kaufmann et al., 2005; Díaz et al., 2006).

In the Canary Islands, the location of the TWI follows a seasonal pattern, occurring in summer between 770 m a.s.l. and 1380 m a.s.l. with an average thickness of about 560 m, while in winter the layer is found at higher altitude (1360 m a.s.l. to 1850 m a.s.l.) and with a reduced average thickness of about 360 m (Torres et al., 2001).

2.3.4. DISCUSSION

2.3.4.1. Dust distribution: spatial and temporal variability

In the NEA region, a strong seasonal variation of mineral aerosol concentration has been observed from the results of long-term sampling in the Canary and Cape Verde Islands. Similar mean atmospheric dust concentrations were measured at the island observation sites of Cape Verde (47.1 ± 55.5 µg m^{-3}) and the Canary Islands (45 ± 82 µg m^{-3}) in the CCLME. The highest mineral dust concentrations are registered during winter and early spring in the Canary Islands and during the late autumn and winter in Cape Verde (Gelado-Caballero et al., 2012; Fomba et al., 2014). This variability is mainly related to the influence of African air mass inflow in the lower atmospheric layer. The highest dust concentrations found in Cape Verde during the winter are strongly influenced by the Harmattan, a characteristic wind transporting Saharan dust at lower heights to the Atlantic Ocean. As a consequence of the seasonal pattern of dust transport, differences are found in the aerosol chemical composition between days with and those without dust events.

Long-term satellite data show a seasonal pattern similar to the *in situ* dust measurements. A mean seasonal pattern of emission and transport over the subtropical North Atlantic has been described by Ben-Ami et al. (2012), consisting of two strong dust seasons and one season with low dust loadings. During the first dust season (November-March), episodic dust events are originated in the Bodélé Depression and dust is transported southward and over West Africa and the Atlantic at ≈5°N. In the second dust season (May-September), the frequency of dust events is more uniform and emissions also have important contributions from the Bodélé Depression and Western Sahara (Figure 2.3.2). The dust plume advances northward to reach about 20°N. The third season with apparent low dust loadings (October-December) is not defined in the same manner according to the different satellite products. As has been mentioned before, island observations have clearly established dust transport towards Cape Verde during the late autumn and winter.

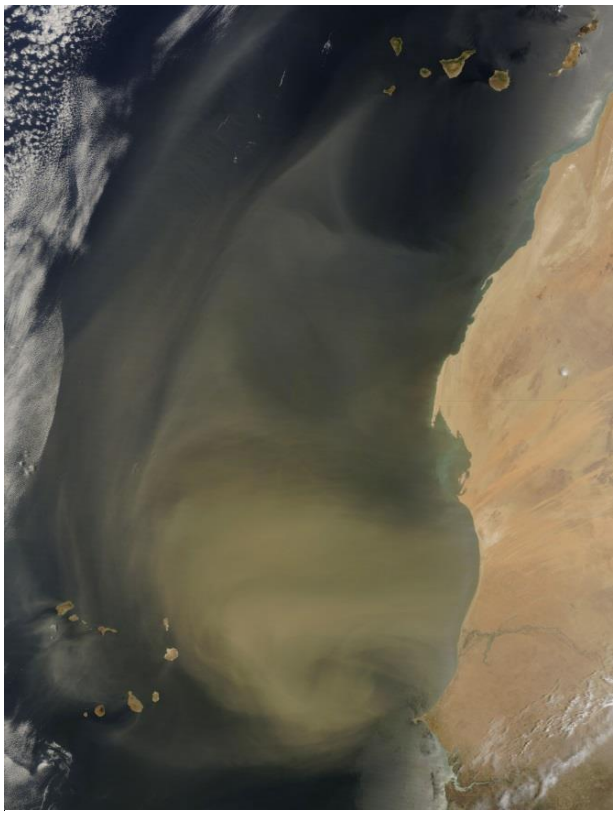

Figure 2.3.2. Dust plumes blew off the west coast of Africa on 9 May 2007. Moderate Resolution Imaging Spectroradiometer (MODIS) image from the Terra satellite (courtesy of Jeff Schmaltz, NASA Earth Observatory, using data from MODIS Land Rapid Response System, NASA Goddar Space Flight Center).

Dust deposition measurements are very scarce in the CCLME region. In the dust sources (i.e. Niger, Mali and Senegal) the dust deposition fluxes are very high, with values of the order of 100 g m^{-2} yr^{-1} (see Bergametti and Forêt, 2014). The deposition flux decreases with the distance from the dust sources. A long-term series of total deposition measurements carried out in Gran Canaria using surrogate surfaces has shown a dust deposition flux of 17 g m^{-2} yr^{-1} (Gelado-Caballero et al., 2012). Dry deposition dominated the particle flux, with wet deposition fluxes of around 10% of the total deposition flux. This deposition flux is consistent with estimates of an annual average deposition resulting from different models for the North Atlantic Basin which range between 140 Tg yr^{-1} and 254 Tg yr^{-1} (Table 2.3.2) (see Engelstaedter et al., 2006). Niedermeier et al. (2014) have estimated the deposition flux in Cape Verde applying five different methods, using meteorological and physical measurements, remote sensing and regional dust transport simulations, resulting in values ten times lower than those measured in the Canary Islands.

Table 2.3.2. Estimates of mean annual dust deposition to the global oceans (GO), North Atlantic Ocean (NAO). Duce et al. (1991) use a scavenging ratio (SR) of 1000 except for NAO (SR=200) whereas Prospero (1996) using the same model applied a SR of 200 globally. *Estimates are based on the sum of the individual ocean basins.

	Deposition (Tg yr^{-1})	
Reference	**GO**	**NAO**
Duce et al. (1991)	910	220
Prospero (1996)	358	220
Ginoux et al. (2001)	478*	184
Zender et al. (2003)	314	178
Luo et al. (2003)	428*	230
Ginoux et al. (2004)	505*	161
Tegen et al. (2004)	422	259
Kauffman et al. (2005)		140 ± 40
Jickells et al. (2005)	134*	202
Mahowald et al. (2010)	477*	276

2.3.4.2. Biogeochemical impacts of dust: nutrients supply

Because of the short residence time and a non-homogeneous spatial and temporal distribution of the dust sources, aerosols are distributed heterogeneously in the troposphere, with a maximum concentration near sources. More than 80% of the total mass of minerals contained in the mineral aerosols collected in Gran Canaria correspond to particles larger than 2.5 microns and contain aluminosilicates, feldspar, quartz, calcite and Fe-rich minerals such as hematite (López-García, 2012). Silicates such as illite, smectite, chloritoid, albite and plagioclase (Kandler et al., 2011) are dominant, accounting for about 60%-70% of the total mass of African mineral aerosols, while feldspars account for approximately 10%, which is a similar composition to that described for aerosols collected in Niger(Chou et al., 2008) and Morocco (Kandler et al., 2009). Calcite and iron-rich minerals are present in higher proportion in the mineral aerosol samples originating in North Africa than in the samples from the Sahel.

During transport, mineral aerosols undergo chemical and physical changes, especially due to cloud processes (i.e. condensation and evaporation), which may result in a substantial increase of dust solubility

and/or significant and relatively fast scavenging by rainfall (typically, in the span of one week). In addition, pH plays an important role in the control of solubility. Iron solubility kinetics for oxides and other minerals are very sensitive to pH variations (low pH increases the solubility). Probably the large variations in pH are related to the cloud processes (condensation and evaporation) around the dust particles. Dust particles can act as cloud condensation nuclei (CCN) and this interaction of dust particles with cloud water, or cloud processing, provides the main mechanism for uptake of acid gases in the atmosphere (Seinfeld and Pandis, 2006). Clouds can form and evaporate repeatedly (from 5 up to 10 times), before the dust is deposited on the ocean surface, and as the pH of the cloud changes in each of these condensation/evaporation processes, the dust particle can be substantially affected.

African mineral dust is relatively depleted in soluble P relative to other nutrients (soluble Fe and N) with respect to phytoplankton requirements for these elements. Measured soluble nutrient concentrations in the dust samples collected in the Canary Islands produced values of between 0.4-2.9 nmol m^{-3} phosphate and 21-64 nmol m^{-3} nitrate + nitrite, resulting in mean N:P, Fe:P and Fe:N ratios of 59, 1.4 and 0.03, respectively (Gelado-Caballero et al., 2012). In all samples the N:P, Fe:P and Fe:N ratios were significantly higher than the Redfield values. The relatively low abundance of P in atmospheric inputs appears to be related to the observed P limitation in the NE Subtropical Atlantic Ocean (Baker et al., 2003; Duarte et al., 2006).

Baker et al. (2013) have estimated total atmospheric input of Fe for the North Atlantic region using aerosol and rainwater samples collected during large-scale research cruises over two periods, April-June (AMJ) and September-November (SON). Soluble and Total Fe estimates were 0.032 and 0.76 Gmol (in AMJ) and 0.027 and 0.92 Gmol (in SON), respectively. The values are reasonably consistent with the results produced by Mahowald et al. (2009) from modelled mineral dust deposition and results from a regional dust transport model (Heinold et al., 2011) in the North Atlantic.

Ohde and Siegel (2010) have studied the biological response to coastal upwelling and dust deposition in the area off Northwest Africa around the Cape Verde Islands. Only six events of 57 strong storms were clearly related to an increase of chlorophyll-a caused by Saharan dust input and not by coastal upwelling processes, with a very small contribution (5%) to the variability of surface chlorophyll-a anomalies.

Increased rates of either primary or export production in response to fertilization by mineral dust input have not been clearly established in the eastern subtropical North Atlantic (Neuer et al., 2004). It has been suggested that iron delivered in dust is important to stimulate N_2 fixation which consequently raises N:P ratios above Redfield levels, making P the limiting nutrient for diazotrophs in the NEA region (Sohm et al., 2011). Although some studies have reported correlations between dissolved Fe concentrations and *Trichodesmium* abundance (Moore et al., 2009; Fernández et al., 2010), Agawin et al. (2013) did not find any correlation with N_2 fixation rates or with the abundance of *Trichodesmium* in the CCLME. Marañon et al. (2010) have suggested that the predominant type of metabolic response to enhanced dust fluxes depends on the ecosystem's degree of oligotrophy. Rubin et al. (2011) have reported that *Trichodesmium* colonies are able to trap dust particles and solubilize them to take advantage of the nutrients they might contain. The absence of a response in the N_2 fixation rates to dust inputs might be explained by the predominance of free trichomes over colonies in non stratified waters suggested by Benavides et al. (2011, 2013a). As long as they are in this form, free trichomes would not be able to solubilize the particles and take advantage of the Fe contained in the dust.

2.3.4.3. Dust models

Regional or global dust models are used to obtain estimates of dust emissions, transport and deposition fluxes (reviews e.g. Tegen 2003; Mahowald et al., 2005). In the last few decades, aerosol modelling has improved their capacities (see for example Nickovic et al., 2001; Ginoux et al., 2004; Huneeus et al., 2011). Nevertheless, this modelling contains substantial uncertainties which may be related to the characteristics of the datasets used: ground-based and satellite remote sensing. Huneeus et al. (2011), comparing the results of 15 global models for the year 2000, found that dust deposition estimates present very large disparities among models, especially in their emissions. These dust models agreed within a factor of ten. This study emphasized the need for satellite observations to better characterize dust loads over source areas.

Using high-resolution data from MODIS Deep Blue in combination with other datasets including land use, Ginoux et al. (2012) have estimated that the anthropogenic dust sources account for 25% of global dust emissions. The study of these anthropogenic sources is essential, as it is estimated that the dust load may have doubled during the 20th century as a consequence of anthropogenic activities (Mahowald et al., 2010).

Despite the fact that the information provided by remote sensing is currently essential for understanding the dust cycle, given the sporadic and highly variable nature of dust inputs, long-term datasets are crucial in order to gain a further understanding of the composition and properties of African mineral dust as well as to constrain models of dust transport and deposition in the region. Accordingly, the sets of long-term measurements of aerosol concentrations over the NEA margin in Cape Verde and the Canary Islands, although discontinued, have established the daily, seasonal and interannual variations of dust concentration and the chemical characterization of aerosols over the NEA region (e.g. Patey, 2010; Gelado-Caballero et al., 2012).

There is a strong seasonal variation in aerosol components in the CCLME but mineral dust is mostly Saharan dust. According to regional dust models (e.g. Schepanski et al., 2009), the Sahara produces a larger amount of dust during summer, but the dust is transported at higher altitudes of up to 10 km within the SAL. In winter the dust is transported along the northeast trade winds at far lower altitudes. This transport pattern is consistent with the seasonal variability observed from *in situ* dust measurements in the region, with high atmospheric particle concentrations during winter. Air masses originating in the Sahel only represent around 10% of the dust events days in the Canary Islands and are observed mainly in the summer.

2.3.5. CONCLUSIONS AND RECOMMENDATIONS

There is a compelling need for long-term measurements to validate the models in the region and to identify the processes affecting dust emissions and transport and in order to understand the composition and properties of African mineral dust. Dust deposition is rarely measured directly and there are only a few sites located in the NE Subtropical Atlantic Ocean where long-term dust observations are carried out. More observations of nutrient deposition variability are needed for a better understanding of the ocean biogeochemistry and to be able to evaluate quantitatively the impact of dust on ocean productivity (Figure 2.3.3).

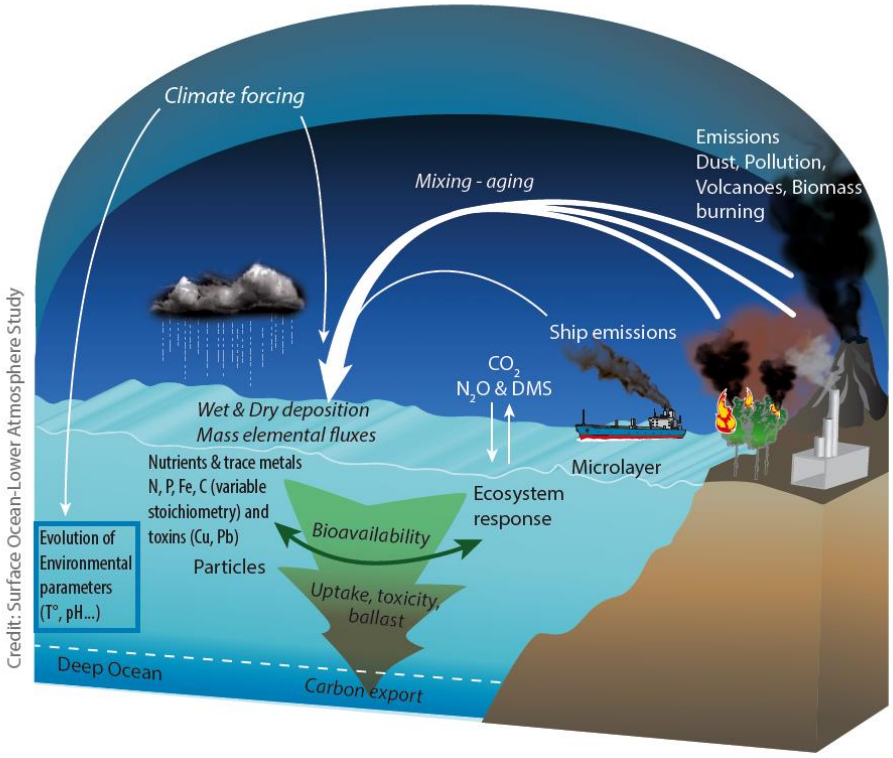

Figure 2.3.3. Conceptual diagram illustrating the main issues, processes and species relating to the SOLAS atmospheric nutrients strategy (Law et al., 2013).

Aerosol deposition is an important supply of macronutrients and trace metals (Fe, Co, Mn, Cu and Al) to the NE Subtropical Atlantic Ocean, which may stimulate the autotrophic components (nitrogen fixation and diatoms). A major effort is required to understand what fraction of these nutrients is bioavailable and what the different responses of phytoplankton communities are to the dust input. This is especially important to improve the estimates of dust impact on ocean biogeochemistry on a global and regional scale.

Human activities may be increasing atmospheric dust in the region as a consequence of land use and climate change. Change in dust deposition is likely to be strongly driven by the changes in precipitation, which alter soil particle structure. According to the projected precipitation, climate change may increase dust emission from dust sources. However, the projections for regions such as sub-Saharan Africa, which are known to be highly active sources today, are uncertain. In addition, an ever-growing demand for water resources for croplands, urban use and grazing may produce an increase of anthropogenic emissions associated with ephemeral water bodies. Dust models need to be improved to reduce uncertainties in dust source distribution and changes therein in response to human activities.

Acknowledgements

The author would like to express their gratitude to the NASA/Goddard Space Flight Center for the provision of VIIRS and MODIS satellite imagery and SOLAS Project for the conceptual diagram illustrating the atmospheric nutrients strategy. Collection of mineral aerosol data in Gran Canaria presented in this work was supported by European FEDER funds (PCT-MAC projects: MACSIMAR MAC/1/A089 and ESTRAMAR MAC/3/C177). The author would also like to thank Dr. Joaquín Hernández-Brito, Dr. José Mangas-Viñuela and Ms. Itahisa Déniz-González for their corrections and comments.

3. HYDROGRAPHIC STRUCTURE AND OCEAN CIRCULATION

3.1. REGIONAL WEATHER DYNAMICS AND FORCING IN TROPICAL AND SUBTROPICAL NORTHWEST AFRICA

Emanuel Francisco SANTOS SOARES

Instituto Nacional de Meteorologia e Geofísica. Cabo Verde

3.1.1. INTRODUCTION

The region under study, herein referred as region or area, comprises tropical and subtropical Northwest Africa (NWA) lying between latitudes 10°N and 35°N and longitudes 5°W and 30°W, including the Canary Current Large Marine Ecosystem (CCLME) area of interest. Most of it consists of an undulating low plateau below 500 m above sea level (a.s.l.), being fringed on the west and south by a coastal plain. It is a region of high insulation with considerable variation in intensity, effectiveness and duration of sunlight in all the different areas and at different times of the year. Mean annual radiation is about 105 kcal m^{-2} near the coast and the equator, resulting from cloud cover in the rainy season, while on the edge of the desert it amounts to up to 205 kcal m^{-2}. The low density of the surface weather observation network has been a great handicap to collecting existent knowledge and sufficient data to conduct a NWA atmospheric circulation systems analysis. The massive use of satellite observations and limited area models (based on the analysis of systematic estimates and meteorological data at higher spatial resolution, as well as regional-scale simulations) has made it possible to reconstruct and further improve the knowledge on weather dynamics over the region and the surrounding ocean basin (Figure 3.1.1). It has been found that most of the prevailing atmospheric circulation structures that affect the weather over the region are thought to impact distant atmospheric dynamics (Kirtman and Pirani, 2009). A continental airmass of surface northwest flow component blows consistently across most of the area. It is a very dry airmass, with maintained subsidence and stability until it reaches equatorial areas.

Another circulation structure, the summer African monsoon, is a primary cause of rainfall distribution over the area, and still today is a very complex mechanism related to diurnal forcing effects. Other mechanisms related to diurnal forcing effects are: large-scale convective events, deep convective systems, and synoptic wave perturbations on convective systems. The intraseasonal time-scale variability of all these atmospheric circulation systems is the result of several superimposed atmospheric and oceanic physical mechanisms, many of them associated with the synoptic variability of the African easterly waves (AEW). These are characterized by peaks of low- to mid-level wind shear and high convective available potential energy in the vicinity of elevated terrain as a response to coherent and organized local convection.

The seasonal time scale of the atmospheric dynamic characteristics of the African monsoon is also associated with the African easterly jet (AEJ), which is developed in response to the inverse latitudinal surface temperature gradient during boreal spring. In the upper levels, between parallels 20°N and 30°N, higher velocity westerly subtropical jet stream (STJ) is developed due to the convergence into low-pressure areas and the divergence in the anticyclonic surface flow. During summer, the baroclinic and barotropic gradients increase due to maritime airmass flow, causing a reverse stream that becomes the tropical easterly jet (TEJ). The interaction of the overall regional dynamic circulation with the ocean forcing

mechanism is still today not well understood, and hence these fields are considered a challenge for future land, ocean and atmospheric fields of research.

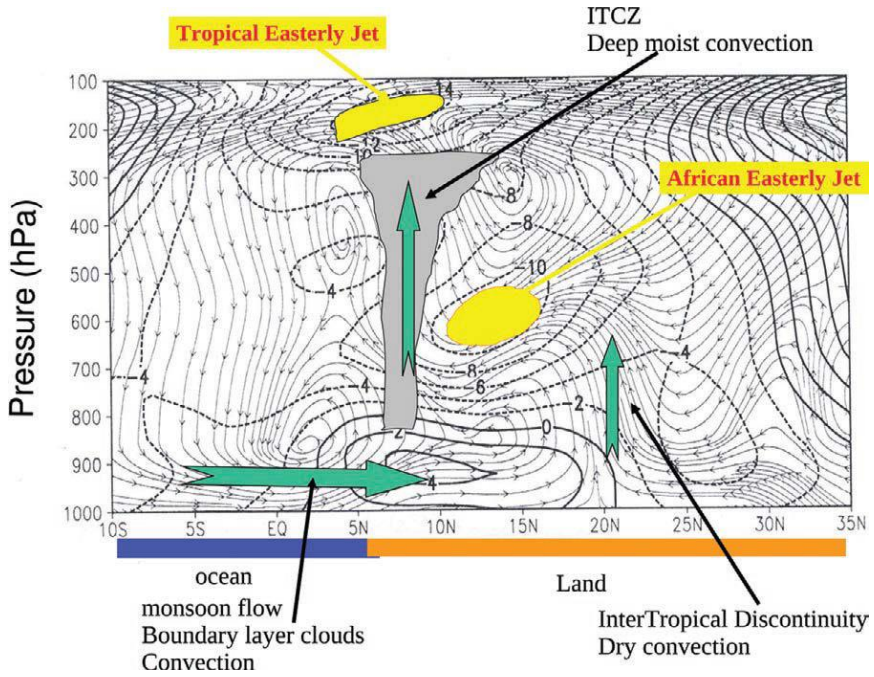

Figure 3.1.1. Summer mean meridional circulation and associated mean winds (m s^{-1}) over NW Africa (reproduced from Hourdin et al., 2010).). This scheme summarizes the interaction between the surface monsoon and westerly (5°N-20°N) stream flow, the AEJ at the 600 hpa level, and the TEJ at 200 hpa, during summer. It also shows the location of the Intertropical Convergence Zone (ITCZ) deep moist convection (5°N-10°N), and the dry convection in the intertropical discontinuity – ITD (20°N). The vertical flows are shown as streamlines. The westerlies (solid lines) and easterlies (dashed lines) are represented as mean speed (m s^{-1}) wind contour lines. The arrows indicate air flow direction. The grey area indicates areas of strong convection, upward movement, and turbulence. The jets are represented by yellow coloured areas. © American Meteorological Society.

3.1.2. DATA

The data used to study this regional tropical and subtropical area resulted from combining several observations and forecast output from a weather prediction model called NCEP_Reanalysis 2. In this model, the probability distributions are associated with observations, and forecasts are merged with dynamical constraints (Kanamitsu et al., 2002). This NCEP_Reanalysis 2 information was provided by the NOAA/OAR/ESRL PSD, United States of America (website at http://www.esrl.noaa.gov/psd/, accessed on 25 February 2015). The data made it possible to analyse wind, temperature and moisture fields in order to identify the 2D and 3D atmospheric regional flow as well as local prevailing structures and interacting forcing mechanisms.

3.1.3. WEATHER ZONES

The NWA region is greatly influenced by the northern, continental Saharan airmass to the north of the intertropical discontinuity (ITD). This is associated with a north southward pulsation of a very narrow line of

a more or less abrupt discontinuity. It is a front which lacks temperature and precipitation contrast between a continental airmass to the north (dry) and a tropical, humid maritime airmass to the south. Basically deriving from precipitation distribution from north to south, the regional climate has been divided into Zones A, B, C and D. To the north of the ITD, Zone A is characterized as having little cloud with periods of dust and haze, low vapour pressure and a large diurnal temperature range, nocturnal temperature inversion near the surface, east-northeasterly moderate winds and prevailing rainless conditions. Zone B lies on the ITD southern side and is humid but mainly rainless due to restriction in cloud development, although afternoon thunderstorms may occur. Fair weather cumulus is the dominant figure. Zone C is an approximately 800-km belt south of Zone B, similar to it but with marked local thunderstorms and westward-moving disturbances with heavy showers. Although it tends to be subdivided, Zone D extends some 300 km to the south of Zone C with almost daily occurrence of persistent precipitation and SW mean steady winds. The movement of the line of discontinuity is a repeating pattern that follows the seasonal movement of the sun, making the tropical and subtropical NWA rainless during winter in regard to its atmospheric forcing over the region.

3.1.4. ATMOSPHERIC CIRCULATION MECHANISMS

3.1.4.1. The Hadley cell

The dominant atmospheric flow is the so-called Hadley cell. Assimilated to a non-rotating globe, in literature this cell is a well understood atmospheric system described as a closed circulation loop, which begins at the equator with warm, moist air lifted aloft in the induced low-pressure areas to the tropopause, and carried poleward. At about 30°N, this air descends into an area consisting of an induced high-pressure subtropical belt that extends more or less continuously around the globe, being neither homogeneous nor continuous. A portion of the descending air travels equatorially along the surface, closing the loop of the northern Hadley cell and creating the trade winds that blow almost throughout the year (Schubert et al., 1991). It is accurate to describe this motion as a figure that follows the sun's zenith point, or a type of thermal equator which undergoes a semiannual north-south migration (Leroux, 2001). It can be considered to be warm air rising in the Gulf of Guinea (low pressure), flowing north towards the pole, descending over the Atlas Mountains of NWA (high pressure) and being redirected to the equator at the low levels. Were it not for the Coriolis Effect, in the northern hemisphere this circulation would be a simple flow due south from the parallel 30°N at the surface and in reverse direction from the equator in the upper level. The Coriolis force turns the northerly blowing winds into northeast trades, and the counter trades aloft westerlies due to the diminishing friction effect with altitude. This basic circulation system is the forcing mechanism that influences the weather over tropical and subtropical northwest Africa and the adjacent Atlantic Ocean waters (Leroux, 2001).

3.1.4.2. The subtropical anticyclone and the trade winds

The anticyclones of Azores in the northern hemisphere and Saint Helen in the southern hemisphere are the two belts that affect directly, and are the main forcing mechanisms over, the atmospheric dynamic flows and tropical and subtropical NWA climates on the north side of the equator, with the first largely overrunning during the boreal winter. The northern high pressure cell tends to disappear over land areas especially during the summer season, although it remains in altitude between 500 hpa and 700 hpa above the Sahara Desert. It has the characteristics of being a cell of subsidence and divergence and remarkable dryness (Laing and Evans, 2011).

The surface flow of the Hadley northern circulation cell is generally from the NE and tends to curve to the west, responding to the anticyclone curvature. This northeast trade wind, a continental airmass called harmattan in the Sudan area, blows over most of tropical and subtropical West Africa almost all year round. It is a very dry airmass that becomes even drier while flowing across the Sahara Desert, with maintained subsidence and stable patterns until reaching equatorial areas where it acquires moisture. Above the Atlantic Ocean it generally stratifies with a slightly lower wet and cool layer and a relatively warm and dry upper layer. It is a well-marked low-level inversion up to the height of approximately 500 m in the proximity of the anticyclonic cell. This property prevents atmospheric upwelling and so inhibits cloud development and precipitation. Over the ocean, the wet layer becomes thicker, with decreasing stability and increasing intensity and frequency of rainfall. With moisture increase, upward motion replaces the horizontal flow and the trade winds become an equatorial mass with vertical precipitation developing structure named Inclined Meteorological Equator (IME) by Leroux (2001). The trade winds are somehow a steering flow for tropical storms that form and move across the Atlantic Ocean, often transporting African dust westward with shallow cumulus clouds seen within. This type of local cloud is capped from becoming taller by the trade wind inversion, due to descending air aloft from within the subtropical ridge. It has been observed that the stronger the trade winds, the less rainfall can be expected in the neighbouring land areas (Giresse, 2008).

3.1.4.3. The subtropical jet stream

In the absence of friction, the wind velocity is significantly higher in the upper levels at approximately 12 km altitude (200 hpa) between 20°N and 30°N, generating the subtropical jet stream (STJ). This westerly wind travels from the Atlantic Ocean to cross NWA with speeds attaining 70 knots, with convergence into low pressure areas and divergence in the anticyclonic flow at the surface. During summer time, the baroclinic and barotropic gradients across tropical and subtropical NWA increase due to the maritime airmass flow. The STJ turns into easterly tropical jet with a mean velocity of approximately 40 knots at the 100 hpa level (15 km a.s.l. to 20 km a.s.l.), and around 13°N to 20°N with a velocity of 20 knots at the 500 hpa level (approximately 5 km a.s.l.). This lower level wind is the AEJ (Leroux, 2001).

3.1.4.4. The low pressures over the Sahara Desert

During summer, an inflow of moist air from the Atlantic Ocean is caused by sensible and latent heat release over the Sahara Desert. This flux of moisture-laden air contributes to the northwest and north displacement of the Azores subtropical anticyclone and the Intertropical Convergence Zone (ITCZ), moving and becoming more active over the northern hemisphere. The sensible and latent heat rise drives the development of low-pressure conditions, as opposed to the reverse condition during winter when relative high-pressure conditions prevail. This situation is intensified by the Saint Helen southern subtropical high that intensifies and expands towards the equator during summer, becoming a very important circulation driving force (Laing and Evans, 2011).

3.1.4.5. The monsoon

During summer, the NWA coastal regions receive humid flows of air from SSW, SW and WSW which curve towards the east while entering the continent in opposition to the prevailing easterly stream flow, extending beyond its boundary. This thick moist layer of about 3 km is an IME (Leroux, 2001), with potential instability and forward and retreat pulses, and strong vertical uplifts of thermal convection and turbulence. It is the main cause of precipitation, of development of cumulonimbus cloud clusters with strong vertical development and convection, and is the development source of periodic complex systems induced by kinematic and frontal processes (Taylor, 2008).

3.1.4.6. The African easterly jet (AEJ) and waves (AEW)

The AEJ (Figure 3.1.2) is a region of the lower troposphere over NWA where the seasonal easterly mean wind speed is the maximum. The jet develops as a result of the land mass heating during the summer, creating a surface temperature and moisture gradient between the Sahara Desert and the Gulf of Guinea. The surrounding atmosphere responds by generating vertical wind shear in order to maintain thermal wind balance (Thorncroft et al., 2008). During January, the stream lies at the height of 3000 m a.s.l. at a latitude of 5°N. The wind speed rises from 30 km h^{-1} in January to 40 km h^{-1} in March. While displacing northward to 7°N, winds within the jet increase to 45 km h^{-1} (Chen and van Loon, 1987). By June, it shifts northward into NWA (Leroux, 2001) The development of the thermal low over northern Africa leads to a low-level westerly jet stream which is in place from June to October at the south of the ITCZ (Cook, 1999). During summer, the mid-level African easterly jet occurs above West Africa between 10°N and 20°N (Pu and Cook, 2008). The jet reaches its zenith in August, lying between the latitudes of 16°N and 17°N. In September, wind velocity can be close to 50 km h1 between the parallels of 12°N and 13°N (Parker et al., 2005). The easterly jet weakens and drops southward during the months of October and December (Leroux, 2001) The low-level AEJ plays a crucial role in the dynamics of the African monsoon (Low, 2005) while, with both barotropic and baroclinic instability, it helps to form the AEW, which are ubiquitous weather disturbances that cross the tropical Atlantic basin during the summer season (Parker et al., 2005; Pu and Cook, 2008; Leroux and Hall, 2009). With a preferred wavelength between 2000 km and 4000 km, the wave is a synoptic and subsynoptic scale structure system associated with nonlinear developments (Reed et al., 1977; Thorncroft et al., 2008) of potential vorticity anomalies generated by convection within the mesoscale convective systems (Schubert et al., 1991). Some mesoscale storm systems are embedded in the waves and are potential developers of tropical cyclones after they move into the tropical Atlantic during the months of August and September (Nicholson et al., 2007). During the rest of the year the wave is further south and its activity is suppressed (Pu and Cook, 2008). The variability on AEJ and wave can considerably affect the regional seasonal weather dynamics, temperature and precipitation (Figure 3.1.2).

3.1.4.7. Intertropical convergence zone (ITCZ)

This dynamic system is characterized by its low intertropical atmospheric pressure derived from the trade wind convergence that results in vertical upward flow. It forms an IME towards the north, with low unstable winds at the ground and is vertically structured on the equator, forming an oblique low troposphere stream flow towards the continent (Schubert et al., 1991). The semiannual movement of the ITCZ is associated with and follows the sun's zenith point. As dry air from the north and humid air from the south meet, it is an area of conflict between northeastward continental and eastward oceanic wind flows, and therefore a region of major turbulence. It influences the northern hemisphere basically from July to September. In consequence, the semi-arid regions to the north experience related precipitation only during peak summer. All year long, there is a persistent easterly midtropospheric wind flow overlying the surface stream flow (Leroux, 2001).

a)

b)

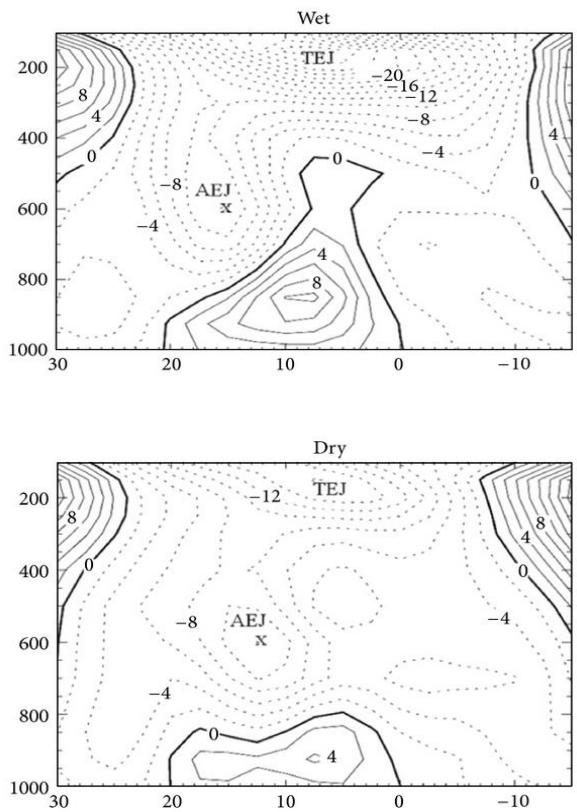

Figures 3.1.2. Vertical cross-sections of zonal winds (m s^{-1}) during wet years (dashed lines = easterlies and solid lines = westerlies), TEJ and the mid-tropospheric AEJ; a) corresponds to wet years and b) dry years (reproduced from Grist and Nicholson, 2001). During wet years, the westerly wind flow is stronger across the WA. It can also reach the 500 hpa pressure level, so forcing the AEJ to move further north at the 600 hpa pressure level. The closed contours lines at 600 hpa and 200 hpa levels indicate the location of the AEJ and the TEJ flows aloft. © American Meteorological Society.

3.1.4.8. Saharan Air Layer (SAL)

The Saharan Desert region of subtropical Africa is the origin of a prevalent atmosphere extending several kilometers from the surface upwards, called SAL (Figure 3.1.3). It is an intensely dry, very hot layer that often overlies the cooler, more humid surface air. As it drives from continental areas out over the ocean, it is normally lifted above the denser marine air causing the trade inversion layer (TWI) where temperature increases with height. Being dry air, the SAL has a temperature dropping steeply with height. Also within the SAL, many disturbances with thunderstorm structures periodically develop over NWA, resulting in large dust and sand storms extending vertically up to 6 km. It has been pointed out that the winds blow twenty percent of dust from a Saharan storm out over the Atlantic Ocean (Braun, 2010), twenty percent of it reaching all the way to the western Atlantic, and the remainder settling out into the ocean or being washed out by precipitation (Dunion, 2007). The dust clouds, often with iron-rich particles visible by satellite, are associated with solar radiation reflectors, being atmospheric coolers as well as reducers of amounts of sunlight reaching and heating the ocean. The SAL has been associated with the suppression of tropical disturbance development and intensification (Evan et al., 2007; Karyampudi and Carlson, 1988), since its particles tend to increase condensation as they drift into the marine layer, but do not lead to precipitation since the drops that are formed are too small and cannot coalesce properly. The drops tend to evaporate when moving into drier air or air mixing takes place (Dunion and Velden, 2004). On account of uncertainties that still remain regarding its forcing mechanism and interaction in the regional atmosphere, SAL is an object of ongoing research in the field of dust particle analysis and interactions (i.e. Saharan Air Layer Experiment or SALEX (website at http://www.aoml.noaa.gov/hrd/project2007/sal.html, accessed 1 April 2015); Sassen et al., 2003; Garrison et al., 2003).

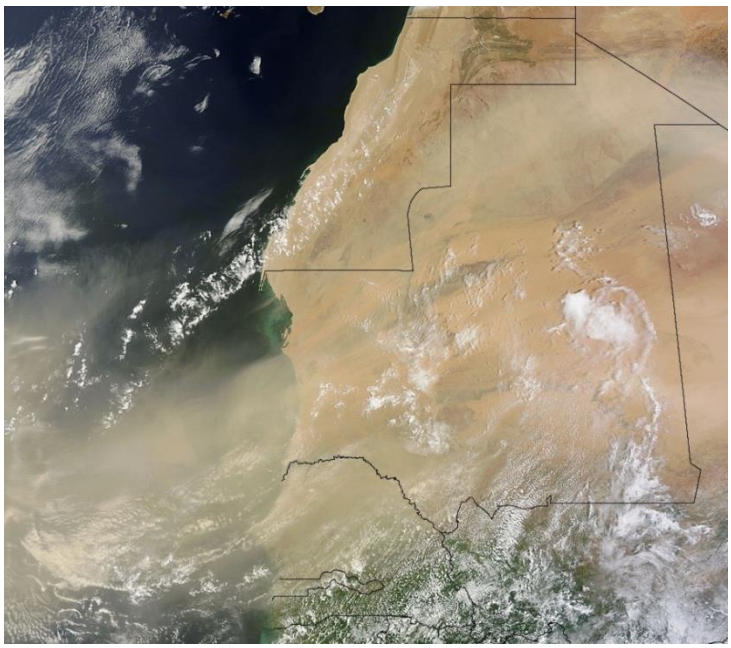

Figure 3.1.3. The image is an example of a natural colour picture of the Saharan Air Layer (SAL) flow off the west coast of Africa. The image taken by the Moderate Resolution Imaging Spectroradiometer (MODIS) on NASA's Terra satellite on July, 2013, shows dust plumes blowing over the NWA and northeast Atlantic (dust is represented by light milky brown colour and clouds in white). These layers of dry and hot air are often transported all the way across the ocean to the western side of the Atlantic (Source: NASA image, by MODIS Rapid Response Team, Goddard Space Flight Center).

3.1.5. ANNULAR INFLUENCE

The seasonal variations of the atmospheric systems over tropical and subtropical Africa are the dominant components of variability over the region, with sensible heating to warm land surfaces more rapidly than the ocean mixing layer. Due to differing heat capacities between land and water, the result is a seasonal monsoon-type circulation in the southern region and a steady northeast stream in the central and northern part, a pattern that affects the overall weather conditions across the region and surrounding ocean basin. These areas experience a remarkable seasonality in terms of atmospheric climate parameters, including pressure, temperature, radiation, evaporation and cloudiness, comprising two basic systems six months apart, wet and dry.

3.1.5.1. The North Atlantic Oscillation

The North Atlantic Oscillation (NAO) is defined as the sea level pressure difference between the Azores high and the Icelandic low. It is a part of the Northern Hemisphere annular mode and a recurrent pattern of atmospheric variability. It consists of a leading mode of variability that can have a considerable influence on temperature and precipitation, expressing variability at multiple monthly and decadal time scales, being the monthly variability that is largely unpredictable (Hurrell et al., 2003) and is associated with changes in the wind speed and direction. It has been found that, more specifically, the positive winter NAO anomalies are consistent with stronger trade winds (Polo et al., 2011).

3.1.5.2. The subtropical moving highs

Mobile polar highs are fast and strong dynamic large circulation systems moving constantly over the region, retaining their original low temperatures while moving across long distances. They are capable of transporting considerable amounts of cold polar air and can drive more deeply into tropical areas. The meridional trajectory and dynamics intensify the cyclonic circulation which enhances poleward energy transfer, involving heat and latent heat through water vapour. The process can also involve air over the ocean with precipitable water potential or continental air with much drier conditions favouring anticyclonic agglutination, possibly reinforcing the trade wind inversion disturbances in middle latitudes, because of

accentuated thermal contrasts when the mobile polar highs are more vigorous, leading to more powerful updrafts. As the anticyclonic agglutination process becomes more vigorous, the westerly jets accelerate and are displaced towards the equator (Leroux, 2001).

Over land, continental agglutination is stronger and anticyclonic conditions last longer. Agglutination also forms at more tropical latitudes, with stability reinforced and presence of inversion. As a result, tropical circulation accelerates, although the trade winds cover only a small area and their energy tends to dissipate on to monsoon fluxes. The greater power of the mobile highs tends to encourage more intense transfers towards the pole. Oceanic surface circulation is accelerated, impelled by colder anticyclonic agglutinations, and the trade winds speed up. These dynamic phenomena basically take place during winter time. In summer, the systems are less intense as a result of a reduced polar thermal deficit as the systems migrate to the north and are less vigorous and almost unnoticed, with the heat low forcing taking over. The reduction causes attenuation of the cyclonic circulation at the leading edges, resulting in a reduced energy transfer towards the poles, although favouring the supply of heat and latent heat. The reduced meridional trajectories prevent the mobile polar highs from reaching or diverting the maximum possible precipitable water potential (Leroux, 2001). Therefore dust is transported because of the deceleration in fluxes in the lower and higher layers.

3.1.5.3. Tropical plumes

Tropical plumes (TPs) are defined as continuous cloud bands (>2000 km) crossing 15°N with temperature anomalies of less than 220 K (Fröhlich et al., 2013). They indicate tropical and extratropical interactions with impacts on radiation and moisture occurring during boreal winter, largely confined to oceanic regions (McGuirk et al., 1988). In fact, in the study region TPs develop more frequently over the eastern Atlantic Ocean extending towards the continent.

These systems often develop downstream of extratropical upper-level troughs propagating into low latitudes, in regions where mean upper-level easterlies do not generally favour equatorward wave propagation (Mecikalski et al., 1998). Blackwell (2000) demonstrated the existence of strong subsidence and convergence in the eastern portion of the ridge upstream of TPs. Accordingly, because of the loss of rotational balance of subtropical flow entering the tropics and the ensuing deceleration, a subtropical jet stream and a TP can be developed, associated with equatorward amplification and the trough zonal contraction.

Convergence results from a prior disturbance of the subtropical jet in the upstream ridge that forces stratospheric air flux to enter the tropical troposphere (Blackwell, 2000). But, according to Mecikalski and Tripoli (1998), changes in the inertial stability field through large-scale advection of low potential vorticity air from tropical convective outflow are responsible for the plume genesis and the initiation of disturbances upstream of the ridge.

With elongated cloud bands (Figure 3.1.4) that often form to the east of the trough axis and extend from the tropics to the subtropics, as minimas in the mid and upper troposphere, the upper-level trough is of great importance in generating precipitation in the midlatitudes and subtropics that usually occurs far east of the trough axis. This precipitation is associated with moisture transported to the eastern side of an upper-level trough and is triggered by upper-level divergence and large-scale uplift due to advection of positive vorticity (Knippertz and Martin, 2005). The upper-level troughs are recognized as cloud bands that play an important role in the transport of momentum and kinetic energy polewards. The existence of dry air at the west side of the trough is due to subsidence.

a)

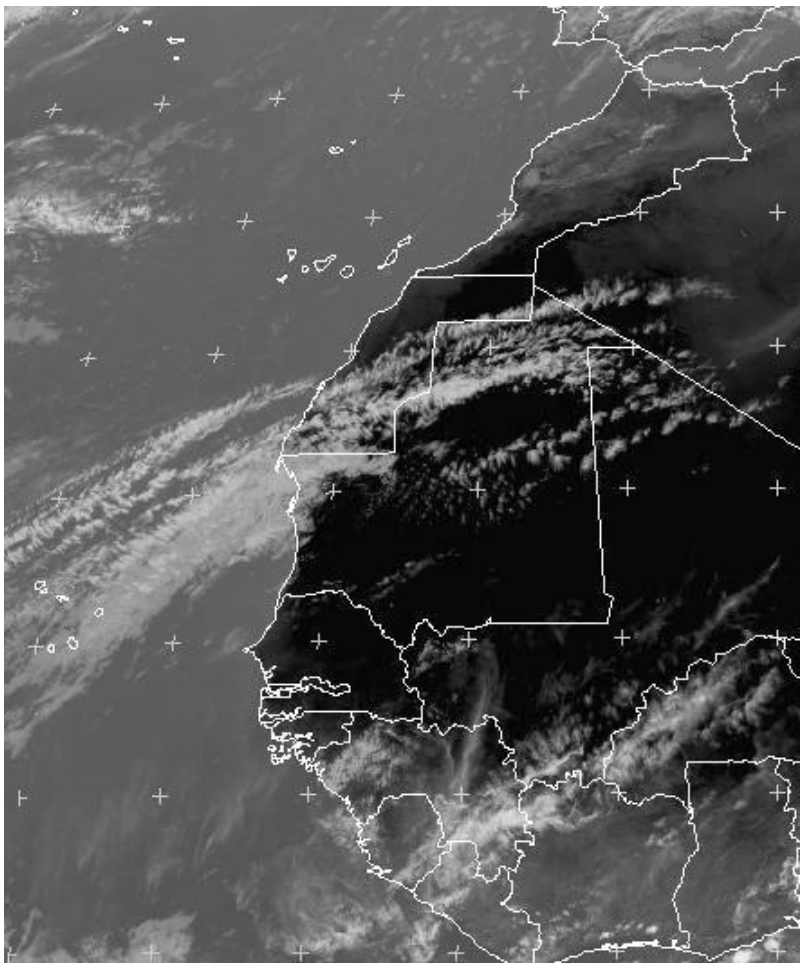

b)

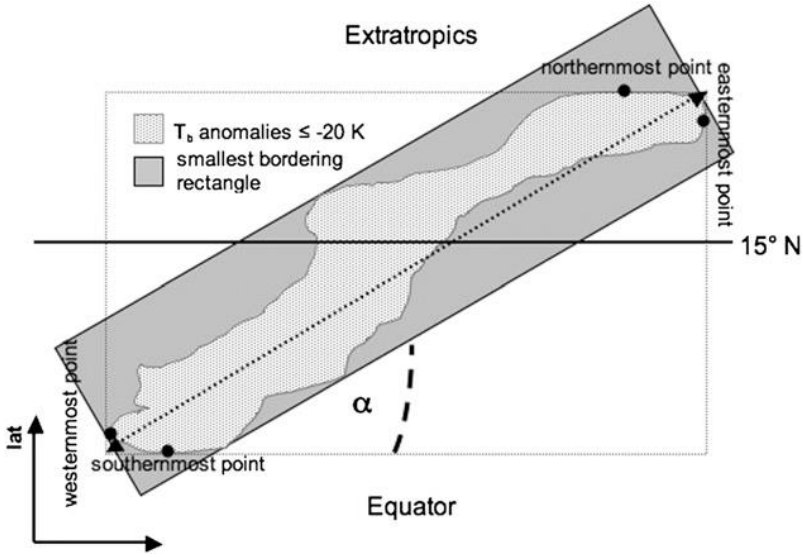

Figure 3.1.4. a) Satellite MET10 infrared imagery at 15:00 UTC 11 Apr 2015 showing the development of a tropical plume over the NWA extending from Cabo Verde to Western Sahara, Mauritania, and Algeria (Source: EUMETSAT, website at http://oiswww.eumetsat.org/IPPS/html/MSG/PRODUCTS/MPE/WESTERNAFRICA/index.htm, accessed on 12 April 2015). b) Schematic illustration of the TP identification procedure for the Northern Hemisphere (reproduced from Fröhlich et al., 2013). The inclination angle (α) between the SW NE direction of the elongated clouds centered at latitude 15°N and the Equator. The grey and light grey correspond to the inclined rectangle range that of the clouds and the temperature anomalies less than or equal to 20 K. © American Meteorological Society.

3.1.6. DISCUSSION AND CONCLUSIONS

The tropical and subtropical NWA climates range from equatorial, tropical wet and dry, tropical monsoon, semi-arid to desert. Except in highland areas and along the fringes, temperate climates remain rare throughout the continent. In fact, it is more realistic to say that the climate of NWA is basically more dependent on rainfall amount than on temperatures. Temperatures are consistently high as a result of the prevailing presence of subtropical high pressure systems.

In this study, using literature research documentation and NCEP reanalysis data it was possible to define the atmospheric circulation dynamic patterns over tropical and subtropical NWA. It has been found that the Azores subtropical high and the monsoon circulation flow are the major structures that influence the weather in the region. The high pressure system causes a surface continental airmass with maintained subsidence and stability to flow consistently from the northeast over most of region. The resulting trade wind flow is a very dry airmass that becomes even drier while flowing across the Sahara Desert. The summer monsoon, of primary importance for the rainfall distribution, is still today a complex mechanism with diurnal forcing effects, which impacts the boundary layer and determines its transition between stable and unstable conditions.

Large-scale convective events and synoptic wave perturbations that move across the continent are figures of considerable importance for field research. Likewise, the regional intraseasonal time-scale variability remains to be well understood as regards the regional atmospheric dynamical interaction of all the atmospheric circulation systems.

Some of the local and regional systems are associated with the synoptic variability of the African easterly perturbations. The seasonal time scale of the atmospheric monsoon dynamic characteristics is associated with the African easterly jet, which is developed in response to the inverse latitudinal surface temperature gradient during spring. In altitude, between the parallels 20°N and 30°N, the westerly subtropical jet streams are characterized by strong velocity, with convergence into low pressure areas and divergence in the anticyclonic surface flow. During summer this is associated with baroclinic and barotropic gradient increases due the maritime airmass flow and the winds become easterlies.

The annular seasonal variability of other atmospheric structures, like the subtropical moving highs, the TPs and the SAL, are also important regional forcing mechanisms that impact the physical and dynamical atmospheric structure, and therefore need further investigation. The interaction between the continental circulation systems and the surrounding ocean basin, yet to be well understood, continues to be considered a major challenge for field research in the CCLME.

Acknowledgments

The author thanks the INMG of Cabo Verde for allowing the use of its facilities during the preparation of the manuscript. NCEP reanalysis data were provided by the National Oceanic and Atmospheric Administration/Office of Oceanic and Atmospheric Research/Earth System Research Laboratory (NOAA/OAR/ESRL) Physical Science Division (PSD) (website at http://www.esrl.noaa.gov/psd/, accessed on 25 February 2015). The SAL image was provided by National Aaeronautics Satellite Administration (NASA) (http://rapidfire.sci.gsfc.nasa.gov/cgi-bin/imagery/single.cgi?image=WestAfrica.A2013211.1140.2km.jpg, accessed on 2 March 2015). The satellite image was provided by EUMETSAT (public weather website at http://oiswww.eumetsat.org/IPPS/html/MSG/PRODUCTS/MPE/WESTERNAFRICA/index.htm, accessed on 12 April 2015). I also thank Itahisa Déniz González for the helpful comments on the manuscript.

3.2. WATER MASSES IN THE CANARY CURRENT LARGE MARINE ECOSYSTEM

María V. PASTOR[1], Pedro VÉLEZ-BELCHÍ[2] and Alonso HERNÁNDEZ-GUERRA[3]

[1] John Abbott College. Canada

[2] Centro Oceanográfico de Canarias, Instituto Español de Oceanografía. Spain

[3] Instituto de Oceanografía y Cambio Global (IOCAG), Universidad de Las Palmas de Gran Canaria. Spain

3.2.1. INTRODUCTION

In the Canary Current Large Marine Ecosystem (CCLME) water masses of very different origin converge. The upper levels, between 100 dbar and 700 dbar, are occupied by North Atlantic Central Waters (NACW) and South Atlantic Central Waters (SACW) that feed the nutrient-rich wind-driven upwelling ecosystem. The NACW are formed by surface subduction of winter water in the North Atlantic, while the SACW are formed in the western South Atlantic Ocean. The Cape Verde Frontal Zone (CVFZ), at approximately 15°N, separates these thermocline waters. The Antarctic Intermediate Water (AAIW) and the warmer and saltier Mediterranean Water (MW) occupy the intermediate layer, between 700 dbar and 1500 dbar. The North Atlantic Deep Water (NADW), formed in the Labrador Sea, occupies the layers deeper than 1500 dbar.

3.2.2. DATA

Since 1996, the Centro Oceanográfico de Canarias of the Instituto Español de Oceanografía together with the Instituto de Oceanografía y Cambio Global of the Universidad de Las Palmas de Gran Canaria, has been carrying out the Radial Profunda de Canarias (RAPROCAN) project with the aim to study the water masses and circulation around the Canary Islands.

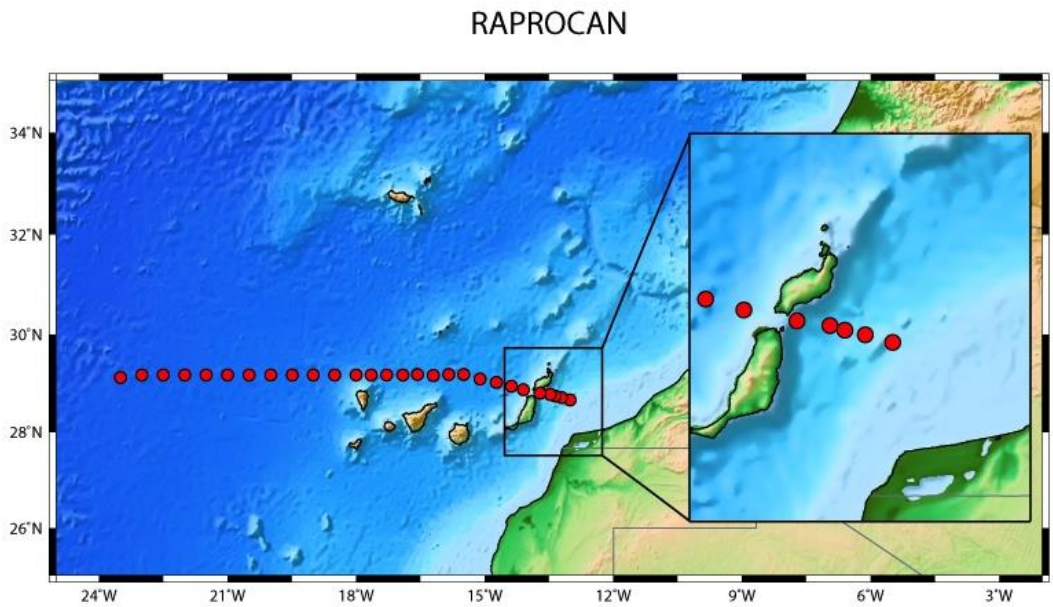

Figure 3.2.1. Stations sampled periodically since 1996, with cruises carried out under the RAPROCAN project. The stations for the Lanzarote Passage are highlighted.

Figure 3.2.1 shows a typical cruise carried out under the RAPROCAN project in September 2006. It consisted of 28 SeaBird 91+ CTD stations from the surface down to 5-10 m above the bottom of the ocean. The station separation is about 50 km except stations in the Lanzarote Passage (LP after Hernández-Guerra et al., 2003) where the separation was reduced to 5-10 km.

During the cruises, the CTD was always equipped with a redundant temperature and salinity sensor for inter-comparison. The salinity data were calibrated using an Autosal instrument, following the World Ocean Circulation Experiment (WOCE) requirements. In addition to these measurements, water samples have been collected during the cruises with a 24-10 L bottle carrousel. Dissolved oxygen and nutrients are estimated from these water samples.

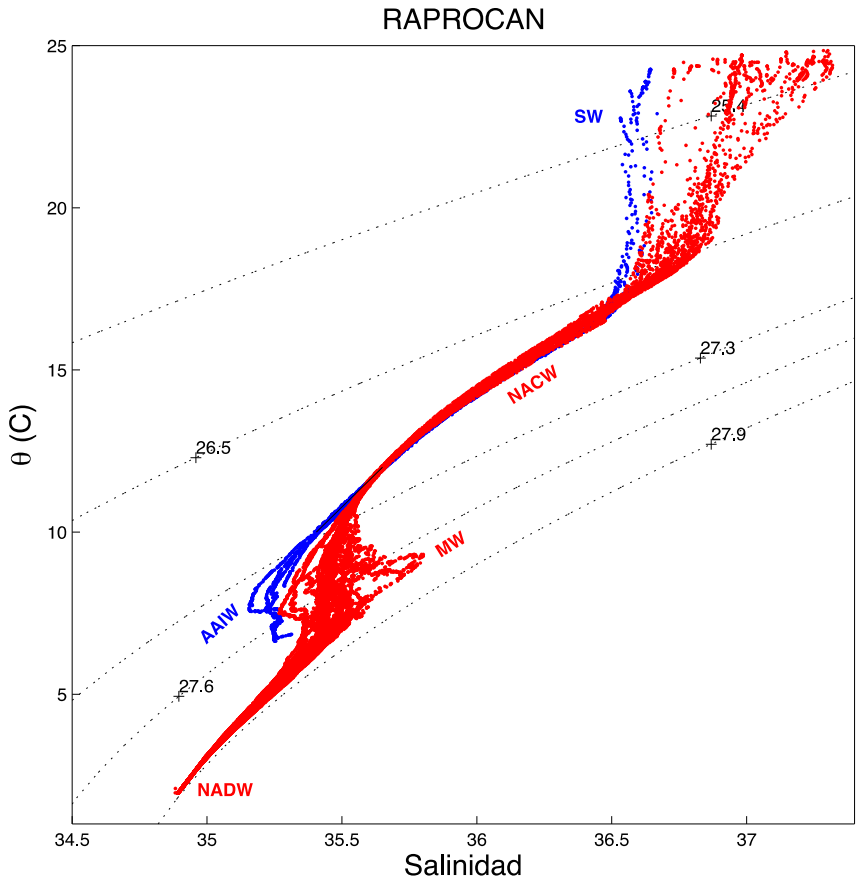

Figure 3.2.2. Potential temperature-salinity diagram with data from the RAPROCAN cruise. The blue and red dots correspond to the stations located in the Lanzarote Passage and west of Lanzarote, respectively.

Figure 3.2.2 shows the diagram of potential temperature and salinity from the RAPROCAN cruise. This diagram shows all the water masses present in the area around the Canary Islands. South of about 21°N, another thermocline water mass is present, the South Atlantic Central Water (SACW), with salinities lower than the NACW. In order to show the characteristics of this water mass, we present the results of the Corriente de contorno oriental - Canarias (CORICA) cruise. This cruise was carried out in September 2003 (Figure 3.2.3), covering most of the CCLME region with the same procedure as for the RAPROCAN cruise. The potential temperature and salinity diagram, obtained using data from the CORICA cruise, clearly illustrates the presence of the relatively fresher SACW (Figure 3.2.4).

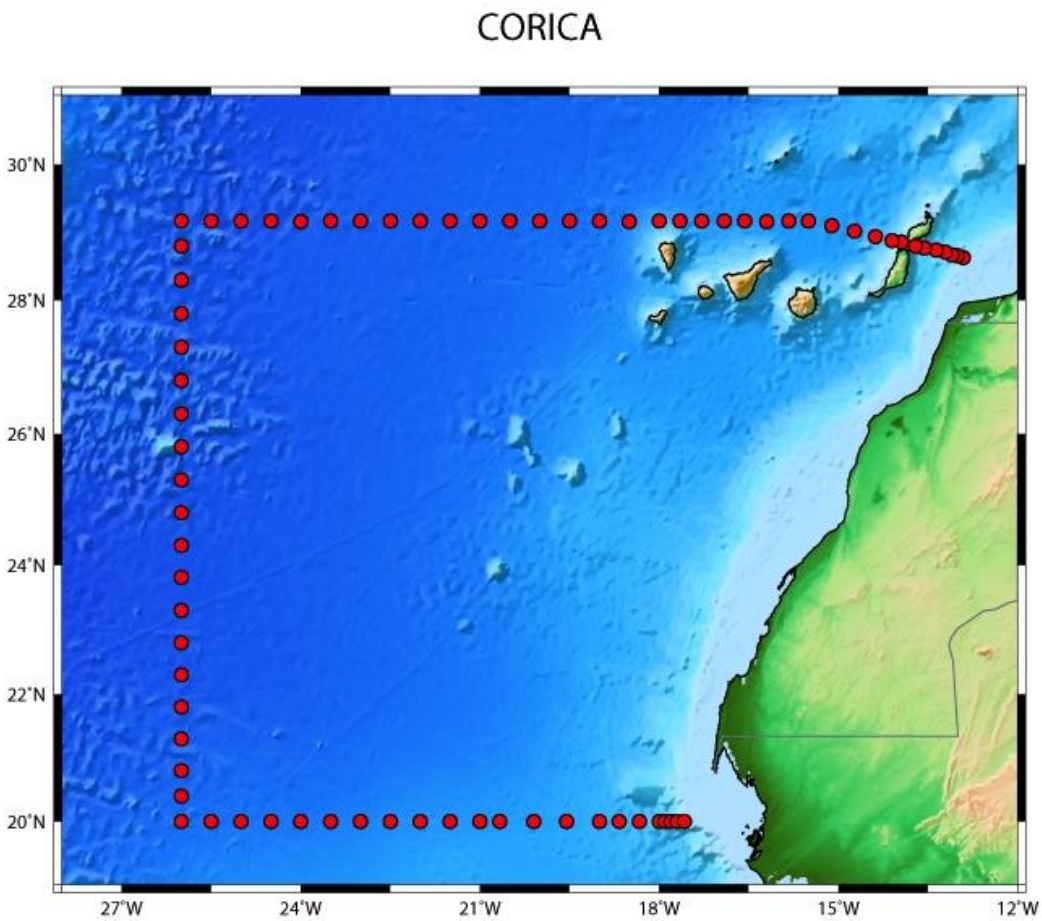

Figure 3.2.3. Stations sampled during the CORICA cruise, carried out in September 2003 (Hernández-Guerra et al., 2005).

3.2.3. SURFACE WATERS

The surface layer (upper 100 dbar, approximately) is characterized by high temperature and salinities, high dissolved oxygen and low nutrient concentrations (Pastor et al., 2008). Winter temperatures decrease progressively with latitude, ranging between about 25°C and 15°C in the southern and northern extremes of the CCLME; summer values may be substantially larger, exceeding 25°C except in the coastal upwelling region. Salinity has a surface maximum close to 37.0 at approximately 25°W, 25°N. The waters also exhibit a shallow subsurface salinity maximum, typically located at the base of the surface mixed layer, which arises because of vertical mixing in the relatively deep winter mixed layer, sometimes referred to as Madeira mode water (Siedler et al., 1987; Bauer and Siedler, 1988).

3.2.4. CENTRAL WATERS

The water masses of the permanent thermocline, known since Sverdrup et al. (1942) as the central water masses, originate at the subtropical gyres of both hemispheres and spread towards the equatorial regions. They extend from approximately 100 dbar to 700 dbar depth and are recognized in a TS-diagram by a nearly linear TS-relationship (Figure 3.2.2). The thermocline waters are essentially divided into NACW and SACW, depending on their origin. Typically, the TS curve of the NACW connects 7°C, 35.0 with 18°C, 36.6, while for the SACW it connects 7.5°C, 34.97 with 20°C, 36.0.

NACW have their source in the North Atlantic subducting zone, defined as where the Ekman pumping velocity is negative, and reach subsurface waters at lower latitudes through the thermocline circulation (Sarmiento et al., 1982; Kawase and Sarmiento, 1985). Only water masses formed in the subducting zone during late winter and early spring may escape the surface layers to be injected into the permanent thermocline; during the rest of the year, subducted waters remain in the mixed-layer as the escape velocities caused by Ekman pumping are less than the seasonal advance of the mixed layer thermocline. Thus, the maximum depth of the winter mixed layer, which varies latitudinally, sets the upper limit of the central water masses. The vertical extension of the NACW in lower latitudes will be determined by the densest winter-outcrop isopycnal within the subducting zone, with a potential density anomaly close to 27.1 (Kawase and Sarmiento, 1985).

SACW are formed in the subducting regions of the South Atlantic subtropical gyre (Stramma and England, 1999). SACW travel through the South Atlantic thermocline into the equatorial current system, from where they are distributed to the tropical and equatorial upper ocean through the system of zonal jets, also reaching the tropical region of the North Atlantic.

NACW is transported to the CCLME region in the anticyclonic circulation of the North Atlantic subtropical gyre through the Azores Current, Portugal Current and Canary Current. SACW also recirculates around the southern subtropical gyre, following the South Atlantic Current, Benguela Current, Equatorial Current, and North Brazil Current. The SACW may then continue north, in the upper layers of the western boundary currents (North Brazil and Guyana Currents), or be transferred eastwards through western boundary retroflections into the equatorial zonal current system to eventually reach the southern part of the CCLME.

Different varieties of both the northern and the southern waters have been identified. Emery and Meincke (1986) subdivided the Central Water of the North Atlantic into Eastern (ENACW) and a Western (WNACW) types. The division reflected different formation regions, south of the Subarctic Front for WNACW and south of the Iceland-Faroe Front for ENACW. Because of its close contact with the fresher underlying subpolar intermediate waters, WNACW has salinities 0.1 to 0.2 lower than ENACW. The higher salinities of the latter variety would also reflect the influence of Mediterranean Water. Conversely, Tomczak and Godfrey (1994) argued that the temperature-salinity changes observed across the ocean basin result from environmental variability within the formation region and thus identify a single water mass of northern origin.

While Emery and Meincke (1986) identified only one type of SACW, Gordon et al. (1992) and Sprintall and Tomczak (1993) showed that central waters formed in the Subtropical Convergence of the Indian Ocean were an important contributor to the thermocline of the Atlantic Ocean, entering the Atlantic basin via the Agulhas Current. This eastern variety has lower salinities than the SACW formed in the subtropical gyre (Sprintall and Tomczak, 1993). Poole and Tomczak (1999) also used this SACW subdivision in their study of the spreading and mixing of the thermocline waters in the Atlantic. As a result of their optimum multi-parameter analysis, they show a strong density stratification of both varieties, with the ESACW variety restricted to the layer from 350 dbar to 600 dbar. Their work also shows that the ESACW variety dominates in the CCLME region, arriving here through the complex zonal equatorial current system.

Poole and Tomczak (1999) examined the entire Atlantic basin, which allowed them to define water types according to the formation region. However, most works done on a regional setting define source water types in the vicinity of the study region, avoiding the need to account for mixing with other water masses along their pathway to the study region. Following this approach, Pastor et al. (2012) identified a distinct type of SACW in coastal hydrographic stations located around 15°N over the continental slope. This water

mass shows lower salinities and higher oxygen concentrations than the surrounding (local) SACW, indicating a more remote tropical origin. Its core is centered at 200 dbar and its zonal average influence reaches as far as 19°N. The spatial distribution of this tropical variety shows that it is advected north by the eastern branch of the cyclonic circulation around the Guinea Dome (Pastor et al., 2012; Peña-Izquierdo et al., 2012).

The CVFZ constitutes the boundary between NACW and SACW and corresponds to the southern limit of the North Atlantic thermocline recirculation (Zenk et al., 1991; Arhan et al., 1994). The CVFZ stretches southwest from 20°N off the coast of Africa to the Cape Verde Islands, and then acquires a more zonal orientation towards the western side of the basin. Both central water masses occupy the same density range – the front is density-compensated because NACW are saltier and warmer than SACW and results in a multitude of intrusions, filaments and lenses (Zenk et al., 1991; Pérez-Rodríguez et al., 2001; Pastor et al., 2008; Martínez-Marrero et al., 2008). Additionally, for any given density level, the inorganic nutrients in the SACW are substantially larger than in the NACW.

3.2.5. INTERMEDIATE WATERS

The intermediate layer in the CCLME area, approximately between 700 dbar and 1500 dbar and denser than 27.3 kg m^{-3}, is occupied by the AAIW and the MW. The AAIW is formed in the Subantarctic Front and advected with the subtropical gyre of the South Atlantic towards the tropics (Suga and Talley, 1995). The AAIW is easily identified by low salinities, with a salinity minimum around 35.1 centered at about 800 dbar depth. Two pathways transport AAIW to the eastern North Atlantic, one is through the western boundary current system and the Azores Current (Kawase and Sarmiento, 1985; Tsuchiya et al., 1992). The second path is through the eastern margin along the African coastline (Machín and Pelegrí, 2009), with a maximum northward penetration during fall (Machín et al., 2010) flowing through the LP (Hernández-Guerra et al., 2003; Fraile-Nuez et al., 2010).

MW is a very salty (hence dense) water mass formed in the Mediterranean Sea, which enters the Atlantic Ocean through the bottom part of the Strait of Gibraltar. After intense initial mixing, it gets substantially diluted and spreads out at intermediate levels, approximately 1200 dbar. The MW follows north along the continental slope of the Iberian Peninsula, what has been named the Mediterranean Undercurrent (Bower et al., 2002), and also spreads west and south as a result of turbulent diffusion, influencing the whole North Atlantic Ocean (Worthington, 1976). Its characteristic high salinity and temperature signature is observed between 1000 dbar and 1500 dbar depth. During the cascading of the outflowing Mediterranean waters along the slope in the Gulf of Cadiz and the Strait of Gibraltar isolated lenses of salty Mediterranean Water, called Meddies (Mediterranean Eddies), are formed. The Meddies propagate into the central Atlantic and the northern part of the CCLME (Hernández-Guerra et al., 2005). The cores of the Meddies are isolated from the surrounding waters and therefore show higher salinity due to lower mixing, as observed in Figure 3.2.4.

Both intermediate waters meet at about 32°N, with AAIW occupying a depth range slightly shallower than MW. Source water properties of intermediate waters are modified by mixing with water above and below, and their TS properties in the study region appear as extreme TS values that tend towards the values found in their formation region (Figures 3.2.2 and 3.2.4).

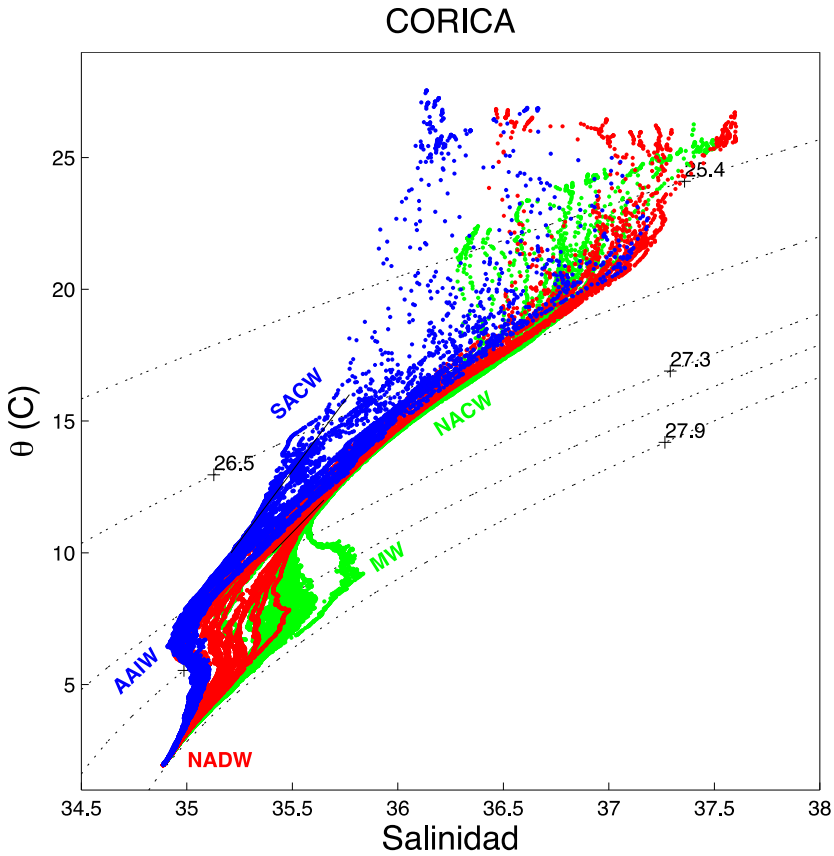

Figure 3.2.4. Potential temperature-salinity diagram with data from the CORICA cruise. Blue, red and green dots correspond to stations in the southern, western and northern transect, respectively.

3.2.6. DEEP WATERS

North Atlantic Deep Water (NADW) is found below the intermediate layer, from about 1500 dbar to the bottom of the ocean and denser than 27.7 kg m^{-3}. The NADW that reaches the eastern North Atlantic has been mainly formed as a mixture between the Iceland Scotland Overflow Water, and the Labrador Sea Water and Lower Deep Water (McCartney, 1992; van Aken, 2000). There are three subclasses of NADW: Upper North Atlantic Deep Water (UNADW), Middle North Atlantic Deep Water (MNADW) and Lower North Atlantic Deep Water (LNADW), differentiated on the basis of their salinity and oxygen distributions. The shallowest deep water is the UNADW, identified by its high salinity values due to mixing with MW. Below the UNADW, a nearly uniform value of oxygen (230-240 µmol kg^{-1}) describes the MNADW. Finally, LNADW is found further deep, characterized by higher oxygen concentrations (>240 µmol kg^{-1}). Figure 3.2.5 shows the vertical section of dissolved oxygen from the CORICA project, from which the spatial distributions of MNADW and LNADW can be discerned.

Acknowledgments

This study has been performed as part of the Instituto Español de Oceanografía RAPROCAN project, the Spanish Ministry of Science through CORICA (REN2001-2649) and Sevacan (CTM2013-48695) projects. The authors would like to thank the comments and suggestions of José Luis Pelegrí.

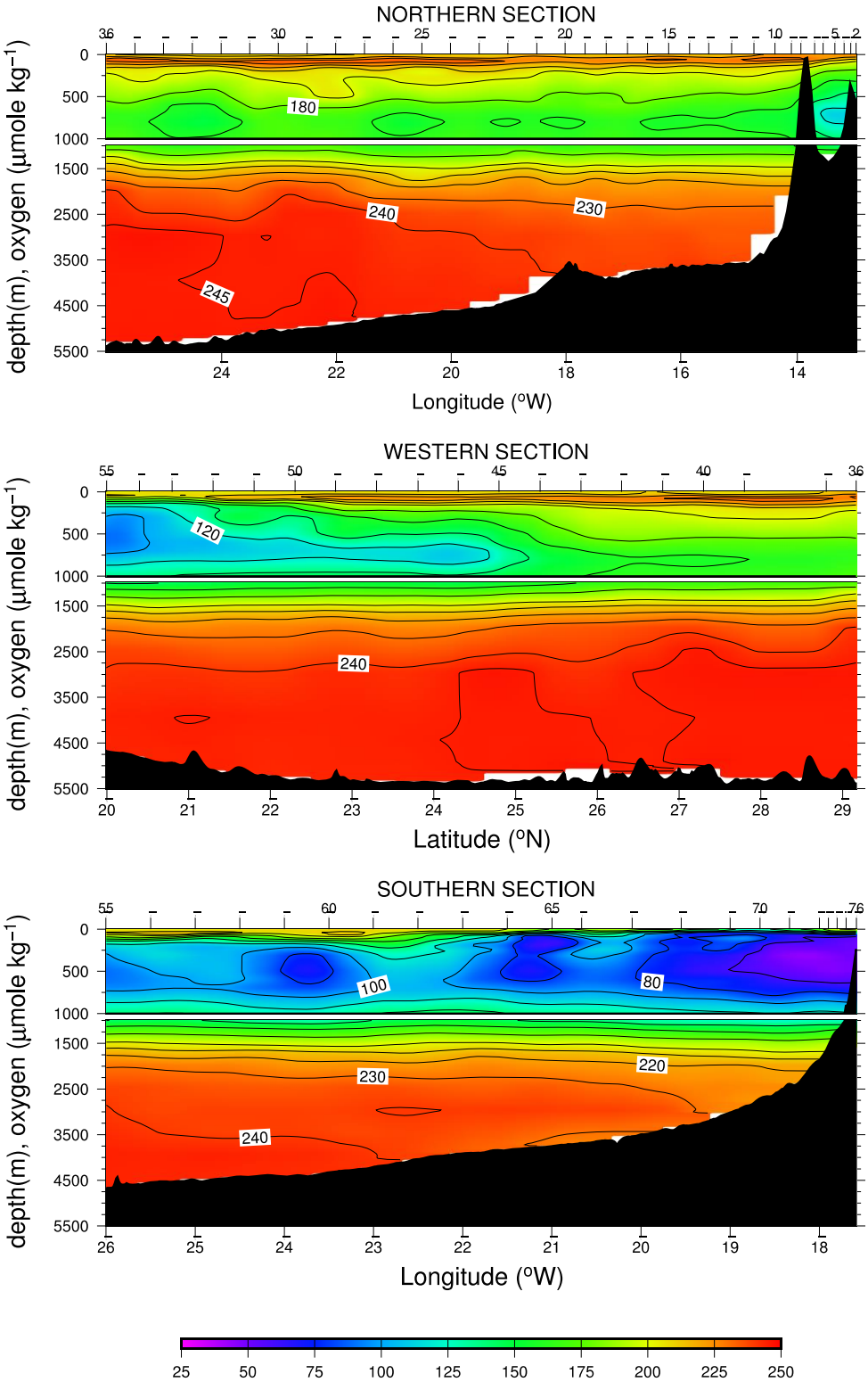

Figure 3.2.5. Dissolved oxygen (µmol kg $^{-1}$) for the (a) north (western end is on the left), (b) west (northern end is on the left), and (c) south (western end is on the left) sections for the CORICA cruise. Note that the vertical scale changes at 1000 dbar depth. The CTD station numbering is indicated in the top axis.

3.3. EASTERN BOUNDARY CURRENTS OFF NORTH-WEST AFRICA

Josep L. PELEGRÍ and Jesús PEÑA-IZQUIERDO

Institut de Ciències del Mar, CSIC. Spain

3.3.1. INTRODUCTION

From an oceanographic perspective, the Canary Current Large Marine Ecosystem (CCLME) may be divided in two major domains: the south-eastern boundary of the North Atlantic subtropical gyre (NASG) and the north-eastern North Atlantic tropical gyre (NATG) (Fig. 3.3.1). These two gyres are formed by surface and upper-thermocline waters – subducted from the sea surface at higher latitudes of both Atlantic hemispheres. The eastern margins of both gyres constitute the boundary current system off North-west Africa (NWA).

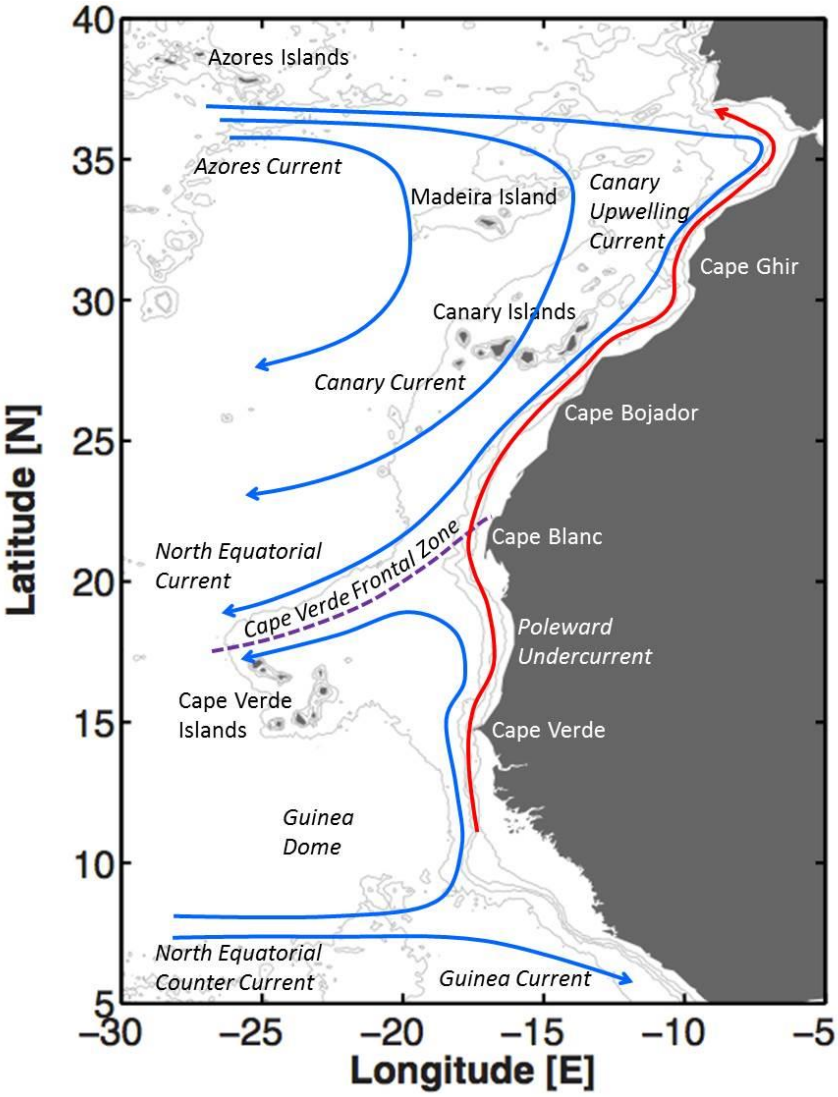

Figure 3.3.1. Scheme illustrating the main geographic features and mean oceanographic currents (italics) in the permanent thermocline of the CCLME; the red line shows the track of the Poleward Undercurrent.

The NASG waters come from the central North Atlantic (North Atlantic Central Waters, NACW) and enter the CCLME region following a relatively direct south-eastward path. The NATG waters, on the other hand, have their origin in the central South Atlantic (South Atlantic Central Waters, SACW) and take a much more intricate route to reach the CCLME: they cross the equatorial region mostly in the western Atlantic, off South America, and arrive to the eastern NATG through a system of zonal jets and recirculations north of the Equator (Rosell-Fieschi et al., 2015; Peña-Izquierdo et al., 2015). The two gyres, and associated water masses, are separated by the Cape Verde Front (CVF), a wide (4-6° of latitude) thermohaline front stretching roughly between Cape Blanc and the northernmost Cape Verde Islands (Fig. 3.3.1) (Zenk et al., 1991; Pérez-Rodríguez et al., 2001). Another frontal system, much shallower (at most 250 m) and narrower (1° of longitude), is found off the African continental slope, extending from the Gulf of Cadiz until Cape Blanc (Cape Vert) in boreal summer (winter) - this is the coastal upwelling front (CUF), separating stratified interior-gyre from more homogeneous slope waters.

In this article we examine the predominant geostrophic currents (annual and seasonal means) of these three upper-thermocline dynamic domains in the CCLME: the south-eastern NASG, the north-eastern NATG, and the upwelling region. We focus on the two main gyres and their seasonal variability, and also look at their connection with the upwelling system (further examined in Pelegrí and Benazzouz, 3.4 this book); other related circulation phenomena are addressed elsewhere in this volume: spatial distribution of water masses (Pastor et al., 3.2 this book) and mesoscale processes (Sangrà, 3.5 this book). For our analysis, we will use the 9-km resolution sea-surface-temperature (SST) and color Moderate Resolution Imaging Spectroradiometer (MODIS) data (2002-2014) from the National Aeronautics and Space Administration (NOAA, 2014) and the Etopo2v2 bathymetry (2' resolution) (NGDC-NOAA, 2006). The wind data (2007-2014) is from the advanced scatterometer (ASCAT) on board the meteorological operational platforms of the Centre de Recherche et d'Exploitation Satellitaire (CERSAT, 2014). The velocity data (1992-2011) comes from the ECCO2 project (Estimating the Circulation and Climate of the Ocean, phase II), a general circulation model (Marshall et al., 1997) with 0.25° horizontal resolution and 50 vertical levels that uses realistic atmospheric forcing and assimilates satellite and in situ data (JPL-NASA, 2014).

3.3.2. ANNUAL-MEAN CURRENTS

3.3.2.1. The subtropical gyre

The NASG is a wind-induced anticyclone, formed by upper-thermocline North Atlantic waters with temperatures down to about 10°C (potential density anomalies about 27.3 kg m^{-3}), reaching some 700-800 m in the eastern boundary and 1000-1100 m in the western boundary (Kawase and Sarmiento, 1985; Machín et al., 2006a). The southeastern margin of the NASG comprises the eastward Azores Current (AC), the southward Canary Current (CC) and Canary Upwelling Current (CUC), and the westward North Equatorial Current (NEC) (Stramma, 1984) (Figs. 3.3.1 and 3.3.2). The NASG experiences wind-induced surface convergence and water subduction, i.e. waters originate near the sea surface and recirculate at depth following an anticyclonic path in near-geostrophic balance (Stommel, 1979; Luyten et al., 1983), so the vertical hydrographic structure reflects the latitudinal changes in the surface formation regions.

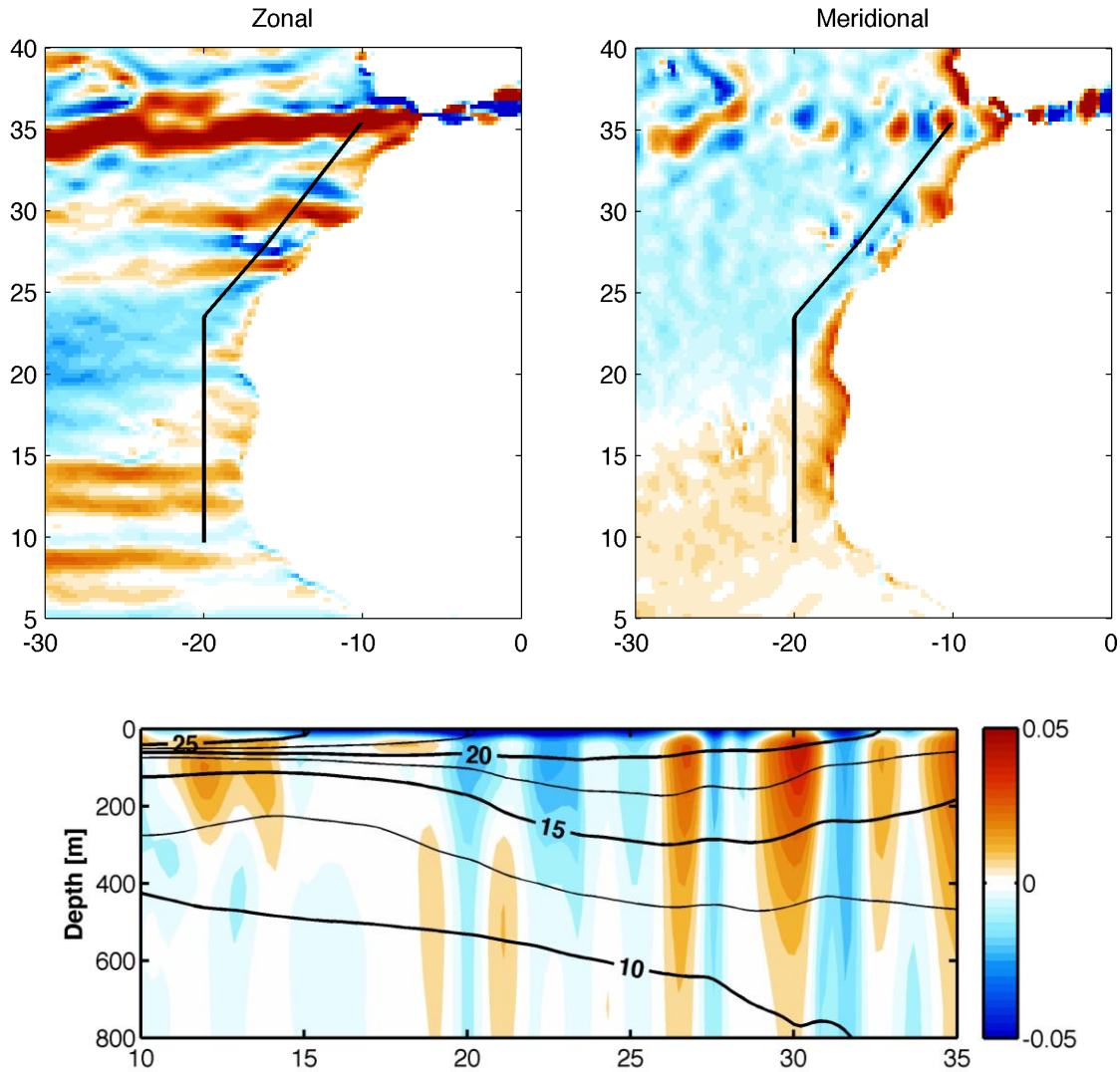

Figure 3.3.2. Mean annual velocities from the ECCO2 model (color-coded, positive values for eastward and northward components; m s^{-1}). Top panel: Zonal and meridional components at 200 m. Bottom panel: component normal to the section in the top panels; temperature (°C) is plotted as solid contours.

Most of the AC flows south as part of the NASG recirculation although about 1 Sv follows into the Mediterranean Sea (Candela, 2001) and another fraction, the Iberian Current, continues north during boreal winter (Haynes et al., 1993). Beyond the Azores Islands, the AC recirculates south as the interior CC (a mean transport of 1 Sv) and the coastal CUC (a mean transport of 1.5 Sv) (Laiz et al., 2012). The gentle eastward rise of the upper-thermocline leads to the southward flowing CC, with mean surface values less than 0.05 m s^{-1}. Closer to the African slope, typically within 2-5°, the upper portion of the water column (about 200 m) rises sharply as a result of wind-induced coastal upwelling, with the appearance of a relatively narrow (100-200 km) and intense (locally in excess of 0.25 m s^{-1}) coastal upwelling jet, the CUC or easternmost branch of the CC (Pelegrí et al., 2005a, 2006). The CUC begins in the Gulf of Cadiz, feeding directly from the AC, and is enhanced through water inflow from the ocean interior, in what is the classical upwelling vertical cell (Pelegrí and Benazzouz, 3.4 this book).

The Canary Islands are a major obstacle to the southward flow (Fig. 3.3.2). The CC follows the deep channels between the main islands, except for an offshore diversion in late boreal fall (Navarro-Pérez and

Barton, 2001; Pelegrí et al., 2005a), and the CUC streams between the eastern islands and the African coast (Hernández-Guerra et al., 2001, 2002). The CC and CUC extend south until near Cape Blanc, where they are fully diverted following the CVF. Between the slope and the CUC, we find the Poleward Undercurrent (PUC), an intense subsurface northward flow which is usually centred at 200-300 m but may occasionally extend from as deep as 800 m to the sea surface (Barton, 1989).

3.3.2.2. The tropical gyre

The NATG covers the zonal band south of the NASG, between the Equator and about 10°N, reaching Cape Blanc (21°N) along the eastern edge. It is a cyclonic region crossed by several seasonally changing zonal jets (Stramma and Schott, 1999; Rosell-Fieschi et al., 2015) (Fig. 3.3.2) – its cyclonic character, with the isothermals rising towards the Equator, is due to the wind-induced equatorial divergence and tropical-subtropical convergence (Castellanos et al., 2015). The eastern NATG extends down some 500 m, reaching down to about 10°C or potential densities of 27.15 kg m^{-3} (less dense than in the subtropical gyre because of its lower salinity), encircled by the westward NEC, the eastward North Equatorial Countercurrent (NECC) and Cape Verde Current (CVC), and the northward Mauritanian Current (MC) and PUC.

The eastward NECC ventilates the southern CCLME between May and December, with maximum zonal speeds of 0.5 m s^{-1} reaching beyond 10°N in August (Rosell-Fieschi et al., 2015). The CVC also flows east between 12°N and 17°N, down to about 300 m, before turning west south of the CVF (Peña-Izquierdo et al., 2015). Along the African slope, the MC is an extension of the NECC and, possibly, the north Equatorial Undercurrent. The PUC has also been found along the continental slope of the NATG during late boreal fall (Peña-Izquierdo et al., 2012), as a continuation of the Guinea Undercurrent (Mittelstaedt, 1976) and possibly the NECC (Rosell-Fieschi et al., 2015; Peña-Izquierdo et al., 2015).

The eastern NATG is classically associated to the south-eastern shadow zone of the NASG, a region which cannot be directly reached by the relatively young waters of the NASG (Luyten et al., 1983). As a result, the NATG thermocline waters are much older; their origin goes back to the subduction regions of the central South Atlantic Ocean and the intermediate waters that upwell near the Equator, reaching the NATG after an intricate path principally along the western Atlantic margin. The interior of the NATG, centred at about (10°N, 20°W) is occupied by the Guinea Dome (GD) (Siedler et al., 1992); the GD intensifies in summer as a result of the northward penetration of the Inter-Tropical Convergence Zone (ITCZ) and the South Atlantic High, bringing westward winds, surface water divergence and upwelling.

3.3.3. THE FRONTAL SYSTEMS

3.3.3.1. The Cape Verde frontal system

The eastern margins of the subtropical and tropical gyres are separated by the CVF, a wide (4-6° of latitude) frontal system with substantial gradients in temperature-salinity and even larger gradients in inorganic nutrients and dissolved oxygen (Pelegrí and Peña-Izquierdo, 4.1 this book), mirroring the remarkable differences between those regions where NACW and SACW are formed. However, the temperature and salinity fields are density-compensating – below the surface mixed layer, along any given density or depth level, the NACW is warmer and saltier than the SACW (Pastor et al., 3.2 this book) – so the cross-frontal density gradients are feeble. This leads to the NEC, a relatively weak along-front geostrophic current

(annual-mean speeds less than 0.05 m s^{-1}), which stretches over several degrees of latitude in the top 300-400 m of the water column.

The confluence of southward (CC and, particularly, the CUC) and northward (PUC and MC) currents along the CVF is the locus of substantial along-shore convergence. This convergence drives chlorophyll- and inorganic-nutrient-rich waters, coming from the tropical gyre and the coastal upwelling region, into the south-eastern edge of the subtropical gyre. The load of inorganic nutrients helps maintain high primary production far from the coast, leading to a giant filament, which appears as a quite remarkable feature in colour satellite images (Fig. 3.3.3) (Gabric et al., 1993; Pastor et al., 2013). The CVF is an effective barrier between the NASG and the NATG but it also acts as a source of lateral mixing. The thermohaline horizontal gradients produce lateral subsurface intrusions (Zenk et al., 1991; Pérez-Rodríguez et al., 2001; Pastor et al., 2008) and the dynamic character of the front generates mesoscale features, in some instances detaching from the adjacent coastal upwelling front (Pastor et al., 2008).

3.3.3.2. The coastal upwelling front

The north-easterly winds along the African coastline cause offshore surface transport and cross-shore water divergence. The result is the CUF, a shallow (typically 200 m) but relatively intense frontal system, found permanently between the Gulf of Cadiz and Cape Blanc, and reaching Cape Vert between late fall and early spring (boreal seasons). The upwelling-frontal region contains the same offshore water masses (NACW/SACW in the subtropical/tropical gyres) yet it truly constitutes a distinct dynamic domain in the CCLME – the coastal transition zone (CTZ) (Barton et al., 1998). The frontal system is usually found offshore from the continental slope, giving rise to the coastal upwelling jet (speeds often in excess of 0.1 m s^{-1}); because of its upstream connection to the Azores Current, this jet constitutes the CUC. Between the CUC and the continental slope we find the relatively homogeneous upwelled waters, typically on top of the subsurface northward PUC.

The CUC and PUC constitute the true skeleton of the CCLME, connecting different latitudes along the CTZ by respectively conveying waters of northern and southern origin. The CUF is also a source of mesoscalar variability, both as eddies (Benítez-Barrios et al., 2011; Ruiz et al., 2014) and filaments (Hagen et al., 1996; Pelegrí et al., 2005b). The size of these eddies is typically the same as the width of the CUF but, west of Cape Bojador, they may be much larger – this happens in late fall as a result of an offshore recirculation which leads to a CUC local reversal (Pelegrí et al., 2005a; Laiz et al., 2012). These coastal eddies, together with those generated downstream of the Canary Islands, propagate westwards as Rossby waves (Sangrà et al., 2009; Mason et al., 2011). Additionally, part of the CUC deviates offshore as surface filaments, mainly at Cape Ghir and, to a lesser degree, off Cape Jubi and Cape Bojador (Hagen et al., 1996; Pelegrí et al., 2005b). For a detailed discussion on the dynamics and characteristics of the CTZ and the associated mesoscalar features, the reader is referred to Pelegrí and Benazzouz, 3.4 this book, and Sangrà, 3.5 this book.

3.3.4. SEASONAL VARIABILITY

The patterns of circulation in the NASG and, very particularly, the NATG display substantial seasonal variability. This is because of the latitudinal motion of the ITCZ and the accompanying high pressure centres (Azores High in the northern hemisphere and South Atlantic High in the southern hemisphere) – along 20°W, the ITCZ moves from 2°N to 14°N between February and August (Hastenrath and Lamb, 1977). In terms of wind forcing, the CTZ may be separated in three domains (all seasons are boreal): between Cape

Vert and Cape Blanc, with north-easterly winds during winter and doldrums and even westerlies during summer; between Cape Blanc and the Canary Islands, with permanent intense north-easterlies; and from the Canary Islands to the Gulf of Cadiz, where the north-easterlies are present all year long but intensify during summer (Fig. 3.3.3).

The changes in wind forcing have several major effects on (a) the intensity and extension of the CUC, (b) the connection between the AC and the CUC, (c) the intensity and extension of the PUC, (d) the recirculation patterns in the NATG, and (d) the flow convergence and offshore export along the CVF. To illustrate these changes we use the seasonal-mean outputs from the ECCO2 model (JPL-NASA, 2014), with the seasons defined as winter (December-February), spring (March-May), summer (June-August), and fall (September-November) (Figs. 3.3.4-3.3.6). In Figure 3.3.4 we present the cross-shore velocities along the same latitudinal section depicted in Fig. 3.3.2; in Figures 3.3.5 and 3.3.6 we show the meridional velocities across four longitudinal sections (30°N, 24°N, 18°N and 12°N), selected to illustrate the seasonal changes north of the Canary Islands, between Cape Blanc and the Canary Islands, and south of Cape Blanc.

3.3.4.1. Coastal upwelling

The remarkable latitudinal extent of the upwelling region shows up clearly in the SST maps (Benazzouz et al., 2014b) (Fig. 3.3.3). During summer and fall, a narrow band of cold upwelled waters extends from the Gulf of Cadiz to Cape Blanc; between Cape Blanc and the Canary Islands, where the winds are most intense, the influence of upwelling reaches far offshore, visible as a second band of surface waters with intermediate SSTs. During winter and spring upwelling reaches Cape Vert, but the band of upwelled waters is much narrower south of Cape Blanc; north of the Canary Islands upwelling still exists but this is hardly visible in the SST images, particularly in winter, because of the relatively low offshore SSTs.

The seasonal variation in the vertical structure of the CUF and the associated CUC may be appreciated from the vertical zonal sections in Figures 3.3.5 and 3.3.6. The CUF is present all year long north of Cape Blanc, 2-4° away from the coast between Cape Blanc and the Canary Islands; during fall, at 30°N and off the slope, the near-surface meridional currents are particularly intense, reflecting a local recirculation south of Cape Ghir (see section 3.3.4.3 below). South of Cape Blanc the CUF is only visible in spring, at 18°N, suggesting that the SST fall and winter patterns (Fig. 3.3.3) correspond to very shallow structures.

3.3.4.2. The Azores Current and the Canary Upwelling Current

The Gulf of Cadiz halts the upstream CUC flow, so the supply necessarily has to come from the AC (Pelegrí et al., 1997, 2005a, 2006; Machín et al., 2006b; Laiz et al., 2012). North of the Canary Islands, the AC transport into the CTZ is larger during winter-spring (2.8 Sv) than during summer-fall (1.9 Sv) (Laiz et al., 2012), possibly because of substantial offshore recirculations (fall and winter panels, Fig. 3.3.4).

The southward transport between the eastern Canary Islands and the continental slope does not change much throughout the year: 1.5 Sv during winter-spring as compared with 1.6 Sv during summer-fall (Laiz et al., 2012). Nevertheless, as a result of local recirculations, the flow through this eastern passage turns north in October-December (Hernández-Guerra et al., 2001, 2002; Laiz et al., 2012).

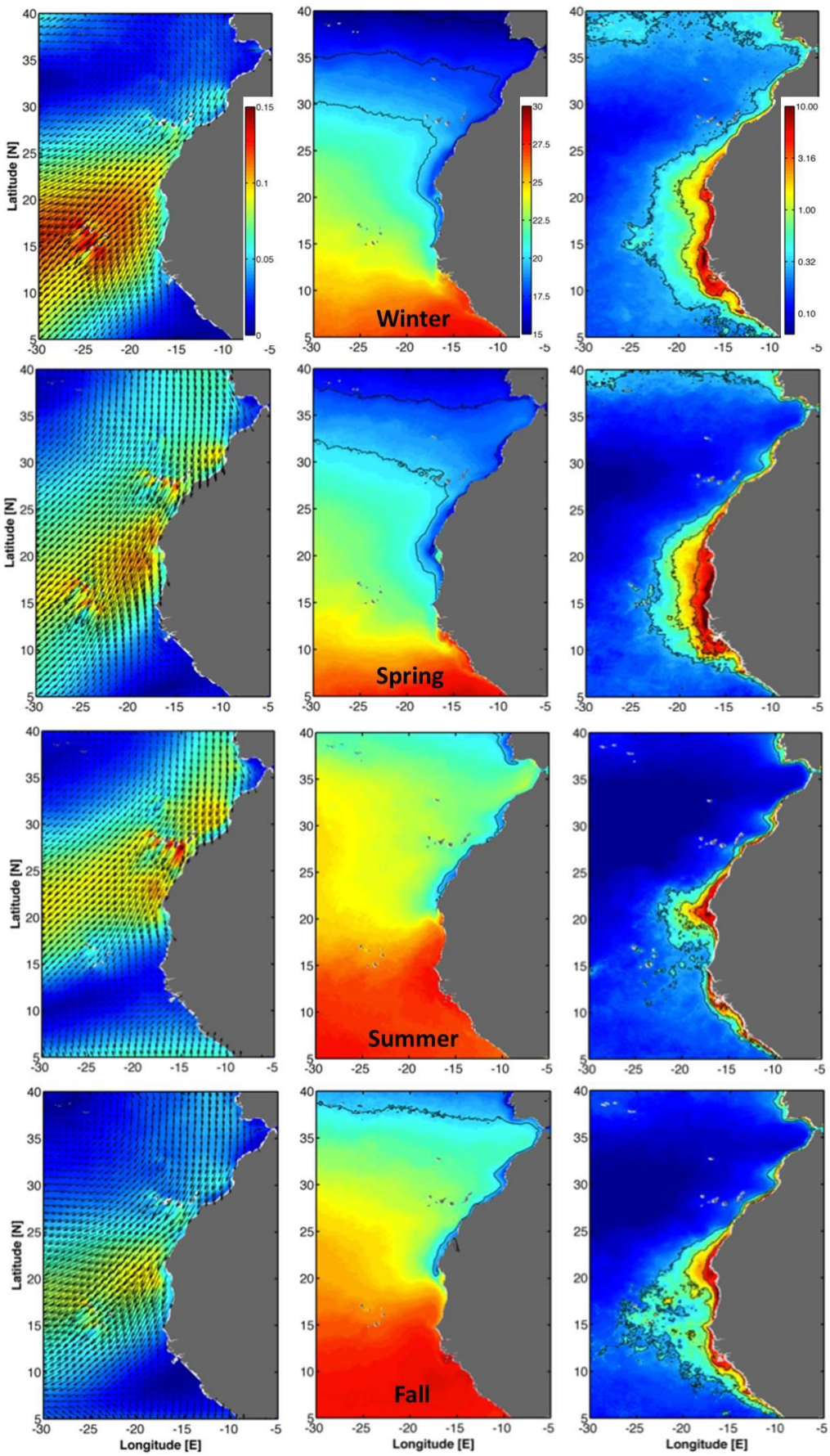

Figure 3.3.3. Boreal season distributions in the CCLME (winter, spring, summer and fall, from top to bottom) of (left) surface winds (m s^{-1}), (middle) SST (°C), and (right) near-surface chlorophyll-a (mg m^{-3}).

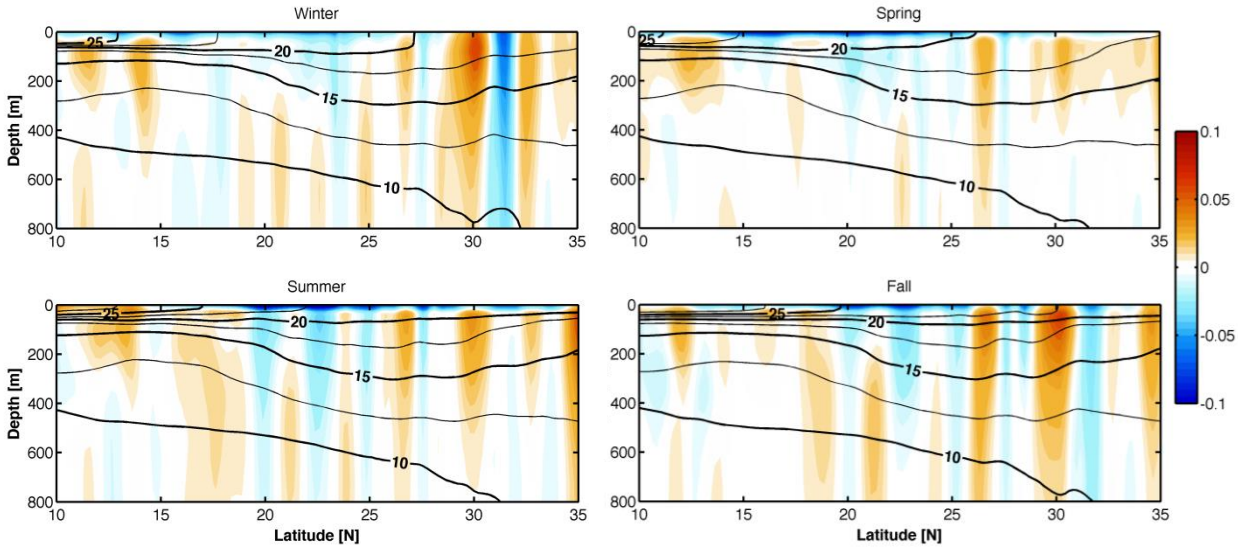

Figure 3.3.4. Mean seasonal distributions of the cross-slope velocity (normal to the meridional section in Figure 3.3.2) as deduced from the ECCO2 model (color-coded, with positive values for onshore velocities; m s^{-1}); temperature (°C) as solid contours.

3.3.4.3. The Poleward Undercurrent

The ubiquity and importance of the PUC is clear in the annual-mean meridional velocity maps (Fig. 3.3.2). The seasonal velocity fields across the four zonal sections confirm the latitudinal continuity of the PUC all along NWA – except south of Cape Blanc during boreal spring (Figs. 3.3.5 and 3.3.6). South of Cape Vert the PUC does not extend very deep, except possibly in boreal summer, and is located further offshore – this surface flow may actually be identified as the northward MC. North of Cape Blanc, the PUC intensifies through onshore intakes located north and south of the Canary Islands and near the CVF (Fig. 3.3.4). During boreal summer and fall, the PUC is particularly intense at 30°N because of a local cyclonic recirculation south of Cape Ghir (Fig. 3.3.6) – during these seasons the northward flow extends to 800 m, as a result of the propagation of intermediate waters (Machín and Pelegrí, 2009; Machín et al., 2010).

3.3.4.4. Circulation in the north-eastern tropical gyre

The results from the model suggest a boreal summer-fall intensification of the CVC (flowing east through 20°W, between 11°N-18°N; Fig. 3.3.4) and the NECC (north through 12°N, west of 20°W; Figs. 3.3.5 and 3.3.6); this coincides with the boreal late-summer and fall growth of the PUC and MC (Lazaro et al., 2005). In boreal winter and spring the GD weakens and the NATG currents decrease.

Because of the semi-enclosed character of the circulation and the weak currents, water parcels have long residence times within the basin, e.g. a parcel moving at 0.1 m s^{-1} would travel less than 800 km in three months, so that the renovation rate depends on the way the Lagrangian pathways are affected by the seasonally changing circulation (Peña-Izquierdo et al., 2015).

3.3.4.5. Flow convergence at the Cape Verde front

According to the model, the zonal band occupied by the CVF (18°N to 21°N) is characterized by year-long near-surface convergence and offshore export, with maximum values during summer and, particularly, fall (Fig. 3.3.4); this result is in agreement with Pastor et al. (2008), who found CVF-related convergence and export to increase from 0.6 Sv to 3.0 Sv between spring and fall. The summer-fall increase in along-slope convergence contrasts with the sea surface color images, where the high surface chlorophyll values occupy their maximum extension during winter and spring (Fig. 3.3.3), see also Pastor et al. (2013); this is likely caused by the seasonal increase in nutrient supply south of Cape Blanc, due to high coastal upwelling and river discharge, brought north by the surface MC.

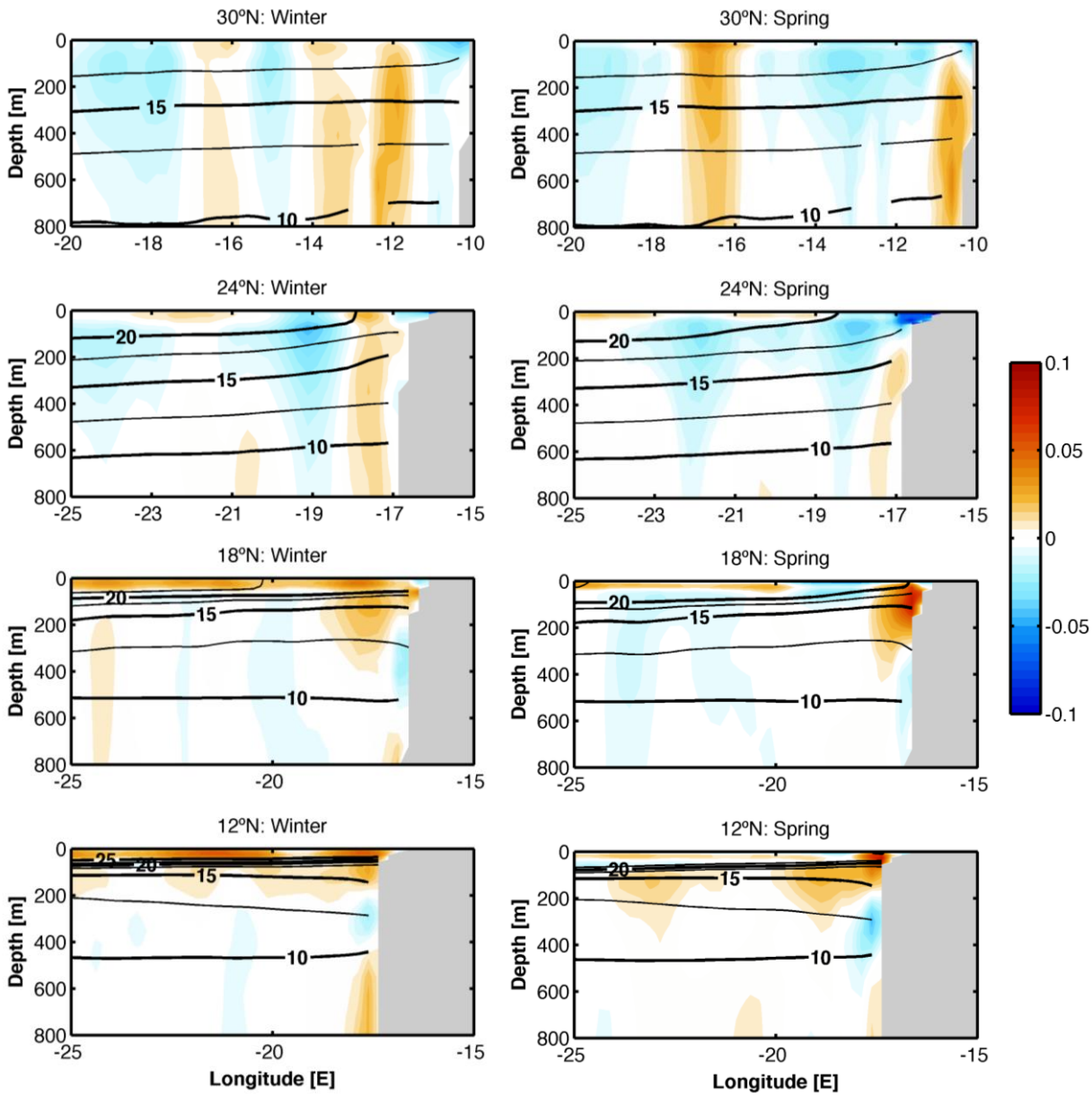

Figure 3.3.5. Mean boreal winter (left) and spring (right) distributions of the meridional velocity along zonal sections (30°N, 24°N, 18°N and 12°N; from top to bottom) as deduced from the ECCO2 model (color-coded, with positive values for onshore velocities; m s^{-1}); temperature (°C) as solid contours.

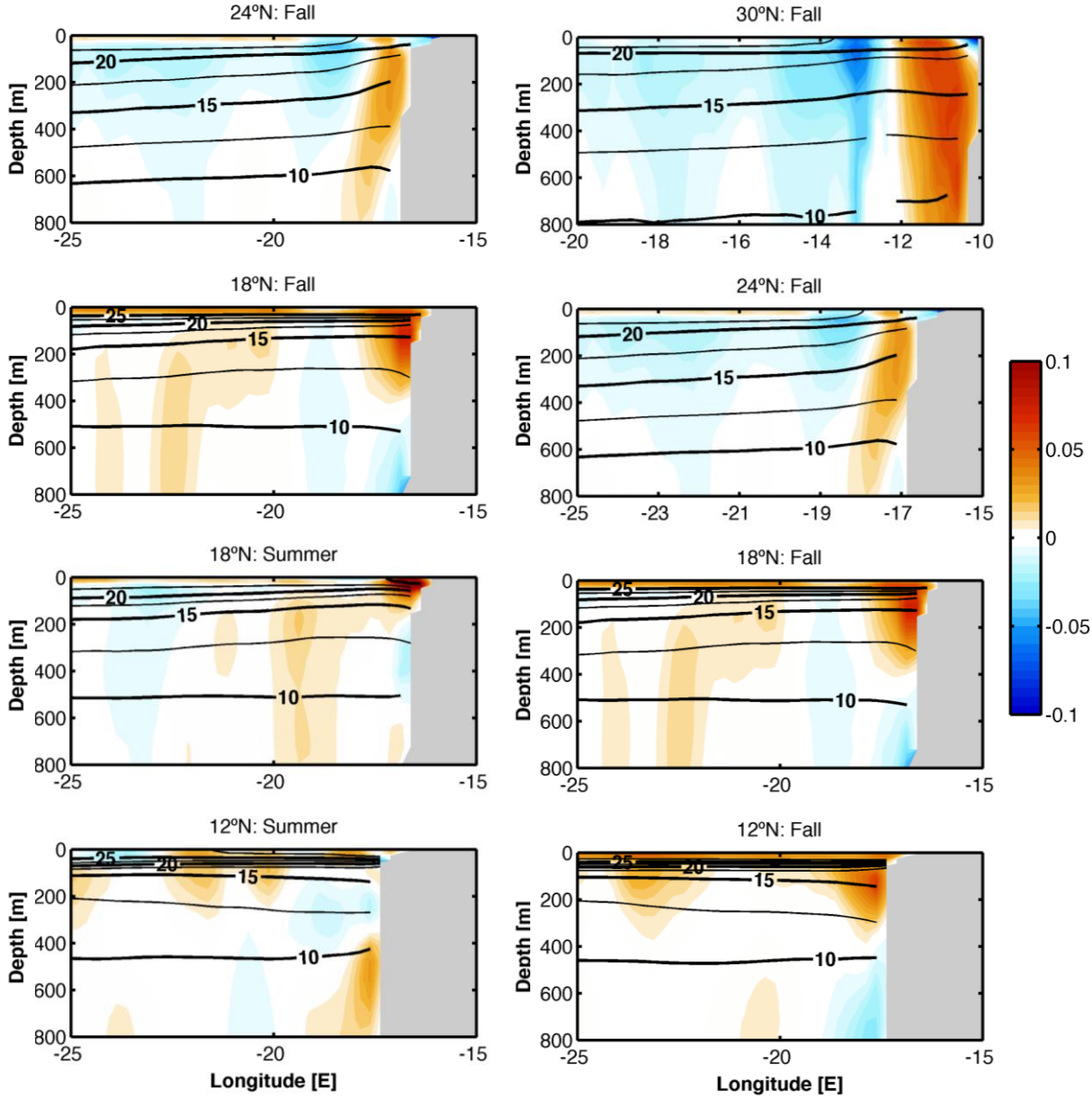

Figure 3.3.6. Mean boreal summer (left) and fall (right) distributions of the meridional velocity along zonal sections (30°N, 24°N, 18°N and 12°N; from top to bottom) as deduced from the ECCO2 model (color-coded, with positive values for onshore velocities; m s^{-1}); temperature (°C) as solid contours.

3.3.5. CONCLUSIONS

The characteristics of the CCLME are controlled by the encountering of the eastern limb of two major ocean gyres: the NASG and the NATG (Fig. 3.3.7). Both these gyres bring water from the interior ocean to the CTZ, where it recirculates meridionally thanks to a system of along-slope currents, predominantly southward in the NASG and northward in the NATG – the two gyres converge into the CVF, where water is expulsed back to the interior ocean. Therefore, despite the presence of offshore meridional currents – the CC in the northern gyre and the cyclonic motions around the GD in the southern gyre – the eastern boundary structure that connects both gyres is the latitudinal current system along the CTZ.

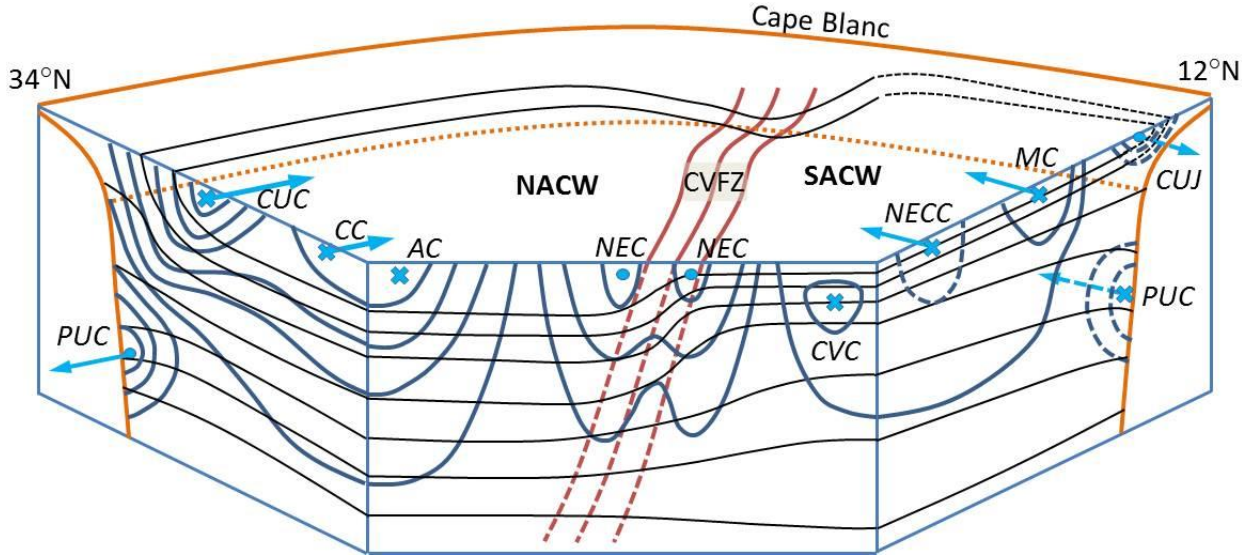

Figure 3.3.7. Cartoon for the principal geostrophic currents in the CCLME, with isopycnals (black lines) and isotachs (blue lines; dashed lines denote seasonal flows); the arrows mark the locus of the peak currents.

The system of along-slope currents is composed by the CUC, flowing south between the Gulf of Cadiz and Cape Blanc, and the PUC, streaming north as a near-surface current until Cape Vert and as a subsurface current till the Gulf of Cadiz and beyond. The way these two currents interact between themselves and with the interior flow is what sets the system of eastern boundary currents (Pelegrí et al., 2005a). Such interaction occurs through both upstream input – the AC for the CUC and the MC for the OUC – and along-track exchange – the vertical upwelling cell for the CUC (Pelegrí and Benazzouz, 3.4 this book) and the interaction between the GD and the CTZ for the PUC.

Our understanding of these boundary systems has greatly increased through the availability of field and satellite observations, as well as thanks to high-resolution numerical circulation models. It could be argued that we now understand the predominant large-scale patterns and their seasonality (Fig. 3.3.8) and are left to learn the inter-annual and longer time-scale variability (Pastor et al., 2013; Benazzouz et al., 2014a, b; Peña-Izquierdo et al., 2015). However, many questions on the annual- and seasonal-mean transports remain open, particularly those related to the exchange of properties across the frontal systems, the way the frontal systems interact among each other, and the spatial and temporal variability of the PUC.

What sets the cross-slope location of both CUC and PUC? What are the principal mechanisms for cross-frontal exchange? What happens with the CUC and MC-PUC in the intersection between the CVF and the CUF? What drives the spatial and temporal variability of the PUC? How the offshore and coastal upwelling systems shape the mean currents in the NATG? What drives localized flow reversals, such as the fall reversal east of the Canary Islands? How are the mean transports affected by the generation of vortices at the frontal systems and their posterior westward propagation? All these questions remain a challenge for the present and future generations of oceanographers.

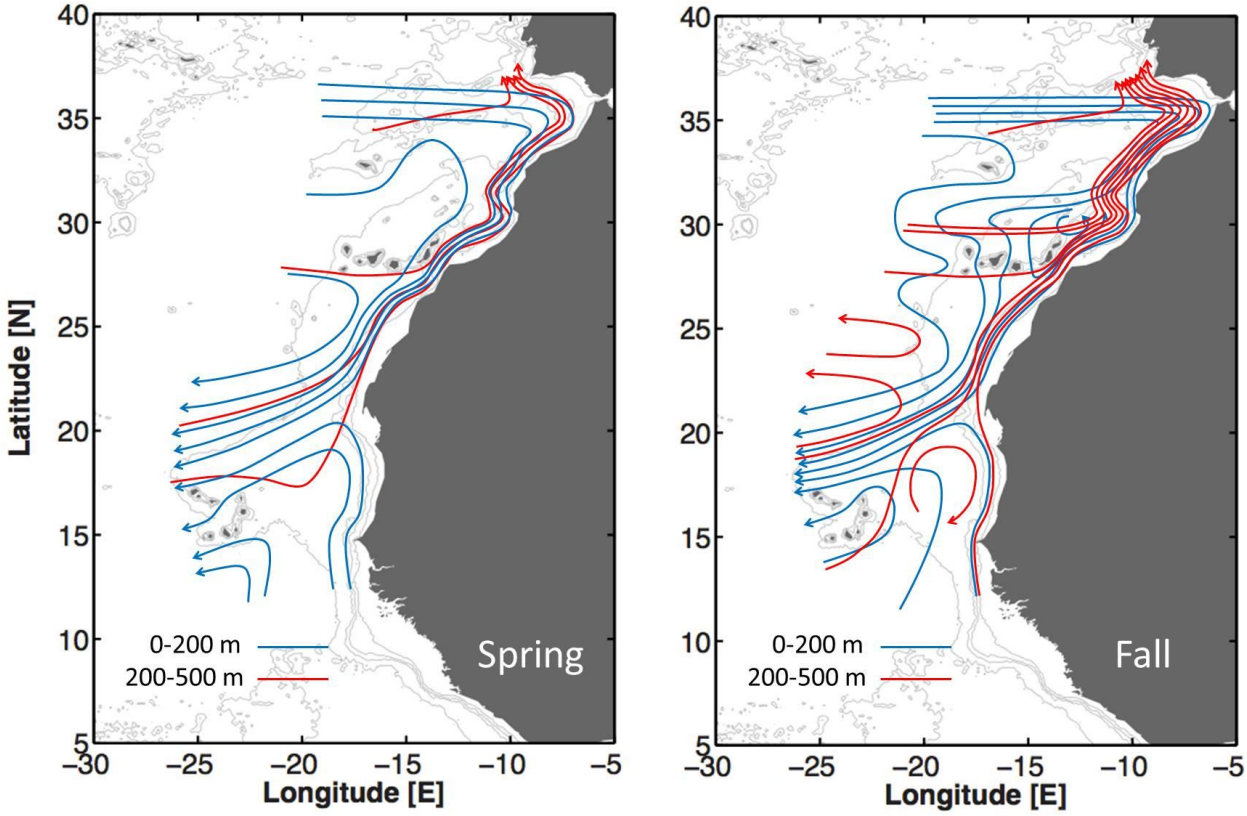

Figure 3.3 8. Scheme with the principal near-surface (50-200 m, in blue) and subsurface (200-500 m, in red) geostrophic currents in the CCLME, as deduced from the ECCO2 model: boreal spring (left) and fall (right).

Acknowledgements

This review synthesizes work on the system of eastern boundary currents in the CCLME linked to several projects carried out during the last two decades, particularly projects CANOA (CTM2005-00444/MAR), MOC2 (CTM2008-06438-C02-01) and TIC-MOC (CTM2011–28867), funded by the Spanish government. Jesús Peña-Izquierdo was funded through a FPI doctoral grant linked to project MOC2. We also wish to thank the NODC and Argo Program for making hydrographic data freely available, and the ECCO2/NASA program for providing the numerical assimilative simulations. Finally, we sincerely thank the many colleagues that have participated with us in these projects, for the hard work carried out together and the many enlightening and joyful conversations, particularly Mikhail Emelianov, Alonso Hernández-Guerra, Irene Laiz, Francisco Machín, Ángeles Marrero-Díaz, Evan Mason, María Pastor, Andry Ratsimandresy, Ángel Rodríguez-Santana, Joaquín Salvador and Pablo Sangrà.

3.4. COASTAL UPWELLING OFF NORTH-WEST AFRICA

Josep L. PELEGRÍ[1] and Aïssa BENAZZOUZ[2]

[1] Institut de Ciències del Mar, CSIC. Spain

[2] Institut National de Recherche Halieutique. Morocco

3.4.1. INTRODUCTION

The north-easterly winds in the Canary Current Large Marine Ecosystem (CCLME) lead to ubiquitous coastal upwelling off North-west Africa (NWA) – a relatively shallow frontal system, typically located within a few degrees from the shelf break and reaching no more than 250 m, with cold upwelled waters on the seashore side and offshore stratified waters (Fig. 3.4.1). This frontal system is also the site of a southward upwelling jet, extending from the Gulf of Cadiz to Cape Blanc in boreal summer and Cape Vert in boreal winter, and a northward undercurrent along the continental slope, which truly are the major meridional conveyors in the CCLME. The transition from the upwelled to the interior waters is characterized by intense mesoscale activity (Barton et al., 1998).

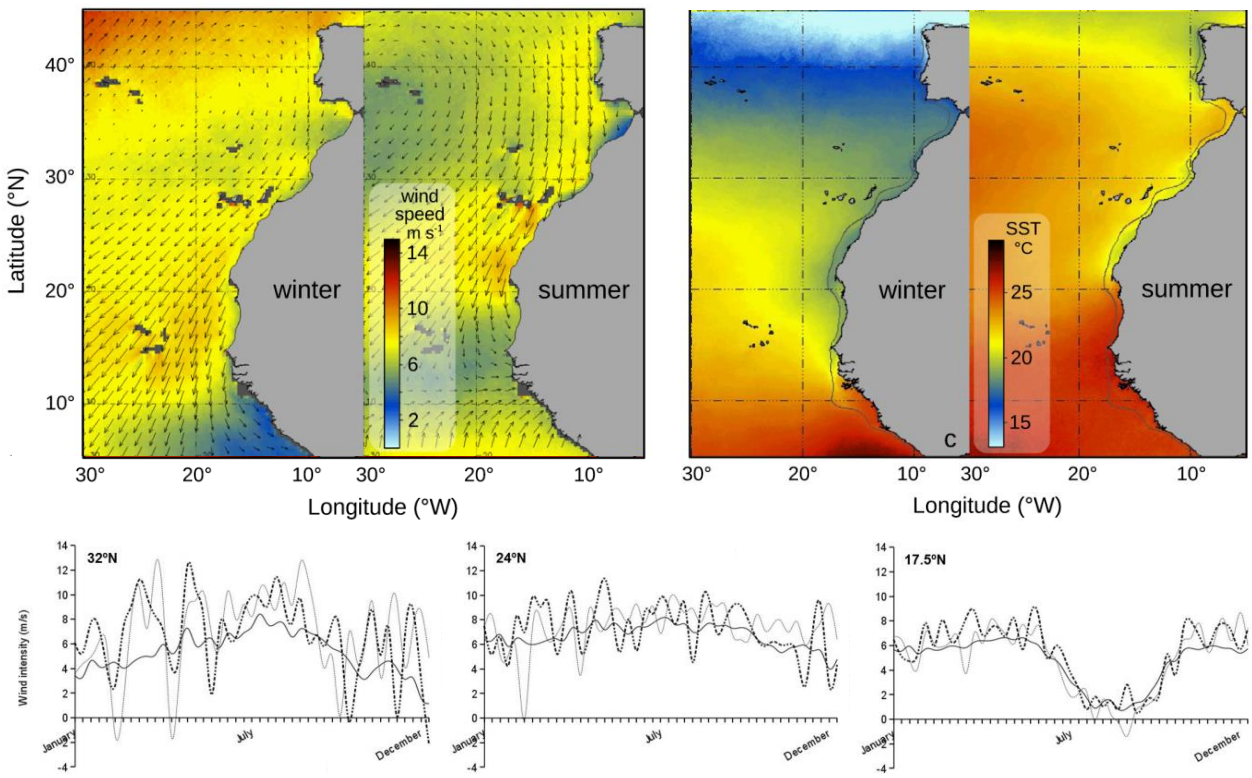

Figure 3.4.1. Mean boreal winter and summer (top-left) surface winds for the 1999-2009 period and (top right) sea surface temperature (SST) for the 1982-2011 period; adapted from Benazzouz et al. (2014a). Bottom: alongshore climatological winds for the 1987-2011 period (solid line), together with the 2007 (dashed line) and 2008 (dotted line) values at 32°N, 24°N and 17.5°N; adapted from Benazzouz et al. (2014b).

The alongshore winds drive a downwind coastal jet, and the Coriolis force associated to this jet induces surface offshore motion. Because of the coastal constraint, this transport raises the subsurface waters and drives an opposing cross-shore pressure gradient that balances the Coriolis force. Remarkably, it is the coastal jet, driven by the winds, which causes offshore transport, and it is this transport that sustains the structure of the frontal system and the jet itself. The frictional forces initiate the jet (surface wind stress), lead to a near-steady state (balance between wind stress and internal friction) and may eventually turn it off (internal friction). These processes are responsible for the classical cross-shore two-dimensional vertical cell, with subsurface onshore flow compensating for the offshore surface transport. Further, they induce a second recirculation: the latitudinal or meridional cell – because of the limited meridional extension of upwelling, the jet feeds upstream from the interior ocean and eventually goes back to it (Fig. 3.4.2).

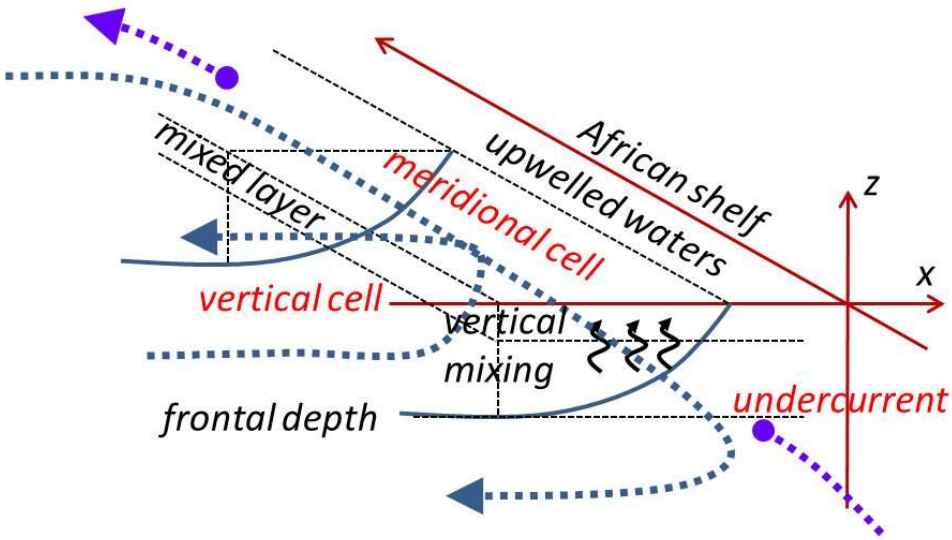

Figure 3.4.2. Schematic diagram illustrating the principal components of the coastal upwelling system.

3.4.2. SEASONAL VARIABILITY

The north-easterly (or trade) winds are associated to the Azores High, the high-pressure atmospheric centre in the North Atlantic Ocean, which moves south-north between the boreal winter and summer (hereinafter, in this article we always refer to boreal seasons). This causes the trade winds to be intense all year long between Cape Blanc and the Canary Islands, reaching Cape Vert during winter and getting intensified north of the Canary Islands during summer (Fig. 3.4.1). As a result, we may talk about three regions with well-differentiated seasonality in upwelling (vertical cell): permanent and intense in a central region, between Cape Blanc and the Canary Islands; weak during winter-spring and intense in summer-fall in the northern area, between the Canary Islands and the Gulf of Cadiz; and present only during winter-spring in the southern domain, between Cape Vert and Cape Blanc (Figs. 3.4.3 and 3.4.4).

Benazzouz et al. (2014a, b) have used satellite, field, climatological (Troupin et al., 2010) and numerical (Mason et al., 2011) data, to analyse the seasonality of coastal upwelling. In the northern and, particularly, central regions the frontal upwelling system is often located several degrees offshore and reaches down to about 200-250 m, with an intense coastal jet, while in the southern domain winter upwelling does not extend below some 100 m and a weak coastal jet is found close to the shelf (Figs. 3.4.3 to 3.4.5). Since the

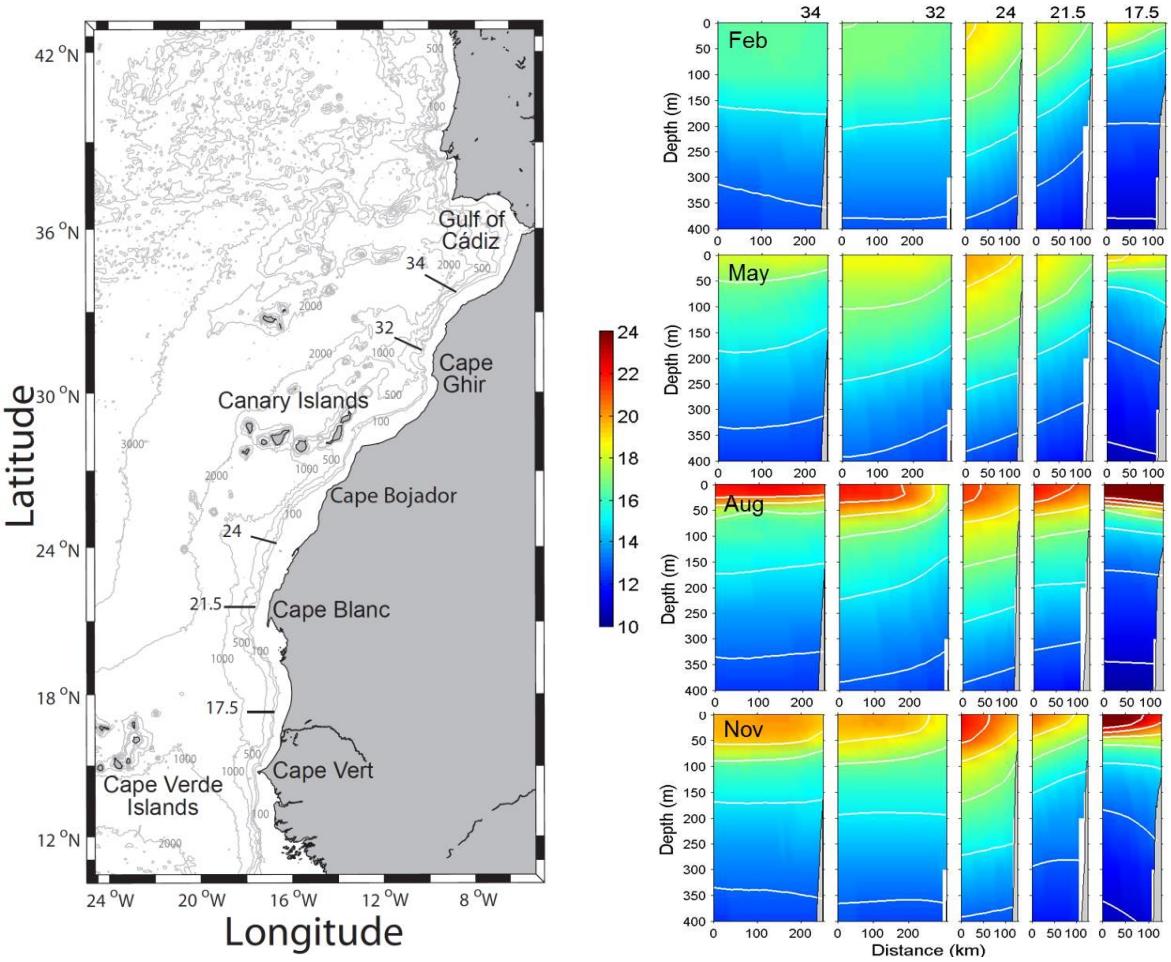

Figure 3.4.3. Left panel: main geographic features and isobaths in the CCLME, with the location of five selected cross-shore sections. Right panel: climatological temperature distributions (°C) along these sections, for February, May, August and November. Adapted from Benazzouz et al. (2014b).

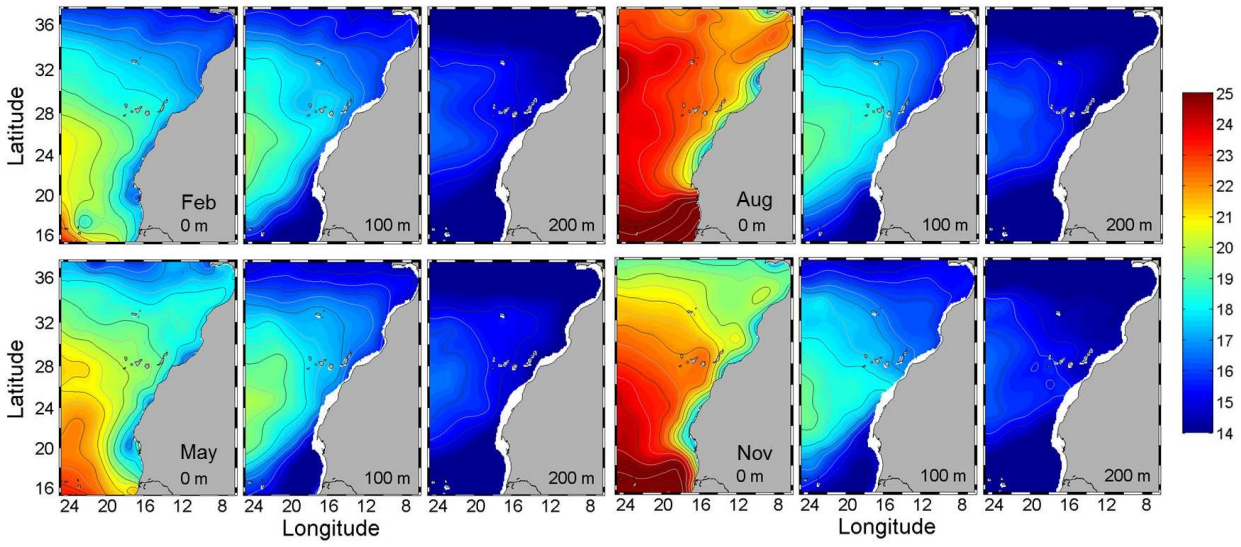

Figure 3.4.4. Climatological temperature fields (°C) for February, May, August and November, at the sea surface, 100 m and 200 m; adapted from Benazzouz et al. (2014b).

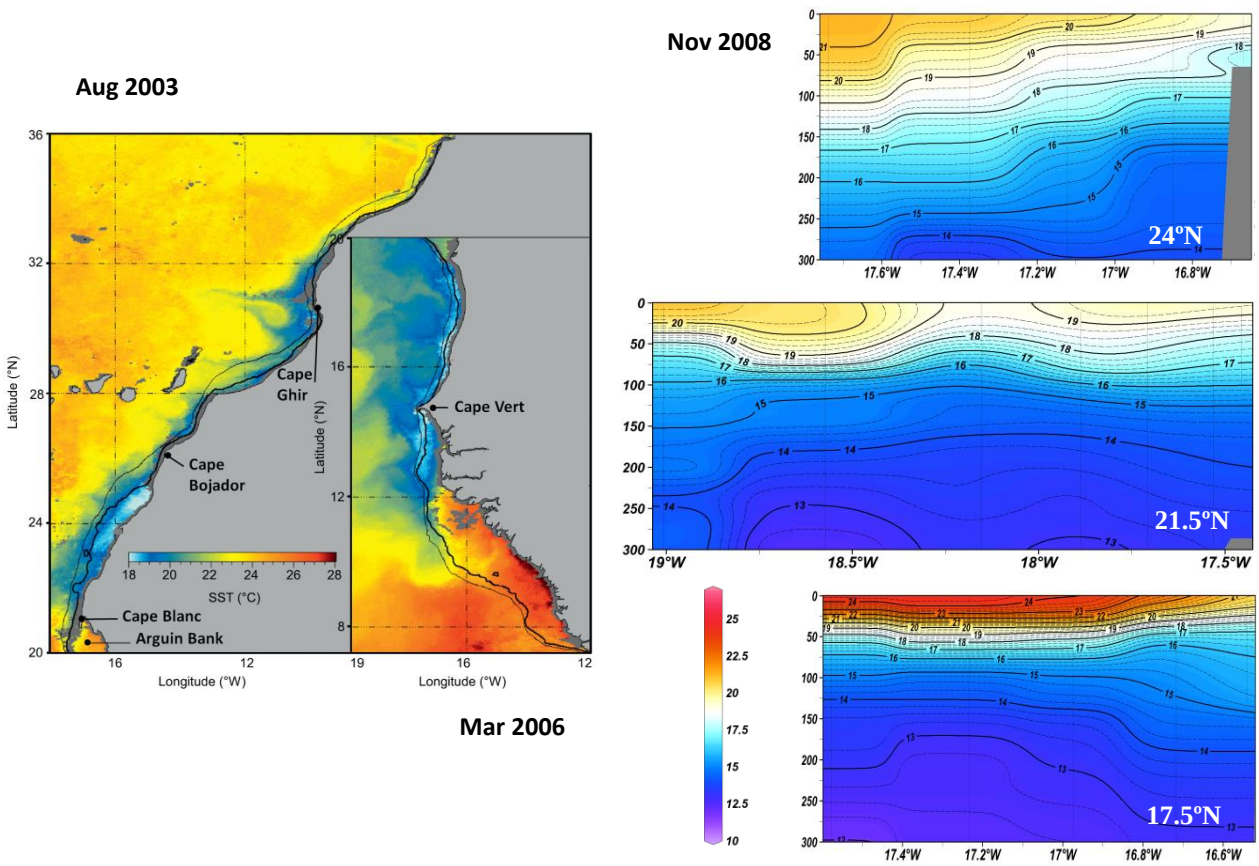

Figure 3.4.5. Left panel: SST fields during boreal summer north of Cape Blanc (1-8 August 2003) and during boreal winter south of Cape Blanc (1-8 March 2006). Right panel: temperature fields in selected cross-sections (see Fig. 3.4.1) for 3-29 November 2008. Adapted from Benazzouz et al. (2014a, b).

structure of the eastern subtropical gyre does not change much from one season to another (Stramma, 1984), the seasonality in coastal upwelling and the associated jet implies substantial variations in the patterns of recirculation between the coastal and deep oceans in the northern and central regions (Pelegrí et al., 2005a; Laiz et al., 2012; Pastor et al., 2008, 2013); in particular, the latitudinal cell intensifies during summer-fall, bringing an increase in the fall-winter zonal recirculations (Pelegrí and Peña-Izquierdo, 3.3 this book).

In the northern and central domains, where upwelling is permanent, the coastal jet becomes the easternmost branch of the Canary Current – the Canary Upwelling Current (CUC) – the true eastern boundary flow for the North Atlantic subtropical gyre (NASG) (Pelegrí et al., 2005a, 2006). In contrast, the upwelling front of the southern domain is too shallow to modify the thermocline circulation in the eastern North Atlantic tropical gyre (NATG) (Peña-Izquierdo et al., 2015). The two gyres meet at the Cape Verde Frontal Zone (CVFZ) (Zenk et al., 1991), stretching between Cape Blanc and the Cape Verde Islands, where along-slope flow convergence and large offshore transport take place (Pelegrí and Peña-Izquierdo, 3.3 this book).

The different characteristics of the northern, central and southern regions may be observed through a principal mode analysis of sea surface temperature (SST) images (Hernández-Guerra and Nykjaer, 1997) (Fig. 3.4.6). The mean field displays a remarkable temperature contrast both across the CVFZ and from the deep ocean to the coastal upwelling meridional band (between Cape Blanc and Cape Ghir). The first two

modes have annual periodicity, respectively accounting for 66% and 10% of the variability. The first mode mainly reflects the seasonal change in insolation, with large offshore warming at high latitudes during summer and low latitudes during winter. Remarkably, the response of the coastal upwelling band is similar to what happens at high latitudes – summer warming, at times when upwelling should intensify – which is understood as an expression of the meridional connection between the interior ocean at latitudes north of Cape Ghir and the coastal upwelled waters as far south as Cape Blanc (Pelegrí et al., 1997, 2005a, 2006). The importance of this first mode explains the simultaneous increase of winds and coastal warming that has occurred during the last 30 years (Benazzouz et al., 6.3 this book): the meridional cell is intensified as a response to the increased winds, bringing to the coastal upwelling band those interior-ocean upper-thermocline waters that have experienced climate warming. The second mode reflects the coastal variations linked to the actual changes in wind pattern, with maximum cooling (the direct effect of wind upwelling) during summer in the central-northern areas and during winter in the southern region.

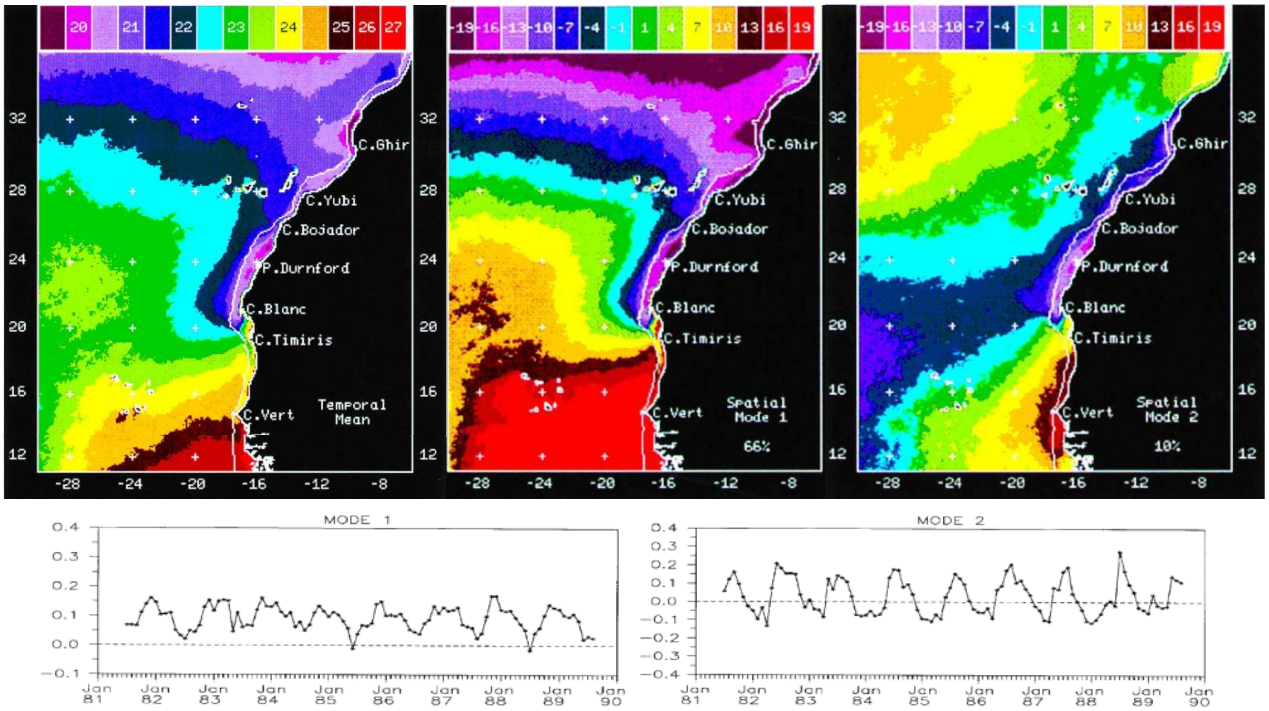

Figure 3.4.6. Mean fields (left), first spatial mode (centre), and second spatial mode of the SST fields for the 1981-1989 period (right). The bottom panels present the time series for the first and second modes. Adapted from Hernández-Guerra and Nykjaer (1997); reprinted by permission of Taylor & Francis LLC.

3.4.3. THE COASTAL UPWELLING FRONTAL SYSTEM

3.4.3.1. The coastal upwelling jet

The principal components of the coastal upwelling frontal system are the relatively homogeneous upwelled waters, the frontal system itself, and the offshore waters overlying the frontal system (Fig. 3.4.2). The vertical circulation cell causes those subsurface waters under the surface mixed layer, in the uppermost permanent thermocline, to flow onshore in order to compensate for the offshore transport in the mixed layer; this raises the isothermals and produces a baroclinic frontal system. If the winds are intense enough, the surface expression of this frontal system, or frontal zone, is found over the continental slope or further

offshore, therefore leaving cold and nutrient-rich waters between the frontal zone and the shelf break – the relatively homogeneous upwelled region. The upwelling jet develops on the offshore side of the frontal zone, on top the raising isothermals. Vertical shear between this jet and the underlying slower waters gives rise to intense vertical mixing which has two roles: eventually compensates for the wind stress so that upwelling is arrested and, when this happens, provides for the mass fluxes necessary to close the vertical cell (Pelegrí and Richman, 1993).

A common index for the intensity of upwelling is the zonal SST difference between the far offshore and the near-shore upwelled waters (Van Camp et al., 1991). If the upwelling jet and frontal system were maintained only through the surface stress granted by the trade winds, this index would be well correlated to the cross-shore Ekman transport (Bakun, 1973). However, for the upwelling region off NWA, the SST difference does not display the high-frequency intermittency of the wind (several days) and follows the Ekman transport with a 1-2 month delay (Fig. 3.4.7). A non-local (cumulative) time index, which takes into consideration both the vertical and meridional cells, leads to a much improved correlation between the winds and the SST difference (Benazzouz et al., 2014b) (Fig. 3.4.8). The long temporal and spatial memory of the upwelling system turns the CUC into a true meridional conveyor of water properties in the uppermost thermocline of the eastern NASG.

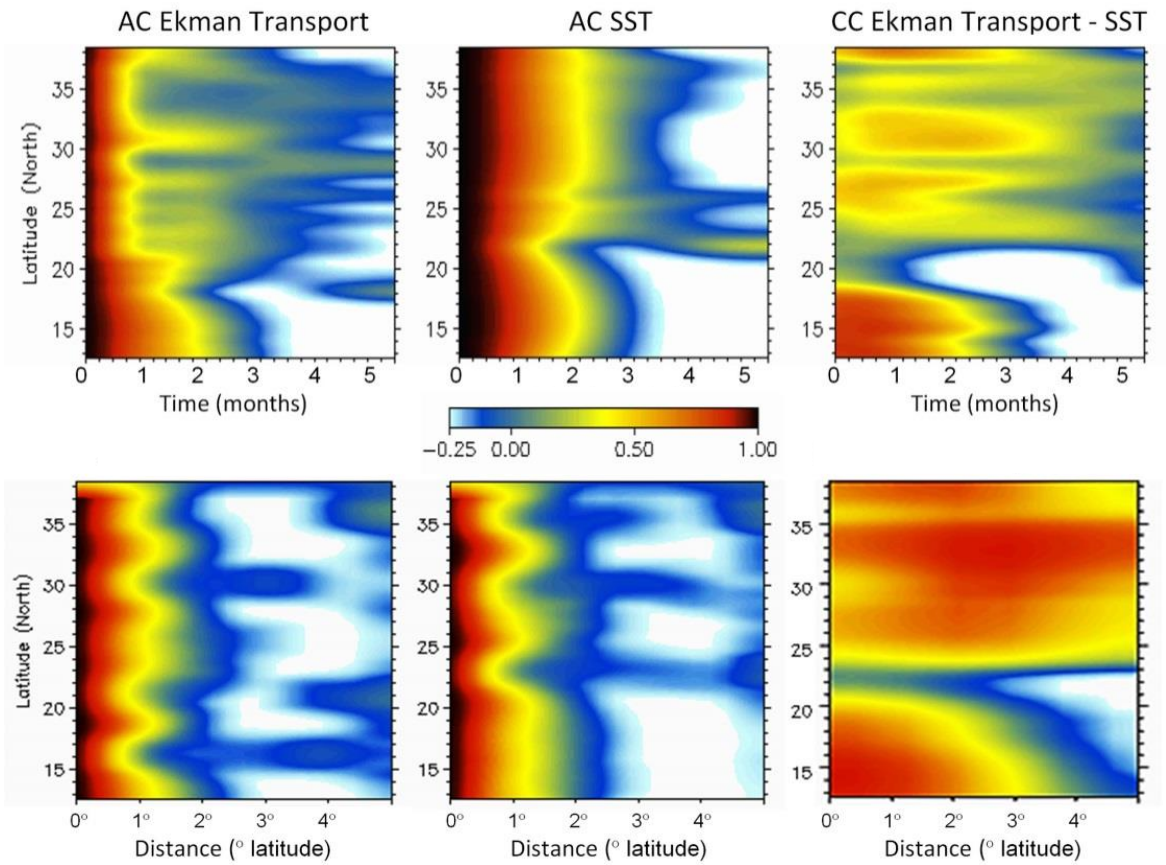

Figure 3.4.7. Auto-correlations for Ekman transport (left) and SST (centre), and cross-correlations between Ekman transport and SST (right), as a function of latitude; temporal (top) and (bottom) annual-mean (bottom) spatial correlations (the latter are to be doubled). Adapted from Benazzouz et al. (2014b).

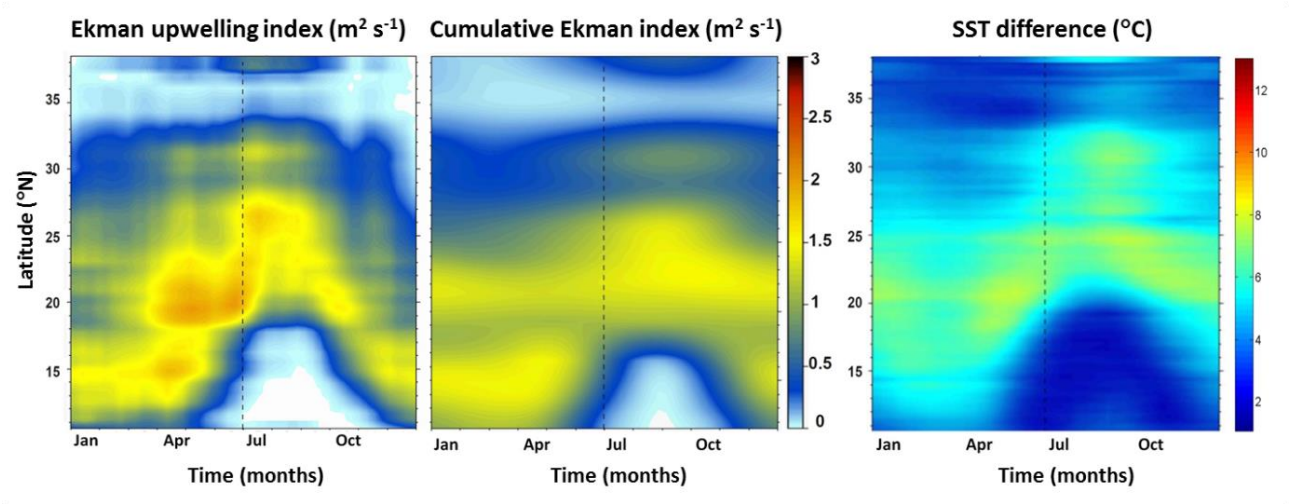

Figure 3.4.8. (Left panel) Local and (centre panel) cumulative Ekman indices; (right panel) SST difference. Adapted from Benazzouz et al. (2014b).

3.4.3.2. Connection between the coastal and interior oceans

The coastal upwelling system is responsible for a close connection between the coastal and interior oceans (Pelegrí et al., 2005a). This takes place through the classical cross-shore vertical cell (e.g. Pelegrí and Richman, 1993) and, for the subtropical gyre, aided by the equally important latitudinal cell (Pelegrí et al., 1997, 2005a, 2006) (Fig. 3.4.2). This subtropical meridional cell starts where the African slope ends, at the Gulf of Cadiz, fed by the Azores Current (Machín et al., 2006b; Laiz et al., 2012) and ends at the CVFZ, where the CUC is diverted offshore after encountering the Mauritanian Current (Pelegrí and Peña-Izquierdo, 3.3 this book). However, there are several locations where water is exported offshore, through surface filaments at coastal capes (Hagen et al., 1996; Pelegrí et al., 2005b; Sangrà, 3.5 this book), and recirculates onshore, such as south of the Canary Islands in late fall (Pelegrí et al., 1997, 2005a, 2006; Machín et al., 2006a; Pelegrí and Peña-Izquierdo, 3.3 this book).

Particle tracking for high-resolution numerical simulations north of the Canary Islands, has confirmed the high relevance of both vertical and meridional water inflow (Mason et al., 2011, 2012), with substantial seasonal variability (Figs. 3.4.9 and 3.4.10). In particular, an along-shore flow reversal is clear in late fall, suggesting that the southward coastal jet has been diverted offshore and recirculates around the Canary Archipelago before re-entering northwards. Another remarkable feature is the presence of latitudinal bands of temporally coherent intensified upwelling, likely linked to geomorphological features, taking place at the submesoscale (order 10 km) (Mason et al., 2012).

All year long, the fate of the CUC is the CVFZ. It is possible that a small fraction of the CUC transport may follow south of this front in winter, when there is a narrow band of shallow upwelling between Cape Vert and Cape Blanc, but even then most of the water is diverted offshore. The result is high along-shore convergence and water, nutrient and chlorophyll export, giving rise to the Cape Blanc giant filament (Gabric et al., 1993; Sangrà, 3.5 this book). Export is increased in winter, as a result of the intensification of the Mauritanian Current, though displaying substantial inter-annual variability (Pastor et al., 2013); asides along-shore convergence, the filament is also the site of substantial vertical mixing and offshore upwelling associated to the horizontal divergence of the wind-induced surface transport (Fig. 3.4.11).

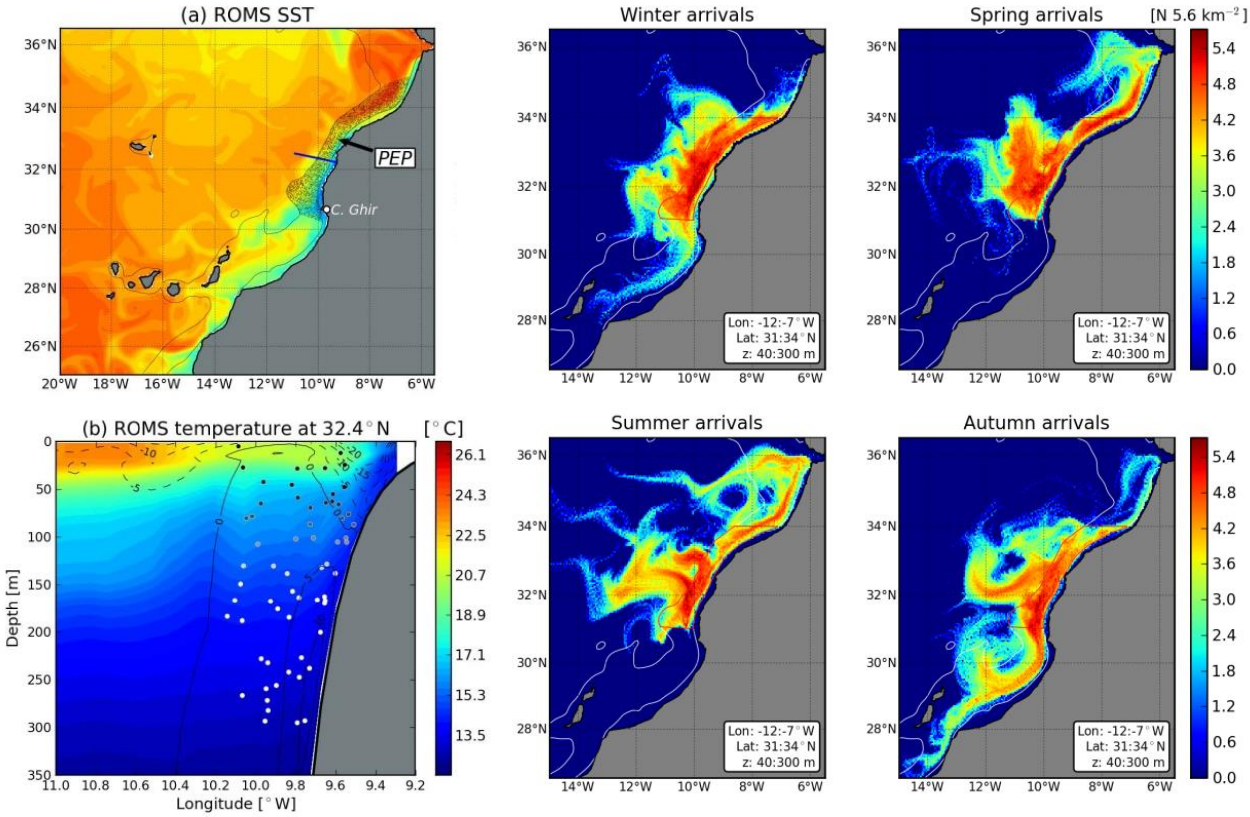

Figure 3.4.9. (Top left panel) Summer snapshot of the numerical SST field, with the region where backtrack particles are released (PEP); bottom left panel SST numerical distribution along the vertical section in the above panel, with the along-shore velocity field (contoured, with positive values – solid lines – representing northward flow; m s^{-1}) and the dots representing random particle release locations; adapted from Mason et al. (2012). (Central and right panels) Seasonal maps of the number of particles per grid element (log scale) 90 days before arriving to the PEP region in the 40-300 m depth range; courtesy of Evan Mason.

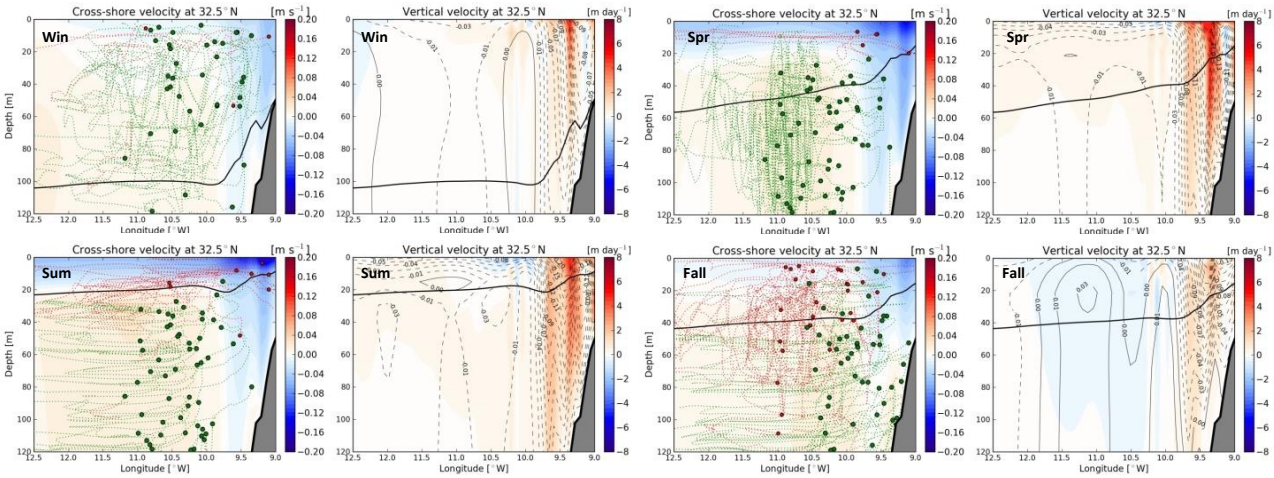

Figure 3.4.10. Pairs of panels showing the mean-seasonal cross-shore, vertical and along-shore velocities. For each pair of panels, the left one shows the cross-shore velocities (positive values denote shoreward flow) together with parcel trajectories (green/red dots represent the end/start of a trajectory), and the right one shows the vertical (color-coded) and alongshore (contoured, solid lines denote northward flow). The solid thick line represents the bottom of the surface mixed layer. Adapted from Mason et al. (2012).

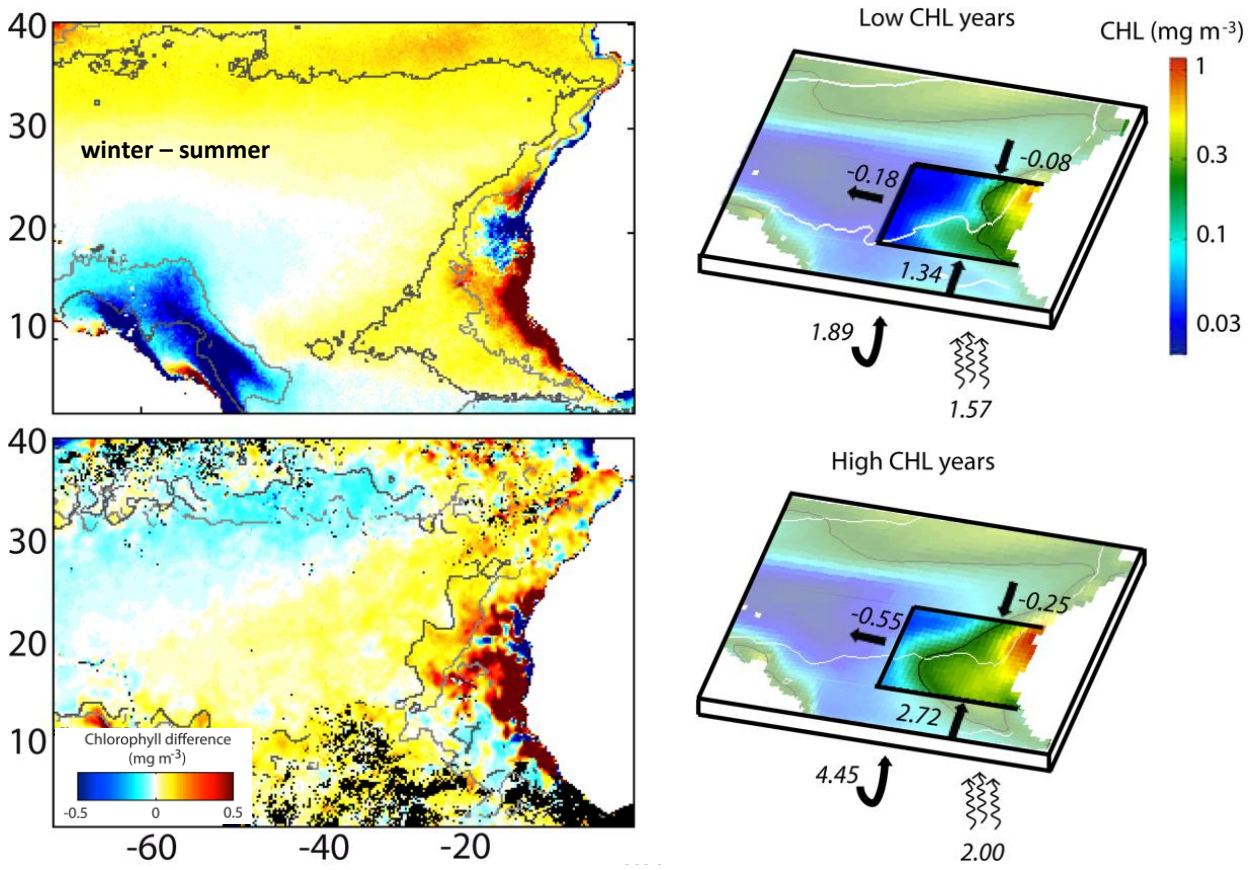

Figure 3.4.11. (Left panels) Seasonal and inter-annual changes of surface chlorophyll in the eastern North Atlantic. Right panels Phosphate fluxes ($\times 10^{-10}$ mol m^2 s^{-1}) during low and high chlorophyll years. Adapted from Pastor et al. (2013).

3.4.3.3. The Poleward Undercurrent

Together with the CUC, the Poleward Undercurrent (PUC) represents an along-slope inter-connector among all latitudes of the CCLME. The PUC flows along the continental slope, typically following the 2000 m isobath; its core is centred near 200-300 m, but often reaches the sea surface, particularly south of Cape Blanc. The PUC may be considered to begin near Cape Vert, as a result of the wind-induced equatorward increase in pressure (Barton, 1989), feeding from both the Mauritanian Current and the complex recirculation of subsurface zonal jets in the north-eastern tropical gyre (Pelegrí and Peña-Izquierdo, 3.3 this book). Numerical simulations with data-assimilating circulation models, also suggest that the PUC intensifies north of Cape Blanc through water input along the CVFZ (Pelegrí and Peña-Izquierdo, 3.3 this book), in agreement with fall observations reported by Peña-Izquierdo et al. (2012).

In contrast to the CUC, the PUC follows (and occasionally intensifies) through the CVFZ; south of Cape Blanc the winter PUC is located off the very shallow near-shore upwelling jet, while north of Cape Blanc the PUC is found in the upwelling region, between the frontal upwelling front and the shelf break. As it flows north, the PUC carries tropical waters (South Atlantic Central Water, SACW), much richer in nutrients than the subtropical waters (North Atlantic Central Waters, NACW). Near the CVFZ, the SACW becomes modified through the addition of old NACW, which has reached this region from far west through the Cape Verde Current system, so the PUC transfers waters to the NASG that are saltier and more oxygen depleted than the SACWs found in the NATG (Peña-Izquierdo et al., 2015).

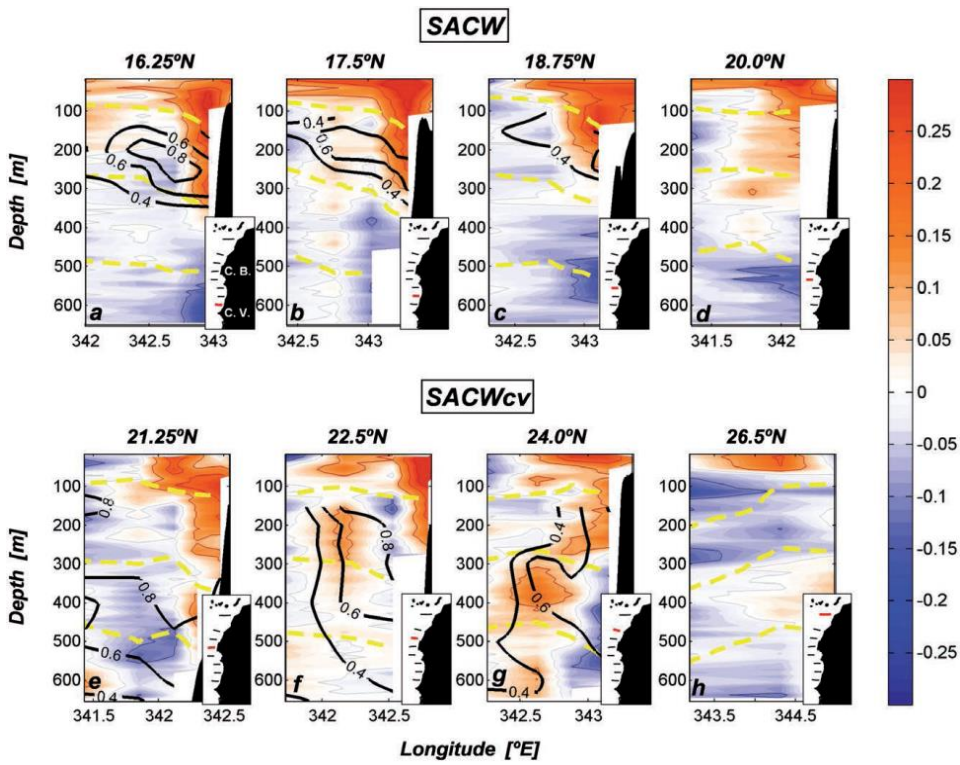

Figure 3.4.12. Alongshore velocities (color-coded, northward flow is positive; m s^{-1}) at different latitudes, plotted with the contributions of the two varieties of SACW (black contours) and selected isopycnals (26.46, 26.85 and 27.10, in yellow). Reproduced from Peña-Izquierdo et al. (2012).

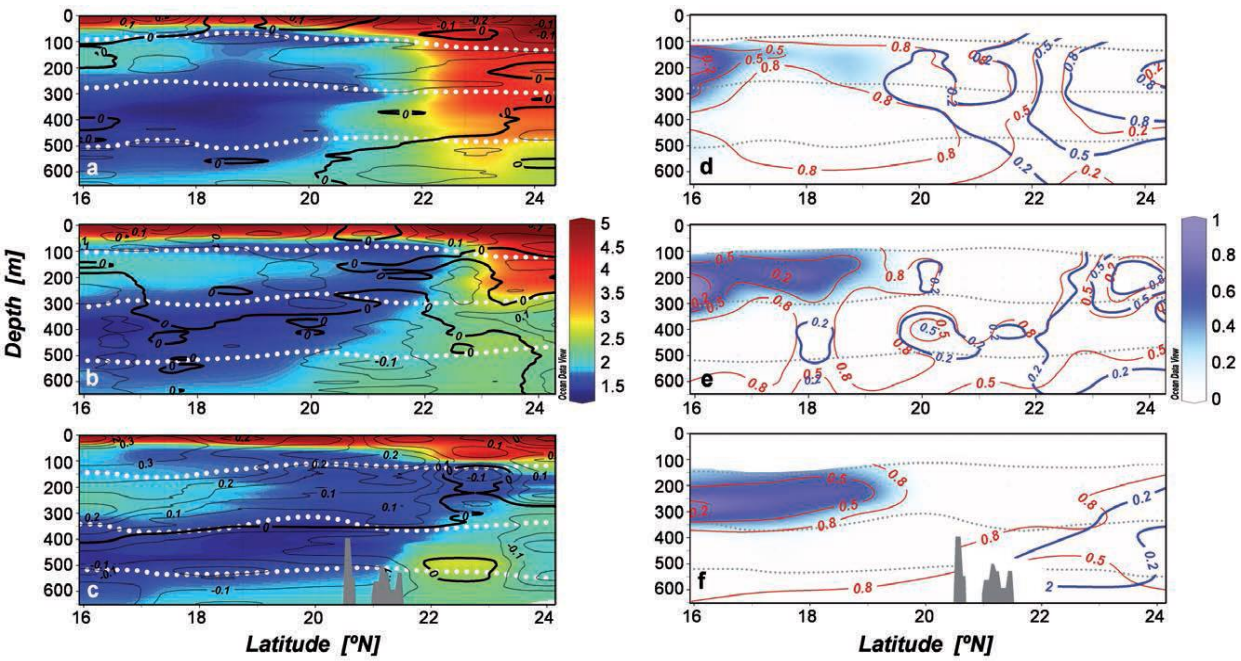

Figure 3.4.13. (Left panels) Oxygen content (color-coded; ml l^{-1}) and meridional velocity (solid lines, positive northward; m s^{-1}). (Right panels) Contribution of the two SACW varieties (color-coded and red contours) and the NACW (blue contours), with selected isopycnals (26.46, 26.85 and 27.10, dotted lines). The top (farther offshore), middle (ca. 2000 m isobath) and bottom (ca. 1000 m isobath) panels correspond to meridional sections separated about 1° in latitude. Reproduced from Peña-Izquierdo et al. (2012).

3.4.4. CONCLUSIONS

The most distinctive oceanographic feature of the CCLME is the coastal upwelling frontal system off NWA – there is a near-surface (typically down to about 200-250 m) high cross-shore contrast in water properties, from the colder vertically-homogeneous and nutrient-rich upwelled waters to the warmer well-stratified and nutrient-depleted offshore interior waters. The vertical circulation cell (wind-driven offshore transport and subsurface onshore compensating flow) associated to this frontal system continuously brings nutrient-rich subsurface waters to the photic layers in the African shelf and slope, therefore sustaining high primary productivity which eventually leads to rich fisheries of small pelagic species. The horizontal circulation cell, in contrast, drives a two-way meridional connection. The southward course is the CUC (the baroclinic jet riding on top the frontal system), connecting the frontal layers (0-250 m) at different latitudes, from the Gulf of Cadiz to Cape Blanc – the CUC constitutes the true eastern boundary branch of the NASG. The northward track follows as the PUC, leaning on the continental slope with its core at depths of about 200-300 m, from Cape Vert, across the CVFZ and reaching at least till the Gulf of Cadiz – the PUC cruises through both the tropical and subtropical regions, carrying northwards the relatively nutrient-rich and oxygen-poor varieties of SACW.

The large-scale meridional currents off NW Africa currents are accompanied by high mesoscale and sub-mesoscale variability, mainly as a result of the instabilities of the coastal upwelling front and the perturbation caused by the Canary Islands to the predominant southward flow. The outcome is a complex meridional and zonal network, responsible for the exchange of water properties between different latitudes and between the coastal and interior oceans, which sets the basis for very high eastern-boundary productivity.

Acknowledgements

This review synthesizes work on coastal upwelling in the CCLME linked to several projects carried out during the last two decades, particularly projects CANOA (CTM2005-00444/MAR), MOC2 (CTM2008-06438-C02-01) and TIC-MOC (CTM2011–28867) funded by the Spanish government. Aïssa Benazzouz was partially supported by the 50th Anniversary Young African fellowship program of the Intergovernmental Oceanographic Commission of UNESCO. We also wish to sincerely thank the many colleagues that have participated with us in these projects, for the hard work carried out together and the many enlightening and joyful conversations, particularly Verónica Benítez, Mikhail Emelianov, Alonso Hernández-Guerra, Ángeles Marrero-Díaz, María Pastor, Jesús Peña-Izquierdo, Ángel Rodríguez-Santana, Joaquín Salvador and Pablo Sangrà.

3.5. CANARY ISLANDS EDDIES AND COASTAL UPWELLING FILAMENTS OFF NORTH-WEST AFRICA

Pablo SANGRÀ

Instituto de Oceanografía y Cambio Global (IOCAG), Universidad de Las Palmas de Gran Canaria. Spain

3.5.1. INTRODUCTION

A distinctive feature of the Canary Current Large Marine Ecosystem (CCLME) is the presence of an archipelago, the Canary Islands, extending ca. 500 km zonally that act as a topographic barrier perturbing the southward flowing of the prevailing winds (Trade Winds) and currents (Canary Current). As a result, oceanic mesoscale eddies are almost continuously spun off by the islands of the archipelago. The CCLME therefore includes a source of mesoscale eddies that is not present in other Eastern Boundary Upwelling Systems (EBUS) and, as we will review in this work, this may have a great impact on the modulation and distribution of physical and biogeochemical properties, both locally and regionally.

The first observations of Canary Island induced eddies were from remote sensing (La Viollete, 1974; Hernández-Guerra, 1990; Hernández-Guerra et al., 1993). The sea surface temperature signature of warm core anticyclonic eddies has been observed southeast of Gran Canaria, Tenerife and El Hierro islands. The sea surface temperature signature of cold core cyclonic eddies has been observed southwest of Gran Canaria, La Palma and El Hierro islands. Arístegui et al. (1994) first described the Canary Island eddies from *in situ* data, revealing their principal characteristics such as diameter, depth and property anomalies in the hydrographic fields. These and further studies were motivated by the search for an explanation of the observed local enhancement of biological productivity by islands, known as the Island Mass Effect (Doty and Ogury, 1956). Later, after a first phase of study concentrated on the eddies hydrography, the focus shifted towards an understanding of their biological effects, taking as a case study the eddies shed from the island of Gran Canaria (Arístegui et al., 1997; Barton et al., 1998; Arístegui and Montero, 2005; Alonso-González et al., 2013; Lasternas et al., 2013). Simultaneously, progress was also made in determining the hydrographic and kinematic characteristics of these eddies, their generation mechanisms, and establishing their Lagrangian evolution (Sangrà et al., 2005, 2007; Piedeleu et al., 2009). Sangrà et al. (2009) observed that Canary Island induced eddies contribute to a zonally oriented eddy corridor that can extend as far as the Mid Atlantic Ridge; this was named the Canary Eddy Corridor (CEC, Figure 3.5.1). This study represented a turning point in understanding of the role that Canary Island induced eddies may play, as their impact may be felt far from the islands, affecting the whole northeastern subtropical Atlantic region.

Upwelling filaments are also typical mesoscale features of the CCLME. They are related with the variability of the coastal upwelling and consist of narrow, O(10 km), and elongated, O(100 km), structures of upwelled water that stretch zonally offshore from the coast, often rooted to major capes (Figure 3.5.2). They are shallow structures, O(100 m), identifiable by low surface temperature and high chlorophyll-a concentration signals. Since the very first remote sensing observations of the northwest African Upwelling System (NAUS), upwelling filaments have been recurrently observed near Cape Ghir (30°38'N), Cape Jubi (27°40'N), Cape Bojador (26°07'N) and Cape Blanc (Figure 3.5.1) (Van Camp et al., 1991; Gabric et al., 1993; Hagen et al., 1996; Pacheco and Hernández Guerra, 1999). In this work we review a number of studies on the Canary Island induced eddies and on the NAUS upwelling filaments system. We also discuss the impact that such mesoscale structures may have on the CCLME.

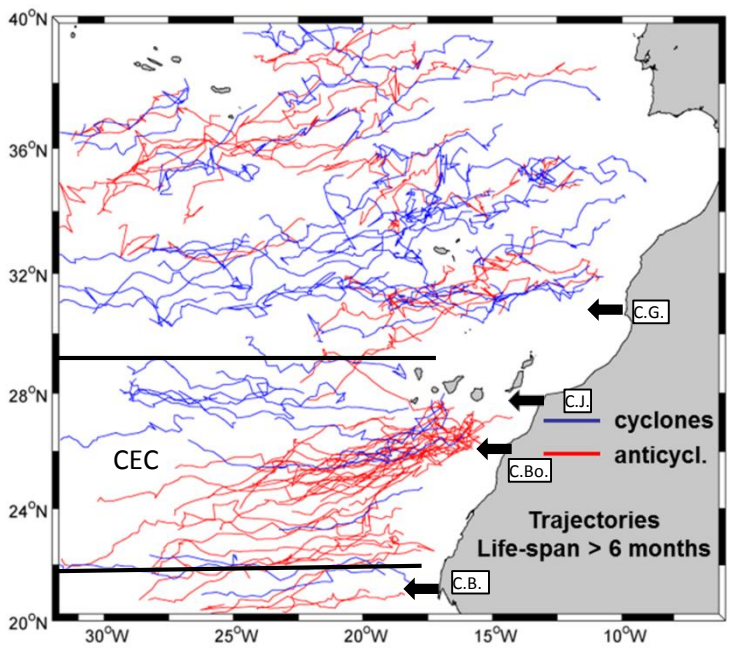

Figure 3.5.1. Westward-propagating eddy trajectories lasting over 6 months, as obtained from 14 years (1992–2006) of merged altimeter data, showing the Canary Eddy Corridor (CEC) extending from 22°N to 29°N. Black arrows indicate the sites of recurrently observed upwelling filaments. They are located in the region near Cape Ghir (C.G.), near and between Cape Jubi (CJ) and Cape Bojador (C.bo.), and near Cape Blanc (C.B.). Adapted from Sangrà et al. (2009).

3.5.2. ISLAND INDUCED EDDIES: FORCING MECHANISMS

Early observational studies of island induced eddies associated the perturbation of the oceanic flow with the island topography, a process referred to as topographic forcing (La Violette, 1974; Hernández-Guerra et al., 1993; Arístegui et al., 1994; Heywood et al., 1996). Laboratory and numerical experiments that consider a flow past an obstacle show that, if the impinging flow is sufficiently energetic, the boundary layer around the obstacle detaches, alternating between flanks and giving rise to the sequential spin off of cyclonic and anticyclonic eddies (Berger and Whille, 1972; Bearman, 1984; Sangrà, 1995; Dong et al., 2007). As a result a Von Kármán like vortex street is formed downstream of the obstacle. This flow regime, and thus the eddy shedding process, is dependent on the Reynolds number,

$$Re = \frac{2\,\varepsilon}{E_H} = \frac{U\,L}{A_H} \tag{1}$$

where U is the characteristic velocity of the incident flow, L is the obstacle diameter, A_H the horizontal eddy diffusivity coefficient, ε the Rossby number, and E_H the horizontal Ekman number. Field and laboratory observations indicate that the eddy shedding process starts at Re≥50-60 (e.g. Pattiaratchi et al., 1986). Assuming A_H and L constant, the flow regime will depend ultimately on the intensity of the impinging oceanic flow, U. Therefore the topographic forcing of oceanic island induced eddies requires a relatively energetic incident flow.

However, island induced eddies have been observed in regions where an energetic incident oceanic flow is absent or very weak, such as is the case for the Hawaii Islands (Calil et al., 2008; Jia et al., 2011). Therefore,

there must be an alternative or additional mechanism to topographic forcing to explain eddy generation during periods of low intensity incident flow. This second mechanism is known as atmospheric forcing, and is associated with wind field perturbation by the orography of tall islands.

In the case of tall islands, prevailing wind perturbations lead to the generation of a downwind wind wake where two counter-rotating stationary wind stress curl cells develop (Chavanne et al., 2002; Jiménez et al., 2008; Mason, 2009). These are the result of the strong wind shear between the wind sheltered region just downstream of the island, and the wind exposed region further away. Observations for the Canary Islands have reported a gradient of the wind intensity between these regions as high as 15 m s^{-1} (Piedeleu, 2014). As proposed by Jiménez et al. (2008), the anticyclonic/cyclonic wind curl cell will induce a divergence/convergence of the Ekman transport that will lead to a downward/upward linear Ekman pumping velocity, which shrinks/stretches the planetary vorticity tubes, spinning up anticyclonic/cyclonic relative vorticity. Therefore, through this process the atmospheric forcing will favor anticyclonic/cyclonic vorticity injection by the wind wake on the right/left side facing upwind.

Piedeleu et al. (2009) and Piedeleu (2014) investigated the relative importance of the topographic and atmospheric forcing on Gran Canaria eddies generation from an observational perspective. They analyzed a two year time series of the eddy signal in the temperature field, the topographic forcing intensity through the Canary Current intensity, and the atmospheric forcing through the wind shear intensity. For those periods where the wind forcing was very low, i.e. when the topographic forcing was the main forcing mechanism, they observed a Canary Current threshold value of U=0.09 m s^{-1} (Re=50, A_H=100 $m^2 s^{-1}$) for triggering of the eddy shedding process. As the Jiménez et al. (2008) model predicts, for such periods of high atmospheric forcing the Canary Current intensity threshold for triggering the eddies shedding process decreases to U=0.05 m s^{-1} (Re=27, A_H=100 $m^2 s^{-1}$). They observed that 50% of Gran Canaria eddies were generated under high topographic and atmospheric forcing mainly in summer, 30% under topographic forcing alone, mainly in winter and spring, and 20% under low topographic and high atmospheric forcing. Moreover, in spite of periods of high atmospheric forcing no eddy shedding was reported in autumn when topographic forcing was absent. This confirms the Jimenez et al. (2008) predictions that, for the case of the Canary Islands, atmospheric forcing alone is not able to trigger the eddy shedding process. Therefore as a corollary we may state that in the Canary Island region the occurrence of an incident oceanic flow is a necessary condition to trigger the eddy shedding process. This can be also extended to Cape Verde islands where the prevailing atmospheric and oceanic flows are oriented meridionally.

3.5.3. EDDY CHARACTERISTICS AND EVOLUTION

Island induced eddies are evolving structures and thus their characteristics will depend on their life stage (Sangrà et al., 2005). The majority of Canary Islands induced eddies were sampled during their early stages when they are located close to the originating island (Arístegui et al., 1994; Sangrà et al., 2007; Piedeleu, 2014). A this stage their radii are close to the climatological first baroclinic Rossby radius of deformation which is ca. 30 km for the Canary Island region (Chelton et al., 1998). The eddies have a typical vertical signature down to about 300 m depth, although intense eddies may initially perturb the full depth range of the North Atlantic Central Water (NACW), reaching 700 m depth (Sangrà et al.; 2007; Piedeleu, 2014). Warm core anticyclonic eddies introduce positive temperature anomalies that may reach +3.5°C, while cold core cyclonic eddies anomalies may attain -4.5°C. Isopycnals and isotherms may deepen/shallow more than 100 m in anticyclonic/cyclonic eddies

Buoy trajectories and hydrographic data indicate that at their initial stage the majority of eddies rotate in near solid body rotation as Rankine-like vortices (Sangrà et al., 2005, 2007; Piedeleu, 2014). Canary Island anticyclonic eddies rotate initially with periods of ca. *T*=2.5 d, two times faster than cyclonic eddies whose initial rotating rates are ca. *T*=5 d (Sangrà et al., 2007; Piedeleu, 2014). These periods coincide with maximum rotating rates permitted by the inertial stability criteria for Rankine-like eddies to be stable to inertial perturbations, and thus for being long lived coherent structures (Sangrà et al., 2007). Given their higher initial rotating rates, it may be expected that anticyclonic eddies will have a much larger life expectancy than cyclonic eddies. This may partly explain why anticyclones dominate in the CEC as we will show in next section. When eddies reach their mature stage they lose their characteristic solid body rotation as the inner core starts to rotate faster than the periphery, evolving into Gaussian like eddies (Sangrà et al., 2005). Eddies propagate southward through advection by the Canary Current, and westward by self advection due to gradient of the local rotating rate known as the β-effect (Cushman-Roisin, 1994; Van Leeuwen, 2007). It has been observed that that mean eddy propagation velocities range between 3.5 and 6 km d^{-1} (Sangrà et al., 2005; Piedeleu, 2014).

3.5.4. NORTHWEST AFRICAN UPWELLING SYSTEM FILAMENTS: STRUCTURE AND GENERATION MECHANISMS

As already introduced, coastal upwelling filaments are recurrently observed near Cape Ghir, Cape Jubi, Cape Bojador and Cape Blanc (Figures 3.5.1 and 3.5.2). Although they have common characteristics, such low temperature and high chlorophyll-a signals, their structure and origin are different. As we detail next, Cape Ghir filament is a quasi-permanent feature and its origin is thought to be on the cyclonic relative vorticity injection by the wind-stress curl (Troupin et al., 2012; Sangrà et al., 2015). Filaments at Cape Jubi and between Cape Jubi and Cape Bojador are smaller, show intermittency and are variable in their location due to their interaction with the eddy field induced by the Canary Islands (Barton et al., 1998, 2004). It has been proposed that their origin is in the entrainment of upwelled water by such offshore eddy field. Cape Blanc filament is also a permanent feature, as the Cape Ghir filament. Its most noticeable feature is its large signature in the chlorophyll-a field: being 200 km wide and stretching 600 km offshore has granted it the name of the Cape Blanc Giant Filament (Gabric et al., 1993). Its great size and permanence is intimately connected with the CVFZ (hereafter, CVFZ) where there is a broad offshore flow associated to the North Equatorial Current and a convergence between North Atlantic Central Water (NACW) and South Atlantic Central Water (SACW). However, at Cape Blanc there are also smaller colds filaments, with a signal very distinct from the chlorophyll-a giant filament (Meunier et al., 2012).

Cape Ghir filament, located in the north part of the NAUS, may stretch up to 200 km offshore from the coastal upwelling as a tongue of cool and rich chlorophyll-a water (Figure 3.5.2a). Sangrà et al. (2015) have recently investigated the anatomy of this filament on scales down to the submesoscale. They describe the filament as a system of three intimately connected structures: a small, shallow and cold filament imbedded within a larger, deeper and cool filament and an intra-thermocline anticyclonic eddy (ITE). Both the cool and cold filaments are bounded by a northern offshore jet and a southern inshore jet, at the submesoscale for the cold filament and mesoscale for the cool filament. A distinctive feature of the Cape Ghir filament is the occurrence of a near stationary ITE between the northern jets of the cold and cool filament, which is linked to the secondary circulation of the filament. The presence of both zonal jets, flowing in opposite directions, and the ITE introduces a relatively strong cyclonic vorticity to the flow. This is coherent with Troupin et al. (2012) numerical experiments, which predict that the origin of the Cape Ghir filament is

caused by the injection of cyclonic relative vorticity by a strong wind curl upstream in the coastal upwelling jet; see Figure 3.5.8a in Troupin et al. (2012). This injected cyclonic relative vorticity disturbs the potential vorticity balance of the upwelling jet, diverting it from its southward path and turning it offshore along zonal contours of cyclonic potential vorticity, thus giving rise to the filament.

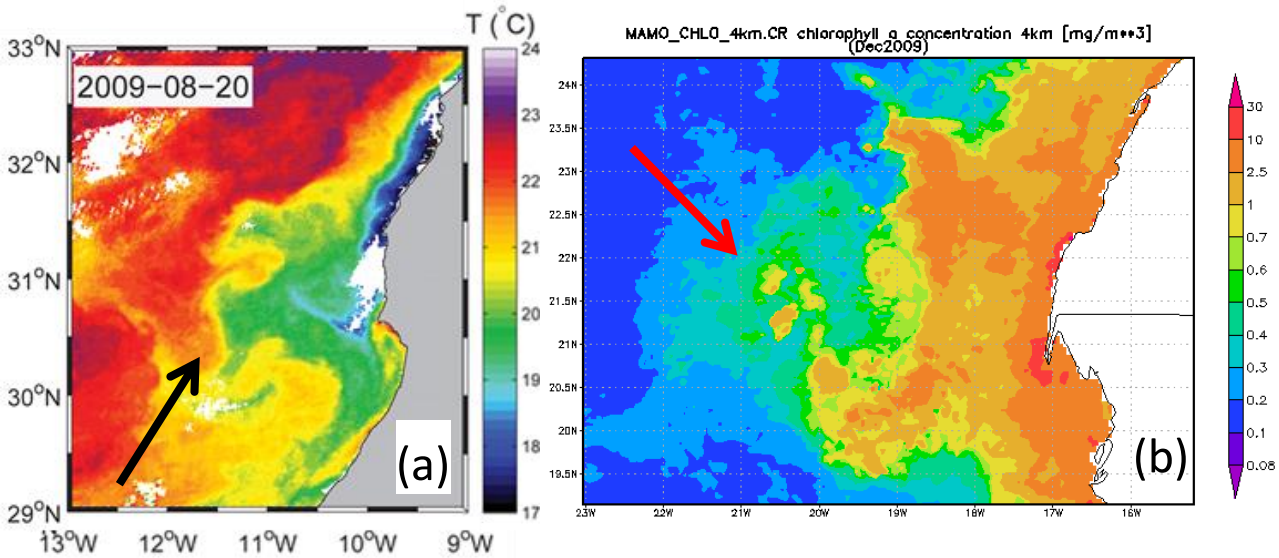

Figure 3.5.2. (a) Signature of the Cape Ghir filament on the SST field. (b) Signature of the Cape Blanc Giant filament on the chlorophyll-a field as obtained from MODIS aqua 4 km resolution data (Giovanni Ocean Color Radiometry Online Visualization and Analysis, http://gdata1.sci.gsfc.nasa.gov/daac-bin/G3/gui.cgi?instance_id=ocean_month, accessed 9 April 2015) for December 2009.

The second region of recurrent upwelling filament generation in the NAUS is between Cape Jubi and Cape Bojador, located near the Canary Islands latitude (Figure 3.5.1). Filaments generated at these locations are highly variable in space and time. SST observations indicate that sometimes a unique filament is located between both capes (Barton et al., 1998) and sometimes one filament in generated simultaneously at each cape (Pacheco and Hernández-Guerra, 1999). Although smaller and shallower (25 m) than Cape Ghir filament, they stretch west interacting with the eddy field induced by the Canary Islands (Barton, 1998; Barton et al., 2004; Sangrà et al., 2005). Barton et al. (2004) proposed that the filament recurrently originated off Cape Jubi is linked to the occurrence of a topographically-trapped cyclonic eddy downstream of the Fuerteventura–Africa channel; in particular, the filament has often been related to an anticyclonic eddy shed by Fuerteventura Island. Filaments occurring simultaneously in both capes have been linked to a system of cyclonic and anticyclonic eddies. The entrainment of upwelled waters by the eddy field has been proposed as the main mechanism for their generation, although the injection of relative cyclonic vorticity by the wind curl field should not be discarded as an additional mechanism. Troupin et al. (2012) have shown that upstream of Cape Juby there is a wind-stress curl as strong as in Cape Ghir – it will inject cyclonic vorticity to the upwelling jet preventing it from continuing southward and detaching it from the coastal region to give rise to the filaments.

Cape Blanc is located in the southern area of the NAUS (Figures 3.5.1 and 3.5.2b). This is a particular and complex region where the Canary Current detaches from the eastern boundary, feeding the North Equatorial Current, and where NACW and SACW converge along the CVFZ (Zenk et al., 1991). The intersection of the NAUS and the CVFZ leads to a complex and dynamic region with an intense eddy field.

The Cape Blanc filament reflects this complexity, having a very distinct signature in the chlorophyll-a and hydrographics fields. As showed in the chlorophyll-a field – see Figure 3.5.2b adapted from Gabric et al. (1993) – the filament shows up as a giant feature stretching 600 km offshore and 200 km wide. Meunier et al. (2012) observed, through the SST and hydrographic fields, a system of much smaller colds filaments rooted over cape Blanc and extending only 300 km offshore and 50 km wide (Figure 3.5.8b). These smaller filaments, as it happens for the Cape Jubi and Cape Bojador filaments, showed high spatial and time variability. The distinct signatures of the chlorophyll-a filament and the cold filaments suggest that the processes involved in their generation are also different. According to Gabric et al. (1993), the Cape Ghir giant filament originates from offshore advection of upwelling waters by the large scale flow, with substantial transfer of chlorophyll-a and probably also nutrients, and the move of the upwelling center to the shelf break area by the wind forcing. On the other hand, the observations by Meunier et al. (2012) support the idea that Cape Blanc colds filaments have their origin on the entrainment of the coastal upwelled water by the eddy field. At this latitude, the potential vorticity of the upwelling jet and the interior ocean are equal, thus the origin of the colds filaments may not be attributed to an injection of cyclonic vorticity by the wind curl as it happens in Cape Ghir.

3.5.5. DISCUSSION

3.5.5.1. Impact of the Canary Eddy Corridor

As mentioned in the introduction, a feature that distinguishes the CCLME from other EBUS is the occurrence of a long lived (life span > 3 months) eddy corridor that was named the Canary Eddy Corridor by Sangrà et al. (2009) (CEC). The CEC may be recognized in Figure 3.5.1 by the high density of long lived eddy tracks located between 22°N and 29°N. It constitutes a major pathway for long lived eddies in the northeastern subtropical Atlantic. Merged altimetry data from which the eddy tracks were derived do have not sufficient resolution to resolve the eddy field close to the coast during their early stage of generation. With this in mind, the majority of the trajectories starts south of the Canary Islands indicating that the CEC is mainly built up by Canary Island induced eddies. However, some trajectories can also be seen to initiate further south, indicating that upwelling system related eddies also feed the CEC. Long lived anticyclonic eddies clearly dominate over cyclonic eddies according to their higher initial rotating rates that increase their life expectancy over cyclones as discussed above. Long lived eddies propagate westward with mean velocities of one degree of longitude per month as a result of their self advection by the β-effect (Van Leeuwen, 2007), although there is also a tendency for southwestward propagation when interacting with the Canary Current flow.

The CEC may play an important role as a zonal conduit carrying both physical and biogeochemical properties from the cold nutrient-rich upwelling eastern boundary towards the interior ocean (Sangrà et al., 2009). As a result the main effect will be to extend the influence of the CCLME to the west. Regarding volume and mass transports, seventeen westward propagating long lived anticyclones are generated yearly. Their estimated westward volume transport is 4.5 Sv corresponding to one-fourth of the southward transport by the Canary Current (Sangrà et al., 2009). The above estimate matches with the values obtained for the westward transport for the region obtained by Hernández-Guerra et al. (2005) using inverse model techniques from a CTD box. This indicates that eddies in the CEC are the main source of westward transport of properties in the northeastern subtropical Atlantic. The CEC is also a source of westward propagating eddy kinetic energy (EKE) that is as high as that transported southward by the Canary Current (Sangrà et al., 2009). The CEC may have also impact the variability of the Atlantic Meridional Overturning Circulation

(AMOC). Chidichimo et al. (2010) related AMOC seasonal variability with density anomalies in the Canary Island region that affect thermocline tilting and hence the AMOC variability. Although these authors discard the impact of Canary Island eddies on such anomalies close to the archipelago, this may be not the case for the observed anomalies within the interior basin located inside the CEC.

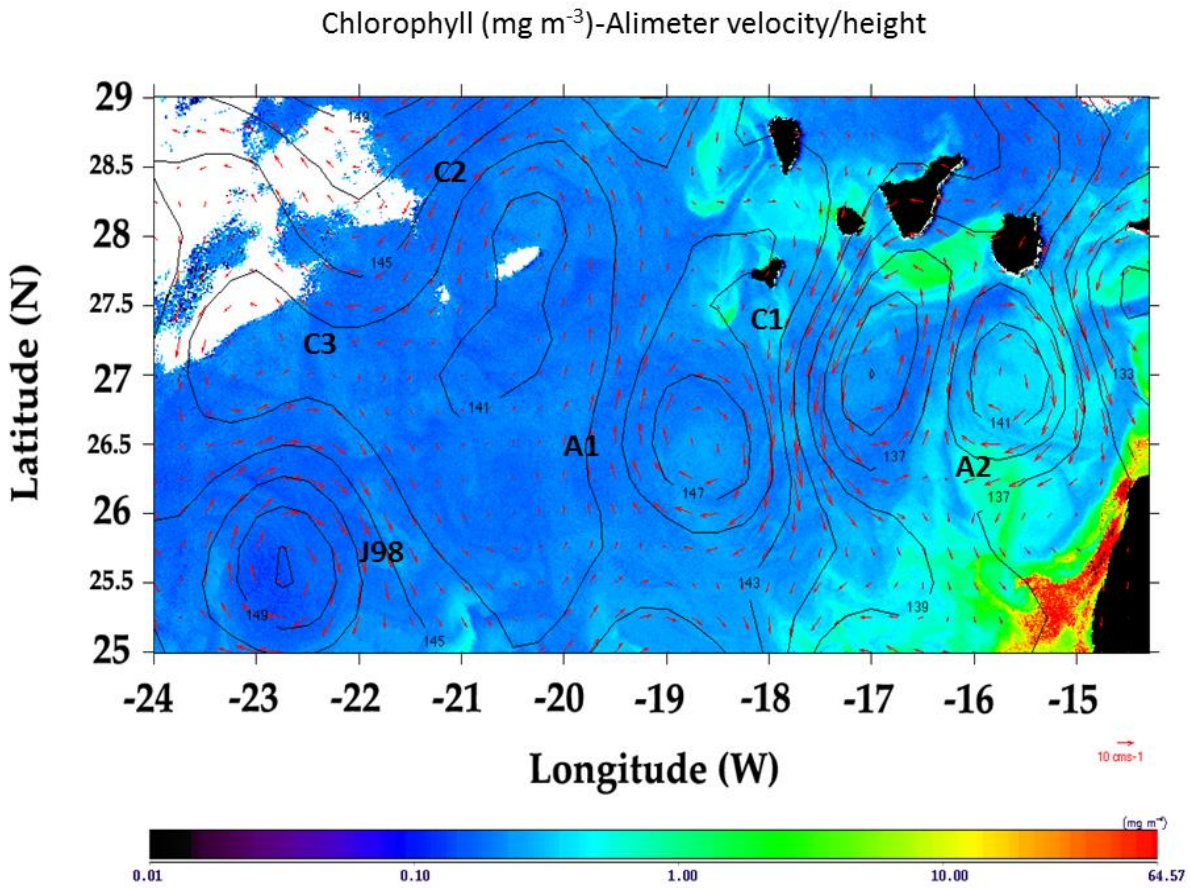

Figure 3.5.5. Chlorophyll concentration (24 April 1999) superposed onto sea-surface height and geostrophic velocity as obtained from merged altimeter data (28 April 1999), showing that eddies in the CEC may enhance chlorophyll concentration. See details in text. Adapted from Sangrà et al. (2009).

It is well known that mesoscale eddies modulate biological production and related biogeochemical fluxes (Benitez-Nelson et al., 2007; McGillicuddy et al., 2007; Lévy, 2008). Thus, the high density of long lived eddies in the CEC may also have a great impact on primary production (PP) and related biogeochemical fluxes. There is growing evidence that indicates that self-induced linear Ekman pumping as a consequence of eddy-wind interaction may lead to upwelling/downwelling in the interiors and of anticyclonic/cyclonic eddies (Martin and Richards, 2001; McGillicuddy et al., 2007; Gaube et al., 2013). Upwelling in the interior of warm core anticyclonic eddies will lead to an increase of PP through nutrient injection to the euphotic zone. Downwelling in the interior of cyclones will lead to depletion of nutrients, although this process may be compensated by the shoaling of the nutricline. Therefore the classical view that inside cyclonic eddies secondary circulation leads to upward velocities, and inside anticyclones to downward velocities, is being abandoned. Eddy-wind interaction through non linear Ekman pumping may also enhance PP at eddy peripheries. The question of which mechanism is more important, linear Ekman pumping at the eddy interior or non linear Ekman pumping at its periphery, is still under discussion (Mahadevan et al., 2008; McGillicuddy et al., 2008). Furthermore, in the case of eddies in the CEC it has also been observed that they

pulsate, hence varying their secondary circulation during their lifetimes (Sangrà et al., 2005, 2009). This is suggestive of a continual switching between upwelling and downwelling modes from birth to death.

Evidence of the enhancement of PP by eddies in the CEC may be extracted from the combined distribution of chlorophyll-a and the eddy field signal in sea surface height as depicted in Figure 3.5.3. At the western flank of the Canary Islands there is a clear increase of chlorophyll. This is related to mixing and an upward linear Ekman pumping velocity linked to the wind stress curl cyclonic cells that promote the generation of cyclonic eddies at the western flanks of the islands (see section 2). Far away from the archipelago we may observe cyclonic eddies C2, C3, and anticyclonic eddies A1 and J98. Cyclonic eddies produce an enhancement of chlorophyll-a most likely related to the shallowing of the nutricline. Enhancement of chlorophyll is also clearly visible in the interior of A1. This eddy is far from the coastal upwelling and hence this increase in chlorophyll-a may not be attributed to the entrainment of rich chlorophyll-a upwelled water; its signal is most likely related to interior self-induced linear Ekman pumping as a consequence of eddy-wind interaction. Eddy J98 also shows an enhancement of chlorophyll-a but only at its periphery, suggesting that eddy-wind interaction through the nonlinear Ekman pumping mechanism is in action at the eddy periphery. During their early stage of generation it is has been recurrently observed that Gran Canaria anticyclones entrain high-chlorophyll water from their interaction with upwelling filaments (Arístegui et al., 1997; Barton et al., 1998; Pacheco and Hernández-Guerra, 1999; Barton et al., 2004). This is the case for anticyclonic eddy A2 shown in Figure 3.5.3. Therefore, eddies in the CEC affect PP both locally and all along the extent of the CEC, producing an enhancement of PP. Sangrà et al. (2009) estimate an average of PP=1 gC m^{-2} d^{-1} per eddy, this being of one order of magnitude higher than the PP measured in the far-field waters (not affected by the eddy field) of the Canary region (Barton et al., 1998).

Sangrà et al. (2009) estimated that 17 annually produced eddies will lead to a total primary production for the CEC of *PTC*=13.3 10^{10} gC d^{-1}. Pelegrí et al. (2005a, b) estimated a mean value of primary production equal to 2.5$\pm$1.5 gC m^{-2} d^{-1} for the NAUS, about twofold higher than our estimate for the CEC. When integrated over the NAUS area between 22°N and 29°N this gives a total primary production for the upwelling region (*PTU*) along the latitude band of the CEC equal to *PTU*=10.5 10^{10} gC d^{-1}. This coincides with the value for the CEC suggesting that the CEC may be as productive as the NAUS. Therefore, the CEC may have a significant impact on biogeochemical fluxes in the northeastern subtropical Atlantic. This poses the question of whether the eastern North Atlantic subtropical gyre can be considered to be an oligotrophic system. Nevertheless, the above estimates should be taken with care as most are based on inference and not direct measurements. An effort is needed to improve these estimates. In particular most of the eddies in the CEC were sampled close to the Canary Islands and there are no corresponding *in situ* observations for eddies far from the islands.

3.5.5.2. Impact of the Northwest African Upwelling filament system on the offshore fluxes

Upwelling filaments may play a key role in transferring phytoplankton (Gabric et al., 1993; Pacheco and Hernández Guerra, 1999; García-Muñoz et al. 2004), nutrients (Barton et al., 1998; García-Muñoz et al., 2005), organic matter (Gracía-Muñoz et al. 2004, 2005, Álvarez-Salgado et al., 2007) and fish larvae (Bécognée et al., 2009; Brochier et al., 2011) from the coastal upwelling eutrophic region towards the interior oligotrophic subtropical gyre, contributing thus to its enrichment and to the setting up the Coastal Transition Zone. Such transport may exceed largely the Ekman transport and may extend several hundred kilometers offshore.

Most of the above studies have focused on the offshore export of particulate and dissolved organic matter by the filaments, since they may represent a significant flux of carbon to the interior ocean (García-Muñoz

et al., 2004, 2005; Álvarez-Salgado et al., 2007). Álvarez-Salgado et al. (2007) have estimated that Cape Ghir, Cape Jubi and Cape Bojador filaments export 35% to 58% of the net community production generated in the coastal upwelling systems as dissolved organic matter (DOM). García-Muñoz et al. (2005) estimated a 65% export for Cape Ghir filament and only a 25% for the Cape Jubi and Cape Bojador filaments. Gabric et al. (1993) estimated that the Cape Blanc filament exports 50% of the coastal primary production, being the carbon export 6×10^{12} g C yr^{-1}. This value is three orders of magnitude larger than those estimated by García-Muñoz et al. (2004, 2005) for the Cape Ghir and Cape Jubi filaments. Therefore, as pointed out by Gabric et al. (1993), the Cape Blanc filament may play a central role in the CCLME carbon cycle.

It has been estimated that offshore transport by filaments might accounts for 2.5 to 4.5 times the offshore carbon export driven by Ekman transport (Álvarez-Salgado et al., 2007), contributing significantly to plankton metabolism in the interior ocean. In particular, it has been suggested that it may partly account for the observed excess of community respiration over primary production in the oligotrophic interior ocean (Duarte et al., 2001, García-Muñoz et al., 2005). However, Álvarez-Salgado et al. (2007) suggested that only less than 16% of the exported carbon may be respired in the interior ocean, pointing out that filaments cannot fully account for the above metabolic imbalance (i.e. net heterotrophy) of the surface waters in the interior ocean. They also suggested that the remainder of the exported organic matter is accumulated within the subtropical gyre.

3.5.6. CONCLUDING REMARKS

The CEC constitutes a unique and distinctive feature between the CCLME and other EBUS. It is mainly the result of continuous eddy shedding from the Canary Islands that act as a topographic barrier to the Canary Current and Trade Winds. Such topographic barriers to the prevailing winds and currents, and thus a source for eddies, is not present in other EBUS. Observations and numerical modelling have contributed to the better understanding of island induced eddy generation mechanisms, eddy evolution, and eddy properties close the islands. However, there are many issues still to be resolved, mainly due to the lack of *in situ* observations of the dominant anticyclonic eddies in the interior of the CEC. In particular: What is the role of anticyclonic eddies in the CEC with respect to deep mixing? Do anticyclonic eddies in the interior of the CEC enhance primary production? What are the effects on the Oceanic Vertical Pump?

To address the above questions a four month old anticyclonic eddy, generated at Tenerife, was sampled in September 2014 near the location of eddy J98 of Figure 3.5.3 during an interdisciplinary cruise in the framework of the project PUMP (http://pump.ulpgc.es, accessed on 15 December 2014). We observed trapping of near inertial waves (NIW) at the base of the eddy at 400 m depth. Trapping of NIW by anticyclonic eddies has been predicted theoretically and observed for anticyclonic eddies close to the Canary Islands (Kunze, 1985; Martínez-Marrero et al., 2014). We also observed from a microstructure turbulence profiler and Lowered Acoustic Doppler Current Profiler (LADCP) data a mixing region as intense as the upper mixed layer, extending from 400 m depth to at least 800 m depth that is associated with the trapped NIW induced shear. These preliminary observations suggest that anticyclonic eddies in the CEC act as deep mixing structures. This may have profound implications in the modulation of AMOC variability and atmosphere-ocean interchanges. Concerning phytoplankton distributions we observed a clear enhancement of micro-phytoplankton biomass at the eddy periphery with respect to the far field. This gives *in situ* data support to the idea discussed in the preceding section about the role of long lived anticyclonic eddies in the CEC in enhancing primary production. However, secondary circulation is still being inferred

and thus the processes involved in the Oceanic Vertical Pump inside this typical anticyclonic eddy of the CEC are still unknown.

NAUS filaments may play a central role in the fluxes of biogeochemical properties for the CCLME. However, there remain many uncertainties that must be solved before it is possible to close the balance. This is mainly due to the lack of high resolution interdisciplinary surveys of the filaments system and the lack of seasonal variability studies. An effort is also needed on implementing coupled high-resolution physical-biogeochemical models. Sangrà et al. (2015) high-resolution study of Cape Ghir filament reveals that the flow structure of filaments may be quite complex, including both onshore and offshore flows at the mesoscale and submesoscale range. The onshore flows may greatly reduce the impact of the overall offshore transport of biogeochemical properties. Moreover, little is known about the secondary circulation and the related oceanic vertical pump (Klein and Lapeyre, 2009) inside filaments. Sangrà et al. (2015) observed a noticeable downward flux of particles related with the occurrence of an ITE linked to the Cape Ghir filament system, and argued that the ITE related secondary circulation may act both as a sink of carbon and to reduce the offshore carbon export by the filament.

Acknowledgements

The Group for High-Resolution Sea Surface Temperature (GHRSST, https://www.ghrsst.org/, accessed 9 April 2015) is acknowledged for providing the SST data. We acknowledge Dr. Charles Troupin (SOCIB) for processing those SST data. We also acknowledge the Ocean Color NASA Earth Data Center (Giovanni Ocean Color Radiometry Online Visualization and Analysis http://gdata1.sci.gsfc.nasa.gov/daac-bin/G3/gui.cgi?instance_id=ocean_month, accessed 9 April 2015) for providing MODIS image. This work has been partly supported by the Spanish government through project PUMP (CTM2012-33355).

3.6. WAVES AND TIDES IN THE CANARY CURRENT LARGE MARINE ECOSYSTEM

Marta GÓMEZ, Begoña PÉREZ-GÓMEZ, Marta DE ALFONSO, Susana PÉREZ and Mª Isabel RUIZ

Puertos del Estado, Ministerio de Fomento. Spain

3.6.1. INTRODUCTION

In recent decades, and in parallel to the increase in the computational capabilities and improvements in telecommunications, a remarkable progress in the development of equipment for marine environment monitoring has been carried out. Many countries are implementing permanent measurement networks, as well as climate forecast and data management systems. The information generated by these tools is distributed to the whole society.

In this context, Puertos del Estado (hereinafter PdE) has developed permanent networks and forecast models of marine physical variables, giving coverage to all of the Spanish national territory and to the routes of navigation starting or ending at Spanish ports.

This article describes waves and tides regime and variability in the Canary Current Large Marine Ecosystem region (CCLME). The study is based on those sources of data with adequate and relevant information (products) that allow a reasonable description of these two oceanographic variables, being PdE equipment and numerical models the main source of information. A review of existing buoys, tide gauges and numerical models available in the region was performed by contacting different institutions from the affected countries as well as international organizations.

3.6.2. WAVES: DATA AND METHODOLOGY

3.6.2.1. *In situ* data

In the CCLME region wave data from PdE wave buoys are available. Figure 3.6.1 shows the position of the existing buoys in the area of interest. All of them belong to PdE networks. Table 3.6.1 shows the location, mooring depth and the data availability for these stations.

The three SeaWatch buoys belong to PdE Deep Water network (Álvarez-Fanjul et al., 2002). They are multipurpose buoys providing parameters of meteorology (wind speed and direction, air temperature and pressure), directional waves since 2003 and subsurface oceanography (currents, sea temperature and salinity). A Directional Waverider wave sensor is installed since 2003. Before this date, the wave sensors were scalar providing only height and period parameters.

The Triaxys buoy is part of PdE coastal buoy network. Due to its mooring location, data provided by this buoy are only representative of the closest surrounding area.

The wave sensor takes samples during approximately 30 minutes every hour. Those samples correspond to vertical (heave) and horizontal displacements respect to the North and East axis.

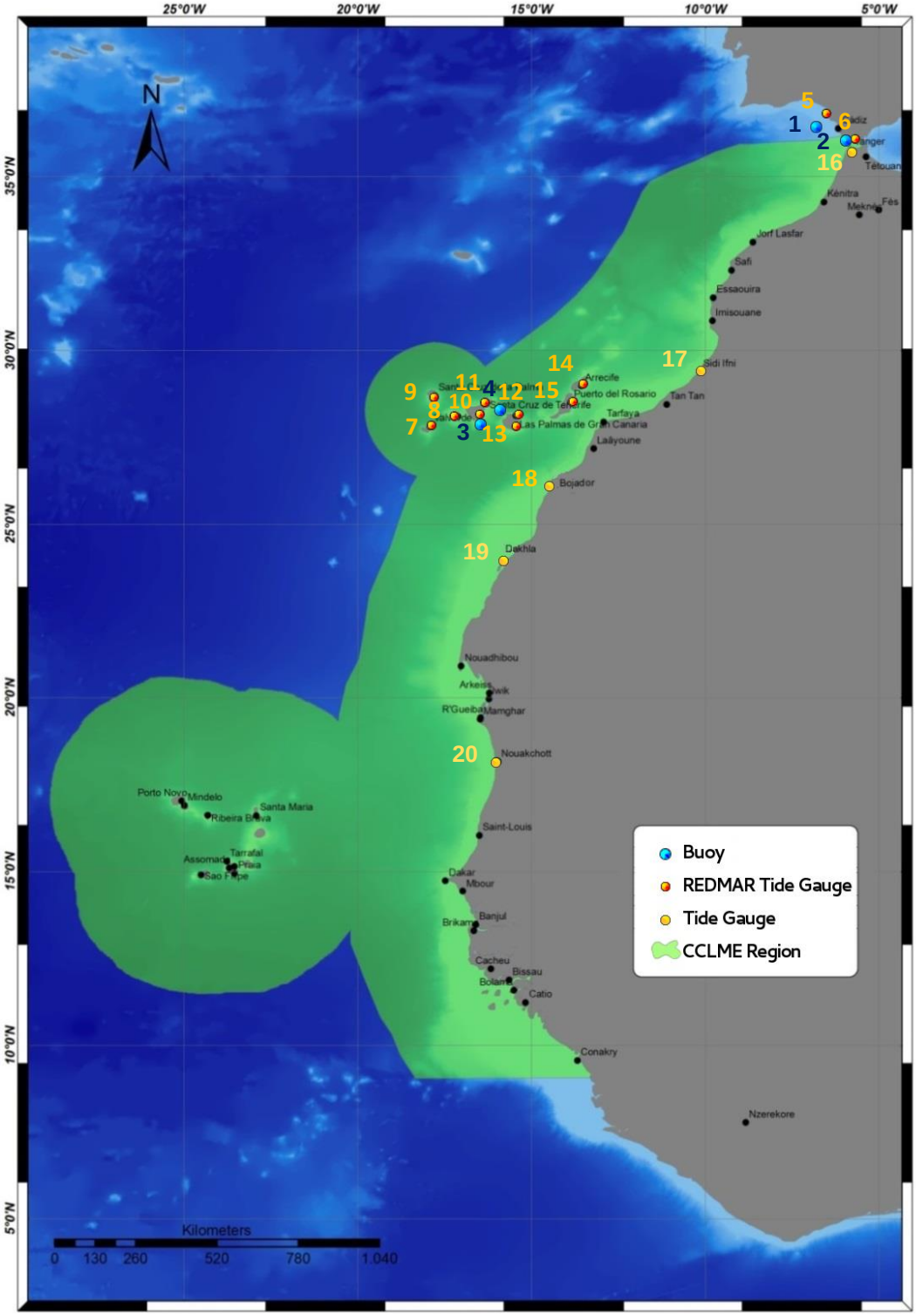

Figure 3.6.1. Area of interest and sensors location. The dark numbers correspond to the buoys listed in Table 3.6.1., and the yellow numbers correspond to the tide gauges listed in Tables 3.6.2 and 3.6.3.

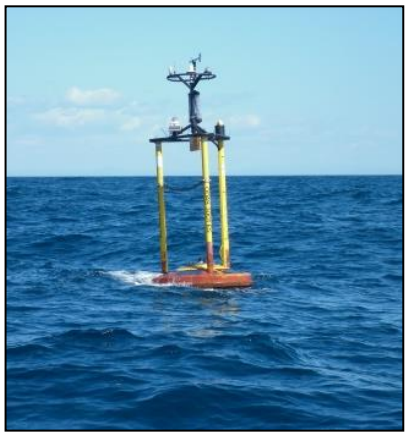

Figure 3.6.2. Left picture: Seawatch buoy from the Deep Water Network; Right picture: Triaxys buoy from the Coastal Network.

Table 3.6.1. Description of the PdE wave measurement stations (number of station corresponds to the number shown on the map in Figure 3.6.1)

Station	Latitude	Longitude	Mooring Depth	Buoy Type	Data availability
1. Golfo de Cádiz	36.48°N	06.96°W	450 meters	SeaWatch	Since 1996
2. Tarifa	36.00°N	05.59°W	33 meters	Triaxys	Since 2008
3. Tenerife	27.99°N	16.58°W	710 meters	SeaWatch	Since 1997
4. Gran Canaria	28.20°N	15.80°W	780 meters	SeaWatch	Since 1996

Buoys have a processor on-board that performs a spectral analysis using the three displacements time-series. As a result, the main spectral parameters are obtained and sent to PdE in real time. These parameters are: significant wave height, mean wave period, peak wave period, mean wave direction and mean wave direction at the spectral peak (Alfonso et al., 2005).

When buoy maintenance is performed, raw displacement series are downloaded from the on-board data logger and then reprocessed at PdE applying an exhaustive quality control procedure and increasing the number of computed parameters (from spectral and zero up crossing analysis).

3.6.2.2. Wave models

PdE has carried out a wave hindcast for the Atlantic Ocean based on the numerical models WAM (WAMDI Group, 1988) and WAVEWATCH III (Tolman, 1991). The boundaries of the area covered by the models, shown in Figure 3.6.3, are: 67°N–20°N, 59°W–8°E, with a variable resolution that goes from 1° in the open waters to 5' in the Gulf of Cadiz and the Canary Islands

This hindcast provides information of all the wave parameters since 1958 to 2005 and it is daily updated with the information provided by the analyzed time series of PdE wave forecast system (Gómez-Lahoz and Carretero-Albiach, 2005). The points shown in Table 3.6.3 have been selected to characterize the waves in the area.

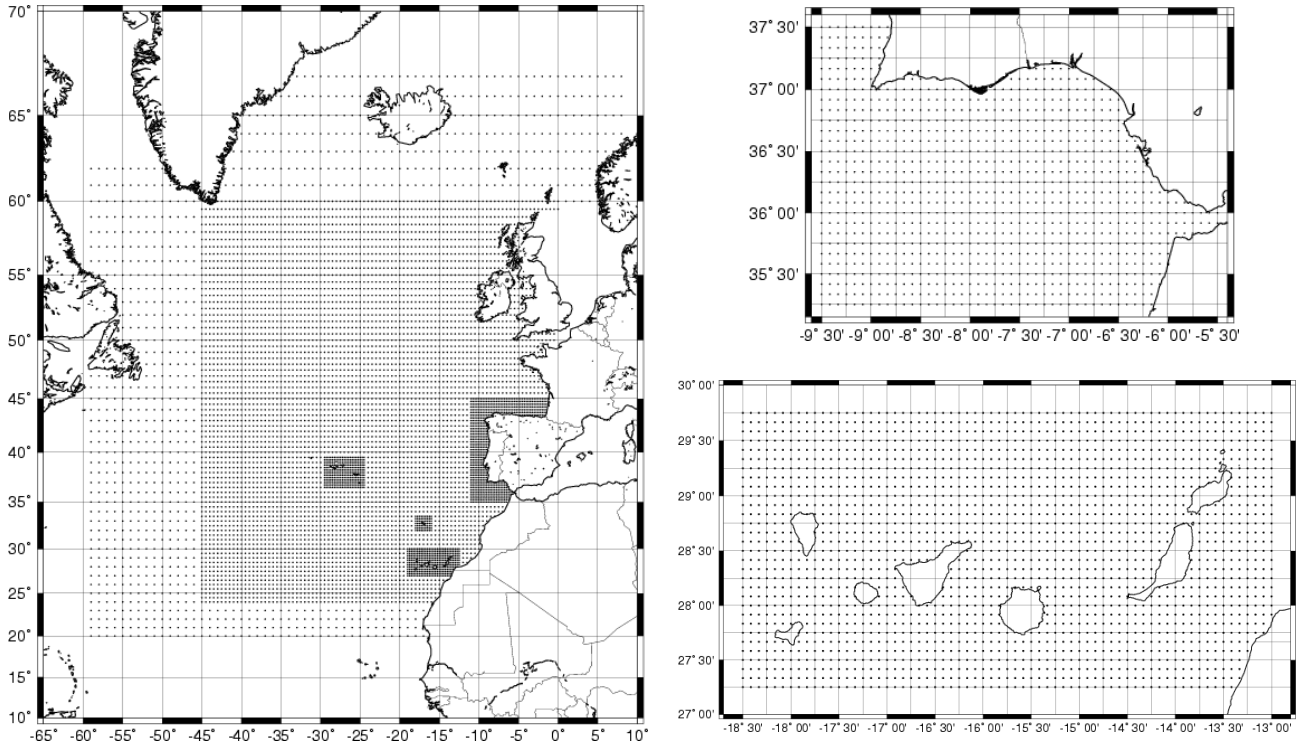

Figure 3.6.3. The Atlantic grid on the left; on the right hand above, the Gulf of Cadiz grid; and on the right hand bellow, the Canary Islands grid.

Table 3.6.2. Wave model selected points (number of station corresponds to the number shown on the map in Figure 3.6.7)

Point	Latitude	Longitude
1. 1040042	35.50°N	10.00°W
2. 1030030	32.50°N	12.50°W
3. 4032028	29.58°N	15.83°W
4. 4010008	27.92°N	17.67°W
5. 4030010	28.08°N	16.00°W
6. 4044008	27.92°N	14.83°W
7. 4066012	28.25°N	13.00°W
8. 1036016	29.00°N	11.00°W
9. 1040024	31.00°N	10.00°W
10. 1044032	33.00°N	09.00°W
11. 1050036	34.00°N	07.50°W
12. 5040000	35.25°N	06.17°W
13. 6048012	35.95°N	05.70°W

The wave hindcast (1958-2005) was forced with ERA40 and ERA-Interim re-analysis. The Wave Forecast System forcing (2006 to present day) is provided by HIRLAM model run by the Spanish Meteorological Agency (AEMET in its Spanish acronym).

Being 20°N the southern limit of PdE application, the area of interest of this project is partially covered by this system. As a matter of fact, the waves propagating from the south that affect the Canary Islands are not reproduced in PdE wave data.

On the other hand, a wave forecast system was developed for the area of interest in the framework of the Marinemet project that was carried out in collaboration between AEMET and PdE (http://www.afrimet.org/marinemet/, accessed on 15 January 2015). The information provided by this system, has not been used in this publication because, although very interesting from the forecast point of view, it is not useful for wave climatic characterization.

3.6.3. TIDES: DATA AND METHODOLOGY

3.6.3.1. *In situ* data

Tide gauges constitute the main and more precise source of tidal constants information along the coast. Most of the information concerning tides has been obtained from PdE tide gauges (REDMAR network) at the Gulf of Cádiz and the Canary Islands (Figure 3.6.1, Table 3.6.3), most of them upgraded to radar sensors (Miros) since 2007. The radar sensors provide sea level measurements and local wind waves at the harbours (Pérez-Gómez et al., 2013; Pérez-Gómez et al., 2014) and consist of an antenna located at the pier well above the higher high water that provides sea level information related to harbour and national datums by emitting radar pulses to the water surface (Figure 3.6.4, right).

The nominal sea level data sampling and latency nowadays is 1-min; at PdE these data are routinely quality controlled in near-real time, processed and filtered to hourly values before computing the harmonic analysis each calendar year by means of the Foreman analysis and prediction package (Foreman, 1977). This allows the study of the annual variability and trends of these harmonic constants (Woodworth, 2010; Pérez-Gómez, 2014). The residual component (mainly meteorological in origin) is obtained after extracting the astronomical tide to the hourly sea level observations.

Additional information on tidal constants was required to other countries as well as other institutions such as Global Sea Level Observing System (GLOSS). Harmonic constants from Nouakchott (Mauritania) were provided by the Laboratory of Atmospheric Physics and Fluid Mechanics, Cote d'Ivoire. The Spanish Hydrographic Institute (hereafter IHM, in its Spanish acronym) on the other hand, provided harmonic constants from Tánger and Ifni (Morocco), and Cape Bojador and Dakhla (Western Sahara). The operation of these stations has been discontinuous in the past and the access to relevant products is not always possible. The Cape Bojador, Ifni and Dakhla harmonic constants were obtained in the 40's by IHM, so their value should be carefully considered here. Finally, tidal constants were also provided by the Instituto Español de Oceanografía (IEO) for Cadiz tide gauge (Gulf of Cadiz, Spain).

Table 3.6.3. Description of sea level (tide) measurement stations (number of station corresponds to the number on the map in Figure 3.6.1).

Station	Latitude	Longitude	Tide Gauge Type	Data availability
5. Bonanza	36.800°N	06.333°W	Miros (radar)	Since 1992
6. Tarifa	36.006°N	05.630°W	Miros (radar)	Since 2009
7. El Hierro	27.780°N	17.900°W	Miros (radar)	Since 2004
8. La Gomera	28.088°N	17.108°W	Miros (radar)	Since 2006
9. La Palma	28.678°N	17.768°W	Miros (radar)	Since 2006
10. Tenerife	28.483°N	16.233°W	Miros (radar)	Since 1992
11. Granadilla	28.090°N	16.490°W	Aanderaa (pressure)	2004-2012
12. Las Palmas	28.150°N	15.330°W	Miros (radar)	Since 1992
13. Arinaga	27.850°N	15.400°W	Aanderaa (pressure)	2004-2012
14. Arrecife	28.900°N	13.530°W	Miros (radar)	Since 2008
15. Fuerteventura	28.500°N	13.850°W	Miros (radar)	Since 2004
16. Tánger	35.783°N	05.800°W	?	May-June, 2005
17. Ifni	29.550°N	10.067°W	?	March-April, 1949
18. C. Bojador	26.117°N	14.500°W	?	Sept.-Oct., 1948
19. Dahkla	23.633°N	16.000°W	?	Nov, 1948-Jan.,1949
20. Nouakchott	17.984°N	16.033°W	?	2007

3.6.3.2. Tidal models

Another important sources of information are global and regional tidal models, which allow a better spatial characterization of the tide in open waters. Their accuracy along the coast will depend on the spatial resolution and the quality of the bathymetry. A new regional tide atlas, provided by Noveltis, Legos and CNES and based on the COMAPI tide model was used (Cancet et al., 2010), with a resolution of 1'x1'. Unfortunately, this high resolution is up to now available only between 22.5°N and 37°N, i.e. we lack information south of Mauritania (Figure 3.6.4, left).

PdE provides operational sea level forecasts for a domain covering the whole Spanish coast, the Mediterranean and the Canary Islands up to 25°N by means of the Nivmar system. This system was established in 1998 based on the combination of the surge or meteorological forecast obtained with the HAMSOM model and the tide forecast obtained at the harbours from the REDMAR network (Álvarez-Fanjul et al., 2001). Nowadays, the system includes the tide forecast at the coast by means of the mentioned high resolution regional tidal atlas for coastal and shelf seas developed by Noveltis, Legos and CNES (COMAPI).

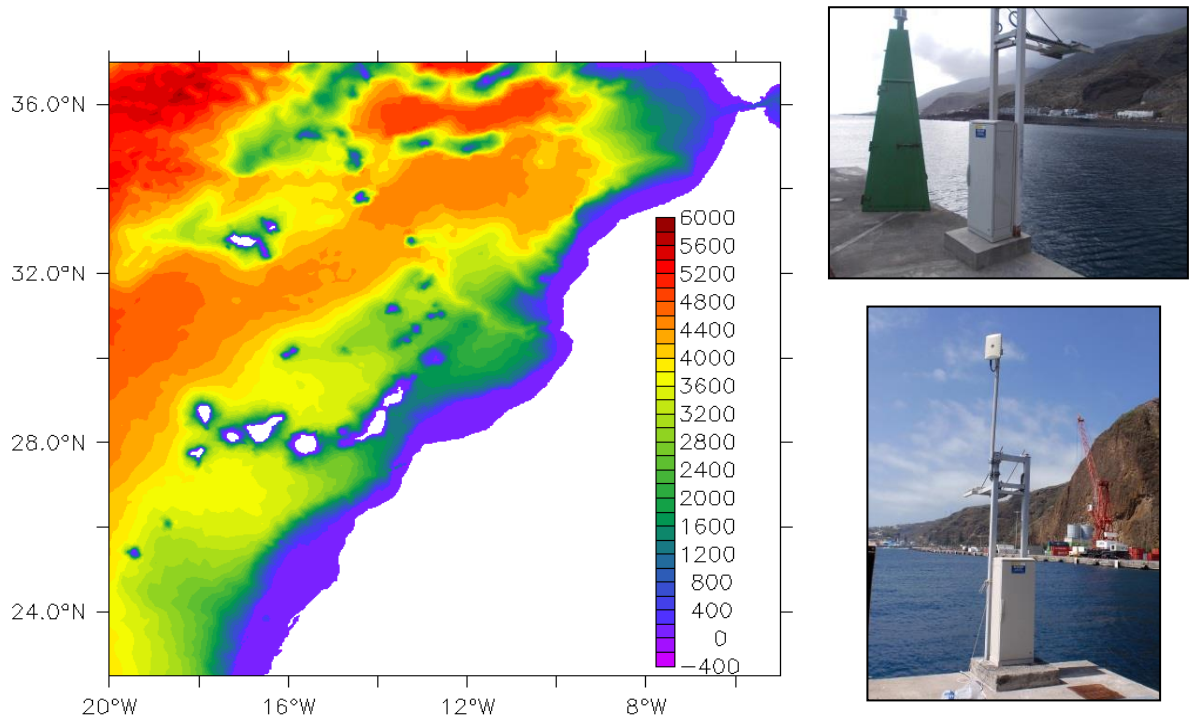

Figure 3.6.4. Left panel: domain and bathymetry of the COMAPI tidal atlas, extracted from the regional product of the North-East Atlantic for the Canary Current region (up to 22.5°N only), one of the sources of data employed for tides description. At right: El Hierro (top) and La Palma (bottom) radar tide gauges from the Spanish REDMAR network.

The domain of the COMAPI tidal atlas for the North East Atlantic (NEA) is a little bit larger at this area than the sea level hindcasts available at PdE (up to 22.5°N) so the analysis of the spatial variation of the main components of the tide is based on this tidal atlas. Its resolution (1'x1') improves significantly in relation to the ones from previous global tidal models such as FES2004, GOT4.7 and TPX07.2, and to the Nivmar system itself (10'x15'). The COMAPI tidal atlas is based on new regional implementations of a hydrodynamic finite element tide model (T-UGOm) combined with altimetry and tide gauge data assimilation; it includes better information of the classical tidal waves near the coast and extension to some of the non-linear constituents. A set of 37 harmonic constituents is available at each grid point.

3.6.4. RESULTS AND DISCUSSION

3.6.4.1. Mean and extreme wave climate

Wave roses of the 4 buoys are presented in Figures 3.6.5 and 3.6.6 while wave roses at 13 model points are shown in Figure 3.6.7. These wave roses represent the percentage of data in each direction for different significant wave height (Hs) intervals that are indicated by different blue tones.

In the case of the buoys the Hs intervals are taken from 0.0 m to 2.5 m with a 0.5 m width, with the last color indicating waves over 2.5 m, and in the case of the model points the intervals go from 0.2 m up to 5 m, with an interval width of 1 m. The last color indicates waves of more than 5 m.

Regarding the directional information, sixteen directions have been considered that indicate the waves incoming direction.

These wave roses give a description of the mean wave climate in each area, as they indicate the main direction from which the waves come and the distribution of the significant wave height.

It is important to distinguish between the wave roses that represent open deep water conditions from those at coastal points, that can be very much affected by the coast line. This remark is especially important at the Canary Islands where, in general, each location is affected by different islands.

It can be said that the wave rose of Golfo de Cádiz buoy (Figure 3.6.5) and of model points number 1, 2 and 3 (Figure 3.6.7), represent open deep water conditions, while the others represent coastal conditions.

At open and deep water locations, the most common wave height is between 1 m and 3 m, being higher at northern locations and decreasing as moving southwards.

In regard with the wave direction, the Gulf of Cadiz is dominated by waves coming from the west and the main directions turn, first to the north and finally to the north-east as we move southwards, being the northeast the main direction at model point number 3 (Figure 3.6.7) at the north of Canary Islands.

As it has been said, the wave conditions at coastal points are very much affected by the coast line and some of them only represent very local wave climate.

This is the case of the Tarifa buoy (Figure 3.6.5), in which there is no presence of waves coming from the west, while in model point number 13 (Figure 3.6.7), that is very close to the buoy, the west is the main direction. It is well known that the wave climate at the Strait of Gibraltar has two main components, from the west and the east respectively, as it is shown in the wave rose of point number 13, but the buoy is protected from this direction by the coast line.

Model points from 8 to 12 (Figure 3.6.7) represent the wave climate along the Moroccan coast. It can be seen that the main direction is the north-west being more northern or western depending on the coast orientation. The most frequent significant wave heights are between 1 m and 3 m, being a little bit lower at points 11 and 12 because they are a little bit protected by San Vicente Cape.

Additionally, at the Canary Islands, the wave climate is represented by the wave roses of Gran Canaria and Tenerife buoys (Figure 3.6.6) and model points from 4 to 7 (Figure 3.6.7). In general, it can be seen that the main direction is north-northeast but, analysing each single case, it depends very much on the point location related with the different islands. The most common significant wave height is between 1 m and 2 m, that is lower than in the locations at open deep water or at the Moroccan coast because of the protection provided by the Islands.

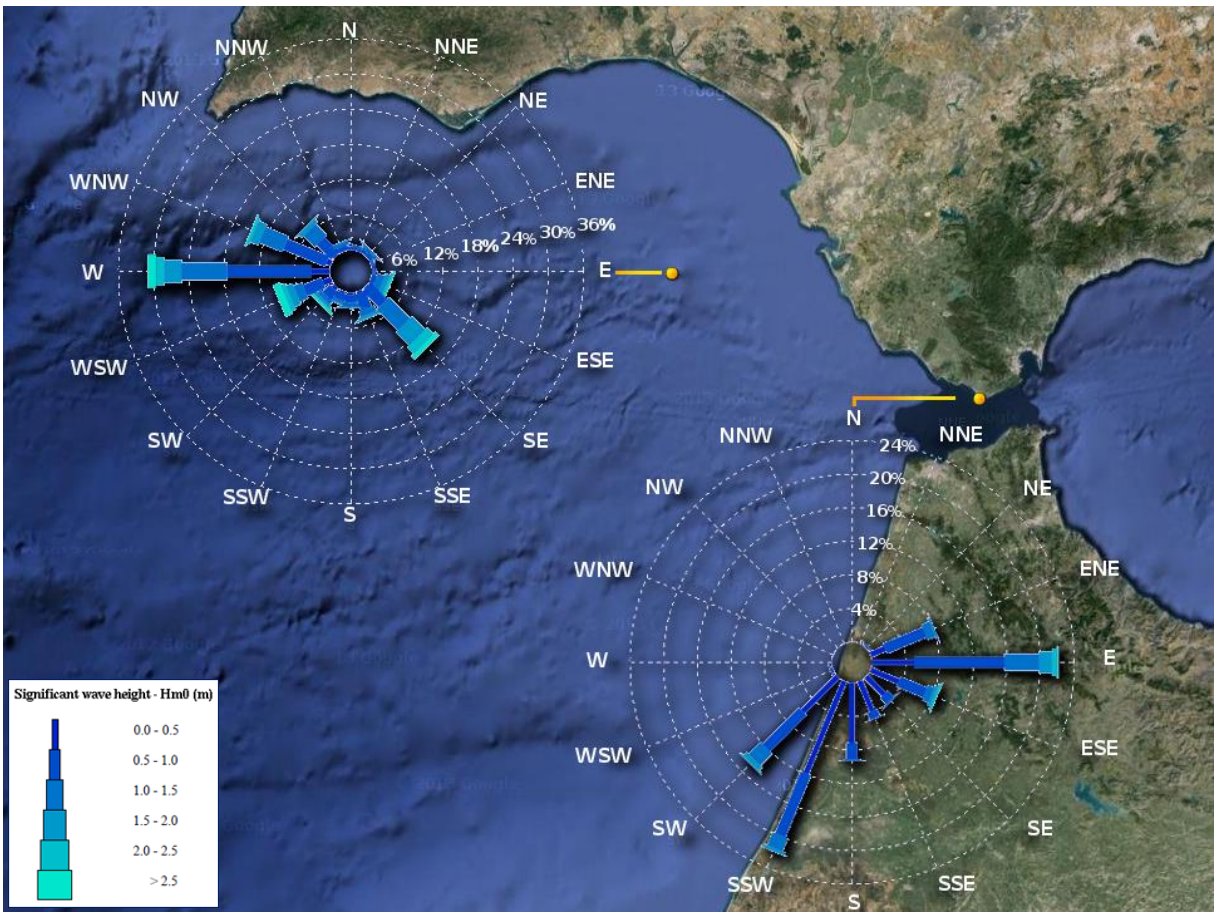

Figure 3.6.5. Wave roses from Golfo de Cádiz (left) and Tarifa (right) buoys (yellow dots)

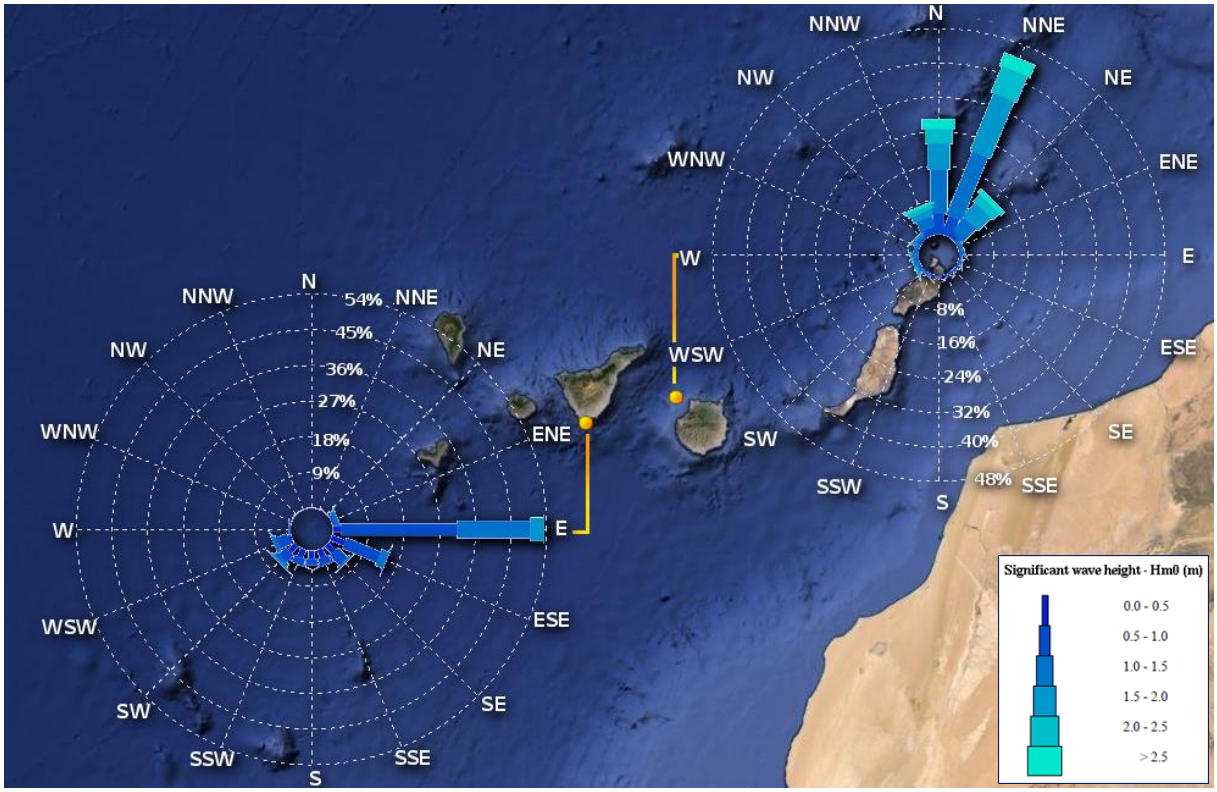

Figure 3.6.6. Wave roses from Tenerife (left) and Gran Canaria (right) buoys (yellow dots).

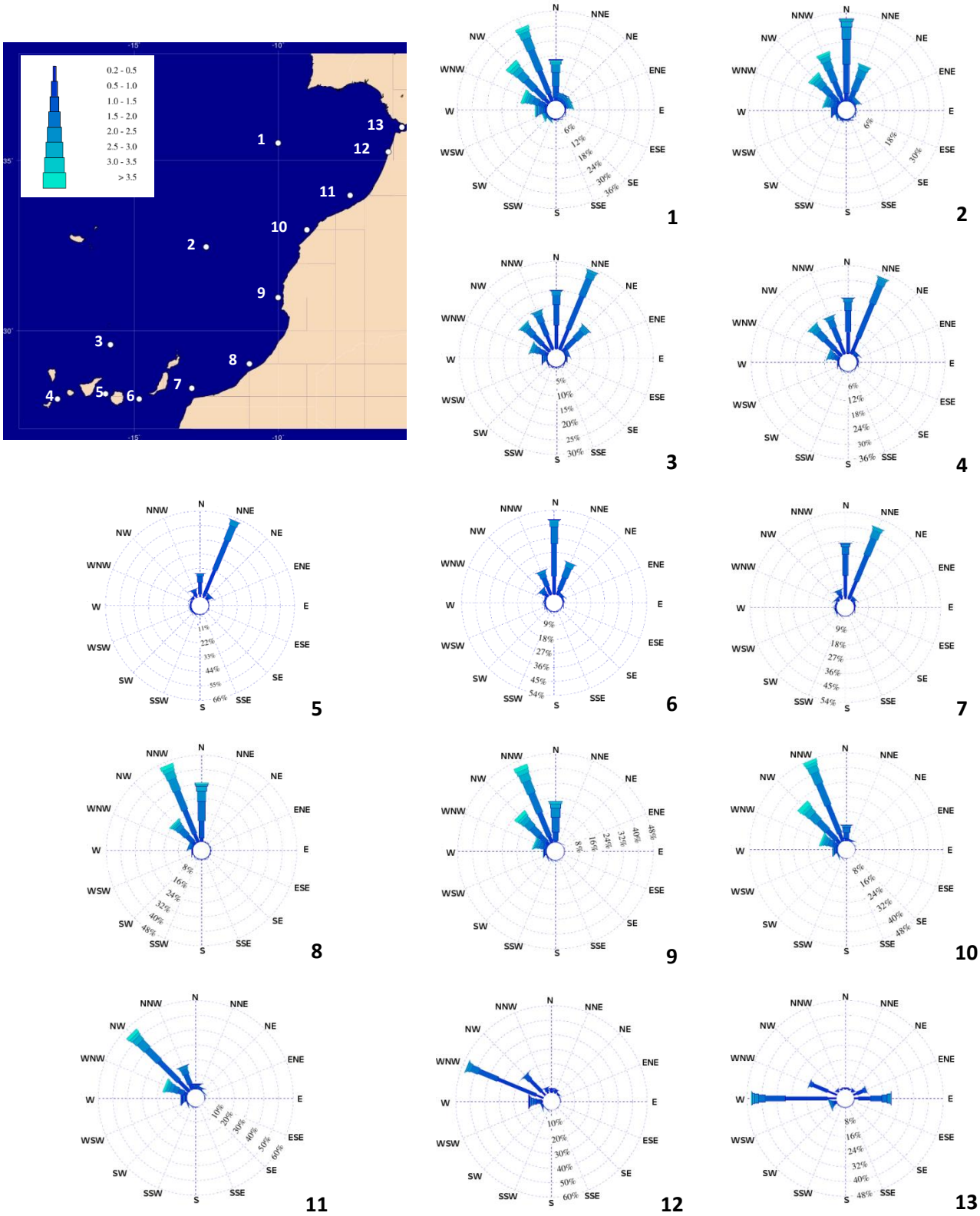

Figure 3.6.7. Wave roses of 13 model points representing different locations of the area of interest.

The most extreme significant wave height ever registered by the 4 buoys and obtained at the 13 model points per season are shown in Tables 3.6.4 and 3.6.5.

Unfortunately, some of the buoys have not always been directional buoys and the extreme events have occurred in dates in which they were not, so there is not information about the direction. In these cases, directional information from the nearest wave model point was used to draw conclusions.

It can be seen that, as expected, the highest extreme storms appear during the winter season. Autumn and spring seasons are very similar while the lowest extreme storms appear in summer. This is valid not only for the significant wave height, but also for the peak period.

The Golfo de Cádiz buoy is an exception because the highest significant wave height was registered in spring. However, it can be considered a rare event, because taking a more general look of this buoy data, most of the highest storms appear during the winter season, as in the other locations.

There is more difference between one location and the others in winter, being the climate more severe in the North than in the South. In summer the extreme wave climate is very similar at all the locations.

Regarding the directions, it can be seen that almost all the extreme events come from the north-west, being slightly more western in winter than in summer.

All the seasonal differences are more evident at the northern locations than at the southern ones.

Table 3.6.4. The highest significant wave height (Hs) ever registered by the 4 buoys, per season (W: winter, Sp: spring, S: summer, A: autumn). The corresponding peak period (Tp), direction and date are also shown. Number of station corresponds to the number on the map in Figure 3.6.1.

Buoy	Season	Max. Hs (m)	Tp (s)	Direction (0-N,90-E)	Date (GMT)	Buoy	Season	Max. Hs (m)	Tp (s)	Direction (0-N,90-E)	Date (GMT)
1. Golfo de Cádiz	W	6.2	10.7	--	1997/12/18 02h	3.Tenerife	**W**	**4.8**	**9.4**	**--**	**1999/01/08 03h**
	Sp	**6.6**	**15.0**	**--**	**2003/04/13 23h**		Sp	3.6	9.1	230	2013/03/03 22h
	S	3.5	8.5	--	1997/06/05 12h		S	2.7	6.4 7.8	90 107	2009/07/25 02h 2013/08/07 01h
	A	3.6	8.5	--	1999/09/19 13h		A	3.2	9.4	--	1998/10/09 14h
2. Tarifa	**W**	**3.6**	**10.5**	**107**	**2010/01/28 01h**	4. Gran Canaria	**W**	**5.7**	**13.5**	**--**	**1999/01/12 09h**
	Sp	3.3	9.0	107	2011/04/05 22h		Sp	5.2	9.8	--	2001/03/13 21h
	S	1.8	7.1	83	2013/06/25 07h		S	3.8	8.5	--	2000/06/10 13h
	A	2.9	8.9	105	2012/11/08 10h		A	5.5	16.6	337	2014 /11/29 06h

The extreme events have lower significant heights at the buoy locations than at the model points because, as it has been said in the previous section, the sensors are placed relatively close to the coast, so they are protected by it. On the other hand, the locations in which the extreme storms are the highest are in the model points 1, 2, 9, 10 and 11 that, as it can be seen in Figure 3.6.7, are the less protected by the coast.

Table 3.6.5. The highest significant wave height (Hs) ever got at each of the 13 the model points, per season (W: winter, Sp: spring, S: summer, A: autumn). The corresponding peak period (Tp), direction and date are also shown (number of station corresponds to the number on the map in Figure 3.6.7).

Point	Season	Max. Hs (m)	Tp (s)	Direction (0-N,90-E)	Date (GMT)
1	**W**	**10.2**	**17.5**	**307**	**1973/01/17 12h**
	Sp	7.8	12.3	77	1955/03/31 21h
	S	4.3	9.3	357	1979/08/16 00h
	A	7.2	16.1	296	1982/11/08 03h
2	**W**	**8.6**	**18.0**	**288**	**1966/02/21 03h**
	Sp	6.7	15.3	299	1989/04/09 09h
	S	4.1	14.8	356	2008/08/19 15h
	A	6.2	15.1	308	2014/11/29 05h
3	W	6.6	13.4	308	1989/12/29 00h
	Sp	5.8	13.8	285	2013/03/05 12h
	S	3.3	9.0	38	2012/07/12 10h
	A	**7.0**	**13.6**	**314**	**2014/11/29 00h**
4	W	5.8	18.0	314	1966/02/21 06h
	Sp	5.4	13.5	290	2013/03/05 04h
	S	4.1	8.3	29	2012/07/15 05h
	A	**6.0**	**14.2**	**321**	**2014/11/29 06h**
5	**W**	**4.9**	**11.0**	**29**	**2014/01/24 10h**
	Sp	4.6	8.5	230	2013/03/03 23h
	S	3.3	8.8	28	2012/06/12 02h
	A	4.6	14.5	343	2014/11/29 10h
6	**W**	**6.3**	**12.2**	**319**	**1972/02/23 06h**
	Sp	4.5	18.9	353	2014/03/04 11h
	S	3.3	8.9	17	2012/07/12 10h
	A	**6.3**	**14.6**	**326**	**2014/11/29 10h**
7	**W**	**5.6**	**11.8**	**10**	**1994/01/17 18h**
	Sp	5.2	11.2	22	1994/04/03 09h
	S	3.7	9.5	10	2007/06/22 21h
	A	4.6	14.9	319	2014/11/29 16h
8	**W**	**8.8**	**18.3**	**322**	**1982/01/12 15h**
	Sp	6.4	17.8	310	1991/03/07 12h
	S	4.7	10.8	357	1966/06/11 00h
	A	6.5	18.1	332	1962/11/07 06h
9	**W**	**10.4**	**18.3**	**309**	**1982/01/12 12h**
	Sp	7.3	17.9	301	1991/03/07 06h
	S	4.7	9.1	358	2012/06/12 20h
	A	7.5	18.1	323	1962/11/07 03h
10	**W**	**9.6**	**18.3**	**290**	**1966/02/21 00h**
	Sp	7.4	17.8	297	1991/03/07 06h
	S	3.7	13.4	322	1961/06/01 00h
	A	8.0	11.7	268	1989/11/19 18h
11	**W**	**9.7**	**18.2**	**283**	**1966/02/21 06h**
	Sp	7.3	17.7	290	1991/03/07 09h
	S	3.7	13.2	309	1961/06/01 00h
	A	8.3	15.9	293	1984/11/05 06h
12	**W**	**8.1**	**17.2**	**293**	**1973/01/17 21h**
	Sp	5.0	14.5	275	1991/03/07 15h
	S	2.6	14.3	296	1985/06/01 09h
	A	4.8	11.5	258	1982/11/07 15h
13	**W**	**6.2**	**10.9**	**272**	**2013/01/19 18h**
	Sp	4.8	11.2	257	2013/03/06 08h
	S	2.5	6.5	83	2013/06/25 11h
	A	4.0	9.1	81	2008/10/11 00h

3.6.4.2. Tides regime

The relative importance of the tide and the meteorological component was estimated by computing the standard deviation of the tidal elevations and the meteorological component for the REDMAR stations during the year 2012 (Figure 3.6.8, left). Examples of the probability density functions or histograms of both components are also displayed in Figure 3.6.8 (right).

Station	Tide Stdv (cm)	Res Stdv (cm)
Bonanza	70.48	6.48
Tarifa	33.46	6.15
Tenerife	55.95	3.88
Granadilla (Tenerife)	49.73	9.44
La Palma	51.99	3.91
La Gomera	46.81	3.70
El Hierro	47.47	4.00
Las Palmas (G. C.)	59.25	4.19
Arinaga (G. C.)	53.89	4.85
Fuerteventura	64.06	3.44
Arrecife (Lanz.)	66.48	3.51

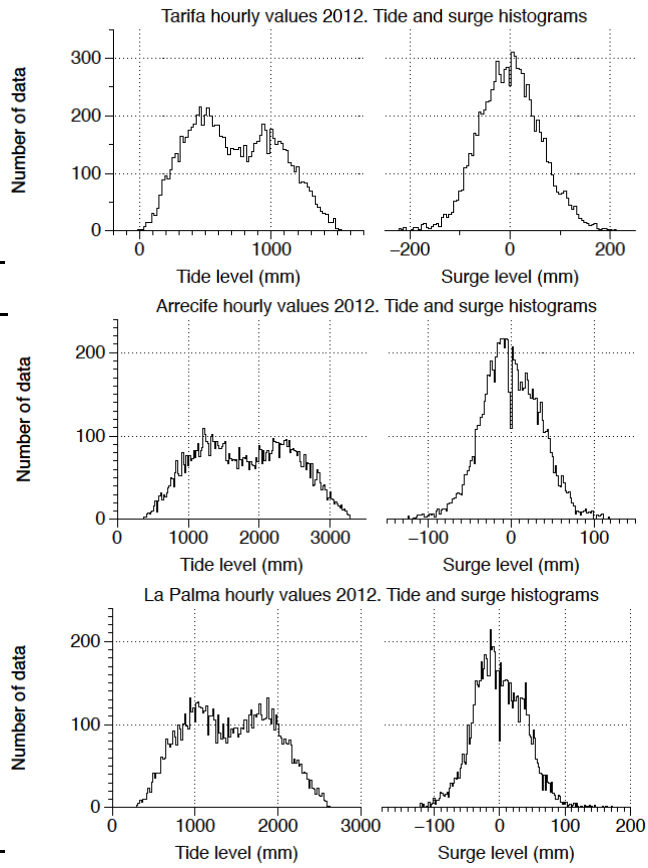

Figure 3.6.8. Left: Standard deviation (Stdv) of the tide and the meteorological or residual component for REDMAR tide gauges in the region (year 2012). Right: From the top to the bottom, tide and surge histograms for Tarifa (Gulf of Cadiz), Arrecife (Lanzarote, Eastern Canary Islands) and La Palma (Western Canary Islands) (hourly data, year 2012).

The amplitudes and phases of the main semidiurnal (M_2, S_2) and diurnal (O_1, K_1) constituents were compiled in Table 3.6.6, not only for the REDMAR stations but also for the ones provided by other organizations. The period of data used for the computation is included, as well as the Form Factor F obtained from the ratio of the amplitudes of these main constituents:

$$F = \frac{A(O_1) + A(K_1)}{A(M_2) + A(S_2)}$$

The value of F is usually employed for tides classification (Pugh, 1987): diurnal, semidiurnal or mixed.

Finally, the spatial variation of the main tidal constituents is shown from COMAPI model at Figures 3.6.9 and 3.6.10.

The Form Factor values in Table 3.6.6, well below 2.5 for all the stations, indicate a clear dominant semidiurnal tide (two highs and two lows per day) in the Canary Current region from the Gulf of Cadiz up to Mauritania. This reflects in the two peaks observed in the tide histograms of Figure 3.6.8 (right), the most probable levels being close to the mean high waters and mean low waters respectively. This is coherent on the other hand with the larger amplitudes of the semidiurnal constituents (M_2 and S_2) in Table 3.6.6, with respect to the diurnal ones at all the stations we could compile.

Table 3.6.6. Amplitude and phase of the main semidiurnal and diurnal tidal constituents, form factor (F) and period of data for its computation. REDMAR stations are shown in bold. Harmonic constants provided by other institutions for those stations shaded in grey.

Station	M_2		S_2		O_1		K_1		F	Years
	Amp (cm)	Phase Lag (o)	Amp (cm)	Phase Lag (o)	Amp (cm)	Phase Lag (o)	Amp (cm)	Phase Lag (o)		
Gulf of Cadiz:										
Bonanza	**89.87**	**63.74**	**30.89**	**90.33**	**6.12**	**322.58**	**6.15**	**60.30**	**0.102**	**2010-2012**
Cádiz	99.67	65.13	35.93	92.82	6.60	307.63	6.76	51.28	0.081	2013
Tarifa	**41.73**	**41.63**	**15.66**	**68.88**	**0.48**	**128.49**	**2.63**	**129.5**	**0.054**	**2010-2012**
Tánger (Morocco)	68.32	65.36	17.92	71.11	4.46	336.13	6.58	60.18	0.128	2005
Canary Islands:										
Tenerife	**70.63**	**28.92**	**27.18**	**52.61**	**4.69**	**292.84**	**6.25**	**40.32**	**0.112**	**2010-2012**
Granadilla (Tenerife)	**61.30**	**25.96**	**24.63**	**47.31**	**4.74**	**292.26**	**5.95**	**40.72**	**0.124**	**2003-2011**
La Palma	**65.16**	**30.30**	**25.51**	**52.96**	**4.58**	**293.65**	**5.78**	**41.64**	**0.114**	**2007-2012**
La Gomera	**57.94**	**23.58**	**23.35**	**45.92**	**4.34**	**290.05**	**5.58**	**32.97**	**0.122**	**2007-2012**
El Hierro	**59.46**	**21.23**	**24.26**	**43.76**	**4.30**	**290.67**	**6.13**	**32.33**	**0.125**	**2010-2012**
Las Palmas (G. Canaria)	**75.27**	**28.38**	**28.97**	**53.17**	**4.88**	**293.45**	**6.19**	**40.05**	**0.106**	**2008-2012**
Arinaga (Gran Canaria)	**68.08**	**28.18**	**26.64**	**50.60**	**4.76**	**292.33**	**6.04**	**37.24**	**0.114**	**2003-2011**
Fuerteventura	**80.89**	**32.33**	**30.53**	**56.21**	**5.18**	**294.34**	**6.14**	**38.53**	**0.102**	**2010-2012**
Arrecife (Lanzarote)	**84.23**	**34.82**	**31.73**	**58.35**	**5.22**	**295.99**	**6.84**	**42.10**	**0.104**	**2008-2012**
West Africa coast:										
Ifni (Morocco)*	91.38	38.47	40.78	76.55	3.53	278.55	4.37	290.1	0.060	1949
C. Bojador (W. Sah.)*	61.55	18.65	33.40	38.24	3.98	283.55	3.02	15.75	0.070	1948
Dakhla (W. Sah.)*	68.55	11.30	19.81	33.47	3.74	279.09	7.69	35.13	0.130	1949
Nouakchott (Maur.)	42.71	28.98	17.37	30.00	4.25	-	6.28	15.04	0.178	2007

The surge or residual component is small in this area (Figure 8, left), with larger standard deviation (between 6-7 cm) at the Gulf of Cadiz (higher latitudes, more prompt to suffer the effect of storms) and lower values at the Canary Islands stations (between 3-5 cm). The small magnitude of the surge component is also related to the narrow shelf, especially at the Canary Islands. We lack information concerning this component of sea level along the coast of Africa, where it is expected to be larger than in the Canary Islands due to the broader continental shelf, and the southern part of the CCLME. Bonanza and Tarifa, in the Gulf of Cadiz, are the stations with larger and lower amplitude of the tide respectively, due to the variability of M_2 and S_2 close to the Strait of Gibraltar, as can be seen also in Figure 3.6.9, from COMAPI model. Maximum tidal ranges are around 1.5 m at Tarifa, 3.5 m at Bonanza, 2.5 m at La Palma and 3.2 m at Lanzarote. The relative importance of meteorological sea level at each station, obtained as Res_Stdv/Tide_Stdv (Table enclosed in Figure 3.6.8) varies between the 18.4% of the tide at Tarifa, due to its small tide amplitude, and the 5% at Arrecife.

In the Canary Islands, there is a longitudinal variation of the tide amplitude, becoming larger for the four main constituents in Table 3.6.6 as we move eastwards and approach the continental slope (African coast); this can also be observed from the spatial variation of their amplitude in Figures 3.6.9 and 3.6.10, for the whole region. This longitudinal variation is most evident in fact for the diurnal constituents (K_1 and O_1).

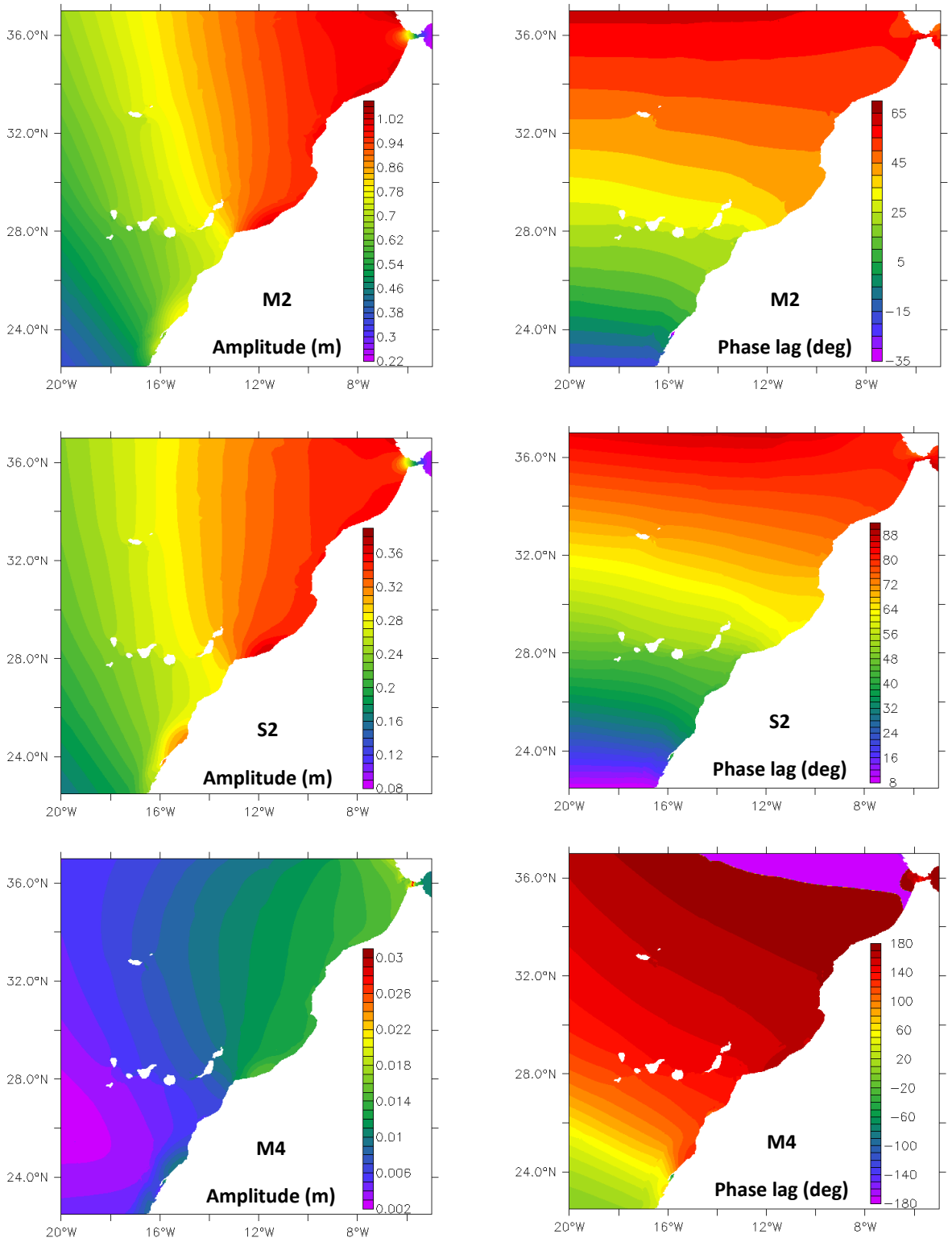

Figure 3.6.9. Spatial variation of amplitude and phase of M_2, S_2 and M_4 harmonic constituents from the COMAPI tidal atlas in the area of interest (resolution 1'×1').

In these figures it is also evident the significant decrease of the tide as we approach the Strait of Gibraltar, with respect to the surrounding Atlantic waters. The phase lag of the main semidiurnal constituents, however, presents a latitudinal variation (Figure 3.6.9, right) due to the propagation of the tidal waves from South to North as a Kelvin wave (with larger amplitude close to the continental shelf).

The higher frequency tidal constituents (such as M_4 and M_6) are usually related to shallow waters non-linear effects. This is why they are not important in the Canary Islands either (amplitudes less than 1 cm), and their magnitude becomes significant at the Gulf of Cadiz (up to 5 cm of M_4 amplitude in Bonanza and 4.7 cm in Tarifa). It should be taken into account that Bonanza station is at the mouth of the Guadalquivir river so shallow water effects are even more important here. For the stations along the west coast of Africa, provided by IHM, the amplitude of M_4 reaches also relatively higher values (3-3.5 cm); the quality of these tidal constants is not clear but the spatial variation observed from COMAPI tidal atlas reveals also a coherent increase of the amplitude of this harmonic towards the shelf (Figure 3.6.9, bottom).

For all the mentioned constituents an increase of the amplitude of the tide is observed at the Western Sahara coast, north of Dakhla (around 24.5°N), most important for S_2 and K_1. Larger tidal amplitudes in the region, according to Figures 3.6.9 and 3.6.10, are found along the Morocco coast. This is not totally coherent however with results from tide gauge observations in Table 3.6.6 which reflect, as already mentioned, the larger tidal amplitudes at Bonanza and Cádiz.

Evaluation of the trends of the main harmonic constants in Las Palmas and Tenerife stations (not shown, see Pérez-Gómez, 2014 for details) do not reveal an increase on the tidal amplitude since 1992. Although the time series is short, this in principle does not confirm the increase of tidal amplitudes observed in other regions of the world (Ray, 2006, 2009; Woodworth, 2010). On the contrary, only M_2 presents a significant negative trend at Las Palmas (Pérez-Gómez, 2014).

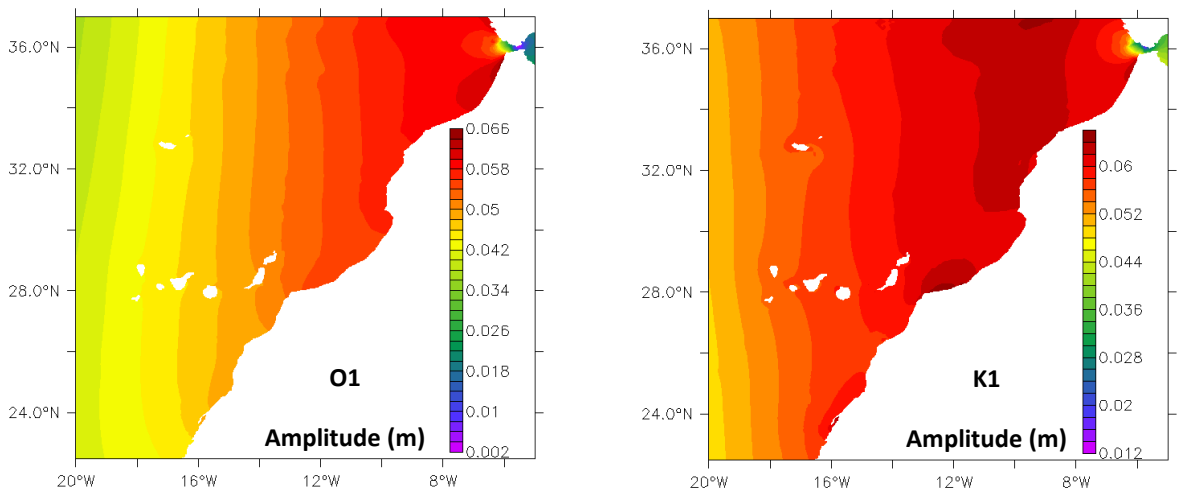

Figure 3.6.10. Spatial variation of the amplitude of the main diurnal constituents (O_1 and K_1) from the COMAPI tidal atlas in the area of interest (resolution 1'×1').

3.6.5. CONCLUSIONS AND RECOMMENDATIONS

Waves

Several wave climates exist in the area of interest. The Strait of Gibraltar, Gulf of Cadiz, Moroccan Coast and Canary Islands wave climates are well described by PdE buoys and models. Golfo de Cádiz buoy (Figure 3.6.5) and model points number 1, 2 and 3 (Figure 3.6.7), represent open deep water conditions, while the other model points and buoys represent local conditions affected by the coastline. South of 20°, unfortunately, there is no source of information on waves available.

The most common significant wave height is between 1 m and 3 m, being higher at northern locations and decreasing as moving southwards. In regard with the wave direction, the Gulf of Cadiz is dominated by waves coming from the west and the main directions turn, first to the north and finally to the north-east as moving southwards to the Canary Islands.

The highest extreme storms appear during the winter season. This is valid not only for the significant wave height, but for the peak period too. The climate is more severe in the north than in the south and the extreme events come from the North West. The extreme events are lowest at the locations close to the coast because they are protected by it.

Tides

With respect to the tide, its variability has been reviewed based on the available tidal constants from tide gauges in the region and the regional tidal atlas based on COMAPI model. The type of tide is mainly semidiurnal for the whole area, with tidal ranges between 1.5 m and 3.5 m and with local variations basically coherent between observations and the model. The meteorological component of sea level is relatively small with respect to the tide, although we lack information from the African coast.

The analysis has been made only for the area north of 22.5°N, covered by COMAPI model. In order to complete the study the domain of this model should be extended to cover the whole region, including Senegal and Cape Verde. There is also a significant lack of tide gauge observations in most of the countries, what would be crucial for detailed information of local tide conditions in the region.

Acknowledgements

We would like to thank Mr. Angora Aman (Laboratory of Atmospheric Physics and Fluid Mechanics, Cote d'Ivoire) and Mr. Salvador Moreno (IHM) for providing tidal constants information of several stations in the African coast and Dr. Florent Lyard (LEGOS) for providing the output of the new high resolution tidal atlas based on the COMAPI model.

4. BIOGEOCHEMICAL CHARACTERISTICS OF THE MARINE ECOSYSTEM

4.1. INORGANIC NUTRIENTS AND DISSOLVED OXYGEN IN THE CANARY CURRENT LARGE MARINE ECOSYSTEM

Josep L. PELEGRÍ and Jesús PEÑA-IZQUIERDO

Institut de Ciències del Mar, CSIC. Spain

4.1.1. INTRODUCTION

The temporal and spatial distribution of inorganic nutrients (IN) and dissolved oxygen (DO) in the ocean responds to the combined effect of physical and biogeochemical processes. Within the surface euphotic layer, primary production (PP) is limited by the availability of sunlight and IN – if the irradiance exceeds some minimum threshold, the higher the flux of IN the higher the PP, hence restraining the maximum IN concentration. The surface waters are typically DO-saturated, as a result of the equilibrium in the partial pressures of oxygen across the air-sea interface – the greater the water temperature, the larger the saturated DO concentration. Within surface waters, as a result of high PP, the concentration of DO may exceed its saturation value.

Below the euphotic depth – in practice meaning below the surface mixed layer and the seasonal thermocline – respiration generally exceeds PP. As a result, organic matter produced at the sea surface gets remineralized in the subsurface layers, along the trajectory of water parcels, and the concentration of IN and DO arises from the interplay between the rate of water supply (bringing upstream concentrations of IN, DO and organic matter) and the local rate of remineralization (which depends largely on water temperature). Therefore, the concentration of IN and DO in subsurface waters reflects both biogeochemical (original IN and DO concentrations at the surface formation regions, the amount of organic materials in these surface waters, and the remineralization processes along the water path) and hydrodynamic (the way the subsurface layers connect to the surface ocean, and the patterns of circulation within the subsurface layers) processes (Fig. 4.1.1).

We begin this article by briefly reviewing how the dynamics of the Canary Current Large Marine Ecosystem (CCLME), together with air-sea exchange and biogeochemical processes, influences the distribution of IN and DO. Afterwards, we continue with a description of the IN and DO spatial distributions, both as horizontal and vertical maps and property-property diagrams, and end up briefly discussing the relevance of the different physical and biogeochemical processes within the CCLME.

4.1.2. PHYSICAL AND BIOGEOCHEMICAL DOMAINS

The CCLME has three well differentiated hydrographic regions: the North Atlantic subtropical gyre (NASG), the north-eastern extension of the North Atlantic tropical gyre (NATG), and the upwelling region off North-west Africa (NWA) (Pelegrí and Peña-Izquierdo, 3.3 this book). The dynamic differences among these regions set distinct biogeochemical domains.

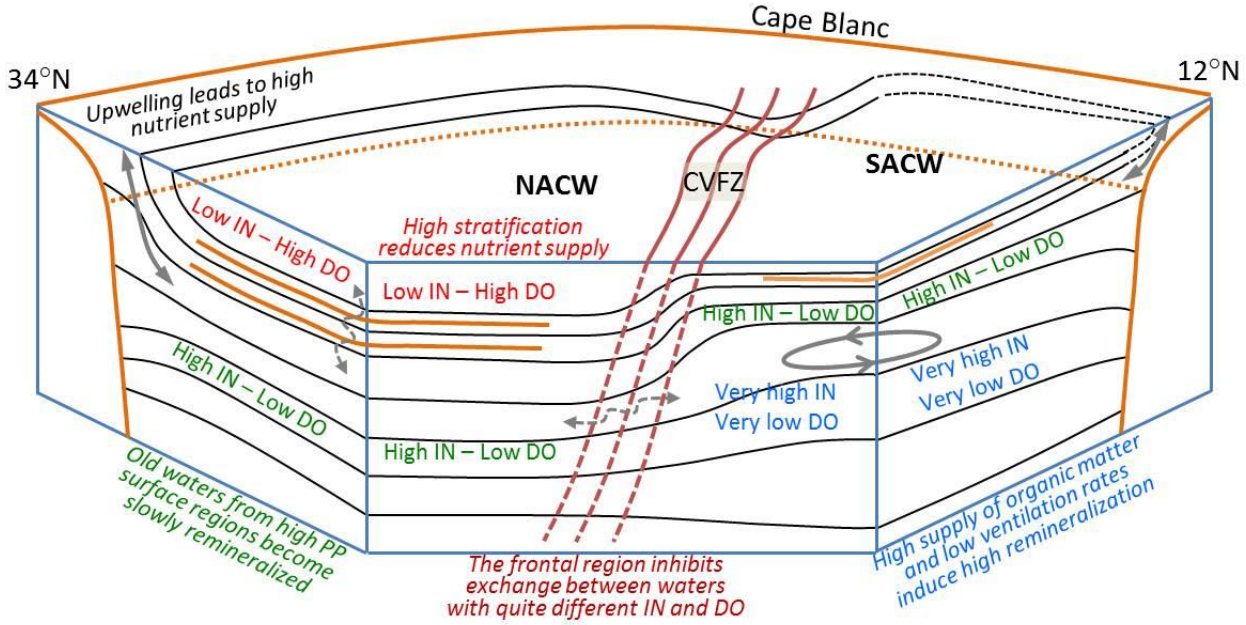

Figure 4.1.1. Schematics of the main processes affecting the distributions of IN and DO in the CCLME, with the isopycnals (black lines) and the main fluxes (advective, solid arrows; diffusive, dashed arrows); the horizontal yellow lines emphasize the role of stratification to inhibit the vertical fluxes.

The NASG is an anticyclonic (clockwise) gyre, constituted by upper-thermocline North Atlantic Central Waters (NACW), with a very intense western boundary current (Gulf Stream) and a much weaker eastern boundary flow (Canary Current system). The anticyclonic flow causes the isopycnals to sink towards the central-western part of the gyre, restricting the connection between the subsurface layers and the euphotic zone; the gyre reaches down to about 600-700 m in the eastern margin and 1000 m in the western margin. Most important, the gyre is a region of water subduction: the sea-surface winds change from intense easterlies at low latitudes to intense westerlies at high latitudes, causing the surface Ekman transport to be convergent and the surface waters to penetrate (subduct) into the subsurface layers (Stommel, 1979; Luyten et al., 1983). The subsurface waters are brought back to the sea surface along the western limb of the gyre, associated with the Gulf Stream and its northern extension (North Atlantic Current), or through relatively slow vertical mixing and boundary upwelling processes. This has two major consequences. First, the surface NASG is an oligotrophic zone. The interior of the gyre is a very low PP region, with shallow subsurface waters having very low nutrient levels except intermittently, near its boundaries, because of lateral inputs through mesoscale activity and thermohaline intrusions. Second, the deeper subsurface layers of the gyre are connected to the sea surface at its margins; in particular, surface to subsurface advection takes place at high latitudes of the northern North Atlantic Ocean, in regions with very high seasonal PP (the spring bloom of the North Atlantic). These surface waters are loaded with organic matter which, after subduction, becomes progressively remineralized and lead to the North Atlantic nutrient-bearing stratum. The deeper the subsurface layer, the higher the nutrient level, up to a maximum located in those layers that outcrop near the loci of maximum westerly winds (approximately defined by the 10°C isothermal); further north the surface waters do not subduct (Sarmiento et al., 1982; Kawase and Sarmiento, 1985).

At latitudes less than Cape Blanc, we find a poorly ventilated upper-thermocline: the shadow zone of the NASG (Luyten et al., 1983), a shallow upper-thermocline (down to about 500 m) which is not directly reached by waters of subtropical origin. As a consequence, this region becomes a north-eastern extension of the NATG, occupied by relatively old South Atlantic Central Water (SACW); the boundary between the NACW and SACW constitutes the Cape Verde Front (CVF) (Zenk et al., 1991), stretching approximately between Cape Blanc and the Cape Verde Islands (15°N-17°N). Because of their old age and the influence of intermediate waters originating in the southern ocean, SACW is distinguished by relatively high IN and low DO concentrations. Additionally, during summer the southern part of this region (between about 8°N and 13°N) experiences wind-induced surface divergence which leads to offshore upwelling. The result is the Guinea Dome, the main supplier of nutrients to the euphotic zone (Pastor et al., 2013). During boreal winter the dome weakens but is accompanied by a narrow band (typically less than 100 km) of shallow (down to about 100 m) coastal upwelling (Pelegrí and Benazzouz, 3.4 this book). The high levels of PP in the Guinea Dome and coastal upwelling regions, together with their low ventilation rate, cause high rates of remineralization and accentuate the characteristics of the SACW, leading to the appearance of a DO minimum and IN maximum zone (Karstensen et al., 2008; Stramma et al., 2008).

The upwelling region off NWA is the result of the year-long northeasterly winds (Pelegrí and Benazzouz, 3.4 this book). These winds induce offshore surface transport which, together with the coastal constraint, brings nutrient-rich subsurface waters to the euphotic zone and gives rise to a coastal band of enhanced PP – the coastal transition zone, typically extending about 2-4° offshore from the continental slope (Barton et al., 1998). Other consequences are the rising of the isopycnals towards the sea surface, leading to the coastal upwelling front with its associated alongshore current (Canary Upwelling Current, CUC), and the creation of alongshore pressure gradients, which sustain the Poleward Undercurrent (PUC) between the frontal system and the slope (Barton, 1989). The CUC and PUC are the true eastern boundary currents of both NASG and NATG, behaving as alongshore water and nutrient conveyors between the Gulf of Cadiz and Cape Vert and providing high spatial and temporal coherence to the whole CTZ (Pelegrí et al., 2005, 2006; Peña-Izquierdo et al., 2012; Benazzouz et al., 2014b; Pelegrí and Peña-Izquierdo, 3.3 this book).

The presence of three dynamic regions results in substantial differences in DO and IN within the CCLME (Fig. 4.1.1). The DO concentration is set at the sea surface through gas exchange with the atmosphere and by PP. Cooling of surface waters reduces the partial pressure of oxygen, hence capturing it from the atmosphere (physical pump); enhanced high PP may cause the surface waters to become oversaturated in DO. Both factors lead to a decrease of DO in warm and nutrient-poor offshore surface waters, and a DO increase in the cold and nutrient-rich coastal upwelling band. Sea surface warming further increases vertical stratification, inhibiting vertical diffusion of IN and DO. In subsurface waters, the enhanced remineralization of organic matter is the main cause for a decrease in DO concentrations and an increase in IN. In highly productive and poorly ventilated areas, such as in the Guinea Dome, the sinking of organic matter and the enhanced water-residence times may lead to a substantial decrease in DO concentration and an increase in IN, resulting in the development of an oxygen minimum zone (OMZ).

4.1.3. SPATIAL DISTRIBUTIONS

In this section we use the temperature, IN and DO fields from the World Ocean Atlas 2013 database (WOA-13, 2013), with a 1° latitude-longitude resolution. We use phosphate to illustrate the spatial IN distributions (Figs. 4.1.2 to 4.1.4), and silicate in the property-property scattered plots (Figs. 4.1.5 and 4.1.6).

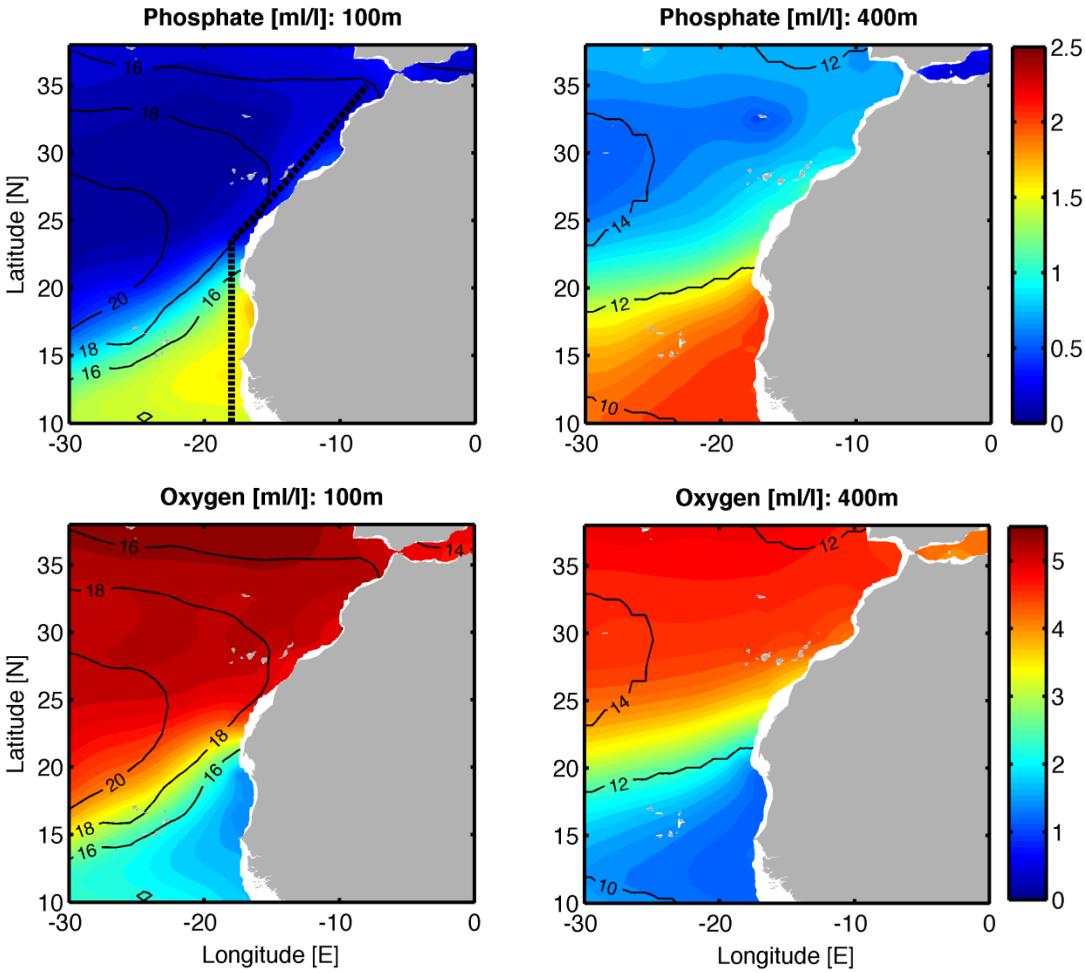

Figure 4.1.2. Annual-mean distributions of phosphate (top) and DO (bottom) concentrations (ml l^{-1}) at 100 m (left) and 400 m (right), with temperature (°C) superimposed as solid contours.

The transition between the tropical and subtropical gyres is clear in the mean annual temperature, IN and DO distributions along a section parallel to the African slope (Fig. 4.1.3). The depth of the upper thermocline (down to 10°C) doubles from the NATG to the NASG. The CVF is evident in the temperature field but the latitudinal IN and DO gradients are even sharper due to the high remineralization in the eastern tropical region (latitudes less than 22°N) and the increased ventilation with latitude along the eastern NASG. The DO distributions show the existence of a local maximum at low latitudes (10-12°N) and shallow depths (200-300 m); this reflects the different regimes in the upper (down to 300 m) and lower (300-500 m) SACW, with the upper layer being oxygenated by the equatorial system of zonal jets and the lower layer subject to very reduced ventilation (Peña-Izquierdo et al., 2015).

The differences between the subtropical and tropical regions are also clear in the annual-mean temperature, IN and DO distributions along zonal sections at different latitudes (Fig. 4.1.4). Those sections in the NASG (30°N and 24°N in Fig. 4.1.4) show a deep thermocline (reaching 800 m at 30°N), with relatively low IN and high DO concentrations, indicative of recently ventilated waters. The CTZ is characterized by the uplifting of isothermals and IN contours; the rise of DO contours is not evident because of the increased air-sea exchange within the cooler coastal waters. Within the NATG (18°N and 12°N in Fig. 4.1.4), the thermocline only extends to about 500 m, with a subsurface IN maximum and DO minimum evidencing much older water masses. The intensity and offshore extent of the IN/DO

concentrations increases/decreases with decreasing latitude, with DO reaching below 1.5 ml l^{-1} near the coast at 12°N, as part of the North Atlantic OMZ (Karstensen et al., 2008; Stramma et al., 2008).

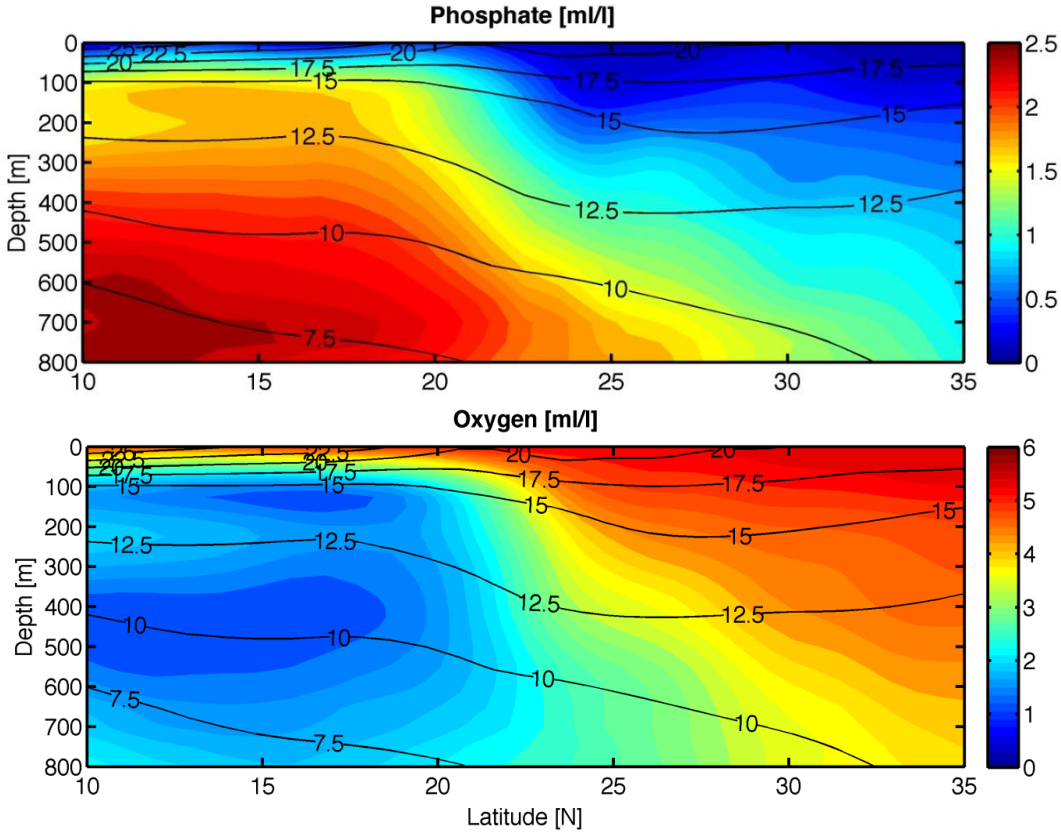

Figure 4.1.3. Annual-mean distributions of phosphate (top) and DO (bottom) concentrations (ml l^{-1}) along the meridional section in the top-left panel of Fig. 4.1.2, with temperature (°C) superimposed as solid contours.

Since we present the mean annual fields, and coastal upwelling develops in the NATG only during boreal winter, the upwelling band is visible only in the NASG, extending about 2-3° from the continental slope. It is interesting to note the deeper location of the IN maximum (700-800 m) as compared with the DO minimum (400-500 m), reflecting the along-slope northward propagation of nutrient-rich intermediate waters (Machín et al., 2006a; Machín and Pelegrí, 2009).

Several decades of observations (Stramma et al., 2008; Brandt et al., 2010) have revealed an expansion and deoxygenation of the world OMZs, with dramatic implications for the highly productive eastern boundary marine ecosystems – all OMZs present hypoxic conditions, with lethal DO concentrations for half of the marine species (Vaquer-Sunyer and Duarte, 2008). The North Atlantic OMZ is the least hypoxic of all the OMZs but its rate of oxygen decline is at least twice faster than any other OMZ (Stramma et al., 2008). This growth in the loss of habitat is threatening the sustainability of the valuable pelagic fisheries and marine ecosystems in the region (Arístegui et al., 2006; Stramma et al., 2012).

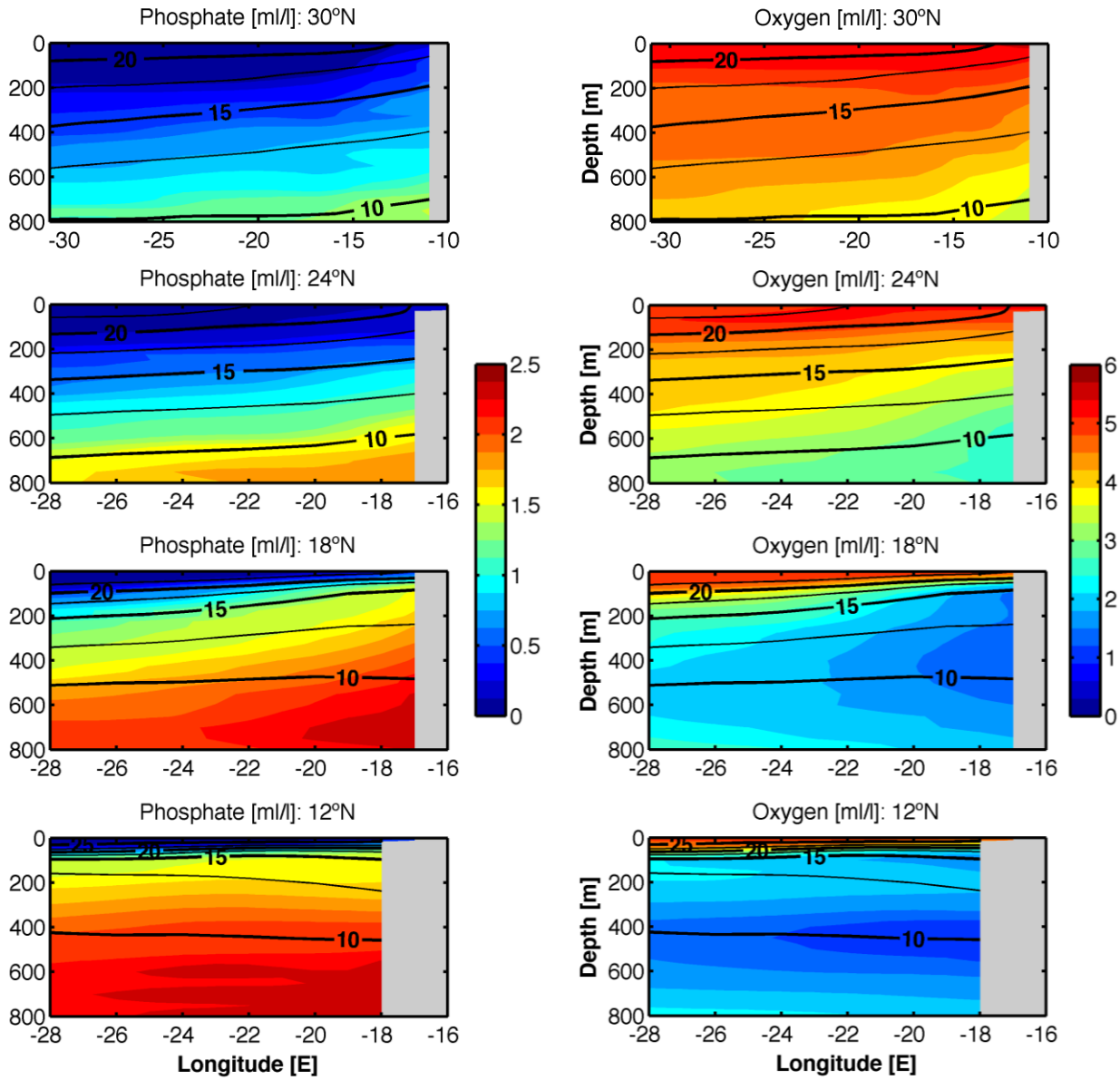

Figure 4.1.4. Annual-mean distributions of phosphate (left) and DO (right) concentrations (ml l^{-1}) along zonal sections (30°N, 24°N, 18°N, 12°N; from top to bottom), with temperature (°C) drawn as solid contours.

4.1.4. NUTRIENT AND OXYGEN RELATIONSHIPS

The differences in IN and DO between NACW and SACW can be identified using scatter plots (or property-property diagrams) (Figs. 4.1.5 and 4.1.6). The meridional transect along the continental slope sharply illustrates that SACW has higher IN and lower DO concentrations than NACW. This is true not only for any given depth but also for the whole water mass, as shown by the shift in data points representative of these two water masses (Fig. 4.1.5). The shift takes place rather abruptly across the CVF. Within the NATG there is a maximum in DO at 200-300 m (see also Fig. 4.1.3), which reflects enhanced ventilation of the upper thermocline by the along-slope PUC (Peña-Izquierdo et al., 2012, 2015).

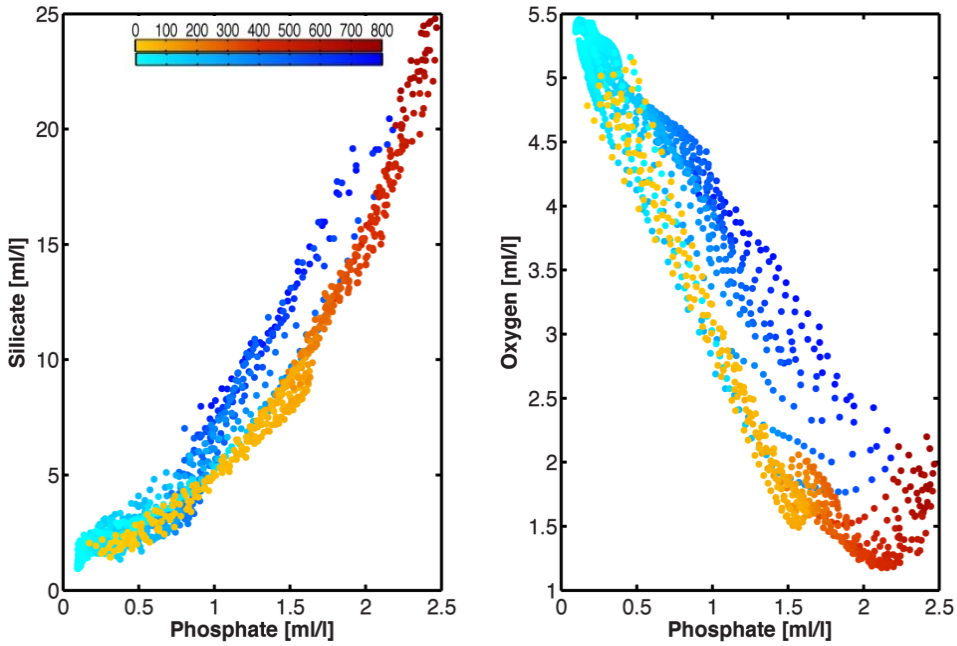

Figure 4.1.5. Scatter plots of silicate-phosphate (left) and DO-phosphate (right) (ml l^{-1}) along the meridional section depicted in the top-left panel of Fig. 4.1.2. The reddish/bluish colours correspond to data points at latitudes less/more than 20°N, with the colour code representing depth (m).

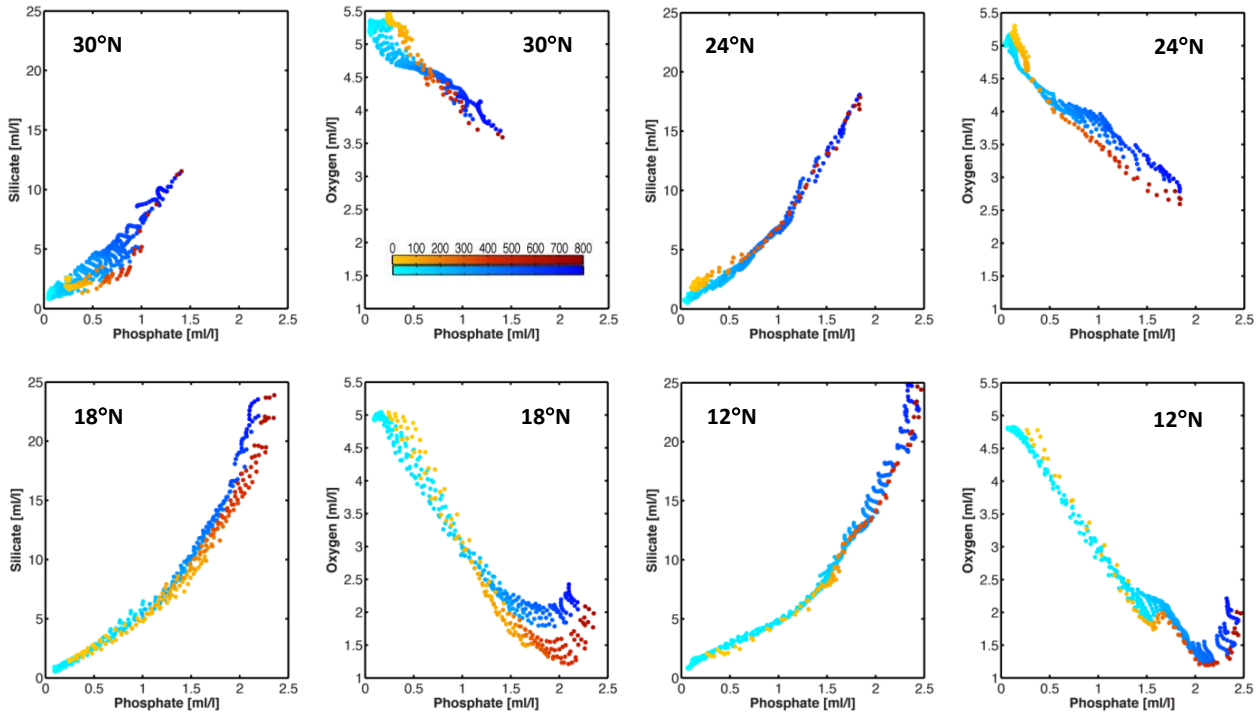

Figure 4.1.6. Scatter plots of silicate-phosphate (left) and DO-phosphate (right) (ml l^{-1}) along the zonal sections in Fig. 4.1.4. The reddish/bluish colours correspond to data points at longitudes east/west of 15°W (30°N), 22°W (24°N), 21°W (18°N), 21°W (12°N); the colour code represents depth (m).

The longitudinal changes at different latitudes show relatively minor differences, visible as small displacements in the scatter plots. The shoreward change in the depth of the isothermals (rising in the NASG and dropping for the NATG) affects the location of any particular set of IN-DO values but does not cause a large shift in the cloud of points. The most significant displacement for the NASG occurs in the DO-phosphate plot, where DO in the cold upwelled waters is relatively high compared with the warm and stratified offshore waters. Regarding the NATG, there is a general increase in DO when moving from 12°N to 18°N, resulting from the transfer of NACW through the CVF (Peña-Izquierdo et al., 2015); an exception occurs at depths between 200 m and 300 m, where the ventilation appears to be related to the northward PUC (Fig. 4.1.3; see Pelegrí and Peña-Izquierdo, 3.3 this book).

4.1.5. CONCLUSIONS

In this article we have described the annual-mean distributions of IN and DO within the surface layers and the permanent thermocline of the CCLME. We have neither discussed their temporal variability nor their relevance on ocean processes such as PP and biodiversity, as these topics are addressed in other articles. Instead, we have focused on those physical and biochemical processes that control the IN and DO distributions, as summarized below (see also Fig. 4.1.1).

4.1.5.1. Physical processes

The physical supply of water mass and associated properties includes both lateral and vertical transports. These arise from processes that range from the regional scale to the small-scale. Becasuse of their spatial and temporal scale, regional patterns are usually considered to be advective processes while mesoscale and small-scale phenomena are commonly thought in terms of mixing processes; the difference, however, resides solely in our skill, and interest, to study the variability acting at certain spatial and temporal scales.

Lateral advection by localized currents, for instance the CUC, leads to the appearance of convergent regions which may undergo water upwelling. One remarkable example is the confluence of the CUC and the Mauritanian Current at the CVF (Pelegrí and Peña-Izquierdo, 3.3 this book); as a result, high PP takes place in this region and surface waters, loaded with organic matter and IN, are exported to the NASG through the Cape Blanc giant filament (Pelegrí and Benazzouz, 3.4 this book). The fronts, however, act not only as a barrier to advection but also as a source of horizontal mixing through the generation of lateral instabilities. The CCLME has two distinctive fronts: the CVF, characterized by double-diffusive intrusions that enhance mixing between the nutrient-rich SACW and the nutrient-poor NACW (Pastor et al., 2008); and the coastal upwelling front, where upwelling filaments and mesoscale eddies lead to offshore transfer of inorganic and organic matter (García-Muñoz et al., 2005; Benítez-Barrios et al., 2011; Ruiz et al., 2014).

Vertical supply takes place as a result of both advection and mixing. Vertical mixing is induced through double diffusion, mainly within the NASG, and localized shear, associated with either frontal jets, mesoscale features or internal waves (Martínez-Marrero et al., 2008); however, the greater the vertical stratification, the greater the vertical shear required to induce mixing. Upward vertical advection, or upwelling, is a widespread and ubiquitous feature along NWA (until Cape Blanc, reaching as far south as Cape Vert only during boreal winter) (Benazzouz et al., 2014b). Upwelling also takes place in the Dome of Guinea and within mesoscale features, such as eddies generated south of the Canary Islands or along the coastal upwelling front (Benítez-Barrios et al., 2011; Pastor et al., 2013).

4.1.5.2. Biogeochemical processes

The main biogeochemical supply of IN occurs in subsurface waters through the remineralization of organic matter in poorly ventilated areas, i.e. where waters have long residence times. Within the CCLME, this takes place in both the subtropical and tropical gyres but in very different ways. The upper-thermocline waters of the NASG originate at the high-latitude sea-surface, in regions of water subduction (Pelegrí and Peña-Izquierdo, 3.3 this book); these subducted waters carry relatively high DO concentrations (the higher the latitude the colder the water and the larger the DO concentration) and a high load of organic matter produced during the North Atlantic spring bloom. The path of these surface waters to the subsurface eastern boundary of the NASG is relatively short, so there is not enough time for the organic matter to be fully remineralized. As a consequence, these waters reach the CCLME with relatively high DO and moderate IN concentrations, with IN increasing and DO decreasing with depth within the permanent thermocline.

The waters arriving to the tropical ocean have high IN and low DO concentrations because of sustained remineralization on route from the South Atlantic (and even the Southern Ocean). These IN and DO concentrations are further increased or reduced as a result of low ventilation (equivalent to high residence times) and the local supply of organic matter (arising from enhanced upwelling and PP in the coastal band and the Dome of Guinea). The outcome is the OMZ, with the highest IN and lowest DO concentrations in the entire North Atlantic Ocean.

The sea surface is saturated in DO because of air-sea exchange; the partial pressure of oxygen within the water decreases with temperature, hence the concentration of sea-surface DO is larger in the coastal upwelling region off NWA than further offshore. This shows up not only at the sea surface but, as a result of intense vertical mixing within the coastal transition zone, also in the subsurface layers. Other IN sources (e.g. coastal, either natural or anthropogenic, or through atmospheric deposition of nitrogen) are generally much smaller and have been neglected (however, see Gelado-Caballero, 2.3 this book, on dust inputs).

4.1.5.3. A complex, hence difficult, forecast

The IN and DO distributions are the outcome of multiple drivers, with important feedbacks between different variables. For example, Stramma et al. (2009, 2013) have presented a scenario with worldwide expansion of the OMZs, possibly as a result of weakened tropical circulation and enhanced stratification (Matear and Hirst, 2003). However, Pastor et al. (2013) have shown that vertical supply in the CCLME is not dominated by vertical mixing but rather by upwelling in the coastal region and, particularly, in the Dome of Guinea. Hence, the warming of surface waters may not significantly reduce the ventilation of the upper-ocean layers. On the contrary, the changes in DO concentration are likely to depend on the long-term variability of the ventilation pathways (Peña-Izquierdo et al., 2015). The answer probably lies in the behaviour of the tropical system of zonal jets (Rosell-Fieschi et al., 2015) and the evolution of the surface winds and their effect on coastal and offshore upwelling (Benazzouz et al., 6.3 this book). A good example is the reported trend of increased trade winds that, non-intuitively, is accompanied by the warming of the coastal upwelled waters: the answer lies on the intensification of the upstream input of interior-ocean waters that have heated up as a result of climate change (Pelegrí and Benazzouz, 3.4.2 this book).

Also relevant is how remineralization may be influenced by climate change, with many possible feedbacks. For example, Llanillo et al. (2013) show that an increase in ventilation leads to a proportionally higher rate of respiration (for the OMZ in the South Pacific), causing a decrease in DO concentration; and Ridder and England (2014) propose that, as a result of global warming, nutrient supply and PP are reduced in the tropics, leading to a decrease in respiration and a contraction of the OMZ. Pelegrí et al. (2006) and Torres-

Valdés et al. (2009) have emphasized the important role of export of nutrients and organic matter from the eastern upwelling region in order to maintain the levels observed within the NASG. In particular, Torres-Valdés et al. (2009) observed significant differences in nitrate and phosphate within the NASG - the former is more abundant (above the Redfield ratio) possibly as a result of nitrogen fixation (Benavides et al., 2013b) – probably causing phytoplankton to respire better dissolved organic phosphorus than nitrogen.

The relevance of the distributions of IN and DO on the trophic chain in the CCLME is unquestionable. The high complexity of the CCLME, i.e. variety of processes controlling the IN and DO distributions, may signify high resilience to anthropogenic perturbations (e.g. MacArthur, 1955); nevertheless, an improved understanding of the physical and biogeochemical processes, and their interactions, is still necessary for predicting how anthropogenic climate change will affect the CCLME future evolution.

Acknowledgements

This review has been supported by projects CANOA (CTM2005-00444/MAR), MOC2 (CTM2008-06438-C02-01) and TIC-MOC (CTM2011–28867), funded by the Spanish government. Jesús Peña-Izquierdo was funded by the Spanish government, through a FPI doctoral grant linked to project MOC2. We also wish to sincerely thank the many colleagues that have participated with us in these projects, for the hard work carried out together and the many enlightening and joyful conversations, particularly Javier Arístegui, Mikhail Emelianov, Alonso Hernández-Guerra, Irene Laiz, Francisco Machín, Ángeles Marrero-Díaz, María Pastor, Grant Pitcher, Ángel Rodríguez-Santana and Pablo Sangrà.

4.2. INORGANIC CARBON, PH AND ALKALINITY IN THE CANARY CURRENT LARGE MARINE ECOSYSTEM

Melchor GONZÁLEZ-DÁVILA and J. Magdalena SANTANA-CASIANO

Instituto de Oceanografía y Cambio Global (IOCAG), Universidad de Las Palmas de Gran Canaria. Spain

4.2.1. INTRODUCTION

Atmospheric carbon dioxide (CO_2) levels have increased by 40% since pre-industrial times, from 280 ppmv (parts per million volume) to 400 ppmv, reached for the first time in 2014. One third of the anthropogenic carbon added to the atmosphere is taken up by the ocean (Le Queré et al., 2014; Sabine et al., 2004). This oceanic CO_2 uptake alters the chemistry of seawater, including pH, carbonate ion concentration as well as calcite and aragonite saturation, which together are commonly referred to as 'ocean acidification'. As the ocean absorbs more anthropogenic CO_2, the CO_2 reacts with the seawater to form carbonic acid (H_2CO_3). This then dissociates to form a bicarbonate ion (HCO_3^-) and a hydrogen ion (H^+), which can react with carbonate ions (CO_3^{2-}) to form bicarbonate (HCO_3^-).This process on its own is independent of any climatic change and the reductions in CO_2 emissions will not reduce ocean acidification of immediate form. Although all CO2 emissions stopped nowadays, it will take thousands of years for the ocean to recover (Caldeira and Wickett, 2003). CO_2 is being absorbed by the ocean so rapidly that the buffering capacity of the surface waters of the oceans will not be able to prevent a substantial lowering of ocean pH (Raven et al., 2005). Increasing temperatures of surface waters reduce the solubility of CO_2 in seawater, consequently the amount of CO_2 the ocean can absorb from the atmosphere decreases. The concern about this, called "the other CO_2 problem" (Turley, 2005), has led us to re-examine the fundamental processes controlling the distributions of dissolved inorganic carbon (C_T) and total alkalinity (A_T) in oceans.

Long-term time series are a powerful tool to investigate any change in ocean bio-geochemistry and its effects on the carbon cycle. They are also the most direct way of estimating the accumulation of anthropogenic CO_2 in the oceans. The ESTOC site (European Station for Time series in the Ocean, the Canary Islands), located off the Canary Islands in the NE Atlantic Ocean (e.g. González-Dávila et al., 2003, 2007, 2010; Santana-Casiano et al., 2001, 2007; Cianca et al., 2013; Bates et al., 2014) has provided evidence about the seasonal and inter-annual changes in the carbonate system for the Canary Island region. Similar role plays the Hawaiian ocean Time Series (HOTS) in the Pacific Ocean and the Bermuda Time Series (BATS) in the West Subtropical Atlantic Ocean (Bates et al., 2014). Physical processes such as turbulent mixing, subduction, advection, and transport of anthropogenic CO_2 from the seasonally mixed layer into deeper water masses will alter the biogeochemical properties there over time. The characterization of these changes requires accurate highly resolved vertical long-term data to be able to adequately identify any observed variation (González-Dávila et al., 2010; Bates et al., 2014). The concentration of CO_2 within the ocean is also critical to the pH of the water and the concentration of carbonate ions. Carbonate ions are needed to build calcium carbonate or limestone structures like coral skeletons and shells for many marine organisms, including shellfish, and marine plankton via calcification (Feely et al., 2004). Therefore, knowledge of the changes in ocean total dissolved inorganic carbon and its speciation, is of utmost importance in understanding and predicting changes in ocean chemistry properties.

The Canary Current Large Marine Ecosystem (CCLME) region, including the adjacent waters of Cape Verde and Guinea Conakry, also includes the Canary Upwelling Ecosystem (CUE) situated Northwest (NW) of

Africa (11°–35°N) with the most active Mauritanian upwelling system (18°-24°N). Several studies have improved our understanding of the Canary Current (Stramma and Siedler, 1988; Lozier et al., 1995; Siedler and Onken, 1996), and have confirmed the existence of a water inflow from the open ocean towards the coastal upwelling region north of the Canary Islands. Therefore the coastal upwelling region has been identified as the eastern boundary condition for the subtropical gyre (Pelegri et al., 2005).

The coastal upwelling system transfers both nutrients and dissolved inorganic carbon to the sun-lit surface ocean (Pelegri et al., 2005). While the first stimulates phytoplankton growth, the second causes low calcium carbonate saturation states in the upper water column, with potentially adverse effects on marine calcifiers. The upwelled seawater also results in high natural variations of CO_2 concentrations and pH reduction in surface seawater compared to most marine environments. As soon as the deeper water with high levels of CO_2 reaches the surface, the temperature increases, and the newly introduced inorganic carbon can be partially or totally consumed through photosynthesis by phytoplankton, causing extensive blooms. This leads to the rapid drawdown of CO_2 and an increase in pH in the more acidic upwelled waters (Santana-Casiano and González-Dávila, 6.5 this book). Phytoplankton can deplete seawater carbon dioxide concentrations in these regions far below current atmospheric levels of ≈400 ppm (Loucaides et al., 2012; Lachkar and Gruber, 2013).

The CUE is an important socio-economic, oceanographic and climatological region. The Canary upwelling area is in one of the major coastal upwelling regions of the world. Others include the Benguela (Hagen et al., 2001), Humboldt (Thiel et al., 2007) and California (Pérez-Brunius et al., 2007) eastern boundary upwelling ecosystems (EBUE). These EBUEs cover approximately 1% of the total ocean surface. Upwelled water is typically denser, cooler and richer in nutrients and in carbon dioxide than surface waters and has significant impacts on coastal climates and marine biology (Miranda et al., 2012). The Upwelling Intensification Hypothesis' (Bakun, 1990), later taken up by Diffenbaugh et al. (2004) and Bakun et al. (2010), suggested that, in a globally warming world, an increase in greenhouse gases will cause reduced night-time continental cooling and increased in day time heating during the warm seasons of the year (spring and summer for the northern Hemisphere subtropics). Consequently the temperature gradient between land and ocean would increase, which would intensify the continental–oceanic pressure gradient. Correspondingly, the along shore wind stress would be strengthened, leading to enhanced coastal upwelling. A considerable amount of literature has emerged since the original hypothesis, showing data and analyses for and against the upwelling intensification mechanism across the four main EBUEs and around the NW African coastline (Barton et al., 2013, Cropper et al., 2014).

4.2.2. DATA SOURCES AND METHODS

4.2.2.1. Research vessels: Time Series Stations

The European Station for Time series in the ocean (ESTOC) (29°10'N, 15°30' W) is located north of the islands of Gran Canaria and Tenerife, and has a depth of 3600 m. The time series station was inaugurated in February 1994 and has continued its monthly operations through to the year 2004. Since 2004, the ESTOC site is been visited seasonally. This station is intended to be representative of the eastern boundary of the northeast Atlantic Ocean, in the Subtropical region. In the eastern region of the subtropical gyre, the water masses are modified by the upwelling processes. The ESTOC website can be found at: http://estoc.plocan.eu, accessed on 20 February 2015.

4.2.2.2. Mooring: Fixed point Open Ocean Observatories

ESTOC and CVOO- (Cape Verde Ocean Observatory, formerly TENATSO Time series station) are both part of the EuroSITES network (http://www.eurosites.info/, accessed on 20 February 2015) which contributes to the global OceanSITES network and the FixO3 network (The Fixed point Open Ocean Observatory network), as a part of the European open ocean fixed point observatories.

4.2.2.3. Cruises

Data for the carbon dioxide variables at the Canary Island region from cruises carried out by single countries or by collaborative projects as a part of national, European or International programs can be found in the Carbon Dioxide Information Analysis Center (CDIAC) web page (http://cdiac.ornl.gov/, accessed on 21 February 2015) and in the websites of the European funded projects CARBOOCEAN (http://www.carboocean.org, accessed on 21 February 2015) and CARBOCHANGE (http://www.carbochange.b.uib.no, accessed on 20 February 2015).

In the Mauritanian upwelling region, between 20.5°N to 21.5°N and 17°W to 19°W, a cruise designed to track an upwelling patch was carried out between April-May 2009. The C_T and A_T values were measured on board as part of the UK SOLAS (Surface Ocean Lower Atmosphere Study).

4.2.2.4. Methodology

Total Alkalinity

Samples for A_T measurements were potentiometrically titrated with HCl to the carbonic acid end point until 2004 (Mintrop et al., 2000). Afterwards, a VINDTA 3C system (Mintrop et al., 2000), which determines both total potentiometric alkalinity and total dissolved inorganic carbon was used. The titration of different certified reference materials (CRM) has been used to test the performance of the titration system. The standard deviation was ± 2 µmol kg^{-1}.

Total Dissolved Inorganic Carbon

C_T has been computed from experimental values of pH_T (Santana-Casiano and González-Dávila, 6.5 this book) and A_T using the carbonic acid dissociation constants by Mehrbach et al. (1973) as in Dickson and Millero (1987). The C_T (pH_T-A_T) values were corrected using certified CRMs with previously determined pH_T and A_T, resulting in a C_T(pH_T-A_T) residual of ± 3 µmol kg^{-1} (n = 90). After 2004, a VINDTA 3C system (Mintrop et al., 2000) with coulometer determination has been used for most of the research groups with a substantially increased precision of ± 1.0 µmol kg^{-1} (www.MARIANDA.com, accessed 21 February 2015) in all cruises in the area.

The C_T and total alkalinity, alongside temperature, salinity, pressure and macronutrient concentrations from all discrete samples, are used to calculate the remaining carbonate chemistry parameters, including saturation state Ω aragonite (Ω_A) and calcite (Ω_C). This was carried out using the CO_2Sys programme with thermodynamic dissociation constants for K_1 and K_2 from Mehrbach et al. (1974) and re-fit by Dickson and Millero (1987).

4.2.3. RESULTS

4.2.3.1. ESTOC Site

The ESTOC site is about 1000 km west of the NW African coast and 100 km north of the Canary Islands. It is far away from the coastal upwelling zone but the effects of upwelling filaments reaching the area on CO_2 system have been described previously (Pelegri et al., 2005; Santana-Casiano et al., 2007; González-Dávila et al., 2007). The ESTOC site is located in the Sub-tropical Gyre and exhibits oligotrophic characteristics (Neuer et al., 2007). A description of the water masses for the Canary region where ESTOC is located has been provided by Pérez et al. (2001), Llinás et al. (2002) where the focus was to describe the distribution of salinity anomalies, and Cianca et al. (2007) and Machín et al. (2006a), presenting mass fluxes. The oxygen dynamics at ESTOC has been discussed by Cianca et al. (2013). The C_T values normalized to a contant salinity of 35 in the surface waters at ESTOC has increased in the last 15 years by 0.9 ± 0.1 µmol kg^{-1} yr^{-1} (Figure 4.2.1) linked to the fCO_2 increase in both the atmosphere and the ocean (Santana-Casiano and González-Dávila, 6.5 this book). The NA_T at the surface remains constant over the years with a value of 2292 ± 2 µmol kg^{-1} (Figure 4.2.1), a similar effect than that observed in the full profile (Figure 4.2.2) (González-Dávila et al., 2010). The stratification of water masses affects the profiles of the carbonate system parameters. Gonzalez-Dávila et al. (2010) provided a description of profiles and trends for the area for each variable. The pH_T at *in situ* conditions decreases with depth to a minimum near 900-1000 m, partly overlapping with the oxygen minimum layer at 800-900 m. After normalization to a constant temperature of 25°C, the pH_T also decreases with depth from a value of around 7.95-7.97 at 200 m to 7.71-7.74 at 1000 m. The C_T and NC_T (the normalized C_T to a constant salinity of 35) distribution increase with depth (Figure 4.2.3), reaching a maximum near 1000-1100 m, with values in the range of 2090 µmol kg^{-1} and 2010 µmol kg^{-1} for the C_T and 2160 µmol kg^{-1} and 2170 µmol kg^{-1} for the NC_T, reflecting the impact of organic matter remineralization. A_T decreases with depth (Figure 4.2.2), but with a distribution strongly related to salinity over the first 600 m in the Eastern North Atlantic Central Water (ENACW) region.

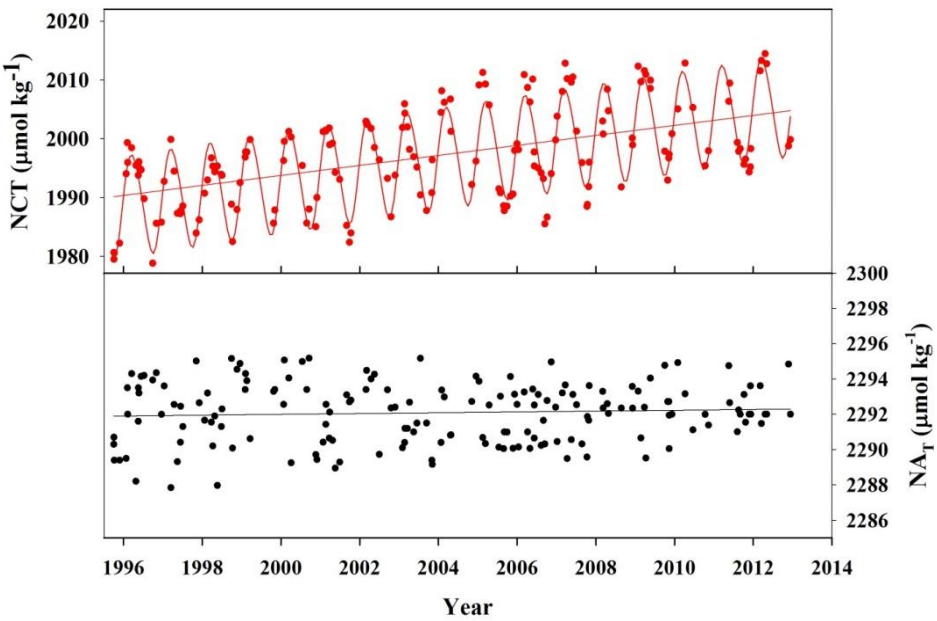

Figure 4.2.1. Long-term trends of surface (10 m) total inorganic carbon and total Alkalinity both of them normalized to a constant salinity of 35, NC_T and NA_T, respectively, at ESTOC. The slope of the regression line for NC_T was 0.9 ± 0.1 µmol kg^{-1} yr^{-1}, while NA_T remains constant at 2292 ± 2 µmol kg^{-1}.

Over the past 15 years the distribution of the carbonate system parameters at the ESTOC station indicated changes in the chemical, biological and physical characteristics of the water column in this area (Figure 4.2.3). A total of 12 depth values were used to define the inter-annual variability for the carbonate system parameters at ESTOC, 7 of which were located over the first 1000 m. In the mixed layer, the NC_T content increased by 0.95 ± 0.6 µmol kg^{-1} yr^{-1}, a similar rate than that indicated above for the surface seawater. At intermediate depths of 300 m, 600 m, and 1000 m, annual increase in the NC_T of 0.69 µmol kg^{-1} yr^{-1}, 0.61 µmol kg^{-1} yr^{-1} and 0.48 µmol kg^{-1} yr^{-1}, respectively, were defined (González-Dávila et al., 2010). The NA_T (normalized A_T to a constant salinity of 35) remains constant over the years at the different water depths. The addition of CO_2 acidifies seawater and lowers its pH. The values for the $pH_{T,25}$ over the first 100 meters decrease at a rate of around 0.0018. The values are statistically significant at 95% confidence level over the first 1000 m, where the $pH_{T,25}$ decreases at a rate of 0.0008 ± 0.0003 units yr^{-1}.

These data were used to compute anthropogenic carbon, C_{ANT}, penetration and carbon storage in the ESTOC area (González-Dávila et al., 2010). The concentration of anthropogenic CO_2 in the 150–200 m depth was 57 ± 4 µmol kg^{-1}, for the year 2000. The yearly average for C_{ANT} was found to increase at a rate of 0.85 ± 0.6 µmol kg^{-1} yr^{-1}, which is in the same range as the observed increase in C_T. The total column inventory of anthropogenic CO_2 was estimated to be 66 ± 3 mol m^{-2} at the ESTOC site for the period 1995-2004.

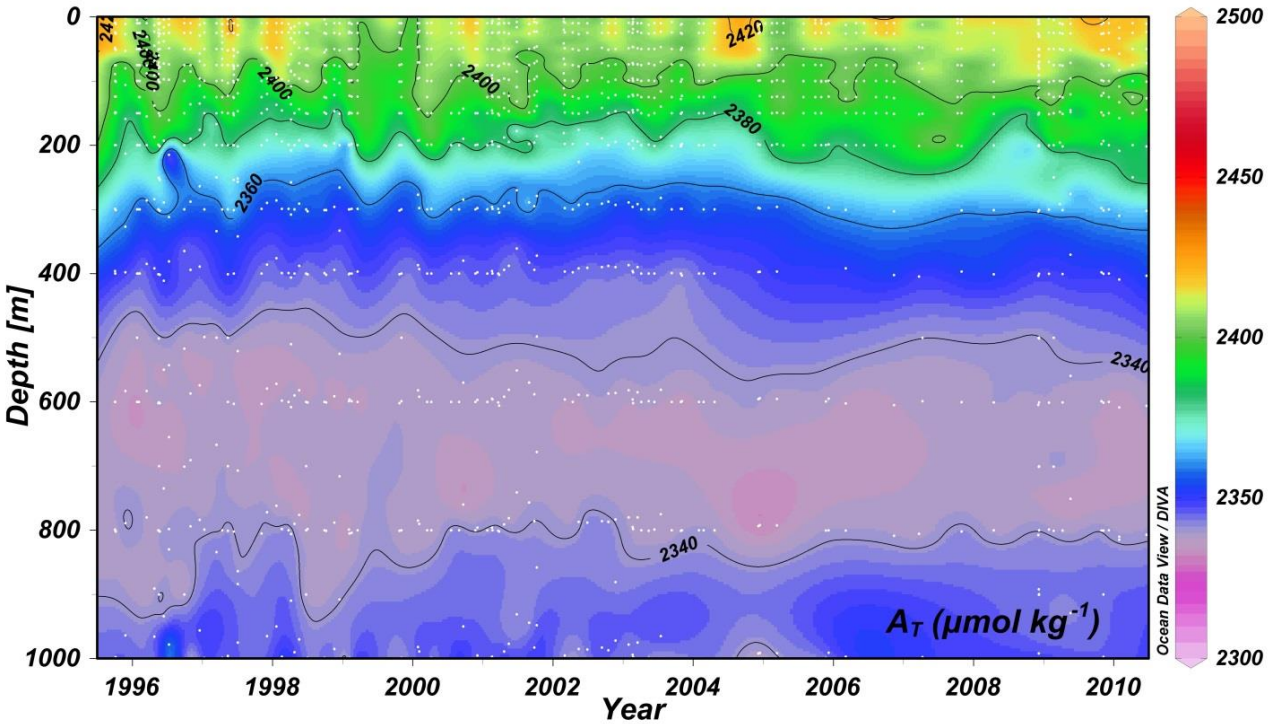

Figure 4.2.2. Hovmöller diagram of the water column A_T evolution for the years 1995 to 2012 (Schlitzer, 2015).

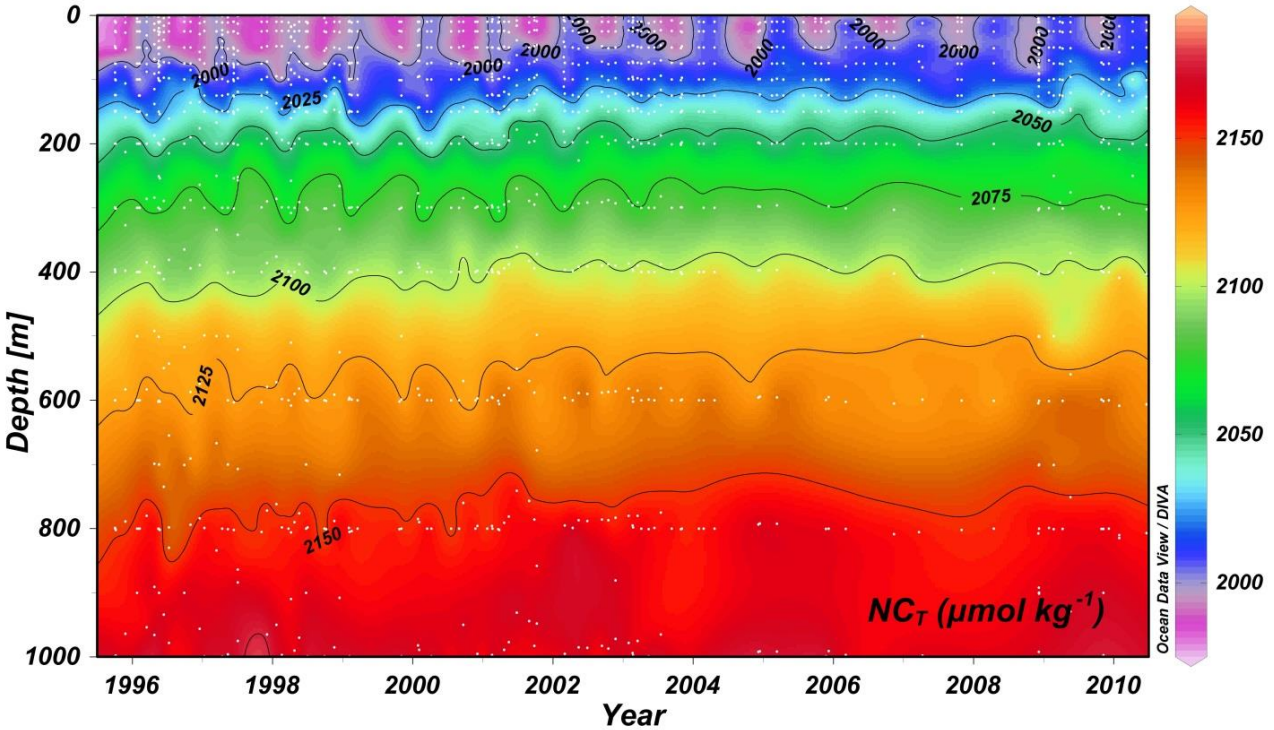

Figure 4.2.3. Hovmöller diagram of the water column NC_T evolution for the years 1995 to 2012 (Schlitzer, 2015).

4.2.3.2. Mauritanian upwelling

The number of CO_2 sutides carried out in the Mauritanean upwelling area is limited. Loucaides et al. (2012) measured C_T and A_T changes in an upwelling filament and detected that average C_T concentrations in the mixed layer decreased during a Lagrangian study. They found the highest C_T levels shortly after upwelling (2168 µmol kg^{-1}) and lowest levels during the last days of the study (2131 µmol kg^{-1}). Average mixed layer A_T concentrations increased during the study. The pCO_2 of the upwelled water decreased by 100-150 µatm after 8 to 9 days. As expected, pH_{tot} values were at their lowest initially and increased by 0.11 units 6 days after. Moreover, the saturation levels of calcite and aragonite increased gradually by 0.8 and 0.6, respectively. Throughout this process, it was observed that C_T in the mixed layer was primarily controlled by biological incorporation into soft tissues and not significantly affected by calcification or dissolution of $CaCO_3$, or vertical exchanges. The observed increase in A_T was caused by nitrate uptake and water mass mixing. In deep waters, the production of C_T was tied to the consumption of oxygen through microbial respiration with a ratio of 0.51, similar to the ratio reported for remineralization in the shallower subsurface layers of the North Atlantic Ocean (Omta et al., 2011]).

The results of the studies on directions in upwelling across the NW African coastline based in satellite wind and sea surface temperature data (Barton et al., 2013; Cropper et al., 2014), that will affect the levels of the different carbon system parameters, are inconsistent with results for and against the upwelling intensification mechanism. Some results support the theory that changes towards upwelling intensification might due to natural inter-annual variability (Cropper et al. 2014 and reference herein). Lachkar and Gruber (2013) have shown that model predicts doubling of the wind-stress doubles net primary production (NPP) north of Cape Blanc (21°N), in the central and northern CUE, which will lead to an enhanced net biological uptake of the upwelled CO_2 and a small change in the CO_2 atmospheric-ocean interchange.

4.2.4. DISCUSSION

The carbonate system in the North East Atlantic Ocean is well represented by measurements conducted at the ESTOC site (Pérez et al., 2001; González-Dávila et al., 2010). The vertical distribution of the carbonate system parameters is affected by the water mass structure. Moreover, the biological/biogeochemical processes related with the production/decomposition of organic matter, the formation/dissolution of calcium carbonates and the differences in the respective carbonate values when each water masses were formed control the final vertical distribution (González-Dávila et al., 2010). In order to identify and quantify the mechanisms controlling the vertical variations of A_T and the C_T distribution, the study took into consideration the changes due to organic matter decomposition and changes due to the carbonate pump caused by carbonate dissolution. The region is characterized by dissolution of surface-produced calcite and aragonite in the upper 1000 m. The dissolution of hard material predominates in deeper water as a result of increased pressure, decreased temperature and longer residence time. The remineralization of organic matter increased with depth. In the first 500 m, 51% of the increase in the C_T can be attributed to remineralization of organic matter. Maximum contribution was obtained at around 900–1000 m, with a value of 80 ± 7 μmol kg^{-1}. It has been determined that the potential contribution of the formation and/or dissolution of $CaCO_3$ and the consumption and/or remineralization of nitrate remain constant with the observed NA_T variability at ESTOC. When the water column C_T was decomposed, the Eastern North Atlantic Ocean, at the area where the ESTOC station is located, showed an increasing storage capacity for excess CO_2 of 0.85 mol m^{-2} yr^{-1}.

Though carbonate system parameter data are scarce for the Mauritanian upwelling region, it is known that the upwelling of waters along the NW African shelf can transport high levels of CO_2 to the sea surface near shore (Copin-Montégut and Avril, 1995; González Dávila et al., 2014). As these waters age and are advected offshore, CO_2 levels decrease, falling well below atmospheric concentrations at the continental shelf break. The initial upwelling leads to low saturation states of $CaCO_3$ in surface waters (Loucaides et al., 2012; Lachkar and Gruber, 2013). However, the uptake of carbon by phytoplankton leads to reduced C_T and upwelling driven CO_2 outgassing. This process, modelled for the northern part of the CUE (Lachkar and Gruber, 2013) consequently raises the saturation states of $CaCO_3$. In the Cape Blanc area, the model applied by Lachkar and Gruber (2013) showed the reduced biological efficiency should produce an enhancement of the CO_2 outgassing. In both regions, the remineralization of sinking organic matter in sub-surface waters would generate CO_2, which causes an increase of C_T and lowers the saturation states of $CaCO_3$.

4.2.5. CONCLUSIONS AND RECOMMENDATIONS

The vertical distribution of the carbon dioxide variables in the Canary Islands region along the last fifteen years have clearly indicated significant changes over, at least, the first 1000 m affecting the inorganic carbon content and the acidity of the seawater. In the surface, the NC_T increased at a rate of 0.9 μmol kg^{-1}, the pH_T decreased each year on average 0.0019 units, while the NA_T keeps constant at a value of 2292 μmol kg^{-1}. This increase in C_T is controlling the total column inventory of anthropogenic CO_2 that has reached a value of 66 ± 3 mol m^{-2} for the reference year 2000. Considering the importance of EBUE in the coastal ocean from a socio-economic, oceanographic and climatological point of view, few studies have been undertaken about the role of this region in inorganic carbon cycling. It has been showed that upwelled waters in the Mauritanian upwelling area provided high contents of inorganic carbon which lead to low calcium carbonate saturation states. The uptake of carbon by phytoplankton acts to decrease C_T and

consequently increase saturation states. Our knowledge about whether coastal upwelling will intensify, or whether upper-ocean warming and the increased stratification will prevail and how these processes will affect the nutrient inputs, carbon exported out of the surface ocean, iron supply, acidification, hypoxia, rainfall patterns and anthropogenic source terms are lacking. Model results indicate the importance of physics and environmental conditions in shaping the sensitivity of CCLME to potential climate change induced upwelling-favorable wind intensification. However, experimental data should be gathered in order to sustain model results.

Acknowledgements

This work has been supported by the European Project CARBOCHANGE 2011-2015 (Changes in carbon uptake and emissions by oceans in a changing climate), GA no: 264879.

4.3. ORGANIC MATTER DYNAMICS IN THE CANARY CURRENT

Xosé Antón ÁLVAREZ-SALGADO[1] and Javier ARÍSTEGUI[2]

[1] Instituto de Investigaciones Marinas, CSIC. Spain

[2] Instituto de Oceanografía y Cambio Global (IOCAG), Universidad de Las Palmas de Gran Canaria. Spain

4.3.1. INTRODUCTION

The primary source of organic matter in the oceans is from the photosynthesis of phytoplankton. Biomass and exudates are processed within the microbial and metazoan food webs, leading to hundreds of thousands of different compounds (Mopper et al., 2007) that span a continuum of size classes from tenths of angstroms to metres (Verdugo, 2012) and lifetimes from hours to thousands of years (Hansell, 2013). Organic matter is operationally classified, according to its size, into particulate (POM) or dissolved (DOM) organic matter, depending on whether it is retained or not by a filter of 0.2–0.7 µm pore size (Fig. 4.3.1). POM consists mainly of a minor portion formed by living organisms (about 10% weight/weight) and a major portion formed by their detritus (about 90% weight/weight). It is classified into suspended (<100 µm, POM_{susp}) and sinking (>100 µm, POM_{sink}) particles, which contribute contrasting ecological roles: whereas POM_{susp} is retained in the parcel of water where it is produced and can be processed and/or transported by coastal and ocean currents, POM_{sink} settles down out of the water parcel where it is produced and is processed in deeper water levels and/or in the coastal, slope or abyssal sediments (Steinberg et al., 2008).

Most of the organic matter in the oceans (>95%) is, however, in the dissolved form, ranging from truly dissolved low molecular weight molecules to large colloidal high molecular weight materials. At the global scale, labile DOM represents a minor fraction of the bulk DOM pool (<0.1%) and is processed within the water parcel where it is produced. Semi-labile DOM represents about 1% of the bulk DOM and it is transported horizontally by the coastal and ocean currents or vertically by convective overturning to be processed, in some cases, thousands of kilometres away from where it was produced (Hansell et al., 2009). Thus, most of the DOM is refractory (>99%), remaining in the oceans for periods of decades to millennia without being used by any living organisms (Hansell, 2013). However, these figures may change in highly productive Eastern Boundary Upwelling Ecosystems (EBUE), such as the Canary Current Large Marine Ecosystem (CCLME), where the proportions of the labile and semi-labile fractions increase dramatically. In this article, we will focus on the role played by POM, either suspended or sinking, and the labile and semi-labile fractions of DOM on the biogeochemistry of the area.

Although organic matter is a key component of the carbon cycle in the CCLME, information relating to its spatial and temporal dynamics and elemental (C:N:P) and chemical composition is scarce. In this work we review the existing literature on ocean colour satellite observations, moored and free-drifting sediment traps, water samples collected during process-orientated studies to resolve the rich mesoscale variability of this area, and the output from coupled physical-biogeochemical models in order to gather an inclusive view of the distribution, composition and role played by the organic materials produced, processed and exported to the ocean water column and sediments adjacent to the CCLME.

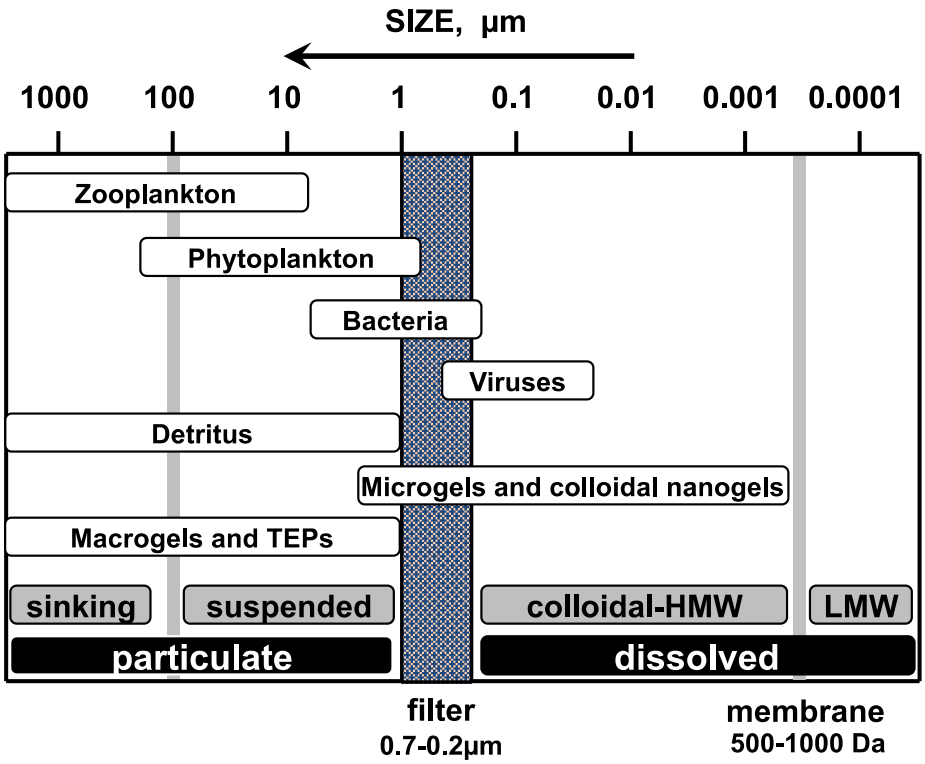

Figure 4.3.1. Size continuum of organic matter in seawater expanding at least 8 orders of magnitude. The separation between dissolved and particulate organic matter is operationally defined by filters of 0.2–0.7 µm cut-off and the separation between truly dissolved and colloidal by filters of 0.5–1 kDa cut-off. TEP, transparent exopolymeric particles. Adapted from Hedges (2002).

Unfortunately, there is an absence of hydrographic monitoring programmes integrating time-series stations and/or repeated transects across the CCLME that include water-column measurements of the concentration of organic matter and its elemental (C:N:P) or molecular composition. Conversely, research efforts on this matter have basically focused on (i) quantifying the flux and elemental (C:N) composition of POM_{sink} using deep-water sediment traps; and (ii) the impact of the mesoscale features resulting from the distortion of the Canary Current by the intricate topography of the coast with its prominent capes, islands and seamounts — producing meanders, filaments and eddies (Sangrà, 3.5 this book) — on POM_{susp} and DOM. Accordingly, we have structured this section into three parts, reviewing the effect of upwelling filaments, intermediate and bottom nepheloid layers, and seamount- and island-generated eddies, on the biogeochemical cycling of organic matter in the CCLME.

4.3.2. COASTAL WATERS AND UPWELLING FILAMENTS

The CCLME is the only EBUE where the effect of filaments of cold upwelled water on the distribution and cycling of organic matter has been studied in some detail (Pelegrí et al., 2005; Arístegui et al., 2009a). These mesoscale structures, which spread into the adjacent ocean from a few hundred kilometres off the Moroccan coast (Van Camp et al., 1991; Pelegrí et al., 2005) to more than one thousand kilometres off Cape Blanc (Helmke et al., 2005), are associated with the most prominent capes along the coast (Álvarez-Salgado et al., 2007; Arístegui et al., 2009a; Sangrà, 3.5 this book). The first evidence of the importance of upwelling filaments in the lateral export of organic matter in the CCLME was provided by Van Camp et al.

(1991) and Gabric et al. (1993) on the basis of sea surface temperature and ocean colour satellite observations. They estimated that about 50% of the POM produced in the coastal area around Cape Blanc (21°N) was exported offshore by the giant filament observed in this region year-round. These observations implied that the lateral export of POM_{susp} could exceed the vertical export of POM_{sink} to the coastal sediments that had previously been considered the fate of primary production in any EBUE (Wilkerson and Dugdale, 2008). It should be noted that neither the satellite observations of Gabric et al. (1993) nor the numerical model developed later by these authors (Gabric et al., 1996) included DOM. A decade later, process-orientated studies were conducted off Capes Juby and Bojador (26°N–28°N; García-Muñoz et al., 2004) and Cape Ghir (30°N–31°N; García-Muñoz et al., 2005) to assess the contribution of POM and DOM to the lateral export of organic matter by the upwelling filaments that develop in these areas. These studies concluded that the concentration of dissolved organic carbon (DOC), which is the major element of organic matter, in the Eastern North Atlantic Central Water (ENACW) that upwelled over the shelf was 50–60 μmol l^{-1} and the corresponding concentrations in the surface waters transported offshore by the filament ranged from 75–90 μmol l^{-1}. Thus, 2/3 of the DOC exported by the filaments consisted of aged materials present in upwelled ENACW and 1/3 was fresh DOC recently produced during the microbial and metazoan processing of the phytoplankton primary production triggered by the massive entry of upwelled inorganic nutrients. Consequently, about 33% of the DOM exported from the productive shelf waters into the oligotrophic adjacent ocean was bioavailable, a proportion much higher than the previously mentioned global estimate of <1% of Hansell (2013).

García-Muñoz et al. (2004, 2005) also showed that the concentration of suspended particulate organic carbon (POC_{susp}) in these filaments was low, 1–4 μmol l^{-1}, which meant that about 90% of the exported fresh organic materials was in the dissolved form. Furthermore, they calculated that from 30% (off Cape Juby) to 60% (off Cape Ghir) of the coastal primary production, estimated to be 750 g C m^{-2} yr^{-1} (Longhurst et al., 1995), was exported horizontally out of the shelf. Given that the Cape Juby-Bojador and Cape Ghir samplings were respectively done under strong upwelling (García-Muñoz et al., 2005) and upwelling relaxation (García-Muñoz et al., 2004) conditions, these ratios should be considered as upper and lower limits of the fraction of new production available for horizontal export from the productive shelf of the CCLME into the oligotrophic open ocean. Despite this experimental evidence of the importance of DOM in the horizontal export of biogenic materials in the CCLME, none of the coupled physical-biogeochemical models recently developed for this area have included this component (Karakas et al., 2006; Machu et al., 2009; Lachkar and Gruber, 2013). These calculations are, however, not applicable to the coastal area south of Cape Blanc, where South Atlantic Central water (SACW) upwells and is characterized by nitrate concentrations 2 to 3 times higher than that of ENACW (Pelegrí and Peña-Izquierdo, 4.1 this book), being further supplemented by nitrate input from River Senegal (Gac and Kane, 1986). DOC concentrations in the upwelled SACW and riverine water are also currently unknown, preventing any calculations specific to this area.

The fate of the organic materials transported by cold filaments in the CCLME remains uncertain. It is known that part of the POM collected by sediments traps in offshore waters of the CCLME is produced in the coastal zone (Romero et al., 2002; Neuer et al., 2002; Helmke et al., 2005; Fischer et al., 2009). This means that either the cold filaments transport POM_{sink} or that further processing of the POM_{susp} within the filaments ends up as POM_{sink}. Neuer et al. (2002) found coastal upwelling particles originating from Cape Ghir in sediment traps deployed at >2900 m depth off the Island of La Palma, about 720 km offshore of their source. They also observed a significant increase with depth of the C:N molar ratio of POM_{sink} from a value of around 7 at 300 m to 10–11 at >2900 m. The value at 300 m depth is not significantly different

from the C:N ratio of the fresh phytogenic materials (6.7; Anderson, 1995; Fraga et al., 1998) currently found in the POM_{susp} transported by filaments. Indeed, Arístegui et al. (2004) obtained an average molar ratio of 6.8 ± 1.5 for the filament off Cape Ghir. The increase in the C:N ratio with depth suggests either (i) elemental fractionation during the mineralization of sinking particles, with the more labile N-rich protein materials being mineralized at shallower levels (Boyd and Trull, 2007); or (ii) lateral input of aged POM from the continental shelf (Bauer and Druffel, 1998; see 4.3.3).

The high proportion of mineral particles imported from the adjacent Sahara desert and recovered in deep-water sediment traps deployed within the area of influence of capes Ghir (Neuer et al., 1997, 2002) and Blanc (Helmke et al., 2005) is also noteworthy. Therefore, it seems that POM_{susp} can be transformed into POM_{sink} mediated by the nucleation properties of dust (Armstrong et al., 2002; Fischer and Karakas, 2009). In this sense, the CCLME is characterized by the largest dust deposition rates worldwide (Jickells et al., 2005; Gelado-Caballero, 2.3 this book) and that POM_{sink} sinking rates ranging from 30 m d^{-1} to 326 m d^{-1} have been recorded in the area (Fischer et al., 2009).

Concerning DOM, it seems that a minor fraction of this material (<16%) is processed by the microbial populations within the coastal transition zone (Álvarez-Salgado et al., 2007), but most of it accumulates in the adjacent oligotrophic subtropical gyre, where high DOM concentrations occur (Hansell et al., 2009). The likely reason for this accumulation is the severe inorganic nutrient limitation in the surface waters of subtropical gyres during summer stratification, although part of these materials are probably processed after winter convection, when inorganic nutrient levels in the mixed layer are not limiting (Hansell et al., 2009). Photochemical decomposition of coloured DOM (CDOM) — i.e. the fraction of DOM that absorbs light in the UV-visible range of the light spectrum — to produce CO, CO_2, NH_4^+ and low molecular weight organic compounds (Moran and Zepp, 1997) is also an expected DOM sink that has been tested during a recent study of the giant filament of Cape Blanc (Kitidis et al., 2014). However, its actual contribution to the DOC loss is still uncertain.

The influence of upwelling filaments on the distribution of organic matter is summarized in the diagram presented in Figure 4.3.2. Cold, nitrate and refractory DOM-rich central water from 150–250 m depth upwells over the shelf, stimulating the growth of diatoms in the surface layer. Southwest displacement of the coastal jet produces an offshore drift of that water, evolving into a cold filament. During this offshore transport nitrate is consumed and the water column stratifies progressively, in such a way that the surface chlorophyll maximum dominated by large diatoms is gradually replaced by a deep, low-chlorophyll maximum dominated by small flagellates (Gabric et al., 1996; García-Muñoz et al., 2005). The biomass of autotrophs also decreases offshore (Arístegui et al., 2004). As a consequence, a transition from a metazoan-dominated food web over the shelf to a microbial-dominated food web offshore may occur. This implies that the biological pump over the shelf is mediated by large fast-sinking POM, whereas in the offshore drifting filament the horizontal export of POM_{susp} + DOM is dominant. This conceptual model is consistent with the drastic 1:5 decrease of POM_{sink} fluxes from the continental slope of the CCLME at 29°N to the Island of La Palma (about 600 km offshore) and the particularly low vertical export ratios — calculated as the ratio between the POM_{sink} flux at 100 m depth and the primary production in the overlying water — of <0.1 obtained for this area (Neuer et al., 2002). This calculation is also consistent with the ranges of vertical export ratio of 0.06 to 0.19 obtained by Arístegui et al. (2004) in the filament of Cape Juby and of 0.16 to 0.24 by Head et al. (1996) in the filament of Cape Ghir, both using free-floating sediment traps deployed at 100 m depth. Nevertheless, although the offshore transport by filaments is 2.5 to 5 times larger than Ekman transport (Pelegrí et al., 2005, Álvarez-Salgado et al., 2007), the return flow of

filament water towards the coastal upwelling jet might reduce the impact of the overall offshore transport, especially south of the Canary Islands, where filaments and island eddies interact (see section 4.3.4).

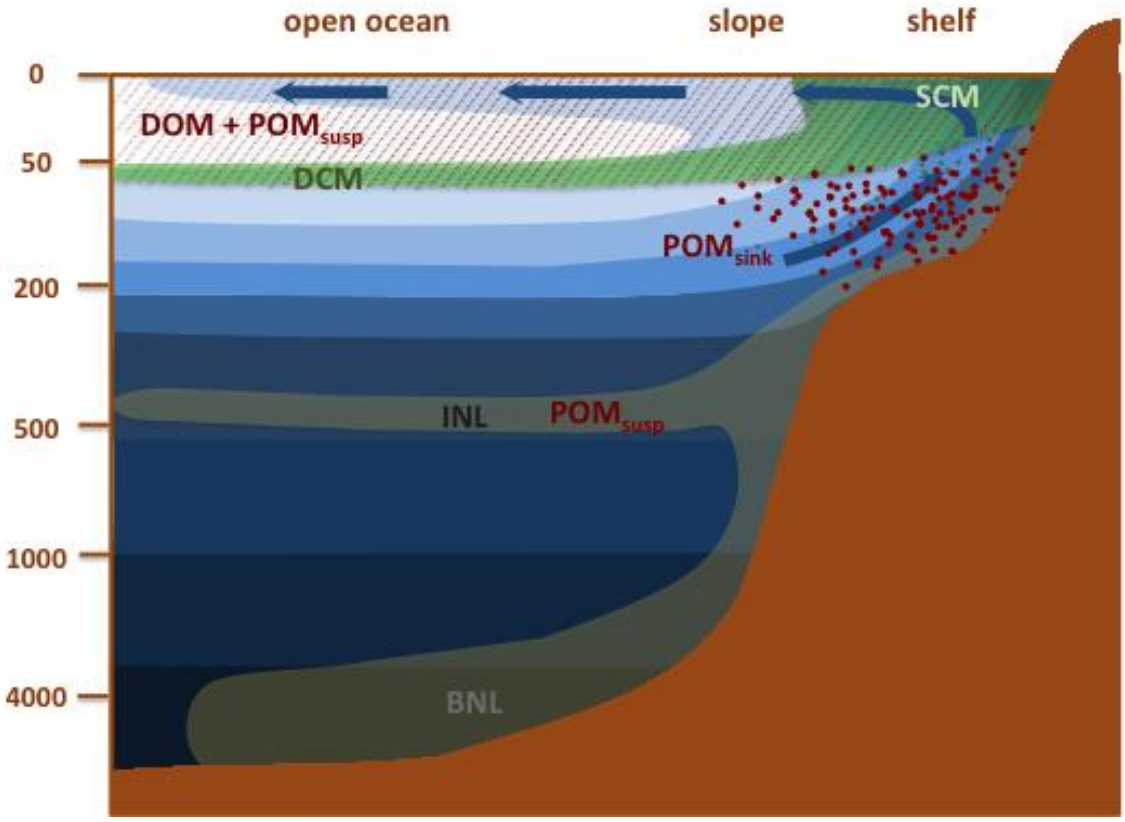

Figure 4.3.2. Schematic showing the off-shelf export of dissolved (DOM), suspended (POM_{susp}) and sinking (POM_{sink}) organic matter by cold upwelling filaments and by intermediate (INL) and bottom (BNL) nepheloid layers in the CCLME. Background colour palette, water temperature (dark to light blue represents colder to warmer waters); dark blue arrows, uplift onto the shelf and offshore transport of cold upwelled waters; green shade, cross-shelf evolution of the chlorophyll distribution from a surface maximum (SCM) over the shelf to a deep maximum (DCM) in the open ocean; oblique stripers, dissolved (DOM) and suspended (POM_{susp}) organic matter transported by the filament; solid circles, sinking of particulate organic matter (POM_{sink}) over the shelf; grey shades, intermediate (INL) and bottom (BNL) nepheloid layers.

4.3.3. NEPHELOID LAYERS

Below the surface nepheloid layer associated with the lithogenic and phytogenic particles transported offshore by upwelling filaments (see 4.3.2), intermediate (INL) and bottom (BNL) nepheloid layers are present in slope and abyssal waters of the CCLME (Fig. 4.3.2; Karakas et al., 2006; Fischer et al., 2009). Nowald et al. (2006), using a particle camera, reported the presence of an INL between 200 m depth and 500 m depth in the open ocean region off Cape Blanc. Supported by a high-resolution coupled physical-biogeochemical model, Karakas et al. (2006) hypothesized that this INL originated from the seaward advection of slow sinking particles (5 m d^{-1}) eroded from shelf or slope sediments by the intense and variable coastal currents. Conversely, particles sinking at 17 m d^{-1} (Karakas et al., 2006) to 30 m d^{-1} (Fischer et al., 2009) seem to be restricted to a bottom layer more than 1000 m thick following downslope to form the BNL. These sinking rates are consistent with the observations of Alonso-González et al. (2010a) who

found that 60% to 75% of the POM collected in Indented Rotating Sphere Carousel (IRSC) sediment traps moored at 250 m south of the Canary Islands consisted of fresh material (C:N molar ratio 7.3-8.5) that sank at <11 md^{-1}. These authors speculate that such slow-sinking particles, which they consider to be POM_{susp}, could result from physical or biological-mediated disaggregation of larger fast-sinking particles but also by assembly of dissolved organic material yielding porous microgels and colloidal nanogels (Fig. 4.3.1).

Deep-water sediment traps also showed evidence of lateral inputs of organic materials transported from the adjacent continental shelf and slope. Neuer et al. (2002) reported an increase in the particle flux and a decrease in the $\delta^{15}N$ of POM with depth in the previously referred to array of sediment traps deployed at about 29°N (European Station for Time series in the ocean (ESTOC) and La Palma Island moorings). These observations can only be explained by an additional lateral input of particles transported by the upwelling filament of Cape Ghir and INLs originating from shelf and slope sediments, especially in areas where the coastal topography is dominated by capes and canyons favouring particle detachment (Fig. 4.3.3). On the basis of $\delta^{15}N$ data, Freudenthal et al. (2001) determined that 50%–75% of the organic nitrogen recovered by the deep-water traps at the ESTOC site was allochtonous. Helmke et al. (2005) and Fischer et al. (2009) also relied on the lateral transport of particles from shelf and slope sediments to explain the particle fluxes observed in the moorings off Cape Blanc. They estimated that the lateral contribution to the organic carbon collected in the traps was 15% on an annual basis, but 63% in the highly productive late winter–early spring period.

A key consequence of the massive offshore transport of organic material produced over the shelf via upwelling filaments, INL and BNL is the relatively low accumulation of fine-grained particles — including phytogenic materials produced in response to coastal upwelling — in continental shelf sediments of the CCLME (Neuer et al., 2002; Karakas et al., 2006). Nevertheless, there is a trend towards increasing accumulation rates of organic material from north to south, which partly reflects a southward increase of productivity, but also an input of clay minerals by the Senegal River and better preservation of organic matter from plankton or terrestrial plants (Arístegui et al., 2006).

In spite of all the experimental evidence and that provided by models, the impact of these intermediate and bottom nepheloid layers in the distribution of organic matter in the region and its potential contribution to the export of biogenic materials produced on the shelf to the adjacent ocean (Fig. 4.3.2), there is almost no information about the overall exchange rate of organic matter between the coast and the open ocean. This is because lateral transport has being estimated by mass balance approaches on the basis of sinking particles (e.g. Ducklow and McAllister, 2005) rather than direct measurements. The first direct estimate of the lateral transport of POM_{susp} in an EBUE was carried out by Alonso-González et al. (2009). These authors reported high concentrations of POC_{susp} in the mesopelagic and bathypelagic zones of the CCLME and estimated, through a box-model approach, that POC_{susp} transported laterally could account for 28% to 59% of the total mesopelagic respiration. These results indicate that the CCLME is probably characterized by higher lateral export of coastally produced POC than was previously assumed.

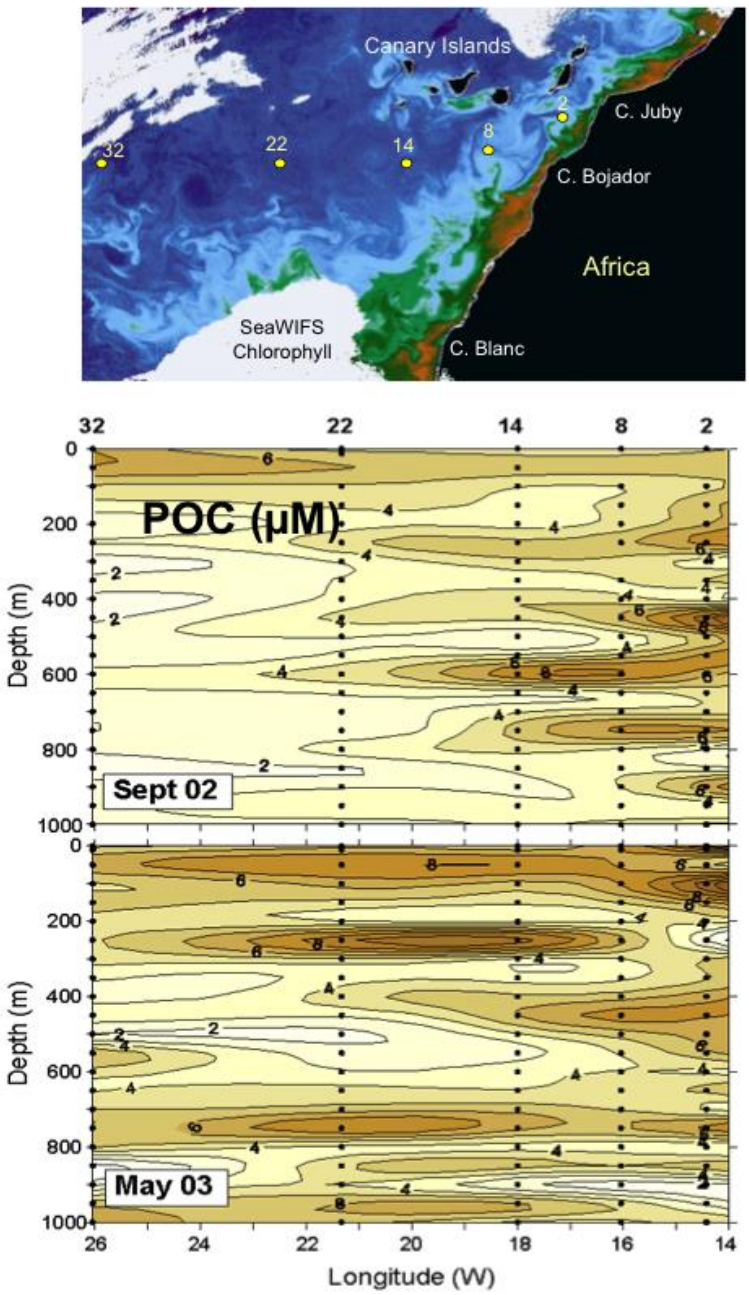

Figure 4.3.3. Vertical distribution of suspended particulate organic carbon (POC_{susp}) across the Canary Islands coastal transition zone. Upper panel: position of the samplings stations on a satellite (SeaWIFS) surface chlorophyll image. Middle panel: POC_{susp} distribution during September 2002. Lower panel: POC_{susp} distribution during May 2003. Notice the coastal-offshore patchy distribution of POC_{susp} in the 200-1000 m depth layer.

4.3.4. ISLAND - AND SEAMOUNT - GENERATED EDDIES

The perturbation of the southward flow of the Canary Current by the Canaries and Madeira archipelagos, as well as by some shallow seamounts, leads to the generation of a strong eddy field in the CCLME with significant implications for the production and cycling of organic matter. Mesoscale eddies can remain trapped off the islands for a variable period of time, or detach and drift along the main flow, or across it, forming part of a westward-flowing eddy corridor (Sangrà et al., 2009).

Shallow seamounts, like Seine seamount to the east of Madeira, may present local accumulations of DOM and POM_{susp} around them. Vilas et al. (2009) argued that the productivity around Seine would not explain the large accumulation of POM found on top of the seamount. They hypothesized that a trapped vortex (like a Taylor Column) would favour the production, accumulation and retention of POM on its shallow summit, as inferred from chlorophyll, POM and biomass measurements (Arístegui et al., 2009b).

In the Canary Islands, cold-core cyclonic and warm-core anti-cyclonic eddies are generated by the combination of flow perturbation and Ekman pumping on the islands' wind shear (Fig. 4.3.4; Arístegui et al., 1994; Barton et al., 2000; Sangrà, 3.5 this book). During their early formation stages ageostrophic cyclonic eddies pump nutrients into their cores, with upwelling velocities of up to 50 m d^{-1} (Barton et al., 1998), enhancing the production of fresh photosynthetic POM (Basterretxea and Arístegui, 2000). The contribution of island eddies to the overall primary production of the Canary Islands has been estimated to be comparable to the coastal upwelling region and locally up to 4 times higher than the background values (Barton et al., 1998; Sangrà et al., 2009). Moreover, recent studies using drifting and moored sediment traps have conclusively demonstrated that the eddy field generated south of the Canary Islands enhance POC export two- to fourfold compared to stations outside of the influence of the eddy field (Alonso-González et al., 2010b; 2013). Cyclonic eddies could therefore act as an efficient organic carbon pump to the ocean interior, accelerating the transfer of fresh organic matter, by favouring the formation of fast-sinking particles in eddy cores (Alonso-González et al., 2013).

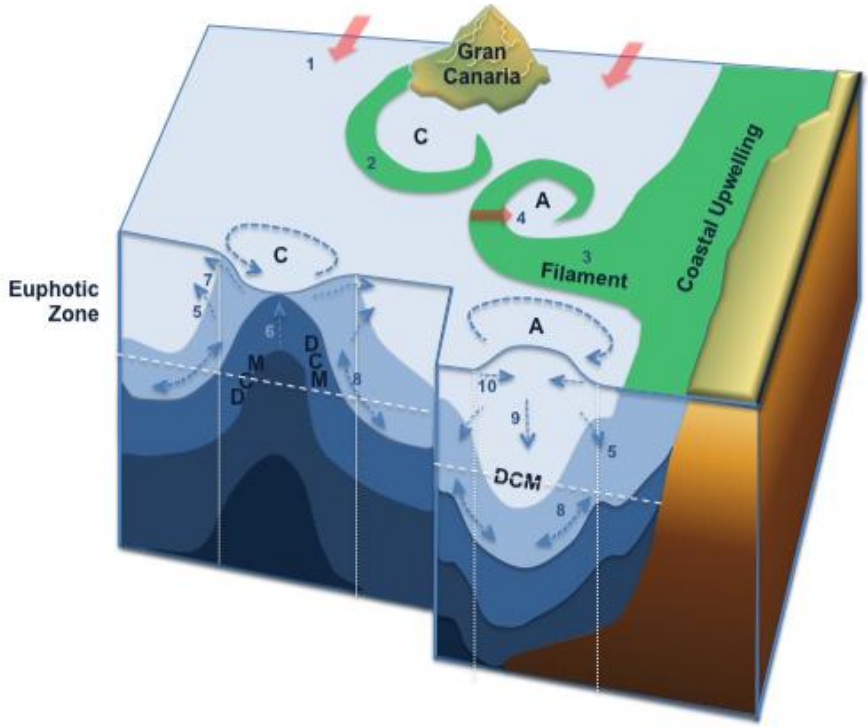

Figure 4.3.4. Schematic showing vertical and horizontal fluxes associated with island-generated cyclonic (C) and anti-cyclonic (A) eddies downstream of Gran Canaria Island. (1) Mean surface flow and wind direction; (2) advection of high-chlorophyll coastal water during cyclonic eddy formation; (3) entrainment of high-chlorophyll water upwelled from the African coast by anti-cyclonic eddy; (4) lateral exchange of chlorophyll between the periphery and the eddy centre; (5) diapycnal mixing; (6) upwelling or uplifting of the thermocline; (7) outward radial advection; (8) isopycnal mixing; (9) downwelling or deepening of the thermocline; (10) inward radial advection. DCM = Deep Chlorophyll Maximum. Adapted from Arístegui et al. (1997).

Eddies can also accumulate and transport in their periphery POM and DOM originating near the islands or trapped in their interaction with upwelling filaments (Fig. 4.3.4; Arístegui et al., 1997; 2004). As a result of this interaction, some of the offshore filament waters can be re-circulated back to the coast. This makes some filaments (such as the one off Cape Juby) less efficient for the offshore export of organic matter than others (e.g. those off capes Ghir and Blanc), particularly in periods of weak upwelling or reduced winds (Arístegui et al., 2004; see 4.3.2). Alternatively, eddies may transport POM and DOM into the adjacent oligotrophic ocean through a corridor of cyclonic and anti-cyclonic eddies that detach from the islands and drift slowly south-westwards for months, while increasing their size and decreasing their rotation speed and eccentricity (Sangrà et al., 2004).

The study of island eddies in the CCLME has been based on satellite observations (Hernández-Guerra et al., 1993, Arístegui et al., 1997; Sangrà, 3.5 this book) and research cruises focused on the hydrographic dynamics of these structures, with particular emphasis on their impact on the distribution of chlorophyll and phytoplankton, microbial respiration and POM sedimentation (e.g. Basterretxea and Arístegui, 2000; Arístegui et al., 2004; Alonso-González et al., 2013). However, process-oriented studies to resolve the distribution, elemental and chemical composition and cycling of organic matter in eddies detached from the Canaries are rare. Therefore, we can hypothesize that fresh material produced *in situ* or trapped by both cyclonic and anti-cyclonic eddies from the islands or the African coast would stimulate microbial respiration (if these materials are dissolved or neutrally buoyant, i.e. DOM+POM_{susp}) or increase sinking rates (if they are in the form of sinking particles, i.e. POM_{sink}) in the coastal transition zone. On the contrary, aged organic materials may accumulate in the core of anti-cyclonic eddies because of the severe nutrient limitation of prokaryotic respiration, referred to earlier, enhanced by the deepening of the nutrient-rich thermocline in the core of these eddies.

4.3.5. CONCLUSIONS AND RECOMMENDATIONS

Despite the considerable efforts made to understand the role played by biogenic dissolved and particulate organic matter in the Carbon cycle of the CCLME, we have identified some gaps that should be addressed: (i) measurements of the concentration, elemental (C:N:P) and molecular composition of POM_{susp} and DOM should be incorporated into existing or future monitoring programmes; (ii) process-oriented studies are needed to quantify the portion of the biogenic organic matter produced on the shelf that is exported seawards by the INL and BNL and its fate within the coastal transition zone — mineralization, aggregation and sinking, or horizontal export to the open ocean; (iii) similarly, there is also a need for studies focused on the corridor of cyclonic and anti-cyclonic eddies detached from the Canary Islands; (iv) the role of POM and DOM in the area south of Cape Blanc — with its distinct hydrography, mediated by the upwelling of low-oxygen SACW and the development of hypoxic conditions on the shelf, and the presence of a large river like the Senegal — merits special attention; and finally (v) coupled physical-biogeochemical models should incorporate DOM and POM_{susp} as key components in forecasting the Carbon cycle in the CCLME under various climate change scenarios.

Acknowledgements

X. A. Álvarez Salgado was supported by the project HOTMIX (grant NºCTM2011-30010-C02-02) and REIMAGE (CTM2011-30155-C03-03) and J. Arístegui by the projects HOTMIX (CTM2011-30010-C02-01) and PUMP (CTM2012-33355). M. J. Pazó helped with illustrations.

4.4. PHYTOPLANKTON AND PRIMARY PRODUCTIVITY OFF NORTHWEST AFRICA

Hervé DEMARCQ[1] and Laila SOMOUE[2]

[1] Institut de Recherche pour le Développement. France

[2] Institut National de Recherche Halieutique. Morocco

4.4.1. INTRODUCTION

Eastern boundary upwelling ecosystems (EBUEs) cover less than 2% of the ocean surface, but contribute 7% of the global marine production. Upwelling systems are a major source of the net primary production (NPP) in tropical and subtropical latitudes and sustain the most productive pelagic fisheries of the world, accounting for 20% to 30% of global marine fisheries production (FAO, 2012a).

The Canary Current Upwelling System (CCUS), which extends from the Iberian Peninsula to Guinea (43°N to 8°N), is one of the most productive coastal upwelling system in the world. It covers the whole Canary Current Large Marine Ecosystem (CCLME). This EBUE is maintained by intense equatorward trade winds (see Soares, 3.1 this volume), persistent in the central part of the region and seasonal in the southern and northern parts, in winter and summer respectively. The wind stress drives offshore surface transport compensated by an inshore and progressively upward flux of nutrient-rich water masses. This upwelling process is adequately modeled by the Ekman transport (Bakun, 1973; Ekman, 1905), used earlier to describe the average seasonal cycle of upwelling in the region (Schemainda et al., 1975; Wooster et al., 1976).

The nutrient concentrations reaching the euphotic layer directly govern the intensity of the phytoplankton blooms during the year (see for example Huntsman and Barber, 1977), simultaneously controlled by the sun light at the sea surface and its vertical penetration.

Phytoplankton are composed of a large diversity of unicellular algae or bacterias and form the base of the marine food web, that constraints all life in the oceans, up to its super-predator part, mostly driven by human consumption through commercial fisheries (Chassot et al., 2010; Watson et al., 2014).

Primary production is the synthesis of organic matter from atmospheric or dissolved carbon dioxide (CO_2), a process that occurs through photosynthesis, a way of harvesting light to convert inorganic carbon to organic carbon. Phytoplankton are mostly composed of photoautotrophic organisms, called primary producers, which are passively transported in water masses. They ultimately supply organic carbon to diverse heterotrophic organisms that obtain their energy solely from the oxydation of organic matter.

Primary production can be considered as net (NPP) or gross (GPP), depending if carbon losses from the respiration of the autotrophic organisms are included. Integrated within the euphotic zone, where sunlight penetrates, the “net ecosystem production” (NEP) from all living organisms is equivalent to the sinking organic carbon, in both particulate or dissolved form.

Despite contributing only 1-2% of the global primary biomass on earth (Falkowski, 1994; Field et al., 1998), oceanic productivity (± 40 GtC yr^{-1}) accounts for about 40% of the total NPP.

This article reviews the various factors that drive NPP in upwelling systems in general and in the CCUS in particular, as well as some ways to estimate it. Quantitative estimates are presented from a remote sensing-based model and the spatio-temporal patterns of productivity are described. The plankton diversity of the region, as detailed from *in situ* determinations in the Moroccan region is also described.

4.4.2. OCEANIC PRIMARY PRODUCTIVITY AND THE GLOBAL CARBON CYCLE

CO_2 concentrations have increased by 40% since pre-industrial times (year 1750) (IPCC, 2013) and more than 25% from any time in the past 420,000 years (Petit et al., 1999). One of the major changes in the global carbon cycle on earth is that the role of the oceans has become predominant. The oceans are now a net sink of CO_2, by removing 2.3 ± 0.7 PgC yr^{-1} from the atmosphere (i.e. about 26% of the anthropogenic emissions), a value similar (2.6 ± 1.2 PgC yr^{-1}) to that of the terrestrial biosphere (IPCC, 2013). It is also estimated that this sink has increased only slightly over the last two decades (Sitch et al., 2015; Wanninkhof et al., 2013), probably because the global temperature increase has reduced the efficiency of the ocean to dissolve CO_2.

Ultimately, only 25% of the carbon fixed in the upper ocean sinks into the interior where it is oxidized by heterotrophic organisms (Falkowski et al., 1998; Laws et al., 2000). This is achieved by the sinking of organic matter before it is returned to dissolved inorganic carbon and dissolved nutrients by bacterial decomposition. Oceanographers often refer to this process as the "biological pump", as it pumps CO_2 out of the surface of the ocean and atmosphere into the voluminous deep ocean (Volk and Hoffert, 1985).

The ocean response to climate change, and particularly the response of EBUEs, that account for 7% of the global marine production, is of primary importance in quantifying the carbon cycle and the way human impacts continue to modify it.

4.4.3. FACTORS LIMITING PRODUCTIVITY

Phytoplankton growth and productivity are affected by several “limiting” factors, including nutrients, light, temperature, circulation, grazing and other biological constraints (Eppley, 1972; Tilman et al., 1982) within the euphotic zone, the upper part of the epipelagic province (0-200m) where light penetrates.

4.4.3.1. Upwelling intensity and nutrient availability

Because of the importance of physical forcing in upwelling systems, the first factor of variability is the supply of nutrient-rich waters to the surface, in direct relationship with the local intensity of the upwelling (see Pelegrí and Benazzouz, 3.4 this volume). The variable width of the continental shelf of the CCUS and the presence of several Capes (from north to south, Cape Ghir, Cape Juby, Cape Bojador and Cape Blanc, see Figure 4.4.1.), contribute to the variable upwelling intensity between different regions, according to the local orientation of the coast line. The resulting enrichment is proportional to the essential nutrient concentrations of the upwelled water that will be used by the phytoplankton in the form of nitrate, phosphate and silicates (see Pelegrí and Peña-Izquierdo, 4.1 this volume).

As described by Tomczak and Hughes (1980) and Barton (1998) the surface waters of the CCUS are formed from North Atlantic Central Water (NACW, 11.00-18.65°C, 35.47-36.76‰ defined by Sverdrup et al. (1942) that dominates the upwelled waters North of Cape Blanc (20°N) in association with deeper intermediate

Eastern North Atlantic Central Water (ENACW, 8.0-18.0°C, 35.2-36.7 ‰ defined by Fiuza and Halpern, 1982). South Atlantic Central Water (SACW, 35.70‰ and 9.70°C, 35.177‰ and 15.25°C), with 3 times higher average nutrient concentration (Fraga, 1974) dominates the southern part of the system, strongly enhancing enrichment of the upwelling system south of Cape Blanc. Coastal upwelling has been shown to be dominated by nitrate-based production, whereas ammonium-based production becomes progressively dominant further offshore: on the shelf off Cape Blanc, Barber and Smith (1981) estimated that regenerated nitrogen accounted for 72% of total nitrogen, whereas close to Cape Ghir, Head et al. (1996) showed bacterial consumption to account for 50% of the total NPP.

4.4.3.2. Light limitation

The second important factor controlling primary production is the availability of sunlight, characterized by daily and seasonal changes in intensity and duration. Sunlight penetrates the semi-transparent water of the euphotic zone, generally defined as the depth where light reaches 1% of its surface value and where photosynthesis occurs. The depth of the euphotic layer varies from less than 10 m in dense or turbid coastal waters to about 80 m in very oligotrophic waters, as those of the tropical oceanic gyres.

An important limit is the “compensation depth” (Sverdrup, 1953), where the rate of photosynthesis exactly matches the rate of respiration, and beyond which no NPP can occur. Because of the dominance of light in phytoplankton growth in upwelling systems, this limit is generally close to the bottom of the euphotic zone.

In the Canary region, light availability is high, especially in the central – cloud free desert region with quasi permanent trade winds from 20°N to 26°N. Light availability decreases on either side of this region: in the north because of a more temperate climate with a summer light maximum, and in the south, from central Mauritania to Guinea, where light is limited in summer because of the high cloud cover due to the northernmost position of the Inter-Tropical Convergence Zone. Nonetheless, on average, the strong seasonality of light moderately impacts the photosynthesis process in the regional areas of upwelling, because of its natural co-occurrence with the trade winds. Because of this compensation effect, Head et al. (1996), did not find any correlation between integrated primary production rates and light intensity in Moroccan inshore waters, despite a two-fold variation of light between winter and summer.

In the euphotic zone, especially in rich coastal upwelling systems, light is significantly limited by self-shading, an important constraint in oceanic NPP (Steemann Nielsen et al., 1962). Mathematical models of self-shading show that settlement characteristics of each species determine, along with nutrient concentrations, the vertical distribution of phytoplankton species (Shigesada and Okubo, 1981). Various experiments support the fact that large phytoplankton species, such as diatoms, induce less self-shading than smaller phytoplankton because of their smaller chloroplast densities and therefore support higher biomasses (Agusti, 1991). Mesocosm experiments show that the self-shading by phytoplankton increasingly constrains abundance as nutrient concentrations increase (Oviatt et al., 1989), leading to a severe drop in the production:biomass (P:B) ratio. Light limitation due to self-shading therefore provides an important negative feedback to phytoplankton abundance and biomass estimation through the water column, with important implications in primary production models, that are almost always based on estimations of biomass, via chlorophyll-a.

4.4.3.3. Secondary limiting elements

The third source of enrichment is represented by elements from sources other than that of the upwelled water, but rather from either the atmosphere or from the sediments. The enrichment from atmospheric

Nitrogen (N) is very low in Northwest Africa (<0.1%) as in the case for most upwelling systems (Mackey et al., 2010) and its benefit are mostly limited to species able to fix dinitrogen gas, such as the cyanobacterium *Trichodesmium*.

At the contrary, iron, a major limiting nutrient, is supplied in the form of atmospheric aerosols. Iron is known to significantly affect phytoplankton growth and therefore oceanic productivity, especially in upwelling regions where high-N and high-P deep water is brought rapidly to the surface (Martin et al., 1988).

The CCUS, especially between Cape Bojador and Cape Blanc, is not affected by iron limitation, first because of its relatively wide continental shelf and because dust deposits coming from the Sahara Desert are very frequent (Jickells et al., 2005; Mills et al., 2004; Gelado-Caballero, 2.3 this book). Manganese, known to limit phytoplankton growth (Dawes, 1998), is also relatively abundant in the coastal waters of Northwest Africa (Shiller, 1997).

The trapping of nutrients on the shelf can be also important (Arístegui et al., 2009a) as the resuspension of sediments may contribute significantly to silicate, generally in excess North of Cape Blanc (Minas et al., 1982) but more rapidly exhausted off Mauritania (Herbland and Voituriez, 1974), where the continental shelf is relatively narrow. This positive effect is more important in the CCUS compared to other EBUEs because of its wider continental shelf, especially south of Cape Bojador (26°N). South of the Cap-Vert peninsula, the considerably nutrient-rich SACW dominates. Except in the extreme south of the system, fresh water runoff plays only a minor role in this enrichment.

4.4.3.4. Biological limitations

The competition between marine species for nutrients and light as well as the diversity of the abiotic environment primarily drives the natural diversity of phytoplankton (see i.e. Margalef, 1978). In EBUEs, this diversity is first measured by the number of species and mostly varies on a cross-shore gradient, determined by spatio-temporal succession of algae.

Zooplankton grazers can significantly decrease phytoplankton density. For example, at a grazing rate of 20%, zooplankton can decrease phytoplankton populations by approximately 75% (Dawes, 1998). On the contrary, high zooplankton grazing pressures may stimulates phytoplankton growth, due to the release of nutrient by the grazers (Strickland, 1972), whereas moderate grazing (10% daily) may produce a doubling of the growth rate (Oviatt et al., 1989). As with other factors affecting phytoplankton production, the effect of grazers is seasonal. Because grazers decline in winter, there is a lag in spring before grazers become effective in controlling spring blooms. For these reasons, the way grazing pressure is integrated into production biogeochemical models if of high importance in their tuning (Hashioka et al., 2013) and in determining the dominance of major phytoplankton groups.

4.4.4. METHODS FOR ESTIMATING PRIMARY PRODUCTION

Whereas the term “primary production” represents a cumulative amount of biomass produced during a given period of time, the term referring to the measurement of a biomass increase over time is “primary productivity”. It is defined as “the rate at which solar energy is converted into chemical energy by photosynthetic and chemosynthetic organisms” (Dillon and Rodgers, 1980), and it is usually expressed as grams of carbon fixed per unit area per unit of time (Dawes, 1998).

The under-sampling of ship-based estimates of global NPP requires significant extrapolation, making it essentially impossible to quantify basin-scale variability from *in situ* measurements. Fortunately, satellite observations contribute to resolving this problem, by providing synoptic measures of ocean color (McClain, 1998). Numerous satellite-based production models exist, either at regional or global scales. A review of the comparison of most models can be found in Carr et al. (2006).

Biogeochemical models, coupled to numerical ocean circulation models (not described here), are also extremely useful in understanding processes in oceans, complementing direct observations. Experiments with the Regional Ocean Modeling System - Pelagic Interaction Scheme for Carbon and Ecosystem Studies (ROMS-PISCES) coupled model are presently set up for the CCUS, but to date only aspects of physical modeling (Marchesiello and Estrade, 2007) have been published. Lagrangian experiments to study the passive drift of planktonic eggs and larvae have been undertaken by Brochier et al. (2008).

Models generally include one or two phytoplankton (and zooplankton) compartments, in order to discriminate between diatom-like large cell species (micro-phytoplankton) and small cells species (nano-plankton). The Dynamic Green Ocean Model (DGOM) is a biogeochemical model that integrates 6 distinct phytoplankton groups (Le Quéré et al., 2005), while some recent models (Goebel et al., 2010) between 50 and 100, based on a reduced number of functional groups. An overview on the scope and history of ocean biogeochemical models can be found in Doney et al. (2003).

4.4.4.1. Direct measurements

The first quantitative studies of primary productivity in the Canary EBUE, made with direct measurements of C14 uptake (first introduced by Steeman-Nielsen, 1952), were mostly made during the 70s (Barber and Smith, 1981; Coste and Minas, 1982; Huntsman and Barber, 1977; Minas et al., 1986; Minas et al., 1982) in March and April 1974 (CINECA-*Charcot V* cruise), in the Cape Blanc region between 21°N and 22°N, the most consistently productive part of the CCLME. Huntsman and Barber (1977) measured NPP values consistently between 1 gC m^{-2} d^{-1} and 3 gC m^{-2} d^{-1}, except in inshore areas where it was assumed that turbidity limited light penetration. Minas et al. (1982) measured values between 0.7 gC m^{-2} d^{-1} and 4.7 gC m^{-2} d^{-1} during the same cruise from a different set of stations in the same area. This large variability is reinforced by the fact that Cape Blanc is located within the mixing region between NACW and SACW. The strong differences in nutrient concentration, combined with the high mesoscale activity of this area (see Sangrà, 3.5. this book) probably explain the large difference in productivity within a relatively small area.

The yearly integrated coastal NPP in the Cape Blanc region has been estimated at 750 gC m^{-2} yr^{-1} (Longhurst et al., 1995), a value similar to those estimated from remote sensing-based production models.

4.4.4.2. Remote sensing-based production models

The era of ocean color observation from space started with the experimental Coastal Zone Color Scanner (CZCS) on board of the Nimbus-7 spacecraft launched in 1978 by the National Aeronautics and Space Administration (NASA). By accurately measuring ocean pigment concentrations (mostly chlorophyll-a), this sensor supplied precious data to the international scientific community until 1986. This was followed by the long-awaited Sea-viewing Wide Field-of-view Sensor (SeaWiFS) in 1997 (data up to 2010 but continuously up to December 2007) and by the MODerate resolution Imaging Spectroradiometer (MODIS) instrument in June 2002, that still operates. More recently (January 2012) the Visible Infrared Imaging Radiometer Suite (VIIRS) instrument has extended and improved the measurements initiated by the MODIS sensor.

Data from platforms other than those operated by NASA have also been successfully used and include the MEdium Resolution Imaging Spectrometer (MERIS) sensor from the European Space Agency (ESA), on board the Envisat platform, between 2002 and 2012.

Standard algorithm-derived ocean color products encompass turbidity, dissolved organic carbon, particulate inorganic carbon, natural fluorescence, etc., but the most widely used product is by far chlorophyll-a (Figure 4.4.1). Because of its specific absorption in the blue and red parts of the visible light, chlorophyll-a algorithms are derived from ratios of light reflected from the sea surface in the blue and green parts of the visible spectra. Chlorophyll-a is the major natural pigment used by plants and unicellular algae to produce chemical energy from sun light through photosynthesis. Therefore, its quantitative estimation from space allows the construction of production models of different complexity, provided that the knowledge of intermediate variables such as the sunlight reaching the sea surface (specifically photosynthetically active radiation – PAR - also estimated from satellite measurements of cloud coverage), the water temperature and various physiological parameters can be estimated, at least for the main groups of algae present in the oceans. Of course, mineral nutrients and temperature (that strongly affects metabolic rates) play crucial roles in regulating NPP in the ocean.

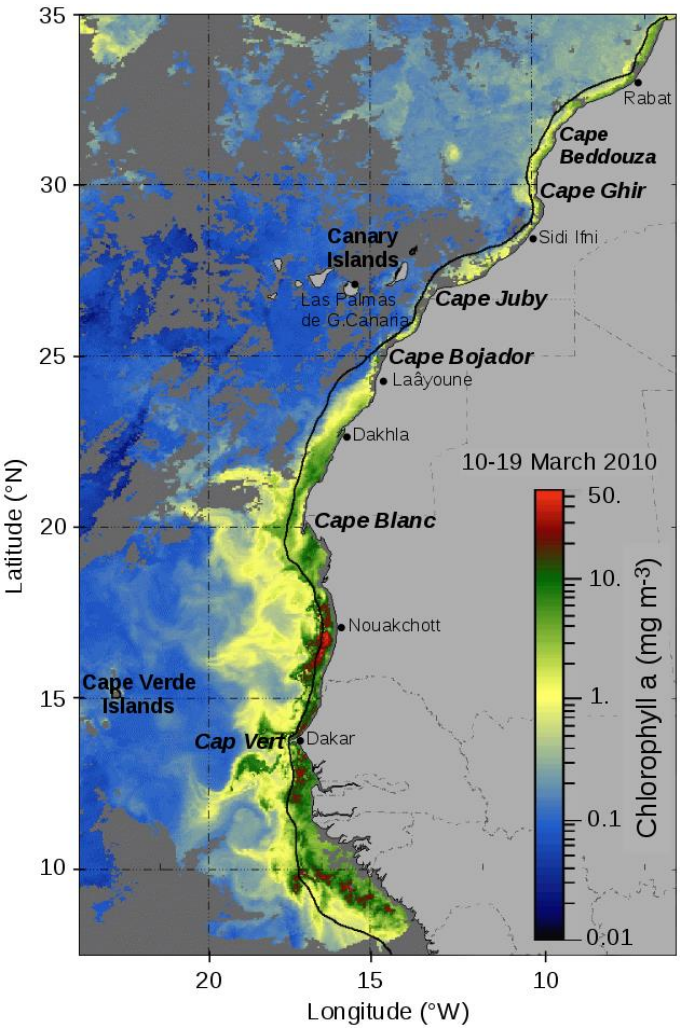

Figure 4.4.1. Average chlorophyll-a computed from MODIS sensor data for the period 10-19 March 2010, during the maximum southward extension of the trade winds concomitant of the maximum intensity of the Mauritanian-Senegalese upwelling. The 200 m bathymetry contour (black line) is added.

For these reasons, remote sensing data provide a powerful source of information by measuring ocean optical properties from which phytoplankton biomass and productivity can be derived (Feldman et al., 1989; Longhurst et al., 1995). Photosynthesis models of varying complexity have been used worldwide (Behrenfeld and Falkowski, 1997; Morel and Berthon, 1989; Platt and Sathyendranath, 1993).

These models integrate numerous uncertainties related to the estimations of the physiological parameters of the models, such as a the carbon:chlorophyll ratio of the different groups of algae, the growth rate of cells according to light and temperature, parameters that vary strongly according to the main functional groups of phytoplankton. Nevertheless, thanks to the availability of continuous fields of chlorophyll-a measured from space, production models provide an unprecedented synoptic view of the oceanic productivity. Size-fractionated production models (Kameda and Ishizaka, 2005; Uitz et al., 2012) integrate various empirical relationships between remote sensing variables in order to split the primary production into its different size classes (micro, nano, and picophytoplankton). Remote sensing of phytoplankton functional types from ocean color (Aiken et al., 2009; Alvain et al., 2008; Hirata et al., 2008; Mustapha et al., 2014; Nair et al., 2008) is also an emerging field, that helps to better understand (for the moment mostly at global scale) the importance of the environment in structuring the marine phytoplankton diversity as well as the mechanisms favouring four different functional types of algae: Synechococcus-like-cyanobacteria, diatoms, Prochlorococcus, Nanoeucaryotes (such as dinoflagellates) and Phaeocystis-like.

In 4.4.5, we show some results from SeaWiFS data, from chlorophyll-a estimates and a generic production model.

4.4.5. PRODUCTIVITY PATTERNS IN THE CCUS

A simple calculation based on SeaWiFS data of chlorophyll-a concentration (a proxy for the phytoplankton biomass) from 1998 to 2007 shows that despite representing only 1.5% of the oceanic surface between 45°S and 45°N, upwelling systems account for 9.3% of the biomass of primary producers.

This computation is based on the limit of 0.5 mg of chlorophyll-a as the best limit to delineate the productive part of the upwelling region as used is previous studies (Demarcq et al., 2007; Nixon and Thomas, 2001). Based on the same chlorophyll-a data, the primary biomass of all four major upwelling systems is approximately 6 times higher than the average of the biomass outside upwelling regions, in the same latitude range of 45°S to 45°N.

Within the same four main upwelling systems, comparative studies (Carr, 2001) show that the CCUS, with a value of 0.33 GtC yr^{-1} would be the second most productive system after the Benguela Current (0.37 GtC yr^{-1}), followed by the Humboldt (0.20 GtC yr^{-1}) and California systems (0.04 GtC yr^{-1}).

The spatio-temporal seasonality of the NPP is computed from the Vertically Generalized Production Model (VGPM) of Behrenfeld and Falkowski (1997). As for most models using chlorophyll-based biomasses, this model estimates NPP from surface chlorophyll using a temperature-dependent description of chlorophyll-specific photosynthetic efficiency and also assumes that phytoplankton biomass is related to a single formulation equating depth-integrated NPP to satellite-measured surface biomass. The other variables are the photoadaptative variable of the maximum production rate under saturating light, the depth of the euphotic zone, the irradiance-dependent function and day length.

The seasonality of the NPP is represented by the monthly averages from all SeaWiFS data from 1998 to 2007 (Figure 4.4.2). It shows high seasonality with minimum productivity in December and a maximum in April-May. Compared to the chlorophyll-a signal from the biomass (see Figure 4.4.1), the production is forced by light (minimum in December and maximum in June) that significantly increases the seasonal contrast. The Figure 4.4.3 shows the average yearly production: (a) as well as the latitudinal/time evolution of the productive areas, first in a qualitative way; (b) by averaging the production values from the coast up to the variable offshore position of the value 1 gC m^{-2} d^{-1} (first contour line on Figure 4.4.3a); and second by a more integrated biomass index (c) from the coast to a fixed offshore distance of 500 km, e.g. approximately the distance of a latitude/longitude square on Figure 4.4.3a.

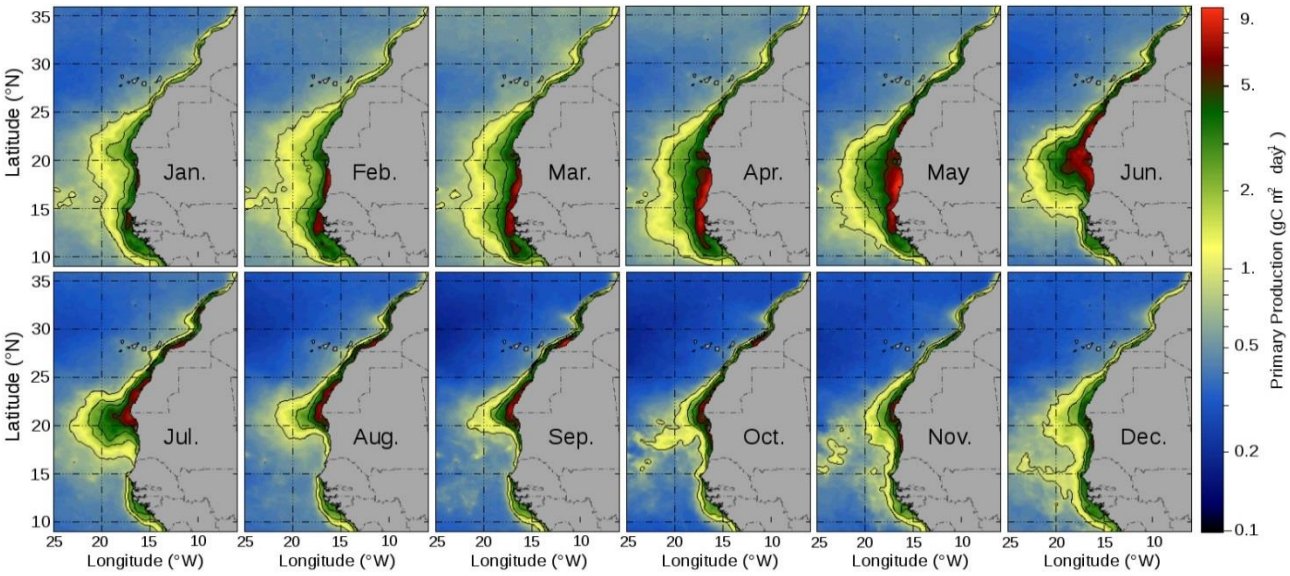

Figure 4.4.2. Seasonal variability of the NPP in the Canary Current from Morocco to Guinea, computed from SeaWiFS data, from 1998 to 2007 (VGPM algorithm, Behrenfeld and Falkowsky, 1998). Values 1 gC m^{-2} d^{-1}, 2 gC m^{-2} d^{-1}, 3 gC m^{-2} d^{-1} and 5 gC m^{-2} d^{-1} are contoured.

The progressive displacement of the most productive areas (values greater than 5 gC m^{-2} d^{-1}) is clearly visible, with a local coastal maximum in Senegal and southern Mauritania from January to May, a maximum in north Mauritania in June that progressively decreases up to December, whereas southern Senegal and Guinea (10°N-15°N) maintain stable average levels (around 2 gC m^{-2} d^{-1}) over the shelf without any upwelling, probably because of the importance of the nutrients from the wide and shallow continental shelf, in addition to nutrient input from several rivers.

Because of the narrowness of the continental shelf, in the central part of the system (from 20°N to 26°N) high levels of productivity show a moderate offshore extension. On the contrary, the region off Cape Blanc (20°N-21°N) shows a strong offshore extension of a constantly windy productive zone, characterized by a giant filament described by several authors (Fischer et al., 2009; Gabric et al., 1993; Meunier et al., 2012).

As mentioned above, the southern part of the system (9°N-21°N) is clearly the most productive (despite a less intense wind regime than the central part, from 21°N to 26°N) because of the exceptional nutrient content of SACW (Fraga, 1974), with enrichment extending as far as the Cape Verde archipelago.

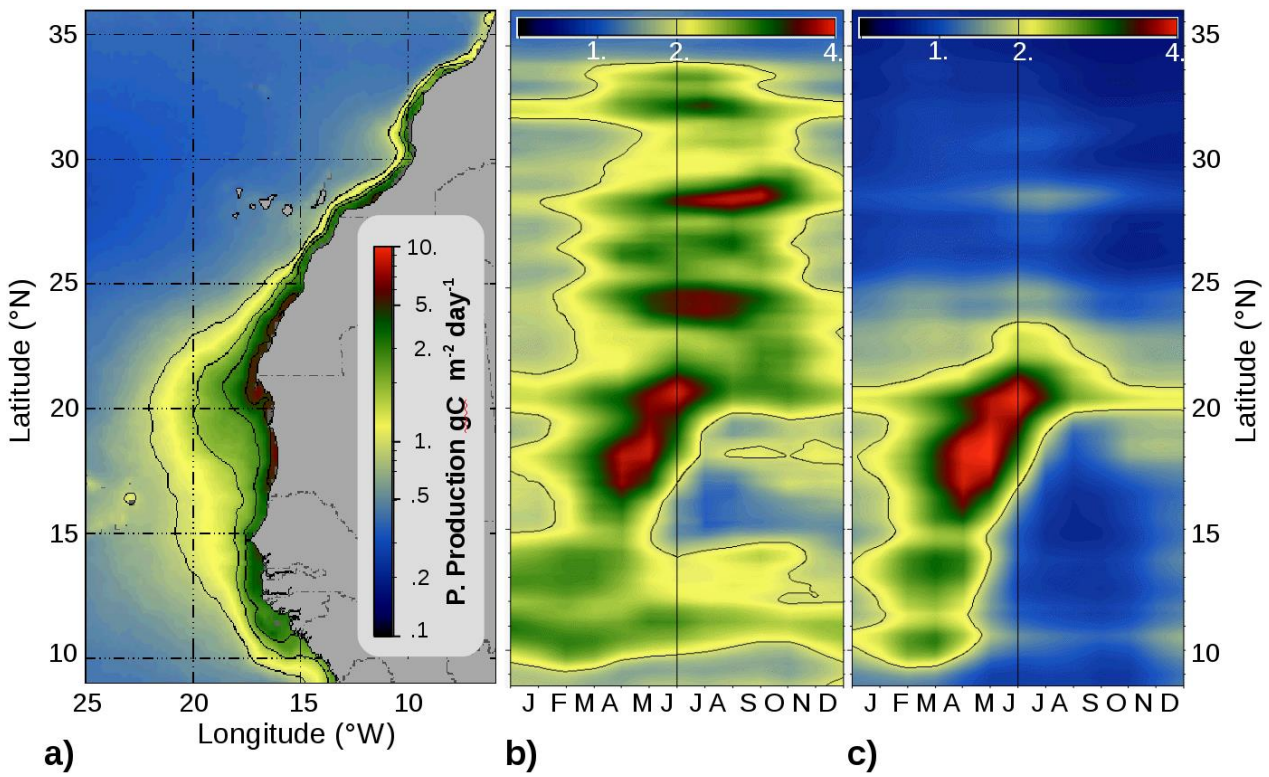

Figure 4.4.3. a) Annual average of the NPP (VGMP model), values 1 gC m^{-2} d^{-1}, 2 gC m^{-2} d^{-1} and 3 gC m^{-2} d^{-1} are contoured, b) local average from the coast to the value 1 gC m^{-2} d^{-1} (most distant contour in Figure 4.4.2a), c) integrated Zonal average from the coast to 500 km. All values are in gC m^{-2} d^{-1}. Isovalue 2 gC m^{-2} d^{-1} is contoured in b) and c).

4.4.6. PHYTOPLANKTON DIVERSITY AND DOMINANT SPECIES

It is recognized that marine phytoplankton diversity worldwide is relatively high, with approximately 4000 species and 500 genera described (Sournia et al., 1991) and probably much more to discover, especially in the bacterial pico-plankton (0.2-2 µm) division. This diversity is higher in freshwater systems, with 15,000 species (Bourrelly, 1985), because of the greater range of environmental conditions.

It has been suggested that this diversity is mostly controlled by the diversity of water masses (Tett and Barton, 1995) and that species richness in phytoplankton is not related to the total productivity of ecosystems (Cermeño et al., 2013). This is particularly true in coastal upwelling systems, where the diversity decreases with the distance from shore.

In upwelling systems, where diatoms dominate because of their competitive advantages in exploiting turbulent waters, they are responsible for ≈40% of the NPP and up to 50% of the organic carbon exported to the ocean interior (Dugdale and Wilkerson, 1998).

High-Performance Liquid Chromatography (HPLC) pigment analysis in the northern Moroccan system (Head et al., 1996) showed that when chlorophyll biomass was high, diatoms were dominant, whereas when it was low, small prymnesiophytes (mostly coccolithophorids), chlorophytes and diatoms were all important. Following upwelling events, the rich diatom-dominated coastal waters are progressively replaced by small flagellates (Arístegui et al., 2004; García-Muñoz et al., 2004), as nitrate is consumed and the system becomes more stratified and progressively replaced by a microbial-dominated system.

Goebel et al. (2013) used a biogeochemical model in the California Current (Goebel et al., 2010) that incorporates a high biodiversity of 78 phytoplanktonic groups. Historical observations (Capone et al., 2008; Head et al., 1996; Wilkerson et al., 2000) confirm the dominance of diatoms in nearshore upwelling regions, but more importantly these biogeochemical models are able to reproduce selectivity processes that explain the local dominance of a relatively low diversity of fast growing diatom species, whereas intermediate off-shore and oligotrophic surface waters are characterized by a lower productivity and a much higher diversity (Goebel et al., 2013).

Determinations of phytoplankton species are undertaken on a yearly basis by Institut National de Recherche Halieutique (INRH, Morocco) (Somoue, 2004). Cell counts are performed with the Utermöhl method (Utermöhl, 1958) by settling 10 ml samples and concentration are expressed in cells l^{-1}. Relative abundances by species and groups are expressed from the relative percentage of individuals.

The microphytoplankton is composed of diatoms, dinoflagellates, silicoflagellates, euglenophytes, coccolithophorids and raphidophytes. It has been found that diatoms regularly dominate the central part of the Coastal upwelling from Cape Blanc to Cape Beddouza (21°N to 32°30'N) with relative abundances of 70-80%, followed by dinoflagellates (10-20%). The other groups are less dominant, both qualitatively and quantitatively (Elghrib et al., 2012; Somoue, 2004; Somoue et al., 2003).

Numerous authors (Margalef, 1978; Smayda and Trainer, 2010; Tilstone et al., 2000), have shown the diatom:dinoflagellate ratio to be closely dependent of the vertical mixing of the water column. Dinoflagellates need for example relatively well stratified waters for optimal growth whereas diatoms have a high ability to be maintained in turbulent water masses (Tilstone et al., 2000), thanks to their extremely high rates of nitrate uptake, leading to maximal growth rates of 1 day^{-1}, even with low iron concentrations (Sunda et al., 1991).

For these reasons upwelling systems are tightly structured by their underlying physical processes: flux of upwelled water, turbulence, offshore displacement and stratification of aged upwelling waters, light penetration, etc. These factors are summarized in Figure 4.4.4.

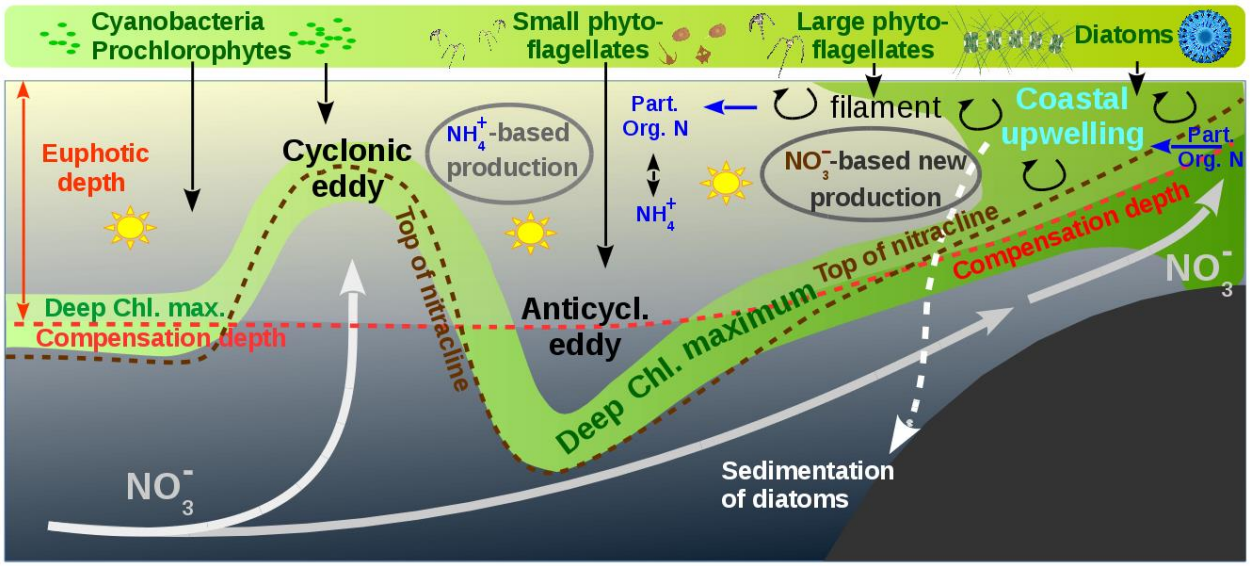

Figure 4.4.4. Schematic representation of the cross-shore section of an upwelling system, from coastal NO_3^- based new production to NH_4^+ based regenerated production, with the influence of the main limiting factors (nutrients and light). The upper rectangle represents the typical size-decreasing algae succession (based in Barton et al., 1998).

In Moroccan waters, 217 taxa of micro-phytoplankton have been identified (Elghrib et al., 2012; Somoue, 2004) from Cape Blanc (21°N) to Cape Beddouza (32°30'N). All taxa are listed in Table 4.4.1. The most abundant diatoms are *Chaetoceros* spp*., Leptocylindrus danicus, Leptocylindrus minimus, Pseudonitzschia* spp*., Thallassiosira* spp*., Melosira* spp. *and Nitzschia* spp. The most common dinoflagellates are: *Protoperidinium* spp*., Alexandrium* spp*., Prorocentrum* spp. and *Gymnodinium* spp. Their relative abundance varies according to the depth and distance from upwelling centers, and according to season and region, mostly because of differences in the local intensity of coastal upwelling (Makaoui et al., 2005).

In the Senegalese upwelling system, historical and partial measurements in December 1981 and March 1982 (Dia, 1986) have shown 5 dominant species present in most locations during the upwelling season (*Thalassionema nitzschioides*, *Pleurosigna elongatum*, *Hemiaulus sinensis*, *Chaetoceros decipiens* and *Rhizosolenia hyalina*) and 5 other species mostly during the onset of the upwelling season, in December (*Nitzschia seriata*, *Chaetoceros affine*, *Chaetoceros curvisetum*, *Rhizosolenia stolterfothii* and *Skeletonema costatum*). Only the two later species are still present at the end of the upwelling season. Due to the coastal position of most stations, dinoflagellates have been more rarely observed. Nevertheless, 5 dinoflagellates species have been recorded during the upwelling season. In Senegal, among 38 diatom species and 6 dinoflagellate species, diatoms represent 93% of the biomass of all species.

4.4.7. CONCLUSIONS AND RECOMMENDATIONS

The knowledge of carbon cycling in the CCUS is dominated by process studies conducted off the Iberian Peninsula, while the knowledge of the diversity of phytoplankton is mostly the consequence of studies from the Iberian and the Moroccan regions.

Extremely few studies concern the southern, yet most productive part of the system, either from a qualitative or quantitative point of view.

At all scales explored, the way productivity is distributed in space and time is directly related to the physics of the upwelling. For example, a nutrient maximum is generally observed 2 to 4 days after a coastal upwelling event and the induced production generally 3 to 10 days after the event and may be sustained for 2-3 days (Jones and Halpern, 1981).

Remote sensing-based observations and modeling are presently the only way to report in both time and space the short-term dynamics of coastal upwelling and its mesoscale structures, as well as to integrate the whole production of the system in space or time.

Combined with process studies, still very scarce in the southern part of the system, a continuous modeling effort would greatly help to better understand the various processes involved in the productivity of the CCUS as well as in the whole CCLME, in order to manage fishing activities in the long term and to preserve still relatively poorly known – albeit heavily exploited – regions of the system.

Table 4.4.1. List of microphytoplankton taxa recorded from Cape Blanc to Cape Beddouza (21°N- 32°30'N).

Diatoms	
Achnanthes brevipes Agardh, 1824	*Hemiaulus* spp.
Achnanthes spp.	*Hemidiscus* spp.
Amphora spp.	*Hyalodiscus radiatus* (O'Meara) Grunow, 1880
Asterionellopsis glacialis (Castracane) Round, 1990	*Lauderia annulata* Cleve, 1873
Asterolampra spp.	*Leptocylindrus danicus* Cleve, 1889
Bacteriastrum spp.	*Leptocylindrus mediterraneus* (Peragallo) Hasle, 1975
Bellerochea spp.	*Leptocylindrus minimus* Gran, 1915
Cerataulina spp.	*Licmophora ehrenbergii* (Kützing) Grunow, 1867
Chaetoceros convolutus Castracane, 1886	*Licmophora* spp.
Chaetoceros danicus Cleve, 1889	*Lyrella* spp.
Chaetoceros decipiens Cleve, 1873	*Melosira* spp.
Chaetoceros densus (Cleve) Cleve, 1899	*Navicula neoventricosa* Hustedt, 1966
Chaetoceros didymus Ehrenberg, 1845	*Navicula* spp.
Chaetoceros eibenii (Grunow) Van Heurck, 1880-1885	*Nitzschia longissima* (Brébisson) Ralfs, 1861
Chaetoceros peruvianus Brightwell, 1856	*Nitzschia rectilonga* Takano, 1983
Chaetoceros socialis Lauder, 1864	*Nitzschia* spp.
Chaetoceros spp.	*Odontella* spp.
Climacodinium frauenfeldianum Grunow, 1868	*Opephora* spp.
Corethron pennatum (Grunow) Ostenfeld, 1909	*Paralia sulcata (*Ehrenberg) Cleve, 1873
Coscinodiscus curvulatus Scmidt, 1878	*Plagiodiscus martensianus* Grunow & Eulenstein
Coscinodiscus spp.	*Plagiotropis* spp.
Ceratoneis closterium Ehrenberg, 1839	*Planktoniella* spp.
Dactyliosolen fragilissimus (Bergon) Hasle, 1996	*Pleurosigma directum* Grunow, 1880
Detonula spp.	*Pleurosigma normanii* Ralfs, 1861
Diploneis bombus (Ehrenberg) Ehrenberg, 1853	*Pleurosigma* spp.
Diploneis crabro (Ehrenberg) Ehrenberg, 1854	*Podosira stelligera* (Bailey) Mann, 1907
Diploneis spp.	*Proboscia alata* (Brightwell) Sundström, 1986
Ditylum brightwellii (West) Grunow, 1885	*Psammodictyon panduriforme* (Gregory) Mann, 1990
Entomoneis spp.	*Pseudo-nitzschia heimii* Manguin, 1957
Epithemia spp.	*Pseudo-nitzschia pungens (*Grunow ex Cleve) Hasle, 1993
Eucampia cornuta (Cleve) Grunow, 1883	*Pseudo-nitzschia seriata* (Cleve) Peragallo, 1899
Eucampia spp.	*Pseudo-nitzschia delicatissima* (Cleve) Heiden, 1928
Eucampia zodiacus Ehrenberg, 1839	*Pseudo-nitzschia* spp.
Fragilaria spp.	*Rhizosolenia acicularis* Sundström, 1986
Gomphonema spp.	*Rhizosolenia antennata* (Ehrenberg) Brown, 1920
Gossleriella tropica Schütt	*Rhizosolenia bergonii* Peragallo, 1892
Grammatophora marina (Lyngbye) Kützing, 1844	*Rhizosolenia clevei var.communis* Sundström, 1984
Guinardia cylindrus (Cleve) Hasle, 1996	*Rhizosolenia curvata* Zacharias, 1905
Guinardia delicatula (Cleve) Hasle, 1997	*Rhizosolenia hebetata f. semispina* (Hensen) Gran, 1905
Guinardia flaccida (Castracane) Peragallo, 1892	*Rhizosolenia imbricata* Brightwell, 1858
Guinardia sp.	*Rhizosolenia polydactyla* Castracane, 1886
Guinardia striata (Stolterfoth) Hasle, 1996	*Neocalyptrella* robusta (Norman ex Ralfs) Hernández-Becerril & Meave del Castillo, 1997
Gyrosigma spp.	*Rhizosolenia setigera* Brightwell, 1858
Hantzschia amphioxys (Ehrenberg) Grunow, 1880	*Rhizosolenia setigera f. pungens (*Cleve-Euler) Brunel, 1962
Helicotheca tamesis (Shrubsole) Ricard, 1890	*Rhizosolenia simplex* Karsten, 1905
Hemiaulus proteus Heiberg, 1863	*Rhizosolenia styliformis* Brightwell, 1858
Hemiaulus hauckii Grunow ex Van Heurck, 1882	*Roperia* spp.
Hemiaulus sinensis Greville, 1865	*Skeletonema costatum* (Greville) Cleve, 1873

Diatoms	
Skeletonema spp.	*Thalassionema nitzschoides (*Grunow) Mereschkowsky, 1902
Stephanopyxis palmeriana (Greville) Grunow, 1884	*Thalassionema pseudonitzschioides (*Schuette & Schrader) Hasle
Surirella spp.	*Thalassionema* spp.
Striatella spp.	*Thalassiosira* spp.
Striatella unipunctata (Lyngbye) Agardh, 1832	*Thalassiothrix longissima* Cleve & Grunow, 1880
Terpsinoë musica Ehrenberg, 1843	*Tryblionella compressa* (Bailey) Poulin, 1990
Thalassionema javanicum (Grunow) Hasle	*Trigonium* spp.

Dinoflagellates	
Amphidinium spp.	*Neoceratium declinatum* (Karsten) Gomez, Moreira & Lopez-Garcia, 2010
Alexandrium spp.	*Neoceratium furca* (Ehrenberg) Gomez, Moreira & Lopez-Garcia, 2010
Archaeperidinium minutum (Kofoid) Jörgensen, 1912	*Neoceratium fusus* (Ehrenberg) Gomez, Moreira & Lopez-Garcia, 2010
Cochlodinium spp.	*Neoceratium horridum* (Gran) Gomez, Moreira & Lopez-Garcia, 2010
Ceratium spp.	*Neoceratium lineatum (*Ehrenberg) Gomez, Moreira & Lopez-Garcia, 2010
Coolia monotis Meunier, 1919	*Neoceratium macroceros* (Ehrenberg) Gomez, Moreira & Lopez-Garcia, 2010
Dinophysis acuminata Claparéde & Lachman, 1859	*Neoceratium pentagonum (*Gourret) Gomez, Moreira & Lopez-Garcia, 2010
Dinophysis acuta Eherenberg, 1839	*Neoceratium symmetricum* (Pavillard) Gomez, Moreira & Lopez-Garcia, 2010
Dinophysis caudata Saville-Kent, 1881	*Neoceratium trichoceros* (Ehrenberg) Gomez, Moreira & Lopez-Garcia, 2010
Dinophysis fortii Pavillard, 1923	*Neoceratium tripos* (Müller) Gomez, Moreira & Lopez-Garcia, 2010
Dinophysis infundibulis Schiller, 1928	*Noctiluca scintillans (*Macartney) Kofoid & Swezy, 1921
Dinophysis odiosa (Pavillard) Tai & Skogsberg, 1934	*Peridinium quinquecorne* Abé, 1927
Dinophysis rudgei Murray & Whitting, 1899	*Peridiniella* spp.
Dinophysis spp.	*Phalacroma oxytoxoides* (Kofoid) Gomez, Lopez-Garcia & Moreira, 2011
Diplopsalis spp.	*Phalacroma* spp.
Dissodinium pseudocalani (Gonnert) Drebes ex Elbrachter & Drebes, 1978	*Pentapharsodinium dalei* Indelicato & Loeblich III, 1986
Goniodoma spp.	*Preperidinium meunieri* (Pavillard) Elbrächter, 1993
Gonyaulax spp.	*Pronoctiluca* spp.
Gymnodinium catenatum Graham, 1943	*Prorocentrum cordatum* (Ostenfeld) Dodge, 1975
Gymnodinium spp.	*Prorocentrum emarginatum* Fukuyo, 1981
Gyrodinium fissum (Levander) Kofoid & Swezy, 1921	*Prorocentrum gracile* Schütt, 1895
Gyrodinium spirale (Bergh) Kofoid & Swezy, 1921	*Prorocentrum lima* (Ehrenberg) Stein, 1878
Gyrodinium spp.	*Prorocentrum mexicanum* Osorio-Tafall, 1942
Heterocapsa circularisquama Horiguchi, 1995	*Prorocentrum micans* Ehrenberg, 1834
Heterocapsa spp.	*Prorocentrum rostratum* Stein, 1883
Karenia mikimotoi (Miyake & Kominami ex Oda) Hansen & Moestrup, 2000	*Prorocentrum* spp.
Katodinium glaucum (Lebour) Loeblich III,1965	*Prorocentrum triestinum* Schiller, 1918
Katodinium spp.	*Protoceratium* spp.
Ostreopsis spp.	*Protoperidinium acanthophorum* (Balech) Balech, 1974
Oxytoxum mediterraneum Schiller	*Protoperidinium areolatum (*Peters) Balech, 1974
Oxytoxum spp.	*Protoperidinium bipes* (Paulsen) Balech, 1974
Oxytoxum tesselatum (Stein, 1883) Schütt, 1895	*Protoperidinium compressum* (Abé) Balech, 1974
Neoceratium candelabrum (Ehrenberg) Gómez, Moreira & López-Garcia, 2010	*Protoperidinium conicum* (Gran) Balech, 1974

Dinoflagellates	
Protoperidinium denticulatum (Gran & Braarud) Balech, 1974	*Protoperidinium* spp.
Protoperidinium depressum (Bailey) Balech, 1974	*Protoperidinium steinii* (Jørgensen) Balech, 1974
Protoperidinium diabolum (Cleve) Balech, 1974	*Protoperidinium tuba* (Schiller) Balech, 1974
Protoperidinium divergens (Ehrenberg) Balech, 1974	*Protoceratium reticulatum* (Claparède & Lachmann) Butschli, 1885
Protoperidinium mastophorum (Balech) Balech, 1974	*Pyrocystis lunula* (Schütt) Schütt, 1896
Protoperidinium ovum (Schiller) Balech, 1974	*Pyrocystis* spp.
Protoperidinium pellucidum Bergh ex Loeblich Jr.& Loeblich III, 1881	*Pyrophacus* spp.
Protoperidinium pentagonum (Gran) Balech, 1974	*Scrippsiella* spp.
Protoperidinium punctulatum (Paulsen) Balech, 1974	*Torodinium robustum* Kofoid & Swezy, 1921
Protoperidinium pyriforme (Paulsen) Balech, 1974	

Coccolithophorids
Coccolithus spp.
Discosphaera tubifer (Murray & Blackman) Ostenfeld, 1900
Pleurochrysis spp.
Rhabdosphaera clavigera Murray & Blackman, 1898
Zygosphaera spp.

Euglenophyceae
Euglena spp.
Eutreptia spp.
Eutreptiella spp.

Raphidophyceae
Chatonella spp.

Silicoflagellates
Dictyocha fibula Ehrenberg, 1839
Dictyocha speculum Ehrenberg, 1839
Dictyocha crux Ehrenberg, 1840
Distephanus polyactis var.literatus Bukry
Dictyocha spp.
Octactis octonaria (Ehrenberg) Hovasse, 1946

Acknowledgments

We are grateful to the NASA Ocean color team (http://oceancolor.gsfc.nasa.gov/, accessed on 27 April 2015) for providing the SeaWiFS data and to the Oregon State University (OSU) (http://www.science.oregonstate.edu/ocean.productivity/, accessed 27 April 2015) for providing the SeaWiFS derived VGPM data used in this study. We are also grateful to the team of the biological oceanography laboratory of INRH for providing the taxa observations.

4.5. HARMFUL ALGAL BLOOM EVENTS IN THE CANARY CURRENT LARGE MARINE ECOSYSTEM

Grant C. PITCHER[1,2] and Santiago FRAGA[3]

[1] Fisheries Management, Department of Agriculture, Forestry and Fisheries. South Africa

[2] University of Cape Town. South Africa

[3] Centro Oceanográfico de Vigo, Instituto Español de Oceanografía. Spain

4.5.1. INTRODUCTION

The major eastern boundary upwelling systems (EBUS) of the world's oceans are susceptible to harmful algal blooms (HABs) because they are highly productive, nutrient-rich environments, prone to high-biomass blooms (Pitcher et al., 2010; Trainer et al., 2010). The majority of species contributing to HABs within these systems constitute regular components of the phytoplankton assemblages of upwelling systems, and their harmful impacts are associated with either their toxic properties or the high biomass such blooms can achieve. Bloom development is dictated through the creation of a mosaic of shifting habitats determined by windstress fluctuations and buoyancy inputs at several scales, and by mesoscale features that interrupt typical upwelling circulation patterns.

As part of an EBUS the Canary Current Large Marine Ecosystem (CCLME) extends from the northwestern tip of Morocco to the south of Guinea-Bissau, and includes the Canary Islands and Cape Verde. The LME is characterized by strong sub-regional variability linked to variable coastline orientation, configuration and shelf width, variable coastal upwelling, nutrient and freshwater input, and retentive or dispersive physical mechanisms (Arístegui et al., 2009b). HABs of the CCLME have been poorly studied although estimates of chlorophyll and primary production, as derived from satellite ocean colour data, have been shown by Chavez and Messié (2009) to be high, indicating in all likelihood a high incidence of HABs.

The sub-regions within the CCLME demonstrate latitudinal variability in satellite derived surface chlorophyll concentrations linked to a southward increase in nutrient concentrations (Lathuiliére et al., 2008; Arístegui et al., 2009b). The northernmost region includes the Moroccan coastline of the Gulf of Cadiz which is unfavourable for upwelling. Further south, between Cape Sim and Cape Blanc, the coasts of Morocco and Western Sahara benefit from year-round upwelling of North Atlantic Central Water (NACW) and are characterized by high mesoscale variability arising from geographical heterogeneity. Here variations in shelf width and the presence of major capes produce extended filaments of elevated chlorophyll. South of Cape Blanc the Mauritanian-Senegalese region is the most productive as a result of winter upwelling of higher-nutrient South Atlantic Central Water (SACW). Also, present within the CCLME are subtropical island archipelagos which span the coastal transition zone from near to open coast providing an additional habitat for HABs. We piece together the few well-documented studies of HABs within these sub-regions to provide a better picture of the incidence and likely causes and impacts of HABs off northwest Africa (NWA). As yet all documented HABs within the region have been associated with the production of one or another toxin.

4.5.2. TOXIN-PRODUCING ALGAE IN THE CCLME

4.5.2.1. Paralytic shellfish poisoning toxins

Paralytic shellfish poisoning (PSP) is associated with the consumption of seafood products contaminated with the neurotoxins collectively known as saxitoxins (STXs) (Etheridge, 2010). Major toxin sources include several species of dinoflagellates of the genera *Alexandrium*, *Gymnodinium* and *Pyrodinium*. Within EBUS *Alexandrium catenella* and *Gymnodinium catenatum* are the most common source of PSP toxins (Trainer et al., 2010). Specific association of *G. catenatum* with the Iberian upwelling system followed a major PSP event on the Galician coast in 1976.

Off NWA records of PSP following consumption of shellfish date back to 1961 on the Moroccan coast with further records in the 1970s and 1980s (Taleb et al., 2003). In 1992 a comprehensive monitoring programme was initiated with the analysis of several species of bivalve molluscs collected fortnightly at 30 stations located on the Atlantic coast of Morocco and off Western Sahara (Taleb et al., 2003). Through implementation of this programme shellfish contaminated with PSP toxins were found in November 1994 to extend from Larache to Essaouira with the highest toxin concentrations of 6000 µg STX eq 100 g^{-1} in mussels (*Mytilus galloprovincialis*) from the Casablanca region (Taleb et al., 1998, 2003). Maximum toxin concentration in oysters (*Crassostrea gigas*) and clams (*Ruditapes decussatus*) was 2608 and 738 µg STX eq 100 g^{-1} respectively. At that time the presence of *Gymnodinium catenatum* (Figure 4.5.1a) in the waters around Casablanca (maximum recorded concentration of $3x10^4$ cells l^{-1}) indicated that it was the most likely cause (Tahri Joutei, 1998); an observation supported by the complex toxin profile of the mussels, that included the presence of dcSTX and the absence of STX (Taleb et al., 2003). In November 1995 shellfish contaminated by PSP toxins were again present near Casablanca although levels of toxicity were much lower.

In 1998 and 1999 shellfish contaminated by PSP toxins were also recorded further south between Agadir and Tan Tan (Taleb et al., 2003). A maximum level of PSP toxins of 1142 µg STX eq 100 g^{-1} was recorded in mussels from Taghazout and the toxin profile of primarily GTX1-4 toxins implicated *Alexandrium minutum* as a possible toxin source; further supported by observations of this species as a component of the plankton (Tahri Joutei et al., 2000).

The prominence of *G. catenatum* within the CCLME has been further demonstrated by its presence in recent sediments of the North Canary Basin (Targarona et al., 1999). Here cysts of *Gymnodinium* species (dominated by *G. catenatum*, Figure 4.5.1b,c), of *Lingulodinium machaerophorum* (=*Lingulodinium polyedrum*), and of *Protoperidinium* species have been found to dominate cyst assemblages occurring in higher numbers in association with the upwelling centers of Cape Ghir and Cape Jubi. These findings support speculation by Ribeiro et al. (2012) that refuge cyst populations off NWA may have been the source of *G. catenatum* blooms off the Iberian coast in the 1970s.

In addition to the threat posed to human health, strong evidence has been provided for PSP toxins as the cause of a mass mortality of Monk Seals in the Cape Blanc peninsula in 1997 (Reyero et al., 1999). The mortality of two-thirds of the population of this endangered species was initially attributed to a morbillivirus (Osterhaus et al., 1997). However, epidemiological, clinical, pathological and toxicological observations were more consistent with poisoning by PSP toxins, and their presence was confirmed in both seal tissue and other fauna (Hernández et al., 1998). Mouse bioassays showed symptoms of PSP, and high performance liquid chromatography (HPLC) supported by mass spectrometry (MS) indicated the presence of dcSTX and neoSTX (Reyero et al., 1999). *G. catenatum* was again considered to be the most likely origin

of these toxins based on the toxin composition of analysed samples and its known presence within the CCLME.

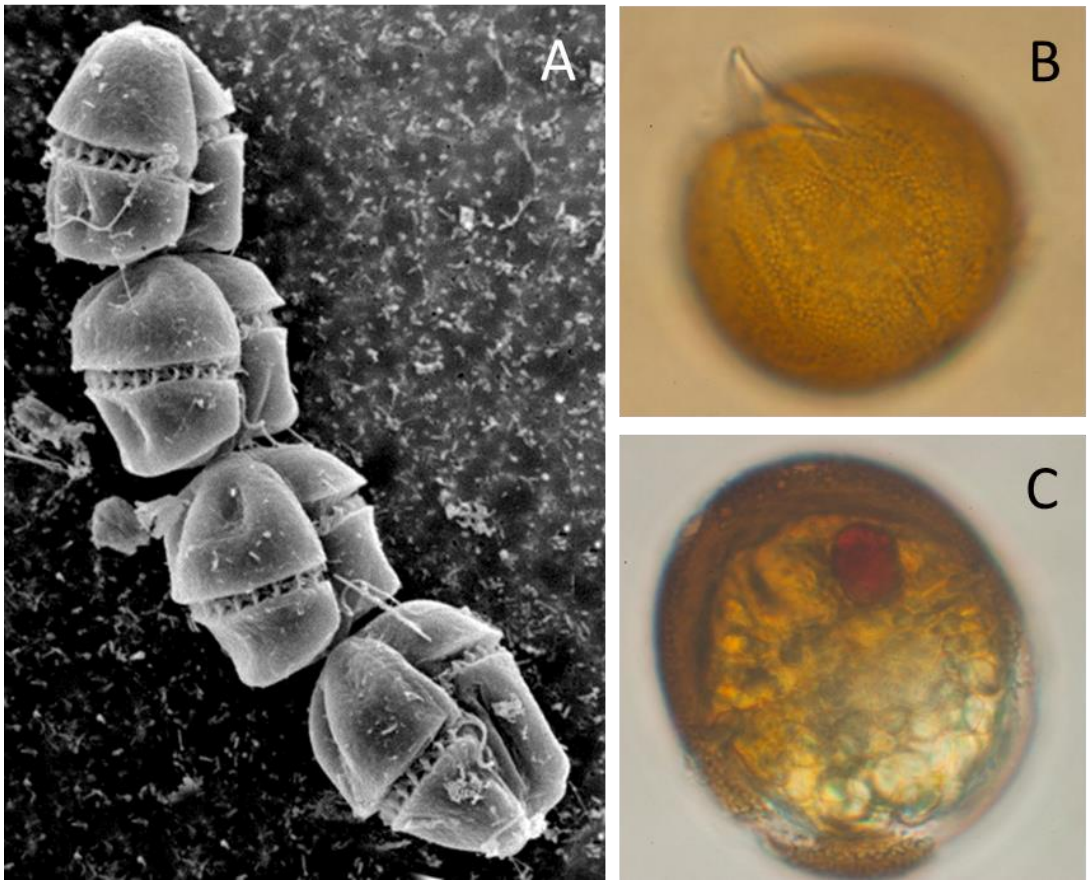

Figure 4.5.1. Scanning electron micrograph of (A) the vegetative stage of the dinoflagellate *Gymnodinium catenatum* (photograph by S. Fraga) the cause of PSP contaminated shellfish on the Moroccan coast (Taleb et al., 2003), and (B and C) light micrographs of the cyst stage of *G. catenatum* (photographs by R. Figueroa) found to dominate recent sediments of the North Canary Basin (Targarona et al., 1999).

4.5.2.2. Diarrhetic shellfish poisoning and other lipophilic toxins

Diarrhetic shellfish poisoning (DSP) is characterized by severe gastrointestinal illness associated with the consumption of filter feeding bivalves (Reguera et al., 2012). Historically three different toxin groups were associated with DSP: okadaic acid (OA) and the dinophysistoxins (DTXs), pectenotoxins (PTXs) and yessotoxins (YTXs) as a result of their co-extraction and single response to the conventional mouse bioassay. However, diarrheagenic effects have only been proven for OA and DTXs, which together with the PTXs are typically produced by species of the dinoflagellate genus *Dinophysis*. Although no longer associated with DSP the YTXs, produced by the dinoflagellates *Protoceratium reticulatum*, *Lingulodinium polyedrum* and *Gonyaulax spinifera*, are lethal to mice following intraperitoneal injection (Tubaro et al., 2010). On the other hand, the more recently discovered azaspiracids (AZAs), produced by the dinoflagellate *Azadinium spinosum*, although never associated with the DSP toxins are known to cause diarrhea in humans (Furey et al., 2010).

DSP toxins, YTXs and the AZAs have all been shown to be present in EBUS and DSP off the Iberian Peninsula, attributed primarily to *D. acuminata*, *D. acuta* and *D. caudata*, is considered to pose the greatest threat to

shellfish harvests in this area (Trainer et al., 2010). Off NWA lipophilic toxins have been recorded almost annually on the Moroccan and Western Saharan coasts since implementation of monitoring in 1999 (Taleb et al., 2006; Elgarch et al., 2008). In 2003 DSP toxins dominated by OA and DTX2 were detected in mussels, clams and oysters extending from El Jadida to Dakhla. In 2006 the presence of DSP toxins was investigated in Oualidia lagoon using liquid chromatography-mass spectrometry (LC-MS) and a quantitative enzyme-linked immunosorbent assay (ELISA) (Elgarch et al., 2008). Sampling from May to August showed OA concentrations to always exceed the regulatory level of 16 µg 100 g^{-1} of edible tissue peaking in June at 135 µg 100 g^{-1}. DTX2 was also present particularly during July and August, contributing between 9 and 23% to the DSP toxins. Unfortunately the causative phytoplankton species were not identified.

In 2004 and 2005 mussels (*Mytilus galloprovincialis*) collected from Oulad Ghanem and Dar El Hamra on the Atlantic coast of Morocco and screened for lipophilic toxins by LC-MS were shown to contain DSP toxins and AZAs responsible for azaspiracid poisoning (AZP) (Taleb et al., 2006). This was the first report of AZAs in the CCLME and showed AZA2 to dominate with lesser quantities of AZA1 and traces of AZA3. In both 2004 and 2005 maximum concentrations of AZAs were recorded in summer and tended to follow peaks in DSP toxins dominated by OA and DTX2. The highest concentration of AZAs of 0.9 µg g^{-1} of digestive gland was recorded in mid-July 2005. AZAs were again detected in 2006, occurring on this occasion in Oualidia lagoon in July and August (Elgarch et al., 2008). On no occasion were the toxins of AZP found to exceed regulatory limits.

Water discolourations caused by blooms of *L. polyedrum* are well known on the Atlantic coast of Morocco (Tahri Joutei et al., 2000) and are consistent with reports of the dominance of *L. polyedrum* cysts in recent sediments (Targarona et al., 1999). Despite the prominence of *L. polyedrum*, YTXs have not been explicitly reported within the Northwest African Upwelling System (NW-AUS). However, following a monospecific bloom of *L. polyedrum* in July and August 1999, shellfish tested positive by means of the mouse bioassay for lipophilic toxins, indicating in all likelihood the presence of YTXs.

4.5.2.3. Domoic acid and amnesic shellfish poisoning

Amnesic shellfish poisoning (ASP) is caused by the neurotoxin domoic acid (DA) produced by some species of the globally distributed diatom genus *Pseudo-nitzschia* (Lelong et al., 2012). The impacts of *Pseudo-nitzschia* and its toxin have been considered by Trainer et al. (2010) to be especially problematic in upwelling systems, particularly in the California Current system where *P. multiseries* and *P. australis* have been identified as posing the greatest risk. Within the Iberian upwelling system, DA was first detected in Galician mussels in 1994, at which time *P. australis* was shown to dominate the plankton and significant amounts of DA were found in concentrated plankton samples (Míguez et al., 1996). This report provided the first account of DA in shellfish in Europe and the first record of *P. australis* in the North Atlantic Ocean.

The only study relating to ASP in the NW-AUS, was the identification by Akallal et al. (2002) of seven *Pseudo-nitzschia* species on the Atlantic coast of Morocco (*P. fraudulenta*, *P. multiseries*, *P. multistriata*, *P. pungens var. cingulata*, *P. subpacifica*, *P. delicatissima* and *P. pseudodelicatissima*), most of which have demonstrated the capability of toxin production. In addition to this study Rijal Leblad et al. (2013) have explored the diversity of *Pseudo-nitzschia* species and the potential risk of ASP in M'diq Bay on the western Mediterranean coast of Morocco in close proximity to the Gibraltar Strait and Atlantic Ocean. Here regular sampling during 2007 revealed the presence of 13 *Pseudo-nitzschia* species, eight of which are known DA producers. Elevated abundance of *Pseudo-nitzschia* spp. was recorded from March through to November and DA concentrations in shellfish were highest in spring, but did not exceed regulatory limits.

4.5.2.4. Ciguatera fish poisoning

Ciguatera fish poisoning (CFP) is a seafood-borne illness caused by consumption of fish that have accumulated lipid-soluble, polyether toxins known as ciguatoxins (CTXs) which have their origin in benthic dinoflagellates of the genus *Gambierdiscus* (Dickey and Plakas, 2010). The microalgae are ingested by herbivorous fish and assimilated and metabolized through multiple trophic levels of the food web. The illness is typically associated with the consumption of carnivorous fish, from tropical and subtropical areas of the Pacific and West Indian Oceans and the Caribbean Sea, producing a complex array of gastrointestinal, neurological and cardiological symptoms.

The CCLME was not considered a ciguatera-endemic region until an incident of poisoning in the Canary Islands in January 2004 provided the first indication of CFP in the northeast Atlantic. The incident followed consumption by five family members of an amberjack (*Serioloa rivoliana*) caught by scuba divers off the coast of the Canary Islands resulting in illness with symptoms of CFP (Pérez-Arellano et al., 2005). A portion of the fish tested positive for CTXs using a commercially available immunoassay (Cigua-Check Test Kit). A further sample of the fish was sent to the Food and Drug Administration (FDA) Gulf Coast Seafood Laboratories (USA) and results were positive indicating a CTX content of 1.0 ng eq g^{-1} as determined by a sodium channel-specific cytotoxicity assay. The toxin CCTX-1 was confirmed by LC-MS/MS and at least 2 other toxins with CTX-like structures were identified.

Further cases of CFP were investigated in the Canary Islands in 2008 and 2009 (Boada et al., 2010). In both cases symptoms followed consumption of amberjack, as in 2004. Toxin activity in both years was detected by cytotoxicity assay, at a level of 0.17 ng eq g^{-1} in 2008 and 0.08 ng eq g^{-1} in 2009. Again LC-MS/MS was used to confirm the presence of CCTX-1 in both years. Following these outbreaks a Surveillance System for Ciguatera poisoning in the Canary Islands (SVEICC) was established in 2009 requiring compulsory notification of all cases of suspected CFP in the healthcare system (Núñez et al., 2012). Between 2008 and 2012 a total of 9 CFP outbreaks have been reported in the Canary Islands affecting 68 people. All cases have been associated with the consumption of large amberjack, but in only three cases has the presence of CTXs been confirmed (Table 4.5.1).

Table 4.5.1. Ciguatera fish poisoning outbreaks off the Canary Islands from 2008-2012 (from Núñez et al., 2012)

Outbreak no.	Date	Island	No. human cases	Fish species	Weight	Origin
1	15 Nov 08	Tenerife	25	*Seriola fasciata*	37	Local market
2	29 Jan 09	Tenerife	4	*Seriola dumerilis*	67	Sport fishing
3	03Sep 09	Gran Canaria	3	*Seriola* spp.	Unknown	Unknown
4	19 Nov 09	Tenerife	2	*Seriola* spp.	Unknown	Sport fishing
5	25 Apr 10	Tenerife	6	*Seriola* spp.	80	Unknown
6	26 Jun 11	Gran Canaria	5	*Seriola* spp.	24	Sport fishing
7	28 Jan 12	Lanzarote	10	*Seriola* spp.	15	Sport fishing
8	04 Apr 12	Lanzarote	9	*Seriola* spp.	26	Sport fishing
9	May 12	Tenerife	4	*Seriola* spp.	Unknown	Local market

In 2007 and 2008 suspected cases of CFP were also recorded from the Madeira archipelago following consumption of fish caught off the Selvagens Islands (Otero et al., 2010). The 2008 incident affected 11 crew members of a fishing boat having caught and eaten amberjack (*Seriola* spp.). Their hospitalization and lengthy recovery period led to a clear diagnosis of CFP. Owing to the implication of *Seriola* spp. in these cases of CFP, two species, *S. dumerili* and *S. fasciata*, were caught off the Selvagens Islands in 2009 for analysis of CTXs. Assays using the Cigua-Check Test Kit provided positive results for both fish species. Ultraperformance liquid chromatography–mass spectrometry (UPLC-MS) revealed the presence of 4 CTX analogues, 2 of which were identified as CTX-1B and CTX-3C. The total toxin concentration as measured by UPLC-MS was 35 ng g^{-1} in *S. fasciata*, and ranged from 33-54 ng g^{-1} in *S. dumerili* depending on the tissue type.

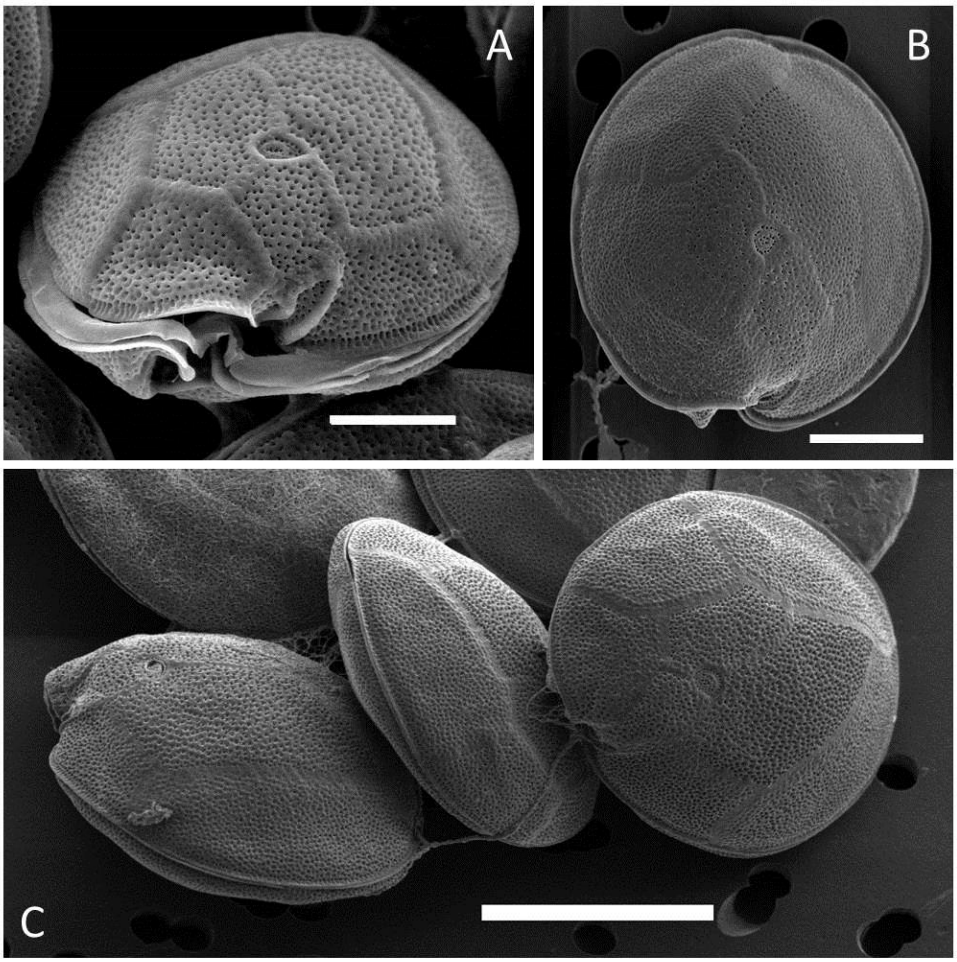

Figure 4.5.2. Three *Gambierdiscus* spp. found to co-occur in tidal pools of rocky shores of the Canary Islands: (A) *G. australes*, (B) *G. silvae* and (C) *G. excentricus* (scale bar = 20 µm; photographs by S. Fraga).

In attempting to establish the causative species of CFP in the Canary Islands, three *Gambierdiscus* spp. have been identified: *Gambierdiscus australes, Gambierdiscus excentricus* and *Gambierdiscus silvae* (Figure 4.5.2) (Fraga et al., 2011; Fraga and Rodríguez, 2014). Although the northeast Atlantic was not considered a ciguatera-endemic zone prior to 2014, it has been suggested by Fraga et al. (2011) that the oldest record of CFP may date back to 1521 in the Gulf of Guinea, and that the first recorded observation of *Gambierdiscus* was in all likelihood made from the Cape Verde archipelago in 1948. Reported at the time as *Goniodoma* sp. by Silva (1956) this species is most likely the same as that recently described as *G. silvae* by Fraga and

Rodríguez (2014). Found as an epiphyte on small seaweeds in tidal pools on the northeast coasts of the islands of Gran Canaria and Tenerife, phylogenetic analyses show strains of *G. silvae* to cluster in a sister clade to *G. polynesiensis*. Previously Fraga et al. (2011) had also described the species *G. excentricus* from the Canary Islands. Shown by phylogenetic analysis to cluster into a well-supported group, with *G. australes* its closest relative, all strains of *G. excentricus* were shown to be toxic indicating the production of both CTX and maitotoxin (MTX)-like compounds. Cell content of CTX was found to range from 0.37-1.1 pg CTX-1B eq $cell^{-1}$, similar to that reported previously for other species of *Gambierdiscus*. However, MTX content ranged from 0.48-1.38 ng $cell^{-1}$, classifying *G. excentricus* as a potent MTX producer. The work of Fraga and Rodríguez (2014) further provided the first identification of *G. australes* in the Atlantic, which was found to co-occur with *G. excentricus* and *G. silvae*.

These reports of *Gambierdiscus* spp. and ciguatoxic fish in the Canary Island and Madeira archipelagos are of further significance in providing evidence of biogeographical expansion, with a shift towards higher latitudes, which has been considered indicative of climate change and increasing sea temperatures in the region (Dickey and Plakas et al., 2010, Otero et al., 2010).

4.5.2.5. Toxin producing cyanobacteria blooms

Several cyanobacteria occurring in fresh, brackish and marine waters produce toxins which are hazardous to the health of livestock and humans. The toxins are classified, according to the target of their toxic action, and include primarily hepatotoxins, neurotoxins and dermatotoxins. Cyanobacteria blooms in marine waters are limited to only a few taxa with *Trichodesmium*, *Richelia*, *Nodularia* and *Aphanizomenon* being most commonly observed (Sellner, 1997).

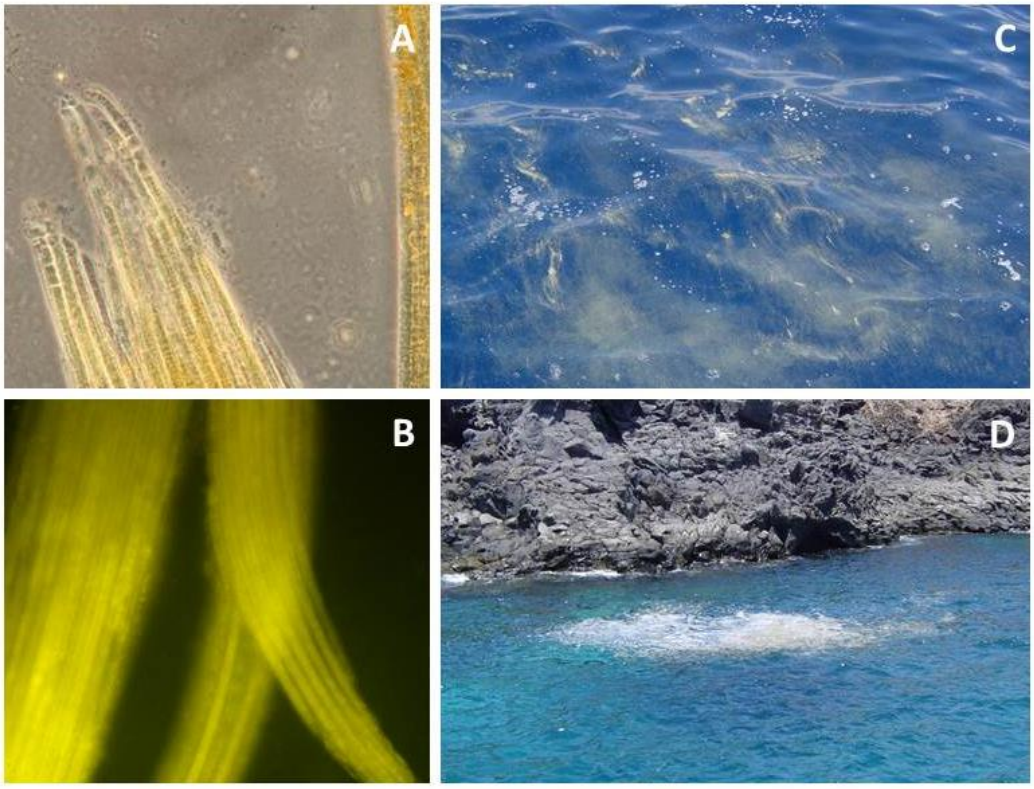

Figure 4.5.3. *Trichodesmium erythraeum* bloom in the Canary Islands in August 2004. Light micrographs of filaments using (A) phase and (B) fluorescence microscopy. Mats of surface filaments (C) and surface foam created by these mats (D) adjacent to the rocky shores of Tenerife (photographs A, B by S. Fraga and C, D by M. Norte).

In August 2004 an extensive bloom of the cyanobacterium *Trichodesmium erythraeum* was observed in the NW-AUS (Ramos et al., 2005b). Water samples collected off the islands of Gran Canaria and Tenerife were found to contain as many as 1240 filaments ml^{-1} of this non-heterocystous diazotrophic cyanobacterium, and in some cases were observed to form filamentous mats in the waters surrounding the islands (Figure 4.5.3). Microcystins were detected by HPLC and confirmed by immunoassay at concentrations from 0.1–1.0 µg microcystin-LR eq g^{-1} dry weight of bloom material. The bloom corresponded to the warmest summer in the Canary Islands since 1912 and followed severe dust storms in the Sahara Desert. Dust deposition is considered to extend over considerable areas of the northeast Atlantic with a significant impact on the biogeochemical cycle of trace elements, specifically providing a source of Fe required for the growth of diazotrophic cyanobacteria. These are considered the first records of extensive *T. erythraeum* blooms off the NW-AUS and may be a function of a general warming of the area (Ramos et al., 2005b).

4.5.3. CONCLUSION

Knowledge of HAB species and their impacts in the major EBUS is disparate between systems and is least studied off NWA. Nevertheless the few documented studies of HABs within this region indicate a similar diversity to that recorded in other upwelling systems, and include those species responsible for PSP, DSP, ASP and AZP. Also present off NWA, but generally absent from the other major upwelling systems, are those species responsible for CFP and microcystin-producing cyanobacterial blooms. Their presence is afforded by the subtropical habitat provided by the island archipelagos found within the CCLME. It is intended that this brief review will provide the foundation and stimulus for further studies of the ecology and dynamics of HABs, of their toxins, and of the public health and socioeconomic impacts of HABs within this region.

Acknowledgements

We thank the Intergovernmental Oceanographic Commission of UNESCO for the invitation to contribute this article through participation in the workshop on *Oceanographic and Biological Features and Trends in the CCLME* in Las Palmas de Gran Canaria from 27-29 January 2015.

4.6. ZOOPLANKTON IN THE CANARY CURRENT LARGE MARINE ECOSYSTEM

Amina BERRAHO[1], Laila SOMOUE[1], Santiago HERNÁNDEZ-LEÓN[2] and Luis VALDÉS[3]

[1] Institut National de Recherche Halieutique. Morocco

[2] Instituto de Oceanografía y Cambio Global (IOCAG), Universidad de Las Palmas de Gran Canaria. Spain

[3] Intergovernmental Oceanographic Commission of UNESCO. France

4.6.1. INTRODUCTION

Eastern boundary upwelling ecosystems, such as the Canary Current Large Marine Ecosystem (CCLME), are marine eco-regions that show the highest productivities in both primary (phytoplankton) and secondary (zooplankton) production and have attracted the attention of biological oceanographers since the mid 1950s. Zooplankton occupies a key position in the food web, and plays an important role in compacting organic matter, which is of paramount importance for the functioning of the biological pump.

Currently, zooplankton is also the focus of research on responses of living organisms to climate change, mostly because of their short life cycles (in the order of weeks) (Hays et al., 2005; Richardson et al., 2009). This community is therefore an ideal candidate for the identification of signatures of change (e.g. changes in phenology, physiological rates, export of organic matter and/or latitudinal displacement of species), which is a major challenge for ecologists. However, an important bottleneck for such research in the CCLME is the lack of routine sampling programmes (e.g. time-series) for such a large area (the CCLME occupies about 5000 km of coastline along Northwest Africa (NWA) and approximately 7600 km if the archipelago coasts are included).

Early studies of zooplankton off the NWA coast focused first on taxonomy and species assemblages (Faure, 1951; Furnestin, 1957; Corral, 1970; Corral and Pereiro, 1974; Boucher, 1982; Boucher et al., 1983), and later on the quantification of abundances and biomasses (Seguin, 1973; Vives, 1975; Furnestin, 1976; Hernández-León, 1988a; Fernández de Puelles and García-Braun, 1989; Somoue et al., 2005). It was more recently that advanced ecological studies on production, respiration, coupling processes and vertical carbon flux were initiated in the CCLME (Hernández-León, 1988b; Hernández-León et al., 2002, 2007).

We have an incipient understanding of the main driving forces determining the peaks in abundance, their variability and patterns in the Canary Current (Makaoui et al., 2005; Arístegui et al., 2006; Benazzouz, 2014; Benazzouz et al., 2013, 2014a). Seasonal changes and upwelling strength show a close link with the production of phytoplankton and zooplankton. Similarly, zooplankton production and its seasonality vary with latitude, with the highest values near Cape Blanc throughout the annual cycle (Pelegrí et al., 2005b). However, these general patterns need to be corroborated and complemented with additional studies at local and regional scales.

This article is an attempt to review (i) the taxonomy and biogeography of the main zooplankton groups in the CCLME and its area of influence northwards and (ii) patterns in the abundance and biomass of zooplankton in the CCLME (with data obtained from international surveys and national sampling programmes); (iii) it also seeks to give an overview of physiological rates (e.g. respiration) and fluxes in this upwelling region.

4.6.2. DATA SOURCES AND METHODS

4.6.2.1. Data sources

Descriptions of taxonomy, species assemblages and biogeography of zooplankton based on copepod species in the CCLME and its area of influence were obtained from several data sources, mainly (i) existing data published in scientific literature (e.g. Morocco, Canary Islands, Senegal, Guinea), (ii) data provided by different authors and (iii) data downloaded from the Ocean Biogeographic Information System (OBIS-www.iobis.org, accessed on 14 January 2015) in order to fill the gaps in data for the waters surrounding the Cape Verde Islands.

In order to compare patterns in the abundance and biomass of zooplankton and their role in carbon fluxes in the CCLME, most data were obtained from the literature, and also from surveys carried out on board Moroccan, Russian and other research vessels in the context of regional programmes and international projects (e.g. data obtained from publications and internal reports provided by the Institut National de Recherche Halieutique of Morocco - INRH).

Physiological rates were obtained from published data obtained from different cruises performed mainly in the area between Cape Ghir and Cape Blanc. During the 1990s and the first decade of this century, the institutions engaged in marine science in the Canary Islands studied the transport of phytoplankton, zooplankton and fish larvae from the rich upwelling area to the oligotrophic ocean. Most of the research was focused on the study of upwelling filaments and their interaction with cyclonic and anticyclonic eddies shed by the Canary Islands. All these studies were carried out under the umbrella of the international Global Ocean and Ecosystem Dynamics (GLOBEC) in an attempt to understand the mechanisms of plankton production and fluxes, as well as the mechanisms of fish larvae drift from the upwelling region to the Canary Islands and the open ocean (Hernández-León et al., 2007).

4.6.2.2. Methodology

The original data provided by Morocco for taxonomy, abundance and biomass were obtained through zooplankton samples collected with a small-size Bongo net (20 cm mouth diameter and 145-150 µm mesh size) equipped with a flow-meter for measuring the water filtered. Zooplankton samples were immediately preserved in 5% borax-buffered formalin. Identification and counting of zooplankton were carried out under a binocular stereoscope. Oceanographic observations and sampling of the entire area localized between Cape Spartel and Cape Blanc were conducted aboard the Russian R/V *AtlantNiro* during the warm (July 1994) and cold seasons (January-February 1995). For other physical, chemical and biological data we refer the reader to the original publications, describing the methodologies followed by the authors.

4.6.3. RESULTS

4.6.3.1. Zooplankton assemblages and biogeography

Zooplankton assemblages in different sectors of the CCLME have been studied by Furnestin (1957), Corral (1970), Corral and Pereiro (1974), Vives (1975), Boucher (1982), Chiahou (1997) and Somoue (2004) among many others, covering both the highly productive coastal waters and the oligotrophic oceanic waters. The holoplanktonic organisms comprised 15 groups: Hydromedusae, Ctenophora, Siphonophora, Polychaeta, Pteropoda, Cladocera, Ostracoda, Copepoda, Anphipoda, Mysidacea, Euphausiacea, Chaetognata,

Appendicularia, Doliolida and Salpida. Meroplanktonic organisms were represented by 9 groups: Gastropoda, Bibalvia, Cirripedia, Natantia, Anomura, Brachiura, Bryozoa, Echinodermata and Teleostei. As expected, copepods dominated the zooplankton in terms of abundance and number of species.

A checklist of copepod species was produced with data available in different regions of the CCLME (Morocco, Canary Islands, Cape Blanc, Guinea and Cape Verde Islands). The region is extraordinarily diverse, including up to 511 copepod species, which is 2.5 times the number of species identified (approximately 200) for the entire Ibero-Atlantic margin (from Santander to the Gulf of Cádiz, even though this coastline is approximately half that of the CCLME). The number of identified copepod species for the different regions were (from North to South): North Cape Bojador, 116; Canary Islands, 286; South Cape Bojador, 104; Cape Blanc, 244; and Cape Verde, 295. Up to 60 species are common to 4 or 5 datasets and these are widely distributed species (Table 4.6.1), making up the bulk of zooplankton; up to 315 species were identified in at least two areas, whereas 196 species were counted in only one dataset.

The similitude analysis of copepod species and assemblages of 13 datasets, 5 from the CCLME[13] plus 8 other datasets from the northern area of the upwelling (the spatial coverage goes from 14°N to 50°N, i.e. 36°N latitude, in other words more than a third of the northern hemisphere), shows two main clusters (Fig. 4.6.1) representing biogeographical and ecological characteristics. One cluster groups together the datasets from Cape Verde, the Canary Islands, Cape Blanc, Madeira and the Gulf of Cádiz, a subregion characterized by tropical and subtropical species and with a low influence of the upwelling nutrient-enriched waters; a second group encompasses the datasets from the North and South Cape Bojador areas, Portugal, Galicia, Asturias, the Bay of Biscay and the Celtic Sea, which is characterized by subtropical and luso-boreal species, with strong seasonality and under the influence of upwelling and coastal nutrient-rich waters.

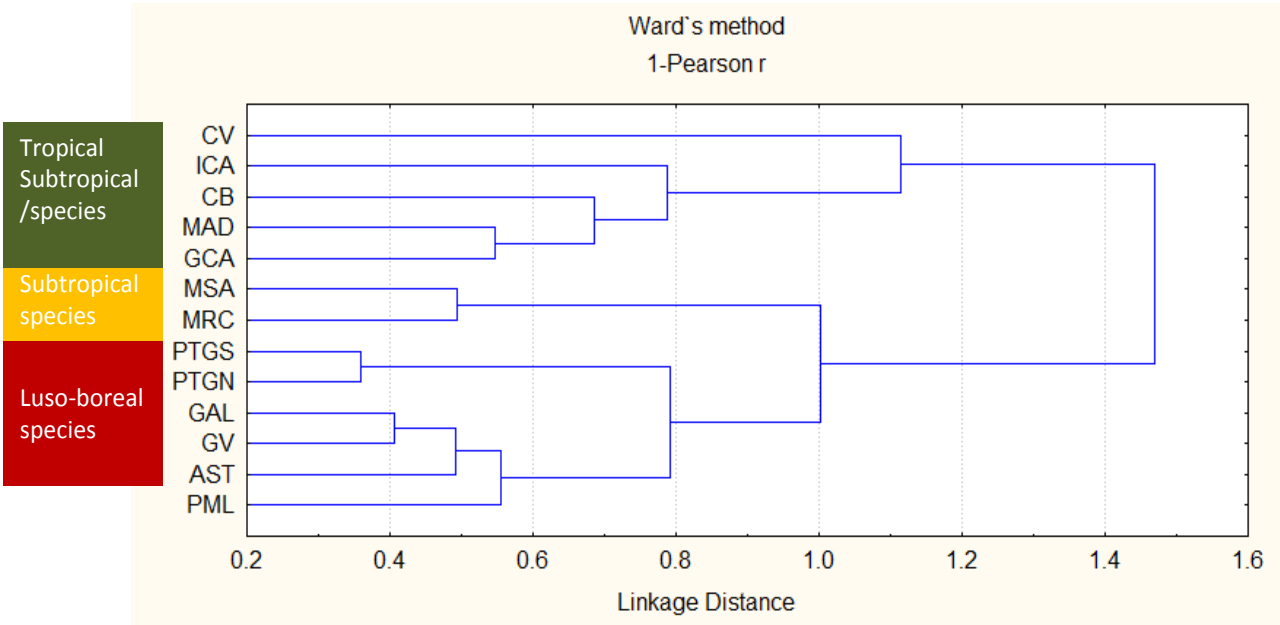

Figure 4.6.1. Ordination of copepod collections at different sampling sites. Cape Verde (CV), Canary Islands (ICA), Cape Blanc (CB), Madeira Islands (MAD), Gulf of Cadiz (GCA), South Cape Bojador (MSA), North Cape Bojador (MRC), South of Portugal (PTGS), North of Portugal (PTGN), Galicia (GAL), Asturias (AST), Bay of Biscay (GV) and the Celtic Sea (PML).

[13] For the similitude analyses we removed the datasets from Guinea as these comprise fewer than 25 species whereas the other catalogues comprise more than 100 species each.

4.6.3.2. Abundance and biomass patterns in the CCLME

As expected, copepod species in the CCLME accounted for 60%–95% of the abundance of zooplankton and makes up the bulk of the mesozooplankton biomass (Fernández de Puelles, 1986; Corral, 1970; Somoue et al., 2005; Salah et al., 2012; Zaafa et al., 2012a). Using available data and published literature, the following patterns in abundance and biomass, from north to south of the CCLME, were observed:

North Cape Bojador area (35°48'N–26°N)

Geographically located between the European temperate zone and the African tropics, this area is characterized by an irregular coastline, seasonal variability and rich shelf sea dynamics. According to these features, two main areas are considered:

- From Cape Spartel to Cape Beddouza (35°48'N–32°30'N): The position of the Azores Current, the presence of the Strait of Gibraltar, and the orientation of the coastline contribute to weak upwelling conditions in this area with strong seasonality and low productivity during the cold season. Biomass distribution in this area was recently studied in relation to seasonality during the warm (July 1994) and cold (January-February 1995) seasons (Fig. 4.6.2A). Average wet zooplankton biomass did not exceed 400 mg m^{-3}, the biomass during the warm season amounting to half of the values observed during the cold season. The distribution did not show a clear pattern other than the coastal influence. However, some mesoscale activity was observed, forcing offshore advection of zooplankton biomass during the cold season.

According to a seasonal sampling (2006-2007) in one transect near Tangier (Zaafa et al., 2012a, b), the zooplankton assemblage was dominated by copepods (93%) representing 85 species belonging to 34 families. Copepod species richness reached a maximum during autumn (December 2006 and November 2007), coinciding with low abundances, indicating a structured and balanced population. During the upwelling season in summer, the population was dominated by a few species with high densities and low richness. The dominant species in this area were *Paracalanus parvus*, *Oncaea venusta*, *Calanus helgolandicus* and *Acartia clausi*.

- From Cape Beddouza to Cape Bojador (32°30'N–26°N): Variability in this area is rather high due to the irregularity of the coastline and the position of the Canary Islands (Fig. 4.6.2B). A strong seasonal upwelling characterizes this area, with pronounced summer peaks in August and early September. Remarkable features of this area are the presence of two mesoscale structures, the giant and quasi-permanent filament off Cape Ghir (30°37'N) and the intermittent upwelling filament off Cape Juby. Both structures have a pronounced impact on the structure of plankton communities as biological tracers of upwelling filaments (Rodríguez et al., 2000; Berraho et al., 2012).

A seasonal study was carried out over two years (2008-2009) in Cape Ghir and Cape Juby to understand the physical functioning (Troupin, 2011; Makaoui et al., 2012) and the structure of plankton communities (Molina, 2013; Salah et al., 2012, 2013; Salah, 2013). Coastal areas surrounding the Cape Ghir and Cape Juby region are zooplankton concentration sites (Fig. 4.6.2B). Contrary to the northern area, the highest biomasses are observed during the warm season, with values exceeding 700 mg m^{-3} in inshore waters. During the cold season, high mesoscale activity again forces the displacement of zooplankton offshore.

In both areas, copepods dominate the zooplankton communities with 65% to 99% of total zooplankton. This group accounted for 86 species in Cape Ghir and 56 in Cape Juby. Dominating species in both Capes were: Acartia clausi, Oithona nana, Oithona similis, Oncaea venusta and Paracalanus parvus. These are neritic species characterized by a wide tolerance to changes in environmental factors and contributing

strongly to the signature of the upwelling filaments, and can be considered to be biological tracers of these filaments.

The copepod community differed between coastal and offshore waters. Offshore, species diversity and evenness were greater and the copepod community was more structured. Near the coast, the community was less structured under the strong influence of the upwelling and the less stable hydrological conditions. Temporally, low copepod diversity was recorded in June, coinciding with the seasonal intensification of the upwelling in both Capes.

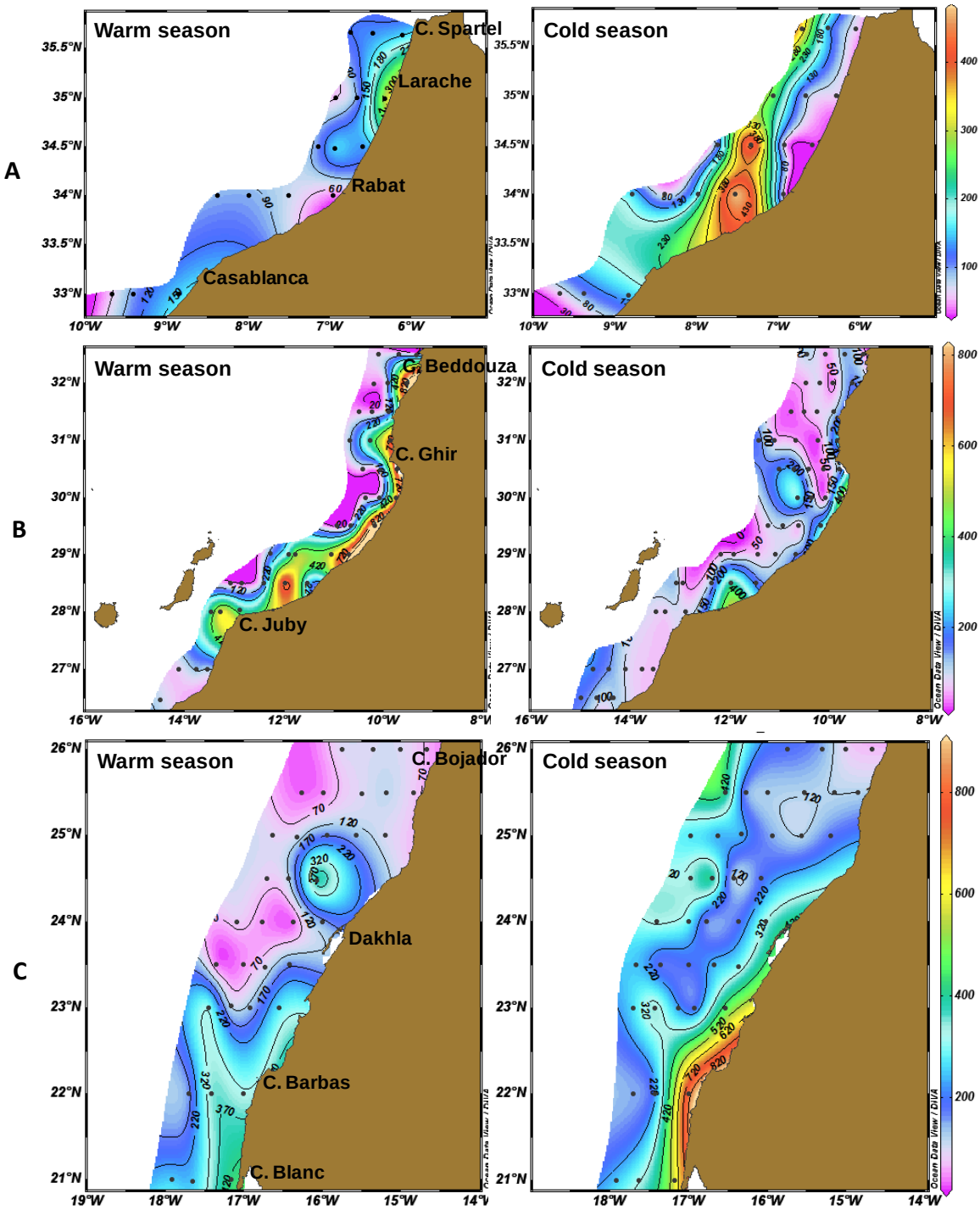

Figure 4.6.2. Distribution of zooplankton biomass expressed as wet weight (mg m^{-3}) in summer (July 1994) and cold (January-February 1995) seasons in North (A and B) and South (C) Cape Bojador areas. Please note the difference in colour scales in the right bar; dots indicate the sampling stations.

Canary Islands (28°N)

The annual cycle (June 1983-February 1985) of mesozooplankton (> 250 µm) was studied by Fernández de Puelles (1986) and Fernández de Puelles and García-Braun (1989) at a sampling site northeast of Tenerife Island (1200 m depth). The annual cycle showed two peaks, in winter and spring. The average abundance was 280 ind m^{-3} with peaks in March and May reaching approximately 900 ind m^{-3}. The zooplankton assemblage was composed of 76% of copepods, with the genus Oncaea (18%), Clausocalanus (18%), Oithona (17%) and Paracalanus (7%) being the most abundant and accounting for 60% of the total copepods. Average biomass (dry weight) of mesozooplankton was 3.99 mg m^{-3}. The bloom observed in the Canary Islands matched the pattern observed in northern Morocco, but was quite the opposite to the pattern shown between Cape Bedouzza and Cape Bojador (which is much closer in distance to the archipelago).

South Cape Bojador area (26°N–21°N)

In this region, the upwelling is strong and quasi-permanent. According to a north-south axis, the 26°N-25°N region corresponds to the active upwelling centre characterized by high turbulence and relatively low biological productivity. In the Dakhla region (25°N-23°N), the presence of mesoscale features (gyres and filaments) caused by warm coastal currents, gives rise to offshore advection of cold water and enhances plankton productivity (Makaoui et al., 2005). Further south, from Cape Barbas to Cape Blanc (23°N-21°N), high biological productivity was normally found throughout the annual cycle. This richness is a result of the upwelling, despite its low intensity, and advection of South Atlantic Central Water (SACW), which is quite rich in nutrients. The Cape Blanc region (20°50'N) constitutes a southern limit of the summer upwelling (Barton, 1998) and an ecological border (Binet, 1991). This was illustrated by the spatial distribution of wet biomass of zooplankton which showed a positive north-south gradient during the warm and cold seasons (Fig. 4.6.2C).

In this area the copepod population is represented by 104 species belonging to 29 families and widely dominated by *Calanus helgolandicus*, *Paracalanus parvus*, *Acartia clausi* and *Corycaeus typicus*. In addition, *Oithona helgolandica*, *Euterpina acutifrons* and *Temora stylifera* normally exhibit a rather high abundance north of Dakhla. Further south, *Calanus helgolandicus*, *C. minor*, *C. carinatus*, *Centropages typicus*, *Paraoithona parvula*, *Paracalanus aculeatus*, *Temora stylifera* and *T. longicornis* were the most abundant species. They are preferential herbivores and colonize regions enriched with nutrients where phytoplankton proliferates. Copepod diversity was generally high in winter and low in summer (Somoue et al., 2005).

Mauritanian area (21°N-16°N)

This region shows the maximum intensity of upwelling during winter (February-April) (Benazzouz et al., 2013, 2014a; Ndoye et al., 2014). Several geographical features in this area, such as the Cape Blanc peninsula, contributed to rather high hydrological variability and the presence of upwelled SACW, as well as multiple upwelling filaments (Kostianoy and Zatsepin, 1996).

Different inventories of copepod species were established in the 1970s (Binet and Dessier, 1971; Seguin, 1973; Vives, 1975). On the basis of these studies, Boucher (1982) concluded the existence of a transition zone along the Mauritanian-Senegal region. This area represents the southern limit of temperate copepod species distribution (i.e. *Calanus helgolandicus*, *Temora longicornis* and *Oncaea curta*) and the northern boundary of tropical species (i.e. *Undinula vulgaris*, *Eucalanus pileatus*, *Euchaeta paraconcinna*, *Acartia*

plumosa, *and Corycaeus africanus*). This faunistic border perfectly matched the hydrological boundary between the North Atlantic Central Water (NACW) and SACW (Minas et al., 1982). However, changes were noted in these two water masses as a result of the northward propagation of the SACW, which relied mainly on the poleward undercurrent associated with the coastal upwelling (Arístegui et al., 2006). Therefore, significant variability of zooplankton biomass, distribution and species diversity was normally observed in the coastal waters of Mauritania during winter (Glushko and Lidvanov, 2012).

Senegambian area (16°N-12°N)

Seasonal variation of zooplankton composition, abundance and biomass in Senegambia was studied by Gaudy and Seguin (1964), Seret (1983) and Medina-Gaertner (1988), among others. Copepod assemblages were determined in different hydrographic seasons (Gaudy and Seguin, 1964). Ten species of Calanoida are perennial in the area: *Eucalanus pileatus, E. subtenuis, Euchaeta marina, Scolecithrix danae, Temora stylifera, T. turbinata, Centropages chierchiae, Candacia pachydactyla* and *C. curta*. It is interesting to note that, although all these species were present in the inventories analysed in the dendrogram shown in Figure 4.6.1, most of them are not included among the most common ones in Table 4.6.1 (red dots), which is consistent with the faunistic boundary indicated in the previous section.

Zooplankton was quite abundant throughout the year (abundances > 2000 ind m^{-3}) with peaks of both biomass and abundance (in the order of 15,000 ind m^{-3}) from November to January (1982-1983) and secondary peaks (5000-10,000 ind m^{-3}) in May and August 1982. Binet (1991) suggested that phytoplankton and zooplankton growth cycles seemed to be coupled, which he related to (i) the Ekman transport of surface waters and (ii) ontogenetic migrations of copepod species coupled with the upwelling of deep waters.

Guinean area (10°N-9°N)

Zooplankton taxonomy and abundances were studied in the vicinity of Conakry (Loos Islands, 9°26'N) by Khlistova and Kéita (1985). A total of 50 copepod species were identified (Calanoida, 50; Cyclopoida, 20; and Harpacticoida, 7). *Paracalanus quasimodo, Oithona brevicornis, O. simplex, O. spinulosa* and *O. nana* were the dominant species, accounting for 80% of total zooplankton abundance. During some periods, other species such as *Corycaeus africanus, Temora turbinate, T. stylifera, Centropages furcatus, Eucalanus pileatus, E. subcrassus, E. mucronatues* and *Euterpina acutifrons* also reached high abundance levels.

Although the sampling site was shallow and under a strong coastal influence, we noted marked consistency in seasonality, with peaks (15,000-18,000 ind m^{-3}) during December and January and low values during February and March (5000-6000 ind m^{-3}). These high numbers were similar to those found in the neighbouring region of Senegambia.

4.6.3.3. Carbon fluxes mediated by zooplankton

Pioneering zooplankton feeding and metabolic studies in the upwelling waters of the CCLME were carried out during the 1970s as part of the CINECA (Cooperative investigation of the central part of the Eastern Central Atlantic) project. Some of the experiments performed at that time are, unfortunately, still unpublished in peer-reviewed journals and remain in different reports. Copepods and euphausiids were the target species commonly used. Concomitantly, other approaches to studies of metabolism were developed. Enzymatic activities like the Electron Transfer System (ETS, Packard et al., 1974), digestive enzymes like amylase (Boucher and Samain, 1974) and proteases (Boucher and Samain, 1975) were used as proxies for respiration, grazing and carnivorism, respectively. An important set of data was generated during that time,

providing the basis for knowledge of the role of zooplankton physiology in upwelling systems. During the 1990s, large projects such as CANIGO (Parrilla et al., 2002), MAST (Barton et al., 1998), and Coastal Transition Zone (Barton et al., 2004) made the major contribution to the knowledge of fluxes mediated by zooplankton.

The general pattern in upwelling areas is a marked decrease in nutrients and chlorophyll from the coast to the ocean (Le Borgne, 1980), which is also coupled with an increase in zooplankton biomass towards the ocean. A succession of small to medium and large calanoids and gelatinous organisms from the upwelled waters to the ocean is normally the rule (Postel, 1990). Zooplankton have longer generation times than primary producers and therefore survive for longer periods, so they could be transported far from the coast. The increase in zooplankton size and temperature and the decrease in food along the offshore drift imply changes in the physiology of the organisms, as shown by Ikeda (1985). These changes were also observed in a switch in the feeding mode of organisms. A phytoplankton-based diet was observed in the inshore upwelling zone. Hernández-León et al. (2002) observed that 90%-100% of feeding in the proper upwelling was phytoplankton, whereas only 10%-20% of the zooplankton diet was pigmented food in the oceanic waters (Fig. 4.6.3). As mentioned, organisms drifting and succession developed towards the ocean. Organisms changed their feeding to non-fluorescent food, to a microzooplankton based diet. This was also observed in fish larvae by Bécognée et al. (2009) and seems to be a general rule for zoo- and ichtyoplankton in the transition zone.

A permanent and prominent feature of upwelling zones is the formation of filaments of colder and fresher waters flowing to the ocean. In the Canary Current, the first observations of filaments were obtained from remote sensing (Van Camp et al., 1991; Hernández-Guerra et al., 1993). They have important consequences for fluxes as they transport phytoplankton (Arístegui et al., 1997), zooplankton (Hernández-León et al., 2002) and fish larvae (Rodríguez et al., 2004) to open ocean waters. As observed by Postel (1990) as a general pattern for the upwelling off NWA, the faunistic composition of filaments showed a clear dominance of small and medium-sized copepods, and large species with a large oil sac (Hernández-León et al., 2007). Zooplankton biomass transported along the filaments also showed the influence of hydrodynamics in their physiology. Hernández-León et al. (2002) and Yebra et al. (2004) studied the effect of these structures on the feeding and metabolic rates of this community. These authors found twofold higher gut fluorescence inside the filaments compared to surrounding waters, indicating increased grazing in the chlorophyll-enriched waters of the filament. Hernández-León et al. (2002) also observed gut fluorescence decreasing as organisms drift to the ocean inside the filament waters. However, although ETS activity also decreased, this proxy for respiration remained at relatively high levels. The growth index used (Aspartate Transcarbamylase Activity, ATC) nevertheless increased towards the ocean (Yebra et al., 2004). Thus, from the physiological standpoint, a succession from the coast to the ocean seemed to occur, with zooplankton feeding heavily on phytoplankton in the upwelled waters and sharply decreasing their grazing towards the ocean as metabolisms remained high and growth increased through the oceanic waters (Fig. 4.6.3). These features indicated a switch from a diet based on phytoplankton to one based on microzooplankton as zooplankters drifted towards the ocean, since their metabolism and growth remained rather high.

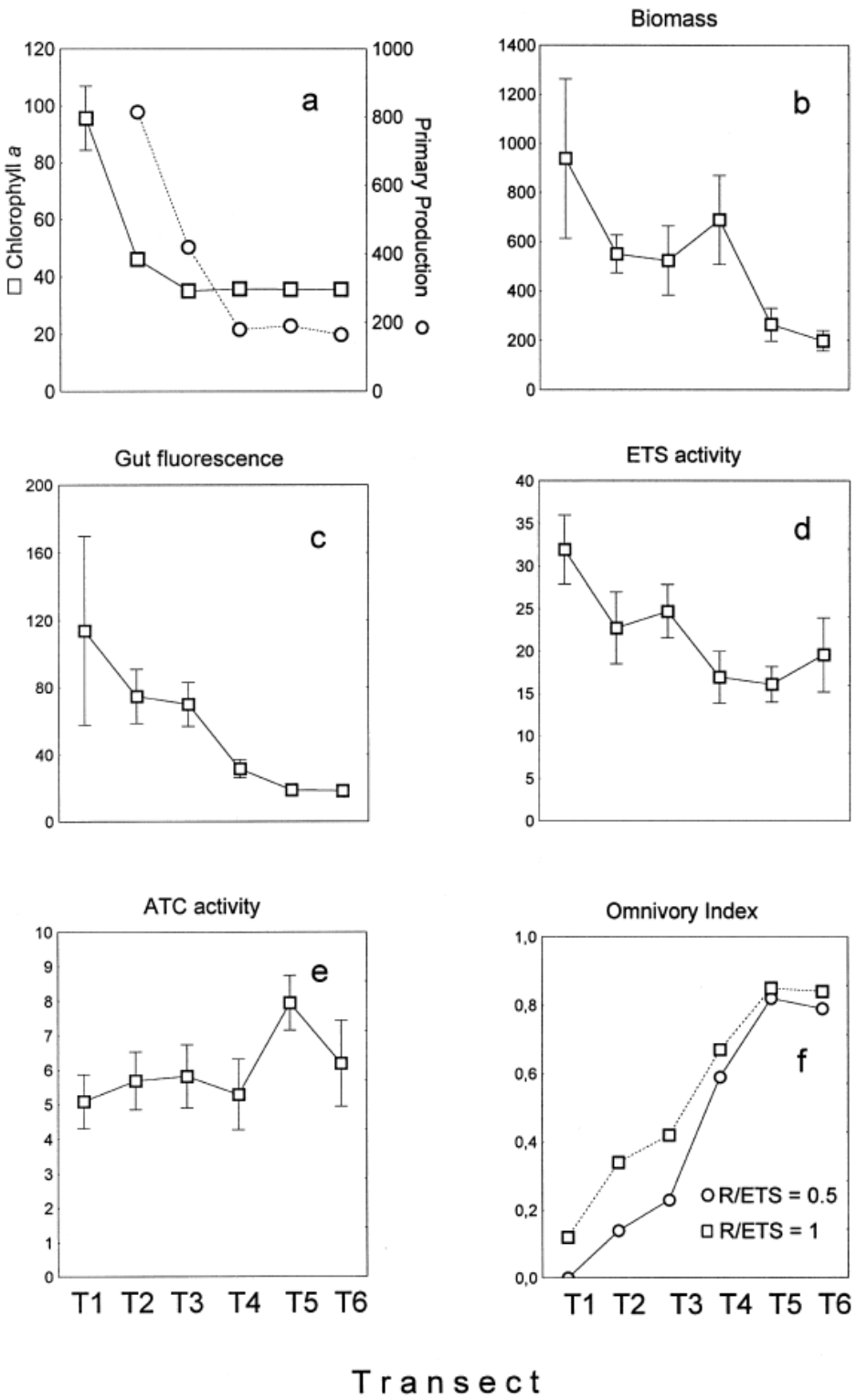

Figure 4.6.3. Average values (±SE) of (a) chlorophyll and primary production (mgC m^{-2} d^{-1}), (b) zooplankton biomass (mg protein m^{-2}), (c) specific gut fluorescence (ng pigments mg^{-1}protein), (d) specific ETS activity (µl O_2 mg^{-1}protein h^{-1}), (e) specific ATC activity (nmol carbamylaspartate mg^{-1}protein min^{-1}), and (f) the index of omnivory (ingestion-grazing/ingestion). The transect T1 is close to the African coast and T6 is oceanic (oligotrophic). Observe the Sharp decrease in chlorophyll followed by primary production and zooplankton biomass, while gut fluorescence and ETS activity decreased offshore, ATC activity remained

constant and the calculated index of omnivory sharply increased toward the ocean (from Hernández-León et al., 2002).

Another important characteristic of the CCLME is the presence of the Canary Islands, a 600 Km barrier in the path of the main current, promoting significant mesoscale activity leeward of the islands. Cyclonic and anticyclonic eddies shed by the islands generates the so-called "Canary Eddy Corridor" (Sangrà et al., 2009; Sangrà, 3.5 of this work). These eddies also have a strong influence on the distribution of phyto- and zooplankton (Hernández-León et al., 2001). While cyclonic eddies produce centrifuge transport, anticyclonic eddies promote downwelling, sinking prokaryotes and phytoplanton (Arístegui et al., 1994; Arístegui and Montero, 2005), and causing an accumulation of zooplankton because of their capacity to swim and avoid sinking (Hernández-León et al., 2001). The increase in primary production in cyclonic eddies also promotes an increase in the metabolic activity of zooplankton, as observed from ETS activity (Hernández-León et al., 2001). The interaction between filaments and eddies shed by the islands fostered a net transport of organic matter to the open ocean which is not fully understood at present.

4.6.3. DISCUSSION AND CONCLUSIONS

The CCLME constitutes one of the four main Eastern Boundary Upwelling Ecosystems (EBUEs) of the world, characterized by their high productivity. The CCLME covers a huge region (9°N-35°N) with marked geographical/topographical diversity. The current knowledge on regional variability in plankton community structure is sparse, with a few well-documented local exceptions, and insufficient to derive geographical patterns of variability (Arístegui et al., 2009a). However, the common feature throughout the CCLME is the dominance of copepods, despite wide variability of biomass, distribution and species diversity from one region to another.

According to Boucher (1982), the comparison of communities that are distant in latitude but connected by similar hydrological, chemical and environmental conditions, offers an opportunity to identify the influence of biogeography and environment conditions on the types of organisms that inhabit them. Upwelling areas are favourable environments for this approach, with a small number of abundant species having similar importance in every region (Table 4.6.1).

In the Moroccan area, zooplankton (mainly copepods) showed a wide biogeographical distribution with many cosmopolitan species from neighbouring regions. Between the Iberian coast and the North Moroccan coast, species exchange is reduced on account of the low flow between the two regions, caused by the interruption of the coastline at the Strait of Gibraltar (Arístegui et al., 2006). However, plankton exchange between the Atlantic Ocean and the Mediterranean Sea through the Strait of Gibraltar is more marked in the Atlantic - Mediterranean direction than in the opposite direction. According to data from 2006-2007, among the 103 species recorded at two transects on both sides of the Strait, 61.2% were common to both sectors, while 21.4% and 17.5% were endemic to the Atlantic Ocean and the Mediterranean Sea, respectively (Zaafa et al., 2012b). The Mediterranean outflow is reduced because of the shallow depth of the Strait (< 300m), and, according to Gómez et al. (2000), microplankton distribution patterns in the Strait of Gibraltar showed an increased abundance from southwest to northeast, a tendency coinciding with a gradual elevation of the Atlantic-Mediterranean depth in the same relative direction.

From Cape Beddouza to Cape Blanc, inventories of copepod fauna showed changes in latitudinal distribution of some species as well as the emergence of other species from distant areas. Boucher (1982)

identified, *Temora longicornis* and *Calanoides carinatus,* reported only in the Mauritania-Guinea sub-region (Furnestin, 1960; Paiva, 1970; Seguin, 1973, 1981). North Atlantic species, such as *Heterocope saliens*, *Calanus hyperboreus* and *Scaphocalanus medius*, and species with quite wide distribution ranges in the Atlantic and Pacific Oceans (e.g. *Scaphocalanus brevicornis*) have also been reported between Cape Bojador and Cape Blanc (Somoue, 2004; Somoue et al., 2005). Recently, *Euchaeta paraconcinna,* a south-central Atlantic species, and the widely tropical *Paracalanus tropicus* (Southeast Atlantic) have also been found in the area (Lidvanov et al., 2013).

In Cape Blanc, *Temora turbinata,* a species indicating the southern origin of the water mass, was dominant in the copepod assemblage during winter 2009/2010 as a result of the inflow of warm waters into northern regions (Glushko and Lidvanov, 2012). In a similar context, analysis of zooplankton assemblages in the Mauritanian coastal waters during summer periods from 1998 to 2004 revealed pronounced increments of the percentage of species, normally observed in the Senegal and Guinea waters. Simultaneously, decreasing upwelling intensity and northward displacement of the boundary between the NACW and the SACW were observed. Thus, the south species abundance on the Mauritania shelf can be attributed to the northward advection of SACW (Sirota and Zhigalova, 2007).

According to Lindley and Daykin (2005) and Valdés et al. (2007), the calanoid copepods *Centropages chierchiae* and *Temora stylifera* have both moved northwards and were found off the Iberian Peninsula in the 1970s and 1980s and into the English Channel in the 1990s. The northward shift of zooplankton species under the effect of increased temperature has been well studied in the Northeast Atlantic region. Here, the range shifts revealed by zooplankton in response to global warming was estimated to be about 200 km per decade (Richardson, 2008), being among the fastest and largest of any group of marine or terrestrial organisms (Richardson et al., 2009). These changes in the distribution and structure of zooplankton communities directly impact the food web, particularly fish species whose diet is planktivorous.

The data presented in this review show that the abundance of zooplankton populations is determined by the seasonality and the upwelling regime. In spite of the different sources of information used in this review, we found a strong consistency in the range of values and the seasonal patterns. However, it must be noted that most of the data available (mainly the annual cycles in short time series) come from studies carried out during the 1980s. More studies are needed to verify that the patterns observed 30-35 years ago are still valid and that climate change and variability of upwelling strength is altering neither the cycles nor the productivity of the CCLME. The zooplankton physiology also deserves future work as these organisms live longer than any other plankton and are the food of diel vertical migrants (large zooplankton and micronekton), which also transport carbon from the ocean upper layers to the deep sea through active flux. This mechanism should shed light on the fate of the huge productivity of upwelling areas.

Table 4.6.1. List of copepod species identified in Northen CCLME area (Cape Spartel-Cape Blanc). Red dots indicate 60 common species inventoried also in Canary Islands, Cape Blanc and Cape Vert.

ACARTIIDAE		**EUCHAETIDAE**	
Acartia clausi Giesbrecht ,1889	●	*Euchaeta pubera (Sars, 1907)*	●
Acartia danae Giesbrecht ,1889	●	*Euchaeta spinosa (Giesbrecht ,1892)*	●
Paracartia grani (Sars ,1904) *(=Acartia grani)*		*Euchaeta sp*	
Acartia longiremis (Lilljeborg ,1853)		*Paraeuchaeta glacialis* (Hansen, 1886)	
Acartia tonsa Dana, 1848		*Paraeuchaeta incisa* (Sars, 1905)	
Acartia discaudata (Giesbrecht,1881)		*Paraeuchaeta norvegica* (Boeck, 1872)	
Acartia margalefi Alkaraz, 1976		*Paraeuchaeta sp.*	
AEGISTHIDAE		*Paraeuchaeta hebes* (Giesbrecht, 1888)	●
Aegisthus dubius Sars, 1916		*Paraeuchaeta gracilis* (G.O. Sars, 1905)	
Aegisthus mucronatus Giesbrecht, 1891		**LUCICUTIIDAE**	
Aegisthus spinulosus Farran ,1905		*Lucicutia magna* (Wolfenden, 1903) (=*Lucicutia atlantica)*	
Aegisthus aculeatus (Giesbrecht,1891)		*Lucicutia tenuicauda* Sars, 1907	
AETIDEIDAE		*Lucicutia flavicornis (Claus, 1863)*	●
Aetideus armatus (Boeck, 1872)	●	*Lucicutia maxima Steuer, 1904*	
Aetideus giesbrechti Cleve, 1904	●	**MACROSETELLIDAE**	
Bradyidius armatus Giesbrecht, 1897		*Macrosetella gracilis* (Dana, 1847)	●
Euchirella curticauda Giesbrecht, 1888		**METRIDINIDAE**	
Euchirella rostrata (Claus, 1866)	●	*Pleuromamma abdominalis* (Lubbock,1856)	●
Gaetanus tenuispinus (Sars, 1900)		*Pleuromamma gracilis* (Claus ,1863)	●
Gaetanus kruppi (Giesbrecht,1904)	●	*Pleuromamma robusta* (Dahl F., 1893)	●
Undeuchaeta plumosa (Lubbock, 1856)	●	*Pleuromamma xiphias (* Giesbrecht, 1889)	●
Unidopsis bradyi Sars, 1884		*Pleuromamma borealis* Dahl F., 1893	●
ARIETELLIDAE		*Pleuromamma piseki* Farran, 1929	●
Arietellus setosus Giesbrecht ,1892		**MONSTRILIIDAE**	
Sarsarietellus abyssalis (Sars, 1905) (=Scotulla abyssalis		*Monstrilla grandis* Giesbrecht, 1891	
Scottula abyssalis (Sars, 1902)		*Monstrilla helgolandica* Claus, 1863	
AUGAPTILIDAE		**NULLOSETIGERIDAE**	
Augaptilus longicaudatus (Claus, 1863)	●	*Nullosetigera bidentata* (Brady, 1883) (=*Phyllopus bidentatus)*	
Augaptilus megalurus Giesbrecht, 1889		**OITHONIDAE**	
Augaptilus spinifrons (Sars, 1907)		*Oithona brevicornis* Giesbrecht, 1891	
Pseudhaloptilus eurygnathus (Sars, 1920)		*Oithona helgolandica* (Claus ,1863)	●
Haloptilus oxycephalus (Giesbrecht, 1889)		*Oithona linearis* Giesbrecht ,1891	
CALANIDAE		*Oithona nana* Giesbrecht ,1891	●
Calanoides carinatus (Kroyer , 1849)	●	*Oithona plumifera* Baird ,1843	●
Calanoides brevicornis (Lubbock, 1856)		*Oithona setigera* Dana, 1849	●
Calanus helgolandicus (Claus, 1863)	●	*Oithona similis* Claus, 1866	
Calanus hyperboreus Kroyer, 1838		*Paraoithona parvula* Farran ,1908	
Nannocalanus minor (Claus, 1863) (=*Calanus minor)*	●	*Oithona sp.*	
Metacalanus inaequicornis (Sars, 1903)		**ONCAEIDAE**	
Neocalanus gracilis (Dana, 1849)	●	*Oncaea curta* Sars ,1916	●
CALOCALANIDAE		*Oncaea media* Giesbrecht, 1891	●
Calocalanus pavo (Dana, 1849)	●	*Oncaea mediterranea* Claus, 1863	●
Calocalanus contractus Farran, 1926		*Oncaea minuta* Giesbrecht ,1892 (=Triconia minuta)	
Calocalanus sp		*Oncaea tennella* Sars, 1916	
CANDACIIDAE		*Oncaea venusta* Philippi,1843	●
Candacia bipinnata (Giesbrecht, 1889)		*Triconia conifera (Giesbrecht, 1891)*	
Candacia elongata (Boeck, 1872)		*Oncaea sp.*	
Candacia varicans (Giesbrecht, 1889)	●	*Oncaea dentipes* (Giesbrecht, 1891)	
Candacia armata (Boeck, 1872)	●	**PARACALANIDAE**	
Candacia longimana (Claus, 1863)	●	*Mecynocera clausi* Thompson I.C., 1888	
Candacia sp.		*Paracalanus aculeatus* Giesbrecht ,1888	●
CENTROPAGIDAE		*Paracalanus nanus* Sars,1907	
Centropages chierchiae Giesbrecht, 1889	●	*Paracalanus pavus* (Claus,1863)	●
Centropages hamatus (Lilljeborg ,1853)		*Paracalanus pygmaeus* (Claus,1863)	
Centropages kroyeri Giesbrecht, 1892		*Paracalanus denudatus Sewell, 1929*	
Centropages typicus Kroyer ,1849		*Paracalanus sp.*	
Centropages violaceus (Claus ,1863)		**PHAENNIDAE**	
Centropages bradyi Wheeler, 1901		*Phaenna spinifera Claus, 1863*	●
Centropages sp		*Xanthocalanus obtusus Farran, 1905*	

CLAUSOCALANIDAE		**PONTELLIDAE**	
Clausocalanus jobei Frost et Fleminger, 1968		*Labidocera wollastoni* (Lubbock, 1857)	
Ctenocalanus vanus Giesbrecht ,1888	●	*Labidocera brunescens* (Czernivsky, 1868) L	
Microcalanus pusillus Sars, 1903		*Labidocera sp*	
Pseudocalanus elongatus (Boeck, 1865)		**SAPPHIRINIDAE**	
Clausocalanus arcuicornis (Dana, 1849)		*Sapphirina opalina* Dana, 1849	
Clausocalanus paululus Farran, 1926		*Copilia mediterranea (Claus, 1863)*	
Clausocalanus pergens Farran, 1926		*Sapphirina iris Dana, 1849*	
Clausocalanus farrani (Sewell, 1929)		*Sapphirina lactens* (Giesbrecht , 1892) BL	
Clausocalanus parapergens (Frost et Fleminger,1968)		*Sapphirina nigromaculata Claus, 1863*	
CLYTEMNESTRIDAE		*Sapphirina sp.*	
Clylemnestra gracilis (Claus, 1891)		**SCOLECITRICHIDAE**	
Clytemnestra scutellata (Dana, 1852)		*Scaphocalanus brevicornis* (Sars ,1900)	
CORYCAEIDAE		*Scaphocalanus echinatus* (Farran, 1905)	●
Corycaeus clausi Fdahl ,1894	●	*Scaphocalanus magnus* (Scott, 1894)	●
Corycaeus speciosus Dana, 1849	●	*Scaphocalanus medius* (Sars ,1907)	
Corycaeus (Agetus) flaccus Giesbrecht, 1891		*Scaphocalanus curtus* (Farran, 1926)	●
Corycaeus (Onychocorycaeus) giesbrechti F. Dahl, 1894		*Scolecithricella ovata* (Farran, 1905)	●
Corycaeus furcifer (Claus, 1863) LRG (=*Urocorycaeus frcifer*)		*Scottocalanus persecans* (Giesbrecht, 1895)	
Corycaeus limbatus (Brady, 1883) L (=*Agetus limbatus*)		*Scolecithricella minor* (Brady, 1883)	
Corycaeus sp		*Scolecithrix bradyi* (Giesbrecht, 1888)	●
Agetus typicus (Kroyer ,1849) (= *Corycaeus typicus*)		*Scolecithrix Danae* (Lubbock, 1856)	●
Ditrichocorycaeus angilicus (Lubbock, 1857) (= *Corycaeus anglicus)*		**SPINOCALANIDAE**	
Farranula carinata (Giesbrecht, 1891) (=Corycella carinata)	●	*Monacilla typica G.O.* Sars , 1905	●
Corycella rostrata (Claus,1863) (=*Farranula rostrata*)		**TACHYDIIDAE**	
DIAIXIDAE		*Euterpina acutifrans* (Dana 1847)	●
Diaixis pygmoea (T. Scott, 1894)		**TEMORIDAE**	
ECTINOSAMATIDAE		*Temora longicornis* (Muller ,1792)	
Microsetella rosea Dana, 1847	●	*Temora stylifera* (Dana ,1849)	●
Microsetella norvegica (Boeck, 1864)		*Heterocope saliens* (Lilljeborg, 1863)	
EUCALANIDAE			
Subeucalanus crassus (Giesbrecht,1888) (=*Eucalanus crassus)*	●		
Eucalanus elongatus (Dana,1848)	●		
Eucalanus hyalinus (Claus, 1866)			
Subeucalanus monachus (Giesbrecht ,1888) *(=Eucalanus monachus)*	●		
Eucalanus spinifer (T. Scott, 1894)			
Rhincalanus cornutus (Dana, 1849)	●		
Rhincalanus nasutus Giesbrecht ,1888	●		
Eucalanus atlanticus (Wolfenden, 1904)			
Eucalanus attenuatus (Dana, 1848)	●		

5. LIFE IN THE SEA

5.1. PELAGIC FISH STOCKS AND THEIR RESPONSE TO FISHERIES AND ENVIRONMENTAL VARIATION IN THE CANARY CURRENT LARGE MARINE ECOSYSTEM

Cheikh-Baye BRAHAM[1] and Ad CORTEN[2]

[1] Institut Mauritanien de Recherches Océanographiques et des Pêches. Mauritania

[2] Ministry of Economic Affairs. The Netherlands

5.1.1. INTRODUCTION

The main stocks of small pelagics are found in the exclusive economic zones (EEZs) of Morocco, Western Sahara, Mauritania, Senegal and The Gambia, most of them being shared by two or more countries of the sub-region. These species constitute essential renewable resources that provide food, employment and income for the local populations and revenues for the government in the form of taxes and licences. Small pelagics have already been exploited for more than a century by both local fishermen and foreign fleets.

This section describes the pelagic resources of the Canary Current Large Marine Ecosystem (CCLME), with an emphasis on the Northwest African area. Furthermore it describes the influence of climatic conditions on the distribution and variability of the exploited fish stocks.

5.1.2. DATA ANALYSIS

The data sources used for this study were obtained from the following sources:

- Reports of the FAO Committee on Eastern Central Atlantic Fisheries (CECAF) Working Group for Small Pelagic Fish in Northwest Africa
- Reports of the International Commission for the Conservation of Atlantic Tunas (ICCAT) Working Group on large pelagic fish
- Acoustic surveys coordinated by the FAO working group
- Data from the United States National Oceanographic Data Center and GHRSST (Group for High Resolution Sea Surface Temperature) obtained by the AVHRR (Advanced Very High Resolution Radiometer) (http://pathfinder.nodc.noaa.gov, accessed on 16 January 2015) Pathfinder Version 5.2 (PFV5.2) were used to monitor sea surface temperature (SST)
- A review of the most recent scientific publications on pelagic fish in the region

5.1.3. RESULTS

The pelagic fish resources of the CCLME area may be divided into small and large pelagics. The most important stocks, both in terms of biomass and commercial value, belong to the small pelagics category. These stocks are generally tied to the coastal areas where food production is highest. On the other side of

the range we find the large pelagic species. These consist of a number of tuna species, some of which have an oceanic distribution and are also exploited by important commercial fisheries. In the following items we shall look at each of these two groups of pelagic resources separately.

5.1.3.1. Small pelagic fish

The small pelagics are the most abundant fish stocks in the CCLME area, and they are mostly shared by several coastal states. They occupy a fundamental place in the upwelling ecosystem because of their intermediate position in the trophic chain and their abundance. The small pelagic stocks exhibit strong natural variations in abundance. These species may control both the abundance of the zooplankton that they eat ("top-down" control) and the abundance of their predators ("bottom-up" control) according to the situation (Bakun, 1996). The reproduction strategy of small pelagics is based on a high growth rate, and their populations may increase by 100% within a few months.

Species of small pelagics

Small pelagics typically have a modal length ranging between 20-40 cm total length. Because of their typical schooling behaviour, they are usually found in schools that may contain many hundreds tons of fish. These dense aggregations may be located either by electronic fish finding devices such as sonar and echo sounders, or by their appearance at the surface. Although the fish have a lower commercial value than other species, the fact that they may be harvested in large quantities makes them an attractive target for commercial fisheries, both industrial and artisanal.

The most important species of small pelagics are shown in Plates 6.1.1 and 6.1.2. These are the sardine (*Sardina pilchardus*), the round and flat sardinellas (*Sardinella aurita* and *Sardinella maderensis*), the bonga (*Ethmalosa fimbriata*), the Cunene and Atlantic horse mackerels (*Trachurus trecae* and *Trachurus trachurus*), the false shad (*Caranx rhonchu*s), the anchovy (*Engraulis encrasicolus*) and the chub mackerel (*Scomber japonicus*). These species may be divided into two categories in the CCLME area on the basis of their temperature preferences. One category contains fish with a preference for cold water, such as the sardine, chub mackerel and Atlantic horse mackerel. The other category contains fish that are associated with warm water, such as the sardinellas and the Cunene horse mackerel.

Apart from the sardine, which is taken mostly in Morocco, the most important species of small pelagics in the CCLME region are the sardinellas. Of the two species involved, the round sardinella (*S. aurita*) is the most important one. This species is taken in about the same quantities in Mauritania and in Senegal. The flat sardinella (*S. maderensis*) is mostly caught in Senegal (Corten et al., 2012).

The general relationship between small pelagics and hydrography in the CCLME area

The abundance of small pelagics in the CCLME area is closely related to the upwelling of nutrient-rich waters that is the basis of the food production for these fish. The largest stocks are therefore found in areas where the upwelling is strongest, i.e. the waters of northern Mauritania and Western Sahara.

The extent of the upwelling area shows seasonal variations, both in latitudinal and longitudinal direction. The upwelling extends furthest south during the cold season, when the vertical temperature gradient of the water is weak, and the wind can easily bring deeper water to the surface. With the warming of surface water during summer, a strong vertical temperature gradient (thermocline) develops, and more energy is required to bring the deeper water to the surface. Infrared satellite pictures show that upwelling becomes an intermittent process, with cold water rising to the surface only during episodes of strong alongshore

wind. When the wind calms down, the cold water sinks again and is covered by warm surface waters. By the end of the summer, the thermocline has become so strong that upwelling retracts to the northern and coastal parts of the Mauritanian zone and the Moroccan coastal zone. These are the only areas where food is still abundant, and hence the small pelagics, in particular the sardinella, concentrate in these areas.

The seasonal variations in water temperature and upwelling have a significant impact on the north/south distribution of the stocks of small pelagics. In general, the cold water species tend to be distributed further to the north than the warm water species. Both groups of species migrate northwards during summer when water temperature rises and upwelling contracts to the north. In winter, when temperature drops and upwelling extends further southwards, both groups of species shift their distribution to the south (Figure 5.1.1).

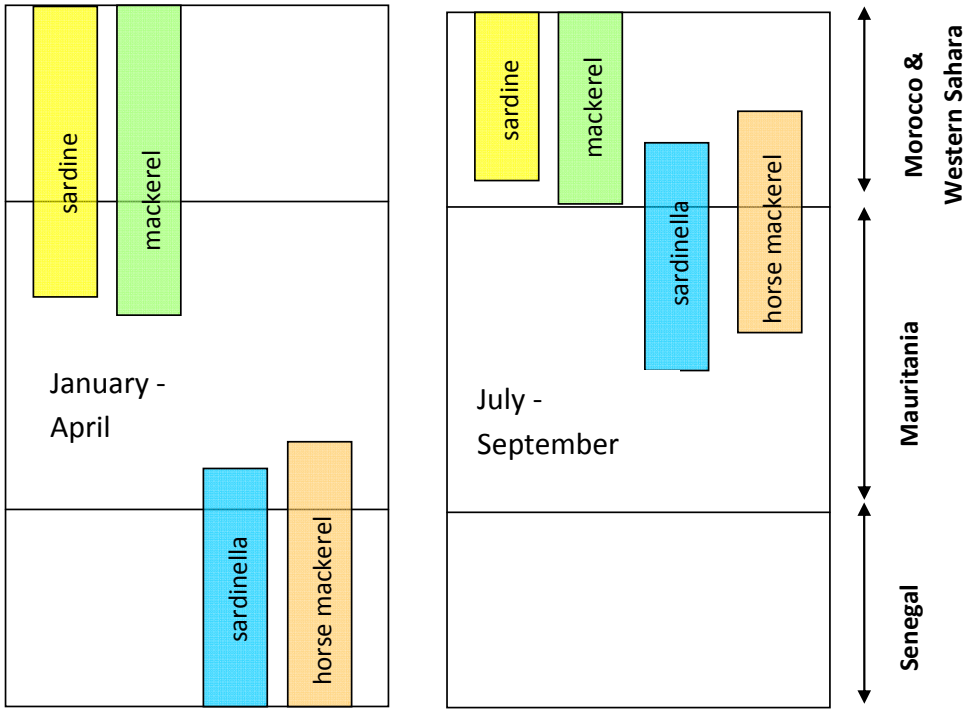

Figure 5.1.1. Simplified scheme of seasonal displacement of small pelagics. "Sardinella" refers to the round sardinella (*S. aurita*) and horse mackerel to the Cunene horse mackerel (*T. trecae*).

The north/south seasonal migrations may be best illustrated by the migrations of the most important species of small pelagics: the round sardinella (*S. aurita*). Figure 5.1.2 illustrates what is presently considered as the most likely hypothesis for the annual migration path of the stock, from the waters of Senegal in winter, to the waters of Mauritania, Western Sahara and Morocco in summer. It should be noted that the migration path in Figure 5.1.2 is a simplified representation, and that a local stock probably remains in northern Mauritania throughout the year.

In addition to the north-south displacements, the round sardinella also exhibits seasonal onshore-offshore migrations. In the second semester of the year, when the upwelling contracts to the coastal zone, the sardinella remains closer inshore than during the first semester. This inshore migration restricts the accessibility of the resource to pelagic trawlers that are banned to fish in the coastal waters of Mauritania.

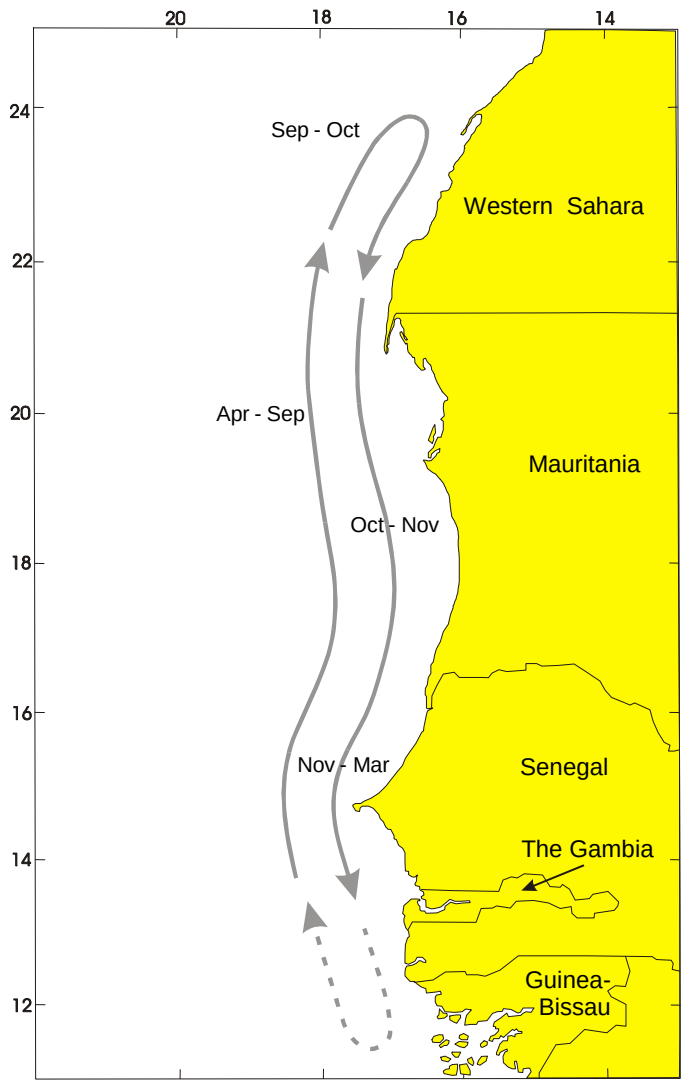

Figure 5.1.2. Seasonal migrations of round sardinella in the CCLME area. The dashed arrows at the southern fringe of the sardinella distribution indicate that is not clear whether the fish in this area also participate in the seasonal migrations towards Mauritania and Western Sahara.

Catch statistics

Catch statistics for the main countries in the CCLME area are updated each year by the FAO Working Group for Small Pelagic Fish in Northwest Africa. These data cover Morocco-Western Sahara, Mauritania, Senegal and The Gambia. A summary of the data available at the last meeting (1990-2013) (FAO, in press a) is presented in Figure 5.1.3.

The total catches of small pelagics in the northwest African zone reached a record level of 2.5 million t in 2010. During the following three years, catches have declined below 2.0 million t (Figure 5.1.3).

Sardine is the dominant species, with catches between 500,000 t and 1,000,000 t. During the last 12 years of the series available, catches have remained fairly constant in absolute terms, fluctuating between 600,000 t and 800,000 t. In relative terms, however, the contribution of the sardine to the total regional catch has declined from more than 60% in 1990, only 35% in 2013 (Figure 5.1.4).

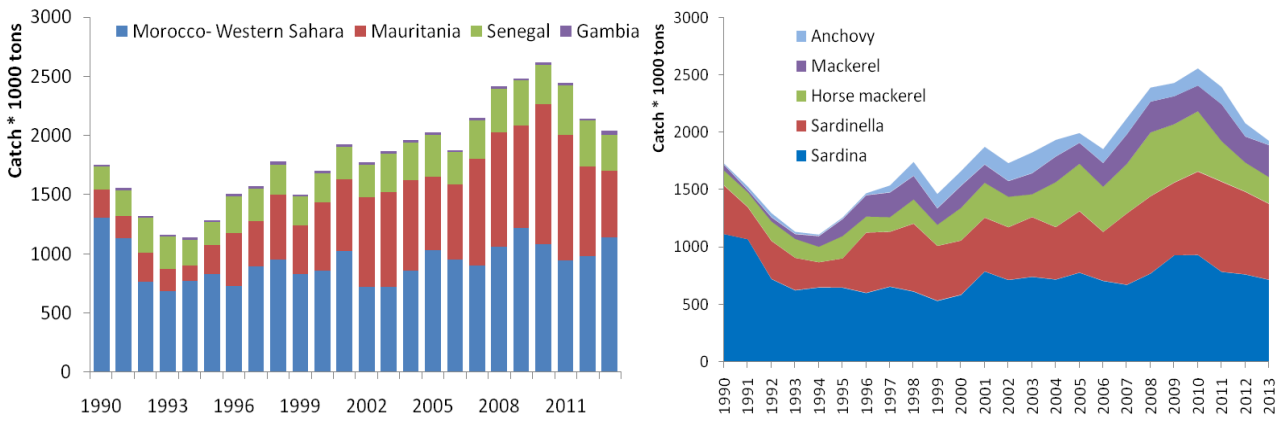

Figure 5.1.3. Catches of small pelagics by country (left) and by species (right) in the area covered by the FAO Working Group on Small Pelagic Fish in NWA. Data presented at 2014 Working Group meeting.

The sardinellas occupy the second place with 32% of the total catches in 2013 (23% round sardinella and 10% flat sardinella). The round sardinella is the most important of the two species. Catches of this species have shown an upward trend since 2006, but they decreased from 611,000 t in 2012 to 458,000 t in 2013 (-25%). The average annual catch for the last 5 years (2009-2013) was about 538,000 t. The average catch of flat sardinella during this period was 154,000 t.

The Cunene horse mackerel is the most important carangid species in the catch, with a share of about 7% (135,000 t) in the total catch. Its average annual catch during the most recent 5 years was around 253,000 t. A continuous decline is observed during the last four years.

Catches of chub mackerel have in general shown an upward trend, from 137,000 t in 2002 to 322,000 t in 2011. The average catch for the period 1990-2013 is estimated at 176,000 t, whereas the average for the most recent 5 years was 259,000 t.

Total catches of anchovy in 2013 were approximately 37,000 t, which was considerably below the catch of 150,000 t in 2011 and of 115,000 t in 2012.

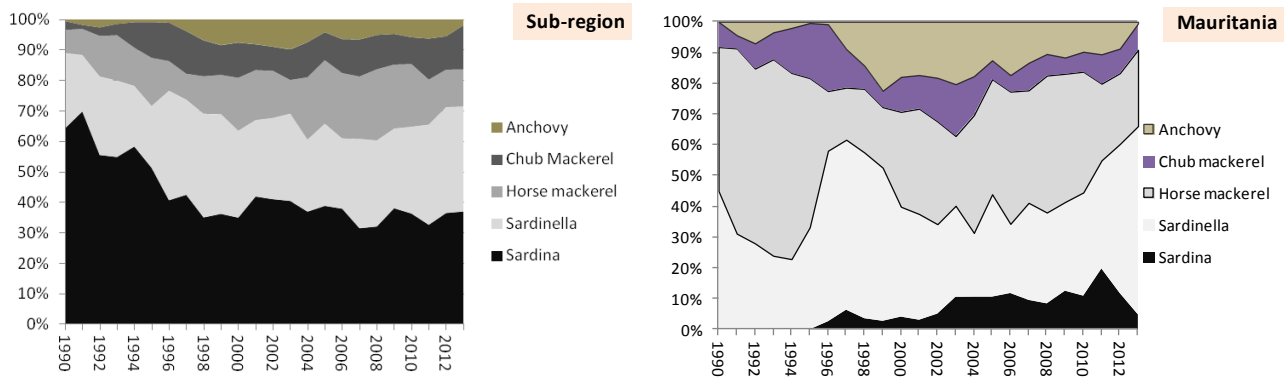

Figure 5.1.4. Changes in species composition of pelagic catches in the area between 9°-35°N (left) and in Mauritania (right). Data from FAO working group and logbooks submitted to Mauritanian authorities.

In the Mauritanian zone, catches of sardinella and horse mackerel show opposite fluctuations. In recent years, opposite fluctuations have also been observed in other species, such as sardine and mackerel (see Figure 5.1.4).

Short-term and long-term variability of small pelagics related to hydrography

Results of acoustic surveys conducted by the R/V *Dr. Fridtjof Nansen* in the CCLME area from 1995 to 2006 show that concentrations of round sardinella are generally found in the same coastal areas year after year (Figure 5.1.5). This must be related to the stability in the upwelling system (Bez and Braham, 2014). However, some long-term changes in the distribution of the round sardinella are observed. The abundance of this species in the southern part of the Moroccan zone has increased since 2001 (Braham et al., 2014). This increase could be related either to a shift in the distribution of the regional stock, or to an increase of a local subpopulations of round sardinella, the existence of which was earlier proposed by Freon (1988). The northward extension of round sardinella, a warm-water species, into Morocco after 2001 could possibly be a function of the long-term upward trend in water temperature in the region (Figure 5.1.6). However, during the same period the sardine, a cold water species, has shown a southward expansion from Morocco and Western Sahara into Mauritania (Figure 5.1.4). This is the opposite of what would be expected on the basis of an upward trend in temperature. The southward extension of the sardine stock into Mauritania, however, might be related to an increase of the stock in the waters of Morocco and the Western Sahara, and not to changes in hydrography.

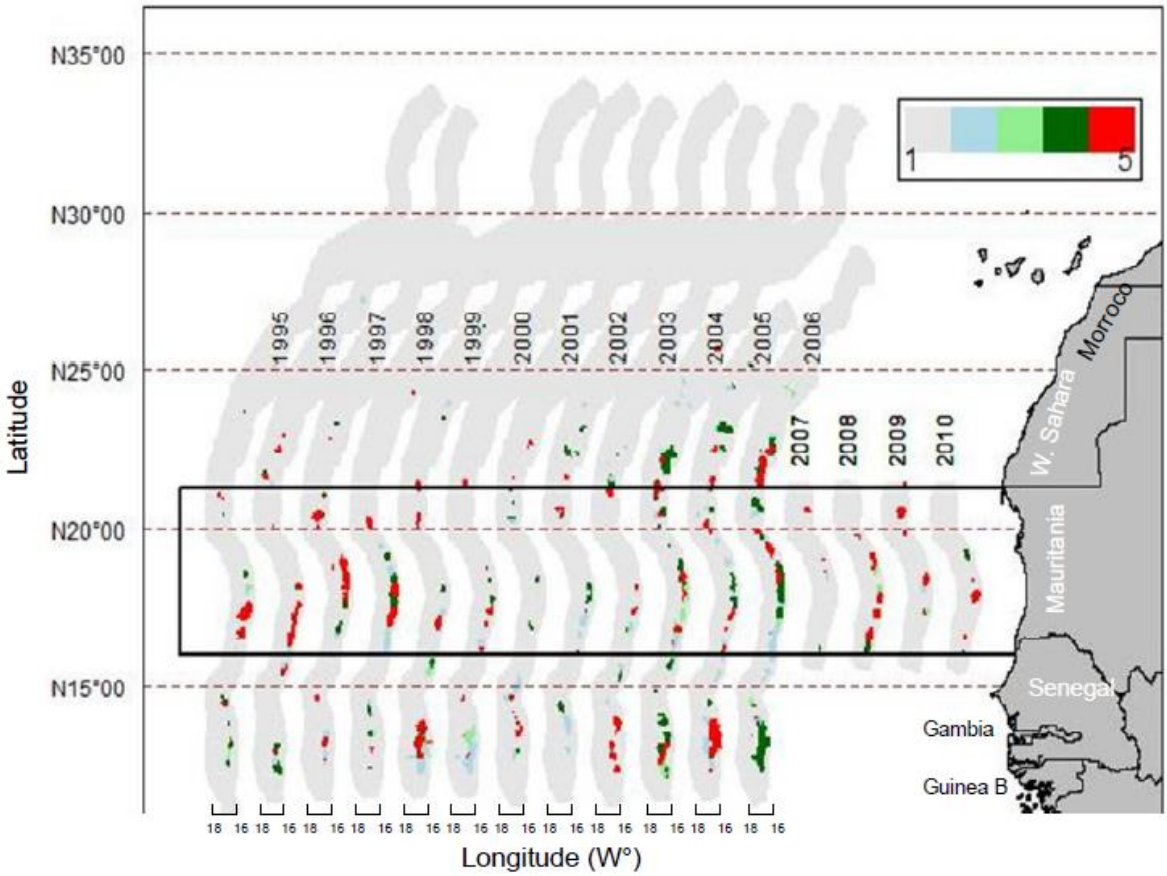

Figure 5.1.5. Distribution of abundance over 5 levels of abundance (1=absence, 2=low, 3=medium, 4 = strong, 5=extremely strong) of round sardinella (*S. aurita*) in North West Africa from 1995 to 2010. The time series of acoustic indices is derived from surveys conducted by R/V *Fridtjof Nansen* in 1995–2006 in the whole sub-region, and by R/V *Al-Awam* in 2007-2010 in the Mauritanian area.

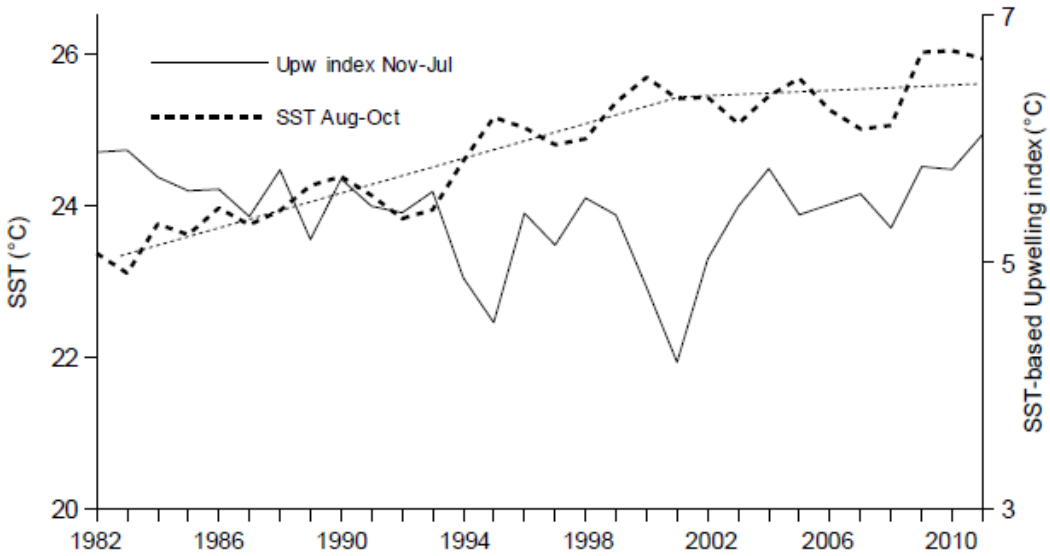

Figure 5.1.6. Interannual changes in upwelling index during the cold season (November–July) and sea surface temperature during the warm season (August–October) for the period 1982–2010 in Mauritania area

Time series of acoustic estimates of round sardinella in the CCLME area show strong inter-annual fluctuations (Figure 5.1.7). It is not quite clear, however, whether these fluctuations represent real variations in abundance or whether they are the result of sampling errors due to variations in the fish distribution and behaviour. The surveys are conducted in November each year, just at the time when the population is migrating from Morocco back to Senegal. Because of the very inshore distribution of the fish at this time of the year, research vessels may miss important concentrations.

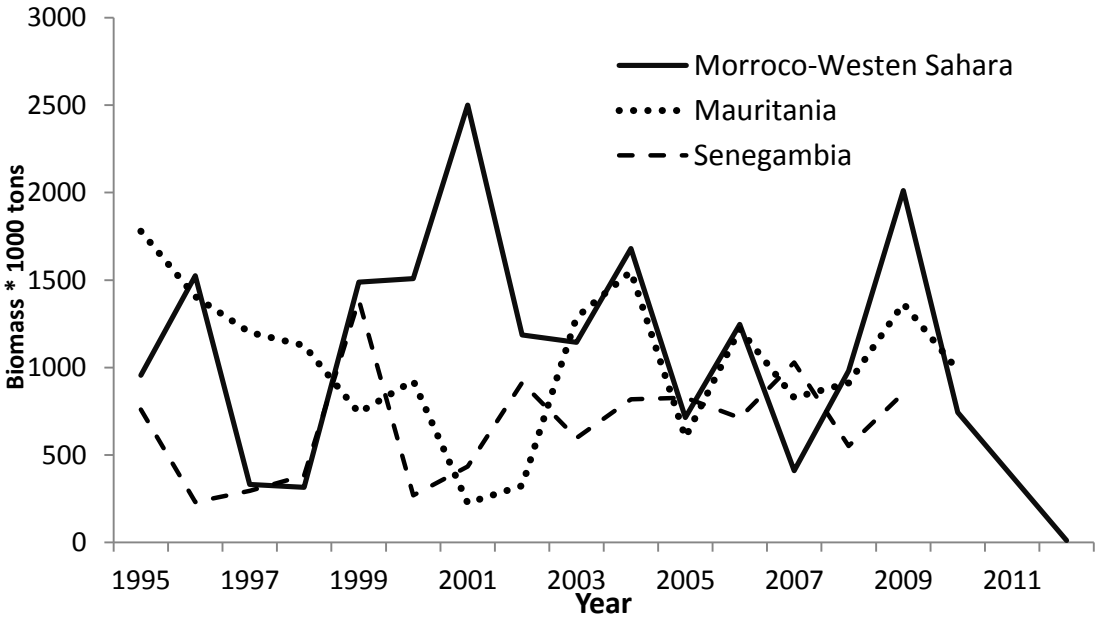

Figure 5.1.7. Trends in biomass of round sardinella from 1995-2012 in the northwest African region as measured by acoustic surveys. In 2011-2012 no surveys were conducted in Mauritania and Senegal.

An analysis of the upwelling index trends over a period of 30 years shows that this was generally high in the last 4 years of the series, the period when sardinella recruitment must have been especially strong (Figure 5.1.6). It has not yet been possible, however, to demonstrate a clear correlation between upwelling and sardinella recruitment. This is mainly due to the lack of good recruitment data for sardinella (no reliable age reading yet) and to the fact that sardinella reproduces over wide areas and long periods. This makes difficult to establish in which area and when a good year-class was produced, and hence what the hydrographic conditions resulted in a good recruitment. Zeeberg et al. (2008) described a regime shift in the north-west African area in 1995 which had considerable effects on the distribution of certain pelagic species, and in particular on the abundance of sardinella.

Another important factor that may affect the distribution and abundance of small pelagic is the primary production, studied through the analysis of the chlorophyll index. As an example, this index shows a clear increase in the years 2004 and 2007 in the Mauritanian zone (Figure 5.1.8). The highest concentrations are generally found each year in July-August, which corresponds to the upwelling peak. According to the distribution of chlorophyll, the Mauritanian area may be divided into three sub-areas, and this division is seen also in the distribution of pelagic fish that are strongly connected to primary production. During the cold season (January-May) the strongest concentrations of chlorophyll are found in the south. In the transition season from cold to warm, the concentrations are higher in the north, and towards the end of the year, the greatest values are observed in the central area.

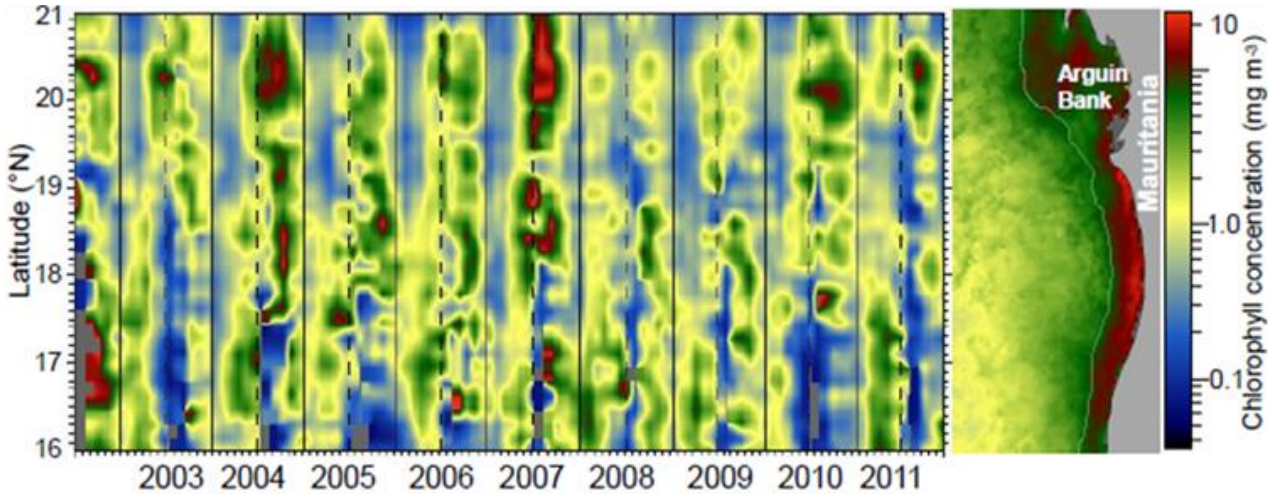

Figure 5.1.8. Evolution of chlorophyll index calculated for the Mauritanian area.

Recent developments in the fishery for small pelagics

The most important developments in the fisheries for small pelagics in the CCLME region in recent years were those related to the sardinella exploitation. Because of the importance of these species for the artisanal fleet in Mauritania, Senegal and The Gambia, the recent developments in these fisheries are discussed in some more detail in the following paragraphs.

Whereas the catch increase of flat sardinella has been moderate over the past 20 years, that of round sardinella has been very significant (Figure 5.1.9). This increase was due mainly to the development of an industrial fishery in Mauritania. Pelagic trawlers from a number of European countries, working under fisheries agreements between Mauritania and the EU, started to target round sardinella from 1996 onwards, which resulted in a strong increase of regional catches. From 1998-2006 catches declined

apparently as a result of overfishing, followed by a new rise after 2007, attributed to good recruitments during certain years. In 2012 Mauritania extended the fishing limits for pelagic trawlers from 13 to 20 nautical miles offshore. This made the industrial fishery for sardinella no longer profitable. In the meantime, Mauritania had developed a fish meal industry based on small pelagics. In 2013, catches of sardinella for fishmeal had risen to 196,000 t yr^{-1}, of which two-thirds consisted of round sardinella. In 2014 there was a further expansion of the fishmeal industry.

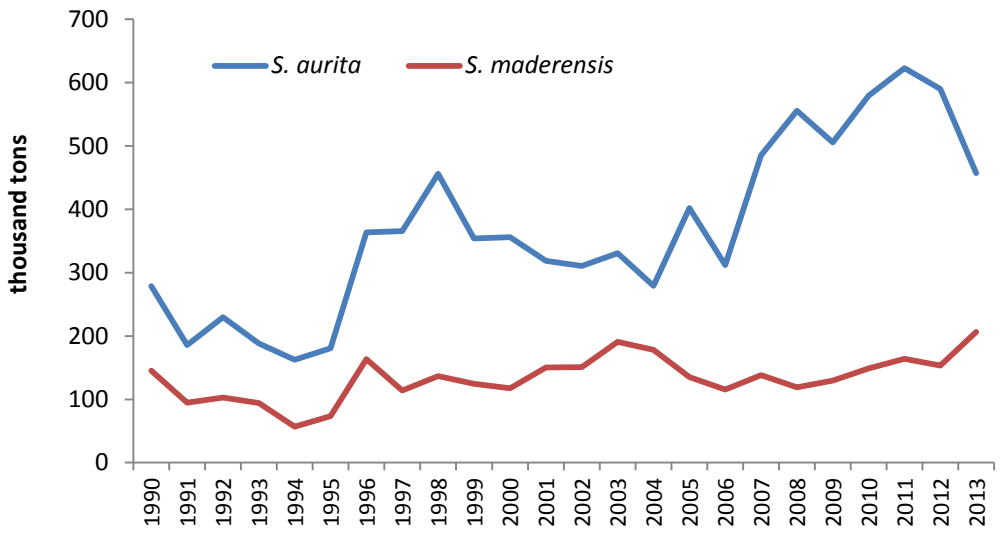

Figure 5.1.9. Landings of the two sardinella species (*S. aurita* and *S. maderensis*) in the CCLME area.

The effect of the increasing effort on round sardinella had an impact on the size decrease of the species, which could be detected from the analysis of the length distribution in the industrial catches of Mauritania (Figure 5.1.10). During the first years of the industrial fishery in Mauritania, the modal total length was around 35 cm, decreasing to 31 cm in 2005, and from then on fluctuating between 30 cm and 32 cm.

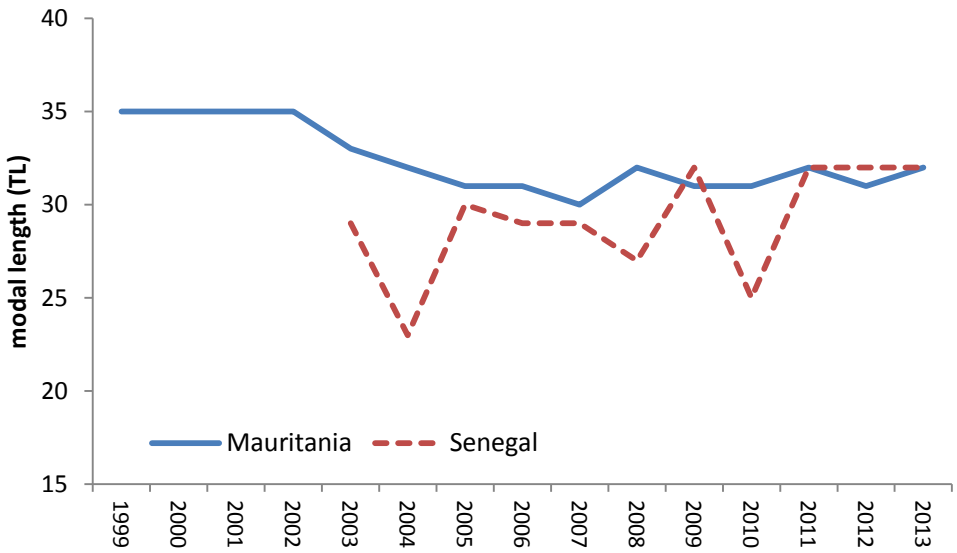

Figure 5.1.10. Modal length (measured as total length) for round sardinella (*S. aurita*) in Mauritania and Senegal. Data reported to the FAO Working Group (in press a).

For Senegal, the reported modal length of round sardinella in the artisanal catches before 2011 used to be smaller than that in Mauritania, indicating that the Senegalese fishermen targeted younger age groups. However, the very strong fluctuations in modal length between 2003 and 2011 raise doubts about the accuracy of the sampling in Senegal during those years. From 2011 onwards the modal length reported for Senegalese catches is the same as the one for Mauritania. This could be related to the expansion of the Senegalese fishery into Mauritanian waters.

Stock assessment of small pelagics

The species of small pelagics that are exploited in a large part of the CCLME region (Morocco, Western Sahara, Mauritania, Senegal and The Gambia) are assessed annually by the FAO Working Group on Small Pelagic Fish in Northwest Africa. A major problem that hampers the use of age structure assessment models in these working groups is the difficulty in age readings, as most research institutes in the region do not possess the expertise to read the age of the fish accurately. In the absence of reliable age readings, the FAO Working Group applies production models or length based assessment for most species. The problem with these methods is that they are based on the assumption of constant recruitment, which is certainly not correct. Another problem is that reliable catch and effort data are hard to obtain. Artisanal fleets usually exploit only a fraction of the total stock, and industrial fleets move from one EEZ to another. Industrial fleets also change target species depending on their abundance and on the market prices. This is an additional problem for using the catch per unit of effort (CPUE) as a true measure of stock abundance, as usually occurs for small pelagic fisheries. Acoustic surveys provided the most useful abundance indices during the period when R/V *Dr. Fridtjof Nansen* conducted annual surveys (1995-2006). However, when national institutes took over these surveys from 2007 onwards, it turned out to be difficult to obtain a full regional coverage each year due to technical and financial problems with the different national research vessels.

In recent years, the FAO Working Group concluded that most of the species of small pelagics in the sub-region were either fully exploited or over-exploited, including sardinella, horse mackerel and chub mackerel. The only exception was the sardine in the area south of Cape Boujdour ("area C"). This stock is still classified as not fully exploited but the working group is aware that this situation may change rapidly depending on recruitment natural fluctuations.

Results of the assessments conducted during the last meeting of this group (May 2014, The Gambia) are summarised in Table 5.1.1, for the stocks in the area covered by the FAO Working Group (Morocco, Mauritania, Senegal and The Gambia).

Management of small pelagics

A number of management measures exists at national level, such as minimum sizes, closed areas and gear restrictions. On a regional level, however, concerted management actions are still lacking. There is no agreement on the limitation of total catches between the total states, nor on the partitioning of total allowable catches (TACs) advised by the FAO working group for the sub-region into national quotas.

Two regional organisations are dealing with the problem of coordinated management action. One is the CECAF that promotes the sustainable utilization of the living marine resources at the international level. The FAO Working Group on Small Pelagic Fish in Northwest Africa is a subgroup of CECAF. The other organisation is the Sub-regional Fisheries Commission (SRFC) that organises meetings at the minister's level, and also technical meetings on various aspects of fisheries management. All the member states in the

region are members of CECAF and participate in meetings of the FAO working Group. Morocco, however, is not member of the SRFC, which presents a problem when it comes to implementing the advice of the FAO working group.

Table 5.1.1. Results of most recent assessment of small pelagic in North West Africa, and corresponding management advice. From FAO, in press a.

Stock	Area	Situation	Management advice
Sardine	Central Morocco	Fully exploited	No increase fishing effort; TAC 360,000 t yr^{-1}
Sardine	South of Cape Bojador	Not fully exploited	Catch should be adjusted according to observed natural changes in the stock
Sardinella spp.	All areas	Overexploited	Reduce fishing effort
Cunene horse mackerel	All areas	Overexploited	Not exceed fishing effort of 2011 TAC 260,000 t yr^{-1} for two species of horse mackerel combined
Atlantic horse mackerel	All areas	Fully exploited	
Chub mackerel	All areas	Overexploited	TAC 257,000 t yr^{-1}

5.1.3.2. Large pelagic fish

Species of large pelagics in the CCLME area

The group of large pelagics consist of a number of tuna species that are distributed both inside and outside the CCLME area. For the CCLME area, the tropical Atlantic species are the most important. These include the skipjack tuna (*Katsuwonus pelamis*), the bigeye tuna (*Thunnus obesus*), and the yellowfin tuna (*Thunnus albacares*) (Plate 6.1.2, photos 4-6). The skipjack is the smallest species, and its distribution is tied most closely to the African continent. The other two species reach much larger size, and their distribution spans the whole tropical Atlantic. The two temperate Atlantic tuna species, bluefin tuna (*Thunnus thynnus*) and albacore (*Thunnus alalunga*), are not found in significant numbers in the CCLME area.

Fisheries for large pelagics

The tuna species are exploited by industrial fisheries and by artisanal fisheries, this especially in the northwest African area. The artisanal fishery for tuna is probably an old tradition in African, but its origin is difficult to trace. The artisanal fleet catch tuna with pole-and-line gears. Main artisanal fisheries are developed in Senegal and in Cape Verde. The industrial fishery for tuna, which occurs in the central-eastern Atlantic, is conducted by three types of fleets: pole-and-line vessels and purse seiners that catch the fish near the surface, and long-liners that catch the fish at greater depths.

The first industrial tuna vessels in the CCLME area were refrigerated pole-and-line vessels from France and Spain, which carried out a seasonal fishery in the EEZs of Senegal and Mauritania in 1953-1956, with excellent results. The fishery was further extended by refrigerated pole-and-line fleets from France and Japan that worked across the Atlantic, including the area around Cape Verde. In the 1990s, the pole-and-line fishery has developed a special strategy for concentrating the tuna underneath the vessel, which

increased its efficiency. The pole-and-line vessels target concentrations of juvenile yellowfin tuna that occur in schools mixed with big-eye and skipjack tuna. Catches contain on average 15% yellow-fin tuna.

In the CCLME area, the oceanic tuna are fished mainly by foreign fleets (Spanish and Japanese, French) that work with private licences or by Fisheries Partnership Agreements between the EU and the coastal countries. These vessels land their catches in foreign ports.

Three main tuna species are exploited in the CCLME area. These are the skipjack tuna (*K. pelamis*) that dominates the catches, followed by the yellowfin tuna (*T. albacares*) and finally the big-eye tuna (*T. obesus*). These three main species represent up to 90% of the tuna landings, and they are fished underneath Fish Aggregating Devices (FADs). In the CCLME area, the skipjack is the main species with average catches around 190,000 t between 2009 and 2013. The average catches of yellow-fin and big-eye tuna in this period were respectively 86,000 t yr^{-1} and 80,000 t yr^{-1}. A drop in catch has been recorded for these two species in the last three years (Figure 5.1.11).

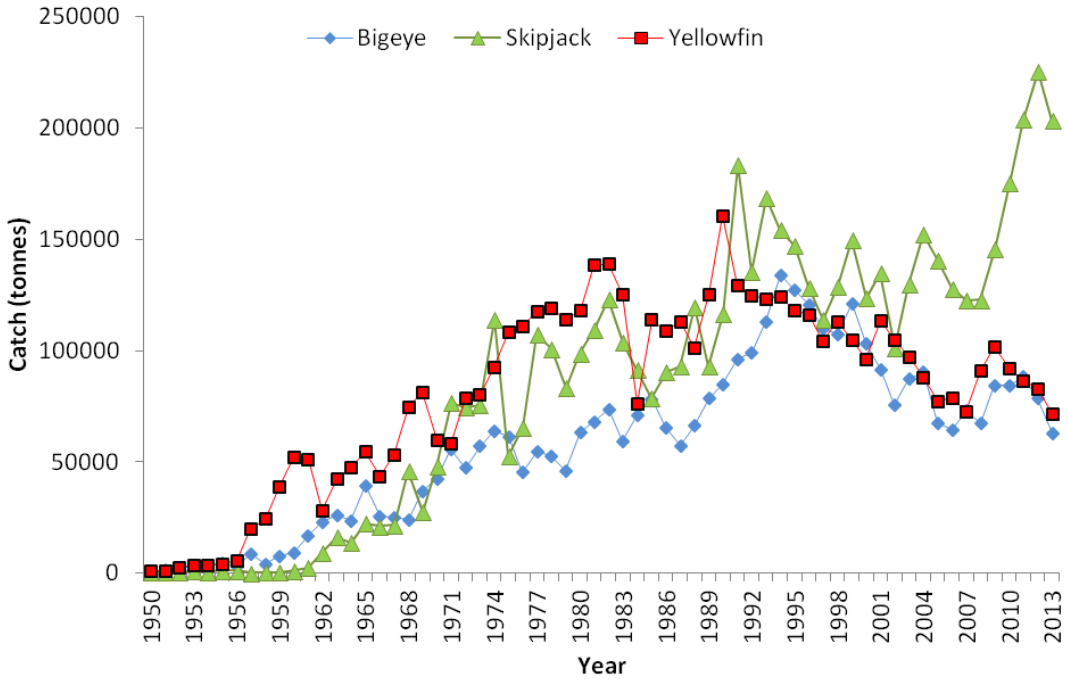

Figure 5.1.11. Trends in the annual catch of large tuna in the eastern Atlantic (Source ICCAT, Report of the standing committee on research and statistics (SCRS), September 2014).

In the Mauritanian zone, a sharp increase in tuna catches was observed in 2012 and 2013 (Figure 5.1.12). The catches, which were negligible in 2011, reached more than 21,000 t in 2012 (+29143% compared to 2011), and increased to more than 47,000 t in 2013 (+123%). Fishing effort, expressed in number of fishing days, also increased, but to a much lesser extent that the catch. The effort increased from 36 days in 2011 to 390 days in 2012 (+983%) and to 963 days in 2013 (+147%). It was an increase in catch-per-unit-of-effort (CPUE) that was primarily responsible for the strong increase in catch. This CPUE increased by 46,059% between 2011 and 2012 and by 123% between 2012 and 2013. This was a level that was never attained before, and it may be explained by several factors. The main cause was the increased use of fish aggregating devices (FADs) that concentrate the fish in certain places. A second reason may have been the decreased catches of small pelagics by the industrial fleet, following the introduction of restrictive measures in Mauritania in 2012. This reduced catch by the industrial fleet will have left more food for the

large pelagics. Finally, the increase of the Minimum Oxygen Layer in the tropical Atlantic in recent years may have reduced the habitat for the tunas, and thereby increased their density in the remaining habitat. We shall return to this point in 5.1.4.

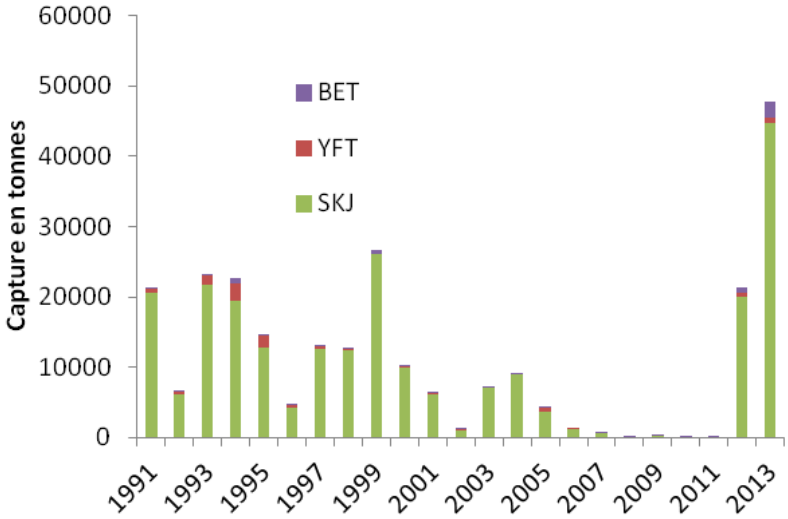

Figure 5.1.12. Annual variations in tuna catches in the Mauritanian EEZ from 1991 to 2013 (Ould Taleb Sidi, communication WG IMROP, 2014). BET: bigeye tuna, YFT: yellowfin tuna, SKJ: skipjack tuna

In the Moroccan zone, tuna catches have reached an average of 4600 t yr^{-1} during the period 2010-2013 (Figure 5.1.13). A record catch was reached in 2006 with more than 7400 t.

The main species at present are skipjack tuna, bluefin tuna and swordfish. Secondary species are big-eye and yellowfin. Catches of bluefin tuna and swordfish have shown an increasing trend over the past years, whereas bluefin and bigeye tuna have declined. Catches of yellowfin have always been small in comparison to the other species.

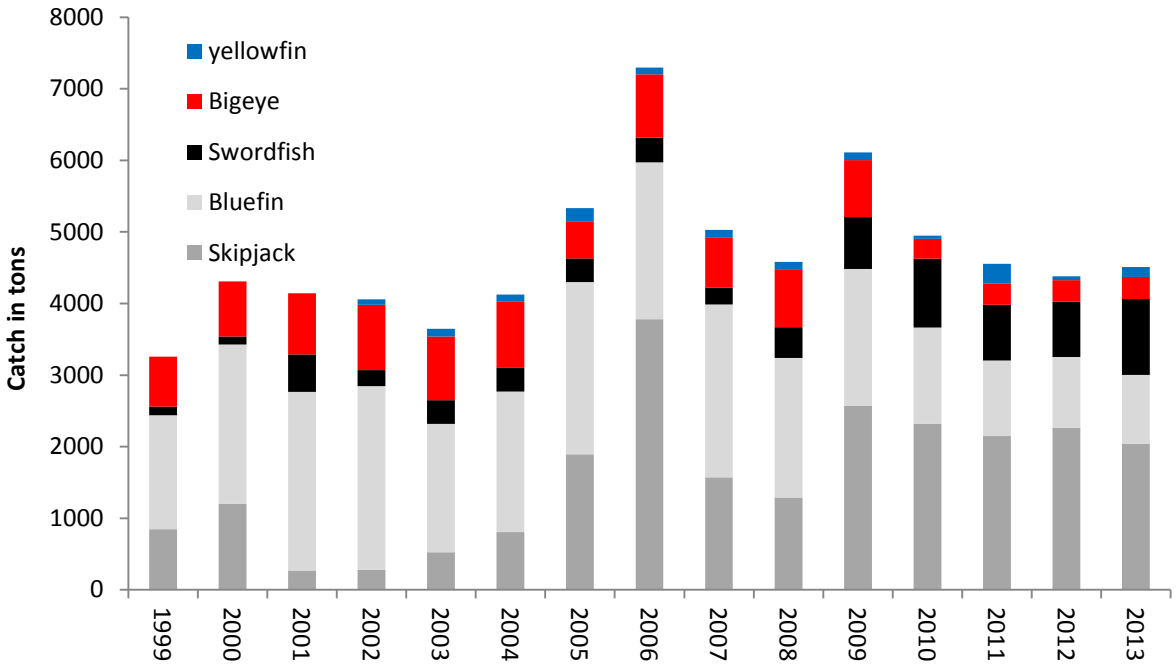

Figure 5.1.13. Tuna catches in the Moroccan zone (ICCAT, 2014)

Stock assessment of large pelagics

The stock situation of the different tuna species is assessed in the framework of ICCAT. For yellow-fin tuna, the last assessment conducted in July 2014 showed that the stock was most likely over-exploited. The analysis of catch data up till 2010 gave conflicting results depending on the assessment method used. Age structured models indicated an increasing trend in fishing mortality and a decrease in stock size, whereas production models indicated the opposite.

For big-eye tuna, data on catches, average fish size and abundance in the years 2003-2013 do not show a clear trend. There is no evidence, therefore, that the stock status has substantially changed since the last assessment in 2010, which means that it is still considered fully exploited (Table 5.1.2).

Finally, for the Eastern Atlantic skipjack, the ICCAT working group in July 2014 was unable to make a reliable quantitative assessment, but it noted there was no evidence of a decline in yield, nor in the average weight of individuals captured. According to a catch-only assessment model, it was unlikely that the eastern skipjack stock was overexploited, but current catches could be at the maximum sustainable yield (MSY) level or even above it.

Table 5.1.2. Stock status assessments of highly migratory, tuna and tuna-like resources (Source: http://www.iccat.int/en/, accessed on 24 December 2014)

Species	**Assessment**
Bigeye tuna	Fully exploited (2010)
Yellowfin tuna	Overexploited (2011)
Skipjack tuna	Overexploited (2008)
Swordfish	Overexploited (2014)
Bluefin tuna	Recovering (2014)

5.1.4. DISCUSSION AND CONCLUSIONS

The pelagic fish stocks play a dominant role in the ecosystem of the CCLME area. Of these stocks, the small pelagics are by far the most important in terms of total weight. They convert the high plankton production caused by upwelling into fish biomass. The pelagic fish constitute an import source of food for other fish species and mammals in the ecosystem, and also for the human population in the coastal states bordering the CCLME area.

The pelagic stocks in the CCLME region are strongly influenced by the hydrographic processes occurring in this ecosystem. The CCLME zone is characterised by the alternation of two clearly separated hydrological seasons and by a large variability in the size and durations of the hydrological processes. The distribution and abundance of the pelagic stocks is very dependent on these processes (Cury and Roy, 1989; Fréon, 1988; Zeeberg et al., 2008; Braham et al., 2014).

The CCLME area stretches across the boundary between temperate and tropical water masses and therefore the ecosystem encompasses two different biogeographical areas, the boundary between which

shifts north and south with the seasons. This results in a high diversity in species composition, and a high variability in catches by the different fishing fleets.

In the CCLME area, climatic changes may influence primary production and thereby the trophic chain, which may have consequences for the biology and distribution of pelagic fish. These consequences, however, are difficult to predict because of possible synergetic effects of the climatically induced changes in the ecosystem.

Allison et al. (2009) have analysed the vulnerability of national economies to the impact of climatic change on the fisheries. Different investigated hypotheses indicate that the areas where fisheries will be most strongly affected by climatic change will be found in Africa, and in particular in northwest Africa where the national economies are strongly dependent on fisheries. Allison et al. (2009) have classified all the countries in the CCLME area as having a "high sensitivity" to climatic change, and a "very low" capacity to adapt to the climatic effects on the fishery. The only exception is Morocco, where the capacity to adapt is classified only as "low", i.e. slightly higher than in the other countries. This is related to the more diversified economy of the country.

The waters of the Canary Current have shown a stronger warming trend during the last three decades than other EBUS (eastern boundary upwelling systems) areas. According to Arístegui et al. (2009a), the observed increase in water temperature is the most likely cause of the observed drop in productivity in the Canary Current system, especially when compared to other EBUS areas (Chavez and Messié, 2009; Demarcq, 2009). However, the observed trends in primary production are not yet reflected in the fish catches in the CCLME area, at least not for the pelagic resources.

On the other hand, the sharp decline of the sardine stock in 1997, 2006 and 2010, and the northward displacement of the sardinella are probably the effect of climatic change (Braham et al., 2014). Another imminent problem, which occurs simultaneously with the increase in water temperature, is the expansion of the minimum oxygen layer (MOL) in the eastern tropical Atlantic (Stramma et al., 2012). The expansion of the MOL decreases the habitat available for the large pelagic species and their prey. The impact on the stocks is not yet known, but it is very important that the effects of the habitat compression are not wrongly interpreted as an increase of abundance.

The dependence of the local populations on the fishery requires a sustainable management of fish stocks. Present attempts to manage these stocks are hampered by a lack of accurate assessments. In addition, the fact that most of these stocks are transboundary and therefore, shared by different countries makes their management even more difficult. For the conservation of the ecosystem, it is important to implement correct management measures based on the best scientific advice. Therefore, assessments should be improved, based on good quality data. We also need to obtain a better insight in the relationship between fish stocks and their environment. Without such insight, it will be impossible to distinguish the effects of the fishing pressure from the natural variations due to hydrographic changes, and hence it will not be possible to provide adequate management recommendations.

Acknowledgements

The authors are grateful for the comments on the manuscript provided by Eva García Isarch and Aboubacar Sidibé during the workshop in Las Palmas de Gran Canaria in January 2015, and also for the help provided by Itahisa Déniz-González in editing the final manuscript.

Plate 6.1.1. (1) Ethmalosa fimbriata © Jean-Dominique Durand. (2) Caranx rhonchus © Oddgeir Alvheim, EAF Nansen project. (3) Engraulis encrasicolus © Oddgeir Alvheim, EAF Nansen project. (4) Sardina pilchardus © Oddgeir Alvheim, EAF Nansen project. (5) Sardinella aurita © Oddgeir Alvheim, EAF Nansen project. (6) Sardinella maderensis © Oddgeir Alvheim, EAF Nansen project.

1

2

3

4

5

6

Plate 6.1.2. (1) Trachurus trecae © Oddgeir Alvheim, EAF Nansen project. (2) Trachurus trachurus © Oddgeir Alvheim, EAF Nansen project. (3) Scomber japonicus © Oddgeir Alvheim, EAF Nansen project. (4) Thunnus obesus © Seinen Chow. (5) Thunnus albacares © Rui Freitas. (6) Katsuwonus pelamis © Rui Freitas.

1

2

3

4

5

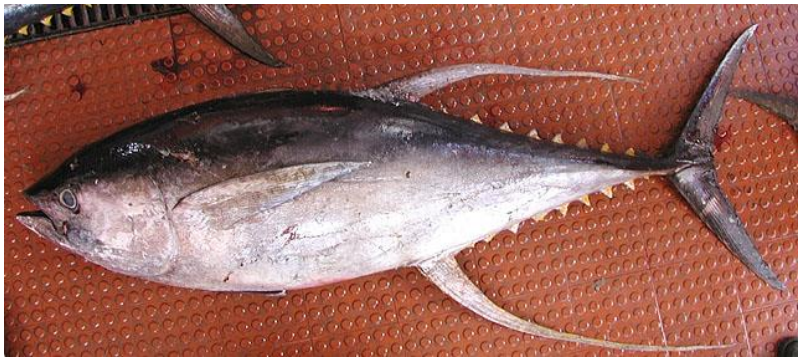

6

5.2. DEMERSAL FISH IN THE CANARY CURRENT LARGE MARINE ECOSYSTEM

Lourdes FERNÁNDEZ-PERALTA[1] and Aboubacar SIDIBÉ[2]

[1] Centro Oceanográfico de Málaga, Instituto Español de Oceanografía. Spain

[2] African Union-Interafrican Bureau for Animal Resources (AU-IBAR), African Union Commission (AUC). Kenya

5.2.1. INTRODUCTION

Until the late 20th century, 90% of the world´s fisheries were in shelf seas. Although upwelling zones made up only 0.1% of worldwide shelf areas, they account over 50% of total catches (Granado Lorencio, 1996). This reflects the significance of major upwelling ecosystems such as the Canary Current Large Marine Ecosystem (CCLME) region, characterized by high biological diversity and significant fisheries resources, which are heavily exploited. Beginning in the 1990s, the fishing pressure on continental shelves led to a displacement of fisheries towards increasingly deeper waters in several parts of the world (Piñeiro et al., 2001), and this is extensive to Large Marine Ecosystems (LME) (Fernández-Peralta et al., 2011, submitted; Fernández-Peralta and Puerto González, submitted).

Demersal ichthyofauna is one of the largest components of marine ecosystems in terms of biomass and biodiversity, and it is very important economically. The role of demersal fish as predators determines the state of lower trophic levels in the food chain, showing that the top-down trophic cascade (Northcote, 1988) is the key factor in the structure of communities (Granado Lorencio, 1996).

Despite the importance of demersal fish in the CCLME region, there are very few biogeographical studies in comparison with other regions such as the North Atlantic. The first studies on this fauna in north-western Africa (NWA), carried out between 1850 and 1950, merely prospected some very shallow waters above the shelf, down to a maximum of 200 m. Highlight the campaigns carried out to this depth in 1936 between Villa Cisneros (now Dakhla) and Sierra Leone in the *Président Théodore Tissier* (Cadenat, 1937; Belloc, 1938) or in the Belgian vessel *Mercator* (Poll, 1949). The first information available on the deeper demersal fish in NWA comes from the campaigns of the *Gérard Treca*, where for the first time sampling was done over the upper slopes (Cadenat, 1953). This was followed by the campaigns of the *Thalassa* in 1962, 1968, 1971 and 1973 (Maurin and Bonnet, 1970; Maurin and Quero, 1981), and the campaign of the *Discovery* in 1976 (Merrett and Domanski, 1985). See Van der Knaap (1985) for a comprehensive list of historical surveys, although detailed information on sampling and data is not available. The Thalassa surveys, carried out from Cape Juby to Cape Verde were the first prospections to depths of 800 m and they published the first inventories and the most complete ichthyological notes in Mauritanian waters (Maigret et al., 1981). Various campaigns over the shelf and upper slopes conducted in 1982 and 1983 by the Mauritanian vessel *N'Diago* and research vessels of the Fisheries Institute of Rostock (German Democratic Republic) enabled Gaudechoux and Richer de Forges (1983) to produce an exhaustive ichthyological inventory of those waters. The Guinean Trawling Survey campaigns (1964-65) were carried out over the shelf and upper slopes of the Gulf of Guinea, outside the CCLME region and they led to the description of tropical demersal fish communities (Williams, 1968; Longhurst, 1969), and many of the species extend as far as the latitude of Cape Blanc. Ramos et al. (1991) provide the most recent information on these demersal communities.

Campaigns conducted between 2002 and 2010 by the *Vizconde de Eza* in Moroccan and Mauritanian waters (down to a depth of 2000 m) and in Guinea-Bissau, down to 1000 m (Hernández-González et al., 2006, 2010; Hernández-González, 2007; García-Isarch et al., 2011; Ramos et al., 2005, 2010) provided valuable information on fish communities (Fernández-Peralta et al., 2008; Fernández-Peralta and Puerto, submitted; Puerto et al., 2012). Lastly, campaigns conducted on board the *Dr. Fridtjof Nansen* in 2011 and 2012 in the CCLME region provided important overall information on fish communities from coastal waters to the slope.

Demersal fish resources have been exploited on a small scale in NWA, first in northern Morocco by Portuguese and Spanish fishermen, who reached Western Sahara waters as early as in 15th century (Balguerías et al., 2000). In the 20th century, the first industrial fisheries began to be developed by foreign fleets extending their ranges as far as the south of the African coast, at the same time the CCLME countries have gradually developed their own small-scale and industrial fisheries. These demersal fish constitute vital renewable natural resources providing food and income for the local population, foreign exchange earnings, revenue for national governments (balance of payments) and employment opportunities in the CCLME countries. The region's coastal-shelf species have been seriously overfished (FAO, in press b, c; Gascuel et al., 2007; Meissa and Gascuel, 2014), leading to a risk that fleets will move to deeper waters, as it which is already occurring (Fernández-Peralta et al., submitted; Fernández-Peralta and Puerto González, submitted).

Knowledge of fish stocks as a whole is vital for maintaining biodiversity. The scientific monitoring of these demersal species is crucial for their protection and sustainable management. This study presents a characterization of the demersal ichthyofauna in the CCLME based on a review of available data. The conclusions provide practical information for the management and biodiversity conservation of the fishery resources of this productive area in a holistic perspective (Jennings, 2004).

5.2.2. METHODS

The data sources used for the characterization of the demersal ichthyofauna in the CCLME were:

- Unpublished results of many surveys carried out in the region.
- Literature review of the main papers available on demersal fish species researched in the area.
- The IEO bottom trawls surveys onboard the R/V *Vizconde de Eza* carried out off Morocco (in 2004 and 2005) (Ramos et al., 2005; Hernández-González et al., 2006), Western Sahara (Hernández-González, 2007), Mauritania (2007 to 2010) (Hernández-González et al., 2010; Ramos et al., 2010) and Guinea-Bissau (2002 and 2010 (García-Isarch et al., 2011). The depths ranged from 500 m to 1850 m (Morocco), 200 m to 1860 m (Western Sahara), 80 m to 1860 m (Mauritania) (Déniz-González et al., 2014) and 20 m to 1000 m (Guinea-Bissau). For a correct identification of the fish species, the specimens were deposited for revision and preservation in the Marine Fauna Collection of the Oceanographic Centre of Málaga (CFM-IEOMA) of the Instituto Español de Oceanografía (IEO) (www.ma.ieo.es/cfm, accessed on 30 March 2015). The specimens have already been extensively reviewed, especially in the case of Mauritania (Fernández-Peralta et al., 2012).
- IEO fisheries data collected observers on board, fisheries statistics and biological sampling of the commercial fish species exploited in the area.
- Reports of the Working Group on the Assessment of Demersal Resources organized by FAO and the Fisheries Committee for the Eastern Central Atlantic (CECAF). The stocks of the northern countries of the

CCLME (Morocco, Mauritania, Senegal and The Gambia) are assessed in Subgroup North, while stocks from Guinea-Bissau and Guinea are assessed in Subgroup South. To assess the exploitation state of the stocks and estimate the population dynamic model parameters, an Excel spreadsheet with an observation error estimator (Haddon, 2001) was used. The model was fitted to the data using the non-linear optimizer built into Excel Solver Tool. Each CCLME country is in charge of its own programme of fishery data collection to carry out these assessments, which are compiled in the different FAO/CECAF reports. The data come from scientific surveys (inventory, abundance, distribution, etc.), fisheries statistics (catch and fishing effort) and biological sampling frequency of some commercial demersal species, with different coverage levels in the different countries.

5.2.3. RESULTS AND DISCUSSION

5.2.3.1. Biogeographical and faunistic considerations

The CCLME area shows a convergence of temperate-water fauna from the north with typically tropical fauna from the south, generating transitional fauna in the central zone. It is characterized by high species richness, although with few endemic species and high biological production. The displacement of the CVFZ from the waters of Guinea-Bissau and Cape Verde to Cape Blanc from June to October, and its southerly descent for the rest of the year (Mittelstaedt, 1991), causes seasonal migrations on the continental shelf of numerous fish species, particularly at their adult stages (Champagnat and Domain, 1978; Garcia, 1982), as well as species having a more deep-water distribution, such as the black hakes, *Merluccius polli* and *M. senegalensis* (Fernández-Peralta et al., 2008, 2011b, submitted).

From a biogeographical viewpoint, Moroccan waters belong to the "Temperate North Atlantic" realm and are contained within the "Lusitanian" province, which shows confluence of species from different ecoregions[14] such as the "South European Atlantic Shelf", the "Saharian upwelling'" and the "Azores, Canaries, and Madeira"(Spalding et al., 2007)". At the north of the CCLME, the same species of commercial interest were found in Ibero-Moroccan Atlantic waters (Maurin, 1968), as well as species of the "Western Mediterranean" and "Alboran Sea" ecoregions (Lloris and Rucabado, 1979, 1998). Noteworthy among these are the European hake (*Merluccius merluccius*) and species belonging to the families Sparidae (*Dentex* spp., *Pagrus caeruleostictus*, *Sparus* spp., *Pagellus acarne*, *P. bogaraveo* and *P. erythrinus*) and Trichiuridae (*Trichiurus lepturus and Lepidopus caudatus*), as well as other economically species such as *Zeus faber* or *Spondyliosoma cantharus*. In the depths between 500 m and 2000 m there are species such as *Hoplostetus mediterraneus* and *Alepocephalus bairdii* and other macrourid species such as *Bathygadus melanobranchus*, *Gadomus longifinis* and *Trachyrincus scabrus*. Deep-water sharks, such as *Deania Calcea* and *Centroscymnus coelolepis* also represent considerable biomass at those depths (Ramos et al., 2005; Hernández-González et al., 2006).

Further south, the Western Sahara coastline represents a transition between the "Atlantic-Mediterranean" and "Tropical" provinces (Bonnet, 1969; Laroche and Idelhaj, 1998). The broad Western Sahara shelf is also dominated by families of Perciformes, and there are large catches of other species of Sparidae, such as *Dentex gibbosus*, *Dentex canariensis*, *P. bellottii* (replacing species of the genus *Pagellus* seen farther north), *Diplodus bellottii* and also *Spondyliosoma cantharus* which, together with some haemulids such as *Plectorhinchus mediterraneus* and *Pomadasys incisus*, and the sciaenid *Argyrosomus regius*, clearly represent transitional coastal fauna in these waters (Maurin, 1968). These are still, however, fauna which

[14] According to Spalding et al. (2007) "ecoregion" is defined as a cohesive unit of the waters up to a depth of 200 m

are more closely linked to temperate waters (Laroche and Idelhaj, 1988) or which are widely distributed; there are few species whose affinity is exclusively tropical. There are also many Pleuronectiformes in these latitudes, such as *Solea* spp. (*S. solea* and *S. vulgaris*; the distribution of the former is limited to Cape Blanc) or *Dicologoglossa cuneata*, Scorpaeniformes (*Scorpaena elongata* and *Pontinus kuhli*) and Anguiliformes, such as *Synaphobranchus kaupii*, which are abundant deeper throughout the Moroccan coast (Maurin, 1968; Merrett and Domansky, 1985; Hernández-González et al., 2006; Hernández-González, 2007). The replacement of species in these waters is obvious in the genus *Merluccius*. The abundance of the European hake, distributed throughout the Moroccan coast, is declining, and even disappearing to the south of Cape Blanc. This species is gradually overlapping, first with *M. senegalensis* (from 33°N) and then with *M. polli* (from 25°N). In Western Sahara waters the three species concur, and this is the world´s only case of three hake species co-distributed over 5° latitude. Only black hake are caught to the south of Cape Blanc, *M. senegalensis* and *M. polli* (Fernández-Peralta et al., submitted); that cape is a major landmark in the distribution of fish species. *M. senegalensis* is a clearly endemic species in the CCLME region, since it disappears in Guinea-Bissau waters.

Mauritanian waters, covering two different realms, the "Temperate Northern Atlantic" and the "Tropical Atlantic" are even more complex from a hydrological and faunistic point of view. The Mauritanian Exclusive Economic Zone (EEZ) occupies the ecoregions of the "Saharan" (around Cape Blanc) and "Sahelian upwellings", the latter is included in the '"West African Transition" province (Spalding et al., 2007). These waters present a contrasting hydroclimate which is due to the passage of the thermal front (CVFZ) to its northern border at Cape Blanc. Over the shallow waters of the shelf there is a community of Sciaenidae with Guinean affinities (Domain, 1986), which was not clearly observed off the Western Sahara coasts. Species as *Arius latiscutatus*, *Cynoglossus canariensis* and *Pomadasys jubelini* are caught in Mauritanian shallower waters, and the other components of this community as *Brachydeuterus auritus*, *Galeoides decadactylus, P. incisus* and *Umbrina canariensis*, are caught also in the north. Nonetheless, the community of Sparidae over the intermediate shelf does not coincide with this situation in both north and south of Cape Blanc (Laroche and Ideljah, 1988). Demersal ichthyofauna in Mauritanian waters is purely transitional from the north to the south, showing this mix of species of different affinities spreading to a depth of almost 1000 m (Fernández-Peralta and Puerto González, submitted). At greater depth, the fauna is composed of cosmopolitan species or widely distributed species belonging to the Macrouridae (*T. scabrus*, *Nezumia* spp., *Bathygadus* spp., *Hymenocephalus* spp. and *Coryphaenoides* spp.) and Alepocephalidae families (*Alepocephalus bairdii*, *A. rostratus* and *A. productus*) but they are present at greater depths in Mauritania (Fernández-Peralta and Puerto González, submitted) than in Morocco and other areas of north Atlantic (Merrett and Marshall, 1981; Massutí et al., 2004). The same occurs with *Synaphobranchus kaupii*, a cosmopolitan deep species which is very abundant in Moroccan waters to 750 m (Merrett and Domansky, 1985; Haedrich and Merrett, 1990), but dominant in Mauritanian waters from 1000 m to 1400 m. These species probably avoid the warming that is taking place in the layers above 300 m throughout the region (Arístegui et al., 2009a), perhaps most evident in Mauritanian slope where the species are deeper (Fernández-Peralta and Puerto González, submitted). The presence of the permanent upwelling in the benthic system (Levin and Gooday, 2003) undoubtedly has a considerable influence on these deep bottoms, with the effect of deepening oligotrophic conditions very far in the oceanic waters offshore, compared to other areas northernmost. An exhaustive review of demersal fish communities in Mauritanian waters from 100 m to almost 2000 m can be found in Fernández-Peralta and Puerto González (submitted).

Consequently a boundary is observed between Western Sahara and Mauritania, probably related to the upwelling's nucleus in Cape Blanc, even at great depth (Fernández-Peralta et al., 2008). This area constitutes the southern edge of the distribution of species with cold-temperate affinities, and the

northern limit of species of subtropical-tropical distribution. Among the Chondrichthyan families, accounting for the highest biomass between 400 m and 2000 m in both Western Sahara and Mauritanian waters, Somniosidae (6 species) was dominant (62%) to the south of Cape Blanc, while Centrophoridae (8 species) was the main family (52%) to the north. Among the Osteichthyes, the Sebastidae family (*Helicolenus dactylopterus* and *Trachyscorpia cristulata echinata*) was more abundant to the north, and the Merlucciidae family (*M. polli* and *M. senegalensis*) to the south. Changes in the proportion of the same species, or replacements of species of the same family or genus by family, as well as some similarity between certain groups in the two areas were observed (Fernández-Peralta et al., 2008).

Tropical species are typical and dominant in Senegalese and Gambian waters. These species are neither found in Cape Blanc border nor in Western Sahara waters, and in some cases not even in Mauritanian waters. The north of the Senegalese EEZ is included, in bio-geographic terms, in the "Sahelian upwelling" ecoregion (belonging to the "West African Transition" province), and the south of the "Gulf of Guinea" province, the westernmost area of the "Tropical Atlantic" realm (Spalding et al., 2007). There are also significant seasonal coastal upwelling regions in these waters, particularly in the northern part, and the thermal front also moves over the shelf. There are numerous trenches and canyons, as in Mauritania, and these structures are very important for the channelling and upwelling of cold water. The Kayar trench is particularly significant. Coastal communities of Sciaenidae (Longhurst, 1969) become more significant as we move further south, reaching their largest size in the CCLME region in Guinean waters. Haemulidae (*Brachydeuterus auritus*, *Pomadays jubelini* and *P. perotaei*), Pleuronectiformes (*Cynoglossus canariensis* and *Syacium micrurum*), and the other species of Sciaenid community (*Pseudotolithus senegalensis*, *Galeoides decadactylus*, *Drepane africana*, *Chloroscombrus crysurus* and *Arius latiscutatus*) are becoming increasingly abundant in the waters of the Senegalese shelf (Franqueville and Freon, 1976; Jouffre et al., 2004). On the intermediate shelf, catches are made of species having a more northern distribution, such as Sparidae (*D. angolensis*, *D. gibbosus* and *P. bellotti*), the Haemulid *P. mediterraneus*, also abundant in the Western Sahara area, or Serranidae such as *Epinephelus aeneus* and *E. goreensis*, as well as cosmopolitan species such as *Pomatomus saltratix* (Domain, 1976; Froese and Pauly, 2015). At greater depth, catches are made of *Dentex macrophthalmus*, *Brotula barbata*, and hakes (Jouffre et al., 2004), *M. polli* and *M. senegalensis*, the latter decreases southward (Caverivière et al., 1986). At greater depth in Senegambia waters, the shortspine African angler, *Lophius vaillanti* (Fernández-Peralta, 2009), is replacing *L. piscatorius* and *L. budegassa* (caught further north in Moroccan waters), and deep-water shark species of the Somniosidae (*Centroscymnus coelolepis*, *C. crepidater* and *Zameus squamulosus*) and Centrophoridae families (*Deania calcea*, *Centrophorus granulosus* and *C. squamosus*) (López-Abellán et al., 1987). This also occurs in the Western Sahara and Mauritania waters.

The marine front reaches the Guinea-Bissau shelf down to the latitude of Cape Verga (Le Loeuff and van Cosel, 1998), although no coastal upwelling is detected. However, it is the widest shelf in western Africa, with strong continental outflows (FAO, 1992), which makes it a productive area of the '"Gulf of Guinea'" province (Spalding et al., 2007). Tropical taxons are dominant in these waters, with a greater diversity of species of the same genus being caught, as is the case with the genus *Pseudotolithus* (*P. senegalensis, P. typus, P. elongatus* and *P. senegallus*), *Arius* (*A. parkii, Carlarius heudeloti* and *A. latiscutatus*), Pomadasys (*P.jubelini, P.incisus, P. perotaei* and *P. rogerii*) and *Cynoglossus* (*C. cadenati, C. senegalensis, C. canariensis* and *C. monodi*) (Table 5.2.1) (Domain, 1976; García-Isarch et al., 2011; Froese and Pauly, 2015). The community of Lutjanidae (*Lutjanus goreensis, L. agennes, Lethrinus atlanticus*), characteristic of hard bottoms and seldom sampled through trawling, is also present in relatively shallow waters, extending as far as the Gulf of Guinea. In Guinean waters, there are also abundant catches of tropical species such as *Pterothrissus belloci*, *Synagrops bellus* and *Fistularia petimba*.

Sparidae species are caught at greater depth in both of the Guineas (*D. maroccanus*, *D. congoensis* and *P. bellottii*), as are Scorpaenidae (*Pontinus accraensis*, *S. normani* and *S. stephanica*) and Triglidae (*Chelidonichthys gabonensis*, *Lepidotrigla cadmani* and *L. carolae*) (FAO, 1992; García-Isarch et al., 2011). *Pseudupeneus prayensis* (Mullidae) is present in these waters (it can be caught down to 200 m), and is also an exploited resource in the waters of Cape Verde. From Mauritanian waters, it replaces species of the genus *Mullus* present in Moroccan waters (*M. barbatus* and *M. surmuletus*). *M. polli* is an important species in the deep shelf and slope ecosystem of Guinea-Bissau, and is caught abundantly between 200 m and 500 m of depth (Fernández-Peralta et al., 2011a; García-Isarch et al., 2011). Other species important at greater depths are *Synagrops microlepis* (also abundant in Mauritanian waters) (Fernández-Peralta and Puerto González, submitted), *Antigonia capros* and species of the families Chlorophthalmidae, Aulopidae (*Aulopus cadenati*) and Macrouridae (*Malacocephalus occidentalis*, *Coelorinchus caelorhincus* and *Nezumia* spp.) (García-Isarch et al., 2011). Among the chondrichthyans, it is worth pointing out the presence of *Squatina oculata*, *Rhinobatos rhinobatos*, *Raja miraletus*, *Mustelus mustelus* and *Centrophorus granulosus*, all of them belonging to different families (García-Isarch et al., 2011). *Diplodus prayensis* is one endemic species in Cape Verde Islands.

The species latitudinal gradient is most evident in the shelf waters, since the deeper-water species are more widely distributed; some of the commercially-exploited species are detected throughout the CCLME region. This occurs with some deep-water species of Sparidae such as *P. bellottii*, *D. macrophthalmus* and *D. gibbosus*, and species such as *Helicolenus dactylopterus*, *Trichiurus lepturus* and *Zeus faber*. These species of the deep slope of the CCLME region are more cosmopolitan, but they are distributed at greater depths here than at those more northern latitudes in Morocco and North Atlantic waters (Fernández-Peralta and Puerto González, submitted).

5.2.3.2. Biodiversity patterns

Due to high fish species richness, it is very difficult to make an exhaustive list of all the demersal ichthyofauna present on the shelf and slope of the CCLME region; furthermore, there are no comparable studies in the area consistently prospected at the same bathymetric ranges. Nonetheless, based on the available data and taking into account the estimates made in other less diverse groups, such as crustaceans (García-Isarch and Muñoz, 5.5 this book), we can affirm that at depths between 80 m and 2000 m the number of fish species throughout the region will be well above 1000.

In the northern CCLME there are 414 fish species on the shelf and upper slope, which are also present in the Alboran Sea (Lloris and Rucabado, 1998). In the recent surveys carried out in Morocco and Western Sahara down to 2000 m, MAROC 0411, MAROC 0511 and MAROC 0611 (Hernández-González et al., 2006; Hernández-González, 2007; Ramos et al., 2005) a greater number of species were caught southwards (240 species up to 30°40'N, 278 between 30°40'N and 26°00'N, and 334 between 26°00'N and 20°40'N). However, in the Western Sahara survey, the bathymetric range extended from 200 m, while in the other two surveys it was from 500 m. Nonetheless, the specific diversity was reflected in an increase with depth that was the clearer still in the case of fish (Hernández-González et al., 2006; Hernández-González, 2007; Ramos et al., 2005). The highest values were found between depths of 1000 m and 1500 m, while the lowest values always occur in the shallowest waters, probably owing to the heavy fishing pressure in the waters of the Morocco shelf (FAO, in press c). The main fish families and their specific richness in Western Sahara waters are shown in Figure 5.2.1.

A quantitative analysis based on the surveys conducted in Mauritania (MAURIT 1107, MAURIT 0811, MAURIT 0911 and MAURIT 1011 surveys; Hernández-González et al., 2010; Ramos et al., 2010) reveal the

presence of 403 fish species belonging to 139 families and the most extensive maximum bathymetric limits of distribution for many species in Atlantic waters cited to date in the scientific literature (Fernández-Peralta and Puerto González, submitted). The most diverse among teleosts were Macrouridae (26 species) and Stomiidae (25), followed by Alepocephalidae and Ophidiidae (each with 17), Myctophidae (12), Sparidae (10), Halosauridae (9) and Sternoptychidae (9) (Fig. 5.2.2).

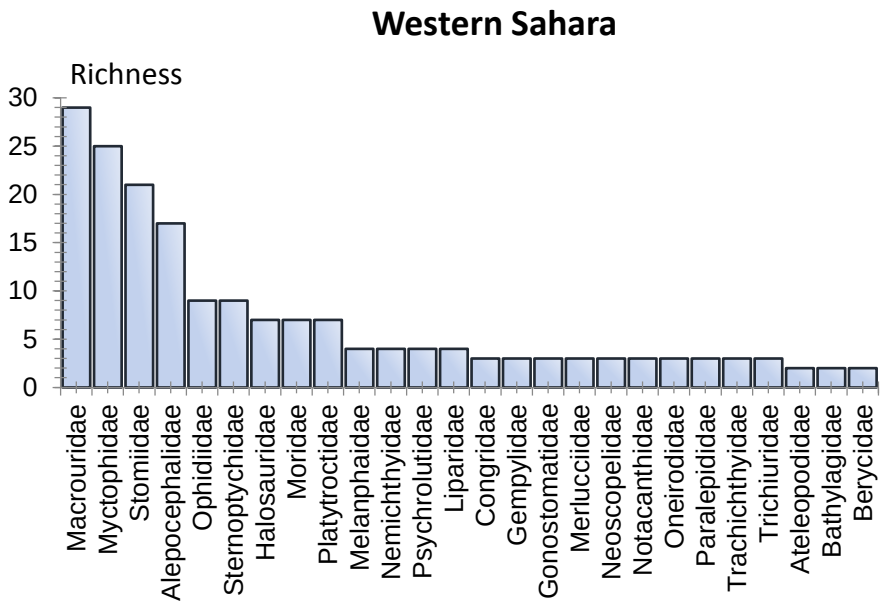

Figure 5.2.1. Specific richness for the main teleost fish families caught during the *Maroc 0611* survey carried out on board the Spanish R/V *Vizconde de Eza,* between 200 m and 1860 m (193 species in the graph). Chondrichthyes are excluded.

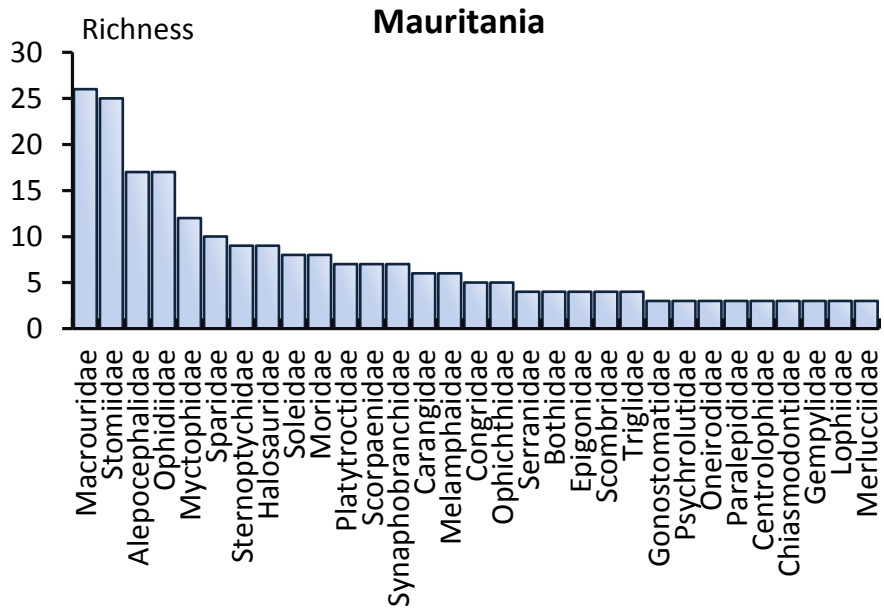

Figure 5.2.2. Specific richness for the main teleost fish families caught during the four *Maurit* surveys (0711, 0811, 0911 and 1011) carried out on board the Spanish R/V *Vizconde de Eza,* between 80 m and 2000 m (231 species in the graph). Chondrichthyes are excluded.

The mean diversity increases with depth, as described in other regions (Merrett and Haedrich, 1997). The observed peaks between 1000 m and 1700 m, as well as the Shannon Index, correspond to a deep middle and lower slope communities (Fernández-Peralta and Puerto González, submitted). This increase is probably due to the coexistence of strictly benthic species with meso- and bathypelagic fishes, such as Stomiidae and Micthopydae, or demersal species of similar behaviour, such as Alepocephalidae, Synaphobranchidae, Macrouridae, Halosauridae and Melamphaeidae. Between 1500 m to1700 m there is a transitional zone for slope fauna, with the fish assemblages changing at these depths. The species richness in these waters is higher than the ones recorded in similar or wider bathymetric ranges of the Atlantic and Mediterranean (Fernández-Peralta and Puerto González, submitted). The Mauritanian fish diversity is similar to that reported for the whole North Atlantic Basin (Merrett, 1994), and is higher than the diversity values recorded in other studies carried out in the area (Merrett and Marshall, 1981; Haedrich and Merrett, 1990). The deep shelf and upper slope assemblages were the least diverse, probably because of intense fishing exploitation (Gascuel et al., 2004, 2007; Fernández-Peralta et al., submitted). Nevertheless, these shallow depths recorded the highest biomass and abundances, due to families with low to medium diversity (Acropomatidae, Sebastidae, Carangidae and Merlucciidae) and represented by one main species each one (*S. microlepis*, *H. dactylopterus*, *T. trecae* and *M. polli*) (Fernández-Peralta and Puerto González, submitted).

The greatest specific richness in Moroccan, Western Saharan and Mauritanian waters is found at considerable depths, where there are resources that have never been exploited. Among other species, that ecosystem is composed of deep-water squaloids (*C. fabriccii, C. coelolepis, C. crepidater* and *Z. squamulosus*), highly vulnerable to fishery exploitation. The deep habitats are reservoirs of biodiversity and certainly must be preserved.

There are no recent data on the southern part of the CCLME region, and particularly on waters deeper than 1000 m. Analyses of data from Senegalese and Guinean waters showed certain stability in both countries' biodiversity, although the authors themselves expressed some caveats on the sensitivity of the indices and the sampling methods used (Domalain et al., 2004). They also draw attention to the correct taxonomic determination of species, including fish species, as a major handicap for the study of biodiversity in that area. Furthermore, the Senegalese and Guinean waters of the shelf are also subject to heavy fishing pressure (Gascuel and Ménard, 1997; Gascuel et al., 2004, 2005; Laurans et al., 2004), which is bound to damage its biodiversity.

So far, a total number of 327 fish species belonging to 124 families have been reported in Guinea-Bissau waters (GUINEA BISSAU 0810 survey; García-Isarch et al., 2011) (Fig. 5.2.3). The greatest specific diversity is found in the following Osteichthyes families: Macrouridae (15 species), Soleidae (12), Serranidae (10), and Alepocephalidae, Carangidae and Sparidae (9 species each).). We observe in these waters a high biodiversity typical from tropical regions.

In addition to the permanent upwelling of Cape Blanc, there are regions of seasonal upwelling in Western Sahara waters and in the Mauritania-Senegal shelf, induced by the regime of trade winds, the topography of the ocean floor and the direction of the coastline. All this contributes to sustain a great fish species richness, even greater than in other zones of major upwelling, such as that of the Namibian waters (Roel et al., 1985). The data are not completely comparable owing to the different depth ranges prospected and seasonal factors, but it can be concluded that diversity is likely to increase in Mauritanian waters, where is noted the greatest mixture of temperate and tropical species, since the two types of fauna converge to a considerable extent. To the north and to the south of Cape Blanc, fish communities are more differentiated

because they belong to two distinct biogeographical realms. Surely, the permanent upwelling of Cape Blanc is a frontier in geographical, hydrological and faunal terms.

Recent surveys in Mauritanian waters have shown a scarcity of the Sparidae family, as well as a great abundance of tropical species such as S. microlepis in the shelf and upper slope during the warm-cold transition season, when the former should be more abundant and the latter less so. These findings could probably be related with the intense fishing exploitation and/or a shift of species distribution caused by a warming of the waters (Cheung et al., 2013), that may affect community composition, inducing potential changes in biodiversity (Fernández-Peralta and Puerto González, submitted; Fernández-Peralta et al., submitted). On the other hand, the possibility of a replacement of Sparidae by cephalopods in the northern fishing grounds of the CCLME, influenced by a combination of factors (fishing, oceanographic variability, competition for food), has already been suggested (Balguerías et al., 2000), pointing to some adjustment in the composition of faunistic communities.

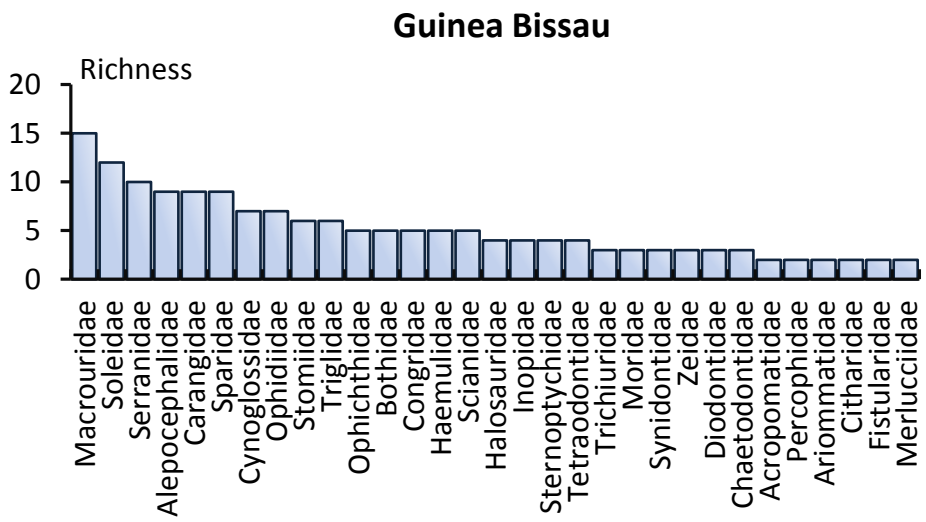

Figure 5.2.3. Specific richness for the main teleost fish families caught during the *Guinea-Bissau 0810* survey carried out on board the Spanish R/V *Vizconde de Eza,* between 20 m and 1000 m (161 species in the graph). Chondrichthyes are excluded.

5.2.3.4. Main commercial stocks

Demersal fish resources of the region are exploited by a great variety of fleets, making it difficult to assess them. The region is characterized by the existence of a large artisan fishing fleet consisting of thousands of small boats operating in shallow waters, from canoes and pirogues to larger craft, and an increasingly developed African industrial fishing fleet. The artisanal fishing fleet is mainly directed to the Sciaenidae, Lutjanidae and coastal Sparidae communities, and the industrial fishing fleet takes deeper demersal fish resources, mostly as by-catch. Foreign fleets, both artisan and industrial (most of the latter being freezer fleets) have been operating in the area for decades, and are either fishing for hake or conducting multi-species fishing or taking considerable volumes of fish demersal species as by-catch (retained and/or discarded), as is the case with cephalopod freezer trawlers (in Guinea-Bissau, for example), or even in pelagic trawlers (in Mauritanian waters) (FAO, in press b, c). Although there has been a considerable reduction in European fleets due to the successive fisheries agreements (Ramos et al., 2000), the region still

sustains large fleets from all over the world extracting fish resources, and their true dimensions are unknown.

Although the region has many demersal fish resources, only a few of these stocks have been studied, monitored and assessed (Gascuel et al., 2004). The latest stock assessments, conducted by FAO/CECAF are shown in Table 5.2.1. In fact, only 21 fish stocks have been assessed in 2011 and 2103, and the condition of the majority of fish stocks is therefore unknown. In the case of some stocks where attempts have been made to evaluate them, no conclusive results have been obtained, as occurred with *Pseudotolithus* spp. in Senegalese-Gambian waters and *P. caeruleostictus* and *D. macrophthalmus* in Moroccan waters. In other cases, the lack of data prevents the assessment from being made, as is the case with *Diplodus* spp. and *P. prayensis* from Cape Verde waters (Table 5.2.2). The collection of fish-related statistics in the area remains a problem, as does the uncertainty contained in the data which are used in some cases (lack of data on the by-catch and on illegal fishing). The fisheries are characterized by *data poor* that only allows the use of relatively rudimentary assessment methods (Gascuel et al., 2004).

The main stocks by catch volume assessed in the area correspond to the families Sparidae (30,000 t), Sciaenidae (28,000 t) and Merlucciidae (12,000 t) (Table 5.2.1). The other major species belong to the families Ariidae (11,000 t), Haemulidae (7000 t), Polynemidae (5000 t) and Cynoglossidae (5000 t), which are components of the Sciaenidae community (Longursth, 1969), which accounts for a yield of 50,000 tonnes yr^{-1}.

Five stocks distributed in Moroccan waters show a state of overexploitation, like *M. merluccius* (exploited only by Moroccan fleets since 1999), the various Sparidae species and the Rubberlip grunt, *Plectorhinchus mediterraneus*, exploited in the south by Moroccan fleets, and less intensely by artisanal fleets from the Spanish Canary Islands. Another three stocks also show signs of overexploitation: the white grouper, *Epinephelus aeneus,* from Mauritania-Senegal-The Gambia, and *Pesudotolithus* spp. and *G. decadactylus* from Guinea and Guinea-Bissau. Six stocks are reported as not fully exploited: *Merluccius* spp. from Mauritania, *P. bellottii* from Mauritania-Senegal-The Gambia, *Arius* spp. both from Senegal-The Gambia and Guinea-Guinea Bissau, and *Cynoglossus* spp. and Sparidae from Guinea-Guinea Bissau. Only three stocks are classified as fully exploited: *Pseudotolithus elongatus* and *Pomadasys* spp. from Guinea-Guinea Bissau, and *Cephalopholis taeniops* from Cape Verde. The situations of five stocks are unknown (Table 5.2.2).

A variety of studies, mostly based on scientific trawl surveys, have shown a fall in the abundance of various demersal fish species in Mauritanian, Senegalese and Guinean waters (Gascuel and Ménard, 1997; Gascuel et al., 2004) and simulations with Ecopath models have shown a decline in the biomass trends for demersal fishes off NWA (Christensen et al., 2004). The study of fishing impacts in the CCLME through trophic spectra analysis indicates that the demersal biomass in the higher species total length range has decreased, while that in the lower range has increased (Gascuel et al., 2005, 2007) and also that substantial changes have occurred in the trophic structure of fish demersal communities in Senegalese and Guinean waters (Laurans et al., 2004). The marked and rapid rise in the fishing mortality in the area prevents catches from increasing and the biomass amount is irremediably trending downwards. Bayesian statistics have also shown widespread overfishing in Mauritanian waters, and a considerable impact on the Sparidae community, among others (Meissa and Gascuel, 2014). Previous studies (Domain, 1979, 1980; Maurin, 1968) and fisheries data (FAO, 1987; Fernández et al., 1998, 2004) showed a great abundance of this community. This overfishing of Sparidae has also been reported in Mauritania on the basis of data surveys (Fernández-Peralta and Puerto, submitted), as well as in Senegal and in the coastal Sciaenidae community (Gascuel and Ménard, 1997; Gascuel et al., 2004).

The fisheries in the region are still typically located on the continental shelf, where severe overfishing is reflected in the shortage of benthic fauna. Currently, only black hake trawlers regularly take their catches from greater depths, up to 1000 m, with the greatest incidence on the depths between 400 m and 800 m (Fernández-Peralta et al., 2011b, submitted).

5.2.4 CONCLUSIONS AND RECOMMENDATIONS

The demersal ichthyofauna of the CCLME is made up of species with more temperate affinities towards the north and more tropical characteristics further south. They converge in the central zone of the region, mainly in Mauritanian waters, and there are few endemic species. This results in very high biodiversity levels in Mauritanian waters, where there is a transition from one fauna type to another. The deep waters show the largest biodiversity in the marine ecosystem, with maximum values between 1000 m and 1700 m, at least in the north and central part of the region (Morocco, Western Sahara and Mauritania), diminishing slightly at greater depths. In shallow waters (less than 200 m), the specific richness is the poorest; this is likely due to heavy fishery pressure on the shelf for the past few decades (Fernández-Peralta and Puerto González, submitted). Changes have been observed recently in fish communities, probably because of fishery exploitation and also temperature increases which have been noted in the area, even in very deep waters (Arístegui et al., 2009a). Species living in the depths of the middle and deep continental slope (such as deep-water sharks), where greater biodiversity is observed, are highly vulnerable and therefore constitute highly sensitive marine ecosystems.

The CCLME supports substantial demersal fish resources, many of them severely affected by over-fishing in the past 10 years. Large individuals are very rare in commercial species populations and total catches are constantly declining. The practice of trawler fishing continues to damage and alter habitats including seabed, spawning and nursery grounds and also to disrupt the food web and threaten marine biodiversity in the CCLME area.

To improve the situation and ensure sustainable exploitation of demersal species, scientific collaboration and technical cooperation must be strengthened to enable countries to continue to benefit from goods and services provided by the CCLME. The efforts of the stakeholders should be joined to obtain systematic information on the variability of physical and biological processes in the CCLME area for a better understanding of the contribution of natural and anthropogenic variability in the demersal fish populations and the associated species. Some important steps to be taken to ensure that all marine resources of the region are preserved, while at the same time being sustainable, are: (i) the establishment of effective monitoring programmes to collect all the data on demersal fish species and implementation of standard system software for the entire region; (ii) studies on discards and enforcement of efficient measures for their reduction; (iii) ecosystem and periodical surveys for biomass assessments and for environmental baseline studies; (iv) stable working groups to reinforce the management system for demersal stocks, especially in the southern area of the CCLME; and (v) international efforts to eradicate illegal fishing.

Table 5.2.1. Fish species or groups of fish species (clustered by families) assessed in the CCLME region within the latest FAO/CECAF Working Groups carried out in 2011 (Subgroup South: Guinea-Guinea Bissau and Cape Verde, FAO, in press b) and 2013 (Subgroup North: Morocco, Mauritania, Senegal-The Gambia and Mauritania-Senegal-The Gambia, FAO, in press c).

Family	Species	CCLME stock area					
		Morocco	Mauritania	Senegal-The Gambia	Mauritania-Senegal-The Gambia	Guinea-Guinea Bissau	Cape Verde
Merlucciidae	*Merluccius merluccius*	X					
	Merluccius spp. *(M. polli, M. senegalensis)*	*	X	*			
Sparidae	*Sparus* spp. (*S. aurata*, *Pagrus auriga*)	X					
	Pagellus spp. (*P. bellottii*, *P. erythrinus*)	X					
	Pagellus acarne	X					
	Pagellus bellottii				X		
	Pagrus caeruleostictus				X		
	Dentex macrophthalmus				X		
	Diplodus spp. (*D. prayensis, D. bellotti*, *D. puntazzo*, *D. sargus, D. vulgaris)*						X
	Sparidae					X	
Haemulidae	*Plectorhinchus mediterraneus*	X					
	Pomadasys spp. (*P. jubelini, P.incisus, P. perotaei, P. rogerii*)					X	
Sciaenidae	*Pseudotolithus* spp. (*P. senegalensis P. typus, P. elongatus, P. senegallus)*			X		X	
	Pseudotolithus elongatus					X	
Serranidae	*Epinephelus aeneus*				X		
	Cephalopholis taeniops						X
Polynemidae	*Galeoides decadactylus*					X	
Ariidae	*Arius* spp. (*A. parkii, Carlarius heudelotii, A. latiscutatus*)			X		X	
Cynoglossidae	*Cynoglossus* spp. (*C. cadenati, C. senegalensis, C. canariensis, C. monodi*)					X	
Mullidae	*Pseudupeneus prayensis*						X
Muraneidae	Muraneidae						X

*Stocks assessed in previous Working Groups.

Table 5.2.2. Demersal fish stocks (common and species names) in the CCLME region and the status assessed in the latest FAO/CECAF Working Groups in 2011 (*Subgroup South: Guinea-Guinea Bissau and Cape Verde) and 2013 (**Subgroup North: Morocco, Mauritania, Senegal-The Gambia and Mauritania-Senegal-The Gambia). The last years of the catches in the assessments were 2010 and 2012, respectively.

Common name	Species	Status	CCLME stock area	Catch last year (tons)
European hake	*Merluccius merluccius*	Over exploited	Morocco	5137
Black hake	*Merluccius* spp.	Not fully exploited	Mauritania	6883
Snapper	*Sparus* spp.	Over exploited	Morocco	4484
Pandora	*Pagellus* spp.	Over exploited	Morocco	4079
Axillary seabream	*Pagellus acarne*	Over exploited	Morocco	569
Red pandora	*Pagellus bellottii*	Over exploited	Mauritania, Senegal, Gambia	5675
Bluespotted seabream	*Pagrus caeruleostictus*	No results from assessment	Mauritania, Senegal, Gambia	6308
Large-eye Dentex	*Dentex macrophtalmus*	No results from assessment	Mauritania, Senegal, Gambia	4021
Bream	*Diplodus* spp.	Not available data	Cape Verde	278
Seabreams	*Sparidae*	Not fully exploited	Guinea, Guinea Bissau	4613
Rubberlip grunt	*Plectorhinchus mediterraneus*	Over exploited	Morocco	4387
Grey grunt	*Pomadasys* spp.	Fully exploited	Guinea, Guinea Bissau	3050
Croaker	*Pseudotolithus* spp.	No results from assessment	Senegal, Gambia	9674
		Over exploited	Guinea, Guinea Bissau	7005
Bobo croaker	*Pseudotolithus elongatus*	Fully exploited	Guinea, Guinea Bissau	11233
White grouper	*Epinephelus aeneus*	Overexploited	Mauritania, Senegal, Gambia	3413
Bluespotted seabass	*Cephalopholis taeniops*	Fully exploited	Cape Verde	248
Threadfins	*Galeoides decadactylus*	Over exploited	Guinea, Guinea Bissau	5265
Marine Catfish	*Arius* spp.	Not fully exploited	Senegal, Gambia	5657
		Not fully exploited	Guinea, Guinea Bissau	5350
Tongue/Sole	*Cynoglossus* spp.	Not fully exploited	Guinea, Guinea Bissau	5168
West African goatfish	*Pseudupeneus prayensis*	Not available data	Cape Verde	33
Moray eels	*Muraneidae*	Fully exploited	Cape Verde	148

*FAO/CECAF Working Group on the Assessment of Demersal resources- Subgroup North. Fuengirola, Spain, 18-27 November 2013 (FAO, in press c).
**FAO/CECAF Working Group on the Assessment of Demersal resources- Subgroup South. Accra, Ghana, 15–25 November 2011 (FAO, in press b).

Plate 5.2.1. (1) *Merluccius polli* (up) and *M. senegalensis* (down) © Ramón García Cancela. (2) *Bathygadus melanobranchus* (up) and *Trachyrincus scabrus* (down) © Ramón García Cancela. (3) *Pagellus bellottii* © Lourdes Fernández Peralta. (4) *Plectorhinchus mediterraneus* © Lourdes Fernández Peralta. (4) (5) *Synaphobranchus kaupii* © Ramón García Cancela. (6) *Alepocephalus rostratus* © Ramón García Cancela.

1

2

3

4

5

6

Plate 5.2.2. (1) *Helicolenus dactylopterus* © Lourdes Fernández Peralta. (2) *Pomadasys perotaei* © Lourdes Fernández Peralta. (3) *Centroscymnus crepidater* (up) *and Centrophorus granulosus* (down) © Ramón García Cancela. (4) *Cynoglossus canariensis* © Lourdes Fernández Peralta. (5) *Lepidotrigla cadmani* © Lourdes Fernández Peralta. (6) *Synagrops microlepis* © Lourdes Fernández Peralta.

1

2

3

4

5

6

5.3. THE BENTHOS OF NORTHWEST AFRICA

Ana RAMOS[1], Fran RAMIL[2], Sidi MOHAMED[3] and Amadou O. BARRY[4]

[1] Instituto Español de Oceanografía. Spain

[2] Universidade de Vigo. Spain

[3] Institut Mauritanien de Recherches Océanographiques et Pêches. Mauritania

[4] Centre de Recherche Scientifique de Conakry-Rogbane. Guinea

5.3.1. INTRODUCTION

Marine benthos is composed of all the organisms that live in close association with the seabed, including microorganisms, plants (macroalgae and sea-grasses), many invertebrates and some vertebrates, such as demersal fishes. These organisms can live buried in the sediments (endobenthos), directly on the bottom, attached to the substrate or enjoying some mobility (epibenthos), or in the water layer close to the sea-bottom (suprabenthos and demersal fishes). The benthos constitutes an essential component of ecosystems, one of the main links in the marine food chains, and also represents an important food source for numerous fish, crustacean and cephalopod species; furthermore, some particular benthic invertebrates, such as sponges and corals, may in certain areas build three-dimensional habitats which host a high biodiversity ("hot-spots"), providing a spawn and nursery refuge area for many commercial species.

During the last decade some studies have clearly demonstrated that overfishing severely degrades marine habitats and results in an irreversible loss of marine biodiversity (Cryer et al., 2002). The depletion of traditional shelf resources is driving fishing fleets into deeper waters, and this is dramatically threatening the integrity of some of the most vulnerable benthic ecosystems of the continental margins, such as cold-water coral reefs, sponge fields, gorgonian forests and seamounts. Knowledge of the benthic realm is therefore essential for biodiversity conservation, responsible management of living resources and sustainable fishing based on a holistic approach.

Following the visit of HMS *Challenger* in 1878, many early expeditions worked off the Northwest African (NWA) coast, collecting fishes and benthic invertebrates from its sea-bottoms. Mythical expeditions like the *Travailleur* and *Talisman*, *Valdivia*, *Princess Alice I*, *Hirondelle II*, *Michael Sars* and *Discovery*, and, more recently, in the mid-20th century, others like the *Atlantide*, *Calypso* or *Thalassa*, travelled along the coasts of Morocco, Western Sahara, the Gulf of Guinea, and the Canary or Cape Verde Islands. To these expeditions, we must add the efforts undertaken by regional research institutes during the colonial and independence periods; especially the Institut Fondamental de l'Afrique Noire (IFAN) and the Office de la Recherche Scientifique et Technique d'Outre-Mer (ORSTOM). Over many decades, these institutes conducted surveys aboard small oceanographic vessels in more limited work areas, particularly in Mauritania, Senegal and Guinea. Although this intense research activity and the surveys were frequently focused on exploitable species, their results, scattered over hundreds of very different publications, provide important information on taxonomy, distribution and bionomy (Maurin, 1968). Thanks to the IFAN research vessel, the *Gerard Treca,* and to the leadership of Cadenat, Marche-Marchad and other prestigious researchers, important faunistic collections were built up, some of them still conserved in the IFAN Museum on Gorée Island (Senegal).

More recently, some large-scale and long-term international projects focused on benthic research have been carried out in NWA. One example is the international multidisciplinary CINECA Programme (Cooperative Investigation of the Northern Part of the Eastern Central Atlantic), which was intended precisely to improve global knowledge on the CCLME area, extending from 10°N to the Straits of Gibraltar (36°N) (Hempel, 1982). The Netherlands' CANCAP programme (1974-1989) aimed to study the biogeography and distribution of benthos in the region, from the coast to 4000 m depth (den Hartog, 1984; Van der Land, 1987). At a more local level, the TYRO-MAURITANIA expedition was conducted in 1988 with the objectives of studying the functioning of the Banc d'Arguin ecosystem, its interactions with the open ocean systems and the quantitative distribution of benthos in northern Mauritania, between Cape Blanc and Cape Timiris (Van der Land, 1988). The main results of this project were compiled in a special volume of the journal *Hydrobiologia* (Wolff et al., 1993).

However, general studies focused specifically on benthic research are quite rare in the region and they are usually confined to the study of specific faunistic groups from coastal and shelf areas. Among the most comprehensive benthic studies carried out in the Canary Current Large Marine Ecosystem (CCLME) are those of Domain (1980), which includes the study of seasonal distribution of benthos abundances on the Senegalese shelf to 100 m depth, Ushakov (1965) and Le Loeuff (1993), focused on the benthic ecosystems of the Guinean shelf to 200 m. Chavance (2002) compiled the old surveys and bibliography on NWA, while Entrambasaguas (2008) made a summary of expeditions collecting marine invertebrates in the waters of the Cape Verde archipelago during the 19th and 20th centuries. Sidi (2010) has resumed the bibliography produced in recent years on benthic studies in the coastal zones of Mauritania and Morocco. In the Canary Islands, many campaigns and projects have contributed to knowledge of the benthos, being summarized in the current marine bibliography on-line (OAG, 2015). Ramos (2011) synthesized the state of benthic knowledge in the CCLME.

Despite the large number of published papers referencing and describing fishes and invertebrates collected by historical expeditions and international projects, according to the latest review of sub-Saharan African biodiversity (Decker et al., 2004) Northwest Africa is among the less known regions of the planet in terms of fauna, particularly with regard to benthic communities.

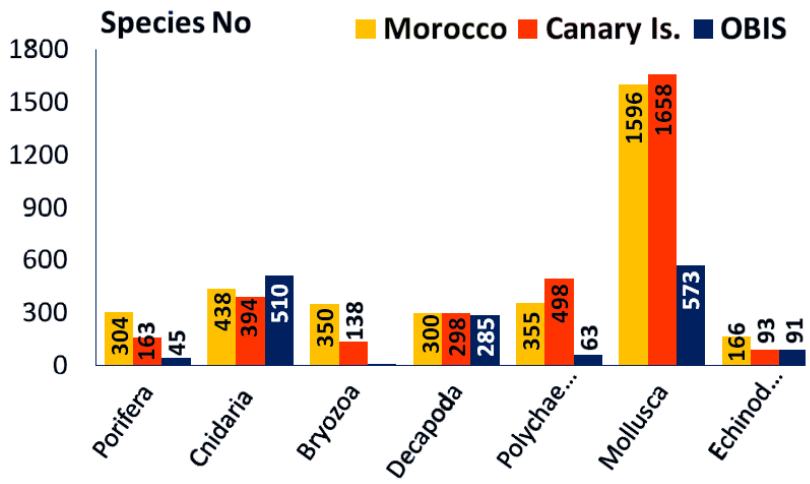

Figure 5.3.1. Diversity of some of main benthic taxa recorded in Morocco (Menioui, 1998), the Canary Islands (Gobierno de Canarias, 2015) and OBIS Database (OBIS, 2015).

The EcoAfrik Project, launched by the Instituto Español de Oceanografía (IEO) in 2009, in collaboration with the Faculty of Marine Science of the University of Vigo (Spain), has sought to address this general gap in the knowledge of biodiversity and benthic ecosystems, particularly in NWA. The project is based on the taxonomic identification and analysis of quantitative data of benthic invertebrates collected in 1350 trawl stations carried out during 12 research surveys in the CCLME on board R/V *Dr. Fridtjof Nansen* and *Vizconde de Eza*, which took place between 2002 and 2012.

This article is based on the bibliographic review of the main historical papers on benthic research developed in the area, as well as on some published results of the Spanish and Norwegian surveys.

5.3.2. A GLOBAL OVERVIEW OF NORTHWEST AFRICAN BENTHOS

5.3.2.1. Biodiversity

The collections made in NWA during the expeditions of the 19th and first part of the 20th centuries have been the subject of many important publications on taxonomy and description of species belonging to numerous groups of benthic invertebrates. It would be impossible to do an exhaustive inventory of all reports containing the results of scientific expeditions carried out over a century and a half. Currently, although remarkable biodiversity studies on some faunal groups or specific habitats (estuaries, bays, islands) have been undertaken in several countries, marine biodiversity inventories are only available for Morocco (Menioui, 1998) and the Canary Islands (Moro et al., 2003; Gobierno de Canarias, 2015). A regional report on biodiversity, including threatened, protected or to protect, harmful and endemic species, has been recently compiled in the framework of the FAO-CCLME project (FAO, 2014b).

Although, because of the heterogeneity of the sampling methods used, comparative analyses are not possible, Le Loeuff and von Cosel (1998) conducted a major review of biodiversity in West Africa, examining reliable systematic works on different benthic invertebrate groups collected in thousands of stations to a depth of 200 m. Their review summarizes 1449 invertebrate species, including 44 gorgonians, 606 polychaetes, 170 brachyurans, 59 pagurids, 380 bivalves and 190 echinoderms.

Although we do not yet have final results on biodiversity since taxonomic identification requires a long study time, preliminary analysis of *Dr. Fridtjof Nansen* surveys shows that the epibenthos of the shelf and upper slope of Northwest Africa seems to be composed of at least 1000-1200 species, belonging to 38 invertebrate groups (Ramos et al., 2012). According to the preliminary results provided by the joint Spanish surveys in Morocco and Mauritania, global benthic diversity in deep water seems to be lower: about 500-600 species inhabit the bottoms from a depth of 200 m to 2000 m in Morocco and Western Sahara (González-Porto et al., 2007) and approximately 700 species were collected in Mauritania between a depth of 80 m and 2000 m (Ramil and Ramos, submitted). In Guinea-Bissau only about 400 megabenthic species were recorded between 20 m and 1000 m depth during the joint Spanish-Guinean Bissau Survey in 2008 (González-Porto et al., 2010). The diversity inventories provided by Menioui (1998) and Gobierno de Canarias (2015) for Morocco and the Canary Islands, respectively, show a global diversity for the main benthic taxa that is very similar in both zones (around 3200-3500 species), but these reviews include littoral, infaunal and small-size species and the Moroccan checklist also includes Mediterranean species.

As occurs in other marine regions, in Morocco and the Canary Islands molluscs, crustaceans, polychaetes and cnidarians are among the most diverse benthic taxa (Menioui, 1998; Gobierno de Canarias, 2015) (Figure 5.3.1). Nevertheless, excepting Cnidaria and Decapoda, highly diverse taxa such as Mollusca,

Polychaeta, Bryozoa and Porifera are scarcely recorded in the OBIS database (OBIS, 2015). Data from ecosystemic surveys show that the richest megabenthic taxon on the shelf and upper slope of NWA is, by far, the decapods (Figure 5.3.2), represented in the region by approximately 250 species and more than 40 families. Prosobranch molluscs account for more than 100 species, being followed in decreasing order by sponges, hydroids, polychaetes, bivalves and gorgonians (Figure 5.3.2). Probably the richness of some groups, such as sponges, hydroids, bivalves and bryozoans will increase once the collections are totally identified.

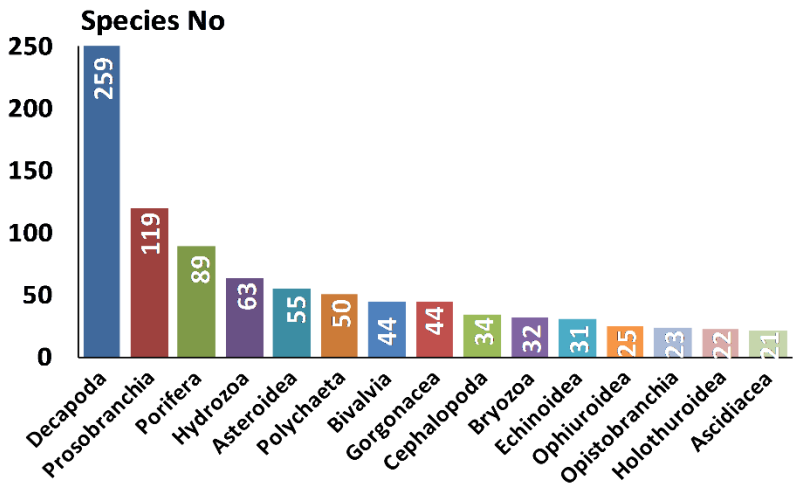

Figure 5.3.2. Preliminary results on biodiversity of CCLME ecosystemic survey in 2011: Species number for the main megabenthic taxa (from Ramos et al., 2012)

The dredging carried out during the *Thalassa* surveys will reveal that the CCLME has an exceptionally rich benthos at all levels, being one of the most productive areas of the oceans. This would explain the abundance of demersal resources (Bonnet et al., 1971). Nevertheless, more recently, Le Loeuff and von Cosel (1998) pointed out that the richness of the main benthic groups in West Africa seems to be of the same magnitude as those of European coasts. In spite of this, if we compare the diversity in the three hydro-climatic zones included in the CCLME (Table 5.3.1, Figure 5.3.3), we can observe that the species richness, as for faunistic groups as for whole fauna, are clearly higher in the alternance zone, between Cape Blanc (Mauritania) and Cape Verga (Guinea-Bissau), where the displacement of a thermal front occurs (Le Loeuff and van Cosel, 1998). Regarding total diversity, 1014 species were found in this area, while only 650-680 were found in areas north of Cape Blanc (Eastern Atlantic Region) and south of Cape Verga (typical tropical region). This finding is also valid for different taxa, with the exception of polychaetes, and it is especially significant in the case of gorgonians, crustaceans and bivalves (Table 5.3.1). The results of Gosselk (1974) and Domain (1980) also provide evidence of the great richness of Senegal's shelf bottoms, in comparison to other Gulf of Guinea areas, such as Sierra Leone, Ivory Coast or Guinea. Rex et al. (1993) pointed out that also in deep-sea waters (500–4000m depth) the richness of bivalves, gastropods and isopods is greater in the Gambia basin than in other Northern Atlantic zones.

Table 5.3.1. Richness of selected benthic groups in the three hydro-climatic zones in the CCLME region (Figure 5.3.3) (based on Le Loeuff and von Cosel, 1998)

	W Sahara	Mau+Sen	Guineas
Gorgonians	18	31	15
Polychaetes	333	333	182
Brachyurans	60	136	85
Pagurids	18	41	35
Bivalves	133	304	228
Echinoderms	67	105	95
Total	650	1014	680

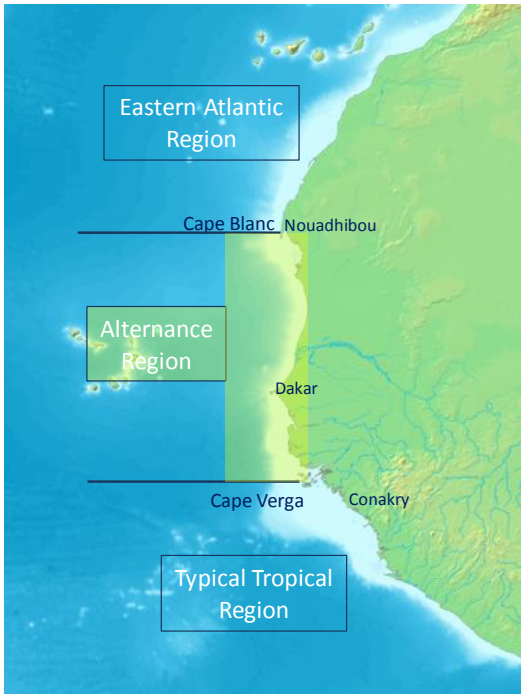

The preliminary results on biodiversity of the *Dr. Fridjof Nansen* ecosystemic surveys in the CCLME show that a diversity pattern directly related to latitude does not exist along the NWA coast, even though González-Porto et al. (2007) showed that specific richness varies significantly with latitude along the Moroccan and Western Saharan slope, seeming clearly higher in the latter. Global megabenthos richness is two times higher in shelf and upper-slope waters north of Cape Blanc (mean = 26-28 species by station, Ramos et al., 2012), than in those of the southern CCLME region (14-18 species by station), being especially high along the Western Saharan slope (mean = 36 species by station) (Figure 5.3.4).

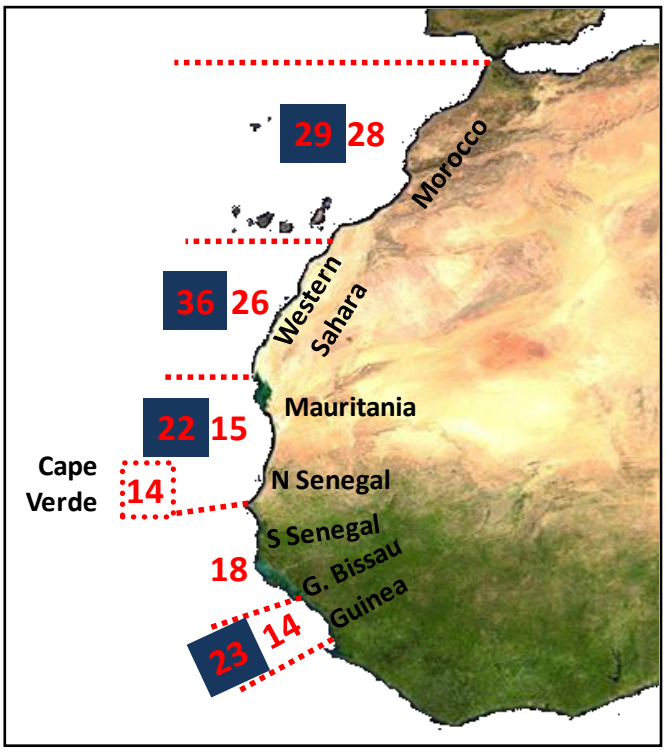

Figure 5.3.4. Mean biodiversity values (specific richness by station) across the CCLME. Data of CCLME ecosystemic surveys (shelf and upper slope area) and joint Spanish surveys (deep-shelf and slope)

Even if the mean biodiversity values of macro- and megabenthos in the deep-shelf and continental slope of Mauritania are lower than those in northern latitudes, specific richness attains local values of 100 species by station, being higher than in European continental margins (Castillo et al., submitted; Ramil and Ramos, submitted). In addition, along the entire Mauritanian coast, a latitudinal gradient also exists for epibenthos: specific richness and diversity indexes are highest in the northern zone (Cape Blanc) (Ramil and Ramos, submitted; Castillo et al., submitted), where the waters, under the influence of a permanent upwelling throughout the year, are highly productive (Arístegui et al., 2009a).

Although its marine biodiversity has not been inventoried, the Cape Verde archipelago shows in general terms high values with species typical of tropical and subtropical areas and includes some endemic species (Ministério do Ambiente, Agricultura é Pescas, 2004). In the Canary Islands, whose global marine diversity has been estimated at 5232 species, 45% of the biodiversity (2379 species) is concentrated in a narrow bathymetric range, from a depth of 5 m to 50 m, as is characteristic of insular systems (Moro et al., 2003). However, in the Canary and Cape Verde islands, different factors, such as steep sea-bottom slopes, the limited extension of the continental shelf and the intertidal zone (due to its volcanic origin), the seasonality of oceanographic phenomena and the shortage of rainfall, have been linked with the low densities of marine organisms in these archipelagos.

In relation to macroalgae, 583 species have been recorded for the entire Gulf of Guinea, between Angola and Mauritania (John et al., 2003), and 639 in the Canary Islands (Moro et al., 2003). Higher algal diversity is found in northern Senegal (274 species), followed by Mauritania (212 species), Western Sahara (81) and The Gambia (62), while the lowest values are found in Guinea-Bissau (21) and Guinea (12) (Figure 5.3.5). The presence of a rocky coastline, that makes algae attachment possible, could explain the high diversity values found in Senegal. Nevertheless, the review of John and Lawson (1997) shows that West African flora is impoverished, in stark contrast to the richness of the flora of the tropical coast of East Africa or of the Caribbean region; this poverty has been related to the lack of coral reefs, the higher wave exposure and the recent recolonization of the region by East Atlantic species after the Pleistocene glaciations. Only five sea-grass species (*Cymodocea nodosa*, *Zostera noltii*, *Halophyla decipiens*, *Halodule wrig*htii and *Ruppia maritima*) colonize the continental and island coasts of NWA, being particularly importants in some ecosystems such as the Banc d'Arguin (Wolff et al., 1993) and the '*sebadales*' of the Canary Islands (Espino et al., 2008).

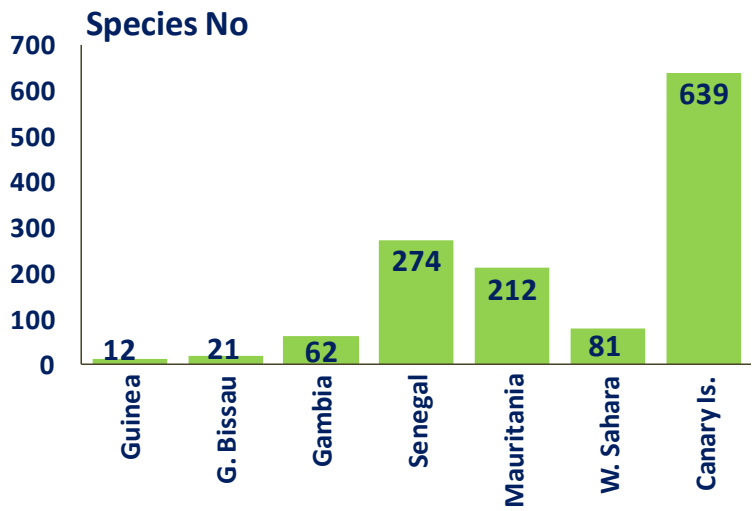

Figure 5.3.5. Algae diversity by country in the CCLME (after John et al., 2003, and Moro et al., 2003, for the Canary Islands)

5.3.2.2. Faunistic composition

The preliminary results of the two *Dr. Fridtjof Nansen* surveys in the CCLME show that the epibenthic communities of NWA, despite the existence of evident differences in their specific composition, seem to maintain similar structures in relation to the dominant groups and trophic strategies (Ramil et al., 2012a). Abundance and biomass in the shelf and upper slope are dominated by decapods and cephalopods in the two hydrological transitional seasons, accounting together for 81%-92% of biomass and 85%-77% of abundance (Ramil et al., 2012a, b).

Decapods constitute 78% of the numerical abundance and 53% of the biomass in the CCLME (Figure 5.3.6). They are dominant mainly between depths of 200 m and 500 m along the upper slope (García-Isarch et al., submitted), and their abundance increases along the NWA coast, from northern Morocco (where they only constitute 59%), to Guinea (where their abundance reaches 96% of the total catch) (Ramos et al., 2012). Among the most characteristic decapods there are, in addition to the important commercial species *Parapenaeus longirostris*, two other shrimps, *Nematocarcinus africanus* and *Plesionika heterocarpus*, some representatives of the Galatheidae familiy, such as *Munida speciosa*, and the brachyuran crabs *Macropipus rugosus* and *Calappa pelli*. Among the cephalopods, *Illex coindettii*, *Todaropsis eblanae*, *Todarodes sagittatus*, *Loligo vulgaris* and *Octopus vulgaris* dominate this group in biomass, while several small species of *Alloteuthis* are the main contributors to abundance levels.

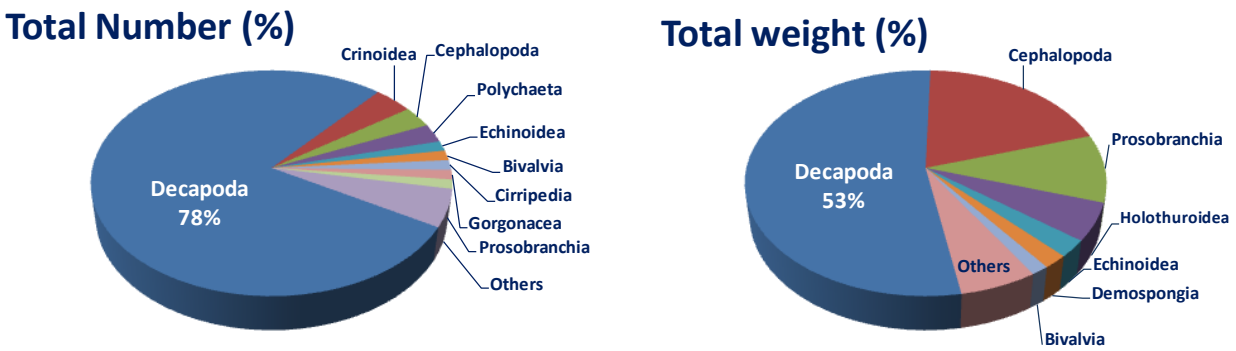

Figure 5.3.6. Global composition of the epibenthos of the Northwest Africa continental region, in individual's number (up) and weight (down) (preliminary data of CCLME ecosystemic surveys, in Ramos et al., 2012)

Despite the high dominance of decapods and cephalopods, other faunistic groups are also important components of the benthic communities inhabiting the shelves and upper slope of the region. Gastropoda, Holothuroidea, Echinoidea, Porifera and Bivalvia constitute an important part of the biomass; and Pennatulacea, Crinoidea, Polychaeta, Bivalvia and Cirripedia constitute an important part of the abundance levels (Ramil et al., 2012a; Ramos et al., 2012).

Among the most characteristic epibenthic species we can cite the regular sea-urchin, *Centrostephanus longispinus*, and the holothurid *Parastichopus regalis*, recorded throughout NWA waters, including Cape Verde and the Canary Islands (Plate 5.3.1). With reference to molluscs, we can highlight the giant gastropod belonging to the *Cymbium* genus, of great commercial importance in the region, and the bivalve *Pinna* sp., whose shells form very rich seabeds in coastal areas. All these species were already recorded in the old fishing maps published by Stassano (1890), Gruvel (1925) and Belloc (1933) more than a century ago, and notably in the first bionomic works resulting from the *Thalassa* expeditions. The *Thalassa* samplings were carried out after 1962 off the Moroccan, Western Saharan and Mauritanian coasts, to depths of 600 m,

800 m or even 1200 m, using different specific benthic samplers. Although only fishes and crustaceans were reported at a specific level on account of their commercial interest, information about other invertebrates was also collected (Maurin, 1968; Maurin and Bonnet, 1969; Bonnet et al., 1971). Thus, *Leptometra* and *Pinna* seabeds and muddy bottoms of *Cidaris*, *Funiculina* and *Isidella*, among others, were already recorded in the old fishing-ground maps of Belloc (1933) and Navarro (1947).

Although the *Princesse Alice II* had already collected some invertebrates in the Cape Verde archipelago at a depth of 6035 m in 1901, information on deep-sea benthos is generally scarce in the CCLME (Decker et al., 2004). According to the results of Spanish joint surveys, the epibenthos of deep waters presents a totally different picture from that of shelf and upper-slope waters, with a clear dominance of echinoderms. Three holothurians, *Benthothuria funebris*, *Paelopatides grisea* and *Enypniastes eximia*, constitute 90% of the biomass, mainly in Mauritanian and Moroccan deep-sea bottoms, where they were always collected deeper than 1000 m. These species were recorded in the Guinea-Bissau slope (González-Porto et al., 2010). *Benthogone rosea* and *Paroriza pallens* are also abundant. Regular sea-urchins belonging to the Echinothuridea order, mainly *Phormosoma placenta* (the species of this order with the widest distribution in deep waters of NWA), and *Hygrosoma petersii*, together with the sea-stars *Pseudarchaster gracilis (*and, in some localities, *Hymenaster roseus)*, are also frequent and abundant in the slope waters (Calero et al., submitted) (Plate 5.3.2).

Important differences in the benthos composition between the south and north of Cape Blanc are observed: from Guinea to Cape Blanc, tropical species are dominant; whereas from Cape Blanc to the Straits of Gibraltar, temperate species are better represented. This faunistic change is especially evident in shallow waters, mainly as regards Prosobranchia and Decapoda, very diverse in the southern area, while the slope species exhibit a much more widespread distribution and species changes are not so obvious (Ramil et al., 2012a). Fifty years ago, Maurin (1968) already revealed the existence of drastic faunistic changes, correlated with a biogeographical and thermal barrier at Cape Blanc latitude, where cold waters from the permanent upwelling are present throughout the year (Arístegui et al., 2009a). Nevertheless, the Canary Current regime seems to favour southwards larval dispersion and hence the entry of northern species into Mauritanian waters, where they coexist with the tropical ones, enhancing the high specific richness (Le Loeuff and von Cosel, 1998; Soest, 1993). In spite of the lack of primary production and matter flux below a depth of 200 m, which limits the food input to the seafloor (Gage and Tyler, 1991), several authors have pointed out that the permanence of one of the most important upwelling systems of the world and the extension of the giant and highly productive Cape Blanc filament to 600 km offshore (Gabric et al., 1993; Fischer et al., 2009; Sangrà, 3.5 this work) would favour food input to deep-sea benthos (Thiel, 1982; Duineveld et al., 1993). In fact, eutrophic conditions at more than 2000 m depth have been described off Cape Blanc (Sibuet et al., 1993; Cosson et al., 1997; Galeron et al., 2000).

Although some studies carried out in NWA forthy years ago remarked on the density of large-size benthic filter-feeders, such as Octocorallia, Crinoidea, Actiniaria and Porifera, from 50 m depth to 350 m depth in the entire upwelling area (Thiel, 1982), our results suggest that suspension-feeders do not currently seem to play an important role in epibenthic communities of deep-shelf and upper-slope waters. However, during the CCLME *Dr. Fridjof Nansen* surveys suspension-feeders (mainly Porifera, Hydrozoa, Octocorals, Bryozoa and Crinoidea) were more abundant in the northern area, namely in Western Saharan and Moroccan waters (Figure 5.3.7, Ramos et al., 2012). Off Western Saharan coasts the most frequent taxa found during the cited surveys were the hydroid *Aglaophenia parvula* (71% of stations) and the gorgonians *Leptogorgia riodouri* and *Eunicella filiformis* (55%) (Ramil et al., 2012a, b).

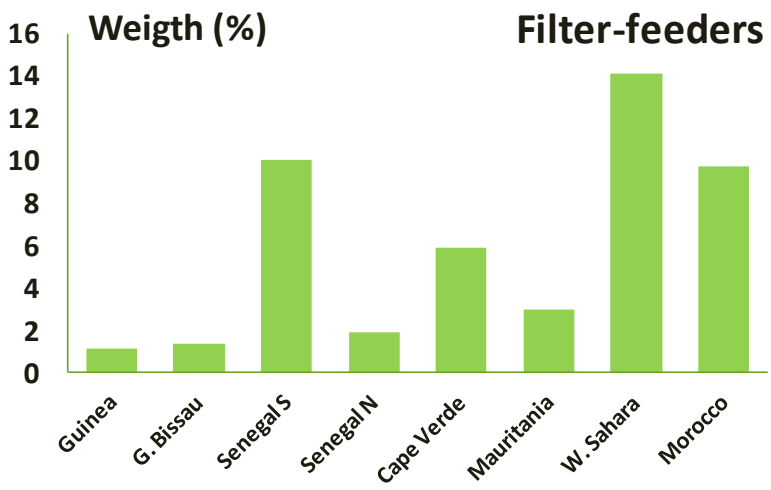

Figure 5.3.7. Weight (in percentage) of suspension-feeder epibenthos in the different areas of the CCLME region (from Ramos et al., 2012)

Also in deep waters of Western Sahara and Morocco, important communities of the hexactinellid *Pheronema carpentieri* and giant Geodidae, mainly *Geodia megastrella* and *Geodia barretti*, were located during the Spanish-Moroccan joint surveys (Palte 5.3.2). In these areas, sponges constitute the main taxa in terms of diversity, abundance and biomass (31%-45% of total biomass) (Ramil et al., 2005; González-Porto et al., 2007). Although the presence of suspension-feeders in shallow waters is mainly related to the planktonic productivity that provides food for their development, in deep waters the existence of this type of community is related to bottom currents, which favour the resuspension, lateral transport and availability of organic matter. In the absence of bottom currents, the organic matter sediments on the bottom and the communities are mainly detritivorous (i.e. Holuthuroidea). This would be the case of Mauritanian slope soft-bottoms, from which megabenthic suspension-feeders are practically absent (Ramil and Ramos, submitted), representing only 9% of the abundance and 1% of epibenthic biomass (Castillo et al., submitted). The scarcity of big suspension-feeders in the deep sea could be related to the impact of fishing pressure in the area, where trawling fleets operate to a depth of 1000 m (FAO, 2006), but also to the unstable conditions on the slope, where turbidity currents and slumping (Ramos et al., 2010) prevent the development and survival of this type of fauna.

5.3.2.3. Vulnerable marine ecosystems

Corals and sponges are found among the invertebrates builders of three-dimensional and vulnerable habitats in coastal and deep waters worldwide. Although corals and other reef cnidarians are abundant in the Cape Verde archipelago (Almeida and Leary, 2011) and in the Canary Islands (Brito and Ocaña, 2004), and some hermatipic coral communities (reef-builders) exist in rocky bottoms of islands and littoral areas of the Gulf of Guinea (Laborel, 1974), in tropical West Africa authentic coral reefs have not been found to date (Sheppard et al., 2010). This feature has been primarily explained by the current hydroclimatic conditions of the region, mainly the existence of numerous rivers whose discharges result in high water turbidity, high sedimentation rates and low salinity, which prevent coral reef development. The Canary Current upwelling system (CCUS), characterized by the presence of cold waters, limits coral-reef formation in the north of the CCLME (Sheppard et al., 2010). Another important element appears to be the paleozoogeography, conditioned by the geological evolution of the Atlantic basin and by the abrupt climatic changes that occurred in West Africa during the glacial and interglacial periods in the Pleistocene, which

produced changes in the sea-level, shifting of permanent upwelling limits and the disappearance of the littoral biotopes, communities and species (Le Loeuff and von Cosel, 1998).

The existence of one, though not continuous, coral barrier of *Dendrophyllia ramea*, running parallel to the coast between 120 m and 180 m depth, from Cape Spartel to, at least, Cape Ghir, was already recorded in the fishing-ground maps of Gruvel (1925, 1929) and described by Maurin (1968). This author, in early bionomic works, and more recently Zibrowius (1980), reported the presence of deep corals, particularly *Lophelia pertusa*, in Moroccan and Western Saharan slopes, although both authors point out that they do not seem to be living corals. Maurin (1968) also described the typically deep cnidarian biocenosis on the Mauritanian slope, constituted by *Lophelia prolifera* (= *L. pertusa*), *Madrepora oculata* and other cnidarians, as well as the frequent presence of patches of *Dendrophyllia cornigera* and *Lophelia* at the edge of the canyons.

Recently, during the four Spanish-Mauritanian surveys (Maurit) carried out in deep waters of Mauritania, seabed maps were produced using multibeam echosounder, as well as the characterization of the geomorphological, oceanographic and faunistic levels of the cold-water coral reef, the canyon systems and a small seamount discovered south of Nouakchott (Ramos et al., 2010). The coral reef, reported for the first time by Colman et al. (2005), constitutes the biggest cold-water coral structure in the world, reaching a height of 100 m from the bottom (Ramos et al., submitted b). The coral structure runs along the Mauritanian slope more than 400 km, parallel to the shelf break, between the Senegalese border and Cape Timiris, and its framework is mostly composed of dead corals, although isolated patches of living *L. pertusa* are reported in several places (Colman et al., 2005; Westphal et al., 2007, 2012; Ramos et al., submitted b) (Plate 5.3.3).

Other important habitats on the Mauritanian continental margin are currently being studied by Spanish and German teams, namely the canyon system of Cape Timiris and Banc d'Arguin, and the seamount, where vulnerable ecosystems constituted by big sponges, corals and other suspension-feeders have been reported (Westphal et al., 2007, 2012; Sanz et al., submitted a, b) (Plate 5.3.3).

5.3.3. CONCLUSIONS

Information on benthos biodiversity is scarce in the CCLME and inventories of marine fauna are only available for Morocco and the Canary Islands; a regional report was recently compiled in the framework of the CCLME project. A major review of benthic biodiversity in West Africa was carried out by Le Loeuff and Von Cosel (1998), who reported the highest specific richness between Cape Blanc (Mauritania) and Cape Verga (Guinea Bissau). Although a latitudinal biodiversity pattern was not observed, preliminary results of R/V *Dr. Fridtjof Nansen* and *Vizconde de Eza* surveys recorded the highest diversity values in Western Sahara and also higher diversity on the shelf and upper slope than in deep waters. An important faunistic change between tropical and temperate biota has been reported at Cape Blanc latitude. The zoobenthos of Cape Verde and the Canary Islands shows some specific features linked to their volcanic origin, insularity and oceanographic conditions.

Epibenthic communities maintain a similar structure throughout the region, despite the differences in their specific composition. Decapods seem to be the most important group, in terms of both abundance and biomass, being other representative taxa molluscs, echinoderms, sponges, cnidarians and polychaetes. Echinoderms, mainly holothuroids, are clearly dominant in deep waters. Suspension-feeder assemblages,

previously recorded in the entire upwelling area, do not seem to play an important role in the current epibenthic communities.

Although tropical coral reefs have not been reported in NWA, vulnerable ecosystems, like the giant cold-water coral reef, canyon systems, seamount and grounds of sponges and gorgonians, still exist in deep waters of the continental slope, despite the intensive fishing exploitation over more than 50 years.

Studies focused on these important vulnerable marine ecosystems, as well as on the currently unknown bottoms of deep-shelf and slope (Senegal, Guinea-Bissau, Guinea and Cape Verde), are strongly recommended in order to protect these deep-water areas threatened by the trawling fleets' displacement and by the oil and mineral resources exploitation.

The assessment of the main benthic taxa during scientific and commercial demersal surveys would improve the ecosystem approach to marine resources management and also help keep track of changes in benthic biodiversity over time. Benthic research in regional marine scientific institutes should be promoted and strengthened and be considered as a highest priority line.

Acknowledgements

The authors wish to express their sincere gratitude to all their helpful colleagues, who for over 10 years have collected and studied the benthos of NWA, both, on board and in the laboratories of the IEO and the University of Vigo. This work was undertaken within the framework of the EcoAfrik project and has been partially funded by the MAVA Fondation pour la Nature (MAVA contract 12/87 AO C4/2012). This is EcoAfrik publication number 24.

Plate 5.3.1. Some diverse ecosystems and main epibenthic species of Northwest African shelf: bottoms of *Munida* and sea-urchins (1), coralinaceans (2), *Pinna* seabeds (3) and tubicoles polychaetes (4), *Centrostephanus longispinus* (5), *Parastichopus regalis* (6), *Munida speciosa* (7), *Cassis tuberosa* (8), *Goniaster tesellatus* (9), *Cymbium* sp. (10) and *Pinna* sp. (11). © Ana Ramos

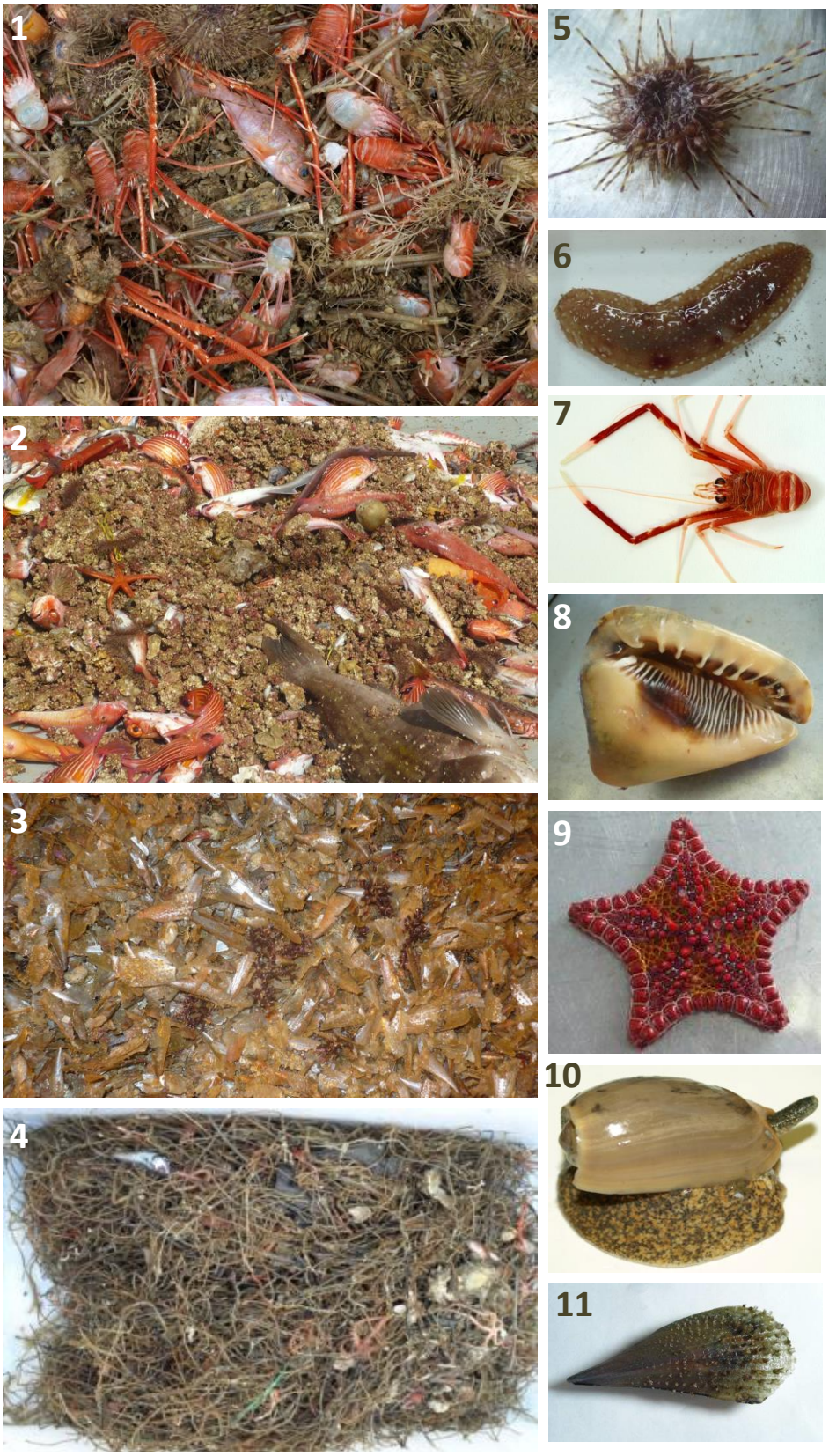

Plate 5.3.2. Deep-sea ecosystems of Northwest African slope: Crustaceans and echinothuroids (12), *Funiculina* bottoms (13), holothurids (14) and sponges (15), *Enypniastes eximia* (16), *Benthothuria funebris* (17), *Phormosoma placent*a (18), *Hymenaster roseus* (19) and *Pheronema carpentieri* (20). © Ana Ramos

Plate 5.3.3. Vunerable marine ecosystems of Northwest African slope and shelf: Cold-water coral, sponges and brittle-star assemblages in the giant reef (21), canyons (22) and seamount (23) off Mauritania; gorgonians over shelf's *Pinna* bottoms (24), *Lophelia pertusa* (25), Geodidae (26), *Leiopathes* sp. (27), *Suberites* sp. (28) and *Leptogorgia* sp. (29). © Ana Ramos

5.4. CEPHALOPODS IN THE CANARY CURRENT LARGE MARINE ECOSYSTEM

Francisco ROCHA[1] and Inejih CHEIKH[2]

[1] University of Vigo. Spain

[2] DDECOMAR. Mauritania

5.4.1. INTRODUCTION

The Canary Current Large Marine Ecosystem (CCLME) ranks third in the world in terms of primary productivity and has one of the highest fisheries production of any African large marine ecosystem with an annual production ranging from 2 to 3 million t (Déniz-González et al., 2014). The CCLME cephalopods are characterized by high abundance, biomass and diversity. In the case of Mauritanian waters a total of 132 species and 39 families have been identified (Rocha et al., submitted). These results concur with the maximum diversity of cephalopods observed in the tropics and subtropics by Nesis (2003). Many species present in CCLME waters have a worldwide distribution or have been previously reported in Atlantic waters (Roper et al., 1984; Nesis, 1987; Mangold, 1998; Jereb and Roper, 2005; Jereb and Roper, 2010; Jereb et al., 2013; Guerra et al., 2014). In this region, species of the families Ommastrephidae, Loliginidae, Octopodidae and Sepiidae represent the main cephalopod resources with high commercial value (Boyle and Rodhouse, 2005), which explains why in this region we find one of the largest cephalopod fisheries in the Eastern Atlantic (Faure et al., 2000; FAO, 2014c).

This work presents a brief review of cephalopod fauna found in CCLME waters in terms of biodiversity, ecology and fisheries.

5.4.2. SPECIES BIODIVERSITY

A recent study (Rocha et al., submitted) shows a high diversity of cephalopod species in the CCLME area. This marine ecosystem presents 139 cephalopod species (Table 5.4.1), including high commercial value groups (Ommastrephids, Loliginids, Octopods and Sepiids).

Sepiids are mainly coastal species associated with the continental shelf and slope up to 500 m depth (Jereb and Roper, 2005). Eight sepiid species have been cited in the area (Table 5.4.1). The most abundant and commercially important sepiid species is *Sepia officinalis* (Nigmatullin, personal communication), although other species such as *S. bertheloti*, *S. elegans*, *S. hierredda* and *S. orbignyana* are also abundant in CCLME coastal waters (Nesis, 1987; Jereb and Roper, 2005; Rocha et al., submitted).

A total of 14 sepiolid species can be observed in this area (Jered and Roper, 2005; Rocha et al., submitted). Of limited commercial interest, probably the most abundant species in the area correspond to *Sepietta oweniana*, *S. neglecta* and *Sepiola rondeletii*.

The unique species of the family Spirulidae, the mesopelagic *Spirula spirula*, is also present in the area (Jereb and Roper, 2005).

Table 5.4.1. CCLME cephalopods checklist with data about their habitat, bathymetry and fishery potential. Abisal (A), Benthic (Be), Demersal (D), Neritic (N), Pelagic (P): Epipelagic (E), Mesopelagic (M), Bathypelagic (Ba), Not determined (?).

Species	Habitat	Deep range (m)	Fishery potential
ORDER: SEPIOIDEA Naef, 1916			
SUBORDER: SEPIIDA Keferstein, 1866			
Family SEPIIDAE Keferstein, 1866			
Sepia angulata Roeleveld, 1972	N	?	?
Sepia bertheloti d'Orbigny, 1835	N	20-160	YES
Sepia elegans Blainville, 1827	N-D	0-500	YES
Sepia elobyana Adam, 1941	N	?	?
Sepia hierredda Rang, 1835	N	0-50	YES
Sepia officinalis Linnaeus, 1758	N	0-200	YES
Sepia orbignyana Férussac in d'Orbigny, 1826	N-D	15-570	YES
Sepiella ornata (Rang, 1837)	N	0-100	YES
SUBORDER SEPIOLIDA Fioroni, 1981			
Family SEPIOLIDAE Leach, 1817			
Subfamily SEPIOLINAE Appellöf, 1898			
Rondeletiola minor (Naef, 1912)	N-D	80-500	YES
Sepiola atlantica Orbigny. 1839-1842	N	0-100	NO
Sepiola knudseni Adam, 1983	N	32-90	?
Sepiola rondeleti Leach, 1834	N-D	0-450	NO
Sepietta neglecta Naef, 1916	N	25-475	YES
Sepietta oweniana (Orbigny, 1839-1841)	N-P(E-M)	0-1000	YES
Sepietta petersi (Steenstrup, 1887)	N	20-350?	?
Subfamily ROSSIINAE Appellöf, 1898			
Austrorossia mastigophora (Chun, 1915)	N	0-640	?
Neorossia caroli (Joubin, 1902)	N-D	40-1750	YES?
Rossia macrosoma (Delle Chiaie, 1830)	N-D	32-900	YES
Subfamily HETEROTEUTHINAE Appellöf, 1898			
Heteroteuthis dagamensis Robson, 1924	?	?	?
Heteroteuthis dispar (Rüppell, 1844)	N-P(M)-Be	0-1600	NO
Stoloteuthis leucoptera (Verrill, 1878)	N-D	160-700	?
Family IDIOSEPIIDAE Appellöf, 1898			
Idiosepius minimus (Orbigny, 1835)	N	0-80	NO
ORDER SPIRULIDA Stolley, 1919			
Family SPIRULIDAE Owen, 1836			
Spirula spirula (Linnaeus, 1758)	P(M)	0-700	NO
ORDER MYOPSIDA Naef, 1916			
Family LOLIGINIDAE Lesueur, 1821			
Afrololigo mercatoris (Adam, 1941)	N	0-50	YES
Alloteuthis africana Adam 1950	N	20-100	YES
Alloteuthis media (Linnaeus, 1758)	N	0-200	YES
Alloteuthis subulata (Lamarck, 1798)	N-D	0-500	YES
Loligo forbesii Steenstrup, 1856	N-D	0-1000	YES
Loligo vulgaris Lamarck, 1798	N-D	0-500	YES
ORDER OEGOPSIDA Orbigny, 1845			
Family ANCISTROCHEIRIDAE Pfeffer, 1912			
Ancistrocheirus lesueurii (d'Orbigny, 1842)	P(E-M)	0-700	YES
Family ARCHITEUTHIDAE Pfeffer, 1900			
Architeuthis dux Steenstrup, 1857	P(M)	200-1000	NO

Species	Habitat	Deep range (m)	Fishery potential
Family BATHYTEUTHIDAE Pfeffer, 1900			
Bathyteuthis abyssicola Hoyle, 1885	P(M-B)	200-1400	NO
Family BRACHIOTEUTHIDAE Pfeffer, 1908			
Brachioteuthis behnii (Steenstrup, 1882)	P(E-M)	50-1000	NO
Brachioteuthis picta Chun, 1910	P	0-3000	NO
Brachioteuthis riisei (Steenstrup, 1882)	P(E-M)	0-1000	NO
Family CHIROTEUTHIDAE Gray, 1849			
Chiroteuthis joubini Voss, 1967	P	?	NO
Chiroteuthis veranyi (Ferussac, 1834)	P	0-1800	NO
Grimalditeuthis bonplandi (Verany, 1839)	P(M-Ba)	200-1000	NO
Planctoteuthis danae (Joubin, 1930)	P	?	NO
Planctoteuthis exophthalmica (Chun, 1908)	P	?	NO
Family CHTENOPTERYGIDAE Grimpe, 1922			
Chtenopteryx canariensis Salcedo-Vargas and Guerrero-Kommritz, 2000	P(M)	200-1000	NO
Chtenopteryx sicula (Verany, 1851)	P(M)	200-1000	NO
Family CRANCHIIDAE Prosch, 1847			
Subfamily CRANCHIINAE Pfeffer, 1912			
Cranchia scabra Leach, 1817	P(M-B)	200-2000	NO
Leachia atlantica (Degner, 1925)	P(E-M)	50-1000	NO
Liocranchia reinhardti (Steenstrup, 1856)	P	50-1200	NO
Subfamily TAONIINAE Pfeffer, 1912			
Bathothauma lyromma Chun, 1906	P	0-2000	NO
Egea inermis Joubin, 1933	P	0-2000	NO
Galiteuthis armata Joubin, 1898	P	0-2500	NO
Helicocranchia joubini (Voss, 1962)	P	100-2000	NO
Helicocranchia pfefferi Massy, 1907	P	0-2000	NO
Liguriella podophthalma Issel, 1908	P	0-1500	NO
Megalocranchia oceanica (Voss, 1960)	P	50-2000	NO
Sandalops melancholicus Chun, 1906	P	0-2000	NO
Taonius pavo (Lesueur, 1821)	P	150-2000	NO
Teuthowenia maculata (Leach, 1817)	P	25-2000	NO
Family CYCLOTEUTHIDAE Naef, 1923			
Cycloteuthis akimushkini Filippova, 1968	P(M)	200-1000	NO
Cycloteuthis sirventi Joubin, 1919	P(M)	200-1000	NO
Discoteuthis discus Young and Roper, 1969	P(M)	200-1000	NO
Discoteuthis laciniosa Young and Roper, 1969	P(M)	200-1000	NO
Family ENOPLOTEUTHIDAE Pfeffer,			
Abralia siedleckyi Lipinski, 1983	P(E-M)	0-600	NO
Abralia veranyi (Rüppel, 1844)	P(E-M)	0-600	NO
Abraliopsis atlantica Nesis, 1982	P(E-M)	0-600	NO
Abraliopsis morissi (Verany, 1839)	P(E-M)	0-600	NO
Enoploteuthis anapsis Roper, 1964	P(E)	0-200	?
Enoploteuthis leptura (Leach, 1817)	P(E)	0-200	YES
Family HISTIOTEUTHIDAE Verrill, 1881			
Histioteuthis arcturi (Robson, 1948)	P(E-M)	0-1000	NO
Histioteuthis bonnellii (Ferussac, 1834)	P(M-Ba)	500-2000	NO
Histioteuthis celetaria (Voss, 1960)	P(E-M)	40-1000	NO
Histioteuthis corona (Voss and Voss, 1962)	P	100-1500	NO
Histioteuthis meleagroteuthis (Chun, 1910)	P	0-2000	NO
Histioteuthis reversa (Verrill, 1880)	P	0-1000	NO
Family JOUBINITEUTHIDAE Naef, 1922			
Joubiniteuthis portieri (Joubin, 1916)	P(M-Ba)	300-2500	NO
Family LEPIDOTEUTHIDAE Pfeffer, 1912			
Lepidoteuthis grimaldii Joubin, 1895	P	100-2000	NO
Family LYCOTEUTHIDAE Pfeffer, 1908			
Subfamily LYCOTEUTHINAE Pfeffer, 1908			
Selenoteuthis scintillans Voss, 1959	P(E-M)	0-600	NO
Subfamily LAMPADIOTEUTHINAE Berry, 1916			
Lampadioteuthis megaleia Berry, 1916	P(E-M)	0-300	NO
Family MAGNAPINNIDAE Vecchione and Young, 1998			
Magnapinna talismani (Fisher and Joubin, 1907)	P	0-3000?	NO

Species	Habitat	Deep range (m)	Fishery potential
Family MASTIGOTEUTHIDAE Verrill, 1881			
Mastigoteuthis agassizii Verrill, 1881	P(M)	700-1000	NO
Mastigoteuthis atlantica Joubin, 1933	P(M)	600-1000	NO
Mastigoteuthis danae (Joubin, 1933)	P(M)	600-1000	NO
Mastigoteuthis flammea Chun, 1910	P-A	100-3500	NO
Mastigoteuthis hjorti Chun, 1913	P(M)	600-1000	NO
Mastigoteuthis magna Joubin, 1913	P(M)	600-1000	NO
Family NEOTEUTHIDAE Naef, 1921			
Neoteuthis thielei Naef, 1921	P(E-M)	100-2000	NO
Family OCTOPOTEUTHIDAE Berry, 1912			
Octopoteuthis danae Joubin, 1931	P(E)	50-100?	NO?
Octopoteuthis megaptera (Verrill, 1885)	P(M-Ba)	200-2000	NO?
Octopoteuthis rugosa Clarke, 1980	P(M)	200-800	NO?
Octopoteuthis sicula Rüppell, 1844	P(M-Ba)	200-2000	NO?
Taningia danae Joubin, 1931	P	0-1300	YES
Family OMMASTREPHIDAE Steenstrup, 1857			
Subfamily ILLICINAE Posselt, 1891			
Illex coindetii (Verany, 1839)	N-D	0-1000	YES
Subfamily OMMASTREPHINAE Posselt, 1891			
Hyaloteuthis pelagica (Bosc, 1802)	P(E-M)	0-800	YES
Ommastrephes bartramii (Lesueur, 1821)	P	0-1500	YES
Ornithoteuthis antillarum Adam, 1957	P	0-1500	YES
Sthenoteuthis pteropus (Steenstrup, 1855)	P	0-1200	YES
Subfamily TODARODINAE Adam, 1960			
Todaropsis eblanae (Ball, 1841)	N-D	20-850	YES
Todarodes sagittatus (Lamarck, 1798)	P(E-M)	0-1000	YES
Family ONYCHOTEUTHIDAE Gray, 1849			
Ancistroteuthis lichtensteini (Férussac, 1835)	P	0-1300	YES
Onychoteuthis banksii (Leach, 1817)	P-A	0-4000	YES
Onykia carriboea Lesueur, 1821	P	0-?	?
Walvisteuthis virilis Nesis and Nikitina, 1986	P(E-M)	0-500	NO
Family PHOLYDOTEUTHIDAE Voss, 1956			
Pholidoteuthis massyae (Pfeffer, 1912)	P(M-Ba)	200-1500	NO?
Family PYROTEUTHIDAE Pfeffer, 1912			
Pterygioteuthis gemmata Chun, 1908	P(E-M)	150-600	NO
Pterygioteuthis giardi Fischer, 1896	P(E-M)	0-500	NO
Pyroteuthis margaritifera (Rüppel, 1844)	P(E-M)	50-800	NO
Family THYSANOTEUTHIDAE Keferstein, 1866			
Thysanoteuthis rhombus Troschel, 1857	P(E-M)	100-800	YES
ORDER OCTOPODA Leach, 1818			
SUBORDER CIRRATA Grimpe, 1916			
Family CIRROTEUTHIDAE Keferstein, 1866			
Cirrothauma magna Hoyle, 1885	P(Ba)-A	1300-3359	NO
Cirrothauma murrayi Chun, 1911	P(Ba)-A	2400-4850	NO
Family OPISTHOTEUTHIDAE Verrill, 1896			
Opisthoteuthis agassizii Verrill, 1883	P(M-Ba)	227-2000	NO
Opisthoteuthis calypso Villanueva, Collins, Sánchez and Voss, 2002	P(M-Ba)	365-2208	NO
Opisthoteuthis grimaldii (Joubin, 1903)	P(Ba)	1135-2287	NO
Opisthoteuthis massyae (Grimpe, 1920)	P(Ba)	1226-1450	NO
Family GRIMPOTEUTHIDAE O'Shea, 1999			
Grimpoteuthis megaptera (Verrill, 1885)	A	4592	NO
Grimpoteuthis wuelkeri (Grimpe, 1920)	P(Ba)	1550-2056	NO
SUBORDER INCIRRATA Grimpe 1916			
Family ALLOPOSIDAE Verrill, 1881a			
Haliphron atlanticus Steenstrup, 1861	P-A	0-6787	NO
Family ARGONAUTIDAE Tryon, 1879			
Argonauta argo Linnaeus, 1758	P(E-M)	0-300	NO
Argonauta hians Lightfoot, 1786	P(E-M)	0-300	NO

Species	Habitat	Deep range (m)	Fishery potential
Family TREMOCTOPODIDAE Tryon, 1879			
Tremoctopus gelatus Thomas, 1977	P(E-M)	0-250	NO
Tremoctopus violaceus Delle Chiaie, 1830	P(E-M)	0-250	NO
Family AMPHITRETIDAE HOYLE, 1886			
Amphitretus pelagicus thielei Robson, 1930	P(E-M)	100-2000	NO
Family OCTOPODIDAE Orbigny, 1840			
Subfamily OCTOPODINAE Grimpe, 1921			
Amphioctopus burryi Voss, 1950	Be	200-400	?
Benthoctopus pseudonymus (Grimpe, 1922)	Be	1600	?
Callistoctopus macropus (Risso, 1826)	Be	0-200	YES
Macrotritopus defilippi (Verany, 1851)	Be	0-200	?
Octopus vulgaris Cuvier, 1797	Be	0-250	YES
Pteroctopus tetracirrhus (Delle Chiaje, 1830)	Be	25-720	YES
Scaeurgus unicirrhus (Delle Chiaje, 1830)	Be	50-500	?
Subfamily ELEDONINAE Grimpe, 1921			
Eledone caparti Adam, 1950	Be	64-150	?
Subfamily BATHYPOLYPODINAE Robson, 1928			
Bathypolypus arcticus (Prosch, 1849)	Be	37-1210	?
Bathypolypus biardii (Verrill, 1873)	Be	20-1545	?
Bathypolypus ergasticus (Fischer and Fischer, 1892)	Be	450-1400	?
Bathypolypus sponsalis (Fischer and Fischer, 1892)	Be	930-1250	?
Bathypolypus valdiviae (Thiele, in Chun, 1915)	Be	200-1000	?
Subfamily GRANELEDONINAE Voss, 1988			
Graneledone verrucosa (Verril, 1881)	Be	850-2300	?
Familia Enteroctopodidae Strugnell et al., 2014			
Muusoctopus fuscus (Taki, 1964)	Be	600-1000	?
Muusoctopus januarii (Hoyle, 1885)	Be	350-750	?
Family OCYTHOIDAE Gray, 1849			
Ocythoe tuberculata Rafinesque, 1814	P(E)	0-200	YES
Family BOLITAENINAE Chun, 1911			
Bolitaena pygmaea (Verrill, 1884)	P	100-1400	NO
Japetella diaphana Hoyle, 1885	P(M)	200-1000	NO
Family VITRELEDONELLIDAE Robson, 1932			
Vitreledonella richardi Joubin, 1918	P(E-M)	0-1000	NO
ORDER VAMPYROMORPHIDA Pickford, 1939			
Family VAMPYROTEUTHIDAE Thiele, in Chun, 1915			
Vampyroteuthis infernalis Chun, 1903	P(M-Ba)	600-1200	NO

Six loliginid squids can be found in coastal waters (Table 5.4.1). Of special importance is *Loligo vulgaris*, one of the most common neritic squids on the northeastern Atlantic and Mediterranean coast. This species lives in the continental shelf and upper slope waters, at up to 500 m depth (Worms, 1983; Jereb and Roper, 2010). In African waters, *L. vulgaris* is distributed over the inner continental shelf, between 50 and 150 m depth, associated with the Mauritanian and Canary currents (Arkhipkin and Laptikhovsky, 2006). Other significant loliginids are *Alloteuthis africana* and *A. subulata*. According to Arkhipkin and Laptikhovsky (2006), from the north to the south, *A. subulata* is distributed over the Mauritanian-Senegalese continental shelf and is gradually replaced by *A. africana* in tropical African waters.

Oegopsid squids represent the most abundant group with 75 species (Table 5.4.1). Most of them correspond to continental slope and oceanic species. Probably the ommastrephids represent the most important group in the area with 7 species. Among these species three seem to be more significant, and we will describe them below. *Todarodes sagittatus* is an oceanic species distributed in the Eastern Atlantic Ocean that inhabits this region from the outer continental shelf to the upper slope, at depths ranging from 65 m to 1800 m (Nigmatullin et al., 2002; Arkhipkin and Laptikhovsky, 2006; Rocha et al., submitted). *Illex coindetii* is a demersal species widely distributed on the continental shelf and upper slope of both eastern

and western coastlines of the Atlantic Ocean (Roper et al., 1998; Sánchez et al., 1998; Jereb and Roper, 2010; González and Guerra, 2013). Its presence in CCLME waters is associated with the continental shelf and upper slope waters, concurring with the findings of Arkhipkin and Laptikhovsky (2006). *Todaropsis eblanae* is a species present in the Eastern Atlantic Ocean (Jereb and Roper 2010). This species presents significant abundance levels associated with the continental shelf and upper slope waters (Arkhipkin and Laptikhovsky, 2006; Rocha et al., submitted). Other species, such as enoploteuthid squids, are relatively abundant in slope waters, although their biomass is not significant because of their small size (Nesis, 1987; Rocha et al., submitted).

Octopods probably represent the less known cephalopod group in the area with 34 species (Table 5.4.1). Shallow-water species are better-known than deep-water species. Of these, *Octopus vulgaris* is the most widely found and studied octopod species in the area (Hatanaka, 1979; Rocha et al., submitted). This is a shallow-water coastal benthic species that lives between the surface and 100 m depth, rarely deeper (Mangold, 1998; Boyle and Rodhouse, 2005). Other species, such as *Pteroptopus tetracirrhus,* are abundant in platform and continental slope waters (Jereb et al., 2013). New records of incirrate octopods of the genus *Muusoctopus* and *Bathypolypus* in Mauritanian waters (Rocha et al., submitted) add to the list of deep benthic cephalopods in the area. *Muusoctopus* species may be a common element of benthic octopod fauna on the CCLME continental slope, as these species can be caught in the region, but these may have been identified as *Benthoctopus* specimens. *Bathypolypus* species may be frequent in deep waters associated with the Canary Current and cold deep waters (Rocha et al., submitted).

Finally, the vampiroteuthid *Vampyroteuthis infernalis* is also reported and seems to be relatively frequent in these waters (Jereb et al., 2013; Rocha et al., submitted).

5.4.3. CEPHALOPOD ASSEMBLAGES AND ECOLOGY

The CCLME constitutes a transitional faunistic region in which tropical, subtropical and boreal species are mixed, probably associated with specific water masses (Arkhipkin and Laptikhovsky, 2006; Rocha et al., submitted).

Table 5.4.1 presents the habitat and distribution deep range of the species present in this region. The cephalopod assemblages in the CCLME area can be divided into three ecological groups in relation to the habitat: bottom, near-bottom and true pelagic species, integrating data about local species, wide distribution species permanently resident in the studied area, and periodical species which inhabit the adjoining waters (Nigmatullin, personal communication). Accordingly, several assemblages can be identified in the zone corresponding to the horizontal speciation and stratification pattern of cephalopod fauna recorded in the world's oceans (Nesis, 2003). Rocha et al. (submitted) identified two assemblages in Mauritanian waters. On the one hand, there is the Shelf Assemblage with two main species, *I. coindetii* and *T. eblanae*, corresponding to bottom-associated neritic species, usually living near the coast (Jereb and Roper, 2010). Other species of this assemblage are benthic or demersal shallow-water species, such as *O. vulgaris* or *S. elegans*, both living close to the coast (Jereb and Roper, 2005; Jereb et al., 2013). On the other hand, the Slope Assemblage is mainly composed of pelagic species such as *T. sagittatus*, which lives outside of continental shelf waters (Jereb and Roper, 2010). This more "pelagic" assemblage is composed of oceanic species and deep benthic and bathyal octopuses (Rocha et al., submitted).

Both assemblages can be divided according to their habitat in: Coastal, Slope, Pelagic and Deep Benthic assemblages (Plates 5.4.1 and 5.4.2). The Coastal Assemblage includes coastal shallow-water species such as *O. vulgaris* and sepiids near the coast and loliginids on the upper slope. The Slope Assemblage includes bottom-associated neritic species such as the ommastrephids *I. coindetii* and *T. eblanae*. The Pelagic Assemblage is composed of pelagic oceanic species such as *T. sagittatus* and *Opisthoteuthis agassizii*. Finally, the Deep Benthic Assemblage includes mainly benthic deep-water octopus species such as *Muusoctopus* and *Bathypolypus.*

The cephalopod fauna of the CCLME is composed of a mixture of tropical to temperate pelagic, demersal and benthic species living over the shelf and in open waters, and cold water benthic species living on the deep slope. Thus, the zone is a transitional area between different zoogeographic provinces, where different water masses from the North and South Atlantic Ocean are present (Nesis, 2003; Arkhipkin and Laptikhovsky, 2006).

5.4.4. CEPHALOPOD FISHERIES

The cephalopod resources in the CCLME represent one of the most substantial fisheries in the Atlantic region (FAO, 2014c), ranging from 80,000 t yr^{-1} to 200,000 t yr^{-1}. The bulk of the catches of cephalopods in the zone are presented in Figure 5.4.1. The level of global cephalopod catches has decreased sharply from a mean of 165,000 t to 91,000 t in the recent period. Most of these catches come from fishing grounds located off the African coast (Fig. 5.4.2). This level of catch is to be seen against catches in other CCLME countries like Guinea-Bissau (approximately 4,000 t in 2012) and Guinea (6,000 t, unpublished data). However, these data include few commercial catch data relating to squid, cuttlefish and octopus species. Most small-scale local fisheries on African coasts lack descriptive statistics making it impossible to identify the species caught. *Octopus vulgaris* is currently the main species exploited by artisanal and industrial fisheries in the coastal waters (Hatanaka, 1979; Balguerías et al., 2002; Jereb et al., 2013).

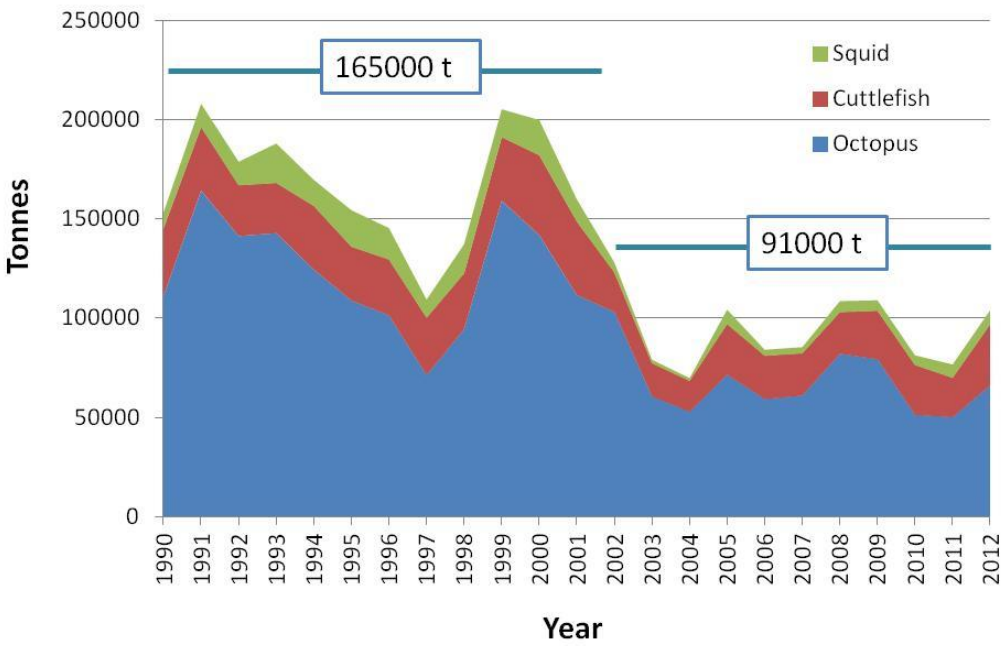

Figure 5.4.1. Cephalopod catches in the area of Morocco (Atlantic), Western Sahara, Mauritania, Senegal and Gambia (derived from CECAF statistics presented in FAO, in press c).

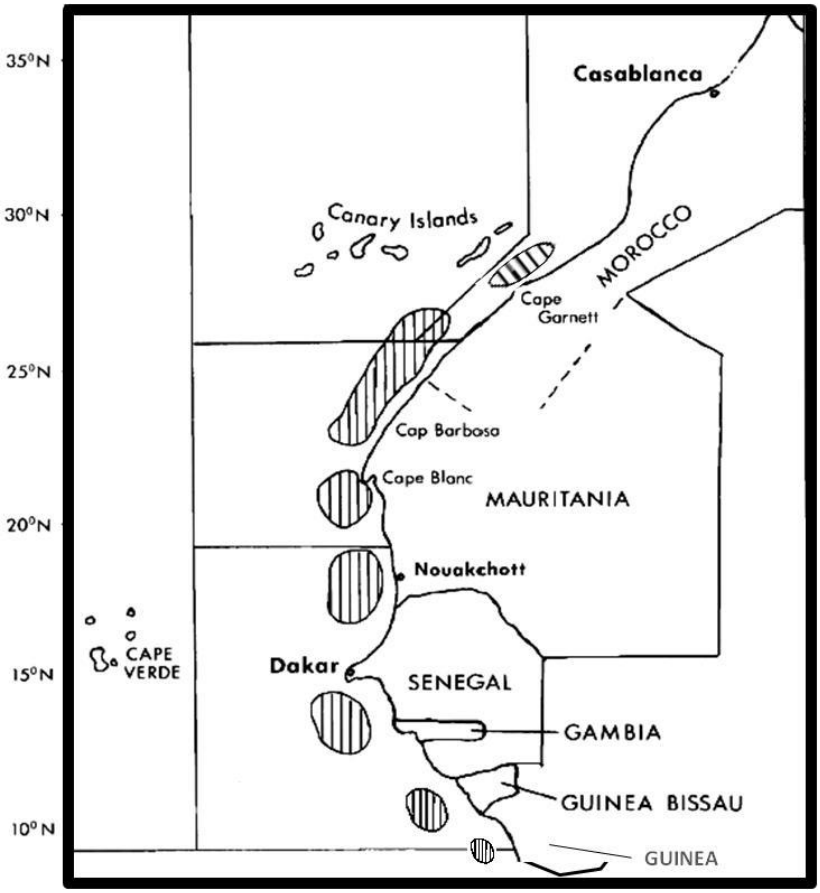

Figure 5.4.2. Main fishing grounds located off the African coast into the CCLME. Based on Grant et al., 1981.

Fishing techniques for cephalopods used in the CCLME, especially along the African coast, are diverse. These species are fished for both artisanal and industrial fisheries, using trawl, traps, diving, jigging and other diverse fishing techniques (Table 5.4.2).

Table 5.4.2. Diversity of the gear used for fishing cephalopods in the CCLME.

Target species	Main fishing technique	Accessory fishing technique
Octopus	Trawl, Pot, Trap, Jig	Diving
Cuttlefish	Trap, Trawl	Jig
Squids	Trawl	

Loliginid and sepiid species constitute substantial resources exploited by coastal fisheries. *Loligo vulgaris* is fished throughout its distributional range by multispecific trawlers and small-scale fishing units. Other species, such as *A. africana* and *A. subulata,* are two small-sized loliginid species caught as bycatch by trawlers, but with no separate statistical data. *Sepia elegans* is the most abundant and commercially important sepiid species (Khromov et al., 1998; Jereb and Roper, 2005, 2010).

Ommastrephid squids probably represent the main potential resource for cephalopod pelagic and trawl fisheries in the area. Three species present great potential for fisheries in the zone. *Todarodes sagittatus* is a potential resource for more pelagic fisheries; it is intermittently fished in Norwegian waters, in the Mediterranean Sea and off the North African coast (Dunning and Wormuth, 1998; Nigmatullin et al., 2002; Jereb and Roper, 2010). *Illex coindetii* is a demersal species caught by bottom trawl and gillnet fleets as bycatch, accounting for a conspicuous fraction of the ommastrephid catches in Mediterranean and Atlantic waters (González et al., 1996; Sánchez et al., 1998; Jereb and Roper, 2010; González and Guerra, 2013). *Todaropsis eblanae* is taken mainly as bycatch in trawl and small-scale fisheries (González et al., 1996; Robin et al., 2002; Jereb and Roper, 2010). In the CCMLE waters this species can present significant abundance levels, also associated with the continental shelf and upper slope waters (Arkhipkin and Laptikhovsky, 2006; Rocha et al., submitted).

5.4.5. CONCLUSIONS

The CCLME waters exhibit a rich cephalopod fauna in comparison with other areas of the world's oceans. These waters are a transitional zone between different Atlantic zoogeographic provinces where tropical, temperate and cold water cephalopod species mix.

Several assemblages can be identified in the coastal, shelf, slope and deep waters. Coastal assemblages are dominated by sepiids, loliginids and shallow-water octopus, while more oceanic assemblages are largely dominated by ommastrephid and deep-water octopus species.

This area shows cephalopod resources that can maintain local and trawl fisheries for these resources, mainly for coastal octopus, neritic loliginids and more pelagic ommastrephids.

Acknowledgements

This work has been partially funded by the MAVA Foundation pour la Nature (MAVA contract 12/87 AO C4/2012). It was undertaken within the framework of the ECOAFRIK project under ECOAFRIK publication number 26.

Plate 5.4.1. Cephalopods species found in Coastal (1, 2, 3) and Slope (4, 5, 6) assemblages of CCLME Region. 1. *Octopus vulgaris* (© Ana Ramos); 2. *Sepia elegans* (© Lourdes Fernández); 3. *Sepia hierredda* (© José F González); 4. *Loligo vulgaris* (© Lourdes Fernández); 5. *Todaropsis eblanae* (© Lourdes Fernández) and 6. *Illex coindetii* (© Lourdes Fernández).

1

2

3

4

5

6

Plate 5.4.2. Cephalopods species found in Pelagic (1, 2, 3) and Deep Benthic (4, 5, 6) assemblages of CCLME Region. 1. *Todarodes saggitatus* (© Lourdes Fernández); 2. *Opisthoteuthis agassizii* (© Ana Ramos); 3. *Galiteuthis armata* (© Ana Ramos); 4. *Muusoctopus januari* (© Ana Ramos); 5. *Bathypolypus ergasticus* (© Ana ramos) and 6. *Bathypolypus valdiviae* (© Ana Ramos).

1

2

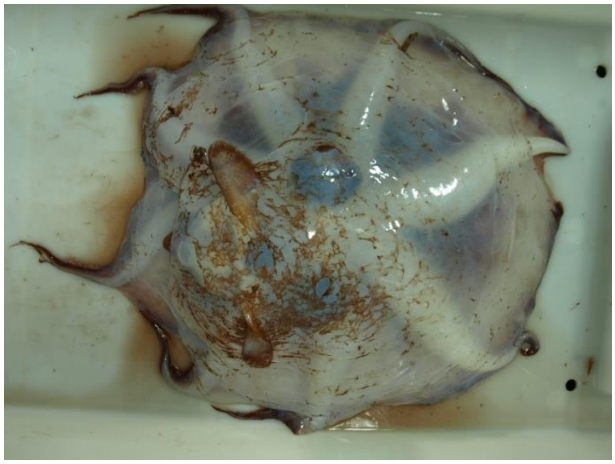

3

4

5

6

5.5. BIODIVERSITY AND BIOGEOGRAPHY OF DECAPOD CRUSTACEANS IN THE CANARY CURRENT LARGE MARINE ECOSYSTEM

Eva GARCÍA-ISARCH[1] and Isabel MUÑOZ[2]

[1] Centro Oceanográfico de Cádiz, Instituto Español de Oceanografía. Spain

[2] Centro Oceanográfico de Santander, Instituto Español de Oceanografía. Spain

5.5.1. INTRODUCTION

Crustaceans constitute one of the most morphologically diverse taxonomic groups on the planet (Martin and Davis, 2001). Among them, decapods are the most studied taxon, mainly on account of the commercial interest of some species and their great diversity. Decapods are mainly composed of marine species that live in waters depths ranging from shallow to deeper than 5000 m. The importance of this group lies in several factors such as the great biomass they represent, their significant role in marine food webs and the commercial interest of many decapod species.

The main morphologic types of Decapoda (the word means "ten legs") include: (i) shrimps and prawns (Dendrobranchiata -Penaeidae- and families Caridea, Stenopodidea and Axiidea), (ii) crabs (Brachyura), (iii) lobsters (infraorders Astacidea and Achelata) and (iv) squat lobsters and hermit crabs (Anomura).

A number of expeditions have been carried out in West African waters since the 19th century with the aim of studying their marine environment and fauna, which involved the first studies on crustaceans including part of the entire Canary Current Large Marine Ecosystem (CCLME) region. This is the case of the *Travailleur* and *Talisman* expeditions in the 19th century (Milne-Edwards and Bouvier, 1892, 1900), and the worldwide voyage of the HMS *Challenger* (Bate, 1888). In the 20th century, the expeditions *Mercator* (1935-1936 and 1938), *Atlantide* (1945 and 1946) and *Calypso* (1956) contributed to a better knowledge of different decapod groups in West Africa (Capart, 1951; Holthuis, 1951; Crosnier and Forest, 1965, 1966; Miyake and Baba, 1970; Saint Laurent and Le Loeuff, 1979). Some crustacean species from Moroccan Atlantic waters, Western Sahara and Mauritania were collected during the cruises on board the R/V *Meteor* in 1967, 1970, 1971 and 1975 (Türkay, 1975, 1976), the R/V *Thalassa* in 1962 (Maurin, 1963), 1968 and 1971 and the R/V *Atlor VII* in 1975 (Anadón, 1981). A significant number of organisms were collected during the CAPCAN expeditions to the Canarian-Caboverdian region (1976-1986) and the MAURITANIA expedition to the Bank d'Arguin (1988) (Fransen, 1991). The material collected in all these expeditions and surveys provided faunal inventories and species descriptions in the CCLME area.

More recently, the surveys carried out by the Instituto Español de Oceanografía (IEO) from 2002 to 2010, on board the R/V *Vizconde de Eza* in several Exclusive Economic Zones (EEZs) of the CCLME region provided excellent material for studying the taxonomy and ecology of decapods in the area. In addition, the analysis of the material collected in the last CCLME Ecosystem surveys conducted on board the R/V *Dr. Fridtjof Nansen* in 2011 and 2012, which is currently under study, will undoubtedly be a valuable tool in furthering knowledge of the crustacean biodiversity in the whole area.

There are certain studies concerning fisheries and biological aspects of some crustacean species (i.e. Maurin and Bonnet, 1969; Crosnier and De Bondy, 1967; Lhomme, 1978, 1979a, b; Bast et al., 1984; Lhomme and Garcia, 1984; Cervantes and Goñi, 1985; García, 1988; Cervantes et al., 1992; Sobrino and

García, 1991, 1992a, 1992b, 1994; Caveriviere and Rabarison Andriamirado, 1997; Laë et al., 2004; Thiaw et al., 2009). Only a few recent works have analysed ecological aspects of the decapod community structure in certain CCLME areas (Muñoz et al., 2012; García-Isarch et al., submitted). Aside from these studies, the literature about decapod crustaceans in the CCLME is rather dispersed and mainly focused on faunal lists and taxonomic aspects of certain species. There is a large number of studies concerning single species or genera. More generally, it is worth mentioning the excellent works carried out in the region by Crosnier and Forest (1973) on deep shrimps (Caridea and Penaidea) and Capart (1951), Monod (1956) and Manning and Holthuis (1981) on Brachyuran crabs. In addition, some excellent taxonomic reviews include West African records such as Zariquiey (1968) for decapods in general; Macpherson (1988) for Lithodidae; Pérez-Farfante and Kensley (1997) for penaeoid shrimps; Holthuis (1991) for lobsters; Galil (2000) for Polychelid lobsters; and McLauguin (2003) for hermit crabs, among others.

In the CCLME, decapod species have been targeted by both artisanal (local) and industrial fisheries. Foreign industrial shrimper fleets have been established in the area since the decade of the 60s, first freely and, since the implementation of the Convention on the Law of the Sea (UNCLOS, 1982), through agreements between the different administrations involved. Later, most CCLME countries developed their own industrial fisheries. The exploitation of these resources has provided significant economic incomes to the coastal States.

The purpose of this article is to present a global overview of the biodiversity of crustaceans in the CCLME region considering the latest information available, supported by an extensive literature review.

5.5.2. METHODS

The main data sources considered for the study of decapod diversity in the CCLME region were:

- IEO surveys. These were carried out in waters off Morocco (2004 and 2005) and Western Sahara (2006), Mauritania (2007, 2008 and 2009) and Guinea-Bissau (2008) on board the R/V *Vizconde de Eza*. Samples were taken by means of bottom trawls, at depths ranging from 229 m to 1861 m (Morocco-Western Sahara), 81 to 1825 m (Mauritania) and 20 to 1000 m (Guinea-Bissau). Decapods taken in each haul were sorted and keyed as specifically as possible to the lowest taxonomic level, counted and weighed. In order to check and complete the species identification, specimens of all the species caught were preserved and transported to the laboratory, where they have already been exhaustively reviewed in the case of Mauritania (García-Isarch et al., submitted) and Guinea-Bissau (Muñoz et al., 2012).

- Decapod specimens deposited in the Collection of Decapod and Stomatopod Crustaceans of the Cádiz Oceanographic Centre (Colección de Crustáceos Decápodos y Estomatópodos del Centro Oceanográfico de Cádiz, CCDE-IEOCD) from the IEO. This collection contains a great number of specimens from West Africa, mainly provided by the IEO and CCLME surveys, together with the IEO programmes of scientific observations on board the shrimper fleet in Mauritania and Guinea Bissau.

- Other sources: IEO databases of commercial fisheries developed in the region.

These data were used to produce a faunal list of the decapods in the area. The island fauna of the CCLME (the Canary Islands and Cape Verde Islands) remained beyond the scope of this study, on account of the lack of data. Considering the different type of sources, only a qualitative analysis was performed, based on

the presence/absence of each species in the CCLME countries. Given the geographical situation of Senegal and The Gambia, both countries were considered the same area.

The sampling coverage level was not the same for all the countries. The areas better sampled and studied were Mauritania and Guinea-Bissau (Muñoz et al., 2012; García-Isarch et al., submitted). The information from Morocco and Western Sahara was quite comprehensive (Ramos et al., 2005; Hernández-González et al., 2006; Hernández-González, 2007), although an in-depth analysis is still needed for a better knowledge of the biodiversity in these waters. However, the data from Senegal, The Gambia and Guinea came only from the material deposited in the CCDE-IEOCD collection, meaning that it does not represent the real diversity in the area. Because of the small number of specimens listed from Guinea, we analysed the decapod fauna of this country together with that of Guinea-Bissau, considering that species occurring in both EEZs were unlikely to be very different, because of the vicinity and similar characteristics of the two areas. Estimations of the species richness by area and by taxonomic group were made using this information.

Taking into account the limitations of our data (not all the areas and depths are similarly represented), the literature available was reviewed to confirm the geographical range of certain species.

5.5.3. RESULTS AND DISCUSSION

5.5.3.1. Species composition and diversity

A total number of 228 decapod species belonging to 54 families are reported in this work for the CCLME. Table 5.5.1 shows the taxonomic list by area (Morocco-Western Sahara, Mauritania, Senegal-The Gambia, Guinea-Bissau-Guinea), indicating the origin of the record (IEO survey, CCDE-IEOCD collection or other sources). Geographical positions of the specimens deposited in the CCDE-IEOCD collection are shown in Figure 5.5.1.

Brachyura, with 87 different species, was the most diversified taxa, followed by Caridea and Anomura with 61 and 33 species, respectively. The most important families in terms of species richness were the Inachidae spider crabs (20 species), followed by the Macropipidae crabs (17 species), the Oplophoridae deep sea shrimps (16), the Pandalidae shrimps (15) and the Penaeidae shrimps (10). Other diverse families were Crangonidae and Pasiphaeidae (8 species each) and the Diogenidae and Paguridae hermit crabs (7 species each). The remaining 45 families were represented by fewer than 6 species each (Figure 5.5.2).

Quantitative data have only been analysed in Mauritania and Guinea-Bissau so far. These analyses revealed quite similar decapod diversities in both areas (H’ = 3.22 in Mauritania and H’ = 3.30 in Guinea-Bissau; H’= Shannon diversity index) (Muñoz et al., 2012; García-Isarch et al., submitted), although samples were obtained at different depth ranges. When comparing the number of species registered in the current study, Morocco-Western Sahara and Mauritania showed the greatest species richness (137 and 134 species, respectively), followed by Guinea-Bissau-Guinea (119 species).

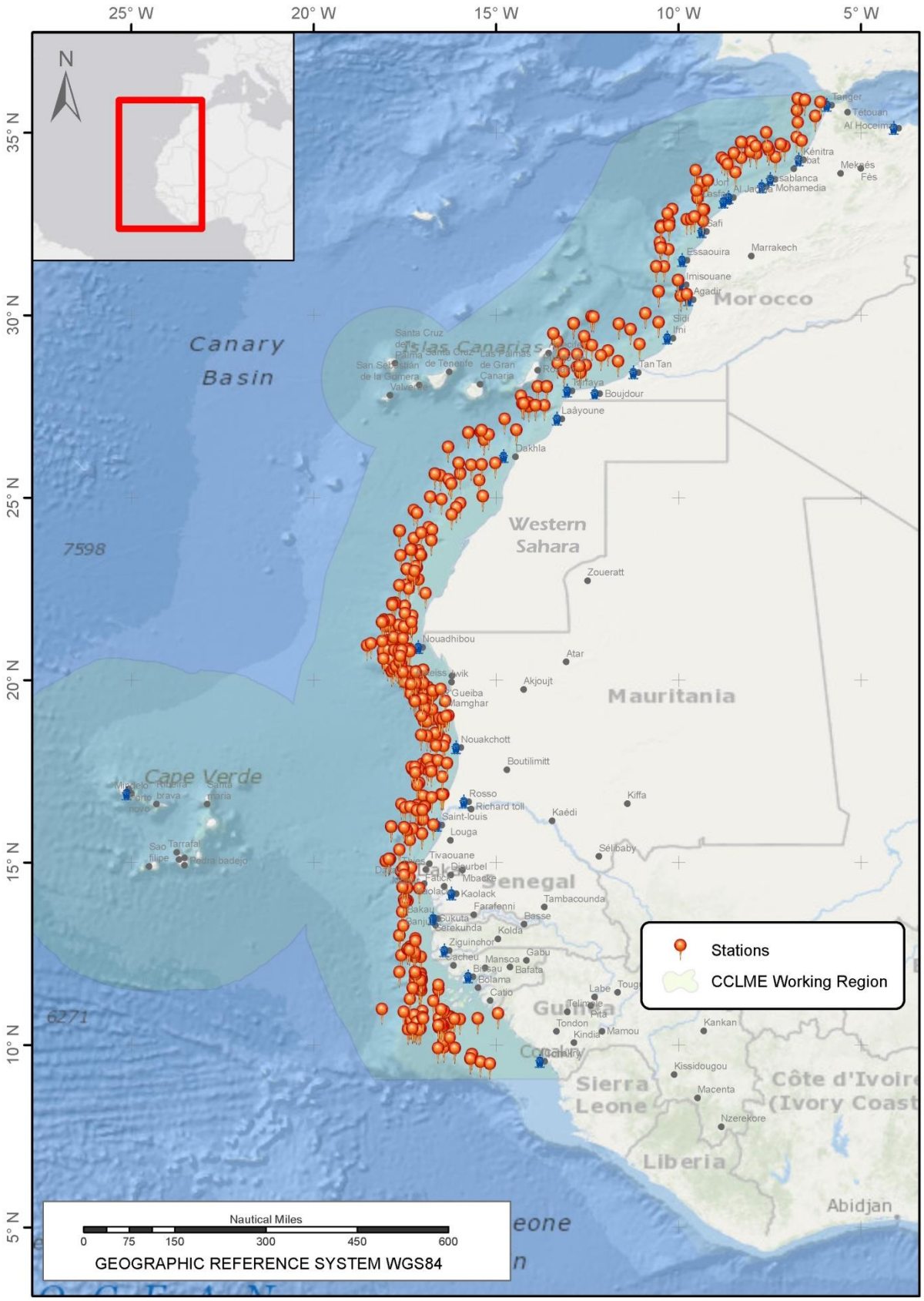

Figure 5.5.1. Geographical situation of the decapod specimens records from the CCLME deposited in the Collection of Decapod and Stomatopod Crustaceans of the Cádiz Oceanographic Centre - in Spanish *Colección de Crustáceos Decápodos y Estomatópodos del Centro Oceanográfico de Cádiz* (CCDE-IEOCD).

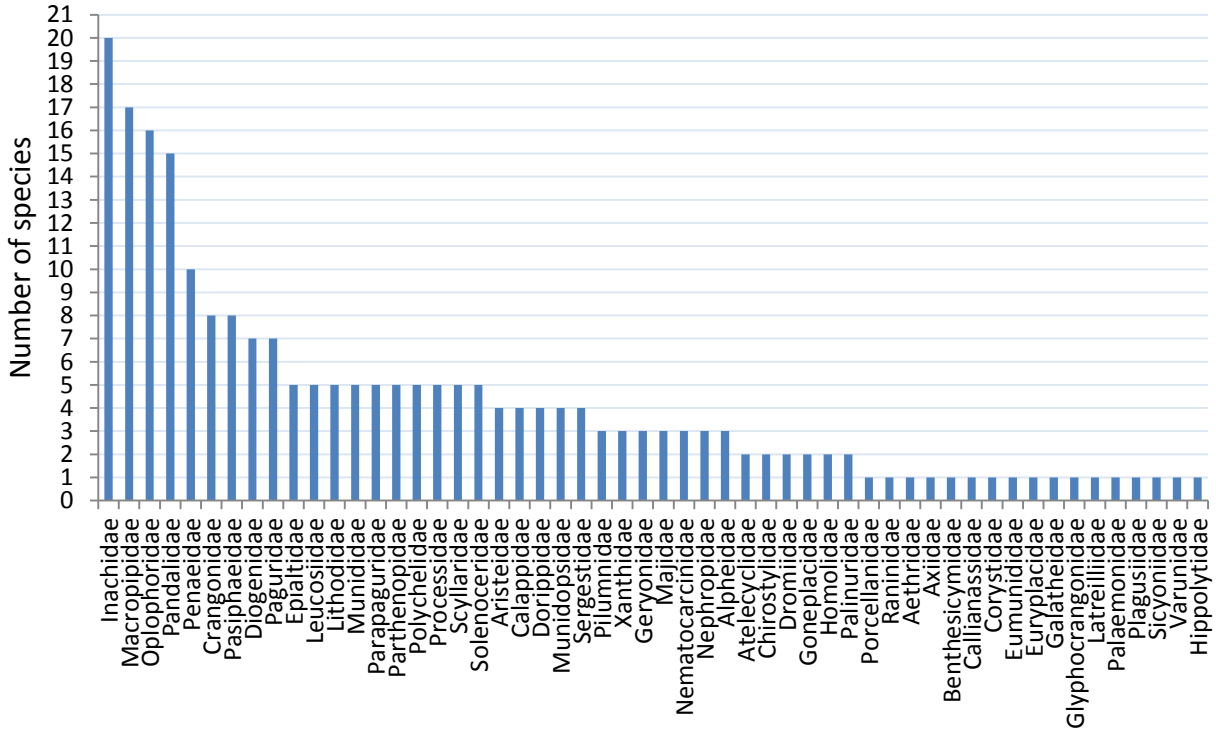

Figure 5.5.2. Species richness by decapod family in the CCLME.

As mentioned before, data from Senegal-The Gambia are not comparable to those of the former countries, because they do not represent the decapods' real diversity. Despite the fact that species richness is supposed to be higher in tropical and subtropical regions as compared to temperate and cold regions (Abele, 1982), the decapod diversity in the most temperate and northern areas of the region (Morocco-Western Sahara and Mauritania) was higher than in the most tropical and southern areas(Guinea-Bissau-Guinea).However, it should be borne in mind that deeper waters were prospected in Morocco-Western Sahara and Mauritania, a fact that may have increased the number of species recorded. In any case, the great diversity of decapods in the temperate area of the CCLME is evident. García-Isarch et al. (submitted) showed the exceptionally high decapod diversity in Mauritania, compared with other temperate areas. This fact gives an idea of the special character of the CCLME, where there is great diversity not only in the tropical southern areas (as typically occurs), but also in more temperate northern waters, in relation to the special hydrographical conditions under the influence of the Canary Current.

It is worth mentioning that our list contains two species that are new to science: *Munidopsis anaramosae* (de Matos-Pita and Ramil, 2014) (Plate 5.5.1(6)) and *Paguristes candelae* (de Matos-Pita and Ramil, 2015) and that some of the observations increased the bathymetric and/or geographic range of certain species in Atlantic waters (Muñoz and García-Isarch, 2013; de Matos-Pita and Ramil, 2014, 2015, submitted; de Matos-Pita et al., submitted, García-Isarch et al., submitted).

5.5.3.2. Biogeographical considerations

In spite of the sampling limitations due to different coverage levels, depth ranges and gears used in different surveys, certain biogeographical considerations are concluded from the available data.

There are some species that are cited only in the northern area of the CCLME region in our work and that have not been reported in southern Morocco-Western Sahara waters or in the literature. This is the case of

the solenocerid shrimp *Hymenopenaeus debilis;* the crangonid *Crangon crangon,* the Processidae *Processa canaliculata, Processa edulis edulis, Processa elegantula,* and *Processa nouveli nouveli;* the Nephropidae *Homarus gammarus* and *Nephrops norvegicus;* the Anomura *Munida curvimana, Pagurus excavatus* and *Strobopagurus gracilipes;* and the Brachyura *Corystes cassivelaunus, Dromia personata, Macropodia tenuirostris, Geryon trispinosus, Liocarcinus depurator, Liocarcinus pusillus, Liocarcinus zariquieyi* and *Polybius henslowii.* Accordingly, Morocco-Western Sahara represents the southern distribution limit for these north-east Atlantic species, which can be considered typically temperate. Other species such as *Notostomus gibbosus* and *Capartiella longipes* found their northern geographical distribution in this area. Waters off the Western Sahara constitute a boundary of zoogeographic regions in West Africa, where species composition changed abruptly (Burukovski, 1998). This may be the transition zone of species belonging to the same genus, as is the case of Solenocera *(S. membranacea* in the North and *S. africana* in the South) and Aristeus (*A. antennatus* in the North and *A. varidens* in the South).

Some other species were recorded only in the waters from Morocco to Mauritania, being considered subtropical-temperate species. This is the case of the solenocerid *Hadropenaeus affinis;* the caridean shrimps *Sabinea hystrix* and *Nematocarcinus ensifer;* the lobster *Palinurus mauritanicus;* and the crabs *Inachus communissimus* and *Macropipus tuberculatus.* The reviewed literature does not report them south of Dakar in Senegal (15°N) or off Cape Verde. More specifically, some of the species in our study only recorded in Mauritania found their southern limit in these waters (i.e. *Ephyrina figueirai figueirai, Munidopsis curvirostra* or *Anapagurus laevis*). Conversely, Mauritania also constitutes the northern known distribution area of other reported species such as *Plesionika holthuisi*, *Neolithodes asperrimus, Inachus nanus, Macropodia hesperiae* and *Macropodia macrocheles.* As mentioned above, two new species were described in Mauritanian waters (*Munidopsis anaramosae* and *Paguristes candelae*) from specimens collected in the IEO surveys. Others, like *Neolithodes grimaldii, Paragiopagurus macroceros* and *Diogenes pugilator are newly recorded* in Mauritanian waters (Muñoz and García-Isarch, 2013; de Matos-Pita and Ramil, 2015). The literature review confirmed that the hippolytid *Lebbeus africanus* has been found only in Mauritanian waters, being a possible endemism. On the open shelf, the boundary between temperate and tropical species occurs around 21°N (Cape Blanc), where a frontal zone is located, due to a coastal upwelling occurrence that changes the characteristics of the water masses. In the case of species living on the shelf edge and continental slope, the northern boundary is situated in the northern part, around 26°N (Burukovski, 1998).

Among the species registered only in Senegal and/or Guinea-Bissau-Guinea, some of them can be considered typically tropical; these include *Penaeus monodon, Acanthephyra kingsleyi, Psathyrocaris infirma, Polycheles perarmatus, Ciliopagurus caparti, Diogenes ovatus, Petrochirus pustulatus* and *Ranilia constricta.* In the absence of a representative number of records from Senegal, the northern limit of these species in Senegalese or southern waters was confirmed with the literature review.

Some 50 species were considered to be distributed in the entire area of the CCLME studied (see Table 5.5.1 and Plate 5.5.2). However, this number may be much higher as the origin of the records reported in this work is limited to certain bathymetric ranges, areas and gear samplers. Most of these widely distributed species inhabit deep waters. At greater depths, physical-geographical characteristics of the water masses are much more homogeneous, which explains the presence of numerous species that are common to the tropical zone and the temperate northern area. In addition, the system of currents in the CCLME contributes to the distribution of many species from the edge of the shelf up to the equatorial zone (Crosnier and Forest, 1973).

Among the species cited, 55 are known only in West African waters, with greater or lesser geographical distribution. They can be considered to be endemisms in the area (see Table 5.5.1.).

It is worth mentioning the presence of the Asian tiger shrimp *Penaeus monodon,* which is an invader species in West Africa. It has been widely farmed outside of its native range in the Indo-West Pacific. Introductions in the late 1980s to West Africa have resulted in the rapid establishment of the species in the wild along the coasts from Senegal to northern Angola, as a result of escapes from aquaculture (Fuller et al., 2014). In our study, it has been registered in Guinea-Bissau.

5.5.3.3. Commercial species

Coastal penaeids such as *Penaeus notialis* and *Penaeus kerathurus* have traditionally been exploited by the local artisanal fleets. The industrial fleets target both coastal shrimps and other species inhabiting deeper waters such as the penaeids *Parapenaeus longirostris* and the aristeids *Aristeus antennatus, Aristeus varidens, Aristaeopsis edwardsiana* or *Aristeomorpha foliacea* (Sobrino and García, 1991, 1992a, 1992b, 1994; FAO, 2012 b, c) (see Plate 5.5.2). Some crabs and lobsters also have great commercial interest (i.e: *Chaceon maritae, Palinurus mauritanicus*). The deep-water rose shrimp *P. longirostris* is the most important commercial species, being fished by industrial fleets in the whole of the region, with average annual catches of around 16,000 t during the period 1990-2012 (FAO b, c, in press). More than 60% of these catches occur in the Moroccan EEZ. The Southern rose shrimp *P. notialis,* with an average annual catch of around 5,000 t in the last 20 years (FAO b, c, in press), constitutes the second most important commercial species, being fished from Mauritania to Guinea. Most catches occur in Senegal-The Gambia (57%), where the species is mainly fished by the industrial fleet. These shrimp stocks are exploited by the coastal countries as well as by foreign fleets, which makes joint action necessary to assess their situation within a scientific framework, provided by the Fishery Committee for the Eastern Central Atlantic (CECAF), a regional fishery body dependent on the Food and Agriculture Organization of the United Nations (FAO). The latest assessments of the FAO/CECAF Working Groups on the Assessment of Demersal Resources were carried out in 2013 (Subgroup North, from Morocco to Senegal-Gambia), and in 2011 (Subgroup South, including Guinea-Bissau and Guinea). These assessments indicated a situation of overexploitation of the Moroccan stock of *P. longirostris* and the Senegal-The Gambia stock of *P. notialis,* while the remaining stocks assessed (*P. longirostris* and *P. notialis* stocks of Mauritania and *P. longirostris* of Guinea-Bissau) were considered not fully exploited. However, it should be kept in mind that abundances of these stocks suffer the typical cyclical fluctuations of short-living species, greatly depending on their annual recruitment and therefore on the environmental conditions.

The magnitude of the impact of trawl fishery on the marine ecosystems in the CCLME area is still unknown.

5.5.4. CONCLUSIONS AND RECOMMENDATIONS

This work constitutes a first contribution to the knowledge of decapod crustaceans in the CCLME region as a whole. The richness of this group in the area is fostered by the special hydrographical conditions of these waters where tropical and temperate species coexist. The detailed analysis of the samples obtained from the most recent surveys conducted in the area, still under study, will provide a better overview of the ecological communities in the region.

One of the main factors adversely affecting the crustacean populations in the CCLME region is the fishing pressure. Some of the species are directly targeted by specific fisheries, or they are captured as by-catch,

thus causing the overexploitation of some stocks, as is the case of the Moroccan stock of *Parapenaeus longirostris* and the Senegal-The Gambia stock of *Penaeus notialis* (FAO b, in press). In addition, there is an indirect impact produced by those fishing activities using certain gears (such as bottom trawls) that affect the benthic communities by disturbing the physical structures and habitats. Other anthropogenic factors such as pollution and eutrophication may affect crustacean populations, especially in shallow areas.

Crustaceans have a significant role in the marine ecosystem, especially in marine food webs, where they link high and low trophic levels (Cartes, 1998). It is therefore recommended first to follow the status and trends of these communities through faunal monitoring programmes in the area. Those especially vulnerable benthic habitats should be protected by specific conservation measures. Thus, protecting benthic habitats as a whole would involve the conservation of their decapod communities.

Another significant conservation measure to be adopted by the coastal countries should be the protection of overexploited stocks, following the recommendations established by the regional fishery organization in charge (FAO/CECAF).

Acknowledgements

We are very grateful to all the participants in the IEO and CCLME surveys, especially to Susana Soto, Fran Ramil, Paqui Salmerón and Caleli Burgos, who contributed to the decapods identifications onboard. We thank Tania Vera and Oscar Valle for their useful and enthusiastic assistance in the general activities of the Collection of Decapod and Stomatopod Crustaceans of the Cádiz Oceanographic Centre (Colección de Crustáceos Decápodos y Estomatópodos del Centro Oceanográfico de Cádiz, CCDE-IEOCD)-IEO. We thank Ana Ramos, Cheikh-Baye Braham and Samir Martins for reviewing the manuscript and Luis Miguel Agudo for providing the map. This work was undertaken within the framework of the ECOAFRIK project, under ECOAFRIK publication number 25.

Table 5.5.1. Decapod taxonomic list by area of the CCLME region: Morocco EEZ (MOR), Mauritania EEZ (MAU), Senegal-The Gambia (SEGAM) and Guinea Bissau-Guinea (GUI), indicating the origin of the record (S=IEO survey, C=collection CCDE-IEOCD, OS=other sources), and endemisms (E). Species highlighted in grey are considered to be distributed along the entire CCLME region.

	Species		MWS	MAU	SEGAM	GUI
Suborder Dendrobranchiata						
Superfamily Penaeoidea						
Family ARISTEIDAE	*Aristaeopsis edwardsiana* (Johnson, 1868)		C-S	S	C	C-S
	Aristaeomorpha foliacea (Risso, 1827)		C-S	C-S		
	Aristeus antennatus (Risso, 1816)		S	C-S		S
	Aristeus varidens Holthius, 1952		S	C-S		C-S
Family BENTHESICYMIDAE	*Benthesicymus bartletti* Smith, 1882		S	C-S		S
Family PENAEIDAE	*Funchalia danae* Burkenroad, 1940		S	S	C	
	Funchalia villosa (Bouvier, 1905)		C-S			
	Holthuispenaeopsis atlantica (Balss, 1914)	E		C	C	C-S
	Penaeus kerathurus (Forskål, 1775)		C	C	OS	OS
	Penaeus monodon Fabricius, 1798					OS
	Penaeus notialis Pérez Farfante, 1967	E		C-S	C	C-S
	Metapenaeopsis miersi (Holthuis, 1952)	E		C-S		
	Parapenaeus longirostris (Lucas, 1846)		C-S	C-S	C	C-S
	Pelagopenaeus balboae (Faxon, 1893)			S	C	
	Penaeopsis serrata Spence Bate, 1881		C-S			
Family SICYONIIDAE	*Sicyonia galeata* Holthuis, 1952	E		C-S	C	C
Family SOLENOCERIDAE	*Hadropenaeus affinis* (Bouvier, 1906)		C	C		
	Hymenopenaeus chacei Crosnier & Forest, 1969	E	C-S	C-S	C	C
	Hymenopenaeus debilis Smith, 1882		C			
	Solenocera africana Stebbing, 1917	E		C-S	C	C
	Solenocera membranacea (Risso, 1816)		C-S	C		
Superfamily Sergestoidea						
Family SERGESTIDAE	*Eusergestes arcticus* (Krøyer, 1855)			S		
	Sergia grandis (Sund, 1920)			C-S		S
	Sergia robusta (Smith, 1882)		S	C-S		S
	Sergia talismani (Barnard, 1947)			C-S		C-S
Suborder Pleocyemata						
Infraorder Caridea						
Superfamily Alpheoidea						
Family ALPHEIDAE	*Alpheus talismani*			C		
	Alpheus sp.1					S
	Alpheus sp.2					S
Family HIPPOLYTIDAE	*Lebbeus africanus* Fransen, 1997			S		
Superfamily Crangonoidea						
Family CRANGONIDAE	*Aegaeon cataphractus* (Olivi, 1792)		C-S	C-S	C	C
	Aegaeon lacazei (Gourret, 1887)		C	C-S		C-S
	Crangon crangon (Linnaeus, 1758)		C			
	Metacrangon bellmarleyi (Stebbing, 1914)	E	S	C-S		S
	Parapontophilus gracilis gracilis (Smith, 1882)	E		C-S	C	
	Philocheras echinulatus (M. Sars, 1862)		C-S			
	Philocheras sculptus (Bell, 1847 [in Bell, 1844-1853])		C			
	Sabinea hystrix (A. Milne-Edwards, 1881)		S	S		
Family GLYPHOCRANGONIDAE	*Glyphocrangon longirostris* (Smith, 1882)		S	C-S		
Superfamily Nematocarcinoidea						
Family NEMATOCARCINIDAE	*Nematocarcinus africanus* Crosnier & Forest, 1973	E	S	C-S	C	C-S
	Nematocarcinus ensifer (Smith, 1882)		S	S		
	Nematocarcinus gracilipes Filhol, 1884		S	C		
Superfamily Oplophoroidea						
Family OPLOPHORIDAE	*Acanthephyra acanthitelsonis* Bate, 1888		S	S	C	S
	Acanthephyra acutifrons (Bate, 1888)		S			S
	Acanthephyra curtirostris Wood-Mason & Alcock, 1891		S	C-S		
	Acanthephyra eximia Smith, 1884		S	C-S		C-S
	Acanthephyra kingsleyi (Bate, 1888)	E				S

	Species		MWS	MAU	SEGAM	GUI
	Acanthephyra pelagica (Risso, 1816)		S	C-S	C	C-S
	Acanthephyra purpurea (A. Milne-Edwards, 1881)		C-S			S
	Ephyrina figueirai figueirai Crosnier & Forest, 1973			C-S		
	Ephyrina ombango (Crosnier & Forest, 1973)					C-S
	Notostomus crosnieri Macpherson, 1984			S		C-S
	Notostomus gibbosus A. Milne-Edwards, 1881		S	S		
	Oplophorus spinosus (Brullé, 1839)		C-S	C-S		
	Systellaspis cristata (Faxon, 1893)		S	C-S		C
	Systellaspis debilis (A. Milne-Edwards, 1881)		C-S	C-S	C	C-S
	Systellaspis pellucida (Filhol, 1885)		C-S	S		C
Superfamily Palaemonoidea						
Family PALAEMONIDAE	*Palaemon serratus* (Pennant, 1777)		C			
Superfamily Pasiphaeoidea						
Family PASIPHAEIDAE	*Glyphus marsupialis* Filhol, 1884		S	C-S	C	C-S
	Parapasiphae sulcatifrons Smith, 1884		S	C-S		
	Pasiphaea multidentata Esmark, 1866		C-S	C-S		C-S
	Pasiphaea semispinosa Holthius, 1951	E		C-S	C	C-S
	Pasiphaea sivado (Risso, 1816)		S			S
	Pasiphaea tarda Krøyer, 1845		S	C-S		C-S
	Psathyrocaris fragilis Wood-Mason & Alcock, 1893		S	C-S	C	
	Psathyrocaris infirma (Alcock & Anderson, 1894)				C	C-S
Superfamily Pandaloidea						
Family PANDALIDAE	*Chlorotocus crassicornis* (A. Costa, 1871)		C			
	Heterocarpus ensifer A. Milne-Edwards, 1881		C-S	C-S	C	C-S
	Heterocarpus grimaldii A. Milne-Edwards & Bouvier, 1900		S	C-S		C-S
	Heterocarpus laevigatus (Bate, 1888)					S
	Plesionika acanthonotus (Smith, 1882)		C-S	C-S	C	C-S
	Plesionika antigai Zariquiey Alvarez, 1955		C			
	Plesionika brevipes (Crosnier & Forest, 1968)			C-S	C	
	Plesionika carinata Holthius, 1951	E	C-S	C-S	C	C-S
	Plesionika edwardsii (Brandt, 1851)		C-S	C-S		C-S
	Plesionika ensis (A. Milne-Edwards, 1881)		C-S	S	C	C-S
	Plesionika giglioli (Senna, 1903)		C			C-S
	Plesionika heterocarpus (A. Costa, 1871)		C-S	C-S	C	C-S
	Plesionika holthuisi (Crosnier & Forest, 1971)			C	C	S
	Plesionika martia (A. Milne-Edwards, 1883)		C-S	C-S	C	C-S
	Plesionika narval (Fabricius, 1787)		C	C-S	C	C-S
	Plesionika williamsi (Forest, 1963)		C-S		C	C-S
Superfamily Processoidea						
Family PROCESSIDAE	*Processa canaliculata* Leach, 1815 [in Leach, 1815-1875]		C			
	Processa edulis edulis (Risso, 1816)		C			
	Processa elegantula Nouvel & Holthuis, 1957		C			
	Processa intermedia Holthuis, 1951		C			
	Processa nouveli nouveli Al-Adhub & Williamson, 1975		C			
Infraorder Polychelida						
Superfamily Erynoidea						
Family POLYCHELIDAE	*Polycheles perarmatus* Holthuis, 1952					C
	Polycheles typhlops Heller, 1862		C-S	S		C-S
	Stereomastis nana (Smith, 1884)		S	C-S		
	Stereomastis sculpta (Smith, 1880)		S	C-S		C-S
	Stereomastis talismani (Bouvier, 1917)	E		C-S	C	
Infraorder Achelata						
Superfamily Palinuroidea						
Family PALINURIDAE	*Palinurus mauritanicus* Gruvel, 1911		C-S	C-S		
	Panulirus regius De Brito Capello, 1864	E			C	C
Family SCYLLARIDAE	*Acantharctus posteli* (Forest, 1963)			C	C	C-S
	Scyllarides latus (Latreille, 1803)					C-S
	Scyllarus arctus (Linnaeus, 1758)		C		C	C-S
	Scyllarus caparti Holthuis, 1952		C	C-S	C	C-S
	Scyllarus subarctus Crosnier, 1970	E	C	C-S	C	C-S

	Species		MWS	MAU	SEGAM	GUI
Infraorder Astacidea						
Superfamily Nephropoidea						
Family NEPHROPIDAE	*Homarus gammarus (Linnaeus, 1758)*		OS			
	Nephrops norvegicus (Linnaeus, 1758)		C-S			
	Nephropsis atlantica Norman, 1882		S	C-S		C-S
Infraorder Axiidea						
Superfamily Axioidea						
Family AXIIDAE	*Calocarides* sp			S		
Superfamily Callianassoidea						
Family CALLIANASSIDAE	*Cheramus oblonga* (Le Loeuff & Intes, 1974)			S		
Infraorder Anomura						
Superfamily Chirostyloidea						
Family CHIROSTYLIDAE	*Gastroptychus formosus* (Filhol, 1884)					C
	Uroptychus concolor (A. Milne Edwards & Bouvier, 1894)					C-S
Family EUMUNIDIDAE	*Eumunida bella* de Saint Laurent & Macpherson, 1990	E		S		
Superfamily Galatheoidea						
Family GALATHEIDAE	*Galathea intermedia* Liljeborg, 1851		C			
Family MUNIDIDAE	*Munida curvimana* A. Milne Edwards & Bouvier, 1894		C			
	Munida guineae Miyake & Baba, 1970	E		S	C	C-S
	Munida intermedia A. Milne Edwards & Bouvier, 1899		C-S			
	Munida rutllanti Zariquiey Álvarez, 1952		C-S	C	C	C
	Munida speciosa von Martens, 1878			C-S	C	C-S
Family MUNIDOPSIDAE	*Munidopsis anaramosae* de Matos-Pita & Ramil, 2014			S		
	Munidopsis chunii Balss, 1913	E		S		
	Munidopsis curvirostra Whiteaves, 1874			S		
	Munidopsis serricornis (Lovén, 1852)			S		
Family PORCELLANIDAE	*Pisidia* sp.					S
Superfamily Paguroidea						
Family DIOGENIDAE	*Areopaguristes mauritanicus* (Bouvier, 1906)	E		S		
	Ciliopagurus caparti (Forest, 1952)	E				C
	Dardanus arrosor (Herbst, 1796)		C	S	C	C-S
	Diogenes ovatus Miers, 1881	E				C-S
	Diogenes pugilator (Roux, 1829)		C	S		
	Paguristes candelae de Matos-Pita & Ramil, 2015			S		
	Petrochirus pustulatus (H. Milne Edwards, 1848)	E				C-S
Family PAGURIDAE	*Anapagurus laevis* (Bell, 1846)			S		
	Pagurus alatus Fabricius, 1775		S	S		
	Pagurus cuanensis Bell, 1845			S		
	Pagurus excavatus (Herbst, 1791)		C			
	Pagurus forbesii Bell, 1846		C	C	C	
	Pagurus prideaux Leach, 1815			S		
	Spiropagurus elegans (Miers, 1881)		C			C-S
Family PARAPAGURIDAE	*Paragiopagurus macrocerus* (Forest, 1955)			S		
	Parapagurus nudus (A. Milne-Edwards, 1891)			S		
	Parapagurus pilosimanus Smith, 1879		S	S		C-S
	Parapaguridae indet.					S
	Strobopagurus gracilipes (A. Milne-Edwards, 1891		C			
Superfamily Lithodoidea						
Family LITHODIDAE	*Lithodes ferox* Filhol, 1885		S	C-S		C-S
	Neolithodes asperrimus Barnard, 1947	E		S		
	Neolithodes grimaldii (A. Milne-Edwards & Bouvier, 1894)			S		
	Paralomis cristulata Macpherson, 1988			S		C-S
	Paralomis erinacea Macpherson, 1988	E		C-S		S
Infraorder Brachyura						
Superfamily Aethroidea						
Family AETHRIDAE	*Sakaila africana* (Manning & Holthuis, 1981)	E			C	C-S
Superfamily Cancroidea						
Family ATELECYCLIDAE	*Atelecyclus rotundatus* (Olivi, 1792)		C			S
	Atelecyclus undecimdentatus (Herbst, 1783)		C	C		

	Species		MWS	MAU	SEGAM	GUI
Superfamily Calappoidea						
Family CALAPPIDAE	*Acanthocarpus brevispinis* Monod, 1946	E		C-S	C	C-S
	Calappa granulata (Linnaeus, 1758)		C-S			
	Calappa pelii Herklots, 1851	E	C	C-S		C-S
	Calappa rubroguttata (Herklots, 1851)	E			C	C-S
Superfamily Corystoidea						
Family CORYSTIDAE	*Corystes cassivelaunus* (Pennant, 1777)		C			
Superfamily Dorippoidea						
Family DORIPPIDAE	*Ethusa mascarone* (Herbst, 1785)		C-S			
	Ethusa sp.					S
	Medorippe lanata (Linnaeus, 1767)		C	C-S		C-S
	Phyllodorippe armata (Miers, 1881)	E			C	
Superfamily Dromioidea						
Family DROMIIDAE	*Dromia personata* (Linnaeus, 1758)		C			
	Sternodromia spinirostris (Miers, 1881)	E	C	C	C	C-S
Superfamily Goneplacoidea						
Family EURYPLACIDAE	*Machaerus oxyacantha* (Monod, 1956)	E			C	C
Family GONEPLACIDAE	*Goneplax barnardi* (Capart, 1951)	E		S	C	C-S
	Goneplax rhomboides (Linnaeus, 1758)		C	S		
Superfamily Grapsoidea						
Family PLAGUSIIDAE	*Euchirograpsus liguricus* H. Milne Edwards, 1853		C	S		
Family VARUNIDAE	*Asthenognathus atlanticus* Monod, 1933		C			
Superfamily Homoloidea						
Family HOMOLIDAE	*Homola barbata* (Fabricius, 1793)		C	C-S	C	C-S
	Paromola cuvieri (Risso, 1816)		C-S	C-S		S
Family LATREILLIIDAE	*Latreillia elegans* Roux, 1830		C-S			
Superfamily Majoidea						
Family EPIALTIDAE	*Apiomithrax bocagei* (Ozorio, 1887)	E				C
	Pisa armata (Latreille, 1803)		C	S		C-S
	Pisa calva (Forest & Guinot, 1966)	E				C-S
	Pisa carinimana Miers, 1879		C	C		
	Rochinia carpenteri (Wyville Thomson, 1873)		C-S			C-S
Family INACHIDAE	*Capartiella longipes* (Capart, 1951)	E	C			
	Dorhynchus thomsoni Thomson, 1873		C			
	Inachus aguiarii de Brito Capello, 1876		C	S		
	Inachus angolensis Capart, 1951	E		C-S	C	C
	Inachus communissimus Rizza, 1840		C	C		
	Inachus dorsettensis (Pennant, 1777)		C			
	Inachus leptochirus Leach, 1817		C	C-S		
	Inachus nanus Manning & Holthuis, 1981			S		
	Inachus thoracicus Roux, 1830		C			
	Inachus sp					S
	Macropodia doracis (Manning & Holthuis, 1981)	E				C-S
	Macropodia gilsoni (Capart, 1951)	E		C-S	C	
	Macropodia hesperiae Manning & Holthuis, 1981	E		S		
	Macropodia linaresi Forest & Zariquiey Alvarez, 1964		C			
	Macropodia longipes (A. Milne Edwards & Bouvier, 1899)		C	C-S		
	Macropodia macrocheles (A. Milne Edwards & Bouvier, 1898	E		S		
	Macropodia rostrata (Linnaeus, 1761)		C	C		S
	Macropodia spinulosa (Miers, 1881)	E			C	C-S
	Macropodia tenuirostris (Leach, 1814)		C			
	Stenorhynchus lanceolatus (Brullé, 1837)		C	C		C-S
Family MAJIDAE	*Eurynome aspera* (Pennant, 1777)			S		
	Maja crispata Risso, 1827		C			
	Maja squinado (Herbst, 1788)		C			
Superfamily Leucosioidea						
Family LEUCOSIIDAE	*Atlantophila cristata* (Miers, 1881)	E		C		C-S
	Ebalia nux A. Milne Edwards, 1883			S		
	Ilia spinosa (Miers, 1881)	E			C	C-S
	Merocryptus obsoletus (A. Milne-Edwards & Bouvier, 1898)	E				C-S
	Pseudomyra mbizi Capart, 1951	E		C-S	C	

	Species		MWS	MAU	SEGAM	GUI
Superfamily Parthenopoidea						
Family PARTHENOPIDAE	*Distolambrus maltzami* (Miers, 1881)			C		
	Parthenopoides massena (Roux, 1830)		C			C-S
	Solenolambrus noordendei (Capart, 1951)	E	C	S	C	
	Spinolambrus macrochelos (Herbst, 1790)		C			
	Spinolambrus notialis (Manning & Holthuis, 1981)	E		S		C-S
Superfamily Portunoidea						
Family GERYONIDAE	*Chaceon affinis* (A. Milne-Edwards & Bouvier, 1894)		S			C
	Chaceon maritae (Manning & Holthuis, 1981)	E	S	C-S	OS	S
	Geryon trispinosus		C			
Family MACROPIPIDAE	*Bathynectes maravigna* (Prestandrea, 1839)		C			C-S
	Bathynectes piperitus Manning & Holthuis, 1981	E		C-S	C	C
	Callinectes amnicola (Rochebrune, 1883)	E				C
	Callinectes marginatus (A. Milne-Edwards, 1861)	E		C		C-S
	Charybdis (Charybdis) hellerii (A. Milne-Edwards, 1867)					C
	Cronius ruber (Lamarck, 1818)					C-S
	Liocarcinus corrugatus (Pennant, 1777)		C	C		S
	Liocarcinus depurator (Linnaeus, 1758)		C			
	Liocarcinus marmoreus (Leach, 1814)		C			S
	Liocarcinus pusillus (Leach, 1816)		C			
	Liocarcinus vernalis (Risso, 1816)		C			
	Liocarcinus zariquieyi Gordon, 1968		C			
	Macropipus rugosus (Doflein, 1904)	E	C-S	C-S	C	C-S
	Macropipus tuberculatus (Roux, 1830)		C	C		
	Portunus (Portunus) hastatus (Linnaeus, 1767)		C			
	Polybius henslowii Leach, 1820		C-S			
	Sanquerus validus (Herklots, 1851)	E			C	S
Superfamily Raninoidea						
Family RANINIDAE	*Ranilia constricta* (A. Milne-Edwards, 1880)					C-S
Superfamily Xanthoidea						
Family PILUMNIDAE	*Pilumnus inermis* A. Milne-Edwards & Bouvier, 1894		C-S			
	Pilumnus spinifer H. Milne Edwards, 1834		C			
	Pilumnus stebbingi (Capart, 1951)	E				C-S
Family XANTHIDAE	*Monodaeus couchii* (Couch, 1851)		C	C		
	Monodaeus cristulatus Guinot & Macpherson, 1988			S		
	Paraxanthias eriphioides (A. Milne Edwards, 1867)					C-S
Number of species	**232**	**54**	**137**	**134**	**59**	**119**

Plate 5.5.1. Five decapod species widely distributed throughout the CCLME: 1. *Nematocarcunus africanus* (© José Francisco González Jiménez, IEO); 2. *Plesionika edwardsii* (© José Franscico González Jiménez, IEO); 3. *Dardanus arrosor* (© Lourdes Fernández Peralta, IEO); 4. *Stenorhynchus lanceolatus* (© Pablo Expósito Martínez, IEO); 5. *Scyllarus subarctus* (© Alberto García García, IEO). Species new to science reported in Mauritanian waters: 6. *Munidopsis anaramosae* (© Ana Ramos Martos, IEO).

1

2

3

4

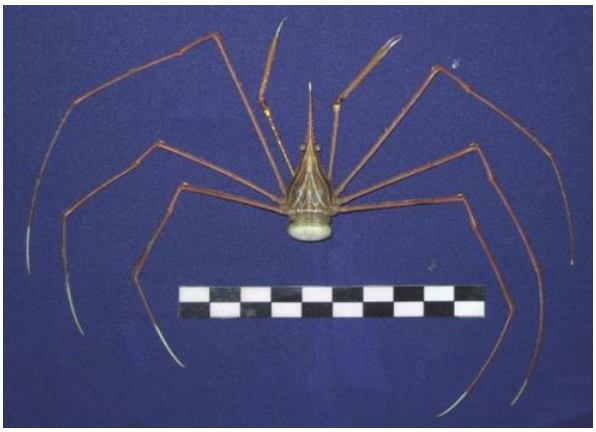

5

6

Plate 5.5.2. Six decapod commercial species of the CCLME. 1. *Parapenaeus longirostris* (© Alberto García García, IEO); 2. *Penaeus notialis* (© Lourdes Fernández Peralta, IEO); 3. *Penaeus kerathurus* (© Lourdes Fernández Peralta, IEO); 4. *Aristaeopsis edwardsiana* (© Alberto García García, IEO); 5. *Aristeus varidens* (© José Francisco González Jiménez, IEO); 6. *Chaceon maritae* (© José Francisco González Jiménez, IEO).

1

2

3

4

5

6

5.6. SEA TURTLES OFF NORTHWEST AFRICA

Adolfo MARCO[1,2] and Samir MARTINS[2]

[1] Estación Biológica de Doñana, Consejo Superior de Investigaciones Científicas. Spain

[2] BIOS.CV. Cabo Verde

5.6.1. INTRODUCTION

Sea turtles are highly migratory mega vertebrates that have extremely important roles in the functioning of marine ecosystems since they first appeared in the Oceans over 100 million years ago. They have been relentlessly exploited for centuries and are currently facing a variety of global changes that are gravely threatening their continued survival. Their status in the Northwestern African waters are of special concern.

The earliest known accounts of sea turtles in the area of the Canary Current Large Marine Ecosystem (CCLME) go as far back as the second half of the XV century. Cadamosto in 1456 and Columbus in 1498 both described how sea turtles were captured for meat consumption in Madeira and the Azores. However, there are no records of reproduction taking place in these archipelagos. There are also accounts on the presence and abundance of sea turtles in the archipelagos of the Canaries and Cape Verde in ancient books that date from the XV to the XIX century (see reviews in Lazar and Holcer, 1998; López-Jurado, 2007; Loureiro and Torrão, 2008). These old texts describe the abundance of sea turtles on several islands as well as the capture of many individuals for meat consumption and for supposed medical remedies. However, it has predominantly been during the past three decades that the feeding grounds and nesting aggregations have become widely known in the scientific community (Brongersma, 1982; Barbosa et al., 1998; Fretey, 2001; López-Jurado, 1992, 2007; Catry et al., 2009).

5.6.2. SPECIES DESCRIPTION

Of the seven existing sea turtle species, six inhabit the waters of the Canary Current (Plate 5.6.1). The loggerhead turtle (*Caretta caretta*) and the green turtle (*Chelonia mydas*) are probably the most common in the CCLME and the only two species that nest regularly on its beaches. The Kemp's ridley sea turtle (*Lepidochelys kempii*), the most restricted and endangered sea turtle in the world, is very rare in the area although migrant juveniles can be found along the northwestern coast of Morocco.

Turtles belonging to the remaining three species (leatherbacks – *Dermochelys coriacea*; hawksbills – *Eretmochelys imbricata;* and olive ridleys – *Lepidochelys olivacea*) can be found in the waters of the Canary Current but are generally tropical nesters. Nevertheless, some nests can sometimes be found in the southern part of the region. Their distribution could change in the next decades if global warming predictions force certain species of sea turtle to select colder beaches in order to guarantee enough male production.

Two very different morphological forms of sea turtle are represented in the region. On one hand, those belonging to the chelonids present a typical turtle form with keratinized scutes covering a hard bony carapace. The other group, dermochelids, also present a bony carapace but in their case it is covered by oily flesh and leather skin.

The loggerhead turtle (*C. caretta*) is a medium-sized sea turtle that can reach up to 125 cm in Straight Carapace Length (SCL) and weigh up to 200 kg (LeBuff, 1990). It has an overly large head with a very thick neck and a strong jaw. Color patterns on its back are brown with reddish or orange shades at the edges, which are more visible on the front. Its plastron is whitish with cream and pale yellow shades. Large juveniles and adults usually have a variety of living organisms, such as seaweeds, tubeworms, barnacles or other crustaceans, attached to their dorsal carapaces. These turtles, in effect, are small moving reefs which act as dispersing agents for a wide range of marine species.

The green turtle (*C. mydas*) is the largest of the hard-shelled sea turtles. Although its external morphology is not geographically uniform, this species usually possesses a dorso-ventrally flat oval carapace, with 5 vertebral scutes, 4 pairs of costal scutes and 4 pairs of inframarginal scutes. The SCL of adults is around 120 cm (71-153 cm). This species is short-necked, has one pair of prefrontal scales and four pairs of postorbital scales. Its upper jaw has a slightly dentate edge, while its lower jaw has a clearer denticulation. Each flipper has a claw, although sometimes they have two. The hatchlings'carapace is predominantly black or dark grey, but will gradually change to dark brown or olive green as it grows up, whereas its plastron is whitish. Coloration is quite variable among adults, and they can have a spotted or striped carapace in brown, grey, black or green tones. The common name of this species is derived from its green body fat. During the subadult and adult stages they feed primarily on marine plants.

The hawksbill turtle (*E.imbricata*) is a medium-sized species with an elongated carapace, overlapping or imbricated scutes and serrated edges. The carapace presents 5 vertebral scutes, 4 pairs of lateral scutes, a variable number of marginal scutes (>10 pairs) and 2 supracaudalscutes, which have a high degree of hardness that is characteristic of the species. Ventrally, the plastron is made up of 4 pairs of inframarginalscutes. The nuchal scute is not in contact with the lateral scutes. The colour of their carapace varies with age; hatchlings are dark brown both dorsal and ventrally. As they grow up, their carapaces develop a characteristic colour pattern on the scutes, with yellow, brown and black spots; this colour remains when they reach maturity. Ventrally, the tone varies from pale yellow to white, sometimes with black spots. They feed on corals and sponges. Their carapace has long been highly valued, and has been traded for decorative purposes.

The two species belonging to the *Lepidochelys* genus are small sea turtles which can grow up to 72 cm in SCL and to 50 kg in weight. They are characterized by having a number of small pores located near the rear margin of every one of the four inframarginal scutes, two claws on each limb (although sometimes adults can lose one of them) and two prefrontal scales on the head. The main difference between the two species of *Lepidochelys* is that the Kemp's ridley has five pairs of costal scutes and the olive ridley has 6 or 7 pairs. Both species have a light olive-green dorsal and a yellow ventral coloration in adults, whereas coloration for immature individuals is grey for the dorsal and white for the ventral area. They can aggregate by the thousands in selected small sections of beaches for diurnal nesting, thus forming the *arribadas*.

The leatherback turtle is the largest species of sea turtle, reaching 200 cm in SCL and weighing up to 900 kg. Their main characteristic is a bony carapace which is completely covered with a leather-like soft tissue, no large scales, with seven longitudinal ridges on its back and five more ridges on its plastron. They are also characterized by their long front flippers and their lack of claws. Their dorsal surface is dark, mottled with pink or white, with a similar color on their ridges and large areas of their heads, necks and limbs. The abdomen color varies but is usually pinkish, white and black. Its head has no scales and its keratinized beak is strong, with smooth edges and a characteristic end adapted to catching slippery prey. The upper side of

their beak's tip is W-shaped. They eat jellyfish, other gelatinous marine invertebrates and, in some cases, they associate themselves with large shoals of jellyfish.

5.6.3. NESTING

Along the oriental coast of the Atlantic Ocean, it is only possible to find a stable loggerhead turtle nesting population in the archipelago of Cape Verde (Marco et al., 2012). This nesting population probably coexisted for centuries with a low human population in the archipelago, unlike on the continental African coast where loggerhead nesting is nowadays considered sporadic. At present, Cape Verde constitutes the third most abundant nesting site of loggerhead turtles in the world, but sadly this does not prevent it from also being considered one of the three most endangered loggerhead turtle populations in the world due to increases in the current extinction risk (Wallace et al., 2011). An average of 15,000 nests are laid annually in Cape Verde varying from 5000 to 30,000 (Fig. 5.6.1). Between 80% and 85% of all nests are laid on just 40 km of the beaches on the eastern half of Boa Vista (Marco et al., 2012). Boa Vista possibly contains the highest nesting density of this species in the world, with more than 2 nests per year for every linear meter of beach in stretches of over 800 m long (Martins, 2012) (Fig. 5.6.2). The islands of Maio, Sal and São Nicolau support a much lower number of nests, with an annual mean of around 1000 nests on each island (Cozens et al., 2011, 2012; Lino et al., 2010; own data). On the remaining islands of the archipelago, nesting is much lower with an estimate of less than 150 nests laid annually per island (Loureiro, 2008, Marco and collaborators, personal observations).

1 2

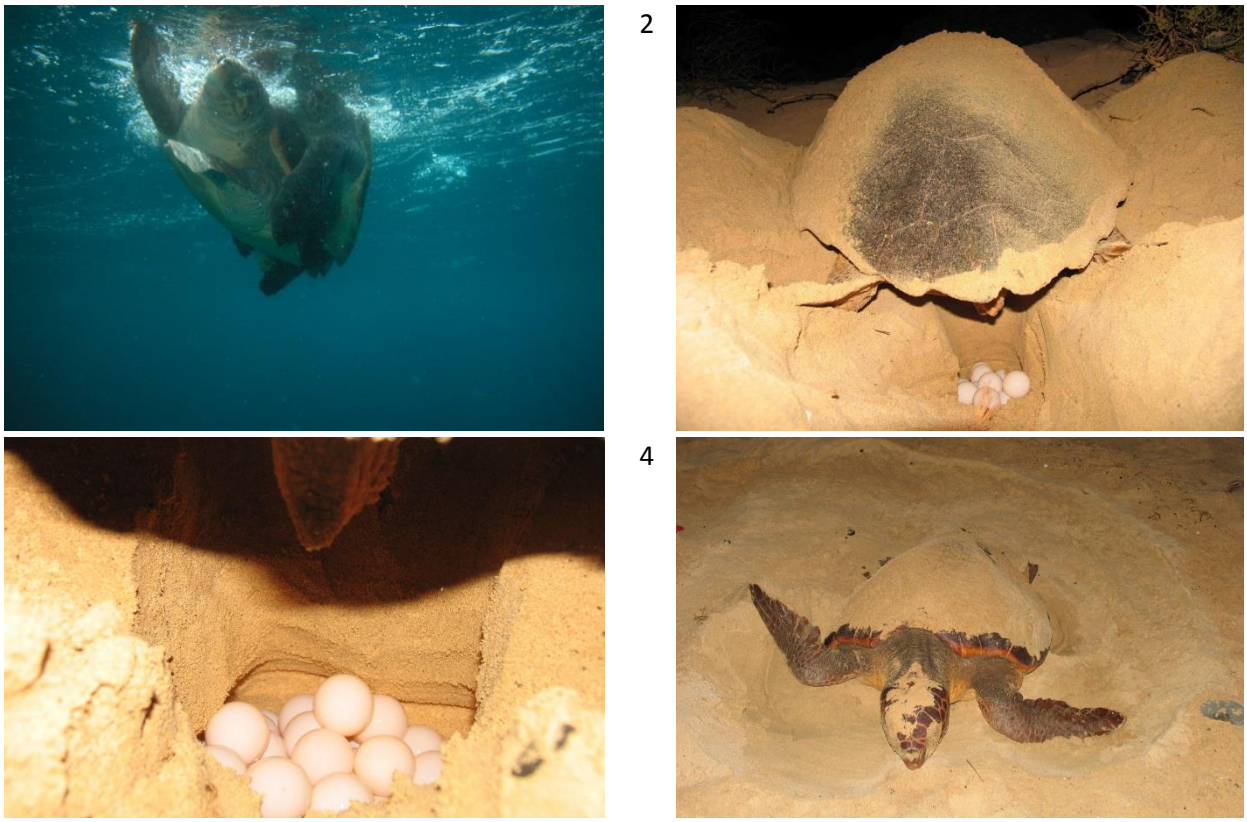

3 4

Figure 5.6.1. Loggerhead (1, © Pedro López) mating, (2, © Adolfo Marco) nesting, (3, © Adolfo Marco) egg-laying and (4, © Adolfo Marco) camouflaging of a nest in Cape Verde.

The island of Poilão in the Bijagós Archipelago, Guinea-Bissau, is known to be an important nesting site for the green turtle, but until recently there were no quantitative estimates of the number of clutches deposited annually. In 2000 a survey was carried out to assess the magnitude of nesting, and an estimated 7400 green turtle clutches were deposited. This study confirmed that Poilão is one of the most important nesting sites for green turtles in the Atlantic, and the largest known nesting colony on the west coast of Africa. Traditionally Poilão has been regarded as a sacred site by the Bijagós people, and this has contributed to the conservation of these turtles. However, the development of fisheries in this region is an emerging threat. To conserve this site a National Marine Park was designated in August 2000 (Fortes et al., 1998, Catry et al., 2009). A significant nesting rookery of olive ridleys turtles also been detected on the same beaches although with a much lower number of nests. The sporadic nesting of olive ridleys, as well as hawksbill, green and loggerhead turtles, has been documented along the continental coast from Mauritania to Guinea-Bissau (Fretey, 2001). Leatherback turtles are much more tropical and nests are very rare on the coast along the CCLME.

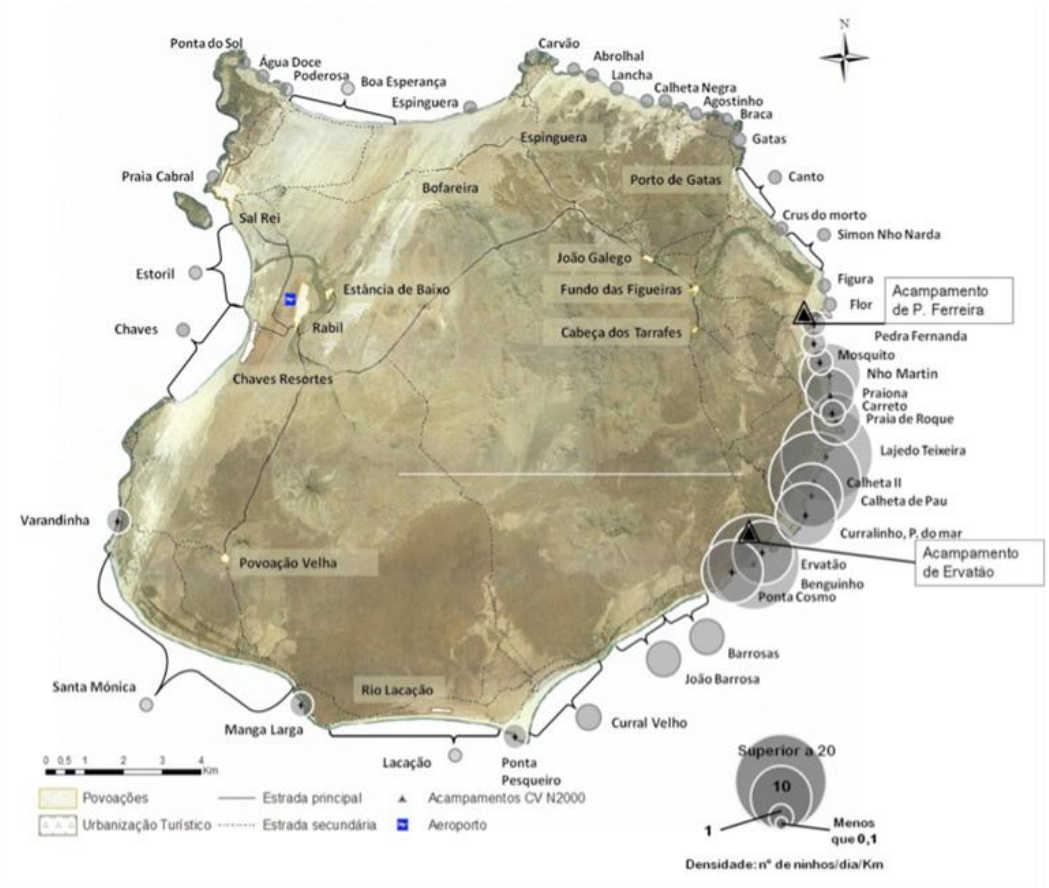

Figure 5.6.2. Annual nest density on the beaches of Boa Vista Island. The highest nest density for the species is found in the Reserva Natural da Tartaruga (southeast), which hosts 60% of the total nestings in Cabo Verde.

5.6.4. THE DISTRIBUTION AND MIGRATION OF ADULTS

Female sea turtles rarely breed annually due to the high energetic costs that are entailed by reproduction and migration. During the remigration interval, loggerheads that nest in Cape Verde move to the continental African coast to feed (Hawkes et al., 2006). The most frequent remigration interval is of 2 years (60%), followed by a 3-year interval (25%) (Gaona et al., in press). Whilst some individuals from the

population make a direct migration eastwards from Cape Verde towards shallow foraging grounds off the coasts of Guinea-Bissau and Senegal, the majority of the population migrates eastwards from the Cape Verde islands but then remains in the oceanic zone, traversing over half a million square kilometers of pelagic foraging habitat (Hawkes et al., 2006; Varo-Cruz et al., 2013). Interestingly, this behavior seems to be linked to body size; only the largest turtles forage in shallow coastal waters, whereas smaller individuals remain in the oceanic zone. In contrast with the females, males from Cape Verde may breed annually (Varo-Cruz et al., 2013). Some males may migrate to the African coast although it appears that others may remain near the nesting area for several months following the nesting season (Varo-Cruz et al., 2013). Oceanic adult loggerheads show a preference for the highly productive upwelling region between Cape Verde and mainland Africa, an area of intense frontal activity. Within the upwelling region, turtles appear to forage epipelagically around mesoscale thermal fronts, exploiting profitable foraging opportunities resulting from physical aggregation of prey (Scales et al., 2015).

Female green turtles from Bissagos lay multiple clutches in any given season and remain close to the islands within the boundaries of the João Vieira and Poilão National Marine Parks during internesting periods which last around 15 days (Fig. 5.6.3b) (Godley et al., 2010). After nesting season some females have short-range movements to locations within the Bissagos archipelago suggesting local residence. However, other females migrate from Poilão to the Park National du Banc D'Arguin, Mauritania (Fig. 5.6.3a), where they remain during long periods to feed (Godley et al., 2010). This post-nesting migration is of over 1000 km along the coastal and near-coastal waters of Gambia, Senegal and Mauritania. For this area, females show a degree of fidelity to shallow water foraging areas.

There seems to be quite an important feeding area along the Mauritanian coast for leatherback turtles coming from the American Atlantic coast (Eckert et al., 2006). Leatherbacks originally from the western African coast (Gabon) may also visit this upwelling area in the Canary Current.

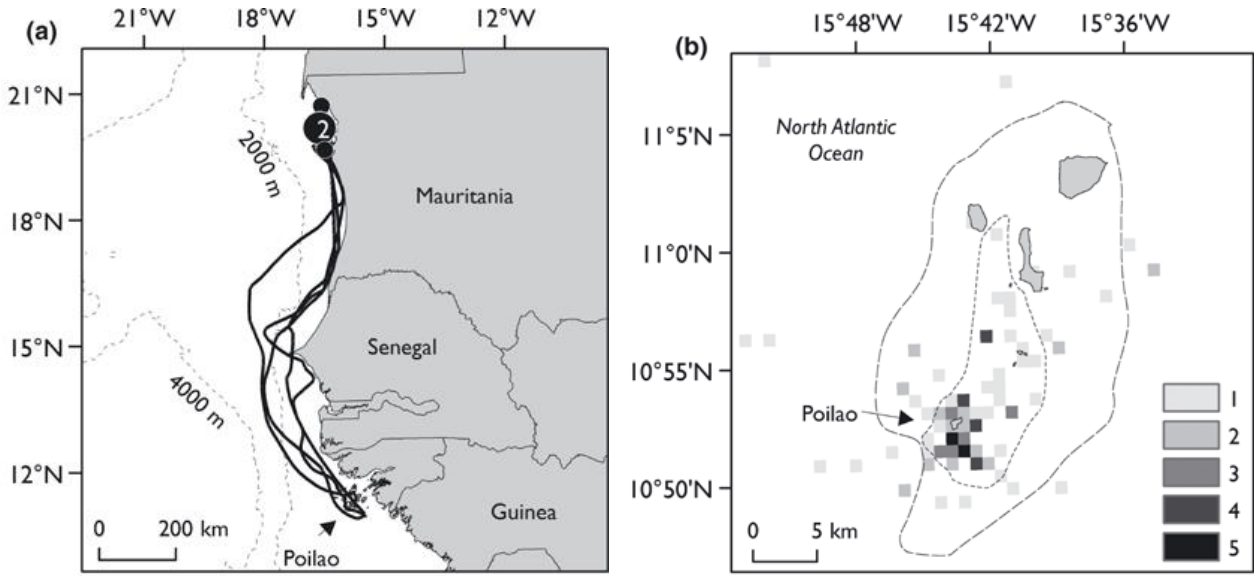

Figure 5.6.3. Satellite tracking offers insights into green turtle distribution and migrational pattern. (a) Post-nesting movements of four females tracked to their foraging sites in the Banq D'arguin National Park (black dot 2). (b) Habitat utilization during the internesting interval. Colors indicate density of occupation (days per km^2). Marks are the limits of the inner and outer zone of the JoãoViera e Poilão National Marine Park. (Figure published in Godley et al., 2010). © 2010 The Authors. Journal compilation © 2010 British Ecological Society.

5.6.5. THE DISTRIBUTION AND MIGRATION OF JUVENILES

Small juvenile turtles are known to disperse extensively on a transatlantic scale (Boltenet al., 1998) and are commonly associated with convergence zones, upwellings, major gyre systems, and eddies (Carr, 1987, Musick and Limpus, 1997) that provide productive foraging grounds by concentrating a variety of planktonic and neustonic organisms.

Juvenile loggerhead turtles from the Cape Verde Islands (Fig. 5.6.4) have been identified in feeding grounds off the Canary Islands, Madeira, the Azores, the Gulf of Cadiz and the southwestern area of the Mediterranean Sea (Monzón-Argüello et al., 2009; Carreras et al., 2011; Clusa et al., 2013). These juvenile turtles share feeding grounds with juveniles of the same species belonging to other Atlantic and/or Mediterranean populations (Monzón-Argüello et al., 2009; Carreras et al., 2011). Genetic studies (Monzón-Argüello et al., 2010a) suggest that less than half of the expected hatchling and juvenile turtles from Cape Verde are subsequently encountered in foraging grounds north of the Cape Verde islands. A significant proportion of juveniles may also disperse to American waters and/or southwards, to waters near the Gulf of Guinea (Monzón-Argüello et al., 2010a). However, due to a relative lack of research effort and funding, the western Atlantic coast of Africa could have other loggerhead feeding grounds yet to be discovered. Future research effort may help in gathering information to fill this important gap in our knowledge on the species. Loggerheads originally from the eastern American coast are frequently observed in the Atlantic archipelagos of Azores, Madeira and the Canaries (Brongersma, 1982; López-Jurado, 1992), as well as the Atlantic coast of Morocco (Aksissou et al., 2006; Benhardouze et al., 2012) where they spend their pelagic juvenile life stage. In these areas loggerhead juveniles and subadults are considered to be abundant.

Data from marine currents and genetic analysis suggest that most green turtle juveniles from Guinea-Bissau disperse to the southwest (Brazil) and the eastern Atlantic, which includes the Canary Current and waters off Senegal, Mauritania and Cape Verde (Godley et al., 2010; Monzón-Argüello et al., 2010b). Green turtle juveniles in the Cape Verde feeding grounds have been found to have come from the Caribbean Sea (Monzón-Argüello et al., 2010b), and hawksbill juveniles have been found to have come from the endangered population of the archipelagos in the Gulf of Guinea (Monzón-Argüello et al., 2011).

Occasionally, juvenile turtles may be displaced from their expected passive dispersal routes (Monzón-Argüello et al., 2012) by oceanic eddies, storm events and/or weather fronts. This appears to have been the case for small numbers of juvenile turtles from Cape Verde that were found stranded along the French coast (Monzón-Argüello et al., 2012).

1

2

Figure 5.6.4. Loggerhead hatchlings on a (1, © Adolfo Marco) beach and at first contact with the (2, © Héctor Garrido) sea.

5.6.6. FEEDING

Juvenile sea turtles are known for their opportunistic feeding behaviour (Bjorndal, 1997; Frick et al., 2009), eating and digesting almost anything they can find. Early on their development they eat small prey which includes micro-algae, marine invertebrates and their eggs (decapods, barnacles, amphipods, hidrozoe, etc.), fish, land insects (diptera, formicidae, aphids, coleoptera, etc.) and fiber, feathers, or any kind of floating inert materials whatsoever (Richardson and McGillivary, 2001). For example, in waters around Madeira, Selvagens Islands, and the Azores, loggerhead turtle diet is rich in siphonophores and but less so in scyphomedusae and hydromedusae (van Nierop and den Hartog, 1984). During their development it is possible for them to undergo several habitat shifts that affect their feeding behaviours.

When turtles get to a large body size they usually specialize their diets and select habitats where they can find appropriate prey (Bjorndal, 1997). Leatherbacks consume jellyfish during their subadult and adult stages (Houghton et al., 2006). Green turtles prefer seagrasses and algae, thus selecting shallow waters that are rich in these species (Cardona et al., 2009). Hawksbills associate with coral reefs and rocky areas to feed on sponges, corals or anemones (Meylan, 1988). Kemp's and olive ridleys prefer muddy and sandy bottoms where they feed on hard prey such as crabs, shrimps, clams and other moluscs (Witherington, 2002). Loggerheads maintain an opportunistic feeding behaviour throughout adulthood (Tomás et al., 2001). In Cape Verde, females show a clear feeding dichotomy (Eder et al., 2012). Most of the individuals feed in pelagic habitats between Cape Verde and the African continental shelf and their diet is very rich in jellyfish. But less than 20% of females, in correspondence with the largest individuals, travel to neritic habitats closer to the Gulf of Guinea where they have a more diverse and nutritive diet (Eder et al*.,* 2012).

A mix of natural and artificial debris is usually found with an alarmingly high frequency in the digestive tract of sea turtles, from plastics to wood, feathers, tar, nylon lines, coal, etc. This fact indicates that debris ingestion may be an important threat to loggerhead sea turtle juveniles in this area, consequence of the loggerhead's opportunistic feeding behavior, their low prey selectivity unluckily coinciding with a high level of marine pollution (Carr, 1987; Tomás et al*.,* 2002; Hamann et al*.,* 2010).

5.6.7. THREATS AND CONSERVATION

All sea turtle species present in the CCLME are globally considered as Endangered (EN) (IUCN, 2014). The loggerhead and green turtles of the CCLME constitute regional management units (Wallace et al., 2010). The loggerhead turtles in the region are genetically different from the other loggerhead populations in the Atlantic Ocean and in the Mediterranean Sea (Monzón-Argüello et al*.,* 2010a; Godley et al., 2010; Shamblin et al., 2014). This genetic distinctiveness indicates a significant reproductive isolation, with little or no gene flow with other populations (Monzón-Argüello et al., 2010a).

Furthermore, the waters of the Canary Current hold a remarkable diversity of sea turtles of different origin, including those from the above mentioned rookeries, as well as turtles from the southeast of the United States of America (Bolten et al., 1998), the Caribbean or the Gulf of Guinea (Monzón-Argüello et al., 2010b, 2010c). These feeding aggregations host individuals from distant populations and that conform different management units, thus any management program involving these management units needs to have a multinational scope in order to include these Eastern Atlantic feeding aggregations. Even complete protection in one region may not be sufficient to save a population if excessive exploitation or mortality occurs in other geographic areas (Bolten et al., 1998).

Additionally, the long lives of sea turtles make them especially vulnerable to depletion and their vast oceanic ranges make them especially difficult to manage. This is why the only time unit by which sea turtle recovery can be measured is in decades (Bowen and Karl, 2007). Only such baseline data on population parameters will allow and enhance our ability to make informed management decisions. Otherwise, in these current times of rapidly changing environments we will not have the necessary information to assess possible impacts on sea turtle populations and apply early and appropriate management practices (Hamann et al., 2003).

Increasing fishing efforts worldwide put all sea turtle species at risk. Pelagic long line fisheries account for a yearly bycatch that is very difficult to quantify accurately. For example, only in Madeira, an estimated 500 turtles are caught every year in black scabbard fisheries using deep drifting longlines (Dellinger and Encarnaçâo, 2000). In fact, for Madeira, several reports indicate that a few hundred loggerhead turtles may be captured every year, especially during the summer months (Serpa, 2000). Swordfish longliners based in the Azores, in the central north Atlantic, capture from 0.04 to 0.75 sea turtles per 1000 hooks (Prieto et al., 2000). In the region of Tangier, on the Atlantic coast of Morocco, the estimated bycatch of the entire fleet using drift nets is 719 (Standard Deviation = 543) captures of loggerheads yr^{-1}. For the longline fleet, the average estimated turtle capture in a year is 142 turtles (range = 20–357 turtles; SD = 31) (Benhardouze et al*.,* 2012). There are no detailed studies regarding the impact of bycatch on loggerheads for the adult's feeding groundps in the waters off Cape Verde, Mauritania and Senegal. However, the intense fishing activities in these areas suggest that the capture of adult loggerheads could be very significant for the population. Similarly, emerging industrial fishing in capeverdian waters may also constitute a severe threat to the loggerhead rookery in the eastern Atlantic.

An additional menace for sea turtles in the pelagic environment is marine debris. Necropsies performed on turtles accidentally caught in fisheries indicate the dimension of the marine litter problem in the open ocean with over 90% of the turtles having marine debris in their stomachs. Although this cannot be ascertained as the ultimate cause of death, it surely has a debilitating effect on the turtles, hence reducing individual fitness.

The high concentration of turtle nesting on small beach stretches of Cape Verde and Guinea-Bissau makes the population extremely vulnerable to any kind of environmental disaster (oil spills, tropical storms, etc.) or artificial impact (urbanization, linear infrastructures, artificial lighting, massive tourism, etc.), putting the survival of the population, and a significant portion of the species' genetic variability, at risk (Catry et al., 2009; Marco et al., 2012). Reports from locals suggest that turtle nesting has significantly declined during the last decades. Many islands where turtles were once common now show virtually no signs of nesting (Catry, 2000; Marco et al., 2011). Similarly, many continental areas where nests of different species were often recorded in the past, now have a much scarcer number of nestings, or they are inexistent altogether (Fretey, 2001).

Turtle-watching activities are known as an alternative source of income for local communities that have historically exploited sea turtles for consumption. When natural resources have been employed for generations in an extractive way to sustain local populations, the transition to a non-extractive and sustainable use takes time. Nonetheless, when natural resources include sea turtles and other threatened species, and there are solid social and cultural changes, triggered by forces like tourist development, ecotourism and turtle-watching may rise as a community-based conservation tool, provided that communities are integrated and actively partake in the development of management plans for these species and their critical habitats.

Plate 5.6.1. Six turtle species that can be found in the CCLME Region. 1. Loggerhead (*Caretta caretta,* © Héctor Garrido); 2. Leatherback, (*Dermochelys coriacea,* © Juan Patiño); 3. Green turtle (*Chelonia mydas,* © Genaro Candella); 4. Olive ridley (*Lepidochelys olivacea,* © Carlos Carreras); 5. Kemp's ridley (*L. kempii,* © Pedro López) and 6. Hawksbill (*Eretmochelys imbricate,* © Adolfo Marco).

1

2

3

4

5

6

5.7. BIODIVERSITY OF CETACEANS IN COASTAL WATERS OF NORTHWEST AFRICA: NEW INSIGHTS THROUGH PLATFORM-OF-OPPORTUNITY VISUAL SURVEYING IN 2011-2013

Abdoulaye DJIBA[1,2], Idrissa Lamine BAMY[3], Abdellahi SAMBA OULD BILAL[4] and Koen VAN WAEREBEEK[2,5]

[1] Musée de la Mer de Gorée, IFAN, Université de Dakar Cheikh Anta Diop. Senegal

[2] Conservation and Research of West African Aquatic Mammals (COREWAM). Senegal

[3] Centre National des Sciences Halieutiques de Boussoura. Guinea

[4] Institut Mauritanien de Recherches Océanographiques et des Pêches. Mauritania

[5] Peruvian Centre for Cetacean Research. Perú

5.7.1. INTRODUCTION

With the exception of the Canary and Cabo Verde Archipelagos, very few dedicated vessel-based surveys have studied the spatio-temporal distribution of cetaceans in most parts of the Canary Current Large Marine Ecosystem (CCLME) (e.g. Diallo et al*.,* 2002, 2004; Boisseau et al*.,* 2007; Wenzel et al., 2009; Bamy, 2011). Historically, modest levels of information on the biodiversity of cetaceans from Northwest Africa (NWA) have been derived mainly from incidental stranding and sighting accounts and more recently from limited directed monitoring of strandings and by-catches (reviewed in e.g. Bayed and Beaubrun, 1987; Reiner et al., 1996; Jefferson et al*.,* 1997; Murphy et al., 1997; Robineau and Vély, 1998; Van Waerebeek et al*.,* 2000, 2003; Bamy et al*.,* 2010; Ritter, 2011; Hazevoet et al., 2010; Perrin and Van Waerebeek, 2012; Mullié et al., 2013). Distributional insights obtained through vessel-based surveys sponsored by Japan (e.g. Diallo et al*.,* 2002, 2004) and from a number of geophysical seismic surveys remain buried in unpublished internal reports. The incomplete record in the CCLME region means that even observer effort from platforms-of-opportunity can contribute significantly to our understanding of marine mammal biodiversity and their spatial and seasonal distribution. The joint Norwegian Ecosystem Approach to Fisheries (EAF) Nansen Project, FAO/CCLME and ODINAFRICA-IODE-IOC-UNESCO projects in 2011-2013 offered a platform for shipboard surveys, preliminary results of which are presented below.

5.7.2. DATA SOURCES AND METHODS

The 56.8 m fisheries research vessel R/V *Dr Fridtjof Nansen* served as a platform of opportunity for three visual marine mammal surveys in passing mode (i.e. the vessel did not close on sightings) off NWA in 2011-2013. The study area stretched from Conakry (9.509°N, 13.712°W) to Tangier (35.767°N, 5.800°W), comprising the continental shelf and (limited) contiguous slope waters off Guinea, Guinea-Bissau, The Gambia, Senegal, Mauritania, Western Sahara and Morocco. In 2012, the survey area included also two deep-water transits to and from Las Palmas de Gran Canaria. The 1-22 May 2013 *Sardinella* spp. stock evaluation cruise was limited to shelf waters between Senegal's Cap-Vert and northern Guinea-Bissau. Cruise tracks were designed for the purposes of fisheries and oceanographic research (e.g. Krakstad et al., 2012) and vessel speed was often reduced (0-5 km h^{-1}). Low, varying speeds impeded the application of line

transect sampling protocol for abundance estimation, with model assumptions unfulfilled, e.g. that animals surveyed should move slowly relative to the observer (Buckland et al., 1993). Mean velocity along tracklines while on-effort was 13.65 km h^{-1}. Cruise speed reached a maximum of 18.5 km h^{-1} (10 knots), which most cetaceans can match or exceed. Observers were vigilant to detect potential re-sightings, both in real-time and at analysis. Continuous use of a hull-mounted multibeam sonar, while some interference was possible, was not thought significantly to affect encounter rates. Many dolphin groups evidently ignored it when approaching and bowriding the ship.

During transits, observers visually scanned 180° forwards with compass-equipped 7x50 marine binoculars and naked eye. When at lowspeed or stationary, 360° were scanned, to anticipate any cetaceans approaching from the stern. In 2013, high-magnification (18x50) image-stabilized binoculars aided with identification. Observers were stationed on the radar deck (eye-height, 17 m) or, rarely, on the forecastle deck (14 m). Standard sighting data protocol comprised 37 variables, including i.a.: species, confirmation, observers, start/end time, position, relative location to ship (estimated angle, initial and minimum radial distance), group size estimates (best-minimum-maximum), group composition, diagnostic and unusual features, behaviour including reaction to vessel, visibility (good>5 km; moderate 1-5 km; poor <1 km), Beaufort sea state, and swell (low<2 m; medium 2-4 m; high>4 m). A numbered paper data form was filled out for each sighting, linked to a GPS waypoint. Group dynamics versus vessel and any relevant features were sketched. Observer effort (duration, distance covered) and the ship's activity were also logged. All sea bottom depths (further "depths") were determined by echosounder.

Overall survey effort covered 13,694 km of transects, for a total effective observer time of 69,812 min (1163 h, 32 min) by four alternating observers (authors), with at any time 1-2 observers on effort. Distance and duration surveyed for each of the three cruises in 2011, 2012 and 2013 (Table 5.7.1) amounted to, respectively, 5334 km (27,238 min), 6278 km (31,153 min) and 2081 km (11,421 min).

Table 5.7.1. Summary parameters of visual observer effort for marine mammals from the R/V *Dr. Fridtjof Nansen,* in CCLME study area, 2011-2013. Observers include (initials, effort in min): A. Djiba (AD, 35,704); I. L. Bamy (ILB, 9079); A. Samba Ould Bilal (ASOB, 7049); and K. Van Waerebeek (KVW, 44,390). Ornithologist P. Robinson (PR) assisted with searching, however secondary to seabird observations.

Code	Cruise transects	Period	Observers	Effort (minutes)	Effort (km)
A	Conakry - Cap-Vert	21 Oct-02 Nov 2011 (13 d)	KVW	6925	1742.1
B	Cap-Vert - Cape Blanc	04 Nov-15 Nov 2011 (12 d)	AD, KVW	5910	1119.53
C	Cape Blanc - Agadir	17 Nov-15 Dec 2011 (27 d)	AD	14,403	2472.72
D	Conakry - Cap-Vert	09 May-25 May 2012 (17 d)	ILB, KVW	9079	2008
E	Cap-Vert - Nouakchott	27 May-03 June 2012 (8 d)	AD, PR	3970	781
F	Nouakchott-Cape Juby-Las Palmas de Gran Canaria	08 June-21 June 2012 (14 d)	ASOB, PR	7049	1206
G	Las Palmas de Gran Canaria–Laayoune-Tangier	27 June-20 July 2012 (24 d)	KVW	11,055	2283
H	Kayar- Guinea-Bissau	01 May-22 May 2013 (22d)	AD, KVW	11,421	2081.85

When species could not be positively confirmed through diagnostic morphological features and behaviour, only genus or family was registered. Confirmed records were routinely supported by photos or video taken with DSLR cameras (Canon EOS-350D, 6D) and 70-300 mm telephoto lenses. Probable records ('like-species') were defined as p>90%. Three relative abundance measures were calculated per species: % of total number of groups sighted, % of total number of individual cetaceans sighted, and an overall encounter rate defined as the total estimated number of individuals sighted per 100 km effective survey effort. Best group estimates or, if missing, minimum estimates were used, implying that for some species a negative bias may exist.

5.7.3. RESULTS

During the three CCLME fisheries research cruises (2011-2013) we collected information on 270 primary sightings (excluding re-sightings), comprising 14 different species. Group composition data are summarized in Table 5.7.2. While searches targeted all marine mammals, only odontocetes (10 species) and mysticetes (4 species) were encountered. Below we succinctly discuss group size, relative densities, population identity, habitat and distributional parameters, including range states, for each species encountered.

5.7.3.1. Short-beaked common dolphins, *Delphinus delphis* Linnaeus, 1758

Common dolphins were by far the dominant marine mammals encountered, accounting for (at a minimum) 28.7% of total sightings, or 32.7% if including probable-*Delphinus* sightings. Common dolphins also represented three quarters (71.3%, or 76.5%) of total number of cetaceans observed (Table 5.7.2). Mean group size was 124.92 (SD=124.37; range 2-450; n=54). Encounter rate was estimated as 81.2 common dolphins 100 km^{-1}, and they were found in all areas surveyed, from nearshore neritic to offshore continental slope waters.

Although many groups that were observed closely were confidently identified as *D. delphis* (Plate 5.7.1 (1) and (2)) many other sightings were at great distance at which it would be unfeasible reliably to differentiate between *D. delphis* and the long-beaked common dolphin *D. capensis.* Positive identification of common dolphins in African seas are hindered by their incompletely resolved taxonomy and a lack of combined morphological and molecular analyses (Van Waerebeek, 1997; Westgate, 2007; Amaral et al., 2009; Mirimin et al*.,* 2009; Pinela et al., 2011). A region-wide study of geographic variation in metric and non-metric cranial and external features would be desirable. A cursory check of colouration patterns documented here indicates significant, but possibly clinal, variation (Plate 5.7.1 (1) and (2)). Some molecular studies suggest a single common dolphin taxon off NWA (Pinela et al., 2011). Nonetheless, population structure of *Delphinus* in West Africa should be compared to these from the Gulf of Guinea and SW African waters (Van Waerebeek, 1997).

5.7.3.2. Common bottlenose dolphins, *Tursiops truncatus* (Montagu, 1821)

Common bottlenose dolphins are frequently observed in coastal waters of Senegal, The Gambia and Guinea-Bissau (Cadenat, 1959a, b; Cadenat and Lassarat, 1959; Spaans, 1990; Murphy et al*.,* 1997; Van Waerebeek et al., 1997, 2000, 2003, 2008a). In 2011-2013, *T. truncatus* was the second-most frequently encountered cetacean (Table 5.7.2) accounting for, at a minimum, 9.56% of total sightings, or 11.4% including probable-bottlenose dolphin sightings. However the estimated 210 (or 285) *T. truncatus* observed represented only 1.35% (or 1.83%) of the total number of cetaceans encountered (Table 5.7.2). Mean group size was 9.30 individuals (SD=10.61, range 2-50, n=23). Encounter rate was estimated at 1.53

bottlenose dolphins 100 km^{-1}. The small group sizes in relatively shallow water, 44.5 m median depth (mean=115.8 m; SD=154.8; range 25.1–538.6 m, n=21), 18 of 21 in neritic waters, are mostly consistent with an inshore ecotype. The largest group of 50 (45-60) dolphins was encountered on the slope (312 m depth) off Guinea-Bissau on 15 May 2012 (Plate 5.7.1 (3)). This raises the question whether, as in many other seas (Wells and Scott, 2009), two partially allopatric ecotypes exist off NWA, a neritic shallow-water population and an offshore population. Additional offshore surveying and morphological and molecular studies are necessary. A presumed offshore ecotype typically associates with short-finned pilot whales over and beyond the continental slope. As co-occurring species they likely feed on similar deep-water prey (Cadenat 1959b), such as squid and small mesopelagic fishes. Stable isotope analysis of food items (Pinela et al*.,* 2010) indicated similar $\delta\ ^{15}N$ values (relative abundance of heavy to light nitrogen) for short-finned pilot whales and bottlenose dolphins in Mauritania, suggesting equivalent trophic level and prey. This adds to the case for a distinct offshore ecotype.

Behavioural traits in five small groups of *T. truncatus* seen nearshore of Ngor Island, Dakar, in April-June 2013 (Van Waerebeek and Djiba, personal observations) concur with the traits of an inshore population, including small groups (median=10; range 1-15) foraging behind the surfzone and slow travel parallel to the coastline. Photo-identification studies are needed to determine the affinity of the Dakar inshore community with the southern riverine communities inhabiting the Gambia and Casamance Rivers (Van Waerebeek et al*.,* 2000, 2003, 2008a). Circumstantial evidence, including fishermen's observations, suggests the latter feed on neritic fish such as mullet (*Mugil* spp.) and bonga fish *(Ethmalosa fimbriata).*

5.7.3.3. Short-finned pilot whales, *Globicephala macrorhynchus* (Gray, 1846)

Reports of pilot whales in NWA are often insufficiently documented, or plainly misidentified, as they may refer to either *G. macrorhynchus* or *G. melas*, considering a range overlap in the study area (Norez and Pérez, 1988). One of the earliest reports of *G. macrorhynchus* consisted of a mass-stranding (n=151) including all age and sex classes, at Yoff, Senegal, in May 1943 (Cadenat, 1947). Another group of minimum 15 individuals live-stranded, and died, at Yoff on 17 August 2005 (Plate 5.7.1 (4)). The only record for The Gambia is a specimen washed ashore at Saniang Point in 1998 (Murphy et al*.,* 1997; Jallow et al*.,* 2005). A single sighting was reported from Guinea (Bamy et al., 2010). *G. macrorhynchus* is fairly common off the Canary Islands (Ritter, 2011). Other range states include Morocco, Mauritania and Cabo Verde (e.g. Jefferson et al*.,* 1997; Van Waerebeek et al*.,* 2000, 2003, 2008b; Hazevoet et al., 2010; Perrin and Van Waerebeek, 2012).

CCLME surveys yielded 5 new sightings of *G. macrorhynchus*, supported by inconspicuous grey saddles and a faint cape and eyestripes (Olson, 2009), all in warm waters. For a small pilot whale group (n=4) off Morocco in November 2011, *G. melas* could not be excluded. In deeper water off Guinea-Bissau, on 15 May 2013, we sighted two groups, one of 30 (20-40) pilot whales at 12°0.051'N, 17°25.725'W (789 m depth), and a smaller group of 10 (10-20) individuals at 11°47.228'N, 17°25.728'W (830 m depth), the first records for Guinea-Bissau. The resting animals moved very slowly in a single direction. The larger group was accompanied by some smaller-sized dolphins, likely *T. truncatus.* Furthermore we recorded three *G. macrorhynchus* sightings off Guinea in 2011-12. Overall encounter rate was estimated as 0.50 pilot whales 100 km^{-1} (or 0.47 confirmed *G. macrorhynchus*).

5.7.3.4. Killer whales, *Orcinus orca* Linnaeus, 1758

We recorded a cluster of three small groups of *O. orca* over a five day-period in 2013. On 9 May, 3 (2-3) females or juvenile orcas moved south (Plate 5.7.1(5)) parallel to shore near Kayar (at 14°51.587'N, 17°15.959'W) in shallow water (42.3 m; SST 21.2°C). The next day, 5 (4-6) orcas, of which 2 subadult males, were seen travelling NE in deep water (1482 m; SST 19.4°C) at 15°46.995'N, 17°19.154'W, south of Cap-Vert Peninsula. On 13 May, 5 (5-6) orcas, of which one adult male, moved in deep water (908 m; SST 22.3°C) at 13°24.701'N, 17°33'W off The Gambia, a new range state for *O. orca.*

While *O. orca* is irregularly documented in West Africa (Hammond and Lockyer, 1988), we compiled 26 records for Senegal, including the earliest case, a female captured near Hann in February 1942, amongst the 17 (65%) around the Cap-Vert Peninsula, and two unusual sightings in the Senegal River (Maigret, 1977). Cadenat (1959a) suggested *O. orca* to be absent from Senegal in the hot season but sightings exist for all seasons, albeit records are still lacking for March-April, August-September and November, and some seasonality is possible. Group sizes have consistently been very small, often 1-2 individuals. Maigret (1977) also observed orcas alone or in pairs in Mauritanian waters.

Confirmed CCLME range states now include Morocco, Mauritania, Senegal, The Gambia, Canary Islands and Cabo Verde (Bayed and Beaubrun, 1987; Hammond and Lockyer, 1988; Van Waerebeek et al., 2000; Hazevoet et al., 2010; Ritter, 2011). *O. orca* has not yet been recorded in Guinea-Bissau and Guinea (Van Waerebeek et al*.,* 2000, 2003; Perrin and Van Waerebeek, 2012) and although it will surely be found there in future, abundance seems higher in Senegal, irrespective of a higher reporting rate. With only three observations the overall encounter rate was a low 0.088 orcas 100 km^{-1}. Population structure in West Africa remains unstudied (Foote et al., 2009), but orcas from Senegal's and Mauritanian coasts likely belong to the same population.

Also, scarce information exists on prey and foraging strategies. Stomach contents of one female captured in Senegal contained remains of 'many fishes' (Cadenat, 1947). Ritter (2011) suggested that orcas in the Canaries follow tuna schools. In 2012, a fisheries officer reported (personal communication to Djiba) that a group of killer whales attacked green turtles (*Chelonia mydas)* nearshore at Joal, Senegal. One photo (Plate 5.7.1(6)) shows a small, obviously juvenile orca pushing and partly lifting a turtle, however this incident remains inconclusive, interpretable as either play or predation. Stable isotope analysis suggested that *O. orca* in Mauritania may be an offshore ecotype preying on fish, while orcas appeared to avoid other marine mammals, including the monk seal (Pinela et al., 2010).

5.7.3.5. Risso's dolphin, *Grampus griseus* (Cuvier, 1812)

A cluster of two confirmed and one probable sighting was recorded off central Morocco within 4 days. Respectively, a slowly moving group of 3 (3-4) at 33°0.753'N, 8°59.789'W on 8 July 2012 (photos archived); a larger group of 15 (12-20) at 34°14.121'N, 7°08.517'W including several large, pale-coloured adults (Plate 5.7.1 (7)) keeping parallel with the ship steaming 10 knots, on 11 July 2012 (09:51); and one hour later (11:02), a very distant group of at least 3 individuals, at 34°14.569'N, 7°03.721'W, their whitish body colouration and large dorsal fins standing out. Bottom depths (and SST) for the location of each sighting were 502 m (18.2°C), 181 m (20.3°C) and 170 m (20.3°C) respectively. These represent first authenticated records of *G. griseus* for Morocco, although an unsupported stranding 31 km north of Agadir in 1984 was mentioned by Bayed and Beaubrun (1987). *G. griseus* is otherwise known from a stranded skull collected in Mauritania (Duguy, 1976) and a pod of 9 individuals sighted at 18.125°N, 16.706' W on 6 December 2012 by one of us (ASOB, personal observations) during an R/V *Al Awam* survey off Mauritania. There are reported

sightings off the Canaries (Ritter, 2011), Cabo Verde (Hazevoet and Wenzel, 2000) and Guinea-Bissau (Van Waerebeek et al., 2000), the latter two unauthenticated. Overall encounter rate is estimated as 0.131 Risso's dolphins 100 km^{-1}.

5.7.3.6. Pantropical spotted dolphin, *Stenella attenuata* (Gray, 1846)

One confirmed and one unconfirmed sightings were made. A small group of 22 (20-30) *S. attenuata* was filmed in deeper water (897 m; SST 27.3°C) at 9°1.5702'N, 15°26.772'W off Guinea, on 22 October 2011, the first documented record for that country. The dolphins approached from the stern and briefly rode the bow wave. A tentative sighting off Senegal, at 13°59.665'N, 17°31.042'W occurred on 20 May 2013. Some 50 (30-80) delphinids, observed at 750 m distance under moderate visibility conditions and 3-4 Beaufort sea state, were tentatively identified as a mixed group of *D. delphis* and *S. attenuata* in continental slope waters (434 m; SST 24.1°C).

The encounter rate for (confirmed) *S. attenuata* was a low 0.163 dolphins 100 km^{-1}. Presumably the species is less rare at the oceanic side of the NWA continental slope which was poorly covered by the 2011-2013 cruises. Hazevoet et al. (2010) documented a live-stranding of 17 *S. attenuata* at Mindelo. Without however referring to other specific cases, they noted that it was one of the commoner dolphin species in Cabo Verde.

S. attenuata has a preference for tropical oceanic waters and may largely avoid the cooler, upwelling-modified neritic habitat of the Canary Current system, which would explain the lack of records between Morocco and Senegal, including the Canaries (Jefferson et al*.,* 1997, Van Waerebeek et al*.,* 2000, 2003; Ritter, 2011; Perrin and Van Waerebeek, 2012).

5.7.3.7. Clymene dolphin, *Stenella clymene* (Gray, 1850)

One of us (K.V.W.) sighted a group of 13 (12-18) *S.clymene* at 15°06.868'N, 17°22.404'W, off Kayar, on 22 May 2013 (depth 603 m; SST 23.3°C), the first documented sighting in Senegal (photos archived). Interestingly, small body size was the most striking phenotypic feature. Their presence near Kayar may be linked to the unusual topography of deep underwater canyons on the north face of the Cap-Vert Peninsula which could facilitate oceanic species to approach nearshore. Several whales, including sperm and one humpback whale are known to have stranded near Kayar.

Based on a few specimens, confirmed CCLME range states for *S. clymene* include Mauritania, Senegal and The Gambia. The northernmost record in the NE Atlantic is 113 km north of Nouakchott at 19°1.9'N, 16°13.5'N (Cadenat, 1959a; Robineau et al*.,* 1994; Van Waerebeek et al*.,* 2000, 2003; Fertl et al., 2003; Perrin and Van Waerebeek, 2012). *S. clymene* is rare in neritic waters off NWA, with an encounter rate of only 0.095 Clymene dolphins 100 km^{-1}. It is as yet unknown from Cabo Verde (Hazevoet et al., 2010) and Canary Islands (Ritter, 2011) despite commercial whale and dolphin-watching. This stands in stark contrast with *S. clymene* status as most-exploited dolphin species in Ghana (Gulf of Guinea) which prompted a Convention on Migratory Species (CMS) Appendix I listing of that population (Van Waerebeek and Perrin, 2007a).

5.7.3.8. Atlantic spotted dolphin, *Stenella frontalis* (Cuvier, 1829)

Five sightings of *S. frontalis* were confirmed, two off Guinea, two off Guinea-Bissau (one associated with *D. delphis*), and one far offshore, closer to the Canaries. Depths ranged widely, from 64.8 m on the Guinean shelf, up to 2379 m (median 583 m; n=5) for the offshore sighting of largely unspotted individuals, probably of a distinct population. Some of the many sightings of unidentified delphinids recorded at great distance were also suspected to be *S. frontalis.* A compact group of 6 (4-10) slowly moving *S. frontalis* at 9°58.041'N, 16°48.849'W, on the Guinea-Bissau continental slope (depth 342 m; SST 25.6°C) on 15 May 2012, comprised heavily spotted individuals (Plate 5.7.1(8)). Another 20 spotted *S. frontalis* formed a mixed group with minimum 150 *D. delphis* (conspecifics herded together in subgroups) when foraging near the vessel (11°33.689'N, 017°24.433'W) after dark (21:30) on 29 October 2011. These represent the first records for Guinea-Bissau (KVW confirmed diagnostics). In the study region, only Morocco and The Gambia have no *S. frontalis* records associated (Perrin and Van Waerebeek, 2012). Encounter rate was 0.32 Atlantic spotted dolphins 100 km^{-1}.

5.7.3.9. Striped dolphin, *Stenella coeruleoalba* (Meyen, 1833)

A single sighting was recorded of this typical oceanic species. The most common cetacean in the Mediterranean Sea, *S. coeruleoalba* is rarely documented in West Africa. We photographed a small herd of 12 (8-15) individuals in Moroccan waters at 32°33.676'N, 9°43.004'W (depth 497.1 m; SST 18.1°C) on 7 July 2012 (Plate 5.7.1(9)). During the brief encounter (13:49-13:55) several dolphins leaped clear and rode the bowwave at 10 knots. This is the first substantiated record of *S. coeruleoalba* for Morocco's Atlantic coast. Encounter rate was a low 0.088 striped dolphins 100 km^{-1}. Other CCLME range states include Cabo Verde (Hazevoet and Wenzel, 2000), Canary Islands (Ritter, 2011), Mauritania and Senegal (Cadenat, 1949; Van Waerebeek et al., 2000; Perrin and Van Waerebeek, 2012). *S. coeruleoalba* is unknown in The Gambia, Guinea-Bissau and Guinea (Bamy et al., 2010). Moreover, the species remains undocumented in coastal waters from Senegal southeast to Angola, bar a unique capture record in Cameroon (Ayissi et al., 2014). Significantly, *S. coeruleoalba* is absent among the many hundreds of verified landings of small cetaceans in Ghana (Debrah et al., 2010).

5.7.3.10. Beaked whales, Ziphiidae

A single unidentified beaked whale, a *Mesoplodon* sp., ca. 3.5-4.5 m in length, was observed in Guinea, at 9°0.078'N, 15°07.431' W (depth 488 m; SST 28.5°C). Dorsally uniformly gray, the triangular dorsal fin was set towards the rear of the back. Either one animal surfaced twice or two similar individuals surfaced sequentially. The minimum encounter rate was 0.007 beaked whales 100 km^{-1}. Mesoplodonts, as well as other beaked whales, are deep-diving species rarely reported for most of the study area, but not infrequently in the Canary Islands, and often from strandings related to navy exercises. Blainville's beaked whale *M. densirostris* is well-known from the Canaries (Ritter and Brederlau, 1999) and Morocco. Sowerby's beaked whale *M. bidens* is also reported from the Canaries; Gervais' beaked whale *M. europaeus* from Mauritania, Canary Islands and Guinea-Bissau (Reiner, 1980; Martín et al., 1990; Robineau and Vély, 1993; Ritter, 2011; Perrin and Van Waerebeek, 2012; Koenen et al., 2013). The large, cosmopolitan Cuvier's beaked whale, *Ziphius cavirostris,* is recorded in Morocco, Canary Islands, Mauritania, Cabo Verde and Senegal (Perrin and Van Waerebeek, 2012).

5.7.3.11. Humpback whale, *Megaptera novaeangliae* (Borowski, 1781)

Arguably the most remarkable cetological finding of the 2011 survey consisted in the discovery of an undescribed stock of humpback whales off NW Africa, thought to comprise the northwestern-most component of the large Southern Hemisphere (SH) breeding assemblage that migrates to and from the Gulf of Guinea in austral winter and spring (Van Waerebeek et al*.,* 2013). Bamy et al. (2010) first formulated a SH stock hypothesis based on a few unseasonal records in Guinea.

M. novaeangliae was the most commonly encountered cetacean (17 confirmed, 4 probable sightings) on the wide Conakry-Dakar shelf, surveyed 21 October–5 November 2011 (Van Waerebeek et al*.,* 2013). None were encountered between Dakar and Agadir, 6 November-15 December 2011. Sighting effort was 468 h over 5334 km. The sum of group sizes totalled 33 whales, or 43 whales (including probable records). Encounter rate was 1.74 or 2.27 humpback whales 100 km^{-1}, respectively, or 0.24 whales 100 km^{-1} for the pooled 2011-2013 effort. Herd sizes ranged 1–6 individuals (median=2). At least 5 of 17 groups (29.4%) consisted of adult–calf pairs, with a minimum crude birth rate ranging 0.060–0.152 (Van Waerebeek et al*.,* 2013). All sightings occurred in very shallow water of 22–60 m (mean=35.0 m). SST was high in 25.5–29.0°C range (mean=27.34°C). *M. novaeangliae* was not encountered during the Conakry–Tangier–Las Palmas survey in May-June 2012.

Cabo Verde, till now, was the only recognised wintering ground in the NE Atlantic (Hazevoet and Wenzel, 2000; Wenzel et al., 2009). Temporal signature of the 2011 records, 6-7 months out-of-phase with mid-season in Cabo Verde, and the presence of small calves strongly suggest that the Conakry–Dakar shelf serves as both wintering and nursery grounds for a South Atlantic stock. Guinea, Guinea-Bissau, The Gambia and Senegal became newly documented range states for *M. novaeangliae* (Bamy et al*.,* 2010; Van Waerebeek et al*.,* 2013).

5.7.3.12. Blue whale, *Balaenoptera musculus* (Linnaeus, 1758)

A herd of three blue whales was sighted above the continental break (depth 383 m; SST 21.2°C) in Gambian coastal waters at 13°17.558'N, 17°33.665'W, on 13 May 2013. A smallish individual (10-12 m), startled by the ship passing closely, blew three times as it fled subsurface exposing a mottled bluish-grey dorsum and a large splash-guard in front of the blowholes, but not its dorsal fin (Plate 5.7.1(10)). At 1 km, it joined a large individual, possibly its mother (Plate 5.7.1(11)). At 2.5 km, a third, adult-sized individual, also a pale bluish-grey, blew with a very tall, vertical columnar blow. Its small dorsal fin at the rear of the back was exposed only seconds before the whale submerged, when its blow had already dissipated. Encounter rate was estimated as 0.022 blue whales 100 km^{-1}.

The winter breeding grounds and austral range of NE Atlantic blue whales remain unknown (Sears and Perrin, 2009). Very few historical records from West Africa are documented to any extent, but two concern vague whaling records. On 10 November 1947, the Soviet *Slava* whaling fleet encountered one and then three more blue whales at 18°10'N, 18°W (SST 25°C) (Kirpichnikov, 1950; Tomilin, 1967). On 1 March 1911, 12 blue whales were observed by other whalers at N16° between Cabo Verde and northern Senegal (Kirpichnikov, 1950). Three blue whales were sighted off La Gomera, Canary Islands, in April 1997 (Ritter and Brederlau, 1998; Ritter, 2001), and one large individual was confirmed off Mauritania at 19°22.44'N, 17°4.2'W on 4 December 2012 (Samba Ould Bilal, personal observations). No specimens of blue whales have been substantiated for any of the CCLME countries (Van Waerebeek et al., 2000, 2003). Two possible historical records include Cadenat's (1947) report of an 'enormous' whale of 25 m length at Malika beach, Dakar, on 5 May 1943, though stranded in April. The size alone would seem to confirm this record.

Maximum known size of northern fin whale *Balaenoptera physalus physalus* is 24 m (Gambell, 1985), an equally rare species off West Africa. Duguy (1976) attributed vertebrae and ribs collected from Rio de Oro (Western Sahara) to blue whale, without diagnostic arguments. According to Sears and Perrin (2009), blue whales sighted recently in winter and spring off the Azores and Canary Islands could be migrating north along the mid-Atlantic ridge to Iceland, where they are seen from May to September. The present record from The Gambia is the southernmost observation of *B. musculus* in the eastern North Atlantic.

5.7.3.13. Balaenopterid whales

Rorquals (*Balaenoptera* spp.) were commonly observed (n=26 groups) in all parts of the study area (encounter rate 0.26 rorquals 100 km^{-1}), however usually from a considerable distance, hampering positive identification. Excluding the *B. musculus* encounter, 3 groups were attributed to Bryde's whale (*B. brydei)*, 6 as Bryde's or sei whale, 1 probable sei whale (*B. borealis),* and 16 groups were unidentified *Balaenoptera* sp. The latter most likely comprise Bryde's and sei whales, two of the three most commonly confirmed rorquals in the study area (Bamy et al., 2010; Van Waerebeek et al., 2000). However, the recent stranding of an Omura's whale (*B. omurai*) in Mauritania (Jung et al., 2015), a first record in the Atlantic Ocean, further complicates the identification process. The smallish North Atlantic minke whale, although not uncommon in the region, was not sighted.

Five black baleen plates with pale, very fine fringe hairs, diagnostic for *B. borealis,* were recovered from demersal trawl haul “station 124” (mean depth=367.5 m,) off Mauritania at 17°40.2'N, 16°37.8'W, on 1 June 2012. At base, the baleen exposed non-decomposed connective tissue (Plate 5.7.1(12)). A small fragment of a sixth plate showed shearing edges, evidently ripped apart forcefully. The baleen may have originated from a recently dead carcass on the seafloor, or the bottom-trawl collided with a live sei whale and shear forces pulled out the baleen (deposited at IMROP collection, Nouadhibou).

5.7.4. DISCUSSION

5.7.4.1. General remarks

Of 270 sightings, 144 (53.3%) could be positively identified to species, and another 57 (21.1%) were tentatively identified as either a 'probable'-species or a rorqual/ziphiid. A quarter of sightings (24.4%) remained 'unidentified Delphinidae', mainly due to great distance and passing mode surveying. That three quarters of sightings were positively or tentatively identified confirms the usefulness of the R/V *Dr. Fridtjof Nansen* as opportunity platform for marine mammal work, despite the obvious limitations of passing mode.

The consistently dominant ecological role common dolphins play in coastal waters of NWA (>69% of total cetaceans) was historically demonstrated by an equivalent preponderance of *Delphinus* skulls at the IFAN-UCAD collection in Dakar, derived from strandings and by-catches, as compared to other marine mammal specimens (Van Waerebeek et al., 2000). *T. truncatus, G. macrorhynchus* and *S. attenuata* came a far second, third and fourth place in relative abundance (respectively, 1.80%, 0.61% and 0.59% of total number of cetaceans observed). Numerically, each of all other species represented less than 0.4% of sighted individuals (Table 5.7.2). Stenellid dolphins were infrequently seen, only 3.3% of sightings for 4 species, explainable due to minimal offshore surveying. However, some stenellids may be locally abundant, e.g. *S. frontalis* is one of the more common dolphins off the Canaries (Ritter, 2011). Also both that species and *S. attenuata* are often reported in the oceanic habitat around the Cabo Verde Islands (Hazevoet et al., 2010).

5.7.4.2. Species not encountered in 2011-2013

Below we briefly discuss 11 cetacean species that are occasionally reported in the CCLME but were not encountered during the 2011-2013 surveys. Only the first three can be considered true CCLME species.

Harbour porpoise (*Phocoena phocoena)* – Adapted to cold temperate waters, the NWA population is closely associated with the Canary Current (Van Waerebeek et al., 2000). Recent stranding records, many from by-catches, suggest that *P. phocoena* is most common in Mauritania (Mullié et al., 2013). Near Cape Blanc, porpoises can be observed year-round from cliff-tops (Van Waerebeek and Jiddou, 2006). *P. phocoena* is notoriously hard to spot with sea states >2 Beaufort, hence it is one of few small cetaceans for which passive acoustic monitoring may be more effective than visual surveys (Boisseau et al., 2007). Morocco, Western Sahara, Mauritania and Senegal are range states for what is a highly discrete population, of not an unrecognized subspecies. Joal-Fadiouth (14°09'N, 16°49'W) is the southern confirmed range boundary (Van Waerebeek et al., 2000).

Atlantic humpback dolphin (*Sousa teuszii*) – This obligate inshore-dwelling delphinid was not sighted, despite the ship occasionally entering shallow (20 m depth), nearshore waters and the study region harbouring five of the eight defined stocks: Dakhla Bay, Banc d'Arguin, Saloum-Niumi, Canal do Geba/dos Bissagos and Guinea (Van Waerebeek et al*.,* 2003, 2004; Van Waerebeek and Perrin, 2007b). Its threatened status is reflected in scarce sightings, small groups and an apparently discontinuous distribution. Few new records exist for Senegal and Guinea since earlier reviews, several of these by-catches (Bamy et al., 2010; Bamy, 2011; Van Waerebeek and Bamy, 2012; Djiba, personal observations).

Common minke whale (*Balaenoptera acutorostrata*) – Its seasonal presence in coastal waters of NWA, as far south as Senegal, is well-documented (Van Waerebeek et al., 1999). No minke whales were sighted, arguably because the 2011-2013 cruises did not cover boreal winter months when *B. acutorostrata* is thought to breed in the study area (Van Waerebeek et al., 1999). The rest of the year, minke whales migrate to cooler, higher latitudes, for feeding.

Another five typically offshore, tropical species which may occasionally be present in the more southern, Guinea Current-influenced, parts of the study area, as well as offshore of the Canary and Cabo Verde archipelagos include:

Spinner dolphin (*Stenella longirostris)* – This small tropical offshore delphinid is seldom recorded in the Canary Current, with only a few specimens known, a capture of four animals in Senegal in 1958 (Van Waerebeek et al., 2000) and a single stranding in the Canary Islands (Ritter, 2011). Four sightings were reported from deep waters off Cabo Verde (Reiner et al., 1996; Hazevoet and Wenzel, 2000).

Fraser's dolphin (*Lagenodelphis hosei)* – is known from a single specimen found stranded at Sangomar Island, Senegal, on 17 November 1997 (Van Waerebeek et al., 2000), a few deep-water sightings off the Canaries (Ritter, 2011) and a recent stranding at Cabo Verde (Torda et al., 2010).

Melon-headed whale (*Peponocephala electra)* – An offshore tropical delphinid infrequently recorded in mainland coastal waters of CCLME: a few strandings in Mauritania (Robineau and Vély, 1998), Senegal and Guinea-Bissau (Van Waerebeek et al., 2000). Two successive mass strandings at Boavista, Cabo Verde, on 17 and 19 November 2007 of healthy animals, with evidence of recent feeding, coincided with the passage of a nuclear submarine possibly using active sonar (Van Waerebeek et al., 2008b). A number of other strandings at Cabo Verde have little associated information (Hazevoet et al., 2010).

Pygmy killer whale *(Feresa attenuata)* – Another mid-sized tropical delphinid seldom encountered in the Canary Current. Known from a single skull retrieved in Senegal in 1966 (Van Waerebeek et al., 2000) and a very few sightings in the Canary and Cabo Verde Islands (Ritter, 2011; Hazevoet et al., 2010; Perrin and Van Waerebeek, 2009).

False killer whale (*Pseudorca crassidens*) - A large, deep-water delphinid rarely seen offshore of the Canary Islands (Ritter, 2011), and known from a few stranded specimens at Cabo Verde (Van Waerebeek et al., 2008b; Hazevoet et al., 2010).

Rough-toothed dolphin (*Steno bredanensis)* – Commonly sighted near the Canary (Ritter, 2011) and Cabo Verde Islands (Hazevoet et al., 2010), *S. bredanensis* is known from only a few strandings on the mainland, in Senegal (Cadenat, 1949) and Mauritania (Duguy, 1976; Perrin and Van Waerebeek, 2012).

Physeterids - Unsurprisingly, no physeterids were recorded, including pygmy sperm whale (*Kogia breviceps)* and dwarf sperm whale (*Kogia sima),* considering their normal distribution in deep oceanic waters (Van Waerebeek et al., 2000; Perrin and Van Waerebeek, 2012). However, KVW and Djiba found a partial skull of a sperm whale (*Physeter macrocephalus*) when beach-combing near Kayar on 3 June 2013. The Kayar canyon system may increase the danger of stranding among normally oceanic species, as they readily come close to shore.

5.7.5. RECOMMENDATIONS

While accessory to fisheries research, the significant amount of relevant marine mammal data obtained underscores the value of surveying efforts from the EAF-Nansen platform-of-opportunity. The 2011-2013 cruises provided useful information on biodiversity, cetacean spatial and seasonal distribution, group composition, relative abundance, in addition to data on variation in external morphology. The incidental nature, in particular the absence of the option for closing on sightings, obviously detracts from the potential efficiency when compared to dedicated marine mammal surveys. However, by obviating ship-time, the results *versus* cost factor is highly beneficial. Hence we strongly recommend to systematically include marine mammal monitoring as an integral part of fisheries and oceanographic research cruises. These initial efforts should be expanded to cover all seasons and all African waters. A massive, multiple-year marine mammal dataset obtained through a long-term programme could ultimately minimize biases and compensate for many of the deficiencies of opportunistic sampling. Moreover, platform-of-opportunity cruises often offer convenient circumstances for training purposes, as to strengthen regional expertise in marine mammal research. Fully dedicated shipboard surveys will surely be needed at some point to obtain absolute abundance estimates, implement targeted sampling or answer specific questions. In the meantime, some limited ship-time (e.g. a few 15 min slots per cruise) could be assigned and selectively applied when particularly high-value observations occur.

A region-wide study of geographic variation in metric and non-metric cranial and external features of common dolphins *Delphinus* spp. would be desirable, to help elucidate population structure in African seas. Also, the feasibility of skin biopsy sampling to collect DNA from bowriding common dolphins (and other species), such as with adapted crossbows, coupled to the documentation of external features and ecological data, merits consideration for future projects.

Due to their wide coastal distribution in the CCLME, *D. delphis, T. truncatus, P. phocoena* and *S. teuszii* are the four small cetacean species most commonly falling victim to net entanglements on the NWA coasts (Van Waerebeek et al., 2000, 2003, 2004; Mullié et al., 2013). Although gillnets and midwater trawls are the

main suspects as problem gear causing detrimental interactions, there are minimal regional data on the dynamics and trends of fisheries-caused mortality. Fisheries observers should be trained and encouraged to consistently record and report marine mammal by-catches. A comprehensive database would allow a more prudent regional management, including the evaluation and introduction of effective mitigation measures.

Acknowledgements

A fair number of people contributed to the success of the CCLME marine mammal survey efforts to all of whom we extend our grateful thanks for their long-term support. Special thanks are due to Paul Robinson and two Senegalese fisheries officers for observer support, to cruise leaders Jens-Otto Krakstad, Kathrine Michalsen and Age Hoiynes and to the captains and crews of the R/V *Dr. Fridtjof Nansen* for efficient and good-humoured collaboration. FAO/CCLME project Regional Coordinating Unit staff Aboubacar Sidibé and Birane Sambe kindly facilitated access to the vessel. Rudy Herman (FUST/ODINAFRICA) and Mika Odido (IOC-UNESCO) kindly offered expert guidance with funding applications. Vassili Papastavrou critically read the manuscript. Marine mammal work and travel was financed by the project «Integrated Data and Information Products and Services for the Management of Oceans and Coastal Zones in Africa – ODINAFRICA-IV» as contribution to the collaboration with FAO/CCLME. The research cruises were conducted as part of the EAF-Nansen project (www.eaf-nansen.org, accessed on 24 February 2015), a partnership between FAO, Norwegian Agency for Development Cooperation (Norad) and the Institute of Marine Research (IMR), in collaboration with the CCLME Project, which covered all vessel-related expenses. K. Van Waerebeek acted as individual UNESCO consultant under short-term contracts. CEPEC provided most of the survey equipment.

Table 5.7.2. Frequency distribution of number of sightings (and % value) per species or higher taxon, and total number (Σ ind.) of individuals (and %) estimated per species or higher taxon, for each of the 2011-2013 surveys, and pooled. Best estimates or, if missing, minimum estimates were used. Mixed species groups were split into its components and considered two sightings for statistical purposes.

TAXON	2011				2012				2013				2011-2013			
	Sights	%	Σ ind.	%	Sights	%	Σ ind.	%	Sights	%	Σ ind.	%	Sights	%	Σ ind.	%
Unidentified Delphinidae	32	26.9	1239	17.2	22	21.8	848	29.6	14	26.9	1000	18.09	68	25.0	3087	19.8
Short-beaked common dolphin	27	22.7	5423	75.3	31	30.7	1522	53.2	20	38.5	4175	75.6	78	28.7	11120	71.3
Probable short-beaked common dolphin	4	3.36	293	4.07	5	4.95	262	9.15	2	3.85	252	4.56	11	4.04	807	5.17
Common bottlenose dolphin	8	6.72	69	0.96	13	12.9	115	4.02	5	9.62	26	0.47	26	9.56	210	1.35
Probable common bottlenose dolphin	2	1.68	44	0.61	3	2.97	31	1.08	0	0	0	0	5	1.84	75	0.48
Pilot whale	3	2.52	24	0.33	2	1.98	4	0.14	2	3.85	40	0.72	7	2.57	68	0.44
Killer whale	0	0	0	0	0	0	0	0	3	5.77	12	0.22	3	1.10	12	0.077
Risso's dolphin	0	0	0	0	2	1.98	18	0.63	0	0	0	0	2	0.73	18	0.11
Probable Risso's dolphin	0	0	0	0	1	0.99	3	0.10	0	0	0	0	1	0.37	3	0.019
Atlantic spotted dolphin	2	1.68	26	0.36	3	2.97	18	0.63	0	0	0	0	5	1.84	44	0.28
Probable Atlantic spotted dolphin	0	0	0	0	1	0.99	5	0.17	0	0	0	0	1	0.37	5	0.032
Pantropical spotted dolphin	1	0.84	22	0.31	0	0	0	0	0	0	0	0	1	0.37	22	0.14
Clymene dolphin	0	0	0	0	0	0	0	0	1	1.92	13	0.24	1	0.37	13	0.083
Striped dolphin	0	0	0	0	1	0.99	12	0.42	0	0	0	0	1	0.37	12	0.077
Unidentified rorquals	4	3.36	5	0.07	10	9.9	17	0.59	2	3.85	2	0.036	16	5.88	24	0.15
Bryde's whale	0	0	0	0	3	2.97	4	0.14	0	0	0	0	3	1.10	4	0.026
Bryde's / sei whale	6	5.04	6	0.08	0	0	0	0	0	0	0	0	6	2.21	6	0.038
Probable sei whale	1	0.84	2	0.03	0	0	0	0	0	0	0	0	1	0.37	2	0.013
Blue whale	0	0	0	0	0	0	0	0	1	1.92	3	0.054	1	0.37	3	0.019
Humpback whale	17	14.3	33	0.46	0	0	0	0	0	0	0	0	17	6.25	33	0.21
Probable humpback whale	4	3.36	10	0.14	0	0	0	0	0	0	0	0	4	1.47	10	0.064
Unidentified cetacean (whale)	8	0	10	0	3	2.97	3	0.10	2	3.84	3	0.054	13	4.78	16	0.10
Beaked whale (Ziphiidae)	0	0	0	0	1	0.99	1	0.03	0	0	0	0	1	0.37	1	0.006
Total	119	100	7206	100	101	100	2863	100	52	100	5526	100	272	100	15595	100

Plate 5.7.1. (1) Short-beaked common dolphin (*Delphinus delphis),* the most widely spread cetacean in the CCLME ecosystem (© Koen Van Waerebeek). (2) Short-beaked common dolphin (*Delphinus delphis).* Note the significant variation in colouration compared to specimen in photo 1. (© Koen Van Waerebeek) (3) Common bottlenose dolphin (*Tursiops truncatus*), 15 May 2012 (© Koen Van Waerebeek) (4) Short-finned pilot whales (*Globicephala macrorhynchus*) live-stranded at Yoff, Senegal, 17 August 2005 (© Abdoulaye Djiba, COREWAM). (5) Small pod of killer whales (*Orcinus orca*) travelling nearshore close to Kayar, Senegal, 9 May 2013 (© Koen Van Waerebeek) (6) Juvenile killer whale (*Orcinus orca*) interacting with green turtle near Joal, Senegal, in 2012 (© Abdoulaye Djiba, COREWAM).

1

2

3

4

5

6

Plate 5.7.2. (1) Adult Risso's dolphin (*Grampus griseus*) off the central Moroccan coast, 11 July 2012 (© Koen Van Waerebeek). (2) A heavily spotted, physically mature Atlantic spotted dolphin (*Stenella frontalis*) (© Koen Van Waerebeek). (3) A first record of the striped dolphin (*Stenella coeruleoalba*) off Atlantic Morocco, 7 July 2012 (© Koen Van Waerebeek). (4) Juvenile blue whale (*Balaenoptera musculus*) fleeing the passing ship, in direction of the adult shown in photo 5. The Gambia, 13 May 2013. Note the mottled bluish-grey dorsum (© Koen Van Waerebeek). (5) Adult blue whale (*Balaenoptera musculus*) surfacing: blow has dissipated but the small dorsal fin, at the rear of the back, is not yet visible (© Koen Van Waerebeek). (6) Fresh baleen plates of sei whale (*Balaenoptera borealis*) recovered from a demersal trawl haul off Mauritania, 1 June 2012 (© A. Samba Ould Bilal).

1

2

3

4

5

6

6. INTERANNUAL, INTERDECADAL AND LONG-TERM VARIABILITY

6.1. OPEN OCEAN TEMPERATURE AND SALINITY TRENDS IN THE CANARY CURRENT LARGE MARINE ECOSYSTEM

Pedro VÉLEZ-BELCHÍ[1], Marta GONZÁLEZ-CARBALLO[2], María Dolores PÉREZ-HERNÁNDEZ[3] and Alonso HERNÁNDEZ-GUERRA[3]

[1] Centro Oceanográfico de Canarias, Instituto Español de Oceanografía. Spain

[2] Observatorio Ambiental de Granadilla. Spain

[3] Instituto de Oceanografía y Cambio Global (IOCAG), Universidad de Las Palmas de Gran Canaria Spain

6.1.1. INTRODUCTION

The Canary Current Large Marine Ecosystem (CCLME) in the Northwest African (NWA) coast is a high productive ecosystem with strong socio-economic impact since it supports a vast and diverse marine population. The high productivity of the CCLME is mainly driven by the trade winds that flows alongshore, parallel to the NWA coastline, and therefore the actual global warming scenario may affect the CCLME by warming the upper ocean waters, but also, as suggested by Bakun (1990), by intensifying the upwelling and therefore cooling the upper ocean waters. Bakun's hypothesis suggested that the increase in greenhouse gases will lead to an increase in the temperature gradient between land and ocean, which would intensify the continental–oceanic pressure gradient, and therefore increase the alongshore wind stress that forces the coastal upwelling. Upwelling favorable wind intensification could benefic marine populating by increasing the nutrient supply to the euphotic layer, however, it could affect also in a negative way by transporting plankton out of the shelve or disrupting trophic interactions.

Although there is not doubt about the increase in global temperatures, the impact on the upwelling ecosystem is controversial. Pardo et al. (2011) estimated the upwelling intensity in the CCLME, using data from the National Centers for Environmental Prediction/National Center for Atmospheric Research (NCEP/NCAR) reanalysis project, and found a general sea-surface warming and weakening of the upwelling intensity between 1970-2010. Using Sea Surface Temperature (SST) images for the period 1987–2006 and remote sensing wind stress Marcello et al. (2011) found intensification of the upwelling system in that period, while the alongshore wind stress remained stable. These authors also found that in the period 1987–2006 upwelled waters off Cape Blanc have increased their offshore spreading. Using different estimates of wind observations, including coastal meteorological stations, Barton et al. (2013) did not found evidences of intensification in upwelling favorable winds, moreover they found a significant increase in sea surface temperature at all latitudes in the CCLME region. Based on that, these authors concluded that there was no evidence for a general increase in the upwelling intensity in the CCLME. Sydeman et al. (2014) carried out a meta-analysis of all the literature focused in understanding the impact of the climate change in the wind intensification of coastal upwelling, and concluded that most of the literature, although subtle and spatially variable, support Bakun's hypothesis. In the case of the CCLME, the authors indicated that wind changes were ambiguous, with warm-season winds as likely to be intensifying as not. These authors found that in the CCLME, studies based on direct observations were significantly more likely to detect intensifying than weakening, while model/data reanalysis products were more likely to detect

weakening winds. Contrarily, Cropper et al. (2014), using a variety of upwelling indices for the period 1981–2010 concluded that there was compelling evidence in favor of the Bakun's hypothesis, with an increase in upwelling-favorable winds north of 20°N, and an increase in downwelling favorable winds south of 20°N.

Estimating upwelling trends from wind data is difficult due to the limited number of observations that can be used to represent ocean winds and that are not under the influence of topographic features, particularly from meteorological stations on the NWA coast. In the case of the California Current Large Marine Ecosystem, the amount of well-measured records was the reason given by Sydeman et al. (2014) to explain the exceptionally coherence between the model-data reanalyzes and the observations, both data types supporting Bakun's hypothesis. Moreover, recently Benazzouz et al. (2014b) have questioned the appropriateness of local indices, based on instantaneous wind forcing, to predict the upwelling due to the long temporal memory of the upwelling system.

Given this controversial about the upwelling intensifying, in this article we have focused in the actual impact of the global warming in the temperature and salinity of the CCLME region. Trends in the surface have been estimated using satellite SST measurements for the whole CCLME, while in the water column data from the only long-term time series available in the area has been used to estimate the impact of the current global warming scenario in the different waters masses.

6.1.2. DATA

SST data was obtained from the National Oceanic and Atmospheric Administration (NOAA) high-resolution blended analysis of Advanced Very High Resolution Radiometer (AVHRR). Daily SST were retrieved, with a spatial resolution of 1/4°, from 1982 to 2013. From the daily data, monthly means were calculated, and the trends were computed using monthly values.

Since 1996, the Centro Oceanográfico de Canarias (COC) of the Instituto Español de Oceanografía (IEO) in collaboration with the Instituto de Oceanografía y Cambio Global (IOCAG) of the Universidad de Las Palmas de Gran Canaria (ULPGC), has been carrying out the Radial Profunda de Canarias project (RAPROCAN, Vélez-Belchí et al., 2014) to study the water masses and circulation around the Canary Islands. With a yearly or twice a year frequency, 50 stations are carried out around the Canary Island archipelago. In each of the stations a Conductivity–Temperature-Pressure (CTD) SeaBird 911+ probe is used from the surface down to 5-10 m above the bottom of the ocean. The station separation is about 30 km in the oceanic waters and 5-10 km for the shelf/coastal stations. The SeaBird 911+ probe is equipped with a redundant temperature and salinity sensor for inter-comparison, and the salinity data is calibrated, following the World Ocean Circulation Experiment (WOCE) requirements, with precise measurements from a guildline-8400B autosal salinometer

The trends were computed using a robust multi-linear regression, which incorporates iteratively reweighted least squares with a bi-square weighting function. This method is insensitive to outliers, but the results are very close to the standard linear least squares trends. The confidence intervals for the slopes were calculated using Student's t test.

6.1.3. RESULTS

6.1.3.1. Surface waters

Overall, the CCLME region shows a warming trend in the yearly averaged SST (Figure 6.1.1b). The mean value for the period 1982-2013 in the region is 0.28°C decade^{-1}, although the mode is 0.25°C decade^{-1}. The minimum values, around 0.02°C decade^{-1} are located west of Cape Beddouza in the weak permanent annual upwelling zone (Cropper et al., 2014), and south of Cape Bojador in the permanent annual upwelling zone. The spatial scale of these minimum values, as can be observed between Cape Juby and then Canary islands, is approximately 30 nm, more than half a degree in longitude at this latitude. The maximum warming trend in the yearly SST, 0.65°C decade^{-1}, is located west of Cape Timiris in the Mauritania-Senegalese upwelling zone. The patterns in the distribution of the warming trends correspond to the dynamical regimes of the region.

Using the mean SST distribution as a proxy that characterized the different dynamical regimes in the region, it is observed (Figure 6.1.1a) that near the coast the minimum values are enclosed by the 20°C isotherm, that characterizes the upwelling regime, except in the area between Cape Ghir and Cape Draa, where the warming is higher than 0.25°C. In this are the coastline is not parallel to the trade winds, and therefore there is weakening in the upwelling. The maximum trend values are between the 24°C and 22°C isotherms, where, in annual average, the influence of the upwelling is weaker that then influence of the downwelling favorable winds during the summer. In the oceanic waters, the area of high warming trends (>0.35°C decade^{-1}), is within in the limits of the Mauritania-Senegalese upwelling zone where Cropper et al. (2014) reported an intensification of the downwelling favorable winds and it is the area where the Canary Current separates from the coast to become the westward flowing North Equatorial Current (Hernández-Guerra et al., 2005). North and south of this area, the warming trends are weaker (<0.25°C decade^{-1}), except of the oceanic waters north of 32°N that are characterized by the Azores Current (Comas-Rodríguez et al., 2011; Pérez-Hernández et al., 2013).

The distribution of the summer (July, August and September) warming trend, confirms the results observed with the yearly data, with a mean summer trend in the region of 0.21°C decade^{-1}. The minimum values are lower than using the yearly data, as expected due to the increase of the upwelling during the summer, and reach -0.14°C decade^{-1} west of Cape Beddouza and south of Cape Bojador in the permanent annual upwelling zone, except in the area between Cape Ghir and Cape Draa, where the warming is higher than 0.25°C. The maximum values are also higher than using the yearly data, as expected due to the increase of the downwelling during the summer, up to 0.90°C decade^{-1} west of Cape Timiris. The distribution of the warming trends during summer also corresponds to the dynamical regimes of the region. Near the coast, the lower, and negative values, are enclosed by the 22°C isotherm, and correspond to the areas with strong upwelling during the summer, while the maximum values are found where the isotherm are perpendicular to the coast, in the area where the downwelling is stronger in summer. As in the annual trends, north of the Azores current region, the warming rates are higher than south of it.

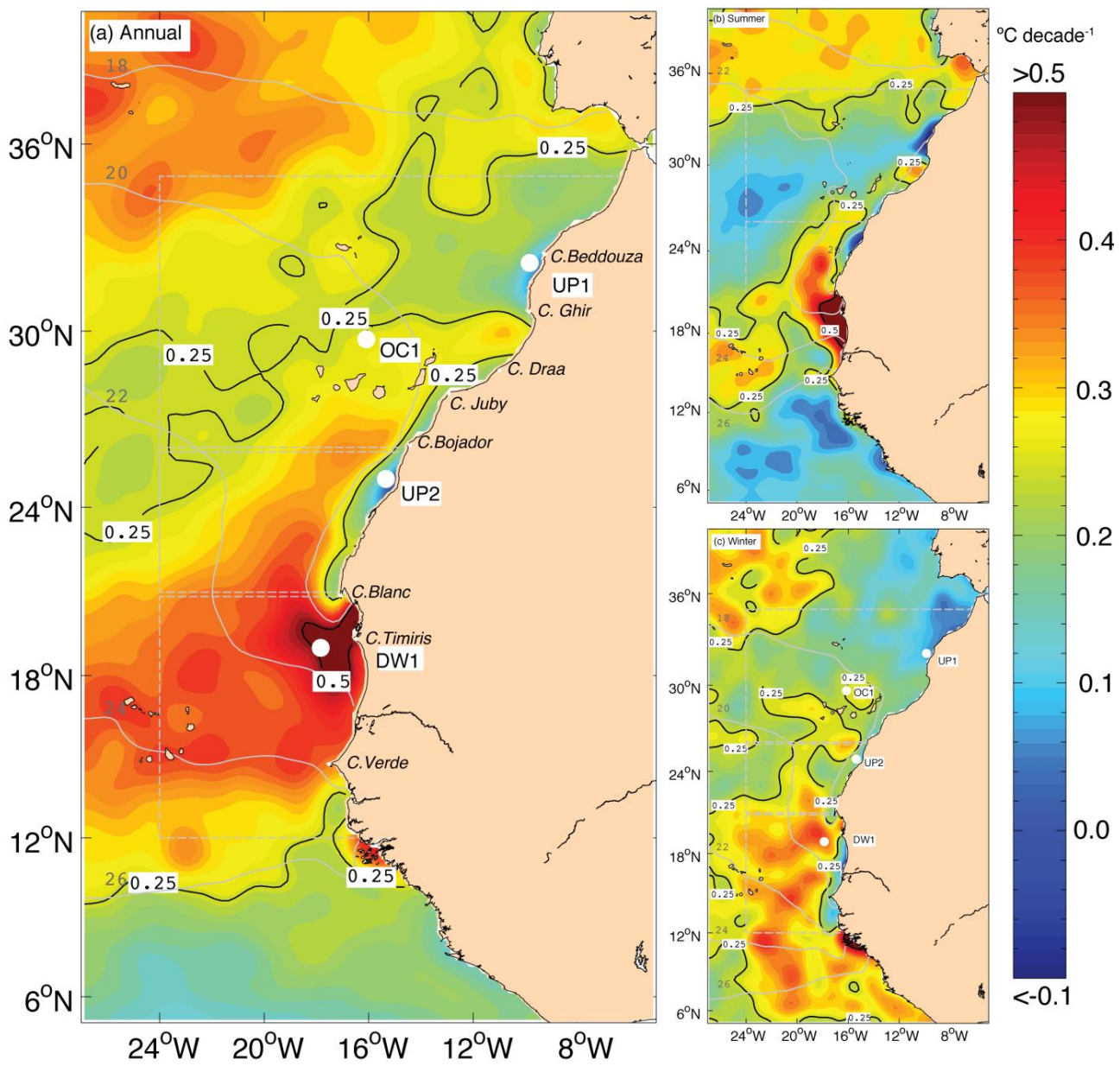

Figure 6.1.1. (a) Sea surface trends (°C decade^{-1}) computed from NOAA high-resolution (1/4°) blended analysis of Daily SST for the 1982–2013 period. (b) as (a) but for the summer (June, July and August, JJA) months, (c) as (a) but for the winter (January, February and March, JFM). The white dots are the location of the time series of Figure 6.1.2. The dashed grey line denote the three upwelling areas as defined by Cropper et al. (2014): the weak annual upwelling zone (26°N-35°N), the permanent annual upwelling zone (21°N-26°N) and the Mauritania-Senegalese upwelling zone (12°N -20°N). The thin solid grey lines correspond to the isotherms (18°C, 20°C, 22°C, 24°C and 26°C) of the mean field for each season. Note that the color scale is the same for the three figures, although the range is different, as describe in the text.

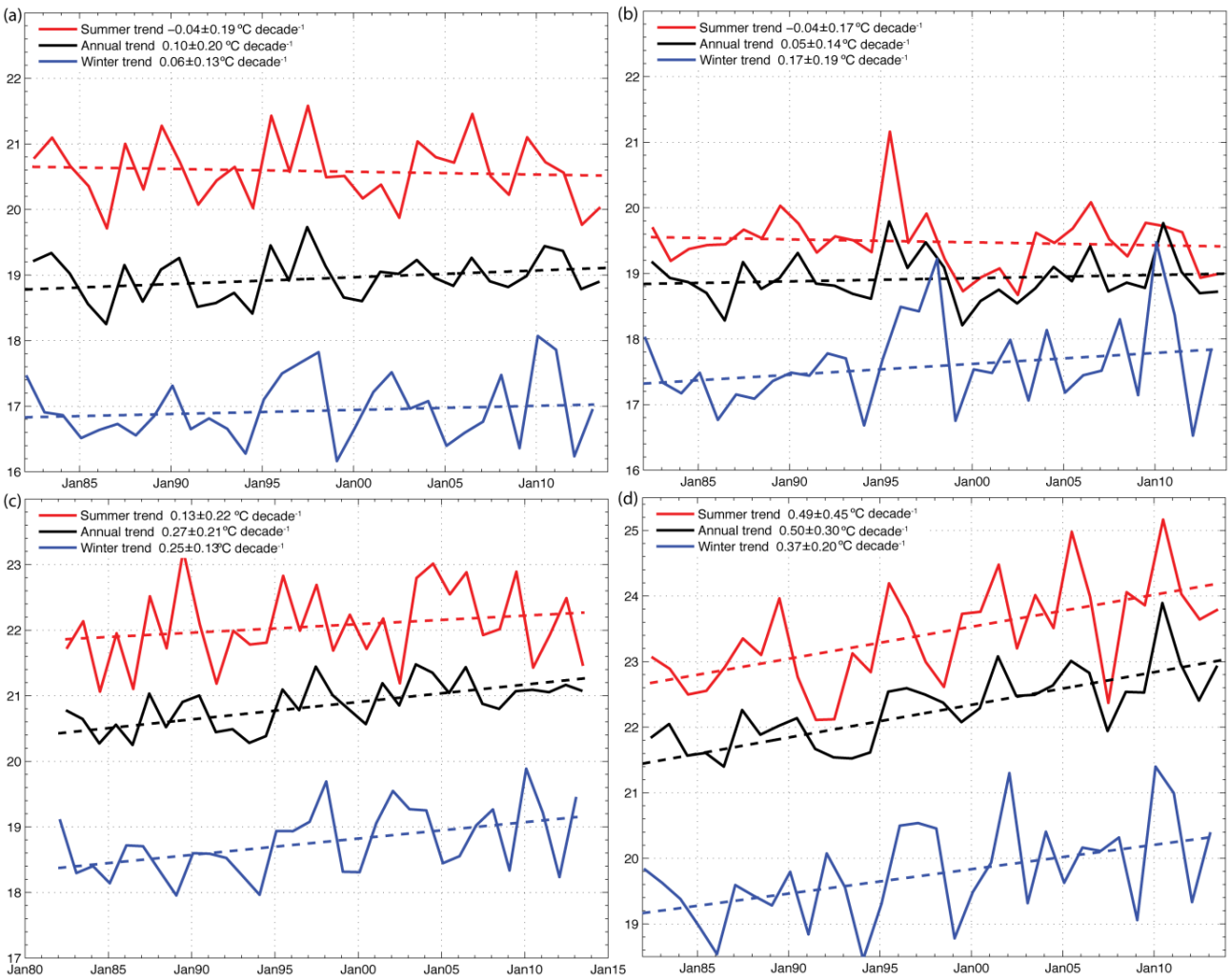

Figure 6.1.2. Yearly values of the SST for the four locations describe in the text and represented in Figure 6.1.1. (a) UP1, west of Cape Beddouza in the weak permanent annual upwelling zone (b) UP2, south of Cape Bojador in the permanent annual upwelling zone (c) OC1, in the oceanic waters north of the Canary Islands, and (d) DW1, west of Cape Timiris, in the Mauritania-Senegalese upwelling zone. In each of the figures, the red line is for the summer mean, the blue for the winter, and the black for the annual average. Trend values (dashed line in °C decade^{-1}), and statistical significant range at the 95% confidence level are indicated in the legend for each one of the locations.

During the winter (January, February and March), warming trends are also coherent with the dynamical regime in the region, with a mean trend winter value in the region of 0.24°C decade^{-1}. The minimum values are found near the coast, north of Cape Beddouza, and in the coast of the Iberian peninsula, in the area, where the upwelling is stronger during the winter, but with trends lower than 0.1°C decade^{-1}. Overall, near the coast, both in the weak permanent annual upwelling zone and in the permanent annual upwelling zones, there are low warming rates, statically not different from zero. Near the coast, in the Mauritania-Senegalese upwelling zone, the trends are lower than during the summer, as low as 0.10°C decade^{-1}, coherent with the fact that during winter there are not downwelling favorable winds in the area. The spatial scale of these patterns of minimum values is approximately 30 nm, more than half a degree in longitude at this latitude.

To confirm the distribution of the observed trends, four locations, representatives of the different dynamical regimes explained before, were selected. The two locations (Figure 6.1.2 a, b) in the weak permanent annual upwelling zone (UP1) and in the permanent annual upwelling zone (UP2) shows trends not statistically different from zero for the yearly averages (0.1 ± 0.20°C decade^{-1} for UP1 and 0.05 ± 0.14°C decade^{-1} for UP2), with negatives values for the summer months (-0.04 ± 0.19°C decade^{-1} for UP1 and -0.04 ± 0.17°C decade^{-1} for UP2), when the upwelling is stronger, and non statistically significant warming trends for the winter months (0.06 ± 0.13°C decade^{-1} for UP1 and -0.17 ± 0.19°C decade^{-1} for UP2). The correlation between the yearly values of the two locations is high, 0.77 ($p<0.01$) for the annually averaged SST and 0.88 ($p<0.01$) for the winter trend, as expected since the two locations are in the same dynamical regime. The location in oceanic waters (OC1, Figure 6.1.2c) shows warming trends statistically significant of 0.27 ± 0.21°C decade^{-1} for the annual and strongly correlated with the locations in the upwelling regime (0.80, $p<0.01$) and in the downwelling regime (0.77, $p<0.01$). The location in the Mauritania-Senegalese upwelling zone (DW1) shows warming trends statistically significant during winter and summer with an annual value of 0.5 ± 0.3°C decade^{-1}. This high warming has been related, by some authors as Cropper et al. (2014), to the recovery of the African monsoon, and the downwelling favorable winds.

6.1.3.2. Water column

Figure 6.1.3a shows the current distribution of hydrographic stations carried out in the framework of the RAPROCAN project, one of the few, if not the only one, long term time series in the Coastal Transition Zone (CTZ) of the Canary Current Large marine ecosystem. Stations from 5 to the 24 have been sampled since 1997.

The area is characterized by four waters masses (Figure 6.1.3b), the North Atlantic Central Waters (NACW), roughly between 200 dbar and 600 dbar and lighter than the 27.25 kg m^{-3} isopycnal; the intermediate waters, mainly Mediterranean (MW) and Antarctic Intermediate Waters (AAIW), between 600 dbar and 1600 dbar, and lighter than the 27.85 kg m^{-3} isopycnal; and the North Atlantic Deep Waters (NADW), deeper than 2600 dbar and heavier than the 27.85 kg m^{-3} isopycnal (Vélez-Belchí et al., 2014).

The trends in temperature and salinity, for the oceanic area (stations 11-24, Figure 6.1.4) and the area in the Lanzarote Passage (LP, stations 5-10, Figure 6.1.5), closer to the upwelling region, were estimated in four different depth stratums, to characterize the trend of the water masses in the area. For the depth stratum (200-600 dbar) that characterize the NACW waters, both the oceanic area and the LP area shows a statistically significant warming trend, 0.20 ± 0.11°C decade^{-1} for the oceanic area and 0.20 ± 0.25°C decade^{-1} for the LP. The variability in the LP is higher due to the proximity of the upwelling region, and the frequent intrusions of upwelling filaments (Hernández-Guerra et al., 2003), and therefore the uncertain is higher in the trend estimations. Similarly, the analysis shows an increase in salinity of 0.03 ± 0.023 decade^{-1} for the oceanic area and of 0.028 ± 0.038 decade^{-1} for the LP. These changes are similar to those found in the subtropical Atlantic at 24°N by Vargas-Yáñez et al. (2002), Vélez-Belchí et al. (2010) and Benítez-Barrios et al. (2008) in the Canary basin. The strong inter-annual variability was also pointed out by Vélez-Belchí et al. (2010). The increase in temperature and salinity almost compensate in density, corroborating that the observed trends are due to deepening of the isoneutral surfaces rather than changes along the isoneutral (Vélez-Belchí et al., 2010).

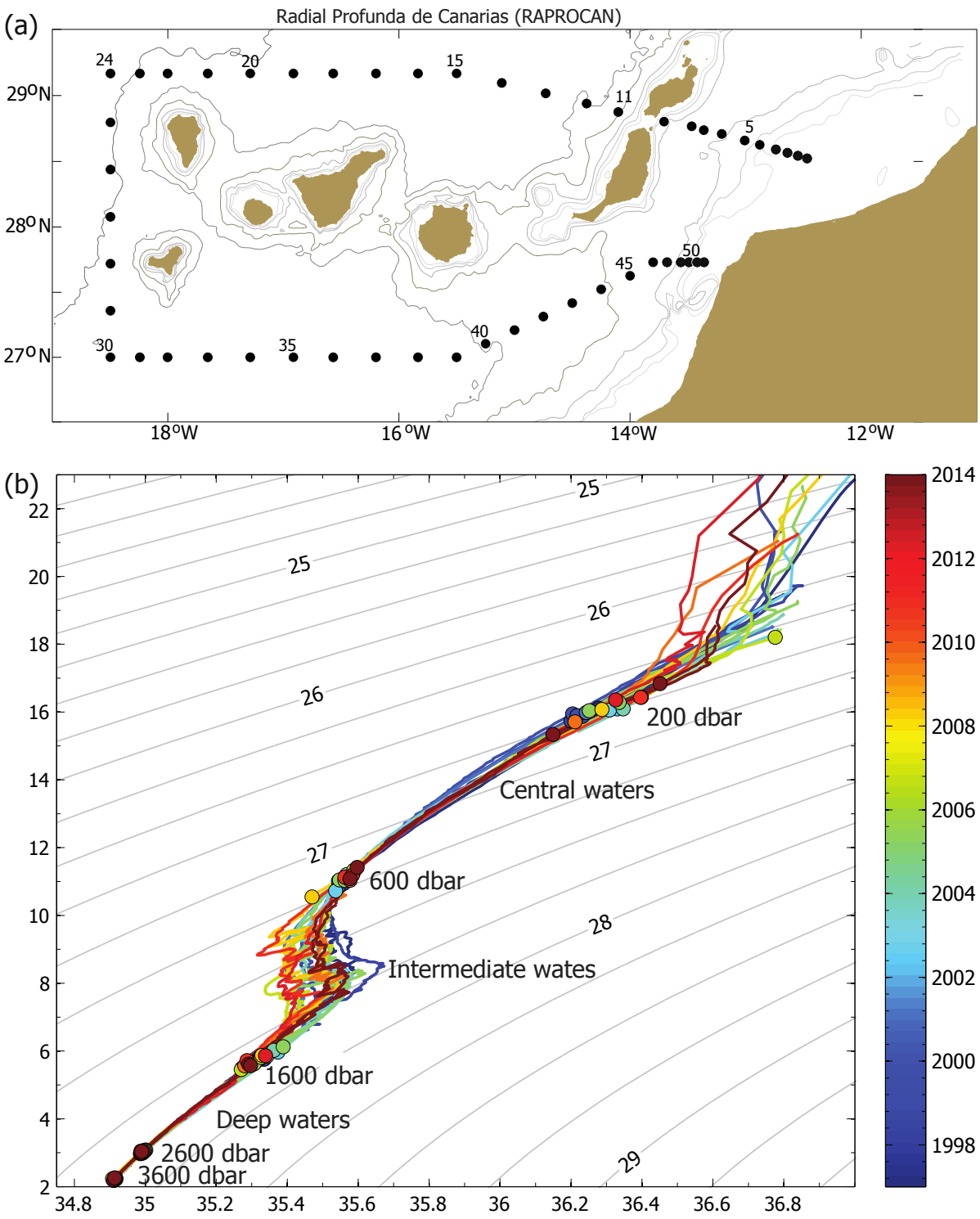

Figure 6.1.3. (a) Localization of the CTD stations currently carried out during the RAPROCAN cruises. (b) Potential temperature/salinity diagram for station 15 (European Station for Time Series in the Ocean, ESTOC), representative of the area. The colors indicated the year of the CTD cast, and the dots are located at 200 dbar, 600 dbar, 1600 dbar, 2600 dbar and 3600 dbar, approximately delimitating the thermocline waters; the central waters (mainly NACW); the intermediate waters (mainly MW and AAIW); and the deep waters (mainly NADW).

The observed trends in temperature in the central waters are very similar to those found using the SST as previously described. The trend in the location OC1 (Figure 6.1.2c), that roughly correspond to station 15, and gave a trend of 0.27 ± 0.21°C decade^{-1}, was reduced to 0.22 ± 0.11°C decade^{-1} when only the time series since 1997 was considered.

In the intermediate waters, the trends for temperature and salinity were not statistically significant, neither in the oceanic region nor in the LP. Both time series (Figure 6.1.4b and 6.1.5b) show high variability due to fact that, as pointed out before, two very different intermediate water masses converge in the region.

For the deep layers, two depth stratums very analyzed. In the shallower one (1700-2600 dbar), corresponding to the upper NADW, there were weak warming and increase in salinity statistically non different from zero. However, in the deeper depth stratums (2600-3600 dbar), where mainly NADW is found, a marginally statistical significant cooling (-0.01 ± 0.01 C decade^{-1}) and freshening (-0.002 ± 0.002°C decade^{-1}) is observed. This freshening corresponds to the reported freshening the of the sub-polar North Atlantic since the 1970s (Curry et al., 2003; Curry and Mauritzen, 2005; Dickson et al., 2002).

6.1.4. CONCLUSIONS

Trends in the open ocean temperature and salinity in the CCLME have been analyzed using satellite high resolution SST that covers the whole region, water column CTD data in the Canary basin and the CTZ with a long-term time series, that goes back to 1997.

The SST for the 32 years in the period 1982-2013, shows a warming trend in the CCLME, with a mean value of is 0.28°C decade^{-1}. However, the warming trend shows significant changes linked to the different dynamical regimes that coexist in the CCLME. Near the coast, in the area closed linked to the upwelling, between Cape Blanc and Cape Beddouza, the warming trend is not statistically different from zero, and during the stronger upwelling months, the summer, there is a cooling trend neither statistically different from zero. The spatial scale of some of these patterns is smaller than one degree, and therefore could only be observed using high resolution SST. Near the coast and in the oceanic waters under the influence of downwelling, between Cape Verde and Cape Blanc, the warming trend is higher (>0.5°C decade^{-1}), and statistically significant, but decreasing towards the west. In the oceanic regions, there is a statistically significant trend of 0.25°C decade^{-1}.

The trends in SST are also observed in waters over the permanent thermocline (200-600 dbar) with a slight weaker statistically significant rate, up to 0.25°C decade^{-1}, that is density compensate with an increase in salinity of 0.02 decade^{-1}. Neither the intermediate waters nor the upper deep waters shows any statistically significant trend, however the deep waters (2600-3600 dbar) in the oceanic waters north of the Canary Islands, shows a warming rate of -0.01°C decade^{-1} and a freshening of -0.002 decade^{-1}.

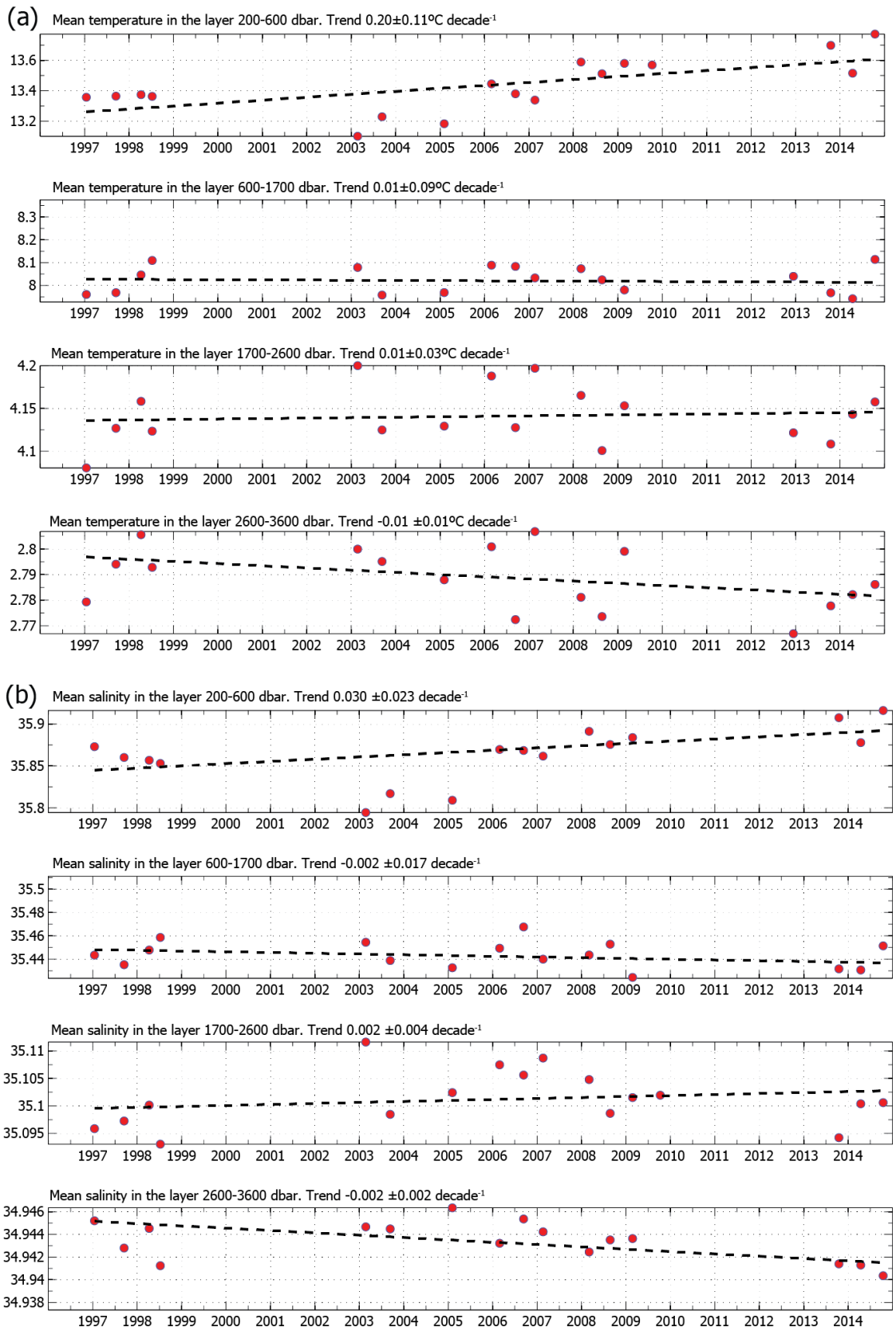

Figure 6.1.4. Time series of (a) mean temperature (°C) and (b) mean salinity between stations 11-24 for four different vertical stratums, representative of the central waters (200-600 dbar), intermediate waters (600-1700 dbar), and deep waters (2600-3600 dbar). Trend (dashed line) and trend values, and statistical significant range at the 95% confidence level are indicated for each depth stratum.

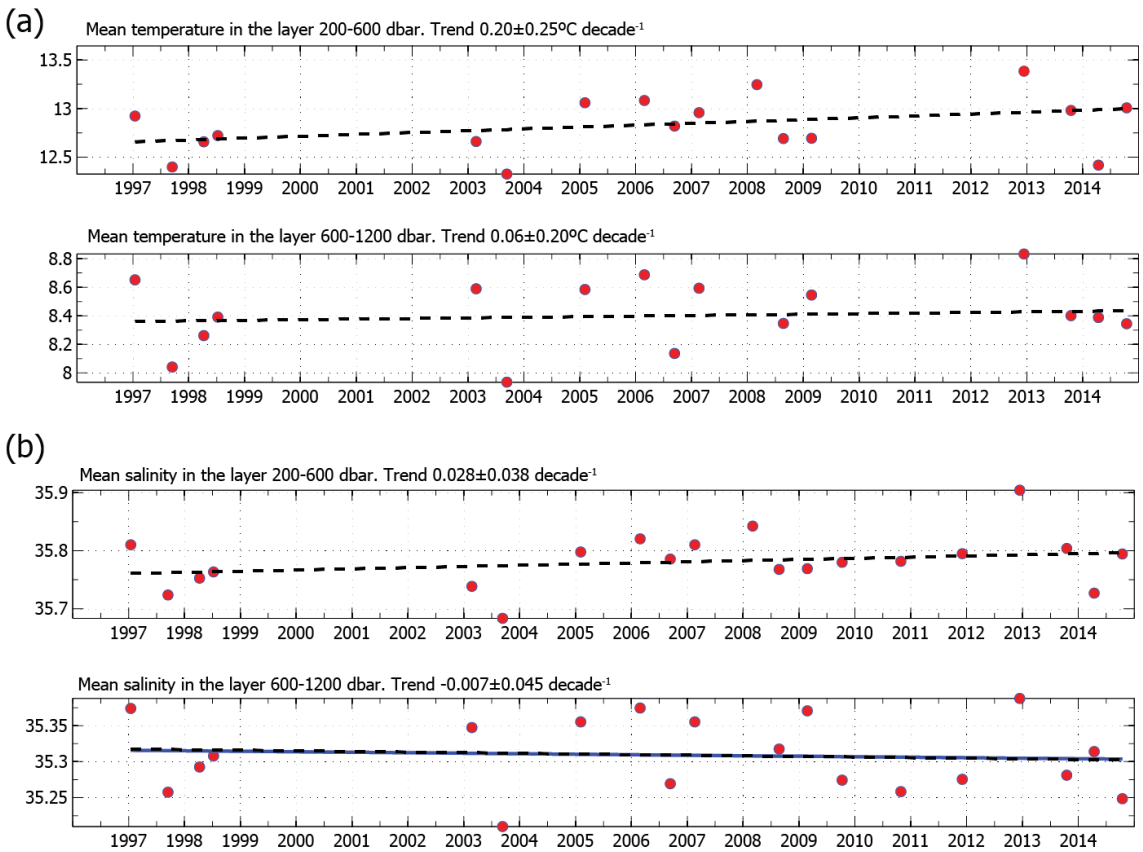

Figure 6.1.5. Same as Figure 6.1.4, but two different vertical stratums, representative of the central waters (200-600 dbar) and intermediate waters (600 dbar-bottom, 1300 m is the maximum depth in the Lanzarote passage).

Acknowledgement

The Instituto Español de Oceanografía supported this study under the RAPROCAN project, part of the IEO's ocean observing system (IEOOS); the Spanish Ministry of Economy and Competitiveness supported this analysis under grants Corica (REN2001-2649) and Sevacan (CTM2013-48695). M. D. Pérez-Hernández was supported by a grant from the Agencia Canaria de Investigación, Innovación y Sociedad de la Información.

6.2. SEA LEVEL VARIABILITY AND TRENDS IN THE CANARY CURRENT LARGE MARINE ECOSYSTEM

Begoña PÉREZ-GÓMEZ[1], Enrique ÁLVAREZ-FANJUL[1], Marta MARCOS[2], Bernat PUYOL[3] and María Jesús GARCÍA[4]

[1] Puertos del Estado. Spain

[2] Instituto Mediterráneo de Estudios Avanzados. Spain

[3] Instituto Geográfico Nacional. Spain

[4] Instituto Español de Oceanografía. Spain

6.2.1. INTRODUCTION

Sea level rise is one of the most alarming consequences of global warming and a threat to coastal settlements in several parts of the world. Caused by thermal expansion of the water and by the melting of glaciers and ice sheets, global sea level rise has accelerated from 1.2-1.5 mm yr^{-1} during last century (Church and White, 2011; Church et al., 2013; Hay et al., 2015) to a present day rate of 3.2 mm yr^{-1} for the last 20 years (Merrifield et al., 2009). Regional and local deviations from these global values are, however, known to be important and probably the most relevant information for practical issues. Long-term mean sea level changes are derived from the around 120 coastal tide gauges in the world with more than 80 years of data (Holgate et al., 2013). Unfortunately these are not evenly distributed and there is a lack of reliable long time series in several parts of the world, such as the African coastline. This problem can be partly overcome thanks to data recovery efforts (e.g. Marcos et al., 2011; Wöppelmann et al., 2014; Talke et al., 2014) and sea level hindcasts carried out with numerical models with realistic forcing (e.g. OCCAM: Coward et al., 2005; SODA: Carton and Giese, 2008). On the other hand the amount of sea level data increased significantly during the last two decades thanks to the densification of the tide gauge networks (including instrumental, maintenance protocols and quality processing improvements) and to the advent of satellite altimetry. It must be noted also that vertical land movements may affect coastal sea level observations and should be considered for any sea level study based on tide gauges. Continuous Global Positioning System (CGPS) measurements are able to monitor their vertical motion; however, they are not yet available at all the coastal stations and, if so, their time length is often too short.

Superimposed to the long-term trends in mean sea level, decadal and interannual variability related to changes of the oceanographic and meteorological forcing are also present. Understanding these changes is critical for a precise knowledge of the causes of observed decadal to multidecadal variations and trends in mean sea level, and their spatial patterns will provide insight into their local influence and/or their propagation.

This article describes these basic aspects of sea level variability for the Canary Current Large Marine Ecosystem region (hereafter CCLME), based on previous publications and existing data from both tide gauges and satellite altimeter. In addition to the temporal and spatial variations of mean sea levels, the evolution of extreme events and the observed relation between altimetry (open waters) and tide gauge data (relative coastal sea level) will be addressed. Two analyses are presented: the first one corresponds to the entire long period for which tide gauge observations are available in the region, starting at the

beginning of the 20th century; the second, more detailed thanks to the larger availability of measurements, corresponds with the so-called altimetric period (1992 onwards). During this second time span, altimetry data and new tide gauges from the Puertos del Estado (PdE) REDMAR network are also available, increasing our capability of diagnoses. In addition an uncertainty analysis is carried out by comparing the measurements from the two independent data sources available for this second period.

6.2.2. DATA SOURCES AND METHODS

6.2.2.1. Data sources

The results presented in this article will be based on tide gauge and altimetry data, as there are no regionalized hindcasts of sea level that cover the CCLME region.

The tide gauges are listed in Table 6.2.1, together with their location, period of operation and institution to which they belong. Note that tide gauges are often located at the same harbour, although with different time spans.

Table 6.2.1. Tide gauge stations employed in this article (also displayed in Figure 6.2.4). IEO: Spanish Institute of Oceanography, PdE: Puertos del Estado, IGN: Spanish National Geographic Institute, UHSLC: University of Hawaii Sea Level Center, IH: Instituto Hidrográfico (Portugal). Those with longest historical records are shaded in grey (from IEO and IGN mainly). New tide gauges from PdE since 1992 (REDMAR network) shaded in blue. White background: stations where trends are not presented: REDMAR stations with shorter records and Dakar and Porto Grande, the only stations from other countries in the CCLME with monthly means found in the PSMSL.

Station	Latitude	Longitude	Institution	Country	Data availability
Bonanza	36.800°N	6.333°W	PdE	Spain	1992-2013
Cádiz	36.540°N	6.286°W	IEO	Spain	1900-2013
Tarifa	36.009°N	5.603°W	IEO	Spain	1943-2012
La Palma I	28.672°N	17.768°W	IEO	Spain	1949-2013
El Hierro	27.780°N	17.900°W	PdE	Spain	2004-2013
La Gomera	28.088°N	17.108°W	PdE	Spain	2006-2013
Tenerife I	28.483°N	16.233°W	IGN	Spain	1927-2012
Tenerife II	28.483°N	16.233°W	PdE	Spain	1992-2013
Las Palmas I	28.147°N	15.407°W	IEO	Spain	1950-2013
Las Palmas II	28.150°N	15.330°W	PdE	Spain	1992-2013
Fuerteventura	28.500°N	13.850°W	PdE	Spain	2004-2013
Arrecife I	28.950°N	13.567°W	IEO	Spain	1949-2012
Arrecife II	28.900°N	13.530°W	PdE	Spain	2008-2013
Dakar	14.683°N	17.417°W	UHSLC	Senegal	1992-2012
Porto Grande	16.883°N	25.000°W	IH	Cape Verde	1990-1995

According to the records of the Permanent Service of Mean Sea Level (PSMSL: http://www.psmsl.org/data/obtaining/map.html, accessed on 15 January 2015), there are monthly values available also for Dakar (Senegal) and Porto Grande (Cape Verde), but in both cases the time series is very short and with important gaps. Unfortunately there is a lack of long time series of sea level data along the African coast.

Another relevant source of information is the altimeter, restricted to the last two decades, but providing spatial coverage of sea level variability in open waters. Use will be made, in particular, of Aviso Mean Sea Level Anomaly (MSLA) maps, a multi-mission product based on the combination of up to four different satellite altimeters at a given time (Topex-Poseidon, Jason-1, Jason-2, Envisat and GFO) that consists of sea surface heights computed with respect to a seven year mean in a 1/3° resolution grid (AVISO-CLS, 2014).

6.2.2.2. Methodology

Mean sea level analysis will be based on monthly mean sea levels from tide gauges and altimetry. Monthly mean sea levels from the Spanish networks (REDMAR, IEO, IGN) are routinely computed following international recommendations, and distributed through their web sites and/or the PSMSL. The REDMAR time series are the result of a recent new quality control designed to generate a unique product at each harbour based on the old (acoustic) and the new (radar) tide gauges, after the upgrade of the whole REDMAR network since 2007 (Pérez-Gómez et al., 2014). For Tenerife I (IGN) and Cádiz (IEO) new historical time series were constructed and analysed in detail by Marcos et al. (2011) and Marcos et al. (2013) respectively, providing the longest records in the CCLME. We summarize here the main conclusions of these relevant data archaeology publications, unique for this region and an important contribution to the global coastal sea level data set during the 20th century.

The Aviso MSLA gridded product has all the environmental and instrumental corrections applied, including the inverse barometer and higher frequency meteorological effects. This includes the DAC (Dynamic Atmospheric Correction) produced by *CLS* Space Oceanography Division using the Mog2D model from *Legos,* and distributed by *Aviso*, with support from *CNES:* http://www.aviso.altimetry.fr/ (accessed on 15 January 2015). The DAC correction was used as provided by Aviso, in a global grid of 1/4° and added to the MSLA maps for direct tide gauge and altimeter comparisons. The altimetry data consist of weekly values that have been averaged to monthly means.

The results and discussion will be separated into two periods: a) long-term mean sea level changes, including the 20th century, mostly based on Tenerife and Cádiz above mentioned works and; b) 1992-2013 period (last two decades, also called the altimetry-period), when more information from the REDMAR network and the altimetry missions will allow a better understanding of recent observations and their spatial patterns for the region. Results for the latter are a particularization of Pérez-Gómez (2014) for the area of interest. In spite of the short time series in this case, these data may be crucial to confirm the mentioned recent sea level rise acceleration and its magnitude in the CCLME region. Also based on the REDMAR network, the seasonal cycle, mean sea level anomalies and the evolution of extremes for this latter period (based on the analysis of the percentile time series following the methodology employed by Woodworth and Blackman, 2004) will be shown.

Finally, the relation between tide gauges and altimetry will also be presented for the REDMAR stations. Taking into account that tide gauges are not corrected for meteorological effects, the DAC correction was

added to MSLA altimetry maps. Correlations, root mean square errors and trends of the difference between tide gauges and altimetry series will therefore be presented. This comparison will serve to analyse the uncertainties on the results derived from two very different data sets.

6.2.3. RESULTS AND DISCUSSION

6.2.3.1. Long-term trends from tide gauges

One of the main problems for assessment of sea level changes for the last century is the limited number of consistent long time series. Tide gauges are in operation since the end of 19th century, with changing technologies, locations inside the harbours, datum references, etc. Recovery of these historical data is a challenging and important task for present-day climate related sea level research. Observed trends for the longest records in the CCLME region are compiled in Table 6.2.2 (a), their value depending strongly on the time period. For Cádiz and Tenerife, as already mentioned, a detailed study after historical data recovery was performed in recent years. Details can be consulted in Marcos et al. (2011) and Marcos et al. (2013), respectively. In the latter work, Tenerife I data, from 2000 onwards, are actually from Tenerife II. Historical records of the IEO stations in Tarifa, Las Palmas, Arrecife and Santa Cruz de la Palma were first recovered and analysed by Fenoglio-Marc and Tel (2010), although datum connection between the periods 1949-1976 and 1996-2013 at Santa Cruz de la Palma, and between 1949-1990 and 1991-2014 at Las Palmas, remain uncertain due to data gaps and changes of location. The IEO has revisited these trends for the present work with the last years of data.

Recently recovered long term tide gauge data at Cádiz (Marcos et al., 2011) reveal that the rate of sea level rise was 1.0 $\pm$ 0.2 mm yr^{-1} during the 20th century, a value lower than the accepted globally averaged sea level rise. The observed sea level trend in Tenerife I is higher with a value of 2.09 $\pm$ 0.04 mm yr^{-1} (Marcos et al., 2013) for the period 1927-2012. These trends are not affected, according to these publications, by land movements so they would reflect absolute sea level rise. However, as they are computed for different periods they are not directly comparable (the trend value obtained for the period 1927-2000 in Tenerife I is 1.9 ± 0.1 mm yr^{-1}). Other values in Table 6.2.2 yield to other interesting facts: sea level trend in Cádiz since 1960 (based on the data of the most modern IEO tide gauge, installed that year) becomes significantly larger: 3.77 $\pm$ 0.64 mm yr^{-1} (IEO, without GPS correction, 3.80 $\pm$ 0.35 mm yr^{-1}, as published by SONEL (http://www.sonel.org/-Sea-level-trends-.html, accessed on 20 January 2015, with GPS correction); the differences on the GPS velocities of the station reported by the two sources of information do not account for this significant increase of the trend. It must be noted that Marcos et al. (2011) found some problems with this tide gauge at the beginning of the record though, that could contaminate the final trend.

The other stations with long time series in Table 6.2.2 started their operation in the 1940's (IEO stations): Tarifa I, La Palma I, Las Palmas I and Arrecife I. We computed the relative sea level trends for these time series finding significantly low values (below 1 mm yr^{-1}) at all of them.

Although with no detailed knowledge of the local land vertical movements at all the stations, we do have estimations of the contribution of the Glacial Isostatic Adjustment (GIA) to these movements, from model estimates such as the ICE-5G Peltier model (Peltier, 2004). This model indicates that the land would be ascending due to GIA at the Gulf of Cádiz (-0.19 mm yr^{-1}at Bonanza, for example) and sinking in most of the Canary Islands (0.09 mm yr^{-1}, 0.05 mm yr^{-1} and -0.01 mm yr^{-1} at El Hierro, Las Palmas and Fuerteventura, respectively). This contribution is nevertheless one to two orders of magnitude lower than the observed

trends in mean sea level, having therefore no influence on the conclusions. Nevertheless other local movements could be present. SONEL reports a vertical land motion at Las Palmas (IEO CGPS station) of -1.56 ± 0.34 mm yr^{-1} (Santamaría-Gómez et al., 2012), and the IGN reports a subsidence of -0.60 ± 0.2 mm yr^{-1} at Tarifa since 2010 (M. Valdés, IGN, personal communication). There is no CGPS information available for La Palma or Arrecife.

It is interesting to point out the range of variability of the trends from long-term time series available in the region. Assuming no errors in the tide gauge measurements, such dispersion is mostly related to the different time periods for which the trends are computed and secondly to the likely different vertical land motions at the tide gauges.

Table 6.2.2. Observed trends and standard error (seasonal cycle removed) for a): the longest time series in the region based on IEO and IGN tide gauges. Grey shaded those trends obtained from recent historical data recovery, detailed quality control and analysis, in the publications shown in column 4; b): trends from IEO and PdE tide gauges for the altimetry period (≈20 years).

Station	Sea level trend (mm yr^{-1})	Data period	Source of data/computed by:
	a) Long term:		
Cádiz	3.77 ± 0.18	1960-2013	IEO/IEO
Cádiz	1.02 ± 0.21	1900-2000	IEO-IGN/Marcos et al. (2011)
Tarifa I	0.93 ± 0.11	1943-2013	IEO/IEO
La Palma I	0.33 ± 0.09	1950-2013	IEO/IEO
Tenerife I	2.09 ± 0.04	1927-2012	IGN/Marcos et al. (2013)
Las Palmas I	0.94 ± 0.11	1949-2013	IEO/IEO
Arrecife I	0.47 ± 0.10	1949-2012	IEO/IEO
	b) Altimetry period (since 1992):		
Bonanza	5.10 ± 0.70	1992-2013	PdE/PdE
Cádiz	1.18 ± 0.69	1992-2013	IEO/IEO
Tarifa I	5.13 ± 0.42	1992-2013	IEO/IEO
La Palma I	1.22 ± 0.52	1997-2013	IEO/IEO
Tenerife II	5.10 ± 0.37	1992-2013	PdE/PdE
Las Palmas I	4.15 ± 0.30	1991-2013	IEO/IEO
Las Palmas II	4.90 ± 0.36	1992-2013	PdE/PdE
Arrecife I	1.10 ± 0.43	1992-2012	IEO/IEO

6.2.3.2. Variability and trends for the altimetry period (1992-2013)

Analysis of tide gauge data:

Relative sea level trends from tide gauges since 1992 are presented in Table 6.2.2 (b), where all tide gauge data sources were included. The time series of Tenerife I for this period is not available at the PSMSL.

There are large differences between stations, some of them relatively close. These could be due to undetected measurement errors at some stations, local movement or/and mesoscale activity.

According to these data, remarkable large trends are obtained for the altimetry period, in agreement with other works in different regions (e.g. Merrifield et al., 2009). These trends exceed the ones during the larger period with the exception of Cádiz, where the trend in the shorter period is similar or even smaller than the trends in the long term section of Table 6.2.2. One reason for this discrepancy in Cádiz tide gauge could be its anomalous operation in the period 1961-1975, explained in Marcos et al. (2011), who suggests a datum shift of about 10 cm during this period.

Seasonal cycle and evolution of mean sea level anomalies (seasonal cycle removed) are shown in Fig. 6.2.1 and 6.2.2 respectively, for all the REDMAR stations in the Canary Islands with more than 5 years of data. This seasonal cycle is obtained averaging the mean monthly values for each calendar month during the whole period. Uncertainties correspond to standard deviations among months. Allowing this short length of the time series explains the appearance of new REDMAR tide gauges in Table 6.2.1 that started their operation after 2004.

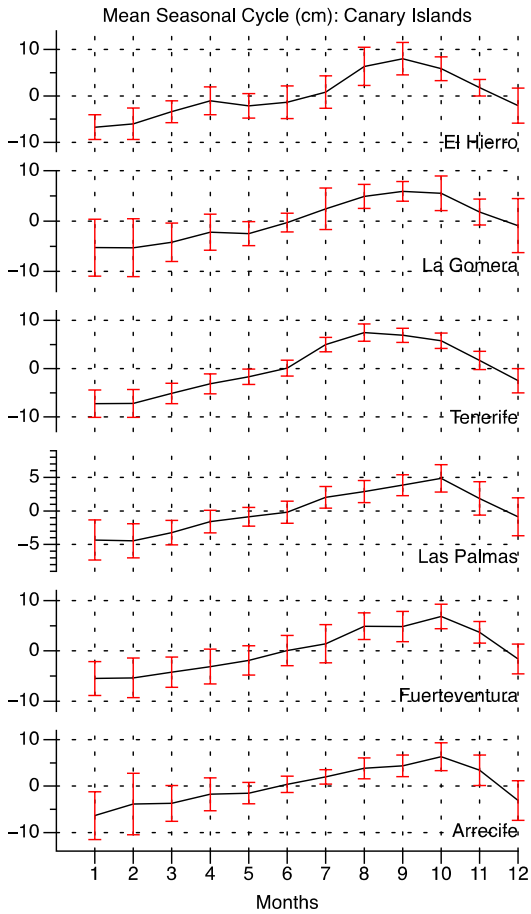

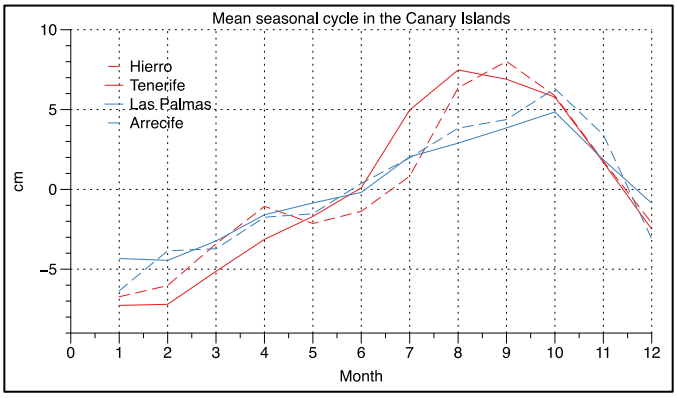

Figure 6.2.1. At the left: mean seasonal cycle for the Canary Islands REDMAR stations with more than 5 years of data (extracted from Pérez-Gómez, 2014). At the right: comparison of the mean seasonal cycle at two stations of the Western Canary Islands (Tenerife and El Hierro, solid and dashed red lines) and at two stations of the Eastern Canary Islands (Las Palmas, Arrecife, solid and dashed blue lines) confirm the different amplitude and peak occurrence associated by García-Lafuente et al. (2004) to seasonal variations of the Canary Current (extracted from Pérez-Gómez, 2014)

The seasonal cycle, mainly composed of annual and semiannual cycles related to cycles in the meteorological forcing, heat content and circulation patterns, presents large spatial correlation. According to García-Lafuente et al. (2004) the semiannual signal is mainly caused by the meteorological forcing while the annual cycle would be mainly explained by the steric (seasonal heating/cooling) effect.

Most of the stations along the Spanish coast (including the ones in the Gulf of Cádiz) present their maximum sea levels in October and November, while this peak happens in September or even August in Tenerife. The annual cycle is dominant, with mean values in the Canary Islands ranging from 6.6 cm in Tenerife to 4.5 cm in Las Palmas (Pérez-Gómez, 2014). The amplitude is slightly larger in the Gulf of Cádiz. According to Pugh (1987), the phase of the annual cycle increases toward the north in the Northern Hemisphere, as it is confirmed by the tide gauge data along the coast. However, an interesting spatial difference is evident within the Canary Islands (Figure 6.2.1, right): the amplitude of the seasonal cycle is lower in Las Palmas and Arrecife stations (eastern islands) than in Tenerife and El Hierro (western islands) while the peak occurs also later (October) in the former. García-Lafuente et al. (2004) consider this difference related to the seasonal variations in the Canary Current (Navarro-Pérez and Barton, 2001), which gets closer to the African coast in summer and further offshore in winter. The lower mean sea levels occur on the other hand in January and February for all the tide gauges employed here within the CCLME.

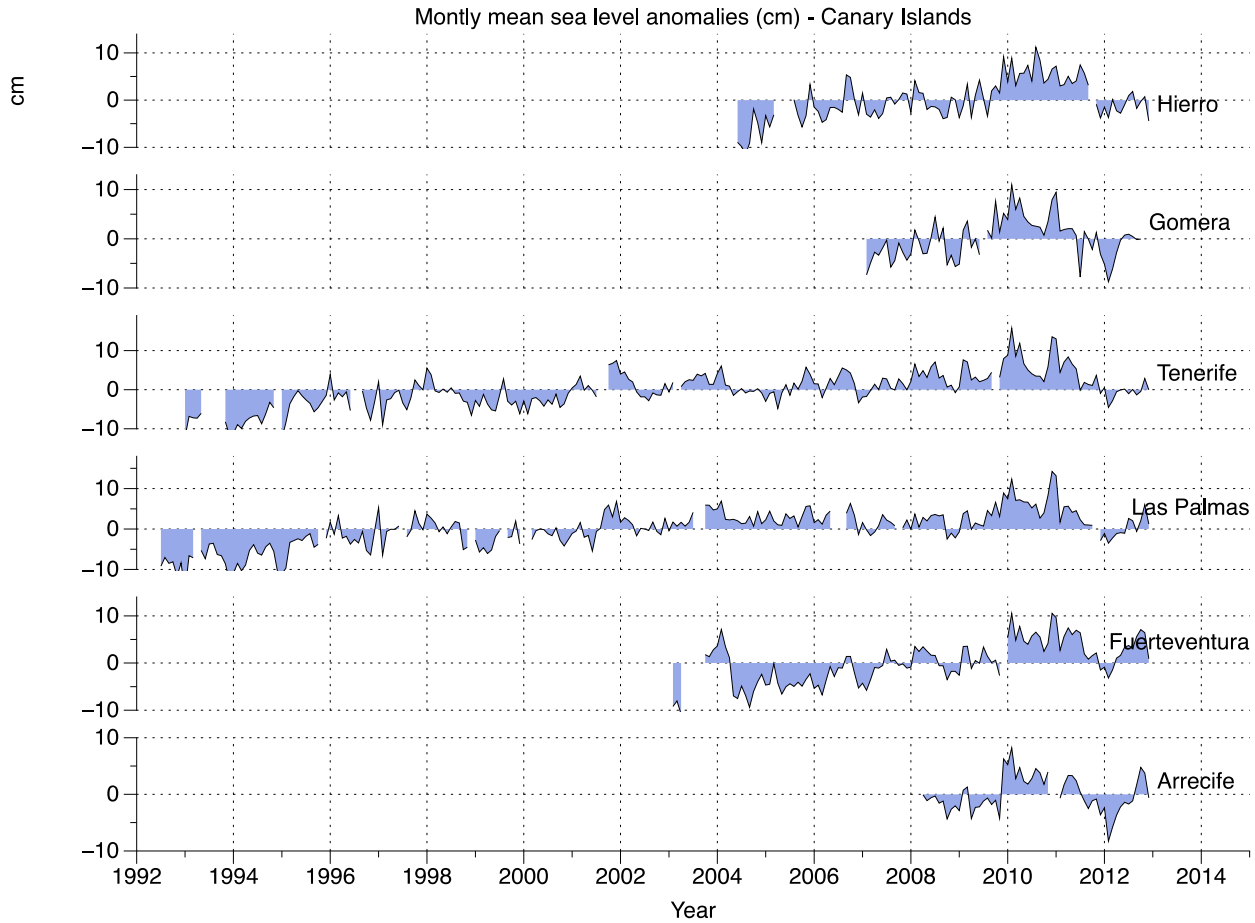

Figure 6.2.2. Monthly mean sea level anomalies at the REDMAR stations in the Canary Islands, since their start date of operation until 2012 (extracted from Pérez-Gómez, 2014).

Interannual variations related to sporadic meteorological and oceanographic events become clear if we remove the seasonal cycle from the monthly means (Figure 6.2.2). This interannual variability is in great part related to the North Atlantic Oscillation (NAO), with a clear negative correlation, along the Atlantic coast of Europe (Woolf et al., 2003; Wakelin et al., 2003). This relation is also apparent still in the Canary Islands, especially since 2002. In fact, the negative value of the NAO Index (not shown) in 2010 coincides with the peak of positive sea level that year at all the stations while the positive NAO Index in 2012 would be in agreement with the lower mean sea levels the same year. Finally Figure 6.2.2 shows again a clear increase of positive sea level events since 2002.

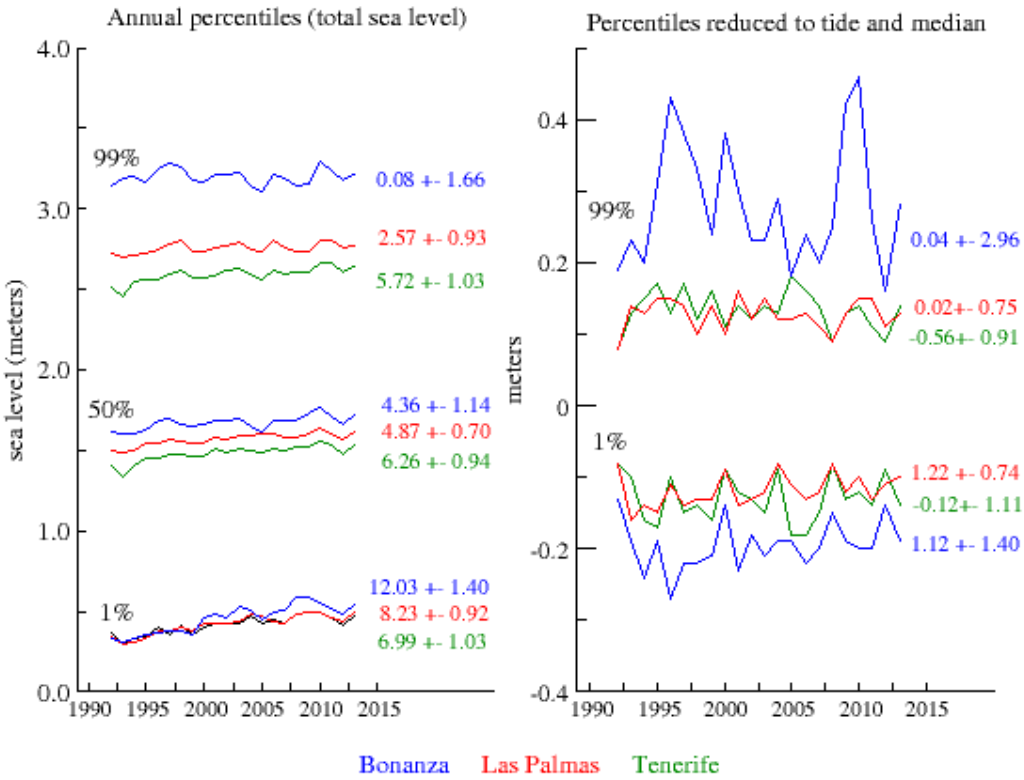

Figure 6.2.3. At the left: evolution of the 1%, 50% and 99% percentiles (from hourly values) for the REDMAR stations of Bonanza (blue), Las Palmas (red) and Tenerife (green), including their trends and standard error in mm yr^{-1} (1992-2013). At the right: evolution of 1% and 99% annual percentiles reduced to tide and median (after harmonic analysis of each year of data). Bonanza larger variability reflects also the impact of Guadalquivir river discharge.

The evolution of the hourly sea levels annual percentiles - 99% (highs), 50% (median, close to mean sea level) and 1% (lows) - are displayed in Figure 6.2.3 (left) for the stations of Bonanza, Tenerife and Las Palmas (the REDMAR stations covering a longer period, 1992-2013, trends in mm yr^{-1}). The evolution of the lowest and highest levels (1% and 99% percentile levels, respectively) reveals a larger positive trend in the lower extremes in comparison to the mean sea level trend (50% percentile) and in comparison to the higher extremes, with an even smaller trend. This is observed both at the Gulf of Cádiz and the Canary Islands (although most evident in other harbours from the REDMAR network, further north, as described in Pérez-Gómez, 2014). This differential trend is still present when the time series are reduced to the median values and, if confirmed in the coming years, would reflect a different origin for the trend of mean sea level and that of extremes. The values for Bonanza could be affected for both instrumentation problems and the

changes observed in the tide in the Guadalquivir River, something that should be confirmed in the future. This difference is on the other hand larger in Las Palmas than in Tenerife. Figure 6.2.3 (right) shows the 99% and 1% percentile series minus those obtained from tidal analysis of each year of data, as in Woodworth and Blackman (2004), i.e. percentiles reduced to tide and median. These reveal the larger variability of non-tidal sea level at Bonanza, as compared to the Canary Islands, where the tidal signal is clearly dominant, and practically negligible trends, what would be in agreement with the statement of Woodworth and Blackman (2004) for other regions of the world: that the observed increase in extremes for the last decades could be an artefact of short-term trends in the extremes of the tide.

Analysis of altimetry data and comparison with tide gauges:

Since 1992 sea level variability and trends are also available in open waters from altimetry observations, as can be seen in Figure 6.2.4, which displays the standard deviation (a measure of the energy or range of variability) and the linear trends derived from monthly means of sea level anomaly from Aviso multi-mission gridded product. In contrast to tide gauges, these are absolute sea level trends. It is important to remark that the atmospheric component has been corrected from this product, by means of the mentioned DAC correction.

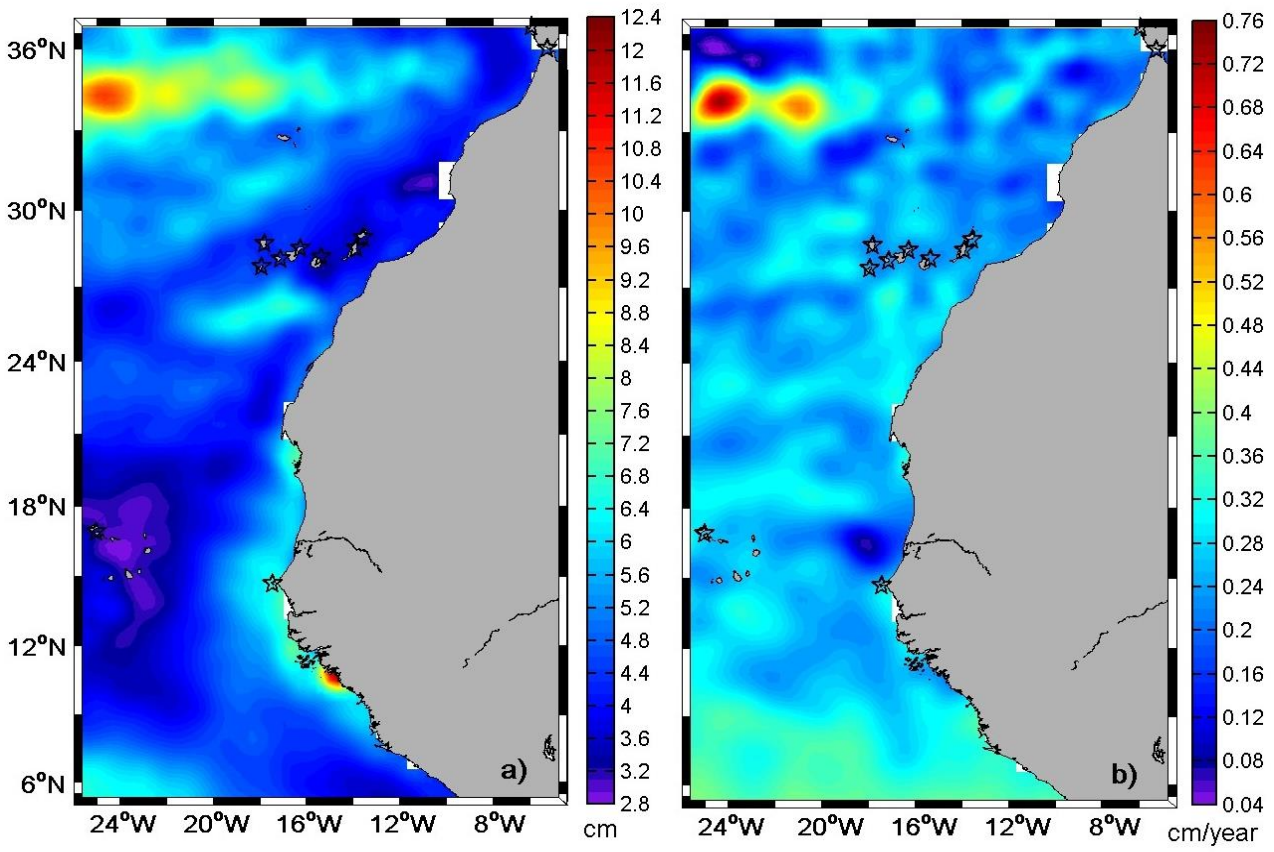

Figure 6.2.4. a) Standard deviation (cm) and b) Trends (cm yr^{-1}) of sea level anomaly (Aviso multi-mission products, 1/3° x 1/3°, period 1992-2013). Black stars: position of the tide gauges in the CCLME.

Figure 6.2.4 (a) reveals, first, two strong signals of mean sea level (MSL) variability in the margins of the region of interest (in the African coast around 11°N and at the northwest corner of the domain, in the middle of the Atlantic). These signals correspond to the mesoscale activity present in the Atlantic, especially north and west off the study domain. Maps covering the whole Atlantic (not included) show this kind of variability around the Gulf Stream and extending over the North Atlantic and Azores current area. In fact, these patterns are the southern more expression of this variability. It is also worth noting a relative increase of energy in mean sea level anomaly at the South of the Canary Islands, extending horizontally from the coast to the open waters, likely related to the mesoscale gyres caused by the interaction of the Canary Current with the islands. A third feature is related to the coastal band of increased energy between the Equator and 22°N, which is probably associated to the along-shore wind effects that generate trapped Kelvin waves travelling northwards (Calafat et al., 2012; Marcos et al., 2013). North of 22°N most of the MSL variability is reduced. Another area of relative increased variability appears in front of the coast south of 22°N (Cape Blanc) without reaching the Cape Verde Islands, possibly related also to the along-shore wind effects.

The spatial variation of sea level trends (Figure 6.2.4-b) shows a general increase of the trend in the domain from North to South, with values between 1.0 mm yr^{-1} and 4.5 mm yr^{-1} (apart from the strong signal in the northwest corner of the domain, out of the CCLME). There is no zonal pattern, however, being the values in open waters not very different from the ones at the coast, especially at the latitude of the Canary Islands and to the north, as stated by Marcos et al. (2013). These spatial patterns show the fingerprint in sea level of the mesoscale activity in the region. The southward increase in the trend is in agreement with a greater contribution to sea level rise since 1990 from the tropical and southern oceans (Merrifield et al., 2009).

Table 6.2.3. Main statistical parameters from the comparison between REDMAR tide gauge and altimeter monthly means, for their common period 1992-2013 (seasonal cycle removed). NVal: number of data (months), Bias (cm): mean difference, RMSE (cm): root mean square error, Rmax (cm): maximum (positive) difference, Rmin (cm): minimum (negative) difference, a0, a1: origin and slope of the altimeter vs. tide gauge linear regression, R: correlation coefficient.

Station	NVal	Bias	RMSE	Rmax	Rmin	a0	a1	R
Bonanza	252	0.04	3.98	11.09	-16.79	0.02	0.53	0.90
Tenerife II	252	0.22	2.08	7.2	-4.64	0.15	0.67	0.91
Las Palmas II	252	-0.02	2.27	7.34	-5.9	-0.01	0.61	0.88

Comparison of tide gauge and altimetry in the vicinity of each station is made to explore the impact of the intrinsic potential differences: local movements of the tide gauges, effect of complex local circulation patterns, etc. (Vinogradov and Ponte, 2011). It will help to assess the uncertainty of the observed sea level trends and to determine the relation of coastal and open ocean sea level signals. To allow the direct comparison of tide gauge and nearby altimeter monthly mean sea levels at the REDMAR stations, the DAC component was added to the MSLA as in Pérez-Gómez (2014). Examples of this comparison, including tide gauge and altimeter trends for the same time period, are presented here for those stations within the CCLME (Figure 6.2.5). The main statistical parameters of this comparison, performed with the average of the altimeter points within a box of 0.5° around the tide gauge, and after removal of the seasonal cycle, are shown in Table 6.2.3.

Correlations and RMSE (root mean square error) are larger than 0.88 and smaller than 2.27 cm in the Canary Islands stations. The RMSE is larger however in Bonanza (3.98 cm). Figure 6.2.5 (extracted from Pérez-Gómez, 2014), on the other hand, reveals a significantly larger trend at the three tide gauges with respect to the trends in the altimeter. This could be due to local unknown movements, as already mentioned. However, if we correct Las Palmas time series of the CGPS derived vertical movement (-1.56 ± 0.34 mm yr^{-1}), this difference is still present. Tide gauges show also in general a larger variability of the mean sea levels.

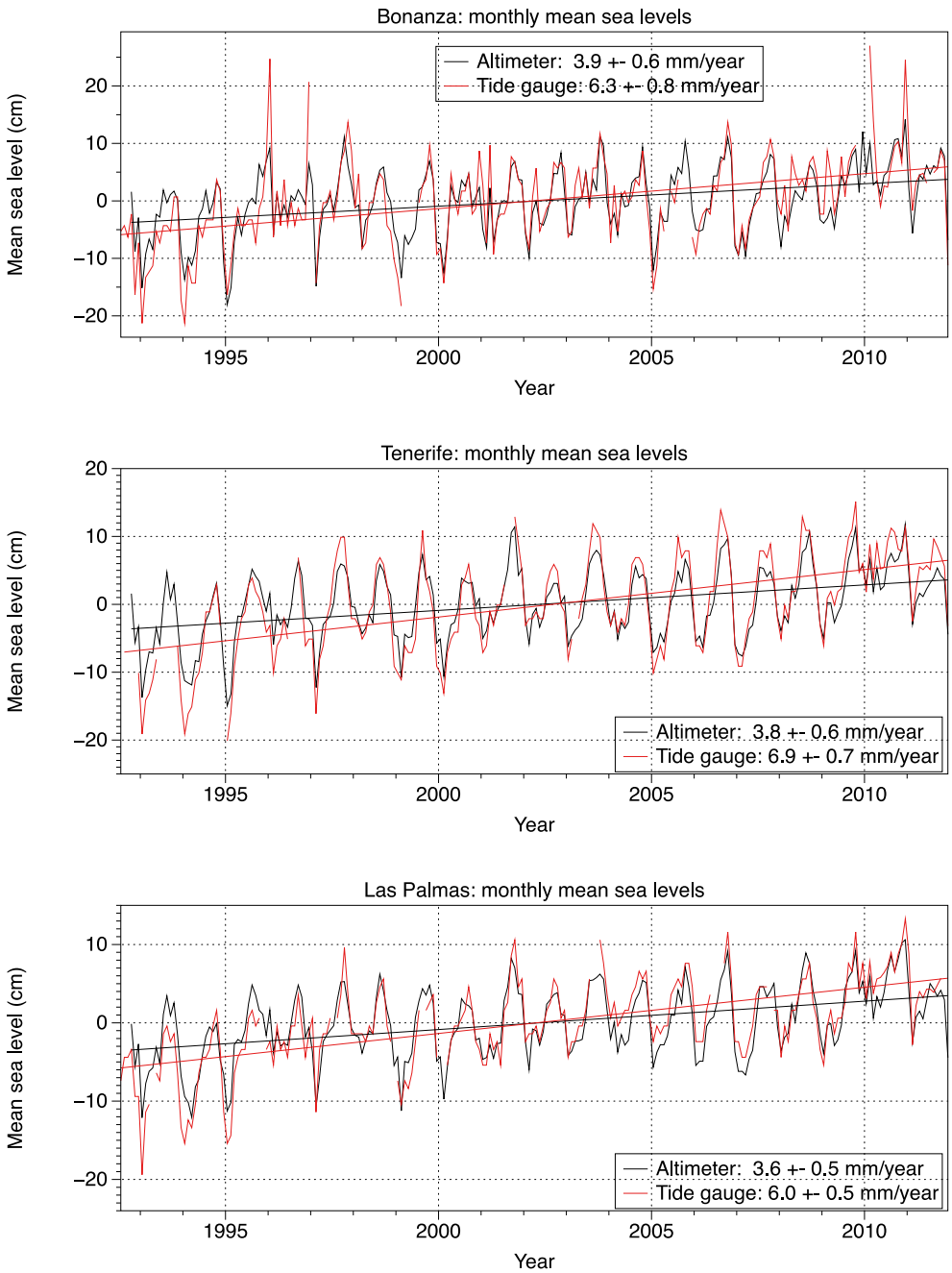

Figure 6.2.5. Monthly means from tide gauges (red) and nearby altimeter data (black) for the period 1992-2011 (extracted from Pérez-Gómez, 2014).

6.2.4. CONCLUSIONS AND RECOMMENDATIONS

A review of published works on long-term mean sea level trends in the CCLME has been combined with new estimates from the longer time series available from tide gauges in the region. There is an evident lack of historical sea level data during the 20th century, of course, but also for the last decades, in the African coastline, so the study is based mainly on Spanish tide gauges. The main difficulty for a direct comparison of the different local trends is the data period employed in each study, as well as the absence of knowledge of local land movements at the stations, needed also for comparing tide gauge observations to altimetry. We know the nowadays value of this vertical movement at Las Palmas and Tarifa stations. Tenerife, according to Marcos et al. (2013), is considered to be a stable site and Cádiz present negligible values (SONEL and Marcos et al., 2011). As the influence of local movements at the rest of the stations considered is still unknown, its determination should be achieved in the future, by installing new CGPS stations close to the tide gauges.

In spite of these difficulties, a comparison of recent trends (last two decades) to the longer-term ones, reveal an increase of the rate of mean sea level rise since the 1990's, coherent with previous publications on global sea level rise (Merrifield et al., 2009; Church et al., 2013). The uncertainty of these trends is addressed by comparison with altimetry data, revealing a general high correlation but a significant difference in the trend that should be further explored in the coming years.

Tide gauge data are also used for a review of interannual and seasonal variations in the region and their relation to oceanographic and meteorological forcing such as the variations of the Canary Current and the NAO; on the other hand, analysis of the extreme percentiles for the last 20 years at these stations reveal positive trends in low sea levels larger than the ones found for mean and high sea levels, but the origin of this discrepancy is so far unknown.

Finally, altimetry data constitute the main source of information for analysis of the spatial variations of sea level variability and trends in the CCLME. Apart from the confirmation of the main oceanographic features in the region, these data reveal larger trends of mean sea level since 1992 in the southern part of the domain, what would be coherent with the increased rates in the tropical regions reported by Merrifield et al. (2009).

Installation and long-term operation of tide gauges and CGPS stations in all the countries of the CCLME region is the main recommendation from this article, for an adequate assessment of long-term sea level variations. In the meantime, implementation of regionalized hindcasts by means of numerical models would provide a better insight on the real causes of observed sea level variations.

Acknowledgements

The altimeter products (MSLA and DAC correction) were produced by Ssalto/Duacs and distributed by Aviso (http://www.aviso.altimetry.fr/duacs/, accessed on 15 January 2015, with support from the Centre National d'Etudes Spatiales (CNES). Monthly means from tide gauges in Dakar and Porto Grande have been downloaded from the Permanent Service for Mean Sea level (http://www.psmsl.org/data/obtaining/map.html, accessed on 15 January 2015) and GPS derived trends for local land movement in Las Palmas was obtained from SONEL (http://www.sonel.org/-Sea-level-trends-.html, accessed on 20 January 2015). Finally the authors would like to thank Javier Soto Navarro (Puertos del Estado) for providing the final altimetry data plots.

6.3. RECENT CHANGES AND TRENDS OF THE UPWELLING INTENSITY IN THE CANARY CURRENT LARGE MARINE ECOSYSTEM

Aïssa BENAZZOUZ[1], Hervé DEMARCQ[2] and Gonzalo GONZÁLEZ-NUEVO[3]

[1] Institut National de Recherche Halieutique. Morocco

[2] Institut de Recherche pour le Développement. France

[3] Centro Oceanográfico de Vigo, Instituto Español de Oceanografía. Spain

6.3.1. INTRODUCTION

The Canary Current Upwelling System (CCUS), which extends from the Iberian Peninsula (IP) (43°N) to the south of Guinea-Bissau (8°N) (Fig. 6.3.1), and includes the Canary Current Large Marine Ecosystem (CCLME), one of the world's four major Eastern boundary upwelling ecosystems (EBUEs). The seasonal variability of the trade winds between winter and summer induces pronounced coastal sea surface temperature (SST) anomalies with a high seasonal contrast, mainly in the southern part of the system (Arístegui et al., 2009a; Barton et al., 2013).

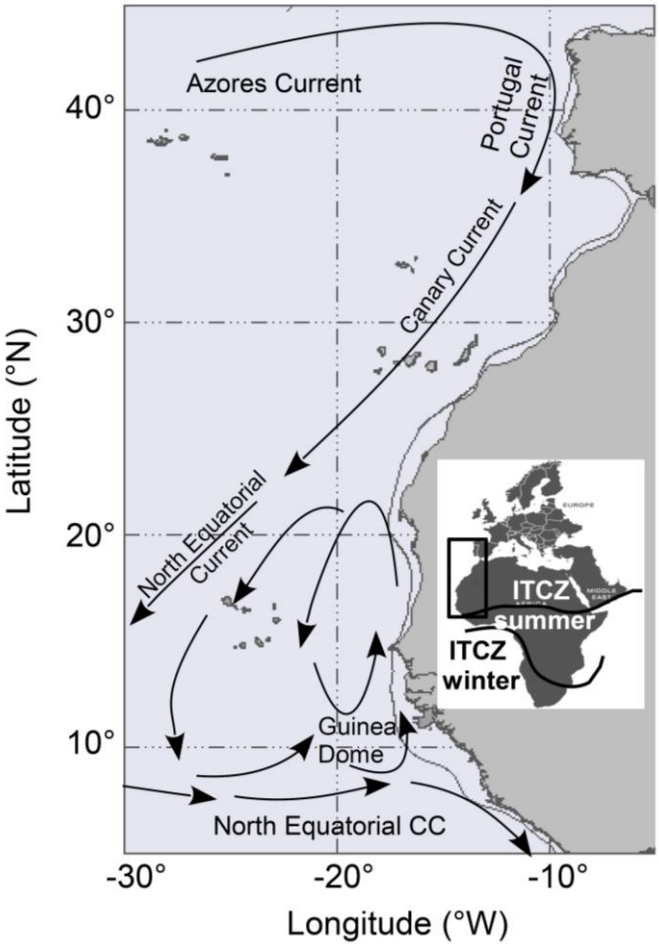

Figure 6.3.1. Study area of the CCLME region with the main surface currents: Azores, Portugal, Canary, North Equatorial current and North Equatorial counter-current. The 200 m isobath is superimposed.

In 1990, Bakun observed a general trend of the upwelling intensification related to the wind intensity increase. Later on, Bakun et al. (2010) hypothesized that in the context of the climatic change due to the global warming, a higher thermal gradient between the land and water masses intensify the alongshore upwelling favorable wind stress that consequently intensify the upwelling process.

This effect has been strongly supported by several authors (García-Reyes and Largier, 2010; McGregor et al., 2007; Narayan et al., 2010). However, contrary to this study, several recent trends in wind and temperature suggest a reduction of upwelling in the Northwest Africa (NWA) and Iberian coast (Alvarez et al., 2008; Lemos and Pires, 2004). In addition, Pardo et al. (2011) have examined the long term variation in the Canaries and other upwelling zones, finding a ‘‘weakening of the upwelling intensity in the Iberian/Canary and NWA regions”. Barton et al. (2013) and Cropper et al. (2014) have found no coherence between wind intensification and coastal SST cooling.

In the context of these conflicting results, our overriding aim is to test the Bakun hypothesis related to the upwelling intensification.

6.3.2. DATASETS

We use two homogeneous datasets from spatial observation: a 30 years SST series from the AVHRR (Advanced Very High Resolution Radiometer) version 5.2 day-time for the time period September 1981 to December 2011 (http://www.nodc.noaa.gov/sog/pathfinder at 4 km resolution, accessed on 15 October 2014), and the global wind CCMP (Cross-Calibrated Multi-Platform) from July 1987 until 2010 funded under the United States National Aeronautics and Space Administration (NASA) Earth Science Enterprise (Atlas et al., 2010).

6.3.3. REGIONAL UPWELLING INDEX DATASET

Our analysis focuses on the coastal-upwelling areas off NWA. The NWA coast is the core area of the eastern North Atlantic upwelling system with the northeast extension covered by the IP.

The definitions of the environmental indices and their regular availability in time are of key importance in the management of coastal upwelling systems. Such indices are derived from physical parameters (wind and SST) and computed on a regular basis, to describe and follow the state of the environment as well as to estimate possible trends.

To quantify upwelling at synoptic time-scales, we have used two different indices that are based on the two different characteristics of the upwelling process. The first index quantifies the physical forcing, the Cross-Shore Ekman Transport (hereafter noted CSET) (Bakun, 1973; Ekman, 1905), the second one considers the physical response of upwelling through the SST (Benazzouz et al., 2014a; Van Camp et al., 1991) and the surface layer during upwelling events (hereafter noted CUI). Statistical analyses have been done on two periods according to the available time series datasets.

The trend is calculated using yearly averaged data. The linear regression is applied for the whole time series, with a least squares (LS) fit used as a linear adjustment.

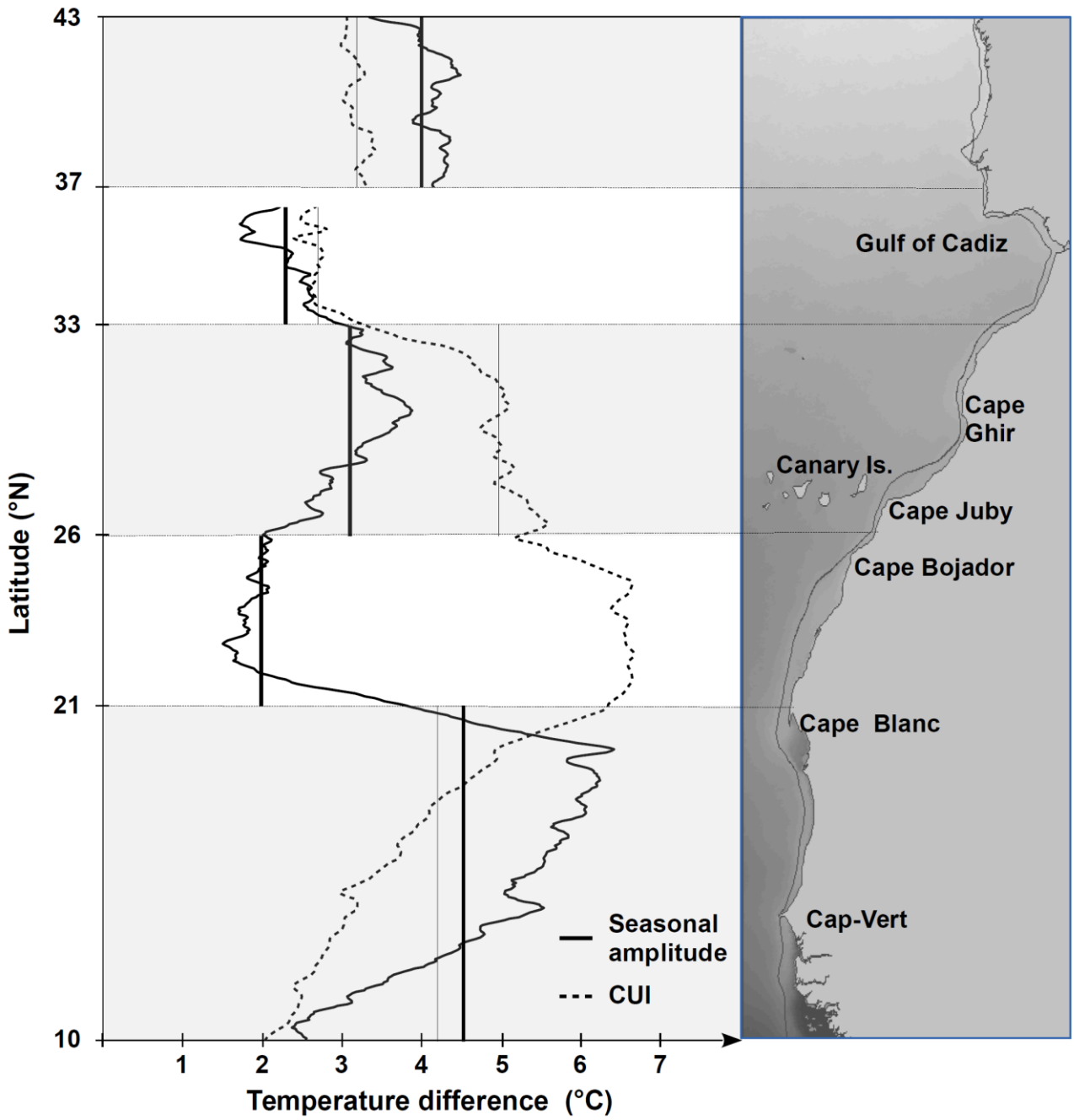

Figure 6.3.2. Latitudinal partition of the study area in five upwelling areas, based on the average value of their thermal zonal difference (CUI) and their seasonal amplitude, both expressed in °C. The vertical bars help to visualize the average values of the parameters.

6.3.4. RESULTS

6.3.4.1. Partitioning of the study area according to average intensity and seasonality

In order to simplify the following results, we use the CUI to define distinct latitudinal regions by combining the intensity of the CUI and its seasonal amplitude. A partition into five regions, from north to south is presented in Figure 6.3.2: the Portuguese coast (37°N-43°N) characterized by a high and stable seasonality; the 33°N–36°N area characterized by a low seasonality and upwelling index; the 26°N–33°N area with a progressively higher index and seasonality; the region between 21°N–26°N with a high index and a very low

seasonality; and the 10°N–21°N region, with a very high but decreasing seasonality associated to regularly decreasing upwelling indices.

6.3.4.2. Interannual variability of the Cross-Shore Ekman Transport

The interannual variability of the CSET showed oscillations that depended on latitude (Fig. 6.3.3).

The five regions previously defined are still very distinct, with the greatest intensity occurring in the coastal strip from 21°N to 26°N, where upwelling is quasi permanent, followed by the strip 26°N–33°N in summer, and south of Cape Blanc in winter.

Particularly, the CSET was very high in the last decade, with the highest values observed in 1999, 2002, 2004, 2007, 2008, 2009 and 2010. The lowest CSET is observed north of Cape Bojador in 1996 and for the whole CCLME region in 1997.

From this figure (Fig. 6.3.3) we can appreciate the acceleration of the trade winds within the study area. This seems to be linked to a general increase in the equatorward winds in the tropical belt worldwide (Demarcq, 2009). This trend is also consistent with the measurements of local coastal wind worldwide, as synthesized by Bakun (1990) who demonstrated a general alongshore wind increased in EBUEs in 1950–1985. Nevertheless, this increase is not uniform in the whole area: the wind is stronger north of Cape Blanc and decreases towards the Cap-Vert region.

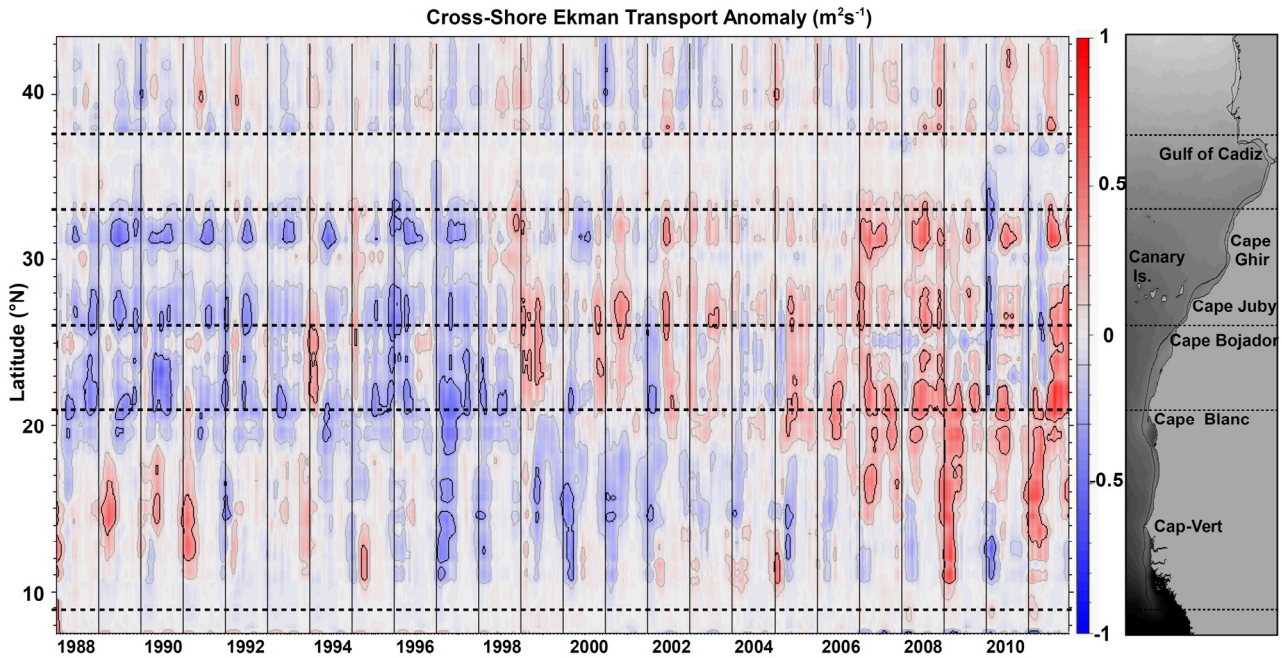

Figure 6.3.3. Space-time Hovmöller plot, illustrating the seasonal and interannual variability of the CSET anomaly from January 1988 to December 2011.

6.3.4.3. Interannual variability of the thermal coastal upwelling indices (CUI)

The space-time diagram of the coastal SST-based upwelling index (CUI), as computed from the 8-day SST (Fig. 6.3.4), shows the seasonal and interannual variations of the upwellings for the period from July 1981 to December 2011 (30 years). It highlights the latitudinal variations in upwelling intensity and seasonality, as well as in terms of spatio-temporal extent.

The interannual variability is more pronounced in the central and northern part of the system, with well-defined continuous latitudinal anomalies.

The whole time period was characterized as having considerable year-to-year variability and oscillations between periods of strong (1982, 1984, 1991, 1993, 1996, 1998, 1999, 2002 and 2005) and anomalously weak upwelling (1983, 1987, 1989, 1990, 1994, 1995, 1997, 1998, 2001, 2005, 2006 and 2009). Nevertheless, only a few years present clear anomalies for the whole system, as 1998–1999 or 2008–2009, where a north to south propagation of the high upwelling intensity is visible. Alternatively, several exceptional upwelling seasons were found to occur in only one portion of the system, for example a very weak upwelling is observed from the end of 1995 to 1997 in the 26°N-33°N area (Fig. 6.3.4), related to an exceptional relaxation of the trade winds (Fig. 6.3.3). These strong anomalies have been associated to a quasi-absence of juveniles in 1996 and 1998, and the collapse of the regional sardine stock between 1996 and 1997 (Machu et al., 2009). On the contrary, some years are associated to strong upwelling seasons only in the southern part of the system, as in 1986, 1996, 1999, 2005, 2009 and 2011.

In general, the interannual variability of the CSET and CUI show a similar pattern: high CSET intensity coincides with positive CUI anomaly in 1999, 2001, 2002, 2007 and 2008; and vice versa, low CSET intensity coincides with negative CUI anomaly in 1995-1998. This last anomalous period (1995-1998) is considered as a Pacific El Niño years, where the zonal wind anomalies act as a bridge linking the two ocean basins (Pacific and Atlantic), and in turn reinforce the inter-basin SST gradient through the atmospheric Walker circulation and associated oceanic processes (Wang et al., 2009).

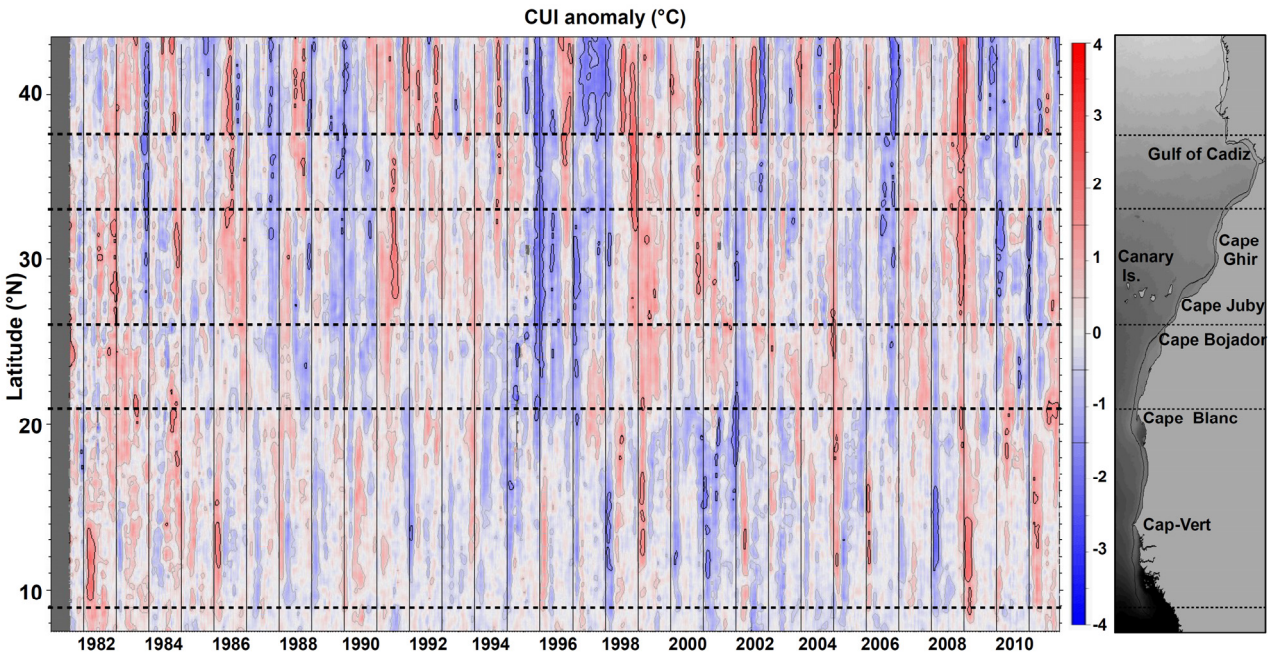

Figure 6.3.4. Space-time Hovmöller plot, illustrating the seasonal and interannual variability of the CUI anomaly from September 1982 to December 2011.

6.3.4.4. Determining the temporal trends in the upwelling time series

Temporal wind trend

The linear trend of the CSET for each upwelling area is documented in Figure 6.3.5a.

The long-term trend of the CSET shows high temporal and regional variability, with a general strengthening of the Ekman transport throughout the whole area. Nevertheless, the order of magnitude off the trend slope varies significantly between areas.

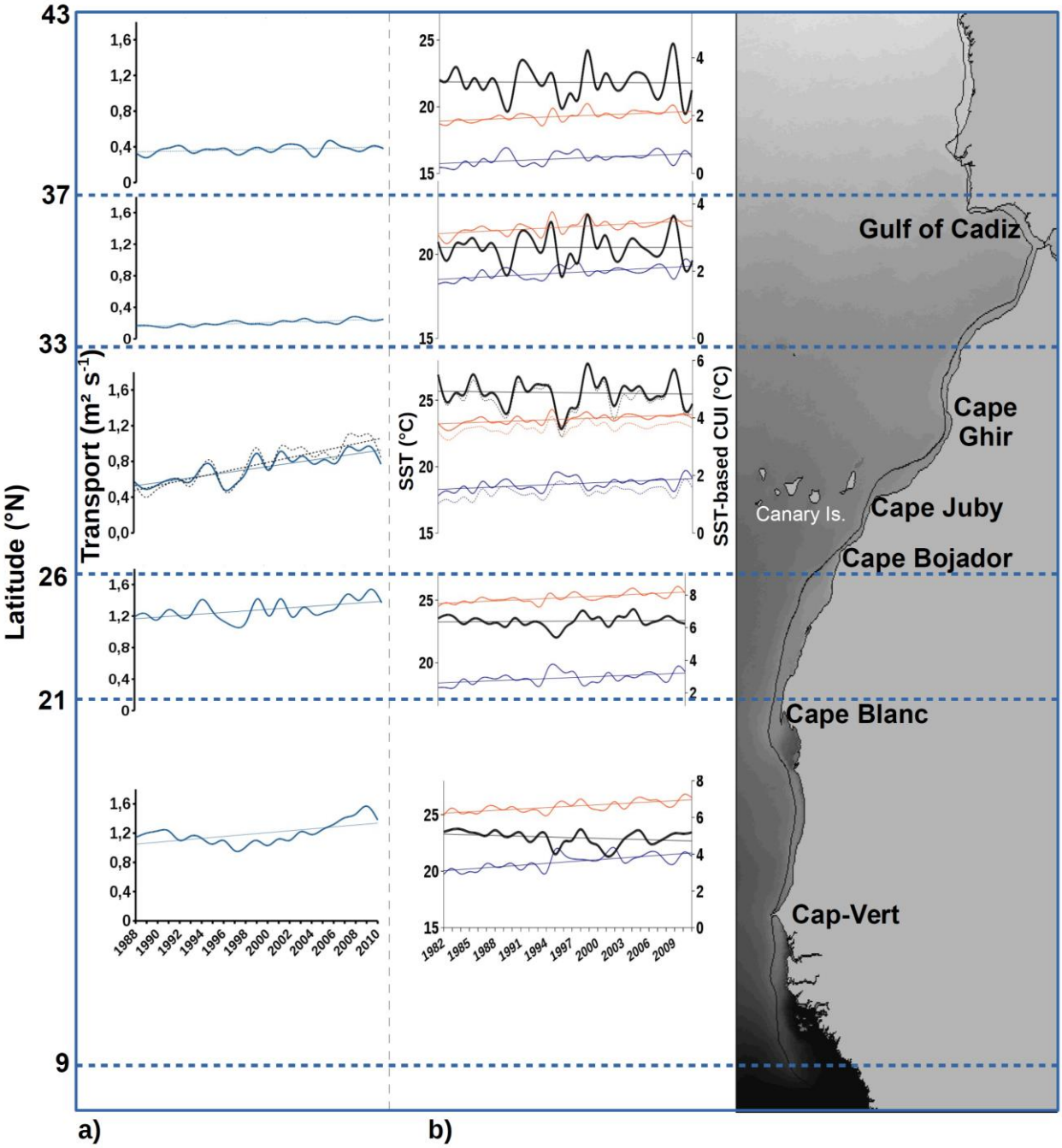

Figure 6.3.5. Linear trends for a) the annual-mean Ekman Transport (m^2 s^{-1}) during 1988-2011 for the five regions of upwelling regimes previously defined, and b) the annual-mean SST during 1982-2011 for SST_{max} (red line), SST_{min} (blue line) and CUI (thick black line).The Cape Ghir trends (dashed lines) are superimposed on the plot for the 26°N-33°N area.

The trends in the CSET are reported in the Table 6.3.1.

The upwelling areas show uniformly significant positive values. An exceptional insignificant trend is observed over the IP, in the northern zone (37°N-43°N).

Table 6.3.1. Linear decadal slopes, associated significance levels, and relative (%) decadal change, computed for the period 1981–2011 for the CSET and for the CUI and its SST components (SST_{min} and SST_{max}) during 1988-2011.

	CSET (m^2s^{-1})		CUI (°C)		SST_{max} (°C)	SST_{min} (°C)
	Slope	Decadal change (%)	Slope	Decadal change (%)	Slope	Slope
37°N-43°N	0.037	16.164	0.007	0.231	0.293**	0.283**
26°N-33°N	0.170**	32.070**	-0.001	-0.015	0.272**	0.275**
21°N-26°N	0.095**	7.825**	0.060	0.945	1.362**	0.265**
17°N-21°N	0.136**	14.242**	-0.134	-2.622	0.428***	0.571**
Cape Ghir	0.252***	52.895***	0.038	0.874	0.260**	0.227**

*Significance level: '***' 0.001 '**' 0.01*

This first result shows, indeed, that there is a trend of the wind generating upwelling. However, this trend is not uniform for the whole area.

The most intense CSET trend is observed in the 26°N-33°N area, which includes the permanent Cape Ghir filament (31.5°N) with a positive slope of 0.170°C $decade^{-1}$. This result is statistically significant at p-value <0.001 and corresponds to an increase of about 32% $decade^{-1}$.

This result corroborates the Bakun hypothesis, stipulating the upwelling-favorable wind intensification. Contradictory to the Bakun's hypothesis, the Iberian system exhibits no positive trend.

The second part of the Bakun hypothesis, which examines the strengthening of cooling as consequence of the wind intensification, is the purpose of the following section.

SST and the CUI trends

The long-term linear trend of the thermal fields is computed for the thermal coastal upwelling index, based on the coastal SST_{min} and offshore $SST_{max,}$ according to the same methodology adopted for the wind.

The annual averaged linear trends are shown in the Figure 6.3.5.

The annual means computed for the 1981-2011 period, both for SST_{min} and SST_{max} (Figure 6.3.5b) show very distinct warming trends over the whole studied area. This result implies that the CCLME is largely affected by global warming.

The warming illustrated by these curves refers to both the coastal upwelling and oceanic waters; this explains that the Atlantic Ocean subtropical basin is warmed in its eastern part, as shown in Demarcq (2009).

In general, both terms (SST_{min} and SST_{max}) evolve in the same way and show significant trends of the annual-mean value in the five regions (Table 6.3.1). In fact, SST_{max} is located mostly at 3000 km offshore, practically in the mid-Atlantic Ocean. Therefore, if both terms (SST_{min} and SST_{max}) are warming simultaneously, they affect the whole eastern part of the Atlantic Ocean interdependently of the upwelling itself which is supposed to be more intense, as a cooling response to the favorable wind strengthening. Nevertheless, the thermal CUI, derived from SST_{max} and SST_{min}, displays an ambiguous trend and is statistically insignificant (Fig. 6.3.5 and Table 6.3.1).

In the light of those results, it should be noted that the linear trend of the thermal fields, as computed from LS, reveals that the whole area is subject to very distinct warming trends, both in its coastal and oceanic parts.

This result can also be considered as contrary to the Bakun hypothesis that stipulates a more intense cooling in response to the wind strengthening.

6.3.5. DISCUSSION

The annual time series highlight the interannual variability as well as the potential existence of the long term trend. Table 6.3.1 summarizes the long term linear trend of the thermal and wind-based indices.

The temporal trend of the CSET shows a statistically significant positive strengthening trend between 17°N and 33°N. The meridional wind has intensified over the whole Moroccan area, with a mean value of 0.3 m s^{-1} $decade^{-1}$ and about 0.8 m s^{-1} $decade^{-1}$ in front of Cape Ghir (results not shown). Between 17°N and 21°N (upwelling seasonal part), the wind speed has increased only about 0.24 m s^{-1} $decade^{-1}$. This weak intensification is of the same order as the magnitude near the IP (0.29 m s^{-1} $decade^{-1}$).

We can conclude that the long term trends resemble those obtained by Bakun, which predicted an increase of the wind stress on the coastal upwelling systems.

However, the results reveal that most of the CCLME has significantly and considerably warmed. This warming concerns the offshore oceanic water as well as the coastal upwelling waters. During the last three decades, the SST_{min} and SST_{max} have increased respectively by 0.28°C $decade^{-1}$ and 0.29°C $decade^{-1}$ in the IP, while in the Senegalese-Mauritanian region the SST_{min} and SST_{max} have increased respectively about 1.71°C (0.57°C $decade^{-1}$) and 1.28°C (0.44°C $decade^{-1}$).

The resulting linear trend of the thermal fields sustain the projection of the Intergovernmental Panel on Climate Change (IPCC, 2013) of a significant increased trend in global SST during the last 100 years, especially the most recent 30 years (Trenberth, 2010).

Furthermore, the coastal upwelling water warming is in contradiction with Bakun hypothesis, which predicts more upwelling water and cooling in response to the strengthening of the upwelling-favorable wind.

In fact, the wind has intensified but this relative strengthening is not accompanied by a significant cooling, instead it displays a clear warming.

The analysis of the CUI variability characterizes in a complementary way the information from the CSET by revealing that:

- The linear trend of the upwelling activity is increasing south of Cape Juby, particularly in the (21°N-26°N) area, while it is visually decreasing south of Cape Blanc (17°N-21°N) and experiences no changes in the rest of the ecosystem.

- According to the CUI index, no trend is statistically significant.

The observed increase over time in the magnitude of the upwelling-favorable wind in the NWA and IP coast is consistent with a recently documented increase of annual-mean upwelling off California, Portugal, Morocco and Peru throughout the 1945-1985 period (Bakun, 1990).

Our results are partially consistent with Bakun's (1990) upwelling intensification hypothesis, which predicts that increased greenhouse gas emissions lead to a stronger thermal gradient between the relatively warm land mass and cool coastal ocean, thereby driving more persistent upwelling-favorable winds in coastal upwelling systems worldwide (Bakun, 1990; Bakun et al., 2010; McGregor et al., 2007; Mendelssohn and Schwing, 2002).However, we predict that these trends would instead be accompanied by coastal warming rather than cooling.

These can be explained in two different ways:

1. - The actual wind could not have sufficient energy to upward the cold water, found at deeper layers. Additionally, it is possible that an increase in wind intensity is constrained by an increasingly stratified water column which would restrict upwelling.

2. - Physical constraints set by the topographic steering and coast line geometry, the width of the continental shelf and the depth of the mixed-layer can potentially alter the long-term variability in a coastal upwelling system.

6.3.6. CONCLUSIONS

In this work we have studied the changes expected on the upwelling trend at the NWA and the IP coast. Studies have been done using different datasets on SST and wind, and the derived indexes. After the study of the behavior of the upwelling in the last three decades, the conclusion is that the wind is actually intensifying. However the temperature at the sea surface is increasing. Also, no trends are observed by the thermal upwelling index in any case: neither in the north, nor in the south.

The general trend of the temperature anomaly during the upwelling season showed an increase of about 0.71°C from 1982 to 2011 (Fig. 6.3.5b). This general trend does not agree with the hypothesis that the strength of upwelling increases due to the global warming signal.

Indeed, the CUI, used as an indicator to quantify the upwelling intensity, shows ambiguous results with quasi absence of a statistically significant trend. Additionally, the surfacing thermal signal which is the oceanic response to the physical forcing process, displays positive warming rates both in the coastal area

and in the offshore water. This result corroborates Barton et al. (2013) conclusion, but contrasts with McGregor et al. (2007) who reported an acceleration of a cooling trend in front of Cape Ghir region during last century.

Nevertheless, the trend of the thermal gradient is quasi null except in front of the Mauritanian region where the thermal difference between the offshore and the inshore is more less decreasing, whatever statistically insignificant. In fact, this visually decreasing trend is due to the increase of the SST_{min} more than SST_{max} (about 1.75°C and 1.28°C, respectively) during the last three decades.

The CUI has been considered to be a complex index, based on a precise spatial analysis of the upwelling structure and its thermal characteristics, granting it a proven robustness. However, we have shown that the surfacing thermal structures on the coastal band are affected by the upwelling process, therefore giving a signal that could be altered by different factors. For example, the reduction of the mixed layer can affect the temperature of the upwelled water and hence the thermal gradient. Equally, storms can drag down the mixed layer and consequently, the wind intensification cannot compensate the stratification or this sinking by the vertical transport. In the Barton et al. (2013) paper, it is mentioned that the analyses at depths of 50 m and 100 m, based on the World Ocean Database 2005 (Boyer et al., 2006) at 50 m and 100 m, show relatively uniform behavior in the sub-tropical North Atlantic, with statistically significant warming across the basin between 15°N and 50°N (Harrison and Carson, 2007). Warming rates approached 0.2°C $decade^{-1}$ in the NWA region at both depths. This result is coherent with what we have found at the sea surface from satellite-based data.

According to these results we can hypothesis that, in the context of the climatic warming, the wind will indeed intensify but the warming of the upwelled water may not take place.

Acknowledgments

The SST data were provided by GHRSST and the US National Oceanographic Data Center, in a project partly supported by a grant from the National Oceanic and Atmospheric Administration (NOAA) Climate Data Record (CDR). CCMP global wind data were obtained from the NASA Physical Oceanography Distributed Active Archive Center at the Jet Propulsion Laboratory.

We are also grateful to the EPURE project (ANR-11-CEPL-005 EPURE) founded by the French National Research Agency that has supported partially this work.

We are grateful to Itahisa Déniz González and Josep Lluis Pelegrí for their helpful comments that substantially improved the manuscript.

6.4. TRENDS IN PHYTOPLANKTON AND PRIMARY PRODUCTIVITY OFF NORTHWEST AFRICA

Hervé DEMARCQ[1] and Aïssa BENAZZOUZ[2]

[1] Institut de Recherche pour le Développement. France

[2] Institut National de Recherche Halieutique. Morocco

6.4.1. INTRODUCTION

The Canary Current Upwelling System is one of the most productive coastal systems in the world, particularly in the subtropical latitudes. It sustains among the most productive monospecific small pelagic fisheries worldwide, mostly composed of clupeids. Catches that account for more than a quarter of the world's marine production (FAO, 2012), showed a strong increase from the 50s to the 90s, with a consistent decrease thereafter (about 15%) until 2011, a trend that explains the 'lose – lose' economic situation of the world's fisheries (Kelleher and Willmann, 2006).

In Northwest Africa (NWA), the contribution of fisheries to the gross domestic product (GDP) is between 2% and 4% for countries such as Senegal, Gambia and Cape Verde (de Graaf and Garibaldi, 2014). The recent trends for NWA countries show a slight but continuous increase in total catches, due primarily to an increase in fishing effort.

It is also well known that small pelagic species, because of their spawning strategy, are naturally very sensitive to environmental constraints (Cury and Roy, 1989; Meiners et al., 2010) and are responsible for most of the variability in the world's catches (Cury et al., 2008; Cury and Shannon, 2004). It is also recognized that regional primary productivity partly constraints natural levels of exploited stocks (Chassot et al., 2010).

The variability of marine primary productivity in the Canary Current Large Marine Ecosystem (CCLME) also plays an important role in the carbon cycle because oceans serve as a net sink of carbon dioxide (CO_2), by removing about 26% of anthropogenic emissions from the atmosphere (IPCC, 2013). It is estimated that this sink has increased only slightly over the last two decades (Sitch et al., 2015; Wanninkhof et al., 2013). The first factor partly controlling this trend is the reduced capability of the ocean to dissolve CO_2 because of continuous warming: the global mean surface temperature over the mean past 20 years (1993–2012) rose at a rate of 0.17°C decade^{-1} from 1979 to 2010 and at 0.24°C ± 0.06°C decade^{-1} from 1979 to 2010 in the northern hemisphere (Morice et al., 2012).

The observed surface warming of the tropical northern Atlantic, particularly for the CCLME region, is one of the highest over the last 30 years, with an average value of 0.30°C decade^{-1}, as computed from AVHRR (Advanced Very High Resolution Radiometer) satellite sea surface temperature (SST) from 1985 to 2007 (Demarcq, 2009; Good et al., 2007) or from more climate-oriented SST datasets (Cropper et al., 2014).

The global long-term warming trend, due to anthropogenic emissions of CO_2, remarkably anticipated by Broecker (1975), is also strongly altered by multidecadal variability (MDV ≈50–80 years). In the North Atlantic, Polyakov et al. (2009) show a general warming trend of 0.031 ± 0.006°C decade^{-1} in the upper 2000 m over the last 80 years of the 20th century, with periods of shorter duration strongly amplified by MDV. For

example, MDV accounts for ≈60% of North Atlantic warming since 1970. The non linear and spatially heterogeneous nature of warming in the CCLME is well described from more than 30 years of satellite-based observations. It is also well established (Hansen et al., 2006) that global warming of more than 1°C (relative to 2000), will constitute a ‘‘dangerous’’ threshold with likely effects on species survival.

The second factor influencing the variability of the carbon cycle is of course the level of marine primary productivity. Likely due to an increase of ocean's stratification, that decreases the vertical exchanges and consequently the enrichment of the surface layer, a decreasing productivity trend has been observed in the world ocean (Behrenfeld et al., 2006; Polovina et al., 2008). In upwelling areas, these trends may be somewhat different as local winds are the major controlling factor in determining trends in productivity (Cropper et al., 2014; Demarcq, 2009).

The most in-depth attempt to compute long-term marine productivity trends from satellite chlorophyll-a data, a common proxy for phytoplankton biomass, was made by Antoine et al. (2005) from two temporally independent spatial missions, the Coastal Zone Color Scanner (CZCS; 1979–1986) and the Sea-viewing WIde Field-of-view Sensor (SeaWiFS, data from 1997–2002). They estimated an average 22% worldwide increase in productivity, mostly in the intertropical areas. It is interesting to note that within the CCLME region, a similar positive trend was observed between 15°N to 30°N for the period 1979-2002, the opposite to that found later in the same region by Demarcq (2009) and several other authors, synthesized by Gregg and Rousseaux (2014) from SeaWiFS data from 1998 to 2007.

Because they partly overlap in time, composite products have been created from SeaWiFS, MODerate resolution Imaging Spectroradiometer (MODIS) and MEdium Resolution Imaging Spectrometer (MERIS) ocean color (OC) data, with the help of a unique chlorophyll-a algorithm (Maritorena et al., 2010). Despite a great improvement in terms of data density and coverage, “clear differences” between sensors have been noted. These differences are explained by differences in calibration and atmospheric corrections, correction of sensor sensitivity drifts and various data processing constraints such as cloud masking and spatial variations in data density. It is therefore not surprising that the combination of all errors lead to significant differences in the retrieval of complex variables such as the chlorophyll-a concentration, in which algorithms differ in the number of sensors and characteristics (see for example Brewin et al., 2013). In the case of MODIS, Shang et al. (2014) noted important and seasonally varying differences between three different published chlorophyll-a algorithms, and *in situ* data. Gregg and Casey (2010) used the Empirical Satellite Radiance-In situ Data (ESRID) methodology (Gregg et al., 2009), an empirical method based on the *a posteriori* re-derivation of SeaWIFS and MODIS bio-optical algorithm coefficients from water-leaving reflectances adjusted from *in situ* data.

Recently, Gregg and Rousseaux (2014) used a new composite method with datasets from two sensors (SeaWiFS and MODIS) combined with the ESRID method, *in situ* data and their assimilation in global biogeochemical models to estimate global trends at the scale of oceanic basins.

The purpose in this work is to define an empirical seasonal bias correction model between the two concomitant chlorophyll-a time series of SeaWiFS and MODIS in complex coastal waters off NWA, in order to include MODIS data from 2008 to 2014 in the determination of trends in chlorophyll-a in the CCLME region. We explore how trends for the whole 17-year period from 2003 to 2014 have evolved in the region since the previous study of Demarcq (2009) for the period 1998-2007 as established from SeaWiFS data for the four major upwelling systems.

6.4.2. DATA AND METHODS

In order to reduce the above-mentioned constraints of using datasets from different sources, data from only SeaWiFS and MODIS-Aqua are used for the 17-year period, from 2003 to 2014. Monthly averages of chlorophyll-a data from the whole SeaWiFS mission from 1998 to 2010 (including major data gaps in 2008 and 2009) and the present MODIS period, from 2003 to 2014 (Table 6.4.1) are examined. Because spatial resolution is an important issue in coastal regions, 9-km monthly SeaWiFS data were downscaled to 4.5 km to match the resolution of level-3 MODIS data.

Table 6.4.1. Temporal coverage of the SeaWiFS and MODIS data used in this study.

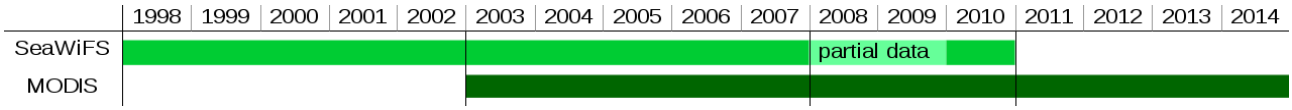

As of March 2015, the current standard OC products, distributed via the National Aeronautics and Space Administration (NASA) Ocean Biology Processing Group (OBPG) (http://oceancolor.gsfc.nasa.gov/cms/, accesed on 16 March 2015) are produced with the reprocessing versions R2010.0 for SeaWiFS and R2013.1 for MODIS-Aqua, and are intended to be equivalent in terms of quality. These versions are used is the present work, and are detailed in http://oceancolor.gsfc.nasa.gov/cms/reprocessing (accessed on 16 March 2015). The previous MODIS-Aqua reprocessing R2013.0 in particular has updated the instrument calibration to improve the late-mission temporal calibration, while the processing algorithms are identical with the previous versions (R2010.0 and R2012.0). The present chlorophyll-a standard algorithms are OC4v6 and OC3M, respectively for SeaWiFS and MODIS.

Ultimately, further data reprocessing (R2014.0) will be soon applied by the OC NASA/OBPG team to all OC missions. This reprocessing will include instrument calibration updates for all sensors to correct raw data for the latest known sensor degradations (such as a decrease in sensitivity over time). Significant changes are likely for some sensors, including SeaWiFS and MODIS-Terra (see http://oceancolor.gsfc.nasa.gov/cms/reprocessing/OCReproc20140.html - accessed 16 March 2015 - for details).

In the present work, special attention has been given to reconstruction of missing SeaWiFS data for the period 2008 to 2009 (2010 does not have full missing months). Fortunately, it has been possible to replace the missing days by the average for the same days of the two surrounding years, in order to minimize the impact of this reconstruction when computing trends.

Trends in primary productivity are derived from chlorophyll-a data. As previously shown (Demarcq, 2009), the results from a biomass-related index are very similar to those from a biomass-based production model such as the Vertically Generalized Production Model (VGPM) (Behrenfeld and Falkowski, 1997), as detailed in Demarcq (2009).

All trends are computed by splitting the time series into two parts. This procedure has been used for its robustness and conservative properties are compared to classic statistical methods (see Demarcq, 2009). In particular, the influence of the first and last years of the time series are greatly reduced in the case of extreme events.

Because of the naturally narrow distribution of the chlorophyll-a data, the adjustment has been made from the decimal logarithm of chlorophyll-a. The relative complexity of the observed biases between both datasets led to a two-step adjustment, utilizing a linear fit for chlorophyll values from 0.01 mg m^{-3} to 0.5 mg m^{-3} and a quadratic fit for higher values.

6.4.3. DIFFERENCES BETWEEN SENSORS

Because the above-mentioned differences between SeaWiFS and MODIS data, differences in chlorophyll-a have been computed separately for the 5-year period from 2003 to 2007 where both datasets are available (Figure 6.4.1). Within the CCLME, except for low chlorophyll-a concentrations, MODIS strongly overestimates measurements (Figure. 6.4.1a) compared to SeaWiFS (Figure 6.4.1b). The differences (Figure 6.4.1c) are high (> 3 mg m^{-3}) in the upwelling area, particularly over the continental shelf, where average concentrations of 10 mg m^{-3} are very common. In the coastal region (10°N-25°N / 15°W-18°W, red rectangle and inserted plot in Figure 6.4.1c), the time series shows a systematic difference of about 2 mg m^{-3} between the datasets. The average yearly difference in this coastal area is 42.5%, but only 32.4% for the greater region, from 15°W to 25°W.

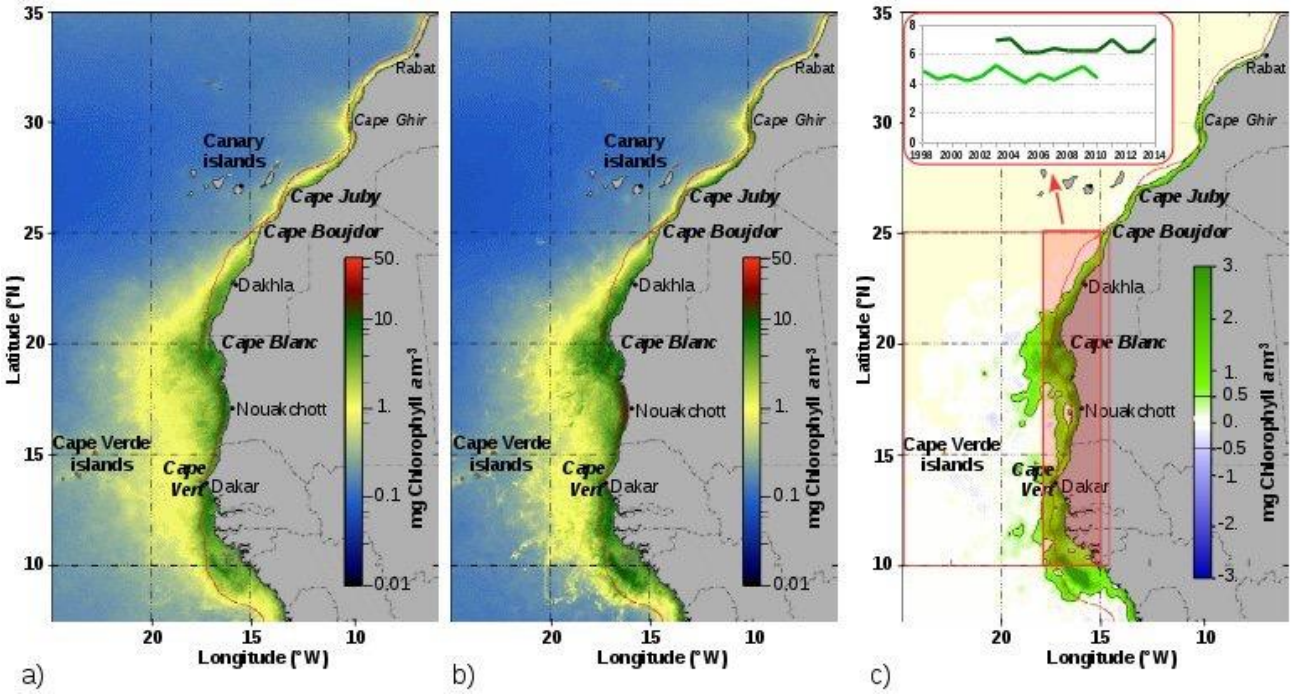

Figure 6.4.1. Average chlorophyll-a concentrations from a) SeaWiFS and b) MODIS data from 2003 to 2007 and c) the MODIS-SeaWiFS difference for the same period. The 200 m depth contour (red line) is superimposed. The insert in plot (c) shows the yearly averages of both sensors from 1998 to 2014 in the coastal area as defined by the red rectangle.

The relative stability of the differences over time shows that a systematic correction of the datasets is possible. The average difference between sensors does vary slightly according to season (not shown), probably because of differences in the atmosphere in this very seasonally variable region of the CCLME.

6.4.4. PARTIAL TRENDS DURING THE 1998-2014 PERIOD

In order to search for coherent temporal trends over the period 1998-2014, partial trends were computed separately for both the SeaWiFS and MODIS sensors for the Mauritanian and Senegalese regions of the CCLME (Figure 6.4.1), where trends were the strongest.

The SeaWiFS trend computed from 1998 to 2007 (Figure 6.4.2a) (Demarcq, 2009) shows mostly negative values with positive trends in the coastal regions of northern Mauritania and Guinea, in the vicinity of the shelf break. The trends computed from MODIS data from 2003 to 2014 (with a 5-year overlap with the previous one) show similar patterns (Figure 6.4.2b) with the dominance of positive trends. Because of the high bias between datasets, no common trend can be computed without preliminary correction.

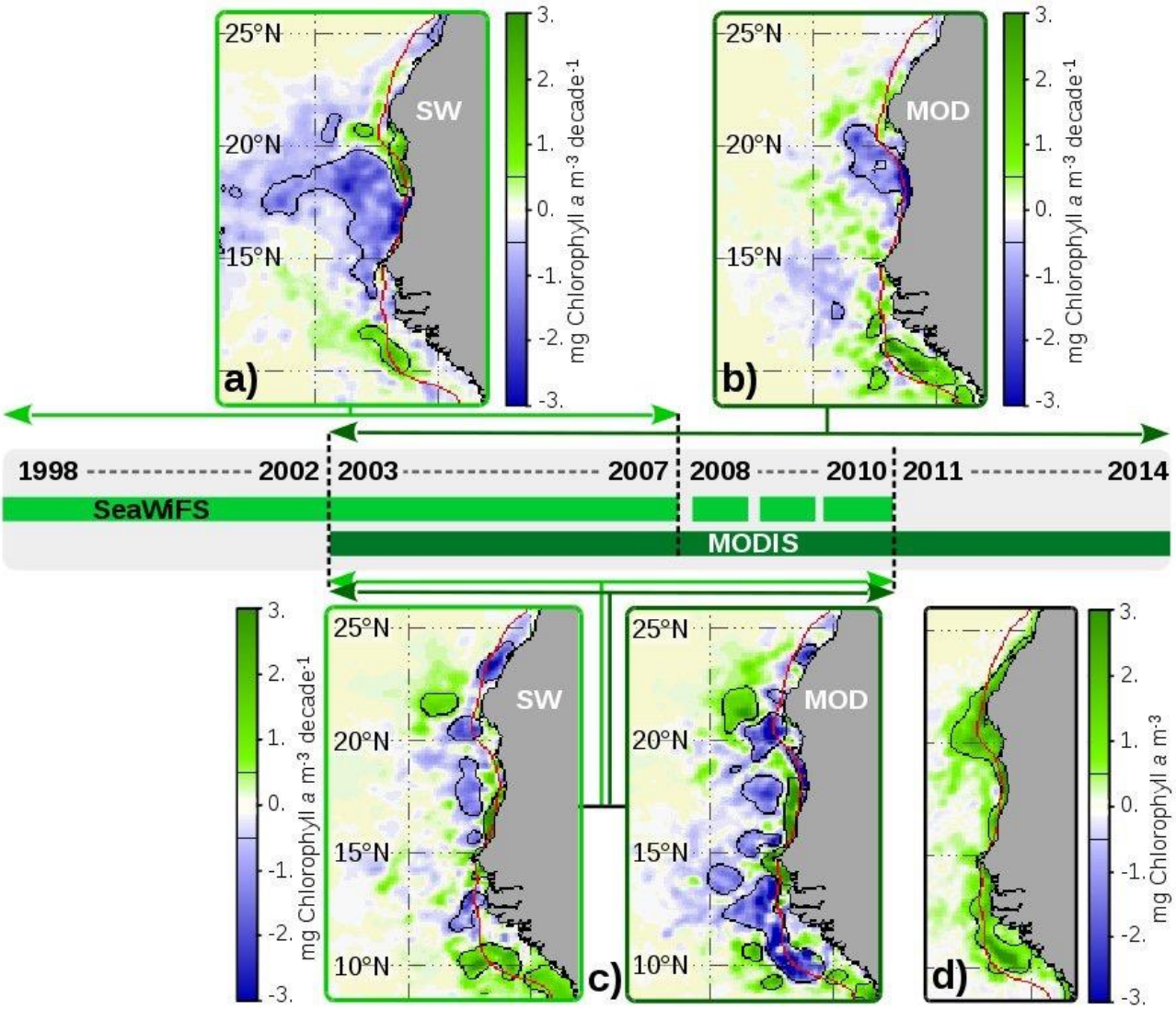

Figure 6.4.2. Partial trends computed for the region 8.5°N to 26°N from the longest homogeneous time series of a) SeaWiFS data from 1998 to 2007; b) MODIS uncorrected data from 2003 to 2014 and c) separately for the common period (2003 to 2010). All values are expressed in mg chlorophyll-a m^{-3} $decade^{-1}$. As a reference, the difference between MODIS and SeaWiFS data from 2003 to 2010 is shown (d). The 200 m isobath is superimposed.

The trends were then separately computed from 2003 to 2010 (Figure 6.4.2c) in order to test the spatial coherency between the datasets. The results show similar spatial patterns (although more contrasted from MODIS), with positive trends over the shelf and negative trends offshore between 14°N to 18°N. This spatial scheme is opposite north of 18°N. The only noticeable difference between both sensors is the large negative trend from MODIS (< -3 mg m^{-3}) over the shelf break between southern Senegal and Guinea (10°N-14°N). This difference is a likely consequence of known artifacts in the MODIS atmospheric correction that leads to incorrect values of chlorophyll-a in the most productive parts of the Senegalese upwelling region (see Figure 6.4.1a and b). Nevertheless, despite a large systematic positive bias in the MODIS data during this period (Figure 6.4.2d), the spatial coherency of these trends demonstrates the possible correction of MODIS data from a SeaWiFS referential for the computation of trends.

6.4.5. CORRECTION OF MODIS CHLOROPHYLL DATA

The monthly differences between SeaWiFS and MODIS chlorophyll-a are systematically examined for the averaged seasonal cycle of the 5-year period from 2003 to 2007 (Figure 6.4.3). It appears that the lower MODIS chlorophyll-a values (generally < 0.4 mg m^{-3}) are generally underestimated when compared to SeaWiFS, with minor seasonal differences. The negative bias of MODIS data is well known and noted by several authors (e.g. Gregg and Casey, 2010) who reported a worldwide difference between sensors of 12.2% during the 1988-2007 period. This difference produces a trend of -15%, instead of -2.6% with SeaWiFS data only.

On the contrary, high values (mostly > 1 mg m^{-3}) were systematically and substantially overestimated in the CCLME. As previously shown, this later part of the correction is of primary importance in upwelling regions where chlorophyll-a values are almost always higher than 1 mg m^{-3} (see Figure 6.4.1). The amplitude of the correction commonly reaches 80% to 120% for chlorophyll-a values higher than 10 mg m^{-3}, again with noticeable seasonal differences, probably caused of variations in the atmosphere and type of aerosols.

After application of the averaged monthly adjustments for the period 2003-2007, the global performance of the correction is estimated for the coastal region of the previous test area (5°N-25°N / 15°W-18°W), where all high chlorophyll-a values are found (see Figure 6.3.1c). The results, summarized in Table 6.4.2, show firstly that the average bias (last line of the table) of the corrected data is close to zero for the whole area and close to 0.01 mg m^{-3} for the coastal region, and secondly that these differences are relatively stable from year to year. The left part of the table shows the differences without MODIS adjustment for comparison.

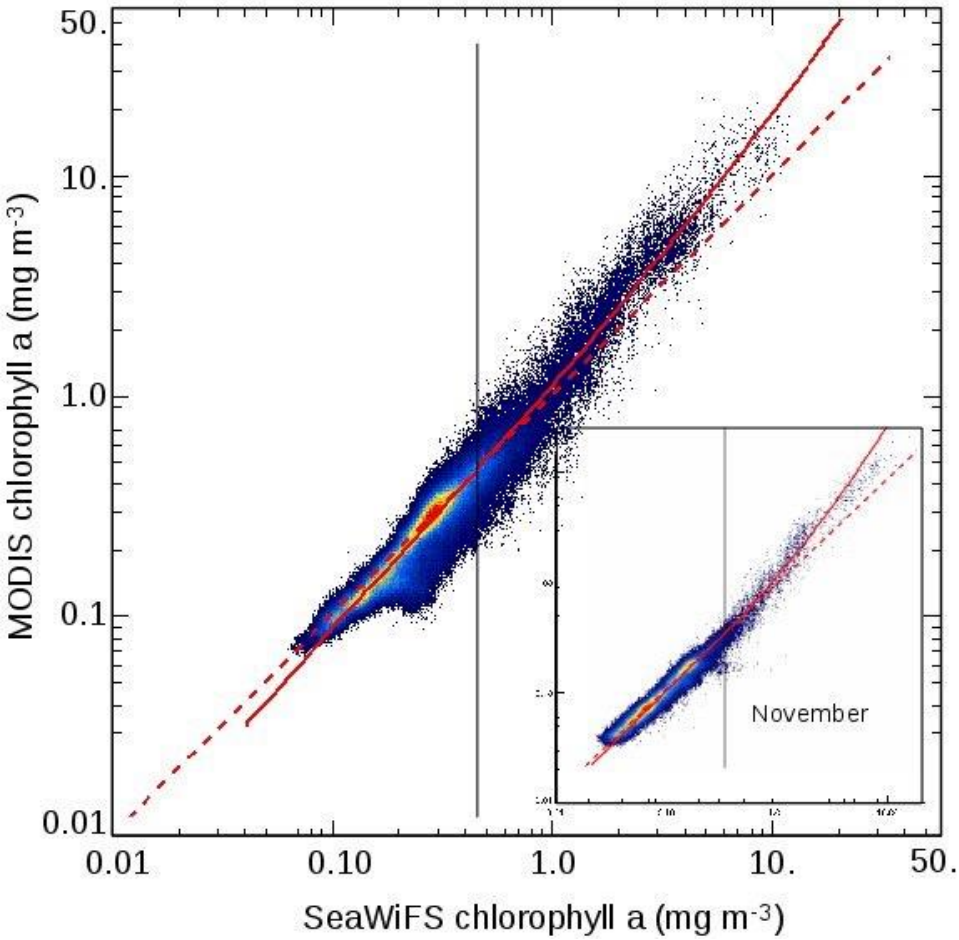

Figure 6.4.3. Example of bidimensional histogram of the MODIS and SeaWiFS chlorophyll-a data (2003-2007 average) including linear and quadratic fits (red lines, respectively for values <0.5 mg m^{-3} and above) for the month of March. The month of November (insert) is presented for comparison.

Table 6.4.2. Averaged biases in chlorophyll-a between MODIS and SeaWiFS data before (raw data) and after adjustment (corrected MODIS data) for the two areas of the Figure 6.4.1c for each year from 2003 to 2007.

Year	**raw data**		**Corrected MODIS data**	
	5-25°N	shelf only	5-25°N	shelf only
2003	0.157	0.696	-0.023	-0.027
2004	0.146	0.682	0.026	0.094
2005	0.132	0.800	-0.005	0.084
2006	0.140	0.585	-0.035	-0.246
2007	0.184	0.780	0.035	0.146
average	**0.152**	**0.709**	**-0.0004**	**0.0102**

Compared to the raw differences in chlorophyll-a between the SeaWiFS and MODIS data from 2003 to 2007 (Figure 6.4.4a), often higher than 3 mg m^{-3} (black areas on Figure 6.4.4a), the spatial structure of the residual (Figure 6.4.4b) shows only minor remaining differences of ± 0.5 mg m^{-3} and are mostly due to the spatial structure of the chlorophyll-a data rather than to the correction method itself.

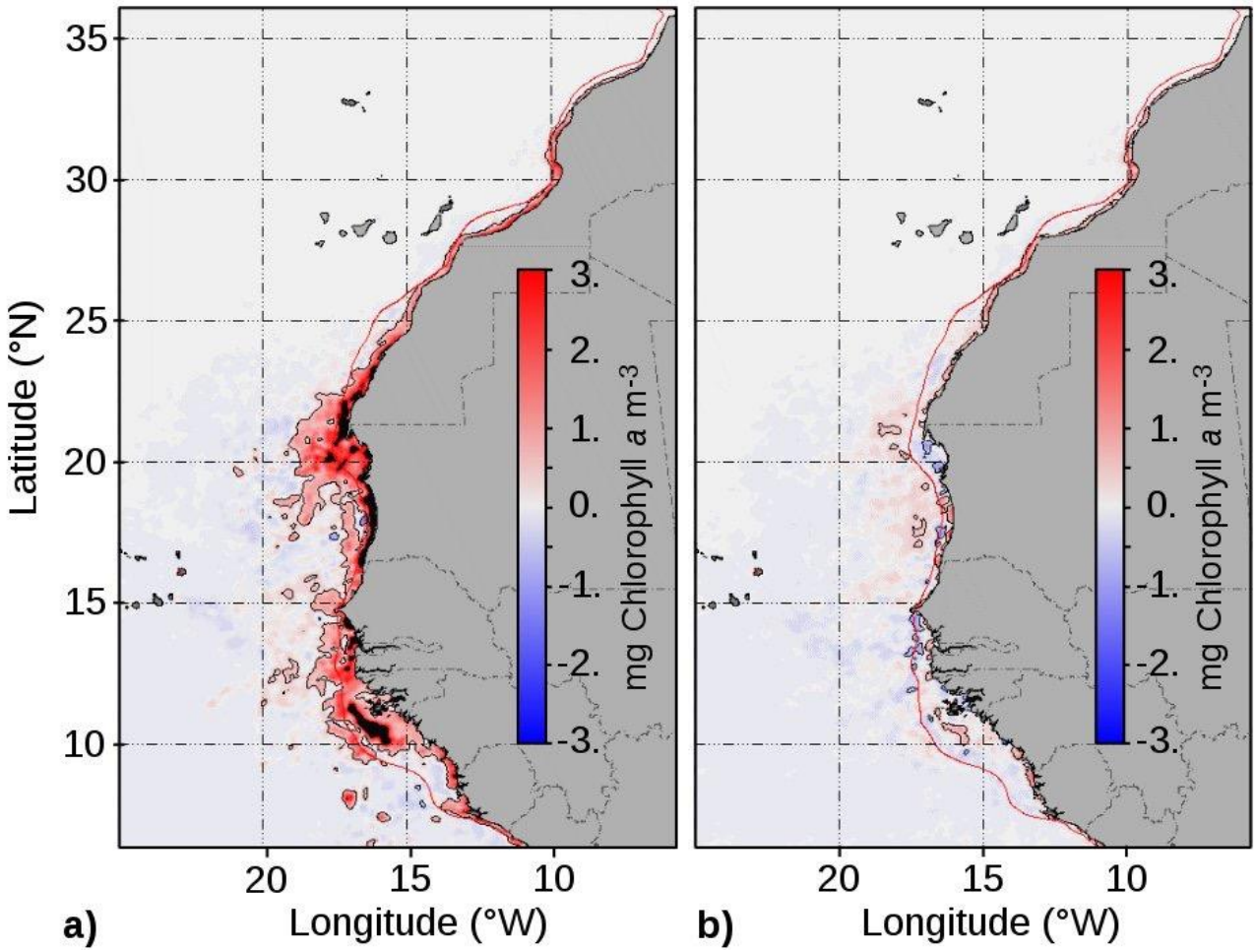

Figure 6.4.4. a) Initial differences between SeaWiFS and MODIS chlorophyll-a data for the period 2003 to 2007, b) same difference after MODIS data correction. The 200 m depth contour (red line) is superimposed.

6.4.6. RESULTING PRODUCTIVITY TRENDS FOR THE WHOLE PERIOD FROM 1998 TO 2014 AND DISCUSSION

It has been previously shown (Demarcq, 2009) that productivity in the CCLME region, computed from the 10-year time series of SeaWiFS data from 1998 to 2007 (Figure 6.4.5a) was clearly decreasing in the large central and southern parts of the system, from 12°N to 25°N, i.e. from the Canary Islands to the south of Senegal. All major anomalies (either negative or positive) were directly associated with the coastal upwelling signature, particularly over the continental shelf.

The few positive trends were mostly found between Cape Blanc (20°N) and central Mauritania (18°N, close to Nouakchott), and between 10°N and 12°N, at the southern tip of the upwelling system, an area where high values of productivity are found especially in June and July and from September to October.

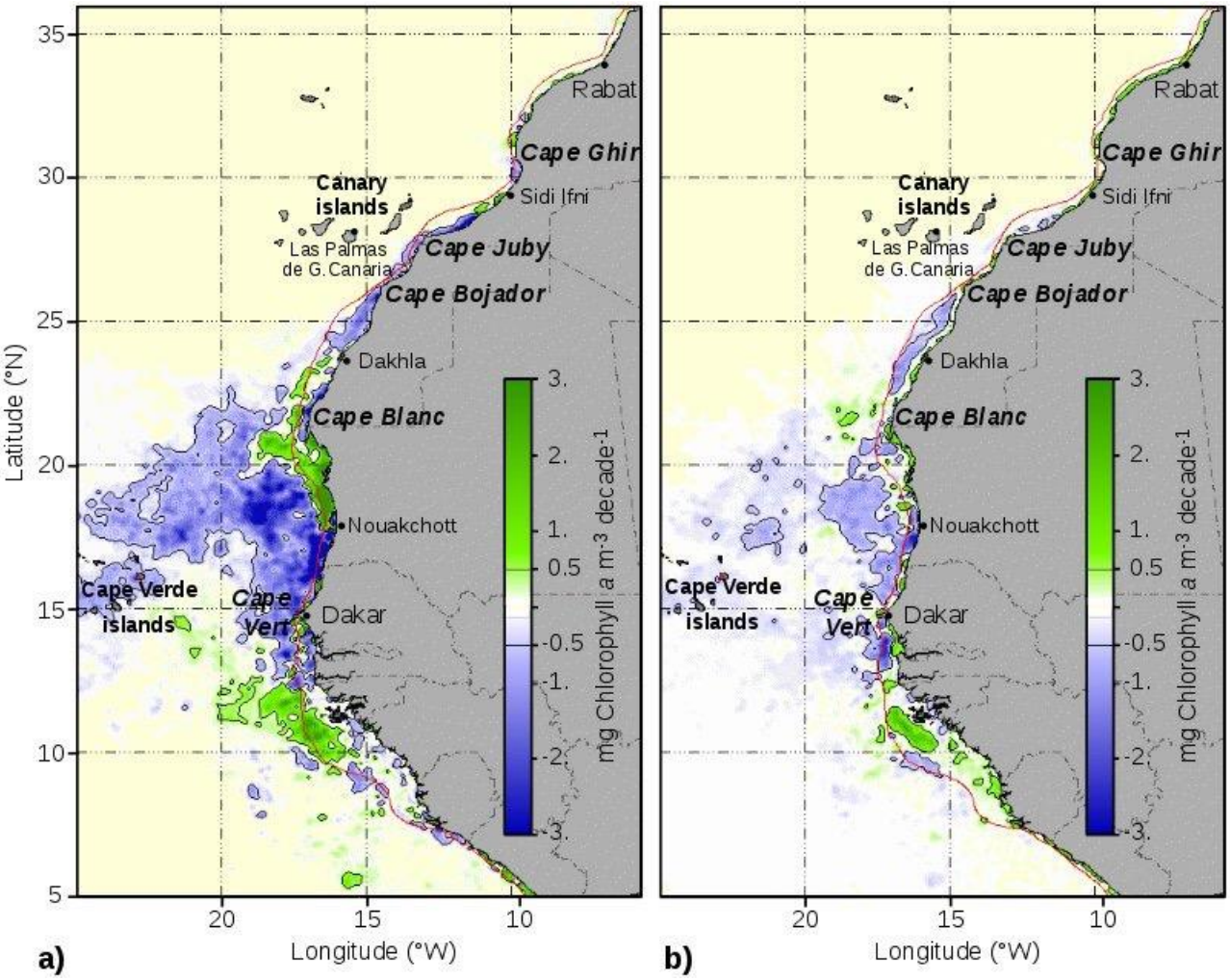

Figure 6.4.5. Trends in chlorophyll-a computed a) from SeaWiFS data from 1998 to 2003 and b) for the whole period 1998 to 2014 from the concatenation of SeaWiFS (up to 2007) and corrected MODIS data (from 2008), according to the method described in the text. Trends are expressed in mg chlorophyll-a m^{-3} $decade^{-1}$. The 200 m depth contour (red line) is superimposed.

The trends in productivity for the 17-year time series, from 1998 to 2014 (Figure 6.4.5b), have been computed from the suite of SeaWiFS data from 1998 to 2007 and MODIS data thereafter. It shows similar spatial patterns to that of the 1998-2007 period, though much less acute in the southern and seasonal part of the system, south of 22°N. The large negative trends previously found between 12°N and 25°N, are much less intense and more uniform in the coastal region, with a maximum signal over the continental shelf. The positive coastal trend found in northern Mauritania from 1998 to 2003 almost disappears, whereas the positive pattern in the extreme south still persists, with a weak extension up to Liberia. No significant trend is found between Cape Bojador and Cape Ghir (26°N-31°N) even close to the coast where upwelling occurs, except for a weak negative trend over the largest part of the continental shelf from 22°N to 26°N. On the contrary, the coastal area north of 28°N, where upwelling is at a maximum during summer, shows systematic positive trends, which progressively intensify to the north, up to the northern part of the Iberian Peninsula (not shown). It has been shown in this area that upwelling favorable winds are favored in summer because of the higher thermal contrast between sea and land (Bakun et al., 2010). The strongest continuous increase of upwelling-favorable wind in the CCLME has been observed between 26°N and 33°N (see

Benazzouz et al., 6.3 this book, Figure 6.3.3) from 1982 to 2011, and persists during the second half of this period, from 2007.

Further South, in the quasi-permanent upwelling region (21°N to 26°N), the trend or increasing winds is much weaker for the same period, except from 2006 (Benazzouz et al., 6.3 this book). This probably explains the weakening of the anomaly in this area compared to the 1998-2007 period, due to an increase in productivity during recent years. For comparison, an average increase of the productivity has been observed in all major upwelling systems from 2005 to 2007 (Demarcq, 2009), consistent with this observation in the CCLME.

The simultaneous increase in productivity extreme latitude within the CCLME (Iberian Peninsula and the region from Guinea to Sierra Leone), previously observed from 1998 to 2007, is still evident for the period 1998-2014 and reinforced in the Iberian Peninsula. This increase was attributed to a widening of the latitudinal Hadley atmospheric circulation cells, also predicted from circulation models (Kang and Lu, 2012; Seidel et al., 2008).

The same “back to normal” situation is also observed in the region of seasonal upwelling south of Cape Blanc, where winds increased again from 2005. This is likely related to the recovery of the productivity observed in this region, associated with the weaker negative trends previously observed.

A specific spatial pattern is observed off southern Senegal in the form of a marked negative anomaly south of Cap-Vert, where the coldest temperatures are recorded. This feature is either due to a local decrease in upwelling intensity or, more likely, to a change in the chlorophyll gradient between the SeaWiFS and MODIS chlorophyll-a products, due to known differences in atmospheric corrections that lead to more frequent erroneous reflectance values that confuse the chlorophyll-a algorithm.

It has also been shown that important dissimilarities exist between satellite-derived wind data series (Benazzouz et al., 2014a), leading to significant differences in upwelling indices and the computation of temporal trends. Such upwelling indices sometimes even disagree with SST-based indices in the CCLME region (see Benazzouz et al., 6.3 this book, Figure 6.3.5). For these reasons, the relationship between productivity and upwelling intensity must be considered with caution because of nonlinearities in the physical and biochemical processes involved.

6.4.7. CONCLUSION

Even if further efforts are required for algorithm development to ensure sensor compatibility over their entire ranges of sensitivity (and especially for high end values), empirical cross-correction of standard products, such as chlorophyll-a, is effective in the construction of longer time series of primary productivity in upwelling systems and in the CCLME in particular, in order to search for more reliable patterns of spatiotemporal variability.

The search for linear trends is always very challenging because of the temptation to systematically link them to global warming. In order to quantify temporal long terms changes, the mid-term oceanic variability associated with the Atlantic multidecadal oscillation (AMO) changes on a multi-decadal and basin scale modes should be considered as well as the North Atlantic oscillation (NAO) that controls the strength of the trade winds in the northern part of the CCLME. Consequently, the use of relatively short time series (less than 20 years) is potentially questionable.

The weakening of the trends related to primary productivity, previously observed in the CCLME region during a 10-year only period (Demarcq, 2009), is reassuring in this respect and is an important result of the present approach.

We show that the relative increase in wind from 1998 is probably responsible of the recent moderate increase in productivity in the CCLME, notwithstanding the fact that SST-based indices may contradict this conclusion.

During the last two decades, and despite global warming that has strongly affected the North-East tropical Atlantic, it is possible to state that the whole CCLME, especially the coastal upwelling region, is relatively stable in terms of primary productivity, more so than the oceanic basins, where a negative decrease if generally observed. Nevertheless, very little is known about the qualitative influences of climatic trends on the marine biodiversity of this diverse region, which is impacted more and more by pelagic fisheries.

It is therefore essential to make optimal use of the numerous time series of satellite-based observations made available over the past three decades in order to disentangle the different ways in which physical forcing influences the productivity of the different regions of the CCLME. Secondly, more effort needs to be directed at the integration of satellite data series in modeling in general, from biogeochemical to ecosystem approaches.

Acknowledgments

We are very grateful to the NASA/OBPG and their web data server (http://oceancolor.gsfc.nasa.gov/, accessed 16 May 2015) for providing the SeaWiFS and MODIS datasets used in this study.

6.5. OCEAN ACIDIFICATION IN THE CANARY CURRENT LARGE MARINE ECOSYSTEM

J. Magdalena SANTANA-CASIANO and Melchor GONZÁLEZ-DÁVILA

Instituto de Oceanografía y Cambio Global (IOCAG), Universidad de Las Palmas de Gran Canaria. Spain

6.5.1. INTRODUCTION

The pH in the open ocean decreases due to increased carbon dioxide (CO_2) concentration in the atmosphere caused by anthropogenic activities, e.g. fossil fuel burning (Orr et al., 2005; Raven et al., 2005). As CO_2 dissolves in seawater, bicarbonate (HCO_3^-) is formed, leading to increasing proton concentration and a consequent reduction in pH, a process known as ocean acidification. Consequently CO_3^{2-} concentration and the saturation states (Ω) of calcium carbonate ($CaCO_3$) minerals such as calcite ($\Omega_{calcite}$) and aragonite ($\Omega_{aragonite}$) decrease. These changes in seawater chemistry have complex direct and indirect impacts on marine organisms and ecosystems (Fabry et al., 2008; Gattuso et al., 2011). Moreover, responses to ocean acidification can interact with other stressors (increasing seawater temperature and deoxygenation) and vary over time, with some potential for organism adaptation (Secretariat of Convention on Biological Diversity, 2014). A report about the impact of ocean acidification on marine diversity (Pinnegar, 2012) indicated that possible implications of ocean acidification on the marine ecosystems are quite different and vary between species, populations and ecosystems depending in their adaptation to the new conditions (Hendriks et al., 2010; Connell et al., 2013; Turley, 2012).

To date the oceanic uptake of CO_2 after pre-industrial time has led to a reduction of the surface seawater pH by 0.1 units. This is equivalent to a 30% increase of acidity (Caldeira and Wickett, 2003). Models predict that pH will decrease by another 0.3-0.4 units, the dissolved inorganic carbon, C_T, may increase by over 12%, and the carbonate ion concentration may decrease by 60% by the end of the century (Caldeira and Wickett, 2003; Orr et al., 2005). Moreover, several studies showed that cold, deep, and upwelling regions are highly vulnerable to ocean acidification (Feely et al., 2008; Hauri et al., 2009; Gruber et al., 2012). The coastal upwelling zones represent only a minor part of the global coastal areas. However, they are a hot spot of global fishing activity. Coastal upwelling systems experience natural ranges in surface seawater CO_2 concentrations and pH that are amongst the most extreme in the ocean. CO_2 levels in surface sea water in upwelling zones can exceed 1000 µatm, and pH can drop as low as 7.6-7.7 (Feely et al., 2008).

The Canary Current Large Marine Ecosystem (CCLME) region including the adjacent waters of Cape Verde and Guinea Conakry is affected by upwelling. These regions are sites of active physical and bio-geo-chemical processes of direct relevance to the global carbon cycle (Borges et al., 2005; Monteiro, 2009). A lower ocean pH affects not only on the carbonate biochemistry, but also the chemistry of the compounds and elements present in seawater, mainly those relating to biological activity, such as nutrients and trace metals (Santana-Casiano and González-Dávila, 2011). Results can be differences in speciation (Santana-Casiano et al., 2006), solubilization (Stumm and Morgan, 1981; Liu and Millero, 2002) and also in the distribution of chemical species, favoring the free dissolved forms of metals, and exerting significant physiological, ecological and toxicological effects on organisms.

6.5.2. DATA SOURCES AND METHODS

6.5.2.1. Data sources

Monitoring and mapping changes in ocean acidification is important for understanding the biological impacts of increased concentrations of anthropogenic CO_2. To way of solving the under-sampling problem in marine carbon cycle research is achieved through the combined use of research vessels, ships of opportunity, autonomous floating systems including carbon sensors, moorings, and time series stations (Feely et al., 2010). Data used to understand trends in ocean acidification in the CCLME region are obtained through different media:

Research vessels: Time Series Stations

The ESTOC site (European station for Time series in the Ocean, the Canary Islands, 29°10'N, 15°30'W) is located approximately 100 km north of the islands of Gran Canaria and Tenerife, at a depth of 3650 m. The time series station was inaugurated in February 1994 and continued its monthly operations through to the year 2004. After 2004, the ESTOC site has been visited seasonally. This station is representative of the eastern boundary of the northeast Atlantic Ocean, in the Subtropical region. In the most eastern region of the subtropical gyre, the water masses are modified by the upwelling processes. (ESTOC website: http://estoc.plocan.eu, accessed on 20 February 2015).

Mooring: Fixed point Open Ocean Observatories

ESTOC is part of the EuroSITES network (http://www.eurosites.info/, accessed on 20 February 2015), which contributes to the global OceanSITES network and it is included in the FixO3 network (the Fixed point Open Ocean Observatory network) as a part of the European open ocean fixed point observatories. A buoy with temperature, salinity, pCO_2 and pH sensors has been deployed in ESTOC sites in 2014 in the framework of the FixO3 project.

VOS lines: Observations from a 'Voluntary Observing Ship'

Research in the CCLME region is also based on observations from "Voluntary Observing Ships" (VOS) lines across the North East Atlantic. A voluntary observing ship line, QUIMA-VOS line, was set up within the framework of the CARBOOCEAN (Marine carbon sources and sinks assessment) Project from July 2005 and the CARBOCHANGE (Changes in Carbon uptake and emission by oceans in a changing climate) Project from 2011 to 2014. The QUIMA VOS line focuses on the subtropical and tropical Atlantic measuring the upwelling at the coast of West Africa and at the equator, which is a major and climate-susceptible driver of ocean carbon dynamics. The VOS line was first developed as part of the CARBOOCEAN Project**.** CARBOOCEAN operated a CO_2 measurement network in the Atlantic Ocean that was based on the use of commercial vessels (VOS) as autonomous measurement platforms (http://www.carboocean.org/, accessed on 20 February 2015). From 2011, the VOS line was part of the CARBOCHANGE Project, a Collaborative Project funded by the European Commission's Seventh Framework Program. CARBOCHANGE investigates the ocean's quantitative role in the uptake of carbon under changing climate conditions, thereby using past and present data to infer the future condition of our ocean (http://carbochange.b.uib.no, accessed on 20 February 2015).

6.5.2.2. Methodology

pCO_2 measurements

An automated underway pCO_2 system (General Oceanic) is used to measure seawater and atmospheric xCO_2 on board the VOS. The mixing ratio of CO_2 in the atmospheric air and in the equilibrator air sample is measured using a differential, non-dispersive infra-red gas analyzer (Licor-6262 CO_2/H_2O analyzer). The samples are measured under dry conditions, and corrected for water vapor following DOE (1994). The fugacity of CO_2 (fCO_2) is derived from calculated pCO_2 values at *in situ* conditions, and corrected using the corresponding virial coefficients (DOE, 1994). The system is calibrated by measuring four different standard gases with mixing ratios of 0.0 µatm, 250 µatm, 380 µatm and 490 µatm of CO_2 in air. These calibrated standards are provided by NOAA-ESRL-GMD (National Oceanic and Atmospheric Administration-Earth System Research Laboratory-Global Monitoring Division), and they are traceable to the World Meteorological Organization (WMO) scale (http://www.esrl.noaa.gov/gmd/ccl/, accessed on 20 February 2015). Seawater from 10 m below the sea surface is pumped continuously from the ships' seawater intake to the equipment, at a flow rate of approximately 60 l min^{-1}. A SBE38 thermometer constantly monitored the seawater temperature.

pH measurements

- Potentiometric technique. A ROSS™ glass pH electrode and an Orion double junction Ag/AgCl reference electrode are used for the determination of pH_T at 25°C. The electrode is calibrated by using a Tris/HCl buffer in synthetic seawater with salinity of 35 (DOE, 1994). The standard deviation of repeated CRM (Certified Reference Material for CO_2 determinations) measurements (n = 90) is 0.003 units.

- Spectrophotometric technique. An automated system based on the spectrophotometric technique of Clayton and Byrne (1993) with m-cresol purple indicator is used (González-Dávila et al., 2003). Repeated measurements of CRMs pH_T showed a standard deviation of 0.0015 (n = 59).

In both cases, the pH is measured in the total scale ($[H^+]_T = [H^+]_F + [HSO_4^-]$, where $[H^+]_F$ is the free proton concentration) (pH_T). The obtained pH_T at 25°C, ($pH_{T,25}$) together with A_T is used to compute the pH in the total scale at *in situ* temperature conditions, $pH_{T,is}$, using the CO2sys program (Lewis and Wallace, 1998).

6.5.3. RESULTS

6.5.3.1. pH and pCO_2

The ESTOC site is a long-term time series station in the ocean with direct determinations of pH, showing that the Eastern Atlantic Ocean has undergone a decrease in $pH_{T,is}$ of -0.0019 ± 0.0003 (Figure 6.5.1). This decrease has been a consequence of the increase in the atmospheric pCO_2 that has produced a change in the seawater pCO_2 of 1.9 ± 0.3 µatm yr^{-1} (Figure 6.5.1). Over the last 15 years, surface seawater pCO_2 has increased by approx. 15-20% (Santana-Casiano et al., 2007; Bates et al., 2014). At ESTOC, the increase in surface pCO_2 is similar to the increase observed in atmospheric pCO_2 and similar to that observed at the time series stations HOT (Hawaii Ocean Time Series) and BATS (Bermuda Atlantic Time Series) (Figure 6.5.2)(e.g. González-Dávila et al., 2010; Rhein et al., 2013; Bates et al., 2014). The pCO_2 at ESTOC presents a seasonal variability of 60-70 µatm, with the minimum values (320-340 µatm) recorded in winter and maximum values (390-410 µatm) in summer. After the year 2005, winter values below 340 µatm have

never been recorded. The seasonal variability is also reflected in the pH which seasonally changes by 0.03-0.05 pH units. The lowest values of pH are observed during the winter convective mixing period, while the pH increases again during the enhanced stratification in summer until October (Santana-Casiano et al., 2007; González-Dávila et al., 2007). These rates are in line with those determined during the past three decades of seawater pCO_2 collected from shipboard underway seawater systems (Bates et al., 2014). Although ESTOC is located in an oceanic area, filaments located off Cape Ghir can reach hundreds of kilometers in extension and approach ESTOC location. Under such an event, anomalies in the chemical and biological measurements have been described (Santana-Casiano et al., 2007).

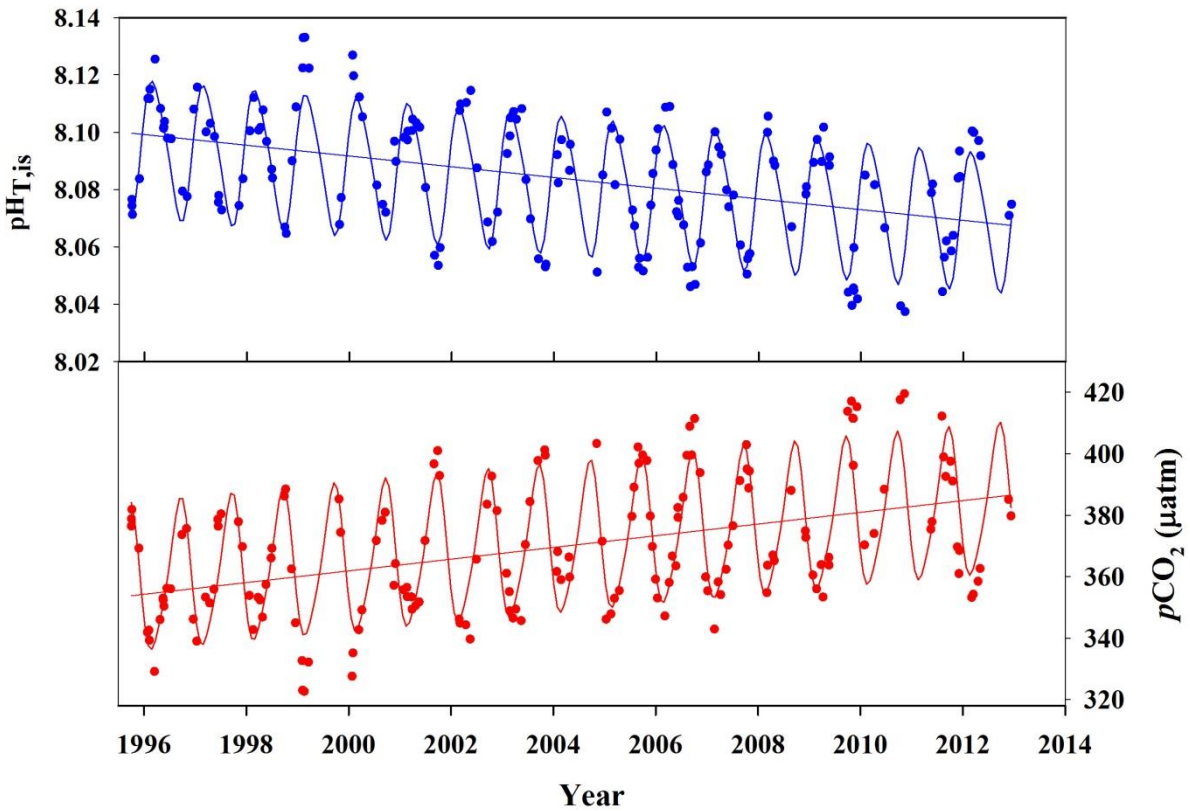

Figure 6.5.1.Time series of surface seawater *in situ* pH($pH_{T,\,is}$), and pCO_2 (µatm) at the ESTOC site.

In the closest to Africa upwelling area, inorganic carbon cycling is driven by a combination of biological and physical processes including the production and remineralization of organic carbon and biogenic carbonates, upwelling of nutrients and dissolved inorganic carbon, and water mass mixing (Borges and Frankignoulle, 2001). In the Mauritanian upwelling, the pCO_2 in seawater shows significant spatial and temporal variability dominated by the presence of the upwelling, reaching the maximum values of 900 µatm at 21°N in spring. At the same longitude but latitude of 27°N, in an area not affected by upwelling, the pCO_2 presents an annual variation similar to that found at the ESTOC site with a classical sinusoidal pattern of amplitude of 40 µatm. At 20°N, the amplitude is much higher, of the order of 150 µatm and the pCO_2 increased at a rate of 4.6 from 2005-2008 (González-Dávila et al., 2014). These high values of pCO_2 generate low values of pH in the upwelling area.

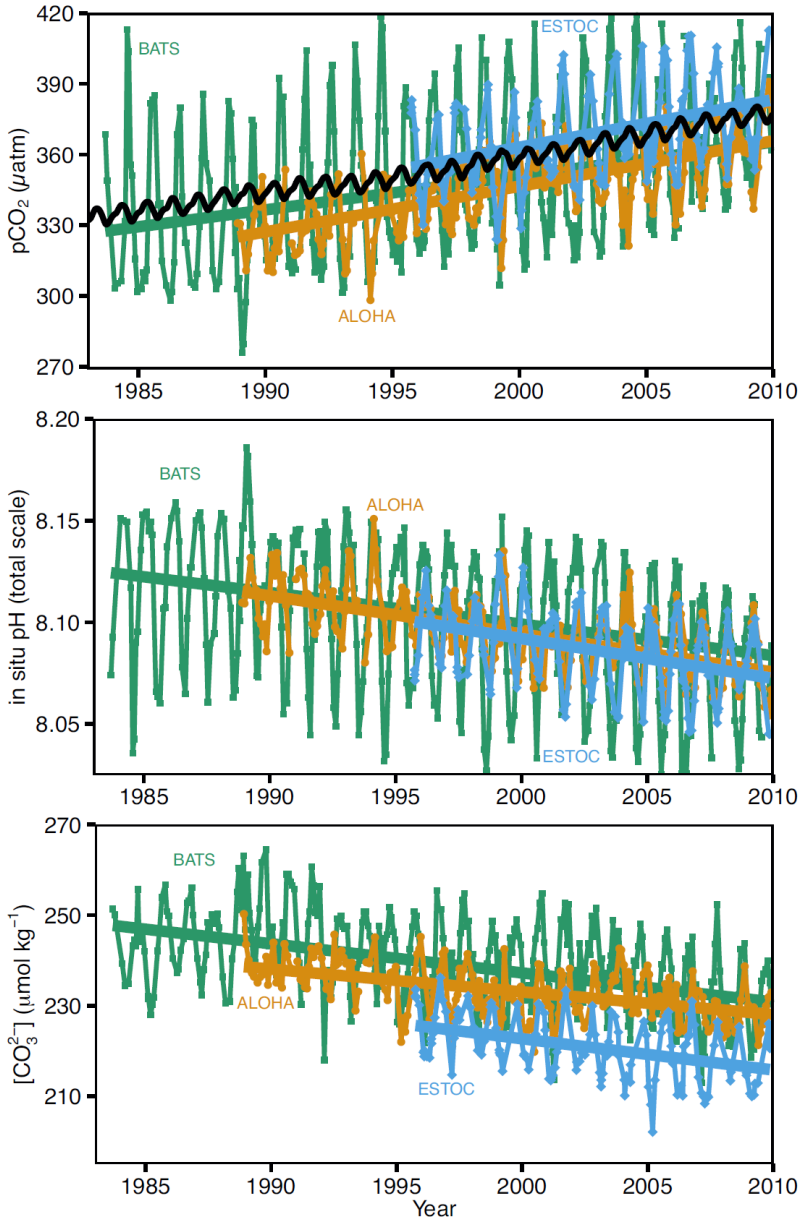

Figure 6.5.2. Long-term trends as shown in Rhein et al. (2013) of surface seawater pCO2 (top), pH (middle) and carbonate ion (bottom) concentration at (a) BATS site (31°40'N, 64°10'W; green) and Hydrostation S (32°10', 64°30'W), (b) HOT site at Station ALOHA (22°45'N, 158°00'W; orange) and (c) ESTOC (29°10'N, 15°30'W; blue). Atmospheric pCO2 (black) from the Mauna Loa Observatory Hawaii is shown in the top panel.

The effect of upwelling filaments on the CO_2 system has been studied in the area near Cape Ghir (Pelegrí et al., 2005a). Comparison of two stations, one within the Cape Ghir filament and the second one just outside of the filament, shows an increase in C_T and in pCO_2 in the former of 13 μmol kg^{-1} and 19 μatm, respectively. Moreover, increase in surface temperature, salinity and pH occur further from the upwelling region towards the open ocean. Temperature increased by 3.9°C and salinity and pH increased by about 0.2 and 0.05 units, respectively. The normalization to the average temperature for the area of 21.5°C does not remove the high variability observed. This indicates that the pCO_2 experiments a large increase in the upwelling region because of the upward pumping of subsurface CO_2 rich waters. The presence of high

normalized pCO_2 values also indicates that biological activity in the region closest to the upwelling is not long enough to overcome the CO_2 excess.

An upwelling filament off the coast of Mauritania and the Western Sahara has also been followed using drifting buoys, determining changes of carbonate chemistry over time as a result of biological, physical and chemical processes (Loucaides et al., 2012). As the plume moved offshore over a period of 9 days, biological uptake of total dissolved inorganic carbon (37 mmol kg^{-1}) reduced pCO_2 concentrations from 540 μatm to 410 μatm, thereby increasing pH from 7.94 to 8.05 and $\Omega_{Calcite}$ and $\Omega_{Aragonite}$ from 3.4 and 2.2 to 4.0 and 2.7 respectively (Loucaides et al., 2012). As this naturally acidified water ages and warms at the surface, phytoplankton blooms consume much of the C_T through photosynthesis. This leads to the rapid drawdown of CO_2 and an increase in pH in the upwelled waters (Loucaides et al., 2012).

6.5.3.2. Buffer capacity, Revelle factor and $CaCO_3$ saturation state

The consequence of the pH reduction observed at the ESTOC station, is a decrease in the buffer capacity (-1.99 ± 0.25 μmol kg^{-1} yr^{-1}), the ability of the seawater to accommodate addition of acid or base without appreciable pH change. Moreover, the Revelle factor that defines the relationship between the changes in pCO_2 (ΔpCO_2) and total dissolved inorganic carbon, C_T (ΔC_T), increases by a factor of 0.2 ± 0.002 yr^{-1}. These changes in these two parameters are followed by $CaCO_3$ dissolution. The Ω_{CaCO3} is decreasing at a rate of 0.018 ± 0.006 units yr^{-1} for calcite, and 0.012 ± 0.004 units yr^{-1} for aragonite (Santana-Casiano and González-Dávila, 2011).

6.5.4. DISCUSSION

The CCLME region covers a series of different oceanographic conditions. The area close to the continental margin is affected by coastal upwelling, whereas the area around the Canary Islands and Cape Verde are affected by the subtropical and tropical regime of the open ocean. The Canary Current is an example of the large-scale interaction between coastal upwelling and open ocean regions, being an open ocean and coastal upwelling coupled system (Pelegrí et al., 2005a). The ESTOC station is an open ocean station representative of the eastern part of the subtropical gyre. Most of the seasonal variability in pCO_2 is explained by the thermodynamic effect of changes in temperature, but in some occasions, it is influenced by upwelling conditions (Santana-Casiano et al., 2007). Generally, the Canary region is affected by the filaments generated in the upwelling zone, south of the islands (Pelegrí et al., 2005a).

The seasonal pCO_2 variability observed in the Mauritanian upwelling area is highly correlated with the upwelling index and it is higher than that observed at the ESTOC site. North of 20°N, the upwelling conditions are favorable throughout the year with the highest upwelling conditions from March to September. This area is characterized by an enrichment of CO_2 in the surface waters. South of 20°N, a marked seasonality is produced, with an important upwelling in winter. South of 15°N, in the Cape Verde area, upwelling conditions are favorable during autumn and winter, being the maximum intensity observed during January and February. This area is also affected by the influence of the Inter-Tropical Convergence Zone (ITCZ), related to maximum precipitation rates that reach north of 10°N from late spring to late summer. As a consequence, a high variability has been observed in the pCO_2. These changes directly affect the decrease in pH (González-Dávila et al., 2014). In the western North Atlantic, the CARIACO (CArbon Retention In a Colored Ocean) site is the only time series station affected by an upwelling process (Taylor et al., 2012; Bates et al., 2014) and it has been selected as a model of an upwelling affected area to explain

the dynamic of CO_2 in an upwelling area. The trends in CARIACO showed a rate of increase of pCO_2 of 2.95 ± 0.43 µatm yr^{-1} and a decrease of pH of -0.0025 ± 0.0004 units of pH yr^{-1}. This is explained by the upwelling of Subtropical Underwater (Taylor et al., 2012). It should be observed that in the Mauritanian area, the pCO_2 has increased at a rate of 4.6 µatm yr^{-1} from 2005 to 2008 (González-Dávila et al., 2014), showing values higher than in the ESTOC or the CARIACO sites, indicating that the decrease in pH here must be even higher than in the previously mentioned stations.

6.5.5. CONCLUSIONS AND RECOMMENDATIONS

The uptake of anthropogenic CO_2 by the ocean and its effect on ocean acidification is being studied through the systematic collection of time-series observations that allow us to know the trends in the carbon system parameters and to quantify the uncertainties in physico-biogeochemical feedbacks in the atmosphere-ocean system. These measurements are required to improve predictions on future CO_2 emissions and the effects of ocean acidification on both the biogeochemical processes and the ecosystems. Bates et al. (2014) reviewed the rates of changes in surface seawater CO_2-carbonate chemistry at seven ocean CO_2 time-series, compiling sustained observations for more than fifteen years, being ESTOC (González-Dávila et al., 2010) one of them. According to these studies, the surface seawater pH has declined in the ocean at rates of -0.0013 yr^{-1} to -0.0025 yr^{-1}. However, there is lacking pH and pCO_2 data to cover the entire CCLME region, in particular the upwelling area. Due to the heterogeneity of this area which evolves from the open ocean to an upwelling coastal margin, it is not possible to generalize the results. From the scarce information available nowadays for upwelling regions, it is known that the pH of surface waters in these areas is lower than in other oceanic regions. However, the rate of decrease of pH in the upwelling areas is the result of complex processes determined by the intensity of the upwelling that can be modified by the variations in oceanographic conditions as a consequence of climate change.

Acknowledgements

This work has been supported by the European Project CARBOCHANGE (264879).

BIBLIOGRAPHY

Abele, L. G. 1982. Biogeography. In: *The biology of Crustacea*, Vol. 1. Bliss, E. (ed.). Academic Press, London, pp. 242-304.

Acosta, J. et al. 2003a. Salt diapirs, salt brine seeps, pockmarks and surficial sediment creep and slides in the Canary Channel off NW Africa. *Marine Geophysical Researches*, Vol. 24, pp. 41-57.

Acosta, J., Uchupi, E., Muñoz, A., Herranz, P., Palomo, C., Ballesteros, M. and EEZ working group. 2003b. Geologic evolution of the Canary Islands of Lanzarote, Fuerteventura, Gran Canaria and La Gomera and comparison of landslides at these islands with those at Tenerife, La Palma and El Hierro. *Marine Geophysical Researches,* Vol. 24, pp. 1-40.

Agawin, N. S. R., Tovar-Sánchez, A., de Zarruk, K. K., Duarte, C. M. and Agustí, S. 2013. Variability in the abundance of *Trichodesmium* and nitrogen fixation activities in the subtropical NE Atlantic. *Journal of Plankton Research*, Vol. 35, pp. 1126-1140. doi:10.1093/plankt/fbt059.

Agusti, S. 1991. Light environment within dense algal populations: cell size influences on self-shading. *Journal of Plankton Research*, Vol. 13 (4), pp. 863–871.

Aiken, J., Pradhan, Y., Barlow, R., Lavender, S., Poulton, A., Holligan, P. and Hardman-Mountford, N. 2009. Phytoplankton pigments and functional types in the Atlantic Ocean: A decadal assessment, 1995–2005. *Deep-Sea Research Part II: Topical Studies in Oceanography*, Vol. 56 (15), pp. 899–917. doi:10.1016/j.dsr2.2008.09.017.

Akallal, R., Billard, C., Fresnel, J., Givernaud, T. and Mouradi, A. 2002. Contribution á l'étude du phytoplancton de la côte atlantique marocaine. II. Le genre *Pseudo-nitzschia* (Bacillariophyceae). *Crytogamie Algologie*, Vol. 23, pp. 187-202.

Aksissou, M., Tiwari, M., Benhardouze, W. and Godfrey, M. H. 2006. The status of marine turtles in Atlantic Morocco. In: *Book of Abstracts. Twenty Sixth Annual Symposium on Sea Turtle Biology and Conservation.* Frick, M., Panagopoulou, A., Rees, A. F. and Williams, K. (compilers). International Sea Turtle Society, Athens, Greece, pp. 121.

Alfonso, M., Lopez, J. D., Alvarez, E. and Ruiz, M. I. 2005. Real time buoy data quality control and exploitation. *The Fifth COPRI International Conference on ocean Wave Measurement and Analysis (WAVES).* Coasts, Oceans, Ports, and Rivers Institute, American Society of Civil Engineers, Madrid.

Ali, M. Y., Watts, A. B. and Hill, I. 2003. A seismic reflection profile study of lithospheric flexure in the vicinity of the Cape Verde Islands. *Journal of Geophysical Research,* Vol. 108, pp. 329-343.

Allison, E. H. et al. 2009. Vulnerability of national economies to the impacts of climate change on fisheries. *Fish and Fisheries*, Vol. 10, pp. 173–196.

Almeida, R. and Leary, R. 2011. Corals of the Cape Verde Islands. www.umassd.edu/specialprograms/ caboverde/corals.htm (Accessed 8 April 2015).

Alonso-González, I. J., Arístegui, J., Vilas, J. C. and Hernández-Guerra, A. 2009. Lateral POC transport and consumption in surface and deep waters of the Canary Current region: A box model study. *Global Biogeochemical Cycles*, Vol. 23, GB2007.doi: 10.1029/2008GB003185.

Alonso-González, I. J., Arístegui, J., Lee, C., Sánchez-Vidal, A., Calafat, A., Fabrés, J., Sangrà, P., Masqué, P., Hernández-Guerra, A. and Benítez-Barrios, V. 2010a. Role of slowly settling particles in the ocean carbon cycle. *Geophysical Research Letters*, Vol. 37, L13608.doi:10.1029/2010GL04382.

Alonso-González, I. J., Arístegui, J., Lee, C. and Calafat, A. 2010b. Regional and temporal variability of sinking organic matter in the subtropical northeast Atlantic Ocean: a biomarker diagnosis. *Biogeosciences*, Vol. 7, pp. 2101–2115.

Alonso-González, I., Arístegui, J., Lee, C., Sánchez-Vidal, A., Calafat, A., Fabrés, J., Sangrà, P. and Mason, E. 2013. Carbon dynamics within cyclonic eddies: insights from a biomarker study. *PLoS ONE*, Vol. 8, No. 12, e82447. doi:10:10.1371/journal.pone.0082447.

Alvain, S., Moulin, C., Dandonneau, Y. and Loisel, H. 2008. Seasonal distribution and succession of dominant phytoplankton groups in the global ocean: A satellite view. *Global Biogeochemical Cycles*, Vol. 22: 15 pp. doi:200810.1029/2007GB003154.

Alvarez, I., Gomez-Gesteira, M., deCastro, M. and Dias, J. M. 2008. Spatiotemporal evolution of upwelling regime along the western coast of the Iberian Peninsula. *Journal of Geophysical Research: Oceans*, Vol. 113 (C7), pp. C07020. doi:10.1029/2008JC004744.

Álvarez-Fanjul, E., Pérez-Gómez, B. and Rodríguez, I. 2001. Nivmar: a storm surge forecasting system for Spanish waters. *Scientia Marina*, Vol. 65, pp. 203-212.

Álvarez-Fanjul, E., Alfonso, M., Ruiz, M. I., Lopez, J. D. and Rodriguez, I. 2002. Real Time Monitoring of Spanish coastal waters: The Deep Water Network. *Proceedings of the Third International Conference on EuroGOOS*. Athens, Greece.

Álvarez-Salgado, X. A., Arístegui, J., Barton, E. D. and Hansell, D. A. 2007. Contribution of upwelling filaments to offshore carbon export in the subtropical Northeast Atlantic Ocean. *Limnology and Oceanography*, Vol. 52, pp. 1287–1292.

Amaral, A. R., Beheregaray, L. B., Sequeira, M., Robertson, K. M., Coelho, M. M. and Möller, L. M. 2009. Worldwide phylogeography of the genus *Delphinus* revisited. International Whaling Commission. Scientific Committee Document SC/61/SM11.

Anadón, R. 1981. Crustáceos Decápodos (excl. Paguridea) recogidos durante la campaña "Atlor VII" en las costas noroccidentales de África (Noviembre 1975). *Resultados de Expediciones Científicas (suplemento de Investigación Pesquera)*, Vol. 9, pp. 151-159.

Ancochea, E. and Huertas, M. J. 2003. Age and composition of the Amanay seamount (Canary Islands). *Marine Geophysics Research*, Vol. 24, pp. 161-169.

Ancochea, E. et al. 2004. *Geología de España.*, Ed. Vera.

Ancochea, E., Huertas, M. J., Hernán, F. and Brändle, J. L. 2010. Volcanic evolution of São Vicente, Cape Verde Islands: the Praia Grande landslide. *Journal of Volcanological and Geothermal Research*, Vol. 198, pp. 143-157.

Anderson, L. A. 1995. On the hydrogen and oxygen content of marine phytoplankton. *Deep-Sea Research Part I: Oceanographic Research Papers*, Vol. 42, pp. 1675–1680.

Anguita, F. and Hernan, F. 2000. The Canary Islands origin: a unifying model. *Journal of Volcanological and Geothermal Research,* Vol. 103, pp. 1-26.

Antobrech, A. A. and Krastel, S. 2006. Morphology, seismic characteristics and development of Cap Timiris Canyon, offshore Mauritania: A newly discovered canyon preserved-off a mayor arid climatic region. *Marine and Petroleum Geology*, Vol. 23, pp. 37-59.

Antobrech, A. A. and Krastel, S. 2007. Mauritania Slide Complex: morphology, seismic characterisation and processes of formation. *International Journal Earth Science*, Vol. 96, pp. 451-472.

Antoine, D., Morel, A., Gordon, H. R., Banzon, V. F. and Evans, R. H. 2005. Bridging ocean color observations of the 1980s and 2000s in search of long-term trends. *Journal of Geophysical Research*, Vol. 110, pp. C06009. doi:10.1029/2004JC002620.

Arhan, M., de Verdière, A. C. and Mémery, L. 1994. The eastern boundary of the subtropical North Atlantic. *Journal of Physical Oceanography*, Vol. 24, pp. 1295-1316.

Arimoto, R. 2001. Eolian dust and climate: relationships to sources, tropospheric chemistry, transport and deposition. *Earth Science Reviews*, Vol. 54, pp. 29-42. doi: 10.1016/S0012-8252(01)00040-X.

Arístegui, J., Sangrà, P., Hernández-León, S., Cantón, M., Hernández-Guerra, A. and Kerling, J. 1994. Island-induced eddies in the Canary Islands. *Deep-Sea Research Part I: Oceanographic Research Papers*, Vol. 41, pp. 1509–1525.

Arístegui, J. et al. 1997. The influence of island-generated eddies on chlorophyll distribution: a study of mesoscale variation around Gran Canaria. *Deep-Sea Research Part I: Oceanographic Research Papers*, Vol. 44, pp. 71–96.

Arístegui, J., Barton, E. D., Tett, P., Montero, M. F., García-Muñoz, M., Basterretxea, G., Cussatlegras, A. -S., Ojeda, A. and de Armas, D. 2004. Variability in plankton community structure, metabolism, and vertical carbon fluxes along an upwelling filament (Cape Juby, NW Africa). *Progress in Oceanography*, Vol. 62 (2–4), pp. 95–113. doi:10.1016/j.pocean.2004.07.004.

Arístegui, J. and Montero, M. F. 2005. Temporal and spatial changes in plankton respiration and biomass in the Canary Islands region: the

effect of mesoscale variability. *Journal of Marine Systems*, Vol. 54, pp. 65– 82.

Arístegui, J., Álvarez-Salgado, X. A., Barton, E. D., Figueiras, F. G., Hernández-León, S., Roy, C. and Santos, A. M. P. 2006. Oceanography and fisheries of the Canary Current/Iberian region of the Eastern North Atlantic (18a,E). In: *The Sea: The Global Coastal Ocean: Interdisciplinary Regional Studies and Syntheses*, Vol. 14B. Robinson, A. R. and Brink, K. H. (eds). Harvard University Press, pp. 877–931.

Arístegui, J. et al. 2009a. Sub-regional ecosystem variability in the Canary Current upwelling. *Progress in Oceanography*, Vol. 83 (1-4), pp. 33–48. doi:10.1016/j.pocean.2009.07.031.

Arístegui, J., Mendonca, A., Vilas, J. C., Espino, M., Polo, I., Montero, M. F. and Martins A. 2009b. Plankton metabolic balance at two north Atlantic seamounts. *Deep-Sea Research Part II: Topical Studies in Oceanography*, Vol. 56, pp. 2646–2655.

Arkhipkin, A. and Laptikhovsky, V. 2006. Allopatric speciation of the teuthid fauna on the shelf and slope of Northwest Africa. *Acta Universitatis Carolinae - Geologica*, Vol. 49, pp. 15-19.

Armstrong, R. A., Lee, C., Hedges, J. I., Honjo, S. and Wakeham, S. G. 2002. A new, mechanistic model for organic carbon fluxes in the ocean based on the quantitative association of POC with ballast minerals. *Deep-Sea Research Part II: Topical Studies in Oceanography*, Vol. 49, pp. 219–236.

Atlas, R., Hoffman, R. N., Ardizzone, J., Leidner, S. M., Jusem, J. C., Smith, D. K. and Gombos, D. 2010. A Cross-calibrated, Multiplatform Ocean Surface Wind Velocity Product for Meteorological and Oceanographic Applications. *Bulletin of the American Meteorological Society*, Vol. 92 (2), pp. 157–174. doi:10.1175/2010BAMS2946.1.

Aviso-CLS. 2014. *User Handbook Ssalto/ Duacs: M(SLA) and M(ADT) Near-Real Time and Delayed-Time Products*, SALP-MU-P-EA-21065-CLS. Edition 4.2, November 2014.

Ayissi, I., Segniagbeto, G. H. and Van Waerebeek, K. 2014. Rediscovery of Cameroon Dolphin, the Gulf of Guinea population of *Sousa teuszii* (Kükenthal, 1892). *ISRN Biodiversity,* Vol. 2014, pp. 1-6. doi: 10.1155./2014/819827.

Baker, A. R., Kelly, S. D. B. K. F., Witt, M. and Jickells, T. D. 2003. Atmospheric deposition of nutrients to the Atlantic Ocean. *Geophysical Research Letters*, Vol. 30, 2296. doi: 10.1029/2003GL018518.

Baker, A. R., Lesworth, T., Adams, C., Jickells, T. D. and Ganzeveld, L. 2010. Estimation of atmospheric nutrient inputs to the Atlantic Ocean from 50°N to 50°S based on large-scale field sampling: Fixed nitrogen and dry deposition of phosphorus. *Global Biogeochemical Cycles*, Vol. 24, GB3006. doi:10.1029/2009GB003634.

Baker, A. R., Adams, C., Bell, T. G., Jickells, T. D. and Ganzeveld, L. 2013. Estimation of atmospheric nutrient inputs to the Atlantic Ocean from 50°N to 50°S based on large-scale field sampling: Iron and other dust-associated elements. *Global Biogeochemical Cycles,* Vol. 27, pp. 755-767. doi:10.1002/gbc.20062.

Bakun, A. 1973. *Coastal upwelling indices, west coast of North America, 1946–1971*. NOAA Technical Report NMFS–SSRF–671: 103 pp., U.S. Department of Commerce, National Marine Fisheries Service, Seattle.

Bakun, A. 1990. Global climate change and intensification of coastal ocean upwelling. *Science,* Vol. 247 (4939), pp. 198-201. doi:10.1126/science.247.4939.198.

Bakun, A. 1996. *Patterns in the ocean: ocean processes and marine population dynamics*. California Sea Grant College System, National Oceanic and Atmospheric Administration, in cooperation with Centro de Investigaciones Biológicas del Noroeste, pp. 1996 - 323.

Bakun, A., Field, D. B., Redondo-Rodriguez, A. and Weeks, S. J. 2010. Greenhouse gas, upwelling-favorable winds, and the future of coastal ocean upwelling ecosystems. *Global Change Biology,* Vol. 16 (4), pp. 1213–1228. doi:10.1111/j.1365-2486.2009.02094.x.

Balguerías, E., Quintero, M. E. and Hernández-González, C. 2000. The origin of the Saharan Bank cephalopod fishery. *ICES Journal Marine Science*, Vol. 57, pp. 15-23.

Balguerías, E., Hernández-González, C. and Perales-Raya, C. 2002. On the identity of *Octopus vulgaris* Cuvier, 1797 stocks in the Saharan Bank (Northwest Africa) and their spatio-temporal variations in abundance in relation to some environmental factors. *Bulletin of Marine Science*, Vol. 71 (1), pp. 147-163.

Bamy, I. L. 2011. *Inventaire des cétacés dans la zone des Iles Tristao*. Projet de Gestion Côtière et Marine de la Biodiversité. Ministère de la Pêche et de l'Aquaculture, Conakry, Guinée: 28 pp.

Bamy, I. L., Van Waerebeek, K., Bah, S. S., Dia, M., Kaba, B., Keita, N. and Konate, S. 2010. Species occurrence of cetaceans in Guinea, including humpback whales with southern hemisphere seasonality. *Marine Biodiversity Records,* Vol. 3, e48, pp. 1-10. doi: 10.1017/ S1755267210000436.

Banda, E., Danobeitia, J. J., Surinach, E. and Ansorge, J. 1981. Features of crustal structure under the Canary Islands. *Earth and Planetary Science Letters*, Vol. 55, pp. 11-22.

Barber, R. and Smith, R. L. 1981. Coastal upwelling ecosystems. *Analysis of Marine ecosystems/AR Longhurst*, pp. 31–68.

Barbosa, C., Broderick, A. C. and Catry, P. 1998. Marine turtles in the Orango National Park (Bijago´s Archipelago, Guinea Bissau). *Marine Turtle Newsletter*, Vol. 81, pp. 6–7.

Barker, A. K., Holm, P. M., Peate, D. W. and Baker, J. A. 2009. A 5 million year records of compositional variations in mantle sources to magmatism on Santiago, southern Cape Verde archipelago. *Contributions to Mineralogy and Petrology,* Vol. 50, pp. 169-193.

Barton, E. D. 1989. The poleward undercurrent on the eastern boundary of the Subtropical North Atlantic. In: *Poleward flows along Eastern Ocean Boundaries.* Neshyba, S., Smith, R. L. and Mooers, C. N. K. (eds). Springer-Verlag Lecture Note Series, pp. 82-95.

Barton, E. D. 1998. Eastern boundary of the North Atlantic: Northwest Africa and Iberia. Coastal segment (18, E). In: *The Sea*, Vol. 11. Robinson, A. R. and Brink, K. H. (eds). John Wiley and Sons Inc., New York, pp. 633– 657.

Barton, E. D. et al. 1998. The transition zone of the Canary Current upwelling region. *Progress in Oceanography*, Vol. 41, pp. 455– 504. doi:10.1016/S0079-6611(98)00023-8.

Barton, E. D., Basterretxea, G., Flament, P., Mitchelson-Jacob, E. G., Jones, B., Arístegui, J. and Felix, H. 2000. Lee region of Gran Canaria. *Journal of Geophysical Research*, Vol. 105, pp. 17173–17193.

Barton, E.D, Arístegui, J., Tett, P. and Navarro-Pérez, E. 2004. Variability in the Canary Islands area of filament-eddy exchanges. *Progress in Oceanography*, Vol. 62, pp. 71-94.

Barton, E. D., Field, D. B. and Roy, C. 2013. Canary current upwelling: More or less? *Progress in Oceanography*, Vol. 116, pp. 167-178. doi:10.1016/j.pocean.2013.07.007.

Basart, S., Pérez, C., Cuevas, E., Baldasano, J. M. and Gobbi, G. P. 2009. Aerosol characterization in Northern Africa, Northeastern Atlantic, Mediterranean Basin and Middle East from direct-sun AERONET observations. *Atmospheric Chemistry and Physics,* Vol. 9, pp. 8265–8282.

Bast, D., Lambert, K., Richer de Forges, B. and Weiss, R. 1984. Etude des principales espèces de crevettes des eaux mauritaniennes (N/R « Eisbar » mars 1984). *Bulletin du Centre National de Recherches Océanographiques et des Pêches*, Vol. 12 (11), pp. 149-163.

Basterretxea, G. and Arístegui, J. 2000. Mesoscale variability in phytoplankton biomass distribution and photosynthetic parameters in the Canary-NW African coastal transition zone. *Marine Ecology Progress Series*, Vol. 197, pp. 27–40.

Bate, C. 1888. Report on the Crustacea Macrura collected by the Challenger during the years 1873-76. Report on the Scientific Results of the Voyage of H.M.S. "Challenger" during the years 1873-7, Vol. 24, No. 52, pp. i-xc and 1-942.

Bates, N., Astor, Y. M., Church, M. W. J., Currie, K., Dore, J. E., González-Dávila, M., Lorenzoni, L., Muller-Karger, F., Olafsson, J. and Santana-Casiano J. M. 2014. Time-Series view of changing surface ocean chemistry due to ocean uptake of anthropogenic CO_2 and ocean acidification. *Oceanography*, Vol. 27 (1), pp. 94-107.

Bauer, E. and Siedler, G. 1988. The relative contributions of advection and diapycnal mixing below the sub-tropical salinity maximum. *Deep-Sea Research A. Oceanographic Research Papers*, Vol. 35, pp. 811-837.

Bauer, J. and Druffel, E. 1998. Ocean margins as a significant source of organic matter to the deep open ocean. *Nature*, Vol. 392, pp. 482-485.

Bayed, A. and Beaubrun, P. C. 1987. Les mammifères marins du Maroc: inventaire préliminaire. *Mammalia*, Vol. 54, pp. 162-164.

Bearman, P. W. 1984. Vortex shedding from oscillating bluff bodies. *Annual Review of Fluids Mechanics,* Vol.16, pp. 195-222.

Bebiano, J. B. 1932. A geologia do Arquipélago de Cabo Verde. *Comunicação do Serviço Geológico de Portugal,* Vol. 18, pp. 1-275.

Becker, J. J. et al. 2009. Global Bathymetry and Elevation Data at 30 Arc Seconds Resolution: SRTM30_PLUS. *Marine Geodesy*, Vol. 32 (4), pp. 355-371. doi: 10.1080/01490410903297766.

Bécognée, P., Moyano, M., Almeida, C., Rodríguez, J. M., Fraile-Nuez, E., Hernández-Guerra, A. and Hernández-León, S. 2009. Mesoscale distribution of clupeoid larvae in an upwelling filament trapped by a quasi-permanent cyclonic eddy off Northwest Africa. *Deep-Sea Research Part I: Oceanographic Research Papers*, Vol. 56 (3), pp. 330–343.

Behrenfeld, M. J. and Falkowski, P. G. 1997. Photosynthetic Rates Derived from Satellite-Based Chlorophyll Concentration. *Limnology and Oceanography*, Vol. 42 (1), pp. 1–20.

Behrenfeld, M. J. et al. 2006. Climate-driven trends in contemporary ocean productivity. *Nature*, Vol. 444 (7120), pp. 752–755.

Belloc, G. 1933. Pêche au chalut. Les fonds chalutables de la côte occidentale d'Afrique (du Cap Vert au Cap Spartel). *Revue des Travaux de l'Office des Pêches Maritimes*, Vol. 6, Fasc. 2, No. 22, pp. 141-196.

Belloc, G. 1938. Liste des poissons pélagiques et bathypélagiques capturés au cours de la cinquième croisière avec diagnose préliminaire de deux espèces nouvelles. *Ibid,* Vol. 11 (3), pp. 281-313.

Ben-Ami, Y., Koren, I., Altaratz, O., Kostinski, A. B. and Lehahn, Y. 2012. Discernible rhythm in the spatio/temporal distributions of transatlantic dust. *Atmospheric Chemistry and Physics,* Vol. 12, pp. 2253-2262. doi:10.5194/acp-12-2253-2012.

Benavides, M., Agawin, N. S. R., Arístegui, J., Ferriol, P. and Stal, L. J. 2011. Nitrogen fixation by *Trichodesmium* and small diazotrophs in the subtropical Northeast Atlantic. *Aquatic Microbial Ecology,* Vol. 65, pp. 43-53. doi:10.3354/ame01534.

Benavides, M., Agawin, N. S. R., Arístegui, J., Cancio, J. L. and Hernández-León, S. 2013a. Short term variability of N2 fixation, *Trichodesmium* and unicellular diazotrophs related to dust deposition in the Canary Islands. *Limnology and Oceanography*, Vol. 58, pp. 267–275. doi:10.4319/lo.2913.58.1.0267.

Benavides, M., Arístegui, J., Agawin, N. S. R., Álvarez-Salgado, X. A., Álvarez, M. and Troupin, C. 2013b. Low contribution of N2 fixation to new production and excess nitrogen in the subtropical northeast Atlantic margin. *Deep-Sea Research Part I: Oceanographic Research Papers*, Vol. 81, pp. 36-48.

Benhardouze, W., Aksissou, M. and Tiwari, M. 2012. Incidental captures of sea turtles in the driftnet and longline fisheries in northwestern Morocco. *Fishery Research*, Vol. 127–128, pp. 125–132.

Benazzouz, A. 2014. *Upwelling côtier et effet de la dynamique océanique à méso-échelle sur la variabilité planctonique dans le système du Courant des Canaries*. PhD Thesis, Faculty of Science Ben M'Sik, University Hassan II Mohammedia-Casablanca: 261pp.

Benazzouz, A. et al. 2013. Changement à long terme et tendance de l'activité de l'upwelling du système du courant des Canaries à partir de l'imagerie satellite. *GeoObservateur*, Vol. 21: 21 pp.

Benazzouz, A., Mordane, S., Orbi, A., Chagdali, M., Hilmi, K., Atillah, A., Pelegrí, J. L. and Demarcq, H. 2014a. An improved coastal upwelling index from sea surface temperature using satellite-based approach – The case of the Canary Current upwelling system. *Continental Shelf Research*, Vol. 81, pp. 38-54. doi:10.1016/j.csr.2014.03.012.

Benazzouz, A., Pelegrí, J. L., Demarcq, H., Machín, F., Mason, E., Orbi, A., Peña-Izquierdo, J. and Soumia, M. 2014b. On the temporal memory of coastal upwelling off NW Africa. *Journal of Geophysical Research: Oceans*, Vol. 119, pp. 6356-6380. doi:10.1002/2013JC009559.

Benítez-Barrios, V. M., Hernández-Guerra, A., Vélez-Belchí, P., Machín, F. and Fraile-Nuez, E. 2008. Recent changes in subsurface temperature and salinity in the Canary region. *Geophysical Research Letters*, Vol. 35, L07603. doi:10.1029/2008GL033329.

Benítez-Barrios, V. M., Pelegrí, J. L., Hernández-Guerra, A., Lwiza, K. M. M., Gomis, D., Vélez-Belchi, P. and Hernández-León, S. 2011. Three-dimensional circulation in the NW Africa coastal transition zone. *Progress in Oceanography*, Vol. 91, pp. 516-533.

Benitez-Nelson, C. R. et al. 2007. Mesoscale eddies drive increased silica export in the Subtropical Pacific Ocean. *Science*, Vol. 316, pp. 1017–1021.

Bergametti, G. and Forêt, G. 2014. Dust Deposition. In: *Mineral Dust. A Key Player in the Earth System.* Knippertz, P. and Stuut, J. -B. W. (eds). Springer, New York, pp. 179-200.

Berger, E. and Whille, R. 1972. Periodic flow phenomena. *Annual Review of Fluids Mechanics*, Vol. 4, pp. 313-340.

Berraho, A. et al. 2012. Distribution des larves de sardine et d'anchois le long du filament du Cap Ghir (région nord-ouest Africaine). *Journal des Sciences Halieutique et Aquatique*, Vol. 6, pp. 178-193.

Bez, N. and Braham, C. -B. 2014. Indicator variables for a robust estimation of an acoustic index of abundance. *Canadian Journal of Fisheries and Aquatic Sciences*, Vol. 71, pp. 709–718.

Binet, D. 1991. Dynamique du plancton dans les eaux côtières ouest-africaines: ecosystèmes équilibrés et déséquilibrés. In: *Pêcheries Ouest Africaines. Variabilité, instabilité et changement*. Cury, P. and. Roy, C. (eds). Editions de l'Office de la recherche scientifique et technique outre-mer, pp. 117-136

Binet, D. and Dessier, A. 1971. Premières données sur les copépodes pélagiques de la région congolaise. *Cahiers ORSTOM, série Océanographie*, Vol. 9 (4), pp. 411-457.

Blackwell, K. G. 2000. Tropical plumes in a barotropic model: A product of Rossby wave generation in the tropical upper troposphere. *Monthly Weather Revue*, Vol. 128, pp. 2288–2302.

Bjorndal, K. A. 1997. Foraging ecology and nutrition of sea turtles. In: *The Biology of Sea Turtles.* Lutz, P. L. and Musick, J. A. (eds). CRC Press LLC, New York, USA, pp. 199-232.

Boada, L. D., Zumbado, M., Luzardo, O. P., Almeida-González, M., Plakas, S. M., Granade, H. R., Abraham, A., Jester, E. L. E. and Dickey, R. W. 2010. Ciguatera fish poisoning on the West Africa coast: an emerging risk in the Canary Islands (Spain). *Toxicon*, Vol. 56, pp. 1516 -1519.

Boisseau, O., Matthews, J., Gillespie, D., Lacey, C., Moscrop, A. and El Ouamari, N. 2007. A visual and acoustic survey for harbour porpoises off North-West Africa: further evidence of a discrete population. *African Journal of Marine Science,* Vol. 293, pp. 403-410.

Bolten, A. B., Bjorndal, K. A., Martins, H. R., Dellinger, T., Biscoito, M. J., Encalada, S. E. and Bowen, B. W. 1998. Transatlantic developmental migrations of loggerhead sea turtles demonstrated by mtDNA sequence analysis. *Ecological Applications*, Vol. 8, No. 1, pp. 1–7.

Bonnet, M. 1969. Les sparides des côtes nord-ouest africaines. *Revue Travaux Institut de Pêches Maritimes,* Vol. 33 (1), pp. 97-116.

Bonnet, M., Duclerc, J. and Pichot, P. 1971. Nouvelle étude sur les fonds de pêche du Banc d'Arguin et de ses abords. Campagne de la «Thalassa», janvier-février 1971. *Science et Pêche, Bulletin Institut de Pêches Maritimes,* No. 203, pp. 1-115.

Borges, A. V. and Frankignoulle, M. 2001. Short-term variations of the partial pressure of CO_2 in surface waters of the Galician upwelling system. *Progress in Oceanography*, Vol. 51 (2-4), pp. 283–302. doi:10.1016/S0079-6611(01) 00071-4.

Borges, A. V., Delille, B. and Frankignoulle, M. 2005. Budgeting sinks and sources of CO_2 in the coastal ocean: Diversity of ecosystems counts. *Geophyical Research Letters*, Vol. 32, L14601. doi:10.1029/2005GL023053.

Bosshard, E. and Macfarlane, D. J. 1979. Crustal structure of western Canary Island from seismic diffraction and gravity data. *Journal of Geophysics Research*, Vol. 75, pp. 4901-4918.

Boucher, J. and Samain, J. F. 1974. L'activité amylasique. Indice de la nutrition du zooplancton: Mise en évidence d´un rythme quotidien en zone d´upwelling. *Tethys*, Vol. 6, pp. 179-188.

Boucher, J. and Samain, J. F. 1975. Étude de la nutrition du zooplankton en zone d´upwelling par la mesure des activités enzymatiques digestives. In: *Proceedings of the 9th European Marine Biology Symposium*. Harold Barnes Ed., pp. 329-341.

Boucher, J. 1982. Peuplement de copépodes des upwellings côtiers nord-ouest africains: I. Composition faunistique et structure démographique. *Oceanologica Acta*, Vol. 5 (1), pp. 49-62.

Boucher, J., Bergeron, J. P. and Gaffet, J. D. 1983. Composition faunistique et distribution du mésozooplancton de l'upwelling côtier Portugais. In: *Remontées d'eaux sur les côtes atlantiques du Portugal, campagne RCA I. Résultats des campagnes á la mer*, Vol. 25. Centre national pour l'exploitation des océans, Paris, pp. 89-94.

Bourrelly, P. 1985. *Les algues d'eau douce: Initiation à la systématique*. Paris (France).

Bowen, B. W. and Karl, S. A. 2007. Population genetics and phylogeography of sea turtles. *Molecular Ecological*, Vol. 16, pp. 4886–4907.

Bower, A. S., Serra, N. and Ambar, I. 2002. Structure of the Mediterranean Undercurrent and Mediterranean Water spreading around the Southwestern Iberian Peninsula. *Journal of Geophysical Research,* Vol. 107 (C10). doi: 10.1029/2001JC001007.

Boyd, P. W. and Trull, T. W. 2007. Understanding the export of biogenic particles in oceanic waters: is there consensus? *Progress in Oceanography*, Vol. 72, pp. 276–312.

Boyer, T. P., Garcia, H. E., Johnson, D. R., Locarnini, R. A., Mishonov, A. V., Pitcher, M. T., Baranova, O. K. and Smolyar, I. V. 2006. *World Ocean Database 2005.* NOAA Atlas NESDIS 60: 190pp.

Boyle, P. and Rodhouse, P. 2005. *Cephalopods Ecology and Fisheries*. Blackwell, London: 452 pp.

Braham, C. -B., Fréon, P., Laurec, A., Demarcq, H. and Bez, N. 2014. New insights in the spatial dynamics of sardinella stocks off Mauritania (North-West Africa) based on logbook data analysis. *Fisheries Research*, Vol.154, pp. 195–204.

Brandt, P., Hormann, V., Körtzinger, A., Visbeck, M., Krahmann, G., Stramma, L., Lumpkin, R. and Schmid, C. 2010. Changes in the Ventilation of the Oxygen Minimum Zone of the Tropical North Atlantic. *Journal of Physical Oceanography*, Vol. 40, pp. 1784–1801.

Braun, S. A. 2010. Reevaluating the role of the Saharan air layer in Atlantic tropical cyclogenesis and evolution. *Monthly Weather Revue*, Vol. 138, pp. 2007-2037.

Brito, A. and Ocaña, O. 2004. *Corales de las islas Canarias.* Francisco Lemus Editor, Santa Cruz de Tenerife: 477 pp.

Brochier, T., Ramzi, A., Lett, C., Machu, E., Berraho, A., Fréon, P. and Hernández-León, S. 2008. Modelling sardine and anchovy ichthyoplankton transport in the Canary Current System. *Journal of Plankton Research*, Vol. 30 (10), pp. 1133–1146. doi:10.1093/plankt/fbn066.

Brochier, T., Mason, E., Moyano, M., Berraho, A., Colas, F., Sangrà, P., Hernández-León, S., Ettahiri. O. and Lett, C. 2011. Ichthyoplankton transport from the African coast to the Canary Islands. *Journal of Marine Marine Systems,* Vol. 87, pp. 109-122.

Broecker, W. S. 1975. Climate Change: Are We on the Brink of a Pronounced Global Warming? *Climate Change: Critical Concepts in the Environment*, Vol. 189, pp. 460–463.

Brongersma, L. D. 1982. Marine turtles of the eastern Atlantic Ocean. In: *Biology and conservation of sea turtles*, *Proceedings of the World Conference on Sea Turtle Conservation, 1979*. Bjorndal, K. A. (eds). Smithsonian Institution Press, Washington D.C., pp. 407-416.

Brust, J. and Waniek, J. J. 2010. Atmospheric dust contribution to deep sea particle fluxes in the subtropical northeast Atlantic. *Deep- Sea Research Part I: Oceanographic Research Papers,* Vol. 57, pp. 988–998. doi:10.1016/j.dsr.2010.04.011.

Buckland, S. T, Anderson, D. R., Burnham, K. P. and Laake, J. L. 1993. *Distance Sampling. Estimating abundance of biological populations.* Chapman & Hall, London: 446 pp.

Burke, K. and Wilson, J. T. 1972. Is the African plate stationary?. *Nature,* Vol. 239, pp. 387-390.

Burukovski, R. N. 1998. On the distribution of shrimp in West African waters. *Journal of Zoology,* Vol. 2 (3), pp. 400-408.

Cadenat, J. 1937. Recherches systématiques sur les poissons littoraux de la côte occidentale d'Afrique, récoltés par le navire Président Théodore Tissier au cours de sa 5ème croisière (1936). *Ibid*, Vol. 10 (4), pp. 425-562.

Cadenat, J. 1947. Observations de Cétacés au Sénégal. *Notes Africaines,* Vol. 34, pp. 20-34.

Cadenat, J. 1949. Notes sur les Cétacés observés sur les côtes du Sénégal de 1941 à 1948. *Bulletin de l'IFAN*, Vol. 11, pp. 1-15.

Cadenat, J. 1953. Notes d'ichthyologie ouest-africaine. VI. Poissons des campagnes du « Gérard Tréca ». *Bulletin de l'IFAN*, Vol. 15 (3), pp. 1051-1102.

Cadenat, J. 1959a. Rapport sur les petits cétacés ouest-africains. Résultats des recherches entreprises sur ces animaux jusqu'au mois de mars 1959. *Bulletin de l'IFAN,* Vol. 21 A (4), pp. 1367-1409.

Cadenat, J. 1959b. Notes sur les Delphinidés Ouest-africains. VI. Le gros dauphin gris *Tursiops truncatus* est-il capable de faire des plongées profondes?. *Bulletin de l'IFAN,* Vol. 21 A (3), pp. 1137-1141.

Cadenat, J. and Lassarat, A. 1959. Notes sur les Delphinidés ouest-africains. III. Notes complémentaires sur *Tursiops truncatus*. *Bulletin de l'IFAN,* Vol. 21A (1), pp. 416-419.

Calafat, F. M., Chambers, D. P. and Tsimplis, M. N. 2012. Mechanisms of decadal sea level variability in the eastern North Atlantic and the Mediterranean Sea. *Journal of Geophysical Research*, Vol. 117, C09022.

Caldeira, K and Wickett, M. E. 2003. Oceanography: Anthropogenic carbon and ocean pH. *Nature*, Vol. 425, p. 365.

Calero, B., Ramil, F. and Ramos, A. Submitted. Echinoderms of Mauritanian deep bottoms. In: *Deep-sea ecosystems off Mauritania: Researching marine biodiversity and habitats in West African deep-waters*. Ramos, A., Sanz, J. L. and Ramil, F. (eds). Springer, Heidelberg.

Calil, P. H. R., Richards, K. J., Jia, Y. and Bidigare R. R. 2008. Eddy activity in the lee of the Hawaiian Islands. *Deep-Sea Research Part II: Topical Studies in Oceanography*, Vol. 55, pp. 1179–1194.

Callot, Y., Marticorena, B. and Bergametti, G. 2000. Geomorphologic approach for modelling the surface features of arid environments in a model of dust emissions: application to the Sahara desert. *Geodinamica Acta,* Vol. 13, pp. 245-270. doi:10.1016/s0985-3111(00)01044-5.

Cancet, M., Lux, M., Pénard, C., Lyard, F., Birol, F., Lemouroux, J., Bourgogne, S. and Bronner, E. 2010. COMAPI: New regional tide atlases and high frequency dynamical atmospheric correction. *Ocean Surface Topography Science Team meeting*, Lisbon, Portugal, 2010.

Candela, J. 2001. Mediterranean water and global circulation. *Ocean Circulation and Climate*. G. Siedler, J. Church and J. Gould (eds). Academic Press, New York, pp. 419–429.

Capart, A. 1951. Crustaces Decapodes Brachyures. Expedition Oceanographique Beige dans les Eaux Cotieres Africaines de I'Atlantique Sud (1948-1949). *Resultats Scientifiques*, Vol. 3 (1), pp. 11-205.

Capone, D. G., Bronk, D. A., Mulholland, M. R. and Carpenter, E. J. 2008. *Nitrogen in the Marine Environment*. Academic Press.

Caquineau, S., Gaudichet, A., Gomes, L., Magonthier, M. C. and Chatenet, B. 1998. Saharan dust: Clay ratio as a relevant tracer to assess the origin of soil-derived aerosols. *Geophysical Research Letters*, Vol. 25, pp. 983-986.

Cardona, L., Aguilar, A., Pazos, L. 2009. Delayed ontogenic dietary shift and high levels of omnivory in green turtles (*Chelonia mydas*) from the NW coast of Africa. *Marine Biology*, Vol. 156, pp. 1487-1495.

Carr, A. 1987. Impact of nondegradable marine debris on the ecology and survival outlook of sea turtles. *Marine Pollution Bulletin,* Vol. 18, pp. 352–356.

Carr, M. -E. 2001. Estimation of potential productivity in Eastern Boundary Currents using remote sensing. *Deep-Sea Research Part II: Topical Studies in Oceanography*, Vol. 49 (1), pp. 59–80.

Carr, M. -E. et al. 2006. A comparison of global estimates of marine primary production from ocean color. *Deep-Sea Research Part II: Topical Studies in Oceanography*, Vol. 53 (5), pp. 741–770.

Carracedo, J. C. 1994. The Canary Islands: an example of structural control on the growth of large ocean-island volcanoes. *Journal of Volcanological and Geothermal Research*, Vol. 60, pp. 225-241.

Carracedo, J. C. 2011. *Geología de Canarias I. Origen, Evolución, edad y volcanismo*. Ed. Rueda S.L., Madrid.

Carracedo, J. C., Day, S., Guillou, H., Rodriguéz-Badiola, E., Canas, J. A. and Pérez-Torrado, F. J. 1998. Hotspot volcanism close to a passive continental margin: the Canary Islands. *Geology Magazine,* Vol. 135, pp. 591-604.

Carreras, C. et al. 2011. Living together but remaining apart: Atlantic and Mediterranean loggerhead sea turtles (*Caretta caretta*) in shared feeding grounds. *Journal of Heredity*, Vol. 102, pp. 666–677.

Cartes, J. E. 1998. Feeding strategies and partition of food resources in deep-water decapod crustaceans (between 400-2300 m). *Journal of the Marine Biological Association of the United Kingdom,* Vol. 78, pp. 509-524.

Carton, J. A. and Giese, B. 2008. A Reanalysis of Ocean Climate Using Simple Ocean Data Assimilation (SODA). *Monthly Weather Review*, Vol. 136, pp. 2999-3017.

Castellanos, P., Pelegrí, J. L., Campos, E. D., Rosell-Fieschi, M. and Gasser, M. 2015. Response of the surface tropical Atlantic Ocean to wind forcing. *Progress in Oceanography*. doi:10.1016/j.pocean.2015.02.005.

Castillo, S., Ramil, F. and Ramos, A. Submitted. Composition and distribution of epibenthic and demersal communities in Mauritanian deep waters. In: *Deep-sea ecosystems off Mauritania: Researching marine biodiversity and habitats in West African deep-waters*. Ramos, A., Sanz, J. L. and Ramil, F. (eds). Springer, Heidelberg.

Catry, P. (ed.). 2000. *Action Plan for the Conservation of Marine Turtles in Guinea-Bissau*. IUCN, Bissau, Guinea-Bissau.

Catry, P., Barbosa, C., Paris, B., Indjai, B., Almeida, A., Limoges, B., Silva, C. and Pereira, H. 2009. Status, ecology, and conservation of sea turtles in Guinea-Bissau. *Chelonian Conservation and Biology*, Vol. 8, pp. 150–160.

Caverivière, A., Thiam, M., Thiam, D. and López Abellán, L. 1986. Rapport de synthèse des quatre campagnes conjointes hispano-sénégalaises de chalutages sur les stocks profonds du Sénégal (1982–1984). Archives Centre de Recherches Océanographiques de Dakar-Thiaroye, No. 151. http://www.sist.sn/gsdl/collect/publi/index/assoc/HASH09b5/bba41e55.dir/doc.pdf (accessed 15 February 2015).

Caverivière, A. and Rabarison Andriamirado, G. A. 1997. Minimal fish predation for the pink shrimp *Penaeus notialis* in Senegal (West Africa). *Bulletin of Marine Science*, Vol. 61 (3), pp. 685-695.

Cermeño, P., Rodríguez-Ramos, T., Dornelas, M., Figueiras, F. G., Marañón, E., Teixeira, I. G. and Vallina, S. M. 2013. Species richness in marine phytoplankton communities is not correlated to ecosystem productivity. *Marine Ecology Progress. Series*, Vol. 488, pp. 1–9.

CERSAT. 2014. *ASCAT on METOP-A Level 4 Monthly Gridded Mean Wind Fields in 0.25° Geographical Grid*. http://cersat.ifremer.fr/ (Accessed December 2014).

Cervantes, A. and Goñi, R. 1985. Descripción de las pesquerías españolas de merluzas y crustáceos de África Occidental al norte de Cabo Blanco. In: *Simposio Internacional sobre las áreas de afloramiento más importantes del Oeste africano (Cabo Blanco y Benguela),* Vol. 2. Bas, C., Margalef, R. and Rubiés, P. (eds). Instituto de Investigaciones Pesqueras, Barcelona, Spain, pp. 825-850.

Cervantes, A., Sobrino, I., Ramos, A. and Fernández, L. 1992. Descripción y análisis de los datos de las pesquerías de merluza y gamba de la flota española que faenó al fresco en África Noroccidental durante el periodo 1983-1988. *Informe Técnico Instituto Español de Oceanografía,* No. 111: 85 pp.

Champagnat, C. and Domain, F. 1979. Migrations des poisons démersaux le long des côtes ouest-africaines de 10° à 24° de latitude nord. Annexe au rapport du groupe de travail ISRA_ORSTOM sur la reproduction des espèces exploitées dans le golfe de Guinée, Dakar (Sénégal), 7-12 novembre 1977. Centre de Recherches Océanographiques de Dakar-Thiaroye ISRA Scientific Document No. 68, pp. 79-110.

Chassot, E., Bonhommeau, S., Dulvy, N. K., Mélin, F., Watson, R., Gascuel, D. and Le Pape, O. 2010. Global marine primary production constrains fisheries catches. *Ecology Letters*, Vol. 13 (4), pp. 495–505. doi:10.1111/j.1461-0248.2010.01443.x.

Chavance, P. N. 2002. Les campagnes scientifiques de chalutage en Afrique de l'ouest: structure des données anciennes (campagnes françaises) et inventaire et bibliographie. *Document Technique Trawlbase-SIAP*, No. 5, pp. 1-25.

Chavanne, C., Flament, P., Lumpkin, R., Dousset, B. and Betamy, A. 2002. Sacatterometer observations of wind variations induced by oceanic islands. Implications for wind-driven ocean circulation. *International Journal of Remote Sensing*, Vol. 28 (3), pp. 466-474.

Chavez, F. P. and Messié, M. 2009. A comparison of Eastern Boundary Upwelling Ecosystems. *Progress in Oceanography*, Vol. 83, pp. 80–96.

Chelton, D. B., Deszoeke, R. A., Schlax, M. G., Naggar, K. and Stwertz, N. 1998. Geographical variability of the first baroclinic Rossby radius of deformation. *Journal of Physical Oceanography*, Vol. 28, pp. 433–460.

Chen, T. C. and van Loon, H. 1987. Interannual variation of the tropical easterly jet. *Monthly Weather Revue*, Vol. 115, pp. 1739–1759.

Cheung, W. W. L., Watson, R. and Pauly, D. 2013. Signature of ocean warming in global fisheries catch, *Nature*, Vol. 497, pp. 365-369.

Chiahou, B. 1997. *Les copépodes pélagiques de la région d'El Jadida (côte Atlantique marocaine). Etude faunistique, écologique et biogéographique*. PhD Thesis, Faculty of Science, University Chouaib Doukkali of El Jadida: 168 pp.

Chiapello, I., Bergametti, G., Gomes, L., Chatenet, B., Dulac, F., Pimenta, J. and Santos Soares, E. S. 1995. An additional low layer transport of Sahelian and Saharan dust over the north-eastern tropical Atlantic. *Geophysical Research Letters*, Vol. 22, pp. 3191-3194. doi: 10.1029/95GL03313.

Chiapello, I., Bergametti, G., Chatenet, B., Bousquet, P., Dulac, F. and Santos Soares, E. 1997. Origins of African dust transported over the northeastern tropical Atlantic. *Journal of Geophysical Research D: Atmospheres*, Vol. 102, pp. 13701-13709. doi: 10.1029/97JD00259.

Chidichimo, M. P., Kanzow, T., Cunningham, S. A. and Marotzke, J. 2010. The contribution of eastern-boundary density variations to the Atlantic meridional overturning circulation at 26.5°N. *Ocean Science*, Vol. 6, pp. 475–490.

Chou, C., Formenti, P., Maille, M., Ausset, P., Helas, G., Harrison, M. and Osborne, S. 2008. Size distribution, shape, and composition of mineral dust aerosols collected during the African Monsoon Multidisciplinary Analysis Special Observation Period 0: Dust and Biomass-Burning Experiment field campaign in Niger, January 2006. *Journal of Geophysical Research D: Atmospheres*, Vol. 113, D00C10. doi:10.1029/2008JD009897.

Christensen, V. et al. 2004. Trends in fish biomass off Northwest Africa, 1960-2000. In: *Pêcheries maritimes, écosystèmes et sociétés en Afrique de l'Ouest: Un demi-siècle de changement.* Chavance, P., Bâ, M., Gascuel, D., Vakily, J. M. and Pauly, D. (eds). Collection des Rapports de recherche halieutique ACP-UE, No. 15. Vol. 1, pp. 377-386.

Church, J. A. and White, N. J. 2011. Sea level rise from the late 19th to the early 21st century. *Surveys in Geophysics*, Vol. 32, pp. 585–602.

Church, J. A. et al. 2013. Sea Level Change. In: *Climate Change 2013: The Physical Science Basis. Contribution of Working Group I to the Fifth Assessment Report of the Intergovernmental Panel on Climate Change*. Stocker, T. F. et al. (eds). Cambridge University Press, Cambridge, United Kingdom and New York, NY, USA.

Cianca, A., Helmke, P., Mouriño, B., Rueda, M. J., Llinás, O. and Neuer, S. 2007. Decadal analysis of hydrography and in situ nutrient budgets in the western and eastern North Atlantic subtropical gyre. Journal *Geophysical Research,* Vol. 112, C07025. doi:10.1029/2006JC003788.

Cianca, A., Santana, R., Hartman, S. E., Martín-González. J. M., González-Dávila, M., Rueda, M. J., Llinás, O. and Neuer. S. 2013. Oxygen Dynamics in the North Atlantic subtropical gyre. *Deep-Sea Research Part II: Topical Studies in Oceanography*, Vol. 93, pp. 135-147.

Clayton, T. D. and Byrne, R. H. 1993. Spectrophotometric seawater pH measurements: Total hydrogen ion concentration scale calibration of m-cresol purple and at-sea results, *Deep-Sea Research Part I: Oceanographic Research Papers*, Vol. 42, pp. 411- 429.

Clift, P. and Acosta, J. (eds). 2005. *Geophysics of the Canary Islands. Results of Spain´s Exclusive Economic Zone Program*. Springer.

Clusa, M. et al. 2013. Mitochondrial DNA reveals Pleistocenic colonisation of the Mediterranean by loggerhead sea turtles (*Caretta caretta*). *Journal of Experimental Marine Ecology and Biology*, Vol. 439, pp. 15–24.

Colman, J. G., Gordon, D. M., Lane, A. P., Forde, M. J. and Fitzpatrick, J. J. 2005. Carbonate mounds off Mauritania, Northwest Africa: status of deep-water corals and implications for management of fishing ad oil exploration activities. In: *Cold-Water Corals and Ecosystems*. Freiwald, A. and Robers, J. M. (eds). Springer-Verlag, Berlin Heidelberg, pp. 417-441.

Comas-Rodríguez, I., Hernández-Guerra, A., Fraile-Nuez, E., Martínez-Marrero, A., Benítez-Barrios, V. M., Pérez-Hernández, M. D. and Vélez-Belchí, P. 2011. The Azores Current System from a meridional section at 24.5 degrees W. *Journal of Geophysical Research: Ocean*, Vol. 116. doi:10.1029/2011JC007129.

Connell, S. D., Kroeber, K. J., Fabricius, K. E., Kline, D. I. and Rusell, B. D. 2013. The other ocean acidification problem: CO_2 as a resource among competitors for ecosystem dominance. *Philosophical Transactions of the Royal Society*, pp.1-9. doi:10.1098/rstb.2012.0442.

Cook, K. H. 1999. Generation of the African easterly jet and its role in determining West African precipitation. *Journal of Climate*, Vol. 12, pp. 1165-1184.

Copin-Montégut., C. and Avril, B. 1995. Continuous pCO_2 measurements in surface water of the northeastern Tropical Atlantic. *Tellus Series B*, Vol. 47 (1-2), pp. 86-92.

Corral, J. 1970. *Contribución al conocimiento del Plancton de Canarias: Estudio cuantitativo, sistemático y observaciones ecológicas de los copepódos epipelágicos en la zona de Santa Cruz de Tenerife en el curso de un ciclo anual*. PhD Thesis, Publicaciones de la Facultad de Ciencias, Sección Biológicas, University of Madrid, No. 129: 280 pp.

Corral, J. E. and Pereiro, J. A. 1974. Estudio de las asociaciones de copépodos planctónicos en una zona de las islas Canarias. *Boletín del Instituto Español de Oceanografía*, Vol. 175: 32 pp.

Corten, A., Asberr, N. M. and Diop, H. 2012. *The sardinella of northwest Africa: fisheries, stock assessment and management.* Technical document Sub-regional Fisheries Commission, Dakar.

Cosson, N., Sibuet, M. and Galeron, J. 1997. Community structure and spatial heterogeneity of the deep-sea macrofauna at three contrasting stations in the tropical northeast Atlantic. *Deep-Sea Research Part I: Oceanographic Research Papers*, Vol. 44 (2), pp. 247–269.

Coste, B. and Minas, H. J. 1982. Analyse des facteurs régissant la distribution des sels nutritifs dans la zone de remontée d'eau des côtes mauritaniennes. *Oceanologica Acta*, Vol. 5 (3), pp. 315–324.

Courtillot, V., Davaille, A., Stock, J. and Besse J. 2003. Three distinct types of hotspots in the Earth's mantle. *Earth and Planetary Science Letters*, Vol. 205, pp. 285-308.

Coward, A. C. and de Cuevas, B. A. 2005. *The OCCAM 66 level model: model description, physics, initial conditions and external forcing.* Southampton Oceanography Centre Internal Document, 99. Southampton Oceanography Centre, Southampton, UK: 83 pp.

Cozens, J., Taylor, H. and Gouveia, J. 2011. Nesting activity of the loggerhead sea turtle *Caretta caretta* (Linnaeus, 1758) on Maio, Cape Verde Islands. *Zoologia Caboverdiana*, Vol. 2 (2), pp. 62–70.

Cozens, J., Pereira, M., Mendes, E. and Miles, R. 2012. First ever population census of nesting loggerheads on Sal island, Cape Verde. In: *Proceedings of the Twenty-ninth Annual Symposium on Sea Turtle Biology and Conservation.* Belskis, L., Frick, M., Panagopoulou, A., Rees, A. F. and Williams, K. (compilers). NOAA Technical Memorandum NOAA NMFS-SEFSC-630, pp. 21–21.

Criado, C. and Dorta, P. 2003. An unusual 'blood rain' over the Canary Islands (Spain). The storm of January 1999. *Journal of Arid Environments*, Vol. 55, pp. 765-783. doi: 10.1016/S0140-1963(02)00320-8.

Cropper, T. E., Hanna, E. and Bigg, G. R. 2014. Spatial and temporal seasonal trends in coastal upwelling off Northwest Africa, 1981–2012. *Deep-Sea Research Part I: Oceanographic Research Papers*, Vol. 86, pp. 94–111. doi:10.1016/j.dsr.2014.01.007.

Crosnier, A. and Forest, J. 1965. Note préliminaire sur les Alpheidae recueillis par la Calypso dans l'Atlantique Oriental Tropical (Crustacea Decapoda Natantia). *Bulletin du Museum Nationelle d'Histoire Naturelle de Paris,* Vol. 2 (36), pp. 602-610.

Crosnier, A. and Forest, J. 1966. Crustacés Décapodes: Alpheidae. In: *Campagnes de la Calypso dans le Golfe de Guinée et aux Iles Principe, Sao Tomé et Annobon (1956), et Campagne aux Iles du Cap Vert* (1959). Part 19: Résultats Scientifiques des Campagnes de la Calypso, Vol. 7, No.27. *Annales de l'Institut Océanographique de Monaco*. 44, pp. 199-314.

Crosnier, A. and De Bondy, E. 1967. Les crevettes commercialisables de la côte ouest de l'Afrique intertropicale. *Initiations, Documentations Techniques ORSTOM*, No. 7: 60 pp.

Crosnier, A. and Forest, J. 1973. Les crevettes profondes de l'Atlantique Oriental Tropical. *Faune Tropicale*, ORSTOM, Paris: 409 pp.

Cryer, M., Hartill, B. and O'Shea, S. 2002. Modification of marine benthos by trawling: toward a generalization for the deep ocean? *Ecological Applications*, Vol. 12 (6), pp. 1824–1839.

Cuñarro, D., Mangas, J., Acosta, J., Rivera, J. and García, L. 2014, Geomorphology of the giant submarine landslides, submarine canyons, volcanic cones and salt diapirs that appear in the seabed surrounding the islands of Fuerteventura and Lanzarote (Canary Islands). Master of Oceanography, Faculty of Marine Science, University of Las Palmas de Gran Canaria: 29 pp.

Curry, R., Dickson, B. and Yashayaev, I. 2003. A change in the freshwater balance of the Atlantic Ocean over the past four decades. *Nature*, Vol. 426, pp. 826–829. doi:10.1038/nature02206.

Curry, R. and Mauritzen, C. 2005. Dilution of the Northern North Atlantic Ocean in Recent Decades. *Science*, Vol. 308, pp. 1772–1774. doi:10.1126/science.1109477.

Cury, P. and Roy, C. 1989. Optimal environmental window and pelagic fish recruitment success in upwelling areas. *Canadian Journal of Fisheries and Aquatic Sciences*, Vol. 46 (4), pp.670-680. doi:10.1139/f89-086.

Cury, P. and Roy, C. 1991. *Pêcheries Ouest Africaines. Variabilité, inestabilité et changement.* Editions de l'Office de la recherche scientifique et technique outre-mer, Paris: 525 pp.

Cury, P. and Shannon, L. 2004. Regime shifts in upwelling ecosystems: observed changes and possible mechanisms in the northern and southern Benguela. *Progress in Oceanography*, Vol. 60, pp. 223–243.

Cury, P., Shin, Y. -J., Planque, B., Durant, J. M., Fromentin, J. -M., Kramer-Schadt, S., Stenseth, N. C., Travers, M. and Grimm, V. 2008. Ecosystem oceanography for global change in fisheries. *Trends in Ecology & Evolution*, Vol. 23 (6), pp. 338–346.

Cushman-Roisin, B. 1994. *Introduction to geophysical fluid dynamics*. Prentice Hall: 313 pp.

Darwin, C. R. 1846. An account of the fine dust which often falls on vessels in the Atlantic ocean. *Quarterly Journal of the Geological Society of London*, Vol.2, pp. 26-30.

Dawes, C. J. 1998. *Marine Botany*. John Wiley & Sons.

d'Almeida, G. A. 1986. A Model for Saharan Dust Transport. *Journal of Climate and Applied Meteorology*, Vol. 25, pp. 903-916. doi:10.1175/1520-0450(1986)025<0903:AMFSDT>2.0.CO;2.

de Graaf, G. and Garibaldi, L. 2014*. The value of African fisheries*. FAO, Rome. FAO Fisheries and Aquaculture Circular*,* No. 1093: 76 pp.

de Matos-Pita, S. S. and Ramil, F. 2014. Squat lobsters (Crustacea: Anomura) from Mauritanian waters (West Africa) with the description of a new species of Munidopsis. *Zootaxa,* No. 3765, pp. 418-434.

de Matos-Pita, S. S. and Ramil, F. 2015. Hermit crabs (Decapoda: Crustacea) from deep waters off Mauritania (NW Africa) with the description of a new species. *Zootaxa,* No. 3926 (2), pp. 151-190.

de Matos-Pita, S. S. and Ramil, F. Submitted.Additions to the thalassinidean fauna (Crustacea: Decapoda) off Mauritanian coasts with the description of a new species.

de Matos-Pita, S. S., Castillo, S. and Ramil, F. Submitted. Contribution to the knowledge of the deep Brachyuran fauna (Crustacea: Decapoda) in waters off Mauritania (NW Africa).

Debrah, J. S., Ofori-Danson, P. K. and Van Waerebeek, K. 2010. *An update on the catch composition and other aspects of cetacean exploitation in Ghana.* International Whaling Commission, Agadir, Morocco. Scientific Committee Document SC/62/SM10.

Decker, C., Griffiths, C., Prochazka, K., Ras, C. and Whitfield, A. (eds). 2004. Marine biodiversity in Sub-Saharan Africa: The Known and the Unknown. *Proceedings of the Marine Biodiversity in Sub-Saharan Africa: The Known and the Unknown.* Cape Town, South Africa, 23-26 September 2003: 310 pp.

Dellinger, T. and Encarnaçâo, H. 2000. Accidental capture of sea turtles by fishing fleet based at Madeira Island, Portugal. In: *Proceedings of the nineteenth Annual Symposium on Sea Turtle Conservation and Biology.* Kalb, H. and Wibbels, T. (eds). NOAA Technical Memorandum NOAA NMFS-SEFSC-443, pp. 218–218.

Demarcq, H. 2009. Trends in primary production, sea surface temperature and wind in upwelling systems (1998-2007). *Progress in Oceanography*, Vol. 83 (1–4), pp. 376–385. doi:10.1016/j.pocean.2009.07.022.

Demarcq, H., Barlow, R. and Hutchings, L. 2007. Application of a chlorophyll index derived from satellite data to investigate the variability of phytoplankton in the Benguela ecosystem. *African Journal of Marine Science*, Vol. 29 (2), pp. 271–282. doi:10.2989/AJMS.2007.29.2.11.194.

Den Hartog, J. C. 1984. An introduction to the CANCAP-project of the Dutch Rijksmuseum van Natuurlijke Historie (RMNH), with special reference to the CANCAP-VI expedition (1982) to the Cape Verde Islands. *Courier Forschungsinstitut Senckenberg*, Vol. 68, pp. 5-15.

Déniz-González, I., Pascual-Alayón, P. J., Chioua, J., García-Santamaría, M. T. and Valdés, L. 2014. *Directory of Atmospheric, Hydrographic*

and Biological datasets for the Canary Current Large Marine Ecosystem. IOC-UNESCO, Paris. IOC Technical Series, No. 110: 214 pp.

Dia, A. 1986. *Biomasse et biologie du phytoplancton le long de la petite côte sénégalaise relations avec l'hydrologie* (Document CRODT). Dakar.

Diallo, S. T. et al. 2002. *Campagne d'observation des cétacés dans les eaux cotières de l'Afrique du Nord Ouest (de la Guinée au Sénégal)*. *Rapport de Mission*. Centre National des Sciences Halieutiques de Boussoura, Republic of Guinea: 16 pp.

Diallo S. T. et al. 2004. *Campagne d'observation des cétacés dans les eaux cotières de l'Afrique du Nord Ouest (de la Guinée au Sénégal). 23 janvier au 10 février 2004*. *Rapport de Campagne.* Centre National des Sciences Halieutiques de Boussoura, Republic of Guinea: 13 pp.

Díaz, A. M., Díaz, J. P., Expósito, F. J., Hernández-Leal, P. A., Savoie, D. and Querol, X. 2006. Air masses and aerosols chemical components in the free troposphere at the subtropical Northeast Atlantic region. *Journal of Atmospheric Chemistry*, Vol. 53, pp. 63-90. doi: 10.1007/s10874-006-264-5.

Dickey, R. W. and Plakas, S. M. 2010. Ciguatera: a public health perspective. *Toxicon*, Vol. 56, pp. 123-136.

Dickson, A. G. and Millero, F. J. 1987. A comparison of the equilibrium constants for the dissociation of carbonic acid in seawater media. *Deep-Sea Research Part I: Oceanographic Research Papers,* Vol. 34, pp. 1733–1743.

Dickson, B., Yashayaev, I., Meincke, J., Turrell, B., Dye, S. and Holfort, J. 2002. Rapid freshening of the deep North Atlantic Ocean over the past four decades. *Nature*, Vol. 416, pp. 832–837. doi:10.1038/416832a.

Diffenbaugh, N. S., Snyder, M. A. and Sloan, L. C. 2004. Could CO(2)-induced land-cover feedbacks alter near-shore upwelling regimes? *Proceeding of the National Academic Science of the United States of America,* Vol. 101, pp. 27–32.

Dillon, C. R. and Rodgers, J. H. 1980. Thermal Effects on Primary Productivity of Phytoplankton, Periphyton and Macrophytes in Lake Keowee, South Carolina. Water Resources Research Institute, Clemson University, S. C., Report No. 81.

Divins, D. L. 2003. *Total Sediment Thickness of the World's Oceans & Marginal Seas*. NOAA National Geophysical Data Center, Boulder, CO.

DOE. 1994. Handbook of methods for the analysis of the various parameters of the carbon dioxide system in sea water; version 2. Dickson, A. D. and Goyet, C. (eds). ORNL/CDIAC-74: 180 pp.

Domain, F. 1976. *Les fonds de pêche du plateau continental ouest-africain entre 17°N et 12°N*. Centre de recherches Océanographiques de Dakar-Thiaroye. Document Scientifique, No. 61: 20 pp.

Domain, F. 1979. Les resources démersales (poissons). In: *Les ressources halieutiques de l'Atlantique Centre-Est. Première partie: Les ressources du Golfe de Guinée de l'Angola à la Mauritanie*. Troadec, J. P. and Garcia, S. (eds). FAO Documents Techniques sur les Pêches, No. 186.1, pp. 79-122.

Domain, F. 1980. *Contribution à la connaissance de l'écologie des poissons démersaux du plateau continental sénégalo-mauritanien. Les ressources démersaux dans le contexte général du Golfe de Guinée*. PhD Thesis, Univerity Pierre et Marie Curie, Paris VI, France: 421 pp.

Domain, F. 1986. *Estimation par chalutage des ressources démersales du plateau continental mauritanien*. FAO, Rome. COPACE/PACE Séries 86/37, pp. 248-273.

Domalain, G., Jouffre, D., Thiam, D., Traore, S. and Wang, C. L. 2004. Évolution de la diversité spécifique et des dominances dans les campagnes de chalutage démersal du Sénégal et de la Guinée. In : *Pêcheries maritimes, écosystèmes et sociétés en Afrique de l'Ouest: Un demi-siècle de changement.* Chavance, P., Bâ, M., Gascuel, D., Vakily, J. M. and Pauly, D. (eds). Collection des Rapports de recherche halieutique ACP-UE, No. 15, Vol. 1, pp. 299-310.

Doney, S. C., Lindsay, K. and Moore, J. K. 2003. Global ocean carbon cycle modeling. In: *Ocean biogeochemistry.* Fasham, M. J. R. (ed.). Springer-Verlag, Berlin Heidelberg, pp. 217–238.

Dong, C. M., McWilliams, J. C and Shchepetkin, A. F. 2007. Island wakes in deep water. *Journal of Physical Oceanography*, Vol. 37 (4), pp. 962–981.

Doty, M. S. and Ogury, M. 1956. The island mass effect. *Journal du Conseil Permanent International pour L´Exploration de la Mer*, Vol. 22, pp. 33-37.

Duarte, C. M., Agustí, S., Arístegui, J., González, N. and Anadón, R. 2001. Compelling evidence for a heterotrophic subtropical NE Atlantic. *Limnology and Oceanography*, Vol. 46, pp. 425– 428.

Duarte, C. M., Dachs, J., Llabrés, M., Alonso-Laita, P., Gasol, J. M., Tovar-Sánchez, A., Sañudo-Wilhemy, S. and Agustí, S. 2006. Aerosol inputs enhance new production in the subtropical northeast Atlantic. *Journal of Geophysical Research G: Biogeosciences*, Vol. 111, G04006. doi: 10.1029/2005JG000140.

Duce, R. A. et al. 1991. The atmospheric input of trace species to the world ocean. *Global Biogeochemical Cycles*, Vol. 5, pp. 193-259. doi: 10.1029/91gb01778.

Ducklow, H. W. and McAllister, S. L. 2005. Biogeochemistry of carbon dioxide in the coastal oceans. In: *The Sea: The global coastal ocean: multiscale interdisciplinary processes*, Vol. 13. Robinson, A. R. and Brink, K. H. (eds). Harvard University Press, pp. 269–315.

Dugdale, R. C. and Wilkerson, F. P. 1998. Silicate regulation of new production in the equatorial Pacific upwelling. *Nature*, Vol. 391 (6664), pp. 270–273. doi:10.1038/34630.

Duguy, R. 1976. Contribution à l'étude des mammifères marins de la côte nord-ouest Afrique. *Revue des Travaux de l'Institut des Pêches maritimes*, Vol. 39 (3), pp. 321-332.

Duineveld, G. C. A., Lavalaye, M. S. S. and Van Noort, G. J. 1993. The trawlfauna of the Mauritanian shelf (Northwest Africa): density, species composition and biomass. In: *Ecological studies in the coastal waters of Mauritania*. Wolff, W. J., Van Der Land, J., Nieuhuis, P. H. and de Wilde, P. A. W. J. (eds). *Hydrobiologia*, Vol. 258 (1-3), pp. 165-174.

Duncan, R. A. 1984. Age progressive volcanism in the New England Seamounts and the opening of the central Atlantic Ocean. *Journal of Geophysical Research,* Vol. 89 (B12), pp. 9980-9990.

Dunion, J. P. 2007. Rewriting the climatology of the tropical North Atlantic and Caribbean Sea Atmosphere. *Journal of Climate*, Vol. 24, pp. 893-908.

Dunion, J. P. and Velden, C. S. 2004. The impact of the Saharan air layer on Atlantic tropical cyclone activity. *Bulletin of American Meteorological Society,* Vol. 84, pp. 353-365.

Dunning, M. C. and Wormuth. J. H. 1998. The Ommastrephid squid genus *Todarodes*: A review of systematics, distribution, and biology (Cephalopoda: Teuthoidea). *Smithsonian Contributions to Zoology*, Vol. 586, pp. 385-391.

Dyhr, C. T. and Holm, P. M. 2010. A volcanological and geochemical investigation of Boa Vista, Cape Verde Islands; 40Ar/39Ar geochronology and field constraints. *Journal of Volcanological and Geothermal Research,* Vol. 189, No. 1–2, pp. 19-32.

Eckert, S. A., Bagley, D., Kubis, S., Ehrhart, L., Johnson, C., Stewart, K. and DeFreese, D. 2006. Internesting and Postnesting Movements and Foraging Habitats of Leatherback Sea Turtles (*Dermochelys coriacea*) Nesting in Florida. *Chelonian Conservation and Biology*, Vol. 5, pp. 239–248.

Eder, E., Ceballos, A., Martins, S., Pérez-García, H., Marín, I., Marco, A. and Cardona, L. 2012. Foraging dichotomy in loggerhead sea turtles *Caretta caretta* off northwestern Africa. *Marine Ecology Progress Series,* Vol. 470, pp. 113–122.

Ekman, V. W. 1905. On the influence of the earth's rotation on ocean-currents. *Arkiv För Matematik, Astronomi Och Fysik*, Vol. 2 (1), pp. 1–52.

Elgarch, A., Vale, P., Rifai, S. and Fassouane, A. 2008. Detection of Diarrheic Shellfish Poisoning and azaspiracid toxins in Moroccan mussels: comparison of the LC-MS method with the commercial immunoassay kit. *Marine Drugs*, Vol. 6, pp. 587-594.

Elghrib, H., Somoue, L., Elkhiati, N., Berraho, A., Makaoui, A., Bourhim, N., Salah, S. and Ettahiri, O. 2012. Phytoplankton distribution in the upwelling areas of the Moroccan Atlantic coast localized between 32°30'N and 24°N. *Comptes rendus biologies*, Vol. 335 (8), pp. 541–554. doi:10.1016/j.crvi.2012.07.002

Emery, W. and Meincke, J. 1986. Global water masses - summary and review. *Oceanologica Acta*, Vol. 9, pp. 383-391.

Engelbrecht, J. P., Menéndez, I. and Derbhysire, E. 2014. Sources of $PM_{2.5}$ impacting Gran Canaria. *Catena,* Vol. 117, pp. 119-132. doi: 10.1016/j.catena.2013.06.017.

Engelstaedter, S., Tegen, I. and Washington, R. 2006. North African dust emissions and transport. *Earth-Science Reviews,* Vol. 79, pp. 73-100. doi: 10.1016/j.earscirev.2006.06.004.

Entrambasaguas, L. 2008. *Estudio faunístico y ecológico de los equinodermos del archipiélago de Cabo Verde*. PhD Thesis, University of Murcia, Spain: 315 pp.

Eppley, R. 1972. Temperature and phytoplankton growth in the sea. *Fishery Bulletin*, Vol. 70 (4), pp. 1063–1085.

Espino, F., Tuyá, F., Blanch, I. and Haroun, R. J. 2008. *Los sebadales de Canarias. Oasis de vida en los fondos arenosos*. BIOGES, University of Las Palmas de Gran Canaria, Spain: 68 pp.

Etheridge, S. M. 2010. Paralytic shellfish poisoning: seafood safety and human health perspectives. *Toxicon*, Vol. 56, pp. 108-122.

Evan, A. T., Dunion, J., Foley, J. A., Heidinger, A. K. and Velden, C. S. 2007. New evidence for a relationship between Atlantic tropical cyclone activity and African dust outbreaks. *Geophysical Research Letters*, Vol. 33.

Fabry, V. J., Seibel, B. A., Feely, R. A. and Orr, J. C. 2008. Impacts of ocean acidification on marine fauna and ecosystem processes. *ICES Journal of Marine Science*, Vol. 65, pp. 414–432.

Falkowski, P. G. 1994. The role of phytoplankton photosynthesis in global biogeochemical cycles. *Photosynthesis Research*, Vol. 39 (3), pp. 235–258.

Falkowski, P. G., Barber, R. T. and Smetacek, V. 1998. Biogeochemical Controls and Feedbacks on Ocean Primary Production. *Science*, Vol. 281 (5374), pp. 200–206. doi:10.1126/science.281.5374.200.

FAO. 1987. *Report of the first ad hoc Working Group on seabreams (Sparidae) stocks in the Northern CECAF zone*. FAO, Rome. CECAF/ECAF Series 86/38: 442 pp.

FAO. 1992. *Groupe de travail COPACE sur les resources démersales du plateau et du talus continental de la Guinée-Bissau, de la Guinée et de la Sierra Leone. Conakry, 4-9 February 1991*. FAO, Rome. COPACE/PACE Séries 91/54: 206 pp.

FAO. 2006. *Report of the FAO/CECAF Working Group on the Assessment of Demersal Resources, Subgroup North; Saly, Senegal, 14-23 September 2004*. FAO, Rome. CECAF/ECAF Series 06/68: 219 pp.

FAO. 2012a. *The State of World Fisheries and Aquaculture 2012.* Rome: 209 pp. http://www.fao.org/docrep/016/i2727e/i2727e00.htm (Accessed 17 April 2015).

FAO. 2012b. *Report of the FAO/CECAF Working Group on the Assessment of Demersal Resources – Subgroup North Banjul, the Gambia, 6-14 November 2007*. FAO, Rome. CECAF/ECAF Series 10/71: 302 pp.

FAO. 2012c. *Report of the FAO/CECAF Working Group on the Assessment of Demersal Resources—Subgroup South, Freetown, Sierra Leone, 9-18 October 2008*. FAO, Rome. CECAF/ECAF Series 11/73: 311 pp.

FAO. 2014a. *The State of World Fisheries and Aquaculture 2014*. Rome: 223 pp.

FAO. 2014b. *Protection du Grand écosystème marin du courant des Canaries (CCLME). Analyse Diagnostique Transfrontalière (ADT)*. Provisional document. FAO and UNEP, Dakar: 168 pp.

FAO. 2014c. FishStatJ program. FAO Fisheries and Aquaculture Department, Statistics and Information Service FishStatJ: Universal software for fishery statistical time series. Copyright 2011.

FAO. In press a. *Report of the FAO Working Group on the Assessment of Small Pelagic Fish off Northwest Africa. Banjul, Gambia, 19-24 May 2014.* FAO Fisheries and Aquaculture Report.

FAO. In press b. *Report of the FAO/CECAF Working Group on the Assessment of Demersal resources- Subgroup South. Accra, Ghana, 15-24 November 2011*. FAO, Rome. CECAF/ECAF Series.

FAO. In press c. Report of the FAO/CECAF Working Group on the Assessment of Demersal resources- Subgroup North. Fuengirola, Spain, 18-27 November 2013. FAO, Rome. CECAF/ECAF Series.

Faure, M. L. 1951. Le zooplancton de la zone côtière du Maroc. Année 1950. Conseil International pour l'Exploration de la Mer. *Annale Biologie*, Vol. 8, pp. 66-68.

Faure, V., Inejih, C. A., Demarcq, H. and Cury, P. 2000. The importance of retention processes in upwelling areas for recruitment of *Octopus vulgaris*: the example of the Arguin Bank (Mauritania). *Fish Oceanography*, Vol. 9 (4), pp. 343-355.

Feely, R. A., Sabine, C. L., Lee, K., Berelson, W., Kleypas, J., Fabry, V. J. and Millero, F. J. 2004. Impact of anthropogenic CO_2 on the $CaCO_3$ system in the oceans. *Science*, Vol. 305 (5682), pp. 362-366.

Feely, R. A., Sabine, C. L., Hernandez-Ayon, J. M., Lanson, D. and Hales, B. 2008. Evidence for upwelling of corrosive 'acidified' water onto the continental shelf. *Science*, Vol. 320, pp. 1490.

Feely, R. et al. 2010. An international observational network for ocean acidification. In: *Proceedings of the OceanObs'09: Sustained Ocean Observations and Information for Society Conference (Vol. 2), Venice, Italy, 21-25 September 2009.* Hall, J., Harrison, D. E. and Stammer, D. (eds). ESA Publication WPP-306. doi:10.5270/OceanObs09.cwp.29.

Feldman, G. et al. 1989. Ocean color: availability of the global data set. *Eos, Transactions American Geophysical Union*, Vol. 70 (23), pp. 634–641.

Fenoglio-Marc, L. and Tel, E. 2010. Coastal and global sea level change. *Journal of Geodynamics*, Vol. 49, pp. 151–160.

Fernández, L., Ramos, A. and González, R. 1998. *La pesquería de volanta en aguas del reino de Marruecos*. Instituto Español de Oceanografía, Spain. Informes Técnicos, No. 170: 84 pp.

Fernández, L., Salmerón, F. and Ramos, A. 2004. Change in elasmobranchs and other incidental species in the Spanish deepwater black hake trawl fishery off Mauritania. *Journal of Northwest Atlantic Fishery Science*, Vol. 35, pp. 325-331.

Fernández, A., Mouriño-Carballido, B., Bode, A., Varela, M. and Marañón, E. 2010. Latitudinal distribution of *Trichodesmium* spp. and N_2 fixation in the Atlantic Ocean. *Biogeosciences*, Vol. 7, pp. 3167−3176.

Fernández de Puelles, M. L. 1986. *Ciclo anual de la comunidad de micro y mesozooplancton, biomasa, estructura, relaciones tróficas y producción en aguas de las islas Canarias*. PhD Thesis, Autonomous University of Madrid: 375 pp.

Fernández de Puelles, M. L. and García-Braun, J. A. 1989. *Dinámica de las comunidades planctónicas en una zona del Atlántico subtropical. Boletín del Instituto Español de Oceanografía*, Vol. 5 (2), pp. 87-100.

Fernández-Peralta, L. 2009. Pêcherie des merlus du Sénégal. Informe Técnico. Banco Mundial, Agencia de Cooperación Francesa and Agencia de Cooperación Española and Desarrollo (AECID), Dakar (Senegal): 50 pp.

Fernández-Peralta, L., Hernández, C., Faraj, A. and Bouzouma, M. 2008. Deep-demersal fish assemblages in the Canary Current ecosystem. *Eastern boundary Upwelling Ecosystems Symposium, Las Palmas de Gran Canaria (Spain), 2-6 June 2008*.

Fernández-Peralta, L., Rey, J. and Puerto, M. A. 2011a. Demersal fish (hake, other finfish and elasmobranchs) stocks exploited by the European fleet under Fisheries Partnership Agreements signed with Morocco, Mauritania and Guinea Bissau. Scientific, Technical and Economic Committee for Fisheries (STECF) Plenary Meeting. Scientific Advice for Fisheries Partnership Agreements Copenhagen, Denmark: 130 pp.

Fernández-Peralta, L., Salmerón, F., Rey, J., Puerto, M. A. and García-Cancela, R. 2011b. Reproductive biology of black hakes (*Merluccius polli* and *M. senegalensis*) off Mauritania. Ciencias Marinas, Vol. 37 (4B), pp. 527–546.

Fernández-Peralta, L., García-Cancela, R., Hernández-González, C., Manchih, K., Meiners, C., Pascual, P., Puerto, M. A., Rey, J. and Salmerón, F. 2012. Fish Fauna Collection online databases off Mauritania. Marine Fauna Collection of the Oceanographic Centre of Malaga (CFM-IEOMA). Instituto Español de Oceanografía. (http://www.gbif.org/dataset/4704d25f-7944-4c1b-89bb-ed4a2007085b/ (accessed on 15 April 2014).

Fernández-Peralta, L. and Puerto González, M. A. submitted. Demersal ichthyofaunal assemblages in Mauritanian waters. In: *Deep-sea ecosystems off Mauritania: Researching marine biodiversity and habitats in West African deep-water*s. Ramos, A., Sanz, J. L. and Ramil, F. (eds). Springer, Heidelberg.

Fernández-Peralta, L., Quintanilla, L. F. and Rey, J. submitted. Overlapped distribution of two sympatric species: the case of black hakes, *Merluccius polli* Cadenat 1960 and *Merluccius senegalensis* Cadenat 1960, off Mauritania. In: *Deep-sea ecosystems off Mauritania: Researching marine biodiversity and habitats in West African deep-waters*. Ramos, A., Sanz, J. L. and Ramil, F. (eds). Springer, Heidelberg.

Fertl, D., Jefferson, T. A., Moreno, I. B., Zerbini, A. N. and Mullin, K. D. 2003. Distribution of the Clymene dolphin *Stenella clymene. Mammal Review*, Vol. 33(3), pp. 253-271.

Field, C. B., Behrenfeld, M. J., Randerson, J. T. and Falkowski, P. 1998. Primary Production of the Biosphere: Integrating Terrestrial and Oceanic Components. *Science*, Vol. 281 (5374), pp. 237–240. doi:10.1126/science.281.5374.237.

Fischer, G. and Karakas, G. 2009. Sinking rates and composition of particles in the Atlantic Ocean: implications for the organic carbon fluxes to the deep ocean. *Biogeosciences*, Vol. 6, pp. 85–102.

Fischer, G., Reuter, C., Karakas, G., Nowald, N. and Wefer, G. 2009. Offshore advection of particles within the Cape Blanc filament, Mauritania: Results from observational and modelling studies. In: *Eastern Boundary Upwelling systems: Integrative and Comparative Approaches*. Freon, P., Barange, M., Arístegui, J. and McIntyre, A. D. (eds). Special Edition, *Progress in Oceanography*, Vol. 83 (1-4), pp. 322-330. doi:10.1016/j.pocean.2009.07.023.

Fiuza, A. F. and Halpern, D. 1982. Hydrographic observations of the Canary Current between 21 N and 25.5 N in March/April 1974. *Rapport et Proces-Verbaux Des Reunions Conseil International Pour l'Exploration de La Mer*, Vol. 180, pp. 58.

Fomba, K. W., Müller, K., van Pinxteren, D., Poulain, L., van Pinxteren, M. and Herrmann, H. 2014. Long-term chemical characterization of tropical and marine aerosols at the Cape Verde Atmospheric Observatory (CVAO) from 2007 to 2011. *Atmospheric Chemistry and Physics,* Vol. 14, pp. 8883-8904. doi:10.5194/acp-14-8883-2014.

Foote, A. D., Newton, S. B., Piertney, E., Willerslev, E. and Gilbert, M. T. P. 2009. Ecological, morphological and genetic divergence of sympatric North Atlantic killer whale populations. *Molecular Ecology*, Vol.18, pp. 5207-5217.

Foreman, F. G. G. 1977. Manual for tidal heights analysis and predictions. *Pacific Marine Science Report,* 77-10, Institute of Ocean Sciences, Patricia Bay, Sidney, B.C.: 58 pp. (2004 revision).

Forster, P. et al. 2007. Changes in atmospheric constituents and in radiative forcing. In: *Climate Change 2007: The Physical Science Basis. Contribution of Working Group I to the Fourth Assessment Report of the Intergovernmental Panel on Climate Change*. Solomon, S., Qin, D., Manning, M., Chen, Z., Marquis, M., Averyt, K. B., Tignor, M. and Miller, H. L. (eds). Cambridge University Press, Cambridge, pp. 129–234.

Fortes, O., Pires, A. J. and Bellini, C. 1998 Green turtle, *Chelonia mydas*, in the island of Poilão, Bolama-Bijagós Archipelago, Guinea-Bissau, West Africa. *Marine Turtle Newsletter*, Vol. 80, pp. 8–10.

Fraga, F. 1974. Distribution des masses d'eau dans l'upwelling de Mauritanie. *Tethys*, Vol. 6 (1-2), pp. 5–10.

Fraga, F., Ríos, A. F., Pérez, F. F. and Figueiras, F. G. 1998. Theoretical limits of oxygen: Carbon and oxygen: nitrogen ratios during photosynthesis and mineralization of organic matter in the sea. *Scientia Marina*, Vol. 62, pp. 161–168.

Fraga, S., Rodríguez, F., Caillaud, A., Diogéne, J., Raho, N. and Zapata, M. 2011. *Gambierdiscus excentricus* sp. nov. (Dinophyceae), a benthic toxic dinoflagellate from the Canary Islands (NE Atlantic Ocean). *Harmful Algae*, Vol. 11, pp. 10-22.

Fraga, S. and Rodríguez, F. 2014. Genus *Gambierdiscus* in the Canary Islands (NE Atlantic Ocean) with description of *Gambierdiscus silvae* sp. nov., a new potentially toxic epiphytic benthic dinoflagellate. *Protist*, Vol. 165, pp. 839-853.

Fraile-Nuez, E., Machín, F., Vélez-Belchí, P., López-Laatzen, F., Borges, R., Benítez-Barrios, V. and Hernández-Guerra, A. 2010. Nine years of mass transport data in the eastern boundary of the North Atlantic Subtropical Gyre. *Journal of Geophysical Research: Oceans*, Vol. 115. doi: 10.1029/2010JC006161.

Francois, R., Honjo, S. and Krishfield R., S. M. 2002. Factors controlling the flux of organic carbon to the bathypelagic zone of the ocean. *Global Biogeochemical Cycles*, Vol. 16, pp. 1087. doi:10.1029/2001GB001722.

Franqueville, C. and Freon, P. 1976. *Rélations poids-longueurs des principales espèces de poissons marins au Sénégal*. Centre de Recherches Océanographiques de Dakar-Thiaroye. Scientific Document No. 60: 37 pp.

Fransen, C. H. J. M. 1991. *Preliminary report on Crustacea collected in the eastern part of the North Atlantic during the CANCAP and MAURITANIA Expeditions of the former Rijksmuseum van Natuurlijke Historie, Leiden*. Nationaal Natuurhistorisch Museum, Leiden: 200 pp.

Fréon, P. 1988. *Réponses et adaptations des stocks de clupéidés d'Afrique de l'ouest à la variabilité du milieu et de l'exploitation: Analyse et réflexion à partir de l'exemple du Sénégal*. PhD Thesis, University of Aix-Marseille: 287 pp.

Fretey, J. 2001. *Biogeography and Conservation of Marine Turtles of the Atlantic Coast of Africa/Biogéographie et conservation des tortues marines de la côte Atlantique de l'Afrique*. UNEP/CMS Secretariat, Bonn, Germany. CMS Technical Series, No. 6: 429 pp.

Freudenthal, T., Neuer, S., Meggers, H., Davenport, R. and Wefer, G. 2001. Influence of lateral particle advection and organic matter degradation on sediment accumulation and stable nitrogen isotope ratios along a productivity gradient in the Canary Islands region. *Marine Geology*, Vol. 177, pp. 93–109.

Frick, M. G., Williams, K. L., Bolten, A. B., Bjorndal, K. A. and Martins, H. R. 2009. Foraging ecology of oceanic-stage loggerhead turtles *Caretta caretta*. *Endangered Species Research*, Vol. 9, pp. 91–97.

Froese, R. and Pauly, D. (eds). 2008. FishBase. World Wide Web electronic publication. www.fishbase.org.

Froese, R. and Pauly, D. (eds). 2015. FishBase. World Wide Web electronic publication. www.fishbase.org, version (02/2015) (Accessed on 15 March 2015).

Fröhlich, L., Fink, A. H., Knippertz, P. and Hohberger, E. 2013. An objective climatology of tropical plumes. *Journal of Climate*, Vol. 26 (14), pp. 5044-5060.

Fuller, P. L., Knott, D. M., Kingsley-Smith, P. R., Morris, J. A., Buckel, C. A., Hunter, M. E. and Hartman, L. D. 2014. Invasion of the Asian tiger shrimp, *Penaeus monodon* Fabicius, 1798, in the western north Atlantic and Gulf of Mexico. *Aquatic Invasions*, Vol. 9, pp. 59-70.

Funck, T. and Schmincke, H. U. 1998. Growth and destruction of Gran Canaria deduced from seismic reflection and bathymetric data. *Journal of Geophysical Research, Solid Earth*, Vol. 103, pp. 15393-15407.

Furey, A., O'Doherty, S., O'Callaghan, K., Lehane, M. and James, K. J. 2010. Azaspiracid poisoning (AZP) toxins in shellfish: toxicological and health considerations. *Toxicon*, Vol. 56, pp. 173-190.

Furnestin, M. L. 1957. Chaetognathes et zooplancton du secteur Atlantique marocain. *Revue des Travaux de l'Institut Technique et Scientifique des Pêches Maritimes*, Vol. 21 (1): 356 pp.

Furnestin, M. L. 1960. Observations sur quelques échantillons de zooplancton d'Afrique occidentale. *Bulletin de l'IFAN*, Vol. 22 A (1), pp. 142-151.

Furnestin, M. L. 1976. Les copépodes du plateau continental marocain et du détroit canarien. I. Répartition quantitative. *Conseil International pour l'Exploration de la Mer*, Vol. 8, pp. 22-46.

Gabric, A. J., García, L., Van Camp, L., Nykjaer, L., Eifler, W. and Schrimpf, W. 1993. Offshore export of shelf production in the Cape Blanc (Mauritania) giant filament as derived from coastal zone color scanner imagery. *Journal of Geophysical Research*, Vol. 98, pp. 4697–4712. doi:10.1029/92JC01714.

Gabric, A. J., Eifler, W. and Schrimpf, W. 1996. A Lagrangian model of phytoplankton dynamics in the Northwest African coastal upwelling zone. *Advances in Space Research*, Vol. 18, pp. 99–115.

Gac, J. Y. and Kane, A. 1986. Le fleuve Sénégal: Bilan hydrologique et flux continentaux de matières particulaires à l'embouchure. *Sciences géologiques bulletin,* Vol. 39 (1), pp. 99–130.

Gage, J. D. and Tyler, P. A. *1991. Deep-Sea Biology: A Natural History of Organisms at the Deep-Sea Floor*. Cambridge University Press, Cambridge: 524 pp.

Galeron, J., Sibuet, M., Mahaut, M. L. and Dinet, A. 2000. Variation in structure and biomass of the benthic communities at three contrasting sites in the tropical Northeast Atlantic. *Marine Ecology Progress Series*, Vol. 197, pp. 121-137.

Galil, B. S. 2000. Crustacea Decapoda: Review of the genera and species of the family Polychelidae Wood-Mason, 1874. In: *Résultats des Campagnes Musorstom*, Vol. 21. Crosnier, A. (ed.). Mémoires du Muséum national d'Histoire naturelle, No. 184, Paris, pp. 285-387.

Gambell, R. 1985. Fin whale *Balaenoptera physalus* Linnaeus, 1758. In: *Handbook of Marine Mammals. The Sirenians and Baleen Whales*, Vol. 3. Ridgway, S. H. and Harrison, R. (eds). Academic Press, London, pp. 171-192.

Gaona, P., Varo-Cruz, N., Abella, E., López, O., Marco, A. and López-Jurado, L. F. In press. Estimation of survival for loggerhead sea turtles nesting in Cape Verde using multi-state models with unobservable states. *Proceedings of the Thirty-Second Annual Symposium on Sea Turtle Biology and Conservation*. NOAA Technical Memorandum.

Garcia, S. (ed.) 1982. Distribution, migration and spawning of the main fish resources in the northern CECAF area. FAO, Rome. CECAF/ECAF Series 82/25: 9 pp.

García, S. 1988. Tropical penaeid prawns. In: *Fish population dynamics* (Second Edition). Gulland, J. A. (ed.). John Wiley and Sons, New York, pp. 219-249.

García-Isarch, E., Burgos, C., Sobrino, I., Mendes de Almeida, A., Barri, I., Assau V., Gomes Correia, R. and Joaquim Gomes, M. 2011. Informe de la campaña de evaluación de recursos demersales de la ZEE de Guinea Bissau a bordo del B/O Vizconde de Eza "Guinea Bissau 0810". Instituto Español de Oceanografía (IEO) and Centro de Investigaçao Pesqueira Aplicada (CIPA): 204 pp. (unpublished).

García-Isarch, E., de Matos-Pita, S. S., Muñoz, I., Mohamed, S. and Ramil, F. Submitted. Decapod assemblages in Mauritanian waters. In: *Deep-sea ecosystems off Mauritania: Researching marine biodiversity and habitats in West African deep-waters*. Ramos, A., Sanz, J. L. and Ramil, F. (eds). Springer, Heidelberg.

García-Lafuente, J., del Río, J., Alvarez-Fanjul, E., Gomis, D. and Delgado, J. 2004. Some aspects of the seasonal sea level variations around Spain. *Journal of Geophysical Research*, Vol. 109 (C9), C09008.

García-Muñoz, M., Arístegui, J., Montero, M. F. and Barton, E. D. 2004. Distribution and transport of organic matter along a filament–eddy system in the Canaries–NW Africa coastal transition zone region. *Progress in Oceanography*, Vol. 62 (1-4), pp. 115–129.

García-Muñoz, M., Arístegui, J., Pelegrí, J. L., Antoranz, A., Ojeda, A. and Torres, M. 2005. Exchange of carbon by an upwelling filament off Cape Ghir (NW Africa). *Journal of Marine Systems*, Vol. 54, pp. 83-95.

García-Reyes, M. and Largier, J. 2010. Observations of increased wind-driven coastal upwelling off central California. *Journal of Geophysical Research: Oceans*, Vol. 115 (C4), pp. C04011. doi:10.1029/2009JC005576.

Garrison, V. H. et al. 2003. African and Asian dust: From desert soils to coral reefs. *BioScience*, Vol. 53 (5), pp. 469-480.

Gascuel, D. and Ménard F. 1997. Assessment of a multispecies fishery in Senegal, using production models and diversity indices. *Aquatic Living Resources*, Vol. 10, pp.281-288.

Gascuel, D., Laurans, M., Sidibé, A. and Barry, M. D. 2004. Diagnostic comparatif de l'état des stocks & évolution d'abondance des resources démersales dans les pays de la C.S.R.P. In : *Pêcheries maritimes, écosystemes et sociétés en Afrique de l'Ouest: Un demi-siècle de changement.* Chavance, P., Bâ, M., Gascuel, D., Vakily, J. M. and Pauly, D. (eds). Collection des Rapports de recherche halieutique ACP-UE, No. 15, Vol. 1, pp. 205-223.

Gascuel, D., Bozec, Y. M., Chassot, E., Colomb, A. and Laurans, M. 2005. The trophic spectrum: theory and application as an ecosystem indicator. *ICES Journal of Marine Science,* Vol. 62, pp. 443-452.

Gascuel, D., Labrosse, P., Meissa, B., Taleb Sidi, M. O. and Guénette, S. 2007. Decline of demersal resources in North-West Africa: an analysis of Mauritanian trawl-survey data over the past 25 years. *African Journal of Marine Science*, Vol. 29 (3), pp. 331-345.

Gattuso, J. -P., Bijma, J., Gehlen, M., Riebesell, U. and Turley, C. 2011. Ocean acidification: knowns, unknowns, and perspectives. In: *Ocean Acidification*. Gattuso, J. -P. and Hansson, L. (eds). Oxford University Press, Oxford, pp. 291-311.

Gaube, P., Chelton, D. B., Strutton P. G. and Behrenfeld, M. J. 2013. Satellite observations of chlorophyll, phytoplankton biomass, and Ekman pumping in nonlinear mesoscale eddies. *Journal of Geophysical Research*, Vol. 118 (12), pp. 6349–6370.

Gaudechoux, J. P. and Richer de Forges, B. 1983. *Inventaire Ichthyologique des eaux mauritaniennes*. Centre National de Recherches Océanographique et des Pêches Document No. 3: 22 pp.

Gaudy, R. and Seguin, G. 1964. Note sur la répartition annuelle des Copépodes pélagiques des eaux de Dakar. *Recueil des Travaux de la Station Marine D'Endoume*. Bulletin 34, Fascicule 50, pp. 211-217.

Gee, M. J. R., Masson, D. G., Watts, A. B. and Allen, P. A. 1999. The Saharan debris flow: an insight into the mechanics of long runout debris flows. *Sedimentology*, Vol. 46, pp. 317–335.

Gelado-Caballero, M. D., Rodríguez, M. J., Hernández, J. J., Brito de Azevedo, E. M., Llinás, O., Collado, C., Cardona, P. and López, P. 2005. Dust deposition fluxes to northeastern subtropical Atlantic (Canary Islands). *Geophysical Research Abstracts,* Vol. 7, 08399.

Gelado-Caballero, M. D., López-García, P., Prieto, S., Patey, M. D., Collado, C. and Hérnández-Brito, J. J. 2012. Long-term aerosol measurements in Gran Canaria, Canary Islands: Particle concentration, sources and elemental composition. *Journal of Geophysical Research D: Atmospheres*, Vol. 117, D03304. doi:10.1029/2011JD016646.

Geldmacher, J. and Hoernle, K. 2000. The 72 Ma geochemical evolution of the Madeira hotspot (eastern North Atlantic): recycling of Palaeozoic (≤500 Ma) basaltic and gabbroic crust. *Earth and Planetary Science Letters*, Vol. 183, pp.73-92.

Geldmacher, J., Hoernle, K., van den Bogaard, P. Zankl, G. and Garbe-Schönberg, D. 2001. Earlier history of the > 70 Ma-old Canary hotspot based on temporal and geochemical evolution of the Selvagens Archipelago and neighbouring seamounts in the eastern North Atlantic. *Journal of Volcanological and Geothermal Research*, Vol. 111, pp. 55-87.

Geldmacher, J., Hoernle, K., van den Bogaard, P., Duggen, S. and Werner, R. 2005. New 40K / 39Ar age and geochemical data from seamounts in the Canary and Madeira volcanic provinces: support for the mantle plume hypothesis. *Earth and Planetary Science Letters*, Vol. 237, pp. 85-101.

Geldmacher, J., Hoernle, K., Hanan, B. B., Blicher-Toft, J. Hauff, F., Gill, J. B. and Schmincke, H. U. 2011. Hafnium isotopic variations in East Atlantic intraplate volcanism. *Contributions to Mineralogy and Petrology,* Vol. 162 (1), pp. 21-36.

Gibbons, W. and Moreno, T. 2002. *The Geology of Spain*. Geological Society of London. London: 664 pp.

Ginoux, P., Chin, M., Tegen, I., Prospero, J. M., Holben, B., Dubovik, O. and Lin, S. J. 2001. Sources and distributions of dust aerosols simulated with the GOCART model. *Journal of Geophysical Research D: Atmospheres,* Vol. 106, pp. 20255-20273. doi:10.1029/2000JD000053.

Ginoux, P., Prospero, J. M., Torres, O. and Chin, M. 2004. Long-term simulation of global dust distribution with the GOCART model: Correlation with North Atlantic Oscillation. *Environmental Modelling and Software*, Vol. 19, pp. 113-128. doi:10.1016/S1364-8152(03)00114-2.

Ginoux, P., Prospero, J. M., Gill, T. E., Hsu, N. C. and Zhao, M. 2012. Global-scale attribution of anthropogenic and natural dust sources and their emission rates based on MODIS Deep Blue aerosol products. *Reviews of Geophysics,* Vol. 50, RG3005. doi:10.1029/2012RG000388.

Giresse, P. 2008. *Tropical and subtropical West Africa: Marine and continental changes during the late Quaternary*. Elsevier, Amsterdam, the Netherlands.

Glushko, O. G. and Lidvanov, V. V. 2012. Composition and Structure of the zooplankton in Coastal Waters of Mauritania in Winter. *Journal of Siberian Federal University, Biology*, Vol. 2, pp. 138-150.

Gobierno de Canarias. *Banco de Datos de Biodiversidad de Canarias.* http//:www.biodiversidadcanarias.es (Accessed 3 February 2015).

Godley, B. J., Barbosa, C., Bruford, M., Broderick, A. C., Catry, P., Coyne, M. S., Formia, A., Hays, G. C. and Witt, M. J. 2010. Unravelling migratory connectivity in marine turtles using multiple methods. *Journal of Applied Ecology,* Vol. 47, pp. 769–778.

Goebel, N. L., Edwards, C. A., Zehr, J. P. and Follows, M. J. 2010. An emergent community ecosystem model applied to the California Current System. *Journal of Marine Systems*, Vol. 83 (3–4), pp. 221–241. doi:10.1016/j.jmarsys.2010.05.002.

Goebel, N. L., Edwards, C. A., Zehr, J. P., Follows, M. J. and Morgan, S. G. 2013. Modeled phytoplankton diversity and productivity in the California Current System. *Ecological Modelling*, Vol. 264, pp. 37–47. doi:10.1016/j.ecolmodel.2012.11.008.

Gómez, F., Echevarría, F., García, C. M., Prieto, L., Ruiz, J., Reul, A., Jiménez-Gómez, F. and Varela, M. 2000. Microplankton distribution in the Strait of Gibraltar: coupling between organisms and

hydrodynamic structures. *Journal of Plankton Research*, Vol. 22 (4), pp. 603-617.

Gómez-Lahoz, M. and Carretero-Albiach, J. C. 2005. Wave Forecasting at the Spanish Coasts. *Journal of Atmospheric and Ocean Science*, Vol. 10 (4), pp. 389-405.

González, A. F., Rasero, M. and Guerra, A. 1996. La explotación de los omastréfidos *Illex coindetii* y *Todaropsis eblanae* (Mollusca, Cephalopoda) en aguas de Galicia. *Nova Acta Científica Compostelana* (*Bioloxia*), Vol. 6, pp. 191-203.

González, A. F. and Guerra, A. 2013. *Illex coindetii*, Broadtail Shortfin Squid. In: *Advances in Squid Biology, Ecology and Fisheries,* Part II. Rosa, R., Pierce, G. and O'Dor, R. (eds.). Nova Science Publishers, New York, pp. 49-71.

Gonzalez-Dávila, M., Santana-Casiano, J. M., Rueda, M. J., Llinás, O. and Gonzalez-Dávila, E. F. 2003. Seasonal and interannual variability of sea surface carbon dioxide species at the European Station for Time Series in the Ocean at the Canary Islands (ESTOC) between 1996 and 2000. *Global Biogeochemical Cycles,* Vol. 17 (3), No. 1076. doi:10.1029/2002GB001993.

González-Dávila, M., Santana-Casiano, J. M. and González-Dávila, E. 2007. Interannual variability of the upper ocean carbon cycle in the northeast Atlantic Ocean. *Geophysical Research Letter,* Vol. 34, L07608. doi:10.1029/2006GL028145.

Gonzalez-Dávila, M., Santana-Casiano, J. M., Rueda, M. J. and Llinás, O. 2010. The water column distribution of carbonate system variables at the ESTOC site from 1995 to 2004. *Biogeosciences,* Vol. 7, pp. 3067–3081.

González-Dávila, M., Santana-Casiano, J. M. and Machin, F. 2014. Seasonal air-sea CO2 fluxes off Northwest Africa. *Geophysical Research Abstracts,* Vol. 16, EGU2014-2734.

González-Porto, M. et al. 2007. A first approach at macroscale level to biodiversity and distribution of deep megabenthic communities from Atlantic Moroccan coast: Megabenthos of Maroc's Surveys. *ISMCC-07 and GLOBEC-IMBER*, Valencia (Spain), 28-31 March 2007.

González-Porto, M., Assau, V., Hernández-González, C. L., de Matos-Pita, S. S., Ramil, F. and Ramos, A. 2010. Biodiversidad del megabentos en aguas de Guinea-Bissau. *XVI SIEBM*, Alicante (Spain), 6-10 September 2010.

Good, S. A., Corlett, G. K., Remedios, J. J., Noyes, E. J. and Llewellyn-Jones, D. T. 2007. The Global Trend in Sea Surface Temperature from 20 Years of Advanced Very High Resolution Radiometer Data. *Journal of Climate*, Vol. 20 (7), pp. 1255–1264. doi:10.1175/JCLI4049.1.

Gordon, A., Weiss, R., Smethie Jr, W. and Warner, M. 1992. Thermocline and intermediate water communication between the South Atlantic and Indian Oceans. *Journal of Geophysical Research*, Vol. 97, pp. 7223-7240.

Gosselk, F. 1974. A quantitative survey of the macro- benthos communities on the continental shelf off North-West-Africa. *ICES,* CM/1974/K30, pp. 1-3.

Goudie, A. S. and Middleton, N. J. 2001. Saharan dust storms: nature and consequences. *Earth-Science Reviews*, Vol. 56*,* pp. 179-204. doi: 10.1016/s0012-8252(01)00067-8.

Granado Lorencio C. 1996. *Ecología de peces*. Universidad de Sevilla, Secretariado de publicaciones, Spain. Serie Ciencias, No. 45: 353 pp.

Grant, W. E., Griffin, W. L. and Warren, J. P. 1981. A Management Model of the Northwest African Cephalopod Fishery. *Marine Fisheries Review*, Vol. 43 (11), pp. 1-10.

Gregg, W. W., Casey, N. W., O'Reilly, J. E. and Esaias, W. E. 2009. An empirical approach to ocean color data: Reducing bias and the need for post-launch radiometric re-calibration. *Remote Sensing of Environment*, Vol. 113 (8), pp. 1598–1612. doi:10.1016/j.rse.2009.03.005.

Gregg, W. W. and Casey, N. W. 2010. Improving the consistency of ocean color data: A step toward climate data records. *Geophysical Research Letters*, Vol. 37 (4), pp. L04605. doi:10.1029/2009GL041893.

Gregg, W. W. and Rousseaux, C. S. 2014. Decadal trends in global pelagic ocean chlorophyll: A new assessment integrating multiple satellites, in situ data, and models. *Journal of Geophysical Research: Oceans*, Vol. 119 (9), pp. 5921–5933. doi:10.1002/2014JC010158.

Griffin, D. W. and Kellogg, C. A. 2004. Dust Storms and Their Impact on Ocean and Human Health: Dust in Earth's Atmosphere. *EcoHealth*, Vol. 1, pp. 284-295. doi:10.1007/s10393-004-0120-8.

Grist, J. P. and Nicholson, E. 2001. A study of the dynamic factors influencing the rainfall variability in the West African Sahel. *Journal of Climate*, Vol. 14 (7), pp. 1337–1359.

Gruber, N., Hauri, C., Lachkar, Z., Loher, D., Frölicher, T. L. and Plattner, G. K. 2012. Rapid progression of ocean acidification in the California Current System. *Science*, Vol. 337, pp. 220-223.

Gruvel, A. 1925. Sur une carte de pêche d'une partie de la côte occidentale du Maroc. *Comptes Rendus de l'Académie des Sciences*, Paris, Vol. 181, No. 15, pp. 469-470.

Gruvel, A. 1929. Sur une carte de pêche d'une partie de la côte occidentale du Maroc. *Comptes Rendus de l'Académie des Sciences*, Paris, Vol. 189, No. 24, pp. 1065-1067.

Guerra, A., González, A. F., Roeleveld, M. and Jereb, P. 2014. Cephalopods. In: *The living resources of the Eastern Central Atlantic, Vol. 1: Introduction, crustacean, chitons and cephalopods*. Carpenter, K. E. and De Angelis, N. (eds). FAO Species Identification Guide for Fisheries Purposes, Rome, pp. 369-638.

Gurenko, A. A., Hoernle, K. A., Hauff, F., Schmincke, H. U., Han, D., Miura, Y. N. and Kaneoka, I. 2006. Major, trace element and Nd-Sr-Pb-O-He-Ar isotope signatures of shield stage lavas from the central and western Canary Islands: insights into mantle and crustal processes. *Chemical Geology,* Vol. 233, pp. 75-112.

Gurenko, A. A., Sobolev, A. V., Hoernle, K. A., Hauff, F. and Schmincke, H. U. 2009. Enriched, HIMU-type peridotite and depleted recycled pyroxenite in the Canary plume: a mixed-up mantle. *Earth and Planetary Science Letters,* Vol. 277, pp. 514-524.

Gutiérrez, M., Casillas, R., Fernández, C., Balogh, K., Ahijado, A., Castillo, C., Colmenero, J. R. and García-Navarro, E. 2006. The submarine volcanic succession of the Basal Complex of Fuerteventura, Canary Islands: a model of submarine growth and emersion of some tectonic volcanic islands. *Geological Society of America Bulletin,* Vol. 118 (7-8), pp. 785-804.

Haddon, M. 2001. *Modelling and quantitative methods in fisheries*. Chapman & Hall/CRC: 406 pp.

Haedrich, R. L. and Merrett, N. R. 1990. Little evidence for faunal zonation or communities in deep sea demersal fish faunas. *Progress in Oceanography,* Vol. 24, pp. 239-250.

Hagen, E., Zülicke, C. and Feistal, R. 1996. Near surface structures in the Cape Ghir filament off Morocco. *Oceanologica Acta*, Vol.19, pp. 577–598.

Hagen, E., Feistel, R., Agenbag, J. J. and Ohde, T. 2001. Seasonal and interannual changes in Intense Benguela Upwelling (1982–1999). *Oceanologica Acta,* Vol. 24, pp. 557–568.

Hamann, M., Limpus, C. J. and Owens, D. W. 2003. Reproductive cycles of males and females. In: *The Biology of Sea Turtles*, Vol. 2. Lutz, P. L., Musick, J. A. and Wyneken, J. (eds). CRC Marine Biology Series, CRC Press, Boca Raton, London, New York, Washington D.C.: 455 pp.

Hamann, M. et al. 2010. Global research priorities for sea turtles: informing management and conservation in the 21st century. *Endangered Species Research*, Vol. 11, pp. 245–269.

Hammond, P. S. and Lockyer, C. 1988. Distribution of killer whales in the eastern North Atlantic. In: *North Atlantic killer whale*s, Vol. 1. Sigurjónsson, J. and Leatherwood, S. (eds). Rit Fiskideildar, pp. 24-41.

Hansell, D. A. 2013. Recalcitrant dissolved organic carbon fractions. *Annual Reviews of Marine Sciences*, Vol. 5, pp. 3.1–3.25.

Hansell, D. A., Carlson, C. A., Repeta, D. J. and Schlitzer, R. 2009. Dissolved organic matter in the ocean: New insights stimulated by a controversy. *Oceanography*, Vol. 22, pp. 52–61.

Hansen, J., Sato, M., Ruedy, R., Lo, K., Lea, D. W. and Medina-Elizade, M. 2006. Global temperature change. *Proceedings of the National Academy of Sciences of the United States of America*, Vol. 103 (39), pp. 14288–14293. doi:10.1073/pnas.0606291103.

Harrison, S. P., Kohfeld, K. E., Roelandt, C. and Claquin, T. 2001. The role of dust in climate changes today, at the last glacial maximum and in the future. *Earth-Science Reviews,* Vol. 54, pp. 43-80.

Harrison, D. E. and Carson, M. 2007. Is the World Ocean Warming? Upper-Ocean Temperature Trends: 1950–2000. *Journal of Physical Oceanography*, Vol. 37 (2), pp. 174–187. doi:10.1175/JPO3005.1.

Hashioka, T. et al. 2013. Phytoplankton competition during the spring bloom in four plankton functional type models. *Biogeosciences*, Vol. 10, pp. 6833-6850. doi:10.5194/bg-10-6833-2013.

Hastenrath, S. and Lamb, P. J. 1977. *Climatic Atlas of the Tropical Atlantic and Eastern Pacific Oceans*. University of Wisconsin Press: 112 pp.

Hatanaka, H. 1979. Studies on the fisheries biology of common octopus off the northwest coast of Africa. *Bulletin Far Seas Fisheries Research Laboratory*, Vol. 17, pp. 13-124.

Hauri, C., Gruber, N., Plattner, G. K., Alin, S., Feely, R. A., Hales, B. and Wheeler, P. 2009. Ocean acidification in the California current system. *Oceanography,* Vol. 22 (4), pp. 60-71. doi:10.5670/oceanog.2009.97.

Hawkes, L. A., Broderick, A. C., Coyne, M. S., Godfrey, M. H., López-Jurado, L. F., López-Suarez, P., Merino, S. E., Varo-Cruz, N. and Godley, B. J. 2006. Phenotypically linked dichotomy in sea turtle foraging requires multiple conservation approaches. *Current Biology*, Vol. 16, pp. 990–995.

Hay, C., Morrow, E., Kopp, R. E. and Mitrovica, X. 2015. Probabilistic reanalysis of twentieth-century sea-level rise. *Nature*, Vol. 0 (1). LETTER. doi:10.1038/nature14093.

Haynes, R., Barton, E. D. and Pilling, I. 1993. Development, Persistence and Variability of Upwelling Filaments off the Atlantic Coast of Iberian Peninsula. *Journal of Geophysical Research*, Vol. 98, pp. 22681-22692.

Hays, G. C., Richardson, A. J. and Robinson, D. C. 2005. Climate change and marine plankton. *Trends in Ecology and Evolution*, Vol. 20, pp. 337–344.

Hazevoet, C. J. and Wenzel, F. W. 2000. Whales and dolphins (Mammalia, Cetacea) of the Cape Verde Islands, with special reference to the humpback whale *Megaptera novaeangliae* (Borowski, 1781). *Contributions to Zoology*, Vol. 69 (3), pp. 197-211.

Hazevoet, C. J., Monteiro, V., López, P., Varo, N., Torda, G., Berrow, S. and Gravanita, B. 2010. Recent data on whales and dolphins (Mammalia: Cetacea) from the Cape Verde Islands, including records of four taxa new to the archipelago. *Zoologia Caboverdiana*, Vol. 1 (2), pp. 75-99.

Head, E. J. H., Harrison, W. G., Irwin, B. I., Horne, E. P. W. and Li, W. K. W. 1996. Plankton dynamics and carbon flux in an area of upwelling off the coast of Morocco. *Deep-Sea Research Part I: Oceanographic Research Papers*, Vol. 43 (11-12), pp. 1713–1738. doi:10.1016/S0967-0637(96)00080-5.

Hedges, J. H. 2002. Why dissolved organic matter? In: *Biogeochemistry of Dissolved Organic Matter*. Hansell, D. A. and Carlson, C. A. (eds). Academic Press, pp. 1–27.

Heileman, S. and Tandstad, M. 2008. Canary Current LME. In: *UNEP Regional Seas Reports and Studies, No. 182*. *LMEs and Regional Seas*. United Nations Environment Programme. Nairobi.

Hein, J. R., Conrad, T. A. and Staudigel, H. 2010. Seamount mineral deposits: a source of rare metals for high-technology industries. *Oceanography*, Vol. 23, No. 1, pp. 184-189.

Heinold, B. et al. 2011. Regional modelling of Saharan dust and biomass burning smoke Part I: Model description and evaluation. *Tellus Series B Chemical and Physical Meteorology*, Vol. 63, pp. 781–799. doi:10.1111/j.1600-0889.2011.00570.x.

Helmke, P., Romero, O. and Fisher, G. 2005. Northwest African upwelling and its effect on offshore organic carbon export to the deep sea. *Global Biogeochemical Cycles*, Vol. 19. doi:10.1029/2004GB002265.

Hempel, G. (ed.). 1982. The Canary Current: Studies of an upwelling system. *Rapports et Procès-verbaux des Réunions du Conseil International pour l'Exploration de la Mer*, Vol. 180: 455 pp.

Hendriks, I. L., Duarte, C. M. and Alvarez, M. 2010. Vulnerability of marine biodiversity to ocean acidification: a meta analysis. *Estuarine Coastal Shelf Science*, Vol. 86, pp. 157-164.

Henrich, R., Hanebuth, T., Krastel, S., Neubert, N. and Wynn, R. 2008. Architecture and sediment dynamics of the Mauritania Slide Complex. *Marine and Petroleum Geology*, Vol. 25 (1), pp. 17-33.

Henrich, R., Cherubini, Y. and Meggers, H. 2010. Climate and sea level induced turbidite activity in a canyon system offshore the hyperarid Western Sahara (Mauritania): The Timiris Canyon. *Marine Geology*, Vol. 275, pp. 178-198.

Herbland, A. and Voituriez, B. 1974. La production primaire dans l'upwelling mauritanien en mars 1973. *Cahiers ORSTOM. Série Océanographie*, Vol. 12, (3), pp. 187–201.

Herman, J. R., Bhartia, P. K., Torres, O., Hsu, C., Seftor, C. and Celarier, E. 1997. Global distribution of UV-absorbing aerosols from Nimbus 7/TOMS data. *Journal Geophysical Research*, Vol. 102, pp. 16911-16922. doi: 10.1029/96jd03680.

Hernández, M. et al. 1998. Did algal toxins cause monk seal mortality? *Nature*, Vol. 393, pp. 28-29.

Hernández-González, C. L. 2007. *Informe preliminar de la campaña Maroc 0611 de prospección por arrastre de los recursos demersales profundos en aguas del sur de Marruecos*. Instituto Español de Oceanografía: 88 pp. (unpublished).

Hernández-González, C. L. et al. 2006. *Informe Final de la campaña MAROC 0511 para la prospección por arrastre de los recursos demersales profundos en aguas del centro de Marruecos*. Instituto Español de Oceanografía-Institut National des Recherches Halieutiques: 526 pp. (unpublished).

Hernández-González, C. L. et al. 2010. Informe de la Campaña 'Maurit-1107' de prospección por arrastre de los recursos demersales profundos en aguas de la República Islámica de Mauritania. Instituto Español de Oceanografía-Institut Mauritanien de Recherches Océanographiques et des Pêches: 416 pp. (unpublished).

Hernández-Guerra A. 1990. *Estructuras oceanográficas observadas en las aguas que rodean las islas Canarias mediante escenas de los sensores AWRR y CZCS*. PhD Thesis, University of Las Palmas de Gran Canaria, Spain.

Hernández-Guerra, A., Arístegui, J., Cantón, M. and Nykjaer, L. 1993. Phytoplankton pigments patterns in the Canary Islands as determined using Coastal Zone Colour Scanner Data. *International Journal of Remote Sensing*, Vol. 14, pp. 1431–1437.

Hernández-Guerra, A. and Nykjaer, L. 1997. Sea Surface temperatura variability off north-west Africa: 1981-1989. *International Journal of Remote Sensing*, Vol. 18, pp. 2539-2558.

Hernández-Guerra, A., López-Laatzen, F., Machín, F., de Armas, D. and Pelegrí, J. L. 2001. Water masses, circulation and transport in the eastern boundary current of the North Atlantic subtropical gyre. *Scientia Marina*, Vol. 65 (S1), pp. 177-186.

Hernández-Guerra, A. et al. 2002. Temporal variability of mass transport in the Canary Current. *Deep-Sea Research Part II: Topical Studies in Oceanography*, Vol. 49, pp. 3415-3426.

Hernández-Guerra, A., Fraile-Nuez, E., Borges, R., López-Laatzen, F., Vélez-Belchí, P., Parrilla, G. and Muller, T. 2003. Transport variability in the Lanzarote passage (eastern boundary current of the North Atlantic subtropical Gyre). *Deep-Sea Research Part I: Oceanographic Research Papers*, Vol. 50 (2), pp. 189–200. doi:10.1016/S0967-0637(02)00163-2.

Hernández-Guerra, A., Fraile-Nuez, E., López-Laatzen, F., Martínez, A., Parrilla, G. and Vélez-Belchí, P. 2005. Canary Current and North Equatorial Current from an inverse box model. *Journal of Geophysical Research: Oceans*, Vol. 110, C12019. doi:10.1029/2005JC003032.

Hernández-León, S. 1988a. Ciclo anual de la biomasa del mesozooplancton sobre un área de plataforma en aguas del Archipiélago Canario. *Investigación Pesquera*, Vol. 52 (1), pp. 3-16.

Hernández-León, S. 1988b. Gradients of mesozooplankton biomass and ETS activity in the wind-shear area as evidence of an island mass effect in the Canary Island waters. *Journal of Plankton Research*, Vol. 10 (6), pp. 1141-1154.

Hernández-León, S., Almeida, C., Gómez, M., Torres, S., Montero, I. and Portillo-Hahnefeld, A. 2001. Zooplankton biomass and indices of feeding and metabolism in island-generated eddies. *Journal of Marine Systems*, Vol. 30, pp. 51-66.

Hernández-León, S., Almeida, C., Portillo-Hahnefeld, A., Gómez, M., Rodríguez, J. M. and Arístegui, J. 2002. Zooplankton biomass and indices of feeding and metabolism in relation to an upwelling filament off northwest Africa. *Journal of Marine Research*, Vol. 60, pp. 327-346.

Hernández-León, S., Gómez, M. and Arístegui, J. 2007. Mesozooplankton in the Canary Current System: The Coastal-Ocean Transition Zone. *Progress in Oceanography*, Vol. 74, pp. 397-421.

Heywood, K. J., Stevens, D. P. and Bigg, R. B. 1996. Eddy formation behind the tropical island of Aldabra, *Deep-Sea Research Part I: Oceanographic Research Papers*, Vol. 43, pp. 555-578.

Hirata, T., Aiken, J., Hardman-Mountford, N., Smyth, T. J. and Barlow, R. G. 2008. An absorption model to determine phytoplankton size

classes from satellite ocean colour. *Remote Sensing of Environment*, Vol. 112 (6), pp. 3153–3159. doi:10.1016/j.rse.2008.03.011.

Hoernle, K. 1998. Trace element and Sr-Nd-Pb isotopic geochemistry of Jurassic ocean crust beneath Gran Canaria (Canary Islands): implications for the generation of OIB reservoirs and for crustal contamination of ascending OIB magmas. *Journal of Petrology,* 39, pp. 859-880.

Hoernle, K. and Tilton, G. 1991. Sr-Nd-Pb isotope data for Fuerteventura (Canary Islands) basal complex and subaerial volcanics: application to magma genesis and evolution. *Schweizerische Mineralogische und Petrographische Mitteilungen,* Vol. 71, pp. 5-21.

Hoernle, K. and Schmincke, H. U. 1993a. The petrology of the tholeiites through melilite nephelinites on Gran Canaria, Canary Islands: crystal fractionation, accumulation and depth of melting. *Journal of Petrology,* Vol. 34, pp.573-597.

Hoernle, K. and Schmincke H. U. 1993b. The role of partial melting in the 15 Ma geochemical evolution of Gran Canaria: a blob model for the Canary hotspot. *Journal of Petrology,* Vol. 34, pp. 599–626.

Hoernle, K., Zhang, Y. S. and Graham, D. 1995. Seismic and geochemical evidence for large-scale mantle upwelling beneath the eastern Atlantic and western and central Europe. *Nature, Vol.* 374, pp. 34-39.

Holgate, S. et al. 2013. New data systems and products at the permanent service for mean sea level. *Journal of Coastal Research*, Vol. 29, pp. 493-504.

Holik J. S., Rabinowitz P. D. and Austin J. A. 1991. Effects of Canary hot spot volcanism on structure of oceanic crust off Morocco. *Journal of Geophysical Research*, Vol. 9, pp. 12039-12067.

Holthuis, L. B. 1951. The caridean Crustacea of Tropical West Africa. *Atlantide Report. Scientific Results of the Danish Expedition to the Coasts of Tropical West Africa 1945-1946*, Vol. 2, pp. 7-187.

Holthuis, L. B. 1991. *FAO Species Catalogue, Vol. 13. Marine Lobsters of the World*. FAO, Rome. FAO Fisheries Synopsis, No. 125, Vol. 3: 292 pp.

Houghton, J. D. R., Doyle, T. K., Wilson, M. W., Davenport, J. and Haysa, G. C. 2006. Jellyfish aggregations and leatherback turtle foraging patterns in a temperate coastal environment. *Ecology*, Vol. 87, pp. 1967–1972.

Hourdin F. et al. 2010. AMMA-Model intercomparison project. *Bulletin of the American Meteorology Society*, Vol. 91, pp. 95-104.

Huntsman, S. A. and Barber, R. T. 1977. Primary production off northwest Africa: the relationship to wind and nutrient conditions. *Deep-Sea Research*, Vol. 24 (1), pp. 25–33. doi:10.1016/0146-6291(77)90538-0.

Huneeus, N. et al. 2011. Global dust model intercomparison in AeroCom phase I. *Atmospheric Chemistry and Physics*, Vol. 11, pp. 7781–7816. doi:10.5194/acp-11-7781-2011.

IEO. 2013a. *Caracterización del Banco de La Concepción*. Informe del Instituto Español de Oceanografía - Centro Oceanográfico de Canarias. Proyecto LIFE+ INDEMARES (LIFE07/NAT/E/000732). Coordination: Fundación Biodiversidad, Madrid: 278 pp.

IEO. 2013b. *Caracterización del Sur de Fuerteventura*. Informe del Instituto Español de Oceanografía - Centro Oceanográfico de Canarias. Proyecto LIFE+ INDEMARES (LIFE07/NAT/E/000732). Coordination: Fundación Biodiversidad, Madrid: 320 pp.

Ikeda, T. 1985. Metabolic rates of epipelagic marine zooplankton as a function of body mass and temperature. *Marine Biology*, Vol. 85, pp. 1-11.

IPCC. 2013. *Climate Change 2013: The Physical Science Basis. Contribution of Working Group I to the Fifth Assessment Report of the Intergovernmental Panel on Climate Change*. Stocker, T. F. et al. (eds). Cambridge University Press, Cambridge, United Kingdom and New York, NY, USA: 1535 pp.

IUCN. 2014. *IUCN Red List of Threatened Species*. Version 2014.2. www.iucnredlist.org (Accessed 30 December 2014).

Jacobi, R. D. and Hayes, D. E. 1982. Bathymetry, microphysiography and reflectivity characteristics of the West African Margin between Sierra Leone and Mauritania. In: *Geology of Northwest African Continental Margin*. Von Rad, W., Hinz, K., Sarnthein, M. and Seibold, E. (eds). Springer-Verlag, New York, pp. 182-210.

Jacobi, R. D. and Hayes, D. E. 1984. Echo character, microphysiography and geologic hazards. In: *Northwest African Continental Margin and Adjacent Ocean Floor off Morocco, Ocean Drilling Program, Regional Atlas Series*. Hayes, D. E., Rabinowitz, P. D. and Hinz, K. (eds). Woods Holes, MA.

Jacobi, R. D. and Hayes, D. E. 1992. Southwest African Plate Margin: Thermal History and Geodynamical Implications. In: *Geologic Evolution of Atlantic Continental Rises*. Van Nostrand Reinhold Ed., New York, pp. 293-326.

Jaenicke, R. 1979. Monitoring and critical review of the estimated source strength of mineral dust from the Sahara. In: *Saharan Dust: Mobilization, Transport, Deposition*. Morales, C. (eds). John Wiley and Sons, New York, pp. 233–242.

Jallow, A. O., Cham, A. M., Barnett, L. K. and Van Waerebeek, K. 2005. Conservation of cetaceans in The Gambia: Whale and Dolphin Field Research. In: *Proceedings from the First Biodiversity Research Symposium The Gambia, May 2005*. Barnett, L. (ed.). Makasutu Wildlife Trust, Darwin Initiative Project, pp. 37-54.

Jefferson, T. A., Curry, B. E., Leatherwood, S. and Powell, J. A. 1997. Dolphins and porpoises of West Africa: a review of records of Cetacea: Delphinidae, Phocoenidae. *Mammalia*, Vol. 61, pp. 87-108.

Jennings, S. 2004. The ecosystem approach to fishery management: a significant step towards sustainable use of the marine environment? *Marine Ecology Progress Series*, Vol. 274, pp. 279-282.

Jereb, P. and Roper, C. F. E. (eds). 2005. *Cephalopods of the world. An annotated and illustrated catalogue of cephalopod species known to date, Vol. 1. Chambered nautiluses and sepioids (Nautilidae, Sepiidae, Sepiolidae, Sepiadariidae, Idiosepiidae and Spirulidae)*. FAO, Rome. FAO Species Catalogue for Fishery Purposes, No. 4, Vol. 1, pp. 1-262.

Jereb, P. and Roper, C. F. E. (eds). 2010. *Cephalopods of the world. An annotated and illustrated catalogue of cephalopod species known to date, Vol. 2. Myopsid and Oegopsid squids*. FAO, Rome. FAO Species Catalogue for Fishery Purposes, No. 4, Vol. 2, pp.1-605.

Jereb, P., Roper, C. F. E., Norman, M. D. and Finn. J. K. (eds). 2013. *Cephalopods of the world. An annotated and illustrated catalogue of cephalopod species known to date, Vol. 3. Octopods and Vampire squids*. FAO, Rome. FAO Species Catalogue for Fishery Purposes, No. 4, Vol. 3, pp. 1-370.

Jia, Y., Calil, P. H. R., Chassignet, E. P.,Metzger, E. J., Potemra, J. T., Richards, K. J. and Wallcraft, A. J. 2011. Generation of mesoscale eddies in the lee of the Hawaiian Islands. *Journal of Geophysical Research*, Vol. 116, pp. C11009.

Jickells, T. D. et al. 2005. Global Iron Connections Between Desert Dust, Ocean Biogeochemistry, and Climate. *Science*, Vol. 308 (5718), pp. 67 –71. doi:10.1126/science.1105959.

Jiménez, B., Sangrà, P. and Mason, E. 2008. A numerical study of the relative importance of wind and topographic forcing on oceanic eddies shedding by deep water islands. *Ocean Modelling*, Vol. 22, pp. 146-157.

John, D. M. and Lawson, G. W. 1997. Seaweed biodiversity in West Africa: a criterion for designating marine protected areas. In: *The Coastal Zone of West Africa: Problems and Management.* Evans, S. M., Vanderpuye, C. J. and Armah, A. K. (eds). Pershaw Press, Sunderland, pp. 111-123.

John, D. M., Lawson, G. W. and Ameka, G. 2003. The marine macroalgae of the tropical West Africa sub-region. *Nova Hedwigia Beihefte* Vol. 125: 217 pp.

Jones, B. H. and Halpern, D. 1981. Biological and physical aspects of a coastal upwelling event observed during March-April 1974 off northwest Africa. *Deep-Sea Research Part A. Oceanographic Research Papers*, Vol. 28 (1), pp. 71–81. doi:10.1016/0198-0149(81)90111-4.

Jouffre, D., Domalain, G., Caveriviere, A. and Thiam, D. 2004. Analysis of demersal fish assemblages on the Senegalese continental shelf considering fishing impact over the decade 1986-1995. IOC-UNESCO, Paris. IOC Workshop Report, No. 188, pp. 105-113.

JPL-NASA. 2014. *Estimating the circulation and climate of the ocean, Phase II: high resolution global-ocean and sea-ice data synthesis*. http://ecco2.jpl.nasa.gov (Accessed December 2014).

Julià-Serdà, G., Cabrera-Navarro, P., Acosta-Fernández, O., Martín-Pérez, P., Batista-Martín, J., Alamo-Santana,F., Rodríguez-de Castro, F. and Antó-Boqué, J. M. 2005. High Prevalence of Asthma Symptoms in the Canary Islands: Climatic Influence?. *Journal of Asthma*, Vol. 42, pp. 507-511. doi: doi:10.1081/JAS-67621.

Jung, J. -L., Mullié, W. C., Van Waerebeek, K., Wagne, M. M., Samba Ould Bilal, A., Ould Sidaty, Z. A., Toomey, L., Méheust E. and Marret, F. 2015. *First specimen record of Balaenoptera omurai off West Africa: interoceanic straggler or indication of a possible Atlantic population?* International Whaling Commission, San Diego, US. Scientific Committee Document SC/66a/SD/1: 9 pp.

Kameda, T. and Ishizaka, J. 2005. Size-fractionated primary production estimated by a two-phytoplankton community model applicable to ocean color remote sensing. *Journal of Oceanography*, Vol. 61 (4), pp. 663–672.

Kanamitsu, M., Ebisuzaki, M., Woollen, J., Yang, S. K., Hnilo, J. J., Fiorino, M. and Potter, J. L. 2002. NCEPDOE AMIPII Reanalysis (R2). *Bulletin of the American Meteorological Society*, pp. 1631-1643.

Kandler, K., Benker, N., Bundke, U., Cuevas, E., Ebert, M., Knippertz, P., Rodríguez, S., Schütz, L. and Weinbruch, S. 2007. Chemical composition and complex refractive index of Saharan Mineral Dust at Izaña, Tenerife (Spain) derived by electron microscopy. *Atmospheric Environment*, Vol. 41, pp. 8058-8074. doi: 10.1016/j.atmosenv.2007.06.047.

Kandler, K. et al. 2009. Size distribution, mass concentration, chemical and mineralogical composition and derived optical parameters of the boundary layer aerosol at Tinfou, Morocco, during SAMUM 2006. *Tellus Series B Chemical and Physical Meteorology*, Vol. 61, pp. 32-50. doi:10.1111/j.1600-0889.2008.00385.x.

Kandler, K. et al. 2011. Ground-based off-line aerosol measurements at Praia, Cape Verde, during the Saharan Mineral Dust Experiment: Microphysical properties and mineralogy. *Tellus Series B Chemical and Physical Meteorology*, Vol. 63, pp. 459-474. doi: 10.1111/j.1600-0889.2011.00546.x.

Kang, S. M. and Lu, J. 2012. Expansion of the Hadley Cell under Global Warming: Winter versus Summer. *Journal of Climate*, Vol. 25 (24), pp. 8387–8393. doi:10.1175/JCLI-D-12-00323.1.

Karakas, G., Nowald, N., Blaas, M., Marchesiello, P., Frickenhaus, S. and Schlitzer, R. 2006. High-resolution modelling of sediment erosion and particle transport across the northwest African shelf. *Journal of Geophysical Research*, Vol. 111, No. C06025. doi: 10.1029/2005JC003296.

Karstensen, J., Stramma, L. and Visbeck, M. 2008. Oxygen minimum zones in the eastern tropical Atlantic and Pacific oceans. *Progress in Oceanography*, Vol. 77, pp. 331–350.

Karyampudi, V. M. and Carlson, T. N. 1988. Analysis and numerical simulations of the Saharan air layer and its effect on easterly wave disturbances. *Journal of Atmospheric Science*, Vol. 45, pp. 3102-3136.

Kaufman, Y. J., Koren, I., Remer, L. A., Tanré, D., Ginoux, P. and Fan, S. 2005. Dust transport and deposition observed from the Terra-Moderate Resolution Imaging Spectroradiometer (MODIS) spacecraft over the Atlantic Ocean. *Journal Geophysical Research D: Atmospheres,* Vol. 110, D10S12. doi:10.1029/2003JD004436.

Kawase, M. and Sarmiento, J. L. 1985. Nutrients in the Atlantic thermocline. *Journal of Geophysical Research*, Vol. 90, pp. 8961–8979.

Kelleher, K. and Willmann, R. 2006. *"The Rent Drain": Towards an Estimate of the Loss of Resource Rents in the World's Fisheries*. Report of the FAO–World Bank Study Design Workshop, January 17–18. World Bank, Washington, D. C.

Khromov, D. N., Lu, C. C., Guerra, A., Dong, Zh. and Boletzky, S. v. 1998. A synopsis of Sepiidae outside Australian waters (Cephalopoda: Sepioidea). *Smithsonian Contributions to Zoology*, Vol. 586, pp. 77-157.

Khlistova, L. M. and Kéita, A. 1985. Variation saisonnière de la composition qualitative et quantitative du zooplancton de la zone côtière du shelf guinéen. *Bulletin du Centre de Rogbané*, Conakry, Guinea, Vol. 1, pp. 28-38.

Kidd, R. B., Hunter, P. M. and Simm, R. W. 1987. Turbidity-current and debris-flow pathways to the Cape Verde Basin: status of long-range side scan sonar (GLORIA) surveys. In: *Geology and Geochemistry of Abyssal Plains, Geological Society Special Publication* 31. Weaver, P. P. E. and Thomson, J. (eds). Blackwell Scientific Publications, Boston, MA, pp. 33-48.

King, S. and Ritsema, J. 2000. African hot spot volcanism: small-scale convection in the upper mantle beneath cratons. *Science*, Vol. 290, pp. 1137-1140.

Kirpichnikov, A. A. 1950. Nablyadeniya nad raspredeleniyem kruphykh Kitoobraznakh v Atlanti cheskom okeane. [Observations on the distribution of large cetaceans in the Atlantic Ocean]. Priroda Leningrad 10, pp. 63-64. Cited in Tomilin, 1967 (original in Russian).

Kirtman, B. and Pirani, A. 2009. The State of the Art of Seasonal Prediction: Outcomes and Recommendations from the First World Climate Research Program Workshop on Seasonal Prediction. *Bulletin of the American Meteorological Society*, Vol. 90, pp. 455–458.

Kitidis, V., Tilstone, G. H., Serret, P., Smyth, T. J., Torres, R. and Robinson, C. 2014. Oxygen photolysis in the Mauritanian upwelling: Implications for net community production. *Limnology and Oceanography*, Vol. 59, No. 2, pp. 299–310.

Klein, P. and Lapeyre, G. 2009. The oceanic vertical pump induced by mesoscale and submesocale turbulence. *Annual Review of Marine Sciences*, Vol. 1, pp. 351-375.

Knippertz, P. and Martin, J. E. 2005: Tropical plumes and extreme precipitation in subtropical and tropical West Africa. *Quarterly Journal of Royal Meteorological Society,* Vol. 131, pp. 2337–2365.

Koenen, F., Magileviciute, E., Rodrigues, J. and Hazevoet, C. J. 2013. First confirmed occurrence of Gervais' beaked whale *Mesoplodon europaeus* (Gervais, 1855) in the Cape Verde Islands. *Zoología Caboverdiana*, Vol. 4 (2), pp. 49-52.

Korhonen, J. V. et al. 2007. *Magnetic Anomaly map of the World; 1st Edition*. Commission for Geologic Map of the Word, supported by UNESCO, Geological Survey of Finland, Helsinki.

Koren, I., Kaufman, Y. J., Washington, R., Todd, M. C., Rudich, Y., Martins, J. V. and Rosenfeld, D. 2006. The Bodélé depression: A single spot in Sahara that provides most of the mineral dust in the Amazon forest. *Environmental Research Let*ters, Vol. 1, 014005. doi:10.1088/1748-9326/1/1/014005.

Kostianoy, A. G. and Zatsepin, A. G. 1996. The West African coastal upwelling filaments and cross-frontal water exchange conditioned by them. *Journal of Marine Systems*, Vol. 7, pp. 349-359.

Krakstad, J. -O. et al. 2012. *Nansen Cruise Report EAF-N/2011/10. CCLME North West Africa Ecosystem Survey, Guinea – Morocc*o. Institute of Marine Research, Bergen, Norway.

Krastel, S., Schmincke, H.-U., Jaacobs, C. L., Rihm, R., Le Bas, T. P. and Alibés, B. 2001. Submarine landslides around the Canary Islands. *Journal of Geophysical Research*, Vol. 106, pp. 3977-3997.

Krastel, S., Wynn, R. B., Hanebuth, T. J. J., Henrich, R., Holz, C., Meggers, H., Kuhlmann, H., Georgiopoulou, A. and Schulz, H. D. 2006. Mapping of seabed morphology and shallow sediment structure of the Mauritania continental margin, North-west Africa: some implications for geohazard potential. *Norwegian Journal of Geology*, Vol. 86, pp. 163-176.

Kunze, E. T. B. 1985. Near-inertial wave propagation in geostrophic shear. *Journal of Physical Oceanography*, Vol. 15, pp. 544-565.

La Violette, P. E. 1974. A satellite-aircraft thermal study of the upwelled waters off the Spanish Sahara. *Journal of Geophysical Research*, Vol. 4, pp. 676-684.

Laborel, J. 1974. West African corals, and hyphothesis on their origin. In: *Proceedings of the 2nd International Coral Reef Symposium*. Cameron, A. M., Cambell, B. M., Cribb, A. B., Endean, R., Jell, J. S., Jones, O. A., Mather, P. and Talbot, F. H. (eds). Great Barrier Reef Committee, Brisbane, Australia, Vol. 1, pp. 425-444.

Lachkar, Z. and Gruber, N. 2013. Response of biological production and air–sea CO2 fluxes to upwelling intensification in the California and Canary Current Systems. *Journal of Marine Systems*, Vol. 109–110, pp. 149–160.

Laë, R., Ecoutin, J. M., Mendy, A., Raffray, J., Weigel, J. Y., Sadio, O. and Djobe, O. 2004. Effects of a targeted shrimp (*Penaeus notialis*) exploitation on fish catches in the Gambia estuary. *Aquatic Living Resources.* Vol. 17 (1), pp. 75-85.

Laing, A. and Evans, J. -L. 2011. *An Introduction to Tropical Meteorology, 2nd edition. A Comprehensive Online & Print Textbook*. University Corporation for Atmospheric Research. http://www.goes-r.gov/users/comet/tropical/textbook_2nd_edition/index.htm (Accessed 14 April 2015).

Laiz, I., Pelegrí, J. L., Machín, F., Sangrà, P., Hernández-Guerra, A., Marrero-Díaz, A. and Rodríguez-Santana, A. 2012. Eastern boundary drainage of the North Atlantic subtropical gyre. *Ocean Dynamics*, Vol. 62, pp. 1287-1310.

Laroche, J. and Idelhaj, A. 1988. Les peuplements démersaux (poissons et céphalopodes) dans les eaux sahariennes de 22°N à 26°N. *Oceanologica Acta*, Vol. 11 (4), pp. 409-422.

Lasternas, S., Piedeleu, M., Sangrà, P., Duarte, C. M. and Agustí, S. 2013 Forcing of dissolved organic carbon release by phytoplankton by anticyclonic mesoscale eddies in the subtropical NE Atlantic Ocean. *Biogeosciences*, Vol. 10, pp. 2129-2143.

Lathuiliére, C., Echevin, V. and Lévy, M. 2008. Seasonal and intraseasonal surface chlorophyll-a variability along the northwest African coast. *Journal of Geophysical Research*, Vol. 113, C05007. doi:10.1029/2007JC004433.

Laurans, M., Gascuel, D., Chassot, E. and Thiam, D. 2004. Changes in the trophic structure of fish demersal communities in West Africa in the three last decades. *Aquatic Living Resources*, Vol. 17, pp. 163-173.

Lazar, B. and Holcer, D. 1998. Notes on the marine turtles of Sal Island, Cape Verde Islands. In: *Proceedings of the Seventeenth Annual Sea Turtle Symposium*. Epperly, S. P. and Braun, J. (eds). NOAA Technical Memorandum NMFS-SEFSC-415, 231pp.

Lazaro, C., Fernandes, M. J., Santos, A. M. P. and Oliveira, P. 2005. Seasonal and interannual variability of surface circulation in the Cape Verde region from 8 years of merged T/P and ERS-2 altimeter data. *Remote Sensing of the Environment*, Vol. 98, pp. 45–62.

Law, C. S. et al. 2013. Evolving research directions in Surface Ocean-Lower Atmosphere (SOLAS) science. *Environmental Chemistry,* Vol. 10, pp. 1-16. doi: 10.1071/EN12159.

Laws, E. A., Falkowski, P. G., Smith, W. O., Ducklow, H. and McCarthy, J. J. 2000. Temperature effects on export production in the open ocean. *Global Biogeochemical Cycles*, Vol. 14 (4), pp. 1231–1246. doi:10.1029/1999GB001229.

Le Bas, M. J., Rex, D. C. and Stillman, C. J. 1986. The early magmatic chronology of Fuerteventura. *Geological Magazine*, Vol. 123, pp. 287-298.

Le Borgne, R. 1980. Les relations entre le zooplancton et le phytoplancton dans trois situations caractéristiques de l´Atlantique intertropical. In: *Production Primaire et Secondaire, Colloque Franco-Soviétique*, Vol. 10. Publication CNEXO, pp. 107-124.

Le Loeuff, P. 1993. La faune benthique des fonds chalutables du plateau continental de la Guinée: premiers résultats en référence à la faune de la Côte-d'Ivoire. *Revue Hydrobiology Tropical*, Vol. 26, pp. 229-252.

Le Loeuff, P. and von Cosel, R. 1998. Biodiversity patterns of the marine benthic fauna on the Atlantic coast of tropical Africa in relation to hydroclimatic conditions and paleogeographic events. *Acta Oecologica*, Vol. 19 (3), pp. 309-321.

Le Quéré, C. L. et al. 2005. Ecosystem dynamics based on plankton functional types for global ocean biogeochemistry models. *Global Change Biology*, Vol. 11 (11), pp. 2016–2040. doi:10.1111/j.1365-2486.2005.1004.x.

Le Quéré, C. et al. 2014. Global Carbon Budget 2014. *Earth System Science Data Discussions*, Vol. 7, pp. 521-610.

LeBuff, C. R. Jr. 1990. *The loggerhead turtle in the Eastern Gulf of Mexico*. Caretta Research, Sanibel Florida, USA: 216 pp.

Lelong, A., Hégaret, H., Soudant, P. and Bates, S. S. 2012. *Pseudo-nitzschia* (Bacillariophyceae) species, domoic acid and amnesic shellfish poisoning: revisiting previous paradigms. *Phycologia*, Vol. 51, pp. 168-216.

Lemos, R. T. and Pires, H. O. 2004. The upwelling regime off the West Portuguese Coast, 1941-2000. *International Journal of Climatology*, Vol. 24, pp. 511–524.

Leroux, M. 2001. *The Meteorology and Climate of Tropical Africa*. Springer, Chichester, UK.

Leroux, S. and Hall, N. M. J. 2009. On the relationship between African Easterly Waves and the African Easterly Jet. *Journal of Atmospheric Science*, Vol. 66, pp. 2303–2316.

Levin, L. A. and Gooday, A. J. 2003. The deep Atlantic Ocean. In: *The Deep Seafloor. Ecosystems of the World.* Tyler, P. A. (ed.) Elsevier, Amsterdam, Lausanne, New York, Oxford, Shannon, Singapore, Tokyo, pp. 111-178.

Lévy, M. 2008. The modulation of biological production by mesoscale turbulence. *Lecture Notes in Physics*, Vol. 744, pp. 219–261.

Lewis, E. D. and Wallace, W. R. 1998. *Program developed for CO_2 system calculations*. Report 105, Oak Ridge National Laboratory, US Department of Energy, Oak Ridge, Tenn.

Lhomme, F. 1978. Biologie et dynamique de *Penaeus duorarum notialis* au Sénégal. Partie 2. Croissance. *Document Scientifique.* Centre de Recherches Océanographiques de Dakar-Thiaroye, No. 64: 52 pp.

Lhomme, F. 1979a. Biologie et dynamique de *Penaeus duorarum notialis* au Sénégal. Partie 3. Reproduction. *Document Scientifique.* Centre de Recherche Océanographique de Dakar-Thiaroye, No. 69: 34 pp.

Lhomme, F. 1979b. Biologie et dynamique de *Penaeus duorarum notialis* (Perez-Farfante, 1967) au Sénégal. Partie 4. Phase juvénile. *Document Scientifique*. Centre de Recherche Océanographique de Dakar-Thiaroye, No. 70: 69 pp.

Lhomme, F. and García, S. 1984. Biologie et exploitation de la crevette pénaeide au Sénégal. In: *Penaeid shrimps: their biology and management*. Gulland, J. A. and Rothschild, B. J. (eds). Farnham: Fishing News Books, pp. 111-144.

Lidvanov, V. V., Kukuev, E. I., Kuderskiy, S. K. and Grabko, O. G. 2013. Mesozooplankton Taxonomic Composition of the Canaries Current Ecosystem (Coast of Morocco). *Journal of Siberian Federal University. Biology,* Vol. 3 (6), pp. 290-312.

Lindley, J. A. and Daykin, S. 2005. Variations in the distributions of *Centropages chierchiae* and *Temora stylifera* (Copepoda: Calanoida) in the north-eastern Atlantic Ocean and western European shelf waters. *ICES Journal of Marine Science*, Vol. 62, pp. 869–877.

Lino, S. P. P., Gonçalves, E. and Cozens, J. 2010. The loggerhead sea turtle (*Caretta caretta*) on Sal Island, Cape Verde: nesting activity and beach surveillance in 2009. *Arquipélago. Life and Marine Sciences*, Vol. 27, pp. 59–63.

Liu, X. and Millero, F. J. 2002. The solubility of iron in seawater. *Marine Chemistry,* Vol. 77 (1), pp. 43-54.

Llanes, P., Herrera, R., Gómez, M., Muñoz, A., Acosta, J., Uchupi, E. and Smith, D. 2009. Geological evolution of the volcanic island La Gomera, Canary Islands, from analysis of its geomorphology. *Marine Geology*, Vol. 264, pp. 123-139.

Llanillo, P. J., Karstensen, J., Pelegrí, J. L. and Stramma, L. 2013. Physical and biogeochemical forcing of oxygen and nitrate changes during El Niño/El Viejo and La Niña/La Vieja upper-ocean phases in the tropical eastern South Pacific along 86°W: 1993 versus 2009. *Biogeosciences*, Vol. 10, pp. 6339-6355.

Llinás, O., Rueda, M., Pérez-Marrero, J., Pérez-Martel, E., Santana, R., Villagarcía, M., Cianca, A., Godoy, J. and Maroto, L. 2002. Variability of the Antartic Intermediate Waters in the northern Canary box. *Deep-Sea Research Part II: Topical Studies in Oceanography*, Vol. 49 (17), pp. 3441–3453.

Lloris, D. and Rucabado, J. 1979. Especies ictiológicas de las expediciones pesqueras realizadas en la plataforma del NW de África (1971-1975). *Resumen Expediciones Científicas,* Vol. 8, pp. 3-151.

Lloris, D. and Rucabado, J. 1998. *Guide FAO d'identification des espèces pour les besoins de la pêche. Guide d'Identification des Ressources Marines Vivantes du Maroc.* Rome, FAO: 263 pp.

Longhurst, A. R. 1969. Species Assemblages in the Tropical Demersal Fisheries. In: *Proceeding of the Symposium on the Oceanography and Fisheries Resources of tropical Atlantic.* Rapport de Synthèse et Communication, UNESCO, Paris, pp. 147-168.

Longhurst, A., Sathyendranath, S., Platt, T. and Caverhill, C. 1995. An estimate of global primary production in the ocean from satellite radioeter data. *Journal of Plankton Research*, Vol. 17 (6), pp. 1245–1272. doi:10.1093/plankt/17.6.1245.

López-Abellán, L. J., Cervantes, A. and de la Serna, J. M. 1987. Exploratory fishing cruise for demersal stocks in waters of the Republic of The Gambia "Gambia 8611". FAO, Dakar. FAO CECAF/TECH/87/87: 187 pp.

López-García, P. 2012. *Flujos de metales derivados de aerosoles africanos en la Cuenca de Canarias*. PhD Thesis, University of Las Palmas de Gran Canaria, Spain.

López-García, P., Gelado-Caballero, M. D., Santana-Castellano, D., Suárez de Tangil, M., Collado-Sánchez, C. and Hernández-Brito, J. J. 2013. A three-year time-series of dust deposition flux measurements in Gran Canaria, Spain: A comparison of wet and dry surface deposition samplers. *Atmospheric Environment*, Vol. 73, pp. 689-694. doi:10.1016/j.atmosenv.2013.07.044.

López-Jurado, L. F. 1992. Synopsis of the Canarian herpetofauna. *Revista Española de Herpertologia*, Vol. 6, pp. 107–118.

López-Jurado, L. F. 2007. Historical review of the archipelagos of Macaronesia and the marine turtles. In: *Marine Turtles. Recovery of Extinct Populations*. López-Jurado, L. F. and Liria, A. (eds). Instituto Canario de Ciencias Marinas, No. 5. Las Palmas de Gran Canaria, Spain, pp. 53–76.

Loucaides, S., Tyrrell, T., Achterberg, E. P., Torres, R., Nightingale, P. D., Kitidis, V., Serret, P., Woodward, M. and Robinson, C. 2012. Biological and physical forcing of carbonate chemistry in an upwelling filament off northwest Africa: Results from a Lagrangian study. *Global Biogeochemical Cycles,* Vol. 26, GB3008. doi:10.1029/2011GB004216.

Loureiro, N. S. 2008. Sea Turtles in Santiago Island, Cape Verde. *Marine Turtle Newsletter,* Vol. 120, pp. 6–8.

Loureiro, N. S. and Torrão, M. M. F. 2008. Homens e Tartarugas Marinhas. Seis Séculos de História e Histórias nas Ilhas de Cabo Verde. *Anais Histórias Além-Mar*, Vol. 9, pp. 37–78.

Low, P. S. 2005. *Climate Change and Africa*. Cambridge University Press, New York, United States.

Lozier, M. S., Owens, W. B. and Curry, R. G. 1995. The climatology of the North Atlantic. *Progress in Oceanography,* Vol. 36, pp. 1-44.

Luo, C., Mahowald, N. M. and del Corral, J. 2003. Sensitivity study of meteorological parameters on mineral aerosol mobilization, transport, and distribution. *Journal of Geophysical Research D: Atmospheres,* Vol. 108, 4447. doi: 10.1029/2003jd003483.

Luyten, J. R., Pedlosky, J. and Stommel, H. 1983. The ventilated thermocline. *Journal of Physical Oceanography*, Vol. 13, pp. 292–309.

MacArthur, R. H. 1955. Fluctuations of animal populations, and a measure of community stability. *Ecology*, Vol. 36, pp. 533-536.

Machín, F., Hernández-Guerra, A. and Pelegrí, J. L. 2006a. Mass fluxes in the Canary Basin. *Progress in Oceanography,* Vol. 70, pp. 416-447.

Machín, F., Pelegrí, J. L., Laiz, I., Marrero-Díaz, A. and Ratsimandresy, A. W. 2006b. Near-surface circulation in the southern Gulf of Cádiz. *Deep-Sea Research Part II: Topical Studies in Oceanography*, Vol. 53, pp. 1161-1181.

Machín, F. and Pelegrí, J. L. 2009. Northward penetration of Antarctic Intermediate Water off northwest Africa. *Journal of Physical Oceanography*, Vol. 39, pp. 512-535.

Machín, F., Pelegrí, J. L., Fraile-Nuez, E., Vélez-Belchi, P., López-Laatzen, F. and Hernández-Guerra, A. 2010. Seasonal flow reversals of Intermediate Waters in the Canary Current System east of the Canary Islands. *Journal of Physical Oceanography*, Vol. 40, pp. 1902-1909.

Machu, E., Ettahiri, O., Kifani, S., Benazzouz, A., Makaoui, A. and Demarcq, H. 2009. Environmental control of the recruitment of sardines (*Sardina pilchardus*) over the western Saharan shelf between 1995 and 2002: a coupled physical/biogeochemical modelling experiment. *Fisheries Oceanography*, Vol. 18 (5), pp. 287–300. doi:10.1111/j.1365-2419.2009.00511.x.

Mackey, K. R. M., van Dijken, G. L., Mazloom, S., Erhardt, A. M., Ryan, J., Arrigo, K. R. and Paytan, A. 2010. Influence of atmospheric nutrients on primary productivity in a coastal upwelling region. *Global Biogeochemical Cycles*, Vol. 24 (4), pp. GB4027. doi:10.1029/2009GB003737.

Macpherson, E. 1988. Revision of the family Lithodidae Samouelle, 1819 (Crustacea, Decapoda, Anomura) in the Atlantic Ocean. *Monografías de Zoología Marina*, Vol. 2 (9), pp. 9-153.

Madeira, J., Mata, J., Mourao, C., Brum da Silveira, A., Martins, S., Ramalho, R. and Hoffmann, D. L. 2010. Volcano-stratigraphic and structural evolution of Brava Island (Cape Verde) based on 40Ar/39Ar, U–Th and field constraints. *Journal of Volcanological and Geothermal Research,* Vol. 196, pp. 219-235.

Mahadevan, A. Thomas, L. N. and Tandon, A. 2008. Comment on "Eddy/Wind Interactions Stimulate Extraordinary Mid-Ocean Plankton Blooms". *Science*, Vol. 320, pp. 448b.

Mahowald, N. M. and Luo, C. 2003. A less dusty future?. *Geophysical Research Lett*ers, Vol. 30, No. 17, 1903. doi:10.1029/2003GL017880.

Mahowald, N. M., Bryant, R. G., del Corral, J. and Steinberger, L. 2003. Ephemeral lakes and desert dust sources. *Geophysical Research Lett*ers, Vol. 30, 1074. doi:10.1029/2002GL016041.

Mahowald, N., Baker, A., Bergametti, G., Brooks, N., Duce, R., Jickells, T., Kubilay, N., Prospero, J. and Tegen, I. 2005. The atmospheric global dust cycle and iron inputs to the ocean. *Global Biogeochemical Cycles,* Vol. 19, GB4025. doi:10.1029/2004GB002402.

Mahowald, N. et al. 2009. Atmospheric Iron deposition: global distribution, variability and human perturbations. *Annual Review of Marine Science,* Vol. 1, pp. 245–278. doi: 10.1146/annurev.marine.010908.163727.

Mahowald, N. M. et al. 2010. Observed 20th century desert dust variability: Impact on climate and biogeochemistry. *Atmospheric Chemistry and Physics,* Vol. 10, pp. 10875–10893. doi:10.5194/acp-10-10875-2010.

Maigret, J. 1977. Les mammifères du Sénégal. II. Les mammifères marins. *Bulletin AASNS,* Vol. 57, pp. 13-30.

Maigret, J. Soukhovershine, V. and Chlibanov, V. 1981. Notes ichthyologiques III. Complément à l'inventaire ichthyologique des côtes de Mauritanie, No. 2. *Bulletin Centre National des Recherches Océanographiques et des Pêches,* Vol. 9 (1), pp. 122-129.

Makaoui, A., Orbi, A., Hilmi, K., Zizah, S., Larissi, J. and Talbi, M. 2005. L'upwelling de la côte Atlantique du Maroc entre 1994 et 1998. *Comptes Rendus Geoscience*, Vol. 337 (16), pp. 1518-1524. doi:10.1016/j.crte.2005.08.013.

Makaoui, A., Orbi, A., Arístegui, J., Benazzouz, A., Laarissi, J., Agouzouk, A. and Hilmi, K. 2012. Hydrological seasonality of cape Ghir filament in Morocco. *Natural Science*, Vol. 4 (1), pp. 5-13.

Mangold, K. 1998. The Octopodinae from the Eastern Atlantic Ocean and the Mediterranean Sea. *Smithsonian Contributions to Zoology*, Vol. 586, pp. 521-528.

Manning, R. B. and Holthuis, L. B. 1981. West African Brachyuran crabs. *Smithsonian Contributions to Zoology*, Vol. 306, pp. xii and 379.

Marañón, E. et al. 2010. Degree of oligotrophy controls the response of microbial plankton to Saharan dust. *Limnology and Oceanography*, Vol. 55, pp. 2339-2352. doi: 10.4319/lo.2010.55.6.2339.

Marcello, J., Hernández-Guerra, A., Eugenio, F. and Fonte, A. 2011. Seasonal and temporal study of the northwest African upwelling system. *International Journal of Remote Sensing*, Vol. 32, pp. 1843–1859. doi:10.1080/01431161003631576.

Marchesiello, P. and Estrade, P. 2007. Eddy activity and mixing in upwelling systems: a comparative study of Northwest Africa and California regions. *International Journal of Earth Sciences*, Vol. 98 (2), pp. 299–308. doi:10.1007/s00531-007-0235-6.

Marco, A., Abella-Pérez, E., Monzón-Argüello, C., Martins, S., Araujo, S. and López-Jurado, L. F. 2011. The international importance of the archipelago of Cape Verde for marine turtles, in particular the loggerhead turtle *Caretta caretta. Zoologia Caboverderdiana*, Vol. 2, pp. 1–11.

Marco, A. et al. 2012. Abundance and exploitation of loggerhead turtles breeding in the Boa Vista island of Cape Verde, their only substantial rookery in the Eastern Atlantic. *Animal Conservation*, Vol. 15, pp. 351–360.

Marcos, M., Puyol, B., Wöppelmann, G., Herrero, E. and García-Fernández, M. J. 2011. The long sea level record at Cadiz (southern Spain) from 1880 to 2009. *Journal of Geophysical Research: Oceans*, Vol. 116, C12003. doi:10.1029/2011JC007558.

Marcos, M., Puyol, B., Calafat, F. M. and Wöppelmann, G. 2013. Sea level changes at Tenerife Island (NE Tropical Atlantic) since 1927. *Journal of Geophysical Research: Oceans*, Vol. 118, pp. 1-12. doi:10.1002/jgrc.20377.

Margalef, R. 1978. Life-forms of phytoplankton as survival alternatives in an unstable environment. *Oceanologica Acta*, Vol. 1 (4), pp. 493–509.

Maritorena, S., d' Andon, O. H. F., Mangin, A. and Siegel, D. A. 2010. Merged satellite ocean color data products using a bio-optical model: Characteristics, benefits and issues. *Remote Sensing of Environment*, Vol. 114 (8), pp. 1791–1804. doi:10.1016/j.rse.2010.04.002.

Marshall, J., Adcroft, A., Hill, C., Perelman, L. and Heisey, C. 1997. A finite-volume, incompressible Navier Stokes model for studies of the ocean on parallel computers. *Journal of Geophysical Research*, Vol. 102, (C3), 5753.

Martí, J., Castro A., Rodriguéz, C., Costa, F., Carrasquilla, S., Pedreira, R. and Bolos, X. 2013. Correlation of magmaevolution and geophysical monitoring during the 2011-2012 El Hierro (Canary Islands) submarine eruption. *Journal of Petrology,* Vol. 54 (7), pp. 1349-1373.

Marticorena, B. and Bergametti, G. 1995. Modeling the atmospheric

dust cycle: 1. Design of a soil-derived dust emission scheme. *Journal of Geophysical Research D: Atmospheres*, Vol. 100, pp. 415–416.

Martin, J. H., Gordon, M. and Fitzwater, S. 1988. Oceanic iron distributions in relation to phytoplanktonic productivity. *EOS: Transactions of the American Geophysical Union*, Vol. 69, pp. 1045.

Martín, V., Vonk, R., Escorza, S. and Montero, R. 1990. Records of Gervais' beaked whale *Mesoplodon europaeus* on the Canary Islands. *European Research on Cetaceans,* Vol.4, pp. 95.

Martin, A. P. and Richards, K. J. 2001. Mechanisms for vertical nutrient transport within a North Atlantic mesoscale eddy. *Deep-Sea Research Part II: Topical Studies in Oceanography*, Vol. 48, pp. 757–773.

Martin, J. W. and Davis, G. E. 2001. An Updated Classification of the Recent Crustacea. Natural History Museum of Los Angeles County, *Science Series,* No. 39: 124 pp.

Martínez del Olmo, W. and Buitrago, J. 2002. Sedimentación y volcanismo al Este de las islas de Fuerteventura y Lanzarote (Surco de Fúster Casas). *Geogaceta*, Vol. 32, pp. 51-54.

Martínez-Marrero, A., Rodríguez-Santana, A., Hernández-Guerra, A., Fraile-Nuez, E., López-Laatzen, F., Vélez-Belchí, P. and Parrilla, G. 2008. Distribution of water masses and diapycnal mixing in the Cape Verde Frontal Zone. *Geophysical Research Letters*, Vol. 35 (7), L07609. doi: 10.1029/2008GL033229.

Martínez-Marrero, A., Sangrà, P., Caldeira, R. M., Aguiar-González, B. and Rodríguez-Santana, A. 2014. Observations of the interaction between near-inertial waves and mesoscale eddies. *EGU General Assembly 2014,* Vienna, 27 April – 02 May 2014.

Martins, S. 2012. The endangered loggerhead (*Caretta caretta*) sea turtle on the Boavista Island, Cape Verde: distribution, abundance, ecology and conservation of nesting females and nests. Master's degree thesis, University of Algarve, Portugal: 132 pp.

Martins, S., Mata, J., Munha-Mendes, A. H., Maerschalk, C., Caldeira, R. and Mattielli, N. 2010. Chemical and mineralogical evidence of the occurrence of mantle metasomatism by carbonate-rich melts in an oceanic environment (Santiago Island, Cape Verde). *Mineralogy and Petrology*, Vol. 99, pp. 43-65.

Mason, E. 2009. *High-resolution modelling of the Canary Basin Oceanic Circulation.* PhD Thesis, University of Las Palmas de Gran Canaria, Spain.

Mason, E., Colas, F., Molemaker, J., Shchepetkin, A. F., Troupin, C., McWilliams, J. C. and Sangrà P. 2011. Seasonal variability of the Canary Current: a numerical study. *Journal of Geophysical Research*, Vol. 116, C06001.

Mason, E., Colas, F. and Pelegrí, J. L. 2012. A Lagrangian study tracing water parcel origins in the Canary Upwelling system. *Scientia Marina*, Vol. 76 (S1), pp. 79-94.

Masson, D. G., Canals, M., Alonso, B., Urgeles, R. and Hühnerbach, V. 1998. The Canary Debris flow: source area morphology and failure mechanisms. *Sedimentology*, Vol. 45, pp. 411–432.

Masson, D. G., Watts, A. B., Gee, M. J. R., Urgeles, R., Mitchell, N. C., Le Bas, T. P. and Canals, M. 2002. Slope failures on the flanks of the western Canary Islands. *Earth Science Reviews*, Vol. 57, pp. 1-35.

Masson, D. G., Harbitz, C. B., Wynn, R. B., Pedersen, G. and LØwholt, F. 2006. Submarine landslides: processes, triggers and hazard prediction. *Philosophical transactions. Series A, Mathematical, physical, and engineering sciences. Royal Society*, Vol. 364, pp. 2009–2039.

Masson, D. G., Le Bas, T. P., Grevenmeyer, I. and Weinrebe, W. 2008. Flank: Collapse and large-scale landsliding in the Cape Verde Island, off West Africa. *Geochemistry, Geophysics, Geosystems (G3)*, Vol. 9, pp. 1-16.

Massutí, M., Gordon, J. D. M., Moranta, J., Swan, S. C., Stefanescu, C. and Merrett, N. R. 2004. Mediterranean and Atlantic deep-sea fish assemblages: Differences in biomass composition and size-related structure. *Scientia Marina*, Vol. 68 (3), pp. 101–115.

Mata, J., Kerrich, R., MacRae, N. D. and Wu, T.W. 1998. Elemental and isotopic (Sr, Nd, and Pb) characteristics of Madeira Island basalts: evidence for a composite HIMU-EM I plume fertilizing lithosphere. *Canadian Journal of Earth Science*, Vol. 35, pp. 980-997.

Matear, R. J. and Hirst, A. C. 2003. Long-term changes in dissolved oxygen concentrations in the ocean caused by protracted global warming. *Global Biogeochemical Cycles*, Vol. 17. doi:10.1029/2002GB001997.

Maurin, C. 1963. Les crevettes capturées par la "Thalassa" au large des Côtes du Rio de Oro et de Mauritanie. Écologie et pêche. *CIEM, Comité des Mollusques et Crustacés*, CM 1963, No. 48: 5 pp.

Maurin, C. 1968. Écologie ichtyologique des fonds chalutables atlantiques de la baie ibéro-marocaine à la Mauritanie et de la Méditerranée occidentale. *Revue Travaux Institut de Pêches Maritimes*, Vol. 32 (1): 130 pp.

Maurin, C. and Bonnet, M. 1969. Le chalutage au large des côtes nord-Ouest africaines. Résultats des campagnes de la Thalassa. *Science et Pêche, Bulletin de l'Institut Scientifique et Techique de Pêches Maritimes,* No. 177, pp. 1-17.

Maurin, C. and Bonnet, M. 1970. Poissons des côtes nord-ouest africaines (Campagnes de la « Thalassa 1962 et 1968). *Revue Travaux Institut de Pêches Maritimes,* Vol. 34 (2): 125 pp.

Maurin, C. and Quero, J. -C. 1981. Poissons des côtes nord-ouest africaines (Campagnes de la «Thalassa 1962, 1968, 1971 et 1973). *Revue Travaux Institut de Pêches Maritimes,* Vol. 45 (1), pp. 5-71.

McCartney, M. 1992. Recirculating components to the deep boundary current of the northern North Atlantic. *Progress in Oceanography,* Vol. 29, pp. 283-383.

McClain, C. R. 1998. Science quality SeaWiFS data for global biosphere research. *Sea Technology*, Vol. 39, pp. 10–16.

McGillicuddy Jr. et al. 2007. Eddy/Wind interactions stimulate extraordinary Mid-Ocean plankton Bloom. *Science*, Vol. 316, pp. 1021–1026.

McGillicuddy Jr., D. J., Ledwell, R. and Anderson, L. A. 2008. Response to Comment on "Eddy/Wind Interactions Stimulate Extraordinary Mid-Ocean Plankton Blooms". *Science*, Vol. 320, pp. 448c.

McGregor, H. V., Dima, M., Fischer, H. W. and Mulitza, S. 2007. Rapid 20th-Century Increase in Coastal Upwelling off Northwest Africa. *Science*, Vol. 315 (5812), pp. 637–639. doi:10.1126/science.1134839.

McGuirk, J. P, Thompson, A. H. and Schaefer, J. R. 1988. An eastern Pacific tropical plume. *Monthly Weather Revue*, Vol. 116, pp. 2505–2521.

McLaughlin, P. A. 2003. Illustrated keys to the families and genera of the superfamily Paguroidea (Crustacea: Decapoda; Anomura), with supplemental diagnoses of the genera of the Paguridae. In: *Biology of the Anomura. Proceedings of a symposium at the Fifth International Crustacean Congress, Melbourne, Australia, 9-13 July 2001*. Lemaitre, R. and Tudge, C. C. (eds). Memoirs of Museum Victoria, No. 60, pp. 111-144.

Measures, C. I., Edmond, J. M. and Jickells, T. D. 1986. Aluminium in the northwest Atlantic. *Geochimica et Cosmochimica Acta*, Vol. 50, pp. 1423-1429.

Mecikalski, J. R. and Tripoli, G. J. 1998. Inertial available kinetic energy and the dynamics of tropical plume formation. *Monthly Weather Revue*, Vol. 126, pp. 2200–2216.

Medina-Gaertner, M. 1988. Analyse des communautés zooplanctoniques de la baie de Dakar et leurs relations avec l'hydrographie. *Investigación Pesquera*, Vol. 52 (1), pp. 17-36.

Mehrbach, C., Culberson, C. H., Hawlay, J. E. and Pytkowicz, R. M. 1974. Measurement of the apparent dissociation constants of carbonic acid in seawater at atmospheric pressure. *Limnology Oceanography,* Vol. 18, pp. 897–907.

Meiners, C., Fernández, L., Salmerón, F. and Ramos, A. 2010. Climate variability and fisheries of black hakes (Merluccius polli and Merluccius senegalensis) in NW Africa: A first approach. *Journal of Marine Systems*, Vol. 80 (3–4), pp. 243–247. doi:10.1016/j.jmarsys.2009.10.013.

Meissa, B. and Gascuel, D. 2014. Overfishing of marine resources: some lessons from the assessment of demersal stocks off Mauritania. *ICES Journal of Marine Science*. doi: 10.1093/icesjms/fsu144.

Mendelssohn, R. and Schwing, F. B. 2002. Common and uncommon trends in SST and wind stress in the California and Peru-Chile current systems. *Progress in Oceanography*, Vol. 53 (2-4), pp. 141–162. doi:10.1016/S0079-6611(02)00028-9.

Menéndez, I., Díaz-Hernández, J. L., Mangas, J., Alonso, I. and Sánchez-Soto, P. J. 2007. Airborne dust accumulation and soil development in the North-East sector of Gran Canaria (Canary Islands, Spain). *Journal of Arid Environments*, Vol. 71, pp. 57-81. doi: 10.1016/j.jaridenv.2007.03.011.

Menioui, M. 1998. *Étude Nationale sur la biodiversité. Faune marine*. Rapport Inédit, Ministère de l'Aménagement du territoire, de

l'Environnement, de l'Urbanisme et de l'Habitat – PNUE. Rabat, Morocco: 133 pp.

Merle, R., Schärer, U., Girardeau, J. and Cornen, G. 2006. Cretaceous seamounts along the continent-ocean transition of the Iberian margin: U-Pb ages and Pb-Sr-Hf isotopes. *Geochemical Cosmochemical Acta*, Vol. 70 (19), pp. 4950-4976.

Merle, R., Jourdan, F., Marzoli, A., Renne, P. R., Grange, M. and Girardeau, J. 2009. Evidence of multi-phase Cretaceous to Quaternary alkaline magmatism on Tore-Madeira Rise and neighbouring seamounts from 40Ar/39Ar ages. *Journal of the Geological Society of London*, Vol. 166, pp. 879-894.

Merrett, N. R. 1994. Reproduction in the North Atlantic oceanic ichthyofauna and the relationship between fecundity and species' size. *Environmental Biology of Fishes,* Vol. 41, pp. 207–245.

Merrett, N. R. and Marshall, N. B. 1981. Observations on the ecology of deep-sea botton-livingfishes collected off northwest Africa (08°-27°N). *Progress in Oceanography*, Vol. 9, pp. 185-244.

Merrett, N. R. and Domansky P. A. 1985. Observations on the ecology of deep-sea bottom-living fishes collected off Northwest Africa. Part II. The Moroccan slope (27-34 N) with special reference to *Synaphobranchus kaupii* Johnson, 1982. *Biological Oceanography*, Vol. 3, pp. 349-399.

Merrett, N. R. and Haedrich, R. L. 1997. *Deep-sea demersal fish and fisheries*. Chapman & Hall, London: 282 pp.

Merrifield, M. A., Merrifield, S. T. and Mitchum, G. T. 2009. An anomalous recent acceleration of global sea level rise. *Journal of Climate*, Vol. 22 (21), pp. 5772–5781.

Meunier, T., Barton, E. D., Barreiro, B. and Torres R. 2012. Upwelling filaments off Cap Blanc: interaction of the NW African upwelling current and the Cape Verde frontal zone eddy field? *Journal of Geophysical Research: Oceans (1978–2012)*, Vol. 117 (C8), C08031. doi:10.1029/2012JC007905.

Meylan, A. B. 1988. Spongivory in hawksbill turtles: a diet of glass. *Science*, Vol. 239, pp. 393-395.

Míguez, A., Fernández, M. L. and Fraga, S. 1996. First detection of domoic acid in Galicia (NW of Spain). In: *Harmful and Toxic Algal Blooms.* Yasumoto, T., Oshima Y. and Fukuyo, Y. (eds). IOC-UNESCO, pp. 143-145.

Miller, R. L., Perlwitz, J. and Tegen, I. 2004. Feedback upon dust emission by dust radiative forcing through the planetary boundary layer. *Journal of Geophysical Research D: Atmospheres*, Vol. 109, D24209. doi: 10.1029/2004jd004912.

Mills, M. M., Ridame, C., Davey, M., La Roche, J. and Geider, R. J. 2004. Iron and phosphorus co-limit nitrogen fixation in the eastern tropical North Atlantic. *Nature*, Vol. 429 (6989), pp. 292-294. doi: 10.1038/nature02550.

Milne-Edwards, A. and Bouvier, E. L. 1892. Observations préliminaires sur les Paguriens recueillis par les expéditions du Travailleur et du Talisman. *Annales des Sciences Naturelles (Zoologie),* Vol. 7 (13), pp. 185-226.

Milne-Edwards, A. and Bouvier, E. L. 1900. Malacostracés. I. Crustaces Decapodes. Premiere Partie: Brachyures et Anomoures. *Expeditions scientifiques du Travailleur et du Talisman pendant les annees 1880,1881, 1882, 1883*. Paris: 396 pp.

Minas, H. J., Codispoti, L. A. and Dugdale, R. C. 1982. Nutrient and primary production in the upwelling region of northwest Africa. *Rapport Conseil International d'Exploration de la Mer*, Vol. 180, pp. 148-183.

Minas, H. J., Minas, M. and Packard, T. T. 1986. Productivity in upwelling areas deduced from hydrographic and chemical fields. *Limnology and Oceanography*, Vol. 31 (6), pp. 1182–1206.

Ministério do Ambiente, Agricultura é Pescas. 2004. *Livro branco sobre o estado do ambiente em Cabo Verde*. Praia. República de Cabo Verde: 229 pp.

Mintrop, L., Pérez, F. F., González Dávila, M., Körtzinger, A. and Santana- Casiano, J. M. 2000. Alkalinity determination by potentiometry: intercalibration using three different methods. *Ciencias Marinas,* Vol. 26, pp. 23-37.

Mirimin, L., Westgate, A., Rogan, E., Rosel, P., Read, A., Coughlan, J. and Cross, T. 2009. Population structure of short-beaked common dolphins *Delphinus delphis* in the North Atlantic Ocean as revealed by mitochondrial and nuclear genetic markers. *Marine Biology*, Vol. 1565, pp. 821-834.

Mittelstaedt, E. 1976. On the currents along the Northwest African coast south of 22° North. *Deutsche Hydrografische Zeitschrift*, Vol. 29, pp. 97-117.

Mittelstaedt, E. 1991. The ocean boundary along the northwest African coast: Circulation and oceanographic properties at the sea surface. *Progress in Oceanography*, Vol. 26, pp. 307-355.

Miyake, S. and Baba, K. 1970. The Crustacea Galatheidae from the tropical-subtropical region of West Africa, with a list of the known species. *Atlantide Report*, No. 11, pp. 61-97.

Molina, V. A. 2013. *The structure of planktonic communities under variable coastal upwelling conditions off Cape Ghir (31°N), in the Canary Current System (NW Africa)*. PhD Thesis, University of Las Palmas de Gran Canaria: 68 pp.

Monod, T. 1956. Hippidea et Brachyura ouest-africains. *Mémoires de l'Institut français d'Afrique noire*, No. 45: 674 pp.

Monteiro, P. M. S. 2009. Carbon fluxes in the Benguela upwelling system. In: *Global Change: The IGBP Series Carbon and nutrient fluxes in continental margin: a global synthesis.* Liu, K. K., Atkison, L., Quiñones, R. and Talau-McManus, L. (eds). Springer-Verlag, New York.

Montelli, R., Nolet, G., Dahlen, F. A. and Masters, G. 2006. A catalogue of deep mantle plumes: new results from finite-frequency tomography. *Geochemistry, Geophysics and Geosystems,* Vol. 7, Q11007.

Monzón-Argüello, C., Rico, C., Carreras, C., Calabuig, P., Marco, A. and López-Jurado, L. F. 2009. Variation in spatial distribution of juvenile loggerhead turtles in the Eastern Atlantic and Western Mediterranean sea. *Journal of Experimental Marine Biology and Ecology*, Vol. 373, pp. 79–86.

Monzón-Argüello, C., Rico, C., Naro-Maciel, E., Varo-Cruz, N., López, P., Marco, A. and López-Jurado, L. F. 2010a. Population structure and conservation implications for the loggerhead sea turtle of the Cape Verde Islands. *Conservation Genetics*, Vol. 11, pp. 1871–1884.

Monzón-Argüello, C., López-Jurado, L. F., Rico, C., Marco, A., López, P., Hays, G. and Lee, P. L. M. 2010b. Evidence from genetic and Lagrangian drifter data for transatlantic transport of small juvenile green turtles. *Journal of Biogeography*, Vol. 37, pp. 1752–1766.

Monzón-Argüello, C., Rico, C., Marco, A., López, P. and López-Jurado, L. F. 2010c. Genetic characterization of eastern Atlantic hawksbill turtles at a foraging group indicates major undiscovered nesting populations in the region. *Journal of Experimental Marine Biology and Ecology,* Vol. 387, pp. 9–14.

Monzón-Argüello, C., Loureiro, N., Delgado, C., Marco, A., Lopes, J. M., Gomes, M. G. and Abreu-Grobois, F. A. 2011. Principe Island hawksbills: genetic isolation of an eastern Atlantic stock. *Journal of Experimental Marine Biology and Ecology*, Vol. 407, pp. 345–354.

Monzón-Argüello, C., Dell'Amico, F., Moriniére, P., Marco, A., López-Jurado, L. F., Hays, G., Scott, R., Marsh, R. and Lee, P. L. M. 2012. Lost at sea: genetic, oceanographic and meteorological evidence for storm-forced dispersal. *Jornal of Royal Society Interface*, Vol. 9, 1725–1732 pp.

Moore, C. M. et al. 2009. Large-scale distribution of Atlantic nitrogen fixation controlled by iron availability. *Nature Geoscience*, Vol. 2, pp. 867-871. doi: 10.1038/ngeo667.

Mopper, M., Stubbins, A. Ritchie, J. D., Bialk, H. M. and Hatche, P. G. 2007. Advanced instrumental approaches for characterization of marine dissolved organic matter: extraction techniques, mass spectrometry, and nuclear magnetic resonance spectroscopy. *Chemical Reviews*, Vol. 107, pp. 419–442.

Moran, M. A. and Zepp, R. G. 1997. Role of photoreactions in the formation of biologically labile compounds from dissolved organic matter. *Limnology and Oceanography*, Vol. 42, pp. 1307–1316.

Morel, A. and Berthon, J. -F. 1989. Surface pigments, algal biomass profiles, and potential production of the euphotic layer: Relationships reinvestigated in view of remote-sensing applications. *Limnology and Oceanography*, Vol. 34 (8), pp. 1545–1562.

Morice, C. P., Kennedy, J. J., Rayner, N. A. and Jones, P. D. 2012. Quantifying uncertainties in global and regional temperature change using an ensemble of observational estimates: The HadCRUT4 data set. *Journal of Geophysical Research: Atmospheres*, Vol. 117 (D8), pp. D08101. doi:10.1029/2011JD017187.

Moro, L., Martín, J. L., Garrido M. J. and Izquierdo, I. (eds). 2003. *Lista de especies marinas de Canarias (algas, hongos, plantas y animales)*.

Consejería de Política Territorial y Medio Ambiente del Gobierno de Canarias: 248 pp.

Müller, R. D., Sdrolias, M., Gaina, C. and Roest, W. R. 2008. Age, spreading rates and spreading symmetry of the world's ocean crust. *Geochemistry, Geophysics, Geosystems (G3)*, Vol. 9, Q 04006.

Mullié, W. C., Wagne, M. M., Ahmed Elmamy C., Mint Yahya, F., Veen, J. and Van Waerebeek, K. 2013. Large number of stranded harbour porpoises *Phocoena phocoena* as by-catch victims in Mauritania. International Whaling Commission, Jeju, Korea. Scientific Committee Document SC/65a/HIM03: 5 pp.

Muñoz, I., García-Isarch, E., Sobrino, I., Burgos, C., Funny, R. and González-Porto, M. 2012. Distribution, abundance and assemblages of decapod crustaceans in waters off Guinea-Bissau (north-west Africa). *Journal of the Marine Biological Association of the United Kingdom,* Vol. 92 (3), pp. 475-494.

Muñoz, I. and García-Isarch, E. 2013. New occurrences of lithodid crabs (Crustacea: Decapoda: Lithodidae) from the coasts of Africa, with the description of a new species of Paralomis White, 1856. *Zootaxa*, Vol. 3670, No. 1, pp. 45-54.

Murphy, P., Van Waerebeek, K. and Jallow, A. 1997. *Cetaceans from Gambian coastal waters*. International Whaling Commission. Scientific Committee Document SC/49/SM11.

Musick, J. A. and Limpus, C. J. 1997. Habitat utilization and migration in juvenile sea turtles. In: *The Biology of Sea Turtles*. Lutz, P. L. and Musick, J. A. (eds). CRC Press, Boca Raton, Florida, pp. 137-163.

Mustapha, Z. B., Alvain, S., Jamet, C., Loisel, H. and Dessailly, D. 2014. Automatic classification of water-leaving radiance anomalies from global SeaWiFS imagery: Application to the detection of phytoplankton groups in open ocean waters. *Remote Sensing of Environment*, Vol. 146, pp. 97–112.

Nair, A., Sathyendranath, S., Platt, T., Morales, J., Stuart, V., Forget, M. -H., Devred, E. and Bouman, H. 2008. Remote sensing of phytoplankton functional types. *Remote Sensing of Environment*, Vol. 112 (8), pp. 3366–3375.

Narayan, N., Paul, A., Mulitza, S. and Schulz, M. 2010. Trends in coastal upwelling intensity during the late 20th century. *Ocean Science*, Vol. 6 (3), pp. 815–823.

Navarro, F. de P. 1947. Exploración oceanográfica del África occidental: desde el Cabo Ghir al cabo Juby: resultados de las campañas del "Malaspina" y del "Xauen" en mayo de 1946 (con una carta provisional de pesca, en escala 1:500.000). Instituto Español de Oceanografía, *Trabajos*, Vol. 20, pp. 1-40.

Navarro-Pérez, E. and Barton, E. D. 2001. Seasonal and interannual variability of the Canary Current. *Scientia Marina*, Vol. 65 (S1), pp. 205– 213.

Ndoye, S, Capet, X., Estrade, P., Sow, B., Dagorne, D., Lazar, A., Gaye, A. and Brehmer, P. 2014. SST patterns and dynamics of the Southern Senegal-Gambia upwelling center. Continental shelf Research. *Journal of Geophysical Research: Oceans*, Vol. 119 (12), pp. 8315–8335.

Nesis, K. N. 1987. *Cephalopods of the world, Squids, Cuttlefishes, Octopuses and Allies*. TFH Publications Inc, United States: 351 pp.

Nesis, K. N. 2003. Distribution of recent Cephalopoda and implications for Plio-Pleistocene events. *Berliner Paläobiollogische Abhandlungen*, Vol. 3, pp. 199-224.

Neuer, S., Ratmeyer, V., Davenport, R., Fischer, G. and Wefer, G. 1997. Deep water particle flux in the Canary Island region: seasonal trends in relation to long-term satellite derived pigment data and lateral sources. *Deep-Sea Research Part I: Oceanographic Research Papers*, Vol. 44, pp. 1451–1466.

Neuer, S., Freudenthal, T., Davenport, R., Llinás, O. and Rueda, M. J. 2002. Seasonality of surface water properties and particle flux along productivity gradient off NW Africa. *Deep-Sea Research Part II: Topical Studies in Oceanography*, Vol. 49, pp. 3561–3567.

Neuer, S., Torres-Padrón, M. E., Gelado-Caballero, M. D., Rueda, M. J., Hernández-Brito, J., Davenport, R. and Wefer, G. 2004. Dust deposition pulses to the eastern subtropical North Atlantic gyre: Does ocean's biogeochemistry respond?. *Global Biogeochemical Cycles*, Vol. 18, pp. 1-10. doi: 10.1029/2004GB002228.

Neuer, S. et al. 2007. Biogeochemistry and hydrography in the eastern subtropical North Atlantic gyre: Results from the European time-series station ESTOC. *Progress in Oceanography,* Vol. 72, pp. 1-29.

NGDC-NOAA. 2006. *2-Minute Gridded Global Relief Data (ETOPO2v2).* http://www.ngdc.noaa.gov/mgg/global/etopo2.html (Accessed December 2014).

Nicholson, S. E., Barcilon, A. I., Challa, M. and Baum, J. 2007. Wave activity on the tropical easterly jet. *Journal of Atmospheric Science*, Vol. 64, pp. 2756–2763.

Nickovic, S., Kallos, G., Papadopoulos, A. and Kakaliagou, O. 2001. A model for prediction of desert dust cycle in the atmosphere. *Journal of Geophysical Research D: Atmospheres*, Vol. 106, pp.18113-18129.

Niedermeier, N. et al. 2014. Mass deposition fluxes of Saharan mineral dust to the tropical northeast Atlantic Ocean: an intercomparison of methods. *Atmospheric Chemistry and Physics*, Vol. 14, pp. 2245–2266. doi:10.5194/acp-14-2245-2014.

Nigmatullin, Ch. M., Laptikhovsky, V. V. and Moustahfid, H. 2002. Brief review on the ecology in the North African population of arrow squid *Todarodes sagittatus* (Cephalopoda: Ommastrephidae). *Bulletin of Marine Science*, Vol. 71 (2), pp. 581-590.

Nixon, S. and Thomas, A. 2001. On the size of the Peru upwelling ecosystem. *Deep-Sea Research Part I: Oceanographic Research Papers*, Vol. 48, pp. 2521–2528. doi:10.1016/S0967-0637(01)00023-1.

NOAA. 2014. *OceanColor Web.* http://oceancolor.gsfc.nasa.gov (Accessed December 2014).

Norez, C. and Pérez, C. 1988. Overlapping range between *Globicephala macrorhynchus* and *Globicephala melaena* in the northeastern Atlantic. *Mammalia,* Vol. 52, pp. 51-55.

Northcote, T. G. 1988. Fish in the structure and function of freshwater ecosystems: a "top-down" view. *Canadian Journal of Fisheries and Aquatic Sciences*, Vol. 45, pp. 361-379.

Nowald, N., Karakas, G., Ratmeyer, V., Fischer, G., Schlitzer, R., Danvenport, R. and Wefer, G. 2006. Distribution and transport processes of marine particulate matter off Cape Blanc (NW Africa): results from vertical camera profiles. *Ocean Sciences Discussions*, Vol. 3, pp. 903–938.

Núñez, D., Matute, P., García, A., García, P. and Abadía, N. 2012. Outbreak of ciguatera food poisoning by consumption of amberjack (*Seriola* spp.) in the Canary Islands, May 2012. *Eurosurveillance*, Vol. 17, pii=20188. http://www.eurosurveillance.org/ViewArticle.aspx?Articleid=20188 (Accessed 12 January 2105).

OBIS. 2015. *Global biodiversity indices from the Ocean Biogeographic Information System*. Intergovernmental Oceanographic Commission of UNESCO. http://www.iobis.org (Accessed 13 January 2015).

Observatorio Ambiental Granadilla (OAG). 2015. *Bibliografía marina de Canarias*. http://www.oag-fundacion.org/index.php/documentosbibliografia/bibliografia-marina (Accessed 8 April 2015)

Ohde, T. and Siegel, H. 2010. Biological response to coastal upwelling and dust deposition in the area off Northwest Africa. *Continental Shelf Research*, Vol. 30, pp. 1108-1119.

Olson, P. A. 2009. Pilot whales *Globicephala melas* and *G. macrorhynchus.* In: *Encyclopedia of Marine Mammals*. Perrin, W. F., Würsig, B. and Thewissen, J. G. M (eds). Academic Press, Elsevier, Amsterdam, pp. 847-852.

Omta, A. W., Dutkiewicz, S. and Follows, M. J. 2011. Dependence of the ocean-atmosphere partitioning of carbon on temperature and alkalinity. *Global Biogeochemical Cycles,* Vol. 25, GB1003. doi:10.1029/2010GB003839

Orr, J. C. et al. 2005. Anthropogenic ocean acidification over the twenty-first century and its impact on calcifying organisms. *Nature*, Vol. 437, pp. 681-686.

Osterhaus, A. et al. 1997. Morbillivirus in monk seal mass mortality. *Nature*, Vol. 388, pp. 838-839.

Otero, P. et al. 2010. First toxin profile of Ciguateric fish in Madeira Arquipelago (Europe). *Analytical Chemistry*, Vol. 82, pp. 6032-6039.

Oviatt, C., Lane, P., French, F. and Donagha, P. 1989. Phytoplankton species and abundance in response to eutrophication in coastal marine mesocosms. *Journal of Plankton Research*, Vol. 11 (6), pp. 1223–1244.

Ozer, P. 2001. Les lithometeores en region sahelienne. *International Journal of Tropical Ecology and Geography*, Vol. 24, pp. 1-317.

Pacheco, M. and Hernández-Guerra, A. 1999. Seasonal variability of recurrent phytoplankton pigment patterns in the Canary Islands

area. *International Journal of Remote Sensing*, Vol. 20, pp. 1405–1418.

Packard, T. T., Harmon, D. and Boucher, J. 1974. Respiratory electron transport activity in plankton from upwelled water. *Tethys*, Vol. 6, pp. 213-222.

Paiva, J. 1970. *Nouvelle contribution à l'étude des copépodes de l'archipel du Cap Vert*. Conseil lnternational de l'Exploration de la Mer, Rapports et procès-verbaux: 159 pp.

Pardo, P. C., Padín, X. A., Gilcoto, M., Farina-Busto, L. and Pérez, F. F. 2011. Evolution of upwelling systems coupled to the long-term variability in sea surface temperature and Ekman transport. *Climate Research*, Vol. 48 (2), 231–246. doi:10.3354/cr00989.

Parker, D., Thorncroft, C., Burton, R. and Diongue Niang, A. 2005. Analysis of the African easterly jet, using aircraft observations from the JET2000 experiment. *Quarterly Journal of Royal Meteorological Society*, Vol. 131, pp. 1461-1482.

Parrilla, G., Neuer, S., Le Traon, P. -Y. and Fernández, E. 2002. Topical Studies in Oceanography: Canary Islands Azores Gibraltar Observations (CANIGO). Vol. 2: Studies of the Azores and Gibraltar regions. *Deep-Sea Research Part II: Topical Studies in Oceanography*, Vol. 49, pp. 3951-3955.

Pastor, M. V., Pelegrí, J. L., Hernández-Guerra, A., Font, J., Salat, J. and Emelianov, M. 2008. Water and nutrient fluxes off Northwest Africa. *Continental Shelf Research*, Vol. 28 (7), pp. 915-936.

Pastor, M. V., Peña-Izquierdo, J., Pelegrí, J. L. and Marrero-Díaz, A. 2012. Meridional changes in water properties off NW Africa during November 2007/2008. *Ciencias Marinas*, Vol. 38 (1B), pp. 223-244.

Pastor, M. V., Palter, J. B., Pelegrí, J. L. and Dunne J. P. 2013. Physical drivers of interannual chlorophyll variability in the eastern subtropical North Atlantic. *Journal of Geophysical Research: Oceans*, Vol. 118, pp. 3871-3886.

Patey, M. D. 2010. *Trace metals and nutrients in aerosols over the tropical and subtropical North Atlantic Ocean.* PhD Thesis, University of Southampton.

Patriat, M. and Labails, C. 2006. Linking the Canary and Cape-Verde Hot-Spots, Northwest Africa. *Marine Geophysical Research,* Vol. 27, pp. 201-215.

Pattiaratchi, C., James, A. and Collins, M. 1986. Island wakes and headland eddies: a comparison between remotely sensed data and laboratory experiments. *Journal of Geophysical Research*, Vol. 92, pp. 783–794.

Pelegrí, J. L. and Richman, J. G. 1993. On the role of shear mixing during transient coastal upwelling. *Continental Shelf Research*, Vol. 13, pp. 1363-1400.

Pelegrí, J. L., Sangrà, P. and Hernández-Guerra, A. 1997. Heat gain in the eastern North Atlantic subtropical gyre. In: *The Mathematics of Models for Climatology and Environment*, NATO ASI Series, Vol. I, Vol. 48. Díaz, J. I. (ed.). Springer-Verlag, Berlin, pp. 419– 436.

Pelegrí, J. L. et al. 2005a. Coupling between the open ocean and the coastal upwelling region off Northwest Africa: Water recirculation and offshore pumping of organic matter. *Journal of Marine Systems*, Vol. 54, pp. 3-37.

Pelegrí, J. L. et al. 2005b. Hydrographic cruises off northwest Africa: The Canary Current and the Cape Ghir region. *Journal of Marine Systems,* Vol. 54 (1-4), pp. 39-63.

Pelegrí, J. L., Marrero-Díaz, A. and Ratsimandresy, A. W. 2006. Nutrient irrigation of the North Atlantic. *Progress in Oceanography*, Vol. 70, pp. 366-406.

Peltier, W. 2004. Global glacial isostasy and the surface of the ice-age Earth: The ICE-5G(VM2) model and GRACE. *Annual Review of Earth and Planetary Sciences*, Vol. 32, pp. 111–149.

Peña-Izquierdo, J., Pelegrí, J. L., Pastor, M. V., Castellanos, P., Emelianov, M., Gasser, M., Salvador, J. and Vázquez-Domínguez, E. 2012. The continental slope current system between Cape Verde and the Canary Islands. *Scientia Marina*, Vol. 76 (S1), pp. 65-78.

Peña-Izquierdo, J., Van Sebille, E., Pelegrí, J. L., Sprintall, J., Mason, E., Llanillo, P. and Machín, F. 2015. Water mass pathways to the North Atlantic Oxygen Minimum Zone. *Journal of Geophysical Research: Oceans*. doi:10.1002/2014JC010557.

Pérez, F. F., Mintrop, L., Llinás, O., González-Dávila, M., Castro, C., Koertzinger, A., Santana-Casiano, M., Alvarez, M. and Ríos, A. F. 2001. Mixing analysis of nutrients, oxygen and inorganic carbon in the Canary Islands region. *Journal of Marine System,* Vol. 28, pp. 183-201.

Pérez-Arellano, J. -L., Luzardo, O. P., Pérez Brito, A., Hernández Cabrera, M., Zumbado, M., Carranza, C., Angel-Moreno, A., Dickey, R. W. and Boada, L. D. 2005. Ciguatera fish poisoning, Canary Islands. *Emerging Infectious Diseases*, Vol. 11, pp. 1981-1982.

Pérez-Brunius, P., Lopez, M., Pares-Sierra, A. and Pineda, J. 2007. Comparison of upwelling indices off Baja California derived from three different wind data sources*. CalCOFI Reports*, Vol. 48, pp. 204–214.

Pérez-Farfante, I. and Kensley, B. 1997. Penaeoid and Sergestoid Shrimps and Prawns of the World: Keys and Diagnoses for the Families and Genera. *Mémoires du Muséum Nationale d'Histoire Naturelle*, Paris, Vol. 175: 233 pp.

Pérez-Gómez, B. 2014. *Design and implementation of an operational sea level monitoring and forecasting system for the Spanish coast.* PhD Thesis, Cantabria University, Santander, Spain: 242 pp.

Pérez-Gómez, B., Álvarez-Fanjul, E., Pérez, S., de Alfonso, M. and Vela, J. 2013. Use of tide gauge data in operational oceanography and sea level hazard warning systems. *Journal of Operational Oceanography*, Vol. 6 (2), pp. 1–18.

Pérez-Gómez, B., Payo, A., López, D., Woodworth, P. L. and Álvarez-Fanjul, E. 2014. Overlapping sea level time series measured using different technologies: an example from the REDMAR Spanish network. *Natural Hazards and Earth System Science*, Vol. 14 (3), pp. 589–610.

Pérez-Hernández, M. D., Hernández-Guerra, A., Fraile-Nuez, E., Comas-Rodríguez, I., Benítez-Barrios, V. M., Domínguez-Yanes, J. F., Vélez-Belchí, P. and De Armas, D. 2013. The source of the Canary current in fall 2009. *Journal of Geophysical Research: Ocean*, Vol. 118, C12019. doi:10.1002/jgrc.20227.

Pérez-Rodríguez, P., Pelegrí, J. L. and Marrero-Díaz, A. 2001. Dynamical characteristics of the Cape Verde frontal zone. *Scientia Marina*, Vol. 65 (S1), pp. 241-250.

Perrin, W. F. and Van Waerebeek, K. 2012. *The small-cetacean fauna of the west coast of Africa and Macaronesia: diversity and distribution.* UNEP/CMS, Bonn, Germany. CMS Technical Series, No. 26, pp. 7-17.

Petit, J. R. et al. 1999. Climate and atmospheric history of the past 420,000 years from the Vostok ice core, Antarctica. *Nature*, Vol. 399 (6735), pp. 429–436. doi:10.1038/20859.

Piedeleu, M. 2014. *Remolinos oceánicos de las Islas Canarias: generación, características y evolución*. PhD Thesis, University of Las Palmas de Gran Canaria, Spain.

Piedeleu, M., Sangrà, P., Sánchez-Vidal, A., Fabrés, J., Gordo, C. and Calafat A. 2009. An observational study of oceanic eddy generation mechanisms by tall deep-water islands (Gran Canaria). *Geophysical Research Letters*, Vol. 36, L14605.

Pim, J., Peirce, C., Watts, A. B., Grevemeyer, I. and Krabbenhoeft, A. 2008. Crustal structure and origin of the Cape Verde Rise. *Earth and Planetary Science Letters,* Vol. 272, pp. 422-428.

Pinela, A. M., Borrell, A., Cardona, L. and Aguilar, A. 2010. Stable isotope analysis reveals habitat partitioning among marine mammals off the NW African coast and unique trophic niches for two globally threatened species. *Marine Ecology Progress Series*, Vol. 416, pp. 295-306.

Pinela, A. M., Borrell, A. and Aguilar, A. 2011. Common dolphin morphotypes: Niche segregation or taxonomy? *Journal of Zoology*, Vol. 2844, pp. 239-247.

Pinnegar, J. 2012. *Climate change and European fisheries: observed changes and future prospects.* European Fisheries and Aquaculture Research Organisations. EFARO Position paper, pp. 1-33.

Piñeiro, C. G., Casas, M. and Bañón, R. 2001. The deep-water fisheries exploited by the Spanish fleets in the Northeast Atlantic: a review of the current status. *Fisheries Research,* Vol. 51, pp. 311-320.

Pitcher, G. C., Figueiras, F. G., Hickey, B. M. and Moita, M. T. 2010. The physical oceanography of upwelling systems and the development of harmful algal blooms. *Progress in Oceanography*, Vol. 85, pp. 5-32.

Platt, T. and Sathyendranath, S. 1993. Estimators of primary production for interpretation of remotely sensed data on ocean color. *Journal of Geophysical Research: Oceans (1978–2012)*, Vol. 98 (C8), pp. 14561–14576.

Poll, M. 1949. *Résultats scientifiques des croisières du navire-école belge Mercator IV. Poissons.* Mémories Institut Royal des Sciences naturelles de Belgique, Serie 2, No. 33, pp. 173-269.

Polo, I., Ullmann, A., Roucou, P. and Fontaine, B. 2011. Weather regimes in the EuroAtlantic and Mediterranean sector, and relationship with West African rainfall over the 1989–2008 period from a self-organizing maps approach. *Journal of Climate*, Vol. 24 (13), pp. 3423–3432.

Polovina, J. J., Howell, E. A. and Abecassis, M. 2008. Ocean's least productive waters are expanding. *Geophysical Research Letters*, Vol. 35 (3), pp. 1–5.

Polyakov, I. V., Alexeev, V. A., Bhatt, U. S., Polyakova, E. I. and Zhang, X. 2009. North Atlantic warming: patterns of long-term trend and multidecadal variability. *Climate Dynamics*, Vol. 34 (2-3), pp. 439–457. doi:10.1007/s00382-008-0522-3.

Poole, R. and Tomczak, M. 1999. Optimum multiparameter analysis of the water mass structure in the Atlantic Ocean thermocline. *Deep-Sea Research Part I: Oceanographic Research Papers*, Vol. 46, pp. 1895-1921.

Postel, L. 1990. *Die Reaktion des Mesozooplanktons, speziell der Biomasse, aufkuÅNstennahen Auftriebvor West afrika*. PhD Thesis, InstitutfuÅN r Meereskunde, Warnemünde: 127 pp.

Prieto, P., Ferreira, R. and Silva, A. 2000. Turtle Bycatch Study in the Longline Fisheries of the Azores. In: *Workshop to design an experiment to determine the effects of longline gear modification on sea turtle bycatch rates*. Bolten, A. B., Martins, H. R. and Bjorndal, K. A. (eds). NOAA Technical Memorandum NMFS-OPR-19, pp. 22–28.

Prospero, J. M. 1996. The atmospheric transport of particles to the ocean. In: *Particle Flux in the Ocean.* Ittekkot, V., Schaefer, P., Honjo, S. and Depetris, P. J. (eds). John Wiley and Sons, Chichester, pp. 19–52.

Prospero, J. M. 1999. Long-term measurements of the transport of African mineral dust to the southeastern United States: Implications for regional air quality. *Journal of Geophysical Research D: Atmospheres*, Vol. 104, pp. 15917-15927.

Prospero, J. M. et al. 1995. Temporal variability of summer-time ozone and aerosols in the free troposphere over the Eastern North Atlantic. *Geophysical Research Letters,* Vol. 22, pp. 2925–2928. doi: 10.1029/95GL02791.

Prospero, J. M., Ginoux, P., Torres, O., Nicholson, S. and Gill, T. 2002. Environmental characterization of global sources of atmospheric soil dust identified with the Nimbus 7 Total Ozone Mapping Spectrometer (TOMS) absorbing aerosol product. *Reviews of Geophysics,* Vol. 40, 1002. doi: 10.1029/2000RG000095.

Prospero, J. M. and Lamb, P. J. 2003. African droughts and dust transport to the Caribbean: Climate Change Implications. *Science*, Vol. 302, pp. 1024-1027. doi: 10.1126/science.1089915.

Pu, B. and Cook, K. H. 2010. Dynamics of the West African westerly jet. *Journal of Climate*, Vol. 23, pp. 6263–6276.

Puerto, M. A., Fernández-Peralta, L., Salmerón, F., Rey, J. and Real, R. 2012. Regionalización biótica de la ictiofauna demersal profunda en aguas de Mauritania. *III International Symposium in Marine Science*, Cádiz (Spain), 24-27 January 2012.

Pugh, D. T. 1987. *Tides, Surges, and Mean Sea-Level*. John Wiley & Sons Ltd.: 472 pp.

Quevedo-González, L. Á., Mangas, J., Acosta, J., Martín-Sosa, P., Arrese, B. and Rivera, J. 2012. Sedimentological characteristics of the submarine sediments associated to the Canarian seamounts of Amanay, El Banquete and Concepcion Bank. *Book of abstracts. MAKAVOL International Conference*. El Hierro (Spain), pp. 17-18.

Quevedo-González, L. Á., Mangas, J., Acosta, J., Martín-Sosa, P., Tauler, E., Arrese, B., Rivera, J., Rodríguez, S. and Menéndez, I. 2014. A leap in seamounts geo-characterization: using a multi-technical approach for origin, nature and evolution of Amanay, Banquete and Concepcion Bank (Canary Islands). LIFE+ INDEMARES (2009-2013). *Book of abstracts. IV Congress of Marine Sciences*. Las Palmas de Gran Canaria (Spain), pp. 201-202.

Ramil, F., Mesfioui, H. and Ramos, A. 2005. La fauna bentónica. In: *Informe de resultados de la Campaña 'Maroc-0411'. Prospección por arrastre de los recursos demersales profundos del norte de Marruecos*. Ramos, A. et al. Report IEO - SGPM (MAPA), pp. 185-201.

Ramil, F., Ramos, A., García-Isarch, E. and de Matos-Pita, S. S. 2012a. Zoobenthos. In: *Cruise Report "Dr. Fridtjof Nansen" CCLME-North West Africa. Ecosystem Survey Guinea–Morocco, 20 October–21 December 2011.* Krakstad, J. -O. et al. FAO-NORAD Project No: GCP/INT/003/ NOR.

Ramil, F., Ramos, A., García-Isarch, E., de Matos-Pita, S. S. and Muñoz, I. 2012b. Zoobenthos. In: *Cruise Report "Dr. Fridtjof Nansen" CCLME-North West Africa. Ecosystem Survey Guinea – Morocco, 05 May – 22 July 2012*. Krakstad, J. -O. et al. FAO-NORAD Project No: GCP/INT/003/NOR.

Ramil, F. and Ramos, A. Submitted. A global overview on biodiversity of bathyal megabenthos off Mauritania. In: Ramos, A., Sanz, J. L. and Ramil, F. (eds). *Deep-sea ecosystems off Mauritania: Researching marine biodiversity and habitats in West African deep-waters*. Springer.

Ramos, A. 2011. *État des connaissances sur le benthos dans la région du CCLME*. Rapport Projet Protection du Grand Écosystème Marin du Courant des Canaries (CCLME), Vigo, Spain: 42 pp. (unpublished).

Ramos, A., Sobrino, I., Fernández, L. and González, J. F. 1991. *Report of "Guinea 90" Survey*. FAO, Rome. CECAF/ECAF SERIES. 91/52: 288 pp.

Ramos, A., González, R., García, T., Sobrino, I. and Fernández, L. 2000. La crisis en el acceso al caladero marroquí: Análisis de la evolución y situación de las pesquerías y recursos de merluzas y crustáceos. Informes Técnicos, Instituto Español de Oceanografía, No. 178: 171 pp.

Ramos, A. et al. 2005a. *Informe de resultados de la Campaña 'Maroc-0411'. Prospección por arrastre de los recursos demersales profundos del norte de Marruecos*. Instituto Español de Oceanografía-Institut National des Recherches Halieutiques: 271 pp. (unpublished)

Ramos, A. G. et al. 2005b. Bloom of the marine diazotrophic cyanobacterium *Trichodesmium erythraeum* in the Northwest African Upwelling. *Marine Ecology Progress Series*, Vol. 301, pp. 303–305.

Ramos, A. et al. 2010. *Estudio de los ecosistemas de la plataforma y margen continental de Mauritania. Informe de resultados de la campaña 'Maurit-0911*'. Instituto Español de Oceanografía-Institut Mauritanien de Recherches Océanographiques et des Pêches: 161 pp. (unpublished).

Ramos, A., Ramil, F., García-Isarch, E., Soto, S., Muñoz, I., Barry, A. O., Mohamed, S. and Zidane, H. 2012. Biodiversité de l'épibenthos du Nord-ouest de l'Afrique: Résultats préliminaires des campagnes écosystémiques dans la Région du CCLME. Paper presented at the First Meeting of the Biodiversity, Habitat and Water Quality Working Group. Nouakchott (Mauritania), 11-12 April 2012.

Ramos, A., Sanz, J. L. and Ramil, F. (eds). Submitted a. *Deep-sea ecosystems off Mauritania: Researching marine biodiversity and habitats in West African deep-waters*. Springer.

Ramos, A., Sanz, J. L., Agudo, L. M., Presas, C. and Ramil, F. Submitted b. The giant cold-water coral mound barrier off Mauritania. In: *Deep-sea ecosystems off Mauritania: Researching marine biodiversity and habitats in West African deep-waters*. Ramos, A., Sanz, J. L. and Ramil, F. (eds). Springer, Heidelberg.

Ratmeyer, V., Fischer, G. and Wefer, G. 1999. Lithogenic particle fluxes and grain size distributions in the deep ocean off northwest Africa: implications for seasonal changes of aeolian dust input and downward transport. *Deep-Sea Research Part I: Oceanographic Research Papers,* Vol. 46, pp. 1289–1337.

Raven, J., Caldeira, K., Elderfield, H., Hoegh-Guldberg, O., Liss, P., Riebesell, U., Shepherd, J., Turley, C. and Watson, A. 2005. Ocean acidification due to increasing atmospheric carbon dioxide. Policy document 12/05. The Royal Society, London: 57 pp.

Ray, R. 2006. Secular changes of the M2 tide in the Gulf of Maine. *Continental Shelf Research*, Vol. 26 (3), pp. 422–427.

Ray, R. 2009. Secular changes in the solar semidiurnal tide of the western North Atlantic Ocean. *Geophysical Research Letters*, Vol. 36, L19601.

Reed, R. J., Norquist, D. C. and Recker, E. E. 1977. The structure and properties of African wave disturbances as observed during phase III of GATE. *Monthly Weather Revue*, Vol. 105, pp. 414-420.

Reguera, B., Velo-Suárez, L., Raine, R. and Park, M. G. 2012. Harmful *Dinophysis* species: a review. *Harmful Algae*, Vol. 14, pp. 87-106.

Reiner, F. 1980. First record of an Antillean beaked whale *Mesoplodon europaeus* Gervais 1855, from República Popular da Guiné-Bissau. *Memórias do Museu do Mar, Serie Zoológica*, Vol. 1(8), pp. 1-8.

Reiner, F., dos Santos, M. E. and Wenzel, F. W. 1996. Cetaceans of the Cape Verde Archipelago. *Marine Mammal Science*, Vol. 123, pp. 434-443.

Represas, P., Cataláo, J., Montesinos, F. G., Madeira, J., Nata, J., Antunes, C. and Moreira, M. 2012. Constraints on the structure of Maio Island (Cape Verde) by a three-dimensional gravity model: imaging partially exhumed magma chambers. Gravity, geodesy and tides. *Geophysical Journal International*, Vol. 190, pp. 931-940.

Rex, M. A., Stuart, C. T., Hessler, R. R., Allen, J. A., Sanders, H. L. and Wilson, G. D. F. 1993. Global-scale latitudinal patterns of species diversity in the deep-sea benthos. *Nature*, Vol. 365 (6447), pp. 636–639.

Reyero, M., Cacho, E., Martínez, A., Vázquez, J., Marina, A. Fraga, S. and Franco, J. M. 1999. Evidence of saxitoxin derivatives as causative agents in the 1997 mass mortality of Monk Seals in the Cape Blanc Peninsula. *Natural Toxins*, Vol. 7, pp. 311-315.

Rhein, M. et al. 2013. Observations: Ocean. In: *Climate Change 2013: The Physical Science Basis. Contribution of Working Group I to the Fifth Assessment Report of the Intergovernmental Panel on Climate Change*. Stocker, T. F. et al. (eds). Cambridge University Press, Cambridge, United Kingdom and New York. http://www.ipcc.ch/pdf/assessment-report/ar5/wg1/WG1AR5_Chapter03_FINAL.pdf (Accessed 20 February 2015).

Ribeiro, S., Amorim, A., Andersen, T. J., Abrantes, F. and Ellegaard, M. 2012. Reconstructing the history of an invasion: the toxic phytoplankton species *Gymnodinium catenatum* in the Northeast Atlantic. *Biological Invasions*, Vol. 14, pp. 969-985.

Richardson, A. J. 2008. In hot water: zooplankton and climate change. *ICES Journal of Marine Science*, Vol. 65, pp. 279–295.

Richardson, J. I. and McGillivary, P. 2001. Post-hatchling loggerhead turtles eat insects in *Sargassum* community. *Marine Turtle Newsletter*, Vol. 55, pp. 2–5.

Richardson, A. J., Bakun, A., Hays, G. C. and Gibbons, M. J. 2009. The jellyfish joyride: causes, consequences and management responses to a more gelatinous future. *Trends in Ecology and Evolution*, Vol. 24, pp. 312–322.

Ridder, N. N. and England, M. H. 2014. Sensitivity of ocean oxygenation to variations in tropical zonal wind stress magnitude. *Global Biogeochemical Cycles*, Vol. 28, pp. 909-926.

Rijal Leblad, B., Lundholm, N., Goux, D., Vernon, B., Sagou, R., Taleb, H., Nhhala, H. and Er-Raioui, H. 2013. *Pseudo-nitzschia* Peragallo (Bacillariophyceae) diversity and domoic acid accumulation in tuberculate cockles and sweet clams in M'diq Bay, Morocco. *Acta Botanica Croatica*, Vol. 72, pp. 35-47.

Ritter, F. 2001. Twenty-one cetacean species off La Gomera (Canary Islands): Possible reasons for an extraordinary species diversity. *Annual Conference of the European Cetacean Society*, Rome, 5-7 May 2001.

Ritter, F. 2011. *Wale und Delfine der Kanarischen Inseln: Beobachten und Bestimmen.* Buchfabrik Halle: 112 pp.

Ritter, F. and Brederlau, B. 1998. First Report of Blue Whales *Balaenoptera musculus* frequenting the Canary Island waters. In: *Proceedings Twelfth Annual Conference of the European Cetacean Society, Monaco, 20-24 January 1998*. Evans P. G. H. and Parsons P. C. M. European Research on Cetaceans, Vol. 12, pp. 95-98.

Ritter F. and Brederlau, B. 1999. Behavioural observations of dense beaked whales *(Mesoplodon densirostris)* off La Gomera, Canary Islands (1995-1997). *Aquatic Mammals*, Vol. 25 (2), pp. 55-61.

Rivera, J., Lastras, G., Canals, M., Acosta, J., Arrese, B., Hermida, N., Micallef, A., Tello O. and Amblas D. 2013. Construction of an oceanic island: Insights from the El Hierro (Canary Islands) 2011–2012 submarine volcanic eruption. *Geology,* Vol. 41 (3), pp. 355-358.

Robin, J. P., Denis, V., Royer, J. and Challier, L. 2002. Recruitment, growth and reproduction in *Todaropsis eblanae* (Ball, 1841), in the area fished by French Atlantic trawlers. *Bulletin of Marine Science*, Vol. 71 (2), pp. 711-724.

Robineau, D. and Vély, M. 1993. Stranding of a specimen of Gervais' beaked whale (*Mesoplodon europaeus*) on the coast of West Africa (Mauritania). *Marine Mammal Science,* Vol. 9 (4), pp. 438-440.

Robineau, D., Vély, M. and Maigret, J. 1994. *Stenella clymene* Cetacea, Delphinidae from the west coast of West Africa. *Journal of Mammalogy,* Vol. 753, pp. 766-767.

Robineau, D. and Vély, M. 1998. Les cétacés des côtes de Mauritanie Afrique du Nord-Est. Particularités et variations spatio-temporelles de répartition: role des facteurs océanographiques. *Revue Ecologie Terre Vie,* Vol. 53, pp. 123-152.

Rocha, F., Fernández, R., Ramil, F. and Ramos, A. Submitted. Cephalopods in Mauritanian waters. In: *Deep-sea ecosystems off Mauritania: Researching marina biodiversity and habitats in West African deep-sea*. Ramos, A., Sanz, J. L. and Ramil, F. (eds). Springer.

Rodríguez, J. M., Braun, J. G. and Garcia, A. 2000. Spatial variability of the mesozooplankton biomass and ichthyoplankton in the Canary region autumn 1991. *Journal of Plankton Research*, Vol. 22 (7), pp. 1377-1391.

Rodríguez, J. M., Barton, E. D., Hernández-León, S. and Arístegui, J. 2004. Taxonomic composition and horizontal distribution of the fish larvae community in the Canaries-Coastal Transition Zone, in summer. *Progress in Oceanography*, Vol. 62, pp. 171-188.

Roel, B., Rucabado, J., Lloris, D. and Lleonart, J. 1985. *Las comunidades de peces demersales del afloramiento de África occidental (Sahara y Namibia).* International Symposium Upwelling West Africa, Barcelona, Instituto de Investigaciones Pesqueras, Vol. 1, pp. 691-699.

Romero, O. E., Lange, C. B. and Wefer, G. 2002. Interannual variability (1988–1991) of siliceous phytoplankton fluxes off northwest Africa. *Journal of Plankton Research*, Vol. 24, No. 10, pp. 1035–1046.

Roper, C. F. E., Sweeney, M. J. and Nauen, C. E. 1984. *FAO Species Catalogue, Vol. 3. Cephalopods of the World. An Annotated and Illustrated Catalogue of Species of Interest to Fisheries*. FAO, Rome. FAO Fisheries Synopsys, No. 125, Vol. 3, pp. 1-277.

Roper, C. F. E., Lu, C. C. and Vecchione, M. 1998. A revision of the systematics and distribution of *Illex* species (Cephalopoda: Ommastrephidae). *Smithsonian Contributions to Zoology*, Vol. 586, pp. 402-423.

Rosell-Fieschi, M., Pelegrí, J. L. and Gourrion, J. 2015. Zonal jets in the equatorial Atlantic Ocean. *Progress in Oceanography*, Vol. 130, pp. 1-18.

Rothwell, R. G., Pearce, T. J. and Weaver, P. P. E. 1992. Late quaternary evolution of the Madeira Abyssal plain, NE Atlantic. *Basin Research*, Vol. 4, pp. 103–131.

Rubin, M., Berman-Frank, I. and Shaked, Y. 2011. Dust-and mineral-iron utilization by the marine dinitrogen-fixer Trichodesmium. *Nature Geoscience,* Vol. 4, pp. 529-534. doi: 10.1038/NGEO1181.

Ruiz, S., Pelegrí. J. L., Emelianov, M., Pascual, A. and Mason, E. 2014. Geostrophic and ageostrophic circulation of a shallow anticyclonic eddy off Cape Bojador. *Journal of Geophysical Research: Oceans*, Vol. 119, pp. 1258-1270.

Sabine, C. L. et al. 2004. The oceanic sink for anthropogenic CO_2. *Science,* Vol. 305, pp. 367–371.

Saint Laurent, M. and Le Loeuff, P. 1979. Campagnes de la Calypso au large des côtes Atlantiques Africaines (1956 et 1959) (suite). 22. Crustacés Décapodes Thalassinidea. I. Upogebiidae et Callianassidae. In: *Résultats Scientifiques des Campagnes de la Calypso*, Vol. 11, No. 22. Forest, J. (ed.), Annales de l'Institut Océanographique, Monaco and Paris, 55 suppl., pp. 29-101.

Salah, S. 2013. *Structure spatio-temporelle du zooplancton dans les deux filaments d'upwelling Cap Ghir et Cap Juby. Effet de la dynamique des filaments sur la dispersion des copépodes*. PhD Thesis, Faculty of Science Ain Chock, University Hassan II Casablanca: 277 pp.

Salah, S., Ettahiri, O., Berraho, A., Benazzouz, A., Elkalay, K. and Errhif, A. 2012. Distribution des copépodes en relation avec la dynamique du filament de Cap Ghir (Côte atlantique du Maroc). *Comptes rendus-Biologies*, Vol. 335, pp.155-167.

Salah, S., Errhif, A., Berraho, A., Benazzouz, A., Makaoui, A. and Ettahiri, O. 2013. Contribution à l'étude de l'influence du filament d'upwelling de Cap Juby (Maroc) sur la distribution des copépodes. *Journal des Sciences Halieutique et Aquatique*, Vol. 6, pp. 207-220.

Sánchez, P., González, A. F., Jereb, P., Laptikhovsky, V. V., Mangold, K. M., Nigmatullin, Ch. M. and Ragonese, S. 1998. *Illex coindetii*. In: *Squid recruitment dynamics. The genus Illex as a model. The commercial Illex species. Influences on variability*. Rodhouse, P. G.,

Dawe, E. G. and O'Dor, R. K. (eds). FAO, Rome. FAO Fisheries Technical Paper, No. 376, pp. 59-76.

Sangrà, P. 1995 *Perturbación de un flujo geofísico por un obstáculo: Aplicación a la isla de Gran Canaria*. PhD Thesis, University of Las Palmas de Gran Canaria, Spain.

Sangrà, P., Hernández-Guerra, A., Marrero-Díaz, A., Martín, J. M., Martínez, A., Ratsimandresy, A. W. and Rodríguez-Santana, A. 2004. Life history of an anticyclonic eddy. *Journal of Geophysical Research*, Vol. 110, C03021. doi: 10.1029/2004JC002526.

Sangrà, P., Pelegrí, J. L., Hernández-Guerra, A., Arregui, I., Martín, J. M., Marrero-Díaz, A., Martínez, A., Ratsimandresy, A. W. and Rodríguez-Santana, A. 2005. Life History of an anticyclonic eddy. *Journal of Geophysical Research*, Vol. 11, C03021.

Sangrà, P., Auladell, M., Marrero-Díaz, A., Pelegrí, J. L., Fraile-Nuez, E., Rodríguez-Santana, A., Martín, J. M., Mason, E. and Hernández-Guerra, A. 2007. On the nature of oceanic eddies shed by the Island of Gran Canaria. *Deep-Sea Research Part I: Oceanographic Research Papers*, Vol. 54, pp. 687-709.

Sangrà, P. et al. 2009. The Canary Eddy Corridor: a major pathway for long-lived eddies in the North Atlantic. *Deep-Sea Research Part I: Oceanographic Research Papers*, Vol. 56, pp. 2100-2114.

Sangrà, P., Troupin, C., Barreiro-González, B., Barton, E. D., Orbi, A. and Arístegui, J. 2015. The Cape Ghir filament system in August 2009 (NW Africa). *Journal of Geophysical Research: Oceans*. doi:10.1002/2014JC010514.

Santamaría-Gómez, A., Gravelle, M., Collilieux, X., Guichard, M., Míguez, B. M., Tiphaneau, P. and Wöppelmann, G. 2012. Mitigating the effects of vertical land motion in tide gauge records using a state-of-the-art GPS velocity field. *Global and Planetary Change*, S. 98-99, pp. 6–17.

Santana-Casiano, J. M., González-Dávila, M. and Laglera, L. M. 2001. Carbon dioxide system in the Canary Region during October 1995. *Scientia Marina,* Vol. 65, pp. 41-49.

Santana-Casiano, J. M., González-Davila, M. and Millero, F. J. 2006. The role of Fe(II) species on the oxidation of Fe(II) in natural waters in the presence of O_2 and H_2O_2. *Marine Chemistry*, Vol. 99, pp. 70-82.

Santana-Casiano, J. M., González-Dávila, M., Rueda, M. J., Llinás, O. and González-Dávila, E. F. 2007. The interannual variability of oceanic CO2 parameters in the northeast Atlantic subtropical gyre at the ESTOC site. *Global Biogeochemical Cycles,* Vol. 21, GB1015. doi:10.1029/2006GB002788.

Santana-Casiano, J. M. and González-Dávila, M. 2011. pH decrease and effects on the Chemistry of Seawater. In: *Oceans and the atmospheric carbon content.* Duarte, P. and Santana-Casiano, J. M. (eds). Springer, pp. 95-114. doi:101007/978-90481-9821-4-5.

Sanz, J. L., Agudo, L. M., Ramil, F. and Ramos, A. Submitted a. *Wolofs*' knoll: A small seamount on the Mauritanian continental slope. In: *Deep-sea ecosystems off Mauritania: Researching marine biodiversity and habitats in West African deep-waters*. Ramos, A., Sanz, J. L. and Ramil, F. (eds). Springer, Heidelberg.

Sanz, J. L., Agudo, L. M., Ramil, F. and Ramos, A. Submitted b. Canyon systems of the Banc d'Arguin, Timiris Cape and Senegal River: Development, evolution and environmental and biological characterization. In: *Deep-sea ecosystems off Mauritania: Researching marine biodiversity and habitats in West African deep-waters*. Ramos, A., Sanz, J. L. and Ramil, F. (eds). Springer, Heidelberg (in edition).

Sarmiento, J. L., Rooth, C. G. and Roether, W. 1982. The North Atlantic tritium distribution in 1972. *Journal of Geophysical Research*, Vol. 87, pp. 8047–8056.

Sassen, K., DeMott, P. J., Prospero, J. M. and Poellot, M. R. 2003. Saharan dust storms and indirect aerosol effects on clouds: CRYSTAL-FACE Results. *Geophysical Research Letters*, Vol. 30, No. 12.

Scales, K. L., Miller, P. I., Varo-Cruz, N., Hodgson, D. J., Hawkes, L. A. and Godley, B. J. 2015. Oceanic loggerhead turtles *Caretta caretta* associate with thermal fronts: evidence from the Canary Current Large Marine Ecosystem. *Marine Ecological Progress Series*, Vol. 519, 195-207.

Schemainda, R., Nehring, D. and Shultz, S. 1975. Ozeanologische Untersuchungen zum Produktionspotential des nordwestafrica-niscben Wasserauftriebs region 1970-1973. *Geodätische Geophysikalische Veröffentlichungen*, Vol. 4 (16), pp. 85.

Schepanski, K., Tegen, I., Laurent, B., Heinold, B. and Macke, A. 2007. A new Saharan dust source activation frequency map derived from MSG-SEVIRI IR-channels. *Geophysical Research Lett*ers, Vol. 34, L18803. doi:10.1029/2007GL030168.

Schepanski, K., Tegen, I., Todd, M. C., Heinold, B., Bönisch, G., Laurent, B. and Macke, A. 2009. Meteorological processes forcing Saharan dust emission inferred from MSG-SEVIRI observations of subdaily dust source activation and numerical models. *Journal of Geophysical Research D: Atmospheres*, Vol. 114, D10201. doi:10.1029/2008JD010325.

Schlitzer, R. 2015. Ocean Data View. http://odv.awi.de (Accessed 28 February 2015)

Schmincke, H. -U. 1973. Magmatic evolution and tectonic regime in the Canary, Madeira and Azores Island Groups. *Geological Society of America* Bulletin*,* Vol. 84, pp. 633-648.

Schmincke, H. -U. 1982. Volcanic and chemical evolution of the Canary Islands. In: *Geology of the Northwest African Continental Margin*. Springer-Verlag, Berlin, pp. 61-68.

Schmincke, H. -U. and Sumita, M. 1998. Volcanic evolution of Gran Canaria reconstructed from apron sediments: synthesis of VICAP project drilling. *In: Proceedings of the Ocean Drilling Program Scientific Results,* Vol. 157. Weaver, P. P. E., Schmincke, H. -U., Firth, J. V. and Duffield, W. (eds). College Station, TX (Ocean Drilling Program), pp. 443–469. doi:10.2973/odp.proc.sr.157.135.1998.

Schmincke, H. -U. and Sumita, M. 2010. *Geological evolution of the Canary Islands*. Ed. Görres Verlag, Koblenz, Germany.

Schubert, W. H., Ciesielski, P. E., Stevens, D. E. and Kuo, H. C. 1991. Potential vorticity modeling of the ITCZ and the Hadley circulation. *Journal of Atmospheric Science*, Vol. 48, pp. 1493-1500.

Schütz, L., Jaenicke, R. and Pietrek, H. 1981. Saharan dust transport over the North Atlantic Ocean. *Geological Society American Special Paper*, Vol. 186, pp. 87-100.

Sea Around Us Project. 2015. *Fisheries, Ecosystems, and Biodiversity*. Fisheries Centre, University of British Columbia, Vancouver, Canada. http://www.seaaroundus.org/lme/27.aspx (Accessed 9 February 2015).

Sears, R. and Perrin, W. F. 2009. Blue whale *Balaenoptera musculus*. In: *Encyclopedia of Marine Mammals. Second Edition.* Perrin, W. F., Würsig, B. and Thewissen, J. G. M. (eds). Academic Press, Elsevier, Amsterdam: pp. 120-124.

Secretariat of the Convention on Biological Diversity. 2014. *An Updated Synthesis of the Impacts of Ocean Acidification on Marine Biodiversity.* Hennige, S., Roberts, J. M. and Williamson, P. (eds). Montreal, Technical Series, No. 75, pp. 99.

Seidel, D. J., Fu, Q., Randel, W. J. and Reichler, T. J. 2008. Widening of the tropical belt in a changing climate. *Nature Geoscience*, Vol. 1, pp. 21–24. doi:10.1038/ngeo.2007.38.

Seguin, G. 1973. *Cycles comparés du zooplancton dans l'Ouest africain et la Méditerranée sud occidentale, étude systématique quantitative et écologique*. PhD Thesis, University of Lille: 168 pp.

Seguin, G. 1981. Dynamique des copépodes pélagiques en rade de Villefranche sur Mer à partir de prélèvements quotidiens (année 1972).*Oceanologica Acta*, Vol. 4, pp. 405-414.

Seinfeld, J. H. and Pandis, S. N. 2006. *Atmospheric chemistry and physics: from air pollution to climate change*, 2nd edn. John Wiley and Sons, New York: 1232 pp.

Sellner, K. G. 1997. Physiology, ecology and toxic properties of marine cyanobacteria blooms. *Limnology and Oceanography*, Vol. 42, pp. 1089-1104.

Seret, C. 1983. Zooplancton de la Côte sud de la presqu'île du cap Vert (Sénégal). In: *Etude de l'environnement côtier au sud du cap Vert (Sénégal).* Rapport Provisoire du Centre de Recherches Océanographiques de Dakar-Thiaroye, pp. 157-188.

Serpa, M. F. 2000. Information on Accidental Capture of Marine Turtles in the Azores. In: *Workshopto design an experiment to determine the effects of longline gear modification on sea turtle bycatch rates*. Bolten, A. B., Martins, H. R. and Bjorndal, K. A. (eds). NOAA Technical Memoramdum NMFS-OPR-19, pp. 17–21.

Shamblin, B. et al. 2014. Geographic patterns of genetic variation in a broadly distributed marine vertebrate: new insights into loggerhead turtle stock structure from expanded mitochondrial DNA sequences. *PLoS ONE*, Vol. 9, pp. e85956.

Shang, S. L., Dong, Q., Hu, C. M., Lin, G., Li, Y. H. and Shang, S. P. 2014. On the consistency of MODIS chlorophyll a products in the northern South China Sea. *Biogeosciences*, Vol. 11, pp. 269–280. doi:10.5194/bg-11-269-2014.

Sheppard, C. R. C, Davy, S. K. and Pilling, G. 2010. *The biology of coral reefs. Biology of habitats.* Oxford University Press: 339 pp.

Sherman, K. 2005. The large marine ecosystem approach for assessment and management of ocean coastal waters. In: *Sustaining Large Marine Ecosystems. The Human Dimension. Large Marine Ecosystems,* Vol. 13. Hennessey, T. M. and Sutinen, J. G. Elsevier, pp. 3-16.

Sherman, K. and Duda, A. 1999. An ecosystem approach to global assessment and management of coastal waters. *Marine Ecology Progress Series*, Vol. 190, pp. 271-287.

Shigesada, N. and Okubo, A. 1981. Analysis of the self-shading effect on algal vertical distribution in natural waters. *Journal of Mathematical Biology*, Vol. 12 (3), pp. 311–326. doi:10.1007/BF00276919.

Shiller, A. M. 1997. Manganese in surface waters of the Atlantic Ocean. *Geophysical Research Letters*, Vol. 24 (12), pp. 1495–1498. doi:10.1029/97GL01456.

Sibuet, M., Albert, P., Charmasson, S., Deming, J., Dinet, A., Galeron, J., Guidi-Guilvard, L., Mahaut, M. -L. 1993. The benthic ecosystem in the three EUMELI sites in the northeast tropical Atlantic Ocean: general perspectives and initial results biological abundance and activities. *Annales de l'Institut Océanographique*, Paris, Vol. 69, pp. 21-33.

Sidi, O. M. B. 2010. Contribution à la connaissance de la macrofaune benthique de la Baie de l'Étoile. Rapport de stage: 29 pp. (unpublished).

Siedler, G., Kuhl, A. and Zenk, W. 1987. The Madeira Mode Water. *Journal of Physical Oceanography*, Vol. 17, pp. 1561-1570.

Siedler, G., Zangenberg, N., Onken, R. and Morlière, A. 1992. Seasonal Changes in the Tropical Atlantic Circulation: Observation and Simulation of the Guinea Dome. *Journal of Geophysical Research*, Vol. 97, pp. 703-715.

Siedler, G. and Onken, R. 1996. Eastern recirculation. In: *The Warm water sphere of the North Atlantic Ocean*. Krauss, W. (ed.). Gebrqder Borntraeger, Berlin, pp. 339– 364.

Sirota, A. and Zhigalova, N. 2007. Investigation of water masses distribution and zooplankton assemblage off Northwest African coast using satellite altimetry data and in-situ observations. *3rd Workshop From Inland to Marine Waters in the framework of the 27th EARSeL Symposium*, Bolzano, Italy.

Silva, E. S. 1956. Contribution a L'étude du microplancton de Dakar et des régions maritimes voisines. *Bulletin de l'Institut Fondamental d'Afrique Noire, Serie A,* Vol. 18, pp. 335-371.

Sitch, S. et al. 2015. Recent trends and drivers of regional sources and sinks of carbon dioxide. *Biogeosciences*, Vol. 12 (3), pp. 653–679. doi:10.5194/bg-12-653-2015.

Smayda, T. J. and Trainer, V. L. 2010. Dinoflagellate blooms in upwelling systems: Seeding, variability, and contrasts with diatom bloom behaviour. *Progress in Oceanography*, Vol. 85 (1–2), pp. 92–107. doi:10.1016/j.pocean.2010.02.006.

Sobrino, I. and García, T. 1991. Análisis y descripción de las pesquerías de crustáceos decápodos en aguas de la República Islámica de Mauritania durante el periodo 1987-1990. *Informe Técnico Instituto Español de Oceanografía,* No. 112: 38 pp.

Sobrino, I. and García, T. 1992a. Análisis y descripción de la actividad de la flota española en las pesquerías de crustáceos decápodos profundos en aguas de la República de Senegal durante el periodo 1987-1990. *Informe Técnico Instituto Español de Oceanografía*, No. 125: 37 pp.

Sobrino, I. and García, T. 1992b. Análisis y descripción de las pesquerías españolas de crustáceos decápodos en aguas de la República de Guinea Bissau durante el periodo 1987-1991. *Informe Técnico Instituto Español de Oceanografía*, No. 135: 38 pp.

Sobrino, I. and García, T. 1994. Biology and fishery of the deepwater rose shrimp, *Parapenaeus longirostris* (Lucas, 1846) from the Atlantic Moroccan coast. *Sciencia marina*, Vol. 58 (4), pp. 299-305.

Sohm, J. A., Webb, E. A. and Capone, D. G. 2011. Emerging patterns of marine nitrogen fixation. *Nature Reviews Microbiology,* Vol. 9, pp. 499-508.

Soest, R. W. M. 1993. Distribution of sponges on the Mauritanian continental shelf. In: *Ecological studies in the coastal waters of Mauritania*. Wolff, W. J., Van Der Land, J., Nieuhuis, P. H. and de Wilde, P. A. W. J. (eds). *Hydrobiologia*, Vol. 258 (1-3), pp. 95-106.

Somoue, L. 2004. *Structure des communautés planctoniques de l'écosystème pélagique de l'Atlantique sud marocain entre Cap Boujdor et Cap Blanc (26°30' – 1°N)*. PhD Thesis, Faculty of Science Ain Chock, University Hassan II Casablanca, Morocco: 211 pp.

Somoue, L., Elkhiati, N., Vaquer, A., Ramdani, M., Ettahiri, O., Makaoui, A. and Berraho, A. 2003. Contribution à l'étude des diatomées dans l'écosystème pélagique côtier au sud de l'atlantique marocain (21°N - 26°30'N). *Journal de Recherche Océanographique*, Vol. 28, pp. 1–13.

Somoue, L., El Khiati, N., Ramdani, M., Lam Hoai, T., Ettahiri, O., Berraho, A. and Do Chi, T. 2005. Abundance and structure of copepod communities along the Atlantic coast of southern Morocco. *Acta Adriatica*, Vol. 46 (1), pp. 63-76.

Sournia, A., Chrdtiennot-Dinet, M. -J. and Ricard, M. 1991. Marine phytoplankton: how many species in the world ocean? *Journal of Plankton Research*, Vol. 13 (5), pp. 1093–1099. doi:10.1093/plankt/13.5.1093

Spaans, B. 1990. Dolphins in the coastal area of Guinea Bissau. *Lutra,* Vol. 33, pp. 126-133.

Spalding, M. D. et al. 2007. Marine Ecoregions of the world: A bioregionalization of coastal and shelf areas. *BioScience*, Vol. 57 (7), pp. 573-583.

Sprintall, J. and Tomczak, M. 1993. On the formation of Central Water and thermocline ventilation in the southern-hemisphere. *Deep-Sea Research Part I: Oceanographic Research Papers*, Vol. 40, pp. 827-848.

Stassano, E. 1890. La pesca sulle spiagge atlantiche del Sahara. Reedition. 1932. *Bollettino di pesca, piscicoltura e idrobiologia*, Vol. 9, No. 2, pp. 219-265.

Staudigel, H. and Schmincke, H. U. 1984. The Pliocene seamount series of La Palma, Canary Islands. *Journal of Geophysical Research,* Vol. 89 (B13), pp. 11195-11215.

Staudigel, H. and Clague, D. A. 2010. The geological history of deep-sea volcanoes. Biosphere, Hydrosphere and lithosphere interactions. *Oceanography*, Vol. 23 (1), pp. 58-71.

Steemann-Nielsen, E. 1952. The use of radioactive carbon (14C) for measuring organic production in the sea. *Journal Du Conseil*, Vol. 18 (2), pp. 117–140. 10.1093/icesjms/18.2.117.

Steemann Nielsen, E., Hansen, V. K. and Jørgensen, E. G. 1962. The Adaptation to Different Light Intensities in Chlorella vulgaris and the Time Dependenee on Transfer to a new Light Intensity. *Physiologia Plantarum*, Vol. 15 (3), pp. 505–517. doi:10.1111/j.1399-3054.1962.tb08054.x

Steinberg, D. K., Van Mooy, B. A. S., Buesseler, K. O., Boyd, P. W., Kobari, T., Karl, D. M. 2008. Microbial vs. zooplankton control of sinking particle flux in the ocean's twilight zone, *Limnology and Oceanography*, Vol. 53, pp. 1327–1338.

Stommel, H. 1979. Determination of water mass properties of water pumped down from the Ekman layer to the geostrophic flow below. *Proceedings of the National Academy of Sciences of the United States of America*, Vol. 76, pp. 3051–3055.

Stramma, L. 1984. Geostrophic transport in the warm water sphere of the eastern subtropical North Atlantic. *Journal of Marine Research*, Vol. 42, pp. 537–558.

Stramma, L. and Siedler, G. 1988. Seasonal changes in the North Atlantic subtropical gyre. *Journal of Geophysical Research,* Vol. 93, pp. 8111 – 8118.

Stramma, L. and England, M. 1999. On the water masses and mean circulation of the South Atlantic Ocean. *Journal of Geophysical Research*, Vol. 104, pp. 20863-20883.

Stramma, L. and Schott, F. 1999. The mean flow field of the tropical Atlantic Ocean. *Deep-Sea Research Part II: Topical Studies in Oceanography*, Vol. 46, pp. 279–303.

Stramma, L., Brandt, P., Schafstall, J., Schott, F., Fischer, J. and Körtzinger, A. 2008. Oxygen minimum zone in the North Atlantic south and east of the Cape Verde Islands. *Journal of Geophysical Research*, Vol. 113 (C4), C04014.

Stramma, L., Visbeck, M., Brandt, P., Tanhua, T. and Wallace, D. 2009. Deoxygenation in the oxygen minimum zone of the eastern tropical North Atlantic. *Geophysical Research Letters*, Vol. 36 (20), L20607.

Stramma, L., Prince, E. D., Schmidtko, S., Luo, J., Hoolihan, J. P., Visbeck, M., Wallace, D. W. R., Brandt, P. and Körtzinger, A. 2012.

Expansion of oxygen minimum zones may reduce available habitat for tropical pelagic fishes. *Nature Climate Change*, Vol. 2, pp. 33–37.

Stramma, L. et al. 2013. Expansion of oxygen minimum zones may reduce available habitat for tropical pelagic fishes. *Nature Climate Change*, Vol. 2, pp 33-37.

Strickland, J. D. 1972. Research on the marine planktonic food web at the Institute of Marine Resources: A review of the past seven years of work. *Oceanography and Marine Biology: An Annual Review*, Vol. 10, pp. 349–414.

Stumm, W. and Morgan, J. J. 1981. *Aquatic Chemistry*, 2nd edition. Wiley, New York.

Sunda, W. G., Swift, D. G. and Huntsman, S. A. 1991. Low iron requirement for growth in oceanic phytoplankton. *Nature*, Vol. 351 (6321), pp. 55–57. doi:10.1038/351055a0.

Suga, T. and Talley, L. D. 1995. Antarctic Intermediate Water circulation in the tropical and subtropical South Atlantic. *Journal of Geophysical Research*, Vol. 100, pp. 13441-13453.

Sverdrup, H. U. 1953. On Conditions for the Vernal Blooming of Phytoplankton. *Journal Du Conseil*, Vol. 18 (3), pp. 287–295. doi:10.1093/icesjms/18.3.287.

Sverdrup, H. U., Johnson, M. W. and Fleming, R. H. 1942. *The Oceans: Their physics, chemistry, and general biology*. Prentice-Hall, New York: 1087 pp.

Swap, R., Garstang, M., Greco, S., Talbot, R. and Kallberg, P. 1992. Saharan dust in the Amazon Basin. *Tellus Series B Chemical and Physical Meteorology,* Vol. 44, pp. 133-149. doi:10.1034/j.1600-0889.1992.t01-1-00005.x.

Sydeman, W. J., Garcia-Reyes, M., Schoeman, D. S., Rykaczewski, R. R., Thompson, S. A., Black, B. A. and Bograd, S. J. 2014. Climate change and wind intensification in coastal upwelling ecosystems. *Science*, Vol. 345, pp. 77–80. doi:10.1126/science.1251635.

Tahri Joutei, L. 1998. *Gymnodinium catenatum* Graham blooms on Moroccan waters. In: *Harmful Algae*. Reguera, B., Blanco, J., Fernández, M. L. and Wyatt, T. (eds). Xunta de Galicia and IOC-UNESCO, pp. 66-67.

Tahri Joutei, L., Berraho, A. and Orbi, A. 2000. Harmful algae blooms and the upwelling regime in Atlantic coastal waters of Morocco. *Book of Abstracts. Ninth International Conference on Harmful Algal Blooms*, Hobart, Australia, 7-11 February 2000, pp.145.

Taleb, H., Idrissi, H. and Blaghen, M. 1998. Seasonality of PSP toxicity in shellfish from the Atlantic and Mediterranean coasts of Morocco. In: *Harmful Algae*. Reguera, B., Blanco, J., Fernández, M. L. and Wyatt, T. (eds). Xunta de Galicia and IOC-UNESCO, pp. 68-69.

Taleb, H., Vale, P. and Blaghen, M. 2003. Spatial and temporal evolution of PSP toxins along the Atlantic shore of Morocco. *Toxicon*, Vol. 41, pp. 199-205.

Taleb, H., Vale, P., Amanhir, R., Benhadouch, A., Sagou, R. and Chafik, A. 2006. First detection of azaspiracids in mussels in North West Africa. *Journal of Shellfish Research*, Vol. 25, pp. 1067-1070.

Talke, S. A., Orton, P. and Jay, D. A. 2014. Increasing storm tides in New York Harbor, 1844–2013. *Geophysical Research Letters*, Vol. 41, pp. 3149–3155. doi:10.1002/2014GL059574.

Targarona, J., Warnaar, J., Boessenkool, K. P., Brinkhuis, H. and Canals, M. 1999. Recent dinoflagellate cyst distribution in the North Canary Basin, NW Africa. *Grana*, Vol. 38, pp. 170-178.

Taylor, C. M. 2008. Intraseasonal land atmospheric coupling in the West African monsoon. *Journal of Climate*, Vol. 21 (24), pp. 6636–6648.

Taylor, G. T. et al. 2012. Ecosystem responses in the southern Caribbean Sea to global climate change. *Proceedings of the National Academy of Sciences of the United States of America*, Vol. 109, No. 47, pp. 19315–19320. doi:10.1073/pnas.1207514109.

Tegen, I. 2003. Modeling the mineral dust aerosol cycle in the climate system. *Quaternary Science Rev*iews, Vol. 22, pp. 1821–1834. doi: 10.1016/S0277-3791(03)00163-X.

Tegen, I., Werner, M., Harrison, S. P. and Kohfeld, K. E. 2004. Relative importance of climate and land use in determining present and future global soil dust emission. *Geophysical Research Letters*, Vol. 31, L05105. doi:10.1029/2003GL019216.

Tett, P. and Barton, E. D. 1995. Why are there about 5000 species of phytoplankton in the sea? *Journal of Plankton Research*, Vol. 17 (8), pp. 1693–1704. doi:10.1093/plankt/17.8.1693.

Thiaw, M., Gascuel, D., Jouffre, D. and Thiaw, O. T. 2009. A surplus production model including environmental effects: Application to the Senegalese white shrimp stocks. *Progress in Oceanography*, Vol. 83, pp. 351-360.

Thiel, H. 1982. Zoobenthos of the CINECA area and other upwelling regions. *Rapport Proces-Verbaux Reunions Conseil International pour l'Exploration de la Mer*, Vol. 180, pp. 323-334.

Thiel, M. et al. 2007. The Humboldt current system of northern and central Chile. Oceanography and Marine Biology: An Annual Review*,* Vol. 45, pp. 195–344.

Thomson M. C., Molesworth A., Djingarey, M. H., Yameogo, K. R., Belanger, F. and Cuevas, L. E. 2006. Potential of environmental models to predict meningitis epidemics in Africa. *Tropical Medicine and International Health,* Vol. 11, pp. 781-788. doi:10.1111/j.1365-3156.2006.01630.x.

Thorncroft, C. D., Hall, N. M. J. and Kiladis, G. N. 2008. Threedimensional structure and dynamics of African easterly waves. Part III: genesis. *Journal of Atmospheric Science*, Vol. 65, pp. 3596-3607.

Tilman, D., Kilham, S. S. and Kilham, P. 1982. Phytoplankton Community Ecology: The Role of Limiting Nutrients. *Annual Review of Ecology and Systematics*, Vol. 13, pp. 349–372.

Tilstone, G., Míguez, B., Figueiras, F. and Fermín, E. 2000. Diatom dynamics in a coastal ecosystem affected by upwelling: coupling between species succession, circulation and biogeochemical processes. *Marine Ecology Progress Series*, Vol. 205, pp. 23–41. doi:10.3354/meps205023.

Tolman, H. L. 1991. A third-generation model for wind waves on slowly varying, unsteady and inhomogeneous depths and currents. *Journal of Physical Oceanography*, Vol. 21, pp. 782-797.

Tomás, J., Aznar, F. J. and Raga, J. A. 2001. Feeding ecology of the loggerhead turtle *Caretta caretta* in the western Mediterranean. *Journal of Zoology,* Vol. 255, pp. 525-532.

Tomás, J., Guitart, R., Mateo, R. and Raga, J. A. 2002. Marine debris ingestion in loggerhead sea turtles, *Caretta caretta*, from the western Mediterranean. *Marine Pollution Bulletin,* Vol. 44, pp. 211–216.

Tomczak, M. and Hughes, P. 1980. Three dimensional variability of water masses and currents in the Canary upwelling region. *"Meteor" Forschungsergebnisse*, Vol. A, No. 21, pp. 1–24.

Tomczak, M. and Godfrey, J. S. 1994. *Regional Oceanography: An Introduction*. Elsevier, New York: 402 pp.

Tomilin, A. G. 1967. *Mammals of the USSR and adjacent countries. Volume X. Cetacea.* Original title: Zveri SSSR i prilezhashchikh stran, Izdatel'stvo Akademi Nauk SSSR, Moskva 1957. Israel Program for Scientific Translations, Jerusalem.

Torda, G., López Suárez, P. and López Jurado, L. F. 2010. First records of Fraser's Dolphin *Lagenodelphis hosei* for the Cape Verde Islands. *Zoologia Caboverdiana,* Vol.1 (1), pp. 71-73.

Torres, C., Cuevas, E., Guerra, J. C. and Carreño, V. 2001. Caracterización de las Masas de Aire en la región Subtropical. In: *Proceedings of the V Simposio Nacional de Predicción.* Instituto Nacional de Meteorología, Madrid.

Torres, P. C., Silva, L. C., Serralheiro, A., Tassinari, C. and Munhá, J. 2002a. Enquadramento geocronológico pelo método K/Ar das principais sequências vulcano-estratigráficas da Ilha do Sal–Cabo Verde. G*arcia de Orta Série Geológica*, Vol. 18, pp. 9–13.

Torres, O., Bhartia, P. K., Herman, J. R., Sinyuk, A., Ginoux, P. and Holben, B. 2002b. A long-term record of aerosol optical depth from TOMS observations and comparison to AERONET measurements. *Journal of the Atmospheric Sciences,* Vol. 59, pp. 398–413.

Torres-Padrón, M. E., Gelado-Caballero, M. D., Collado-Sánchez, C., Siruela-Matos, V. F., Cardona-Castellano, P. J. and Hernández-Brito, J. J. 2002. Variability of dust inputs to the CANIGO zone. *Deep-Sea Research Part II: Topical Studies in Oceanography*, Vol. 49, pp. 3455-3464. doi: 10.1016/S0967-0645(02)00091-7.

Torres-Valdés, S. et al. 2009. Distribution of dissolved organic nutrients and their effect on export production over the Atlantic Ocean. *Global Biogeochemical Cycles*, Vol. 23 (4), GB4019.

Trainer, V. L., Pitcher, G. C., Reguera, B. and Smayda, T. J. 2010. The distribution and impacts of harmful algal bloom species in eastern boundary upwelling systems. *Progress in Oceanography*, Vol. 85, pp. 33-52.

Trenberth, K. E. 2010. Global change: The ocean is warming, isn't it? *Nature*, Vol. 465 (7296), pp. 304–304. doi:10.1038/465304a.

Troupin, C. 2011. *Study of the Cape Ghir upwelling filament using variational data analysis and regional numerical model*. PhD Thesis, University of Liège: 224 pp.

Troupin, C., Machín, F., Ouberdous, M., Sirjacobs, D., Barth, A. and Beckers, J. M. 2010. High-resolution climatology of the northeast Atlantic using Data-Interpolating Variational Analysis (Diva). *Journal of Geophyscal Research*, Vol. 115, C08005.

Troupin, C., Mason, E., Beckers, J. M. and Sangrà, P. 2012. Generation of the Cape Ghir upwelling filament: a numerical study. *Ocean Modelling*, Vol. 41, pp. 1–15.

Tsuchiya, M., Talley, L. and McCartney, M. 1992. An eastern Atlantic section from Iceland southward across the equator. *Deep-Sea Research Part A. Oceanographic Research Papers*, Vol. 39, pp. 1885-1917.

Tubaro, A., Dell'Ovo, V., Sosa, S. and Florio, C. 2010. Yessotoxins: a toxicological overview. *Toxicon*, Vol. 56, pp. 163-172.

Türkay, M. 1975. Decapoda Reptantia vom Kap Blanco. Auswertung der Fahrt 26 (1972) von F.S. "Meteor". "Meteor" Forschungserg., (D) 20: 71-75, Abb.1-6; Berlin and Stuttgart.

Türkay, M. 1976. Decapoda Reptantia von der portugiesischen und marokkanischen Küste. Auswertung der Fahrten 8, 9c (1967), 23 (1971) und 36 (1975) von F.S. "Meteor". "Meteor" Forschungserg., (D) 23 : 23-44, Abb.1-35; Berlin and Stuttgart.

Turley, C. 2005. The other CO2 problem, open Democracy. https://www.opendemocracy.net/globalization-climate_change_debate/article_2480.jsp (Accessed 19 April 2015).

Turley, C. 2012. Future biological and ecosystem impacts of ocean acidification and their socioeconomic - policy implications. *Current opinion in environmental sustainability*, Vol. 4, pp. 278. doi:10.1016/j.cosust.2012.05.007.

Uchupi, E., Emergy, K. O., Bowin, C. O. and Phillips, J. D. 1976. Continental margin off western Africa: Senegal to Portugal. *American Association of Petroleum Geologists Bulletin,* Vol. 60, pp. 809-878.

Uitz, J., Stramski, D., Gentili, B., D'Ortenzio, F. and Claustre, H. 2012. Estimates of phytoplankton class-specific and total primary production in the Mediterranean Sea from satellite ocean color observations. *Global Biogeochemical Cycles*, Vol. 26 (2), pp. GB2024. doi:10.1029/2011GB004055.

UNCLOS-UN. 1982. United Nations Convention of the Law of the Sea of December 1982: 208 pp.

UNESCO. 2010. *UNESCO Science Report 2010*. The Current Status of Science around the World. Schneegans, S. (ed.). UNESCO Publishing, Paris: 520 pp. http://unesdoc.unesco.org/images/0018/001899/189958e.pdf (Accessed on 15 April 2015).

Urgeles, R., Canals, M., Baraza, J., Alonso, B. and Masson, D. G. 1997. The most recent megaslideson the Canary Islands: the El Golfo Debris avalanche and the Canary Debris flow. *Journal of Geophysical Research*, Vol. 102, pp. 20305–20323.

Ushakov, P. V. 1965. The bionomic features of the littoral zone in the Guinea Republic, West Africa. *Okeanologiya*, Vol. 5 (3), pp. 507-517.

Utermöhl, H. 1958. Zur vervollkommnung der quantitativen phytoplankton-methodik. *Mitt. Int. Ver. Theor. Angew. Limnol.*, Vol. 9, pp. 1–38.

Valdés, L. et al. 2007. A decade of sampling in the Bay of Biscay: What are the zooplankton time series telling us? *Progress in Oceanography*, Vol. 74 (2-3), pp. 98-114.

van Aken, H. M. 2000. The hydrography of the mid-latitude northeast Atlantic Ocean: I: The deep water masses. *Deep-Sea Research Part I: Oceanographic Research Papers*, Vol. 47, pp. 757-788.

Van Camp, L., Nykjaer, L., Mittelstadt, E. and Schlittenhardt, P. 1991. Upwelling and boundary circulation off Northwest Africa as depicted by infrared and visible satellite observations. *Progress in Oceanography*, Vol. 26 (4), pp. 357–402.

Van den Bogaard, P. 2013. The origin of the Canary Island Seamount Province - New ages of old seamounts. *Nature Scientific Reports*, Vol. 3, No. 2107.

Van der Land, J. 1987. Report on the CANCAP-Project for Marine Biological research in the Canarian - Cape Verdean Region of the North Atlantic Ocean (1976-1986). Part I. List of stations. *Zoologische Verhandelingen*, Vol. 243 (1), pp. 1-94.

Van der Land, J. 1988. *Shipboard report of the Tyro Mauritania-II Expedition 1988*: 36 pp.

Van der Knaap, M. 1985. *Preliminary annotated inventory of the scientific expeditions and resource surveys carried out in the CECAF Area*. FAO, Dakar. CECAF/TECH/85/64: 168 pp.

Van Leeuwen, P. J. 2007. The propagation mechanism of a vortex on the plane. *Journal of Physical Oceanography*, Vol. 37, pp. 2316-2330.

Van Nierop, M. M. and Den Hartog, J. C. 1984. A study on the gut contents of five juvenile loggerhead turtles, *Caretta caretta* (Linnaeus) (Reptilia, Cheloniidae), from the south-eastern part of the North Atlantic Ocean, with emphasis on coelenterate identification. *Zoologische Mededelingen*, Vol. 59, pp. 35–54.

Van Waerebeek, K. 1997. *Long-beaked and short-beaked common dolphins sympatric off central-west Africa*. International Whaling Commission. Scientific Committee Document SC/49/SM46: 5 pp.

Van Waerebeek, K., Diallo, M., Djiba, A., Ndiaye, P. and Ndiaye, E. 1997. *Cetacean research in Senegal 1995-97, an overvie*w. International Whaling Commission, Bournemouth, UK. Scientific Committee Document SC/49/SM10.

Van Waerebeek, K., André, M., Sequeira, M., Martin, V., Robineau, D., Collet, A., Papastavrou, V. and Ndiaye, E. 1999. Spatial and temporal distribution of the minke whale *Balaenoptera acutorostrata* Lacépède 1804 in the southern Northeast Atlantic and the Mediterranean Sea, with comments on stock identity. *Journal of Cetacean Research and Management,* Vol. 1 (3), pp. 223-237.

Van Waerebeek, K., Ndiaye, E., Djiba, A., Diallo, M., Murphy, P., Jallow, A., Camara, A., Ndiaye, P. and Tous, P. 2000. *A survey of the conservation status of cetaceans in Senegal, The Gambia and Guinea-Bissau*. *WAFCET-1 Report*. UNEP/CMS Secretariat, Bonn, Germany: 80 pp.

Van Waerebeek, K. et al. 2003. *Conservation of Cetaceans in The Gambia and Senegal 1999-2001, and status of the Atlantic humpback dolphin. WAFCET-2 Report*. UNEP/CMS, Bonn, Germany: 55 pp.

Van Waerebeek, K. et al. 2004. Distribution, status and biology of the Atlantic humpback dolphin *Sousa teuszii* Kükenthal, 1892. *Aquatic Mammals*, Vol. 301, pp. 56-83.

Van Waerebeek, K. and Jiddou, A. 2006. *Deuxième cours de formation théorique et pratique sur l'identification des mammifères aquatiques de l'Afrique de l'Ouest et méthodologies de collecte de données.* Rapport de Progrès à la Fondation Internationale du Banc d'Arguin: 13 pp.

Van Waerebeek, K. and Perrin, W. F. 2007a. Conservation status of the Clymene dolphin in West Africa. *14th Meeting of the CMS Scientific Council*, Bonn, Germany, 14-17 March 2007. CMS/ScC14/Doc.5: 9 pp.

Van Waerebeek, K. and Perrin, W. F. 2007b. Conservation status of the Atlantic humpback dolphin, a compromised future?. *14th Meeting of the CMS Scientific Council*, Bonn, Germany, 14-17 March 2007. CMS/ScC14/Doc.6: 10 pp.

Van Waerebeek, K, Bamy, I. L., Jiddou, A. M., Sequeira, M., Diop, M., Ofori-Danson, P. K., Tchibozo, S. and Campredon, P. 2008a. *Indeterminate status of West African populations of inshore common bottlenose dolphins Tursiops truncatus cautions against opportunistic live-capture schemes*. Technical Report FIBA, Fondation Internationale du Banc d'Arguin: 9 pp.

Van Waerebeek, K., Hazevoet, C. J., López-Suárez, P., Simão Delgado Rodrigues, M. and Gatt, G. 2008b. *Preliminary findings on the mass strandings of melon-headed whale Peponocephala electra on Boavista Island in November 2007, with notes on other cetaceans from the Cape Verde Islands.* Technical Report FIBA, Fondation Internationale du Banc d'Arguin: 9 pp.

Van Waerebeek, K. and Bamy, I. L. 2012. Exploratory nearshore survey for Atlantic humpback dolphin *Sousa teuszii* at Tristao Islands, Guinea. In: *Marine Mammal Survey 2012 CCLME, Final Report to UNESCO/FAO,* pp. *30-36.*

Van Waerebeek, K., Djiba, A., Krakstad, J. -O., Samba Ould Bilal A., Almeida, A. and Mass Mbye, E. 2013. New evidence for a South Atlantic stock of humpback whales wintering on the Northwest African continental shelf. *African Zoology,* Vol. 48 (1), pp. 177-186.

Vaquer-Sunyer, R. and C. Duarte. 2008. Thresholds of hypoxia for marine biodiversity. *Proceedings of the National Academy of Sciences of the United States of America*, Vol. 105, pp. 15452–15457.

Vargas-Yáñez, M., García Lafuente, J., Sarhan, T., Vargas, J. and Vélez-Belchí, P. 2002. About the seasonal variability of the Alboran Sea circulation. *Journal of Marine Systems*, Vol. 35, pp. 229–248.

Varo-Cruz, N., Hawkes, L. A., Cejudo, D, López, P., Coyne, M. S., Godley, B. J. and López-Jurado, L. F. 2013. Satellite tracking derived insights into migration and foraging strategies of male loggerhead turtles in the eastern Atlantic. *Journal of Experimental Marine Biology and Ecology,* Vol. 443, pp. 134–140.

Vélez-Belchí, P., Hernández-Guerra, A., Fraile-Nuez, E. and Benítez-Barrios, V. 2010. Changes in Temperature and Salinity Tendencies of the Upper Subtropical North Atlantic Ocean at 24.5°N. *Journal of Physical Oceanograph*y, Vol. 40, pp. 2546–2555. doi:10.1175/2010JPO4410.1.

Vélez-Belchí, P. et al. 2014. Monitoring the Oceanic Waters of the Canary Islands: the deep hydrographic section of the Canaries. *IV Congress of Marine Sciences*, Las Palmas de Gran Canaria, Spain, 11-13 June 2014.

Verdugo, P. 2012. Marine microgels. *Annual Reviews of Marine Sciences*, Vol. 4, pp. 375–400.

Vilas, J. C., Arístegui, J., Kiriakoulakis, K., Wolf, G., Espino, M., Polo, I., Montero, M. F. and Mendonca, A. 2009. Seamounts and organic matter – is there an effect? The case of Sedlo and Seine Seamounts Part I. Distributions of dissolved and particulate organic matter. *Deep-Sea Research Part II: Topical Studies in Oceanography*, Vol. 56, pp. 2618-2630.

Vinogradov, S. V. and Ponte, R. M. 2011. Low-frequency variability in coastal sea level from tide gauges and altimetry. *Journal of Geophysical Research: Oceans*, Vol. 116, C07006.

Vives, F. 1975. *Zooplancton et hydrographie des environs du Cap Blanc (N.O. de l'Afrique).* Commission Conseil Permanent lnternational d'Exploration de la Mer, CM 1 L.

Volk, T. and Hoffert, M. I. 1985. Ocean Carbon Pumps: Analysis of Relative Strengths and Efficiencies in Ocean-Driven Atmospheric CO2 Changes. In: *The Carbon Cycle and Atmospheric CO2: Natural Variations Archean to Present.* Sundquist, E. T. and Broecker, W. S. (eds). American Geophysical Union, pp. 99–110.

Von Rad, U. and Ryan, W. B. F. (eds). 1979. *Initial reports of the Deep Sea Drilling Project*. US Government Printing Office, Washington D.C.: 835 pp.

Von Rad, U., Hinz, K., Sarnthein, M. and Seibold, E. (eds). 1982. *Geology of the Northwest African Continental Margin*. Springer-Verlag, Berlin Heidelgerg and New York: 703 pp.

Wakelin, S. L., Woodworth, P., Flather, R. and Williams, J. 2003. Sea level dependence on the NAO over the NW European Continental Shelf. *Geophysical Research Letters*, Vol. 30 (7), pp. 1403.

Walker, G. P. L. 1990. Geology and volcanology of the Hawaiian Islands. *Pacific Science*, Vol. 44, pp. 315-347.

Wallace, B. P. et al. 2010. Regional Management Units for marine turtles: a novel framework for prioritizing conservation and research across multiple scales. *PLoS ONE*, Vol. 5, pp. e15465.

Wallace, B. P. et al. 2011. Global conservation priorities for marine turtles. *PLoS ONE*, Vol. 6, pp. e24510.

WAMDI Group et al. 1988. The WAM model: a third-generation ocean wave prediction model. *Journal of Physical Oceanography*, Vol. 18, pp. 1775-1810.

Wang, C., Kucharski, F., Barimalala, R. and Bracco, A. 2009. Teleconnections of the tropical Atlantic to the tropical Indian and Pacific Oceans: A review of recent findings. *Meteorologische Zeitschrift*, Vol. 18 (4), pp. 445–454. doi:10.1127/0941-2948/2009/0394.

Wanninkhof, R. et al. 2013. Global ocean carbon uptake: magnitude, variability and trends. *Biogeosciences*, Vol. 10 (3), pp. 1983–2000. doi:10.5194/bg-10-1983-2013.

Watson, R., Zeller, D. and Pauly, D. 2014. Primary productivity demands of global fishing fleets. *Fish and Fisheries*, Vol. 15 (2), pp. 231–241. doi:10.1111/faf.12013.

Wells, R. S. and Scott M. D. 2009. Common bottlenose dolphin. In: *Encyclopedia of Marine Mammals*. Perrin, W. F., Würsig, B. and Thewissen, J. G. M (eds). Academic Press, Elsevier, Amsterdam, pp. 249- 255.

Wenzel, F. W. et al. 2009. Current knowledge on the distribution and relative abundance of Humpback Whales (*Megaptera novaeangliae*) off the Cape Verde Islands, Eastern North Atlantic. *Aquatic Mammals,* Vol. 35, pp. 502–510.

Westgate, A. J. 2007. Geographic variation in cranial morphology of short-beaked common dolphins *Delphinus delphis* from the North Atlantic. *Journal of Mammalogy*, Vol. 883, pp. 678-688.

Westphal, H., Freiwald, A., Hanebuth, T., Eisele, M., Gürs, K., Heindel, K., Michel, J. and Reumont, J. 2007. *Report and preliminary results of Poseidon Cruise 346-MACUMA. Integrating carbonates, siliciclastics and deep-water reefs for understanding a complex environment*. Report of the Department of Geosciences, University of Bremen, Las Palmas, Spain: 49 pp.

Westphal, H. et al. 2012. *Report of the Cruise of the Maria S. Merian 16/3 - Phaeton - Paleoceanographic and paleo-climatic record on the Mauritanian shelf. Maria S. Merien-Beritche,* Leibnitz-ZMT, Bremen: 136 pp.

Widom, E., Hoernle, K. A., Shirey, S. B. and Schmincke, H. U. 1999. Os isotope systematics in the Canary Islands and Madeira: Lithospheric contamination and mantle plume signatures. *Journal of Petrology,* Vol. 40 (3), pp. 279-296.

Wien K., Kölling, M. and Schulz, D. H. 2007. Age models for the Cape Blanc Debris Flow and the Mauritania Slide Complex in the Atlantic Ocean off NW Africa. *Quaternary Science Reviews*, Vol. 26, pp. 2558-2573.

Wilkerson, F. and Dugdale, R. G. 2008. Coastal Upwelling. In: *Nitrogen in the Marine Environment.* Capone, D. G., Bronk, D. A., Mulholland, M. R. and Carpenter, E. J. (eds). Academic Press, pp. 771–807.

Wilkerson, F. P., Dugdale, R. C., Kudela, R. M. and Chavez, F. P. 2000. Biomass and productivity in Monterey Bay, California: contribution of the large phytoplankton. *Deep-Sea Research Part II: Topical Studies in Oceanography*, Vol. 47 (5–6), pp. 1003–1022. doi:10.1016/S0967-0645(99)00134-4.

Williams, F. (ed.) 1968. Report on the Guinean Trawling Survey. General Report, Vol. 1. Organization of African Unity, Scientific, Technical and Research Commission, Lagos. OAU/STRC Publication No. 99: 827 pp.

Witherington, B. E. 2002. Ecology of neonate loggerhead turtles inhabiting lines of downwelling near a Gulf Stream front. *Marine Biology,* Vol. 140, pp. 843-853.

WOA-13. 2013. World Ocean Atlas 2013. http://www.nodc.noaa.gov/OC5/woa13/ (Accessed December 2014).

Wolff, W. J., van der Land, J., Nieuhuis, P. H. and de Wilde, P. A. W. J. (eds). 1993. *Ecological studies in the coastal waters of Mauritania*. *Hydrobiologia*, Vol. 258 (1-3): 222 pp.

Woodworth, P. L. 2010. A survey of recent changes in the main components of the ocean tide. *Continental Shelf Research*, Vol. 30 (5), pp. 1680-1691.

Woodworth, P. L. and Blackman, D. L. 2004. Evidence for systematic changes in extreme high waters since the mid-1970s. *Journal of Climate*, pp. 1190–1197.

Woolf, D. K., Shaw, A. G. P. and Tsimplis, M. N. 2003. The influence of the North Atlantic Oscillation on sea-level variability in the North Atlantic region. *Journal of Atmospheric & Ocean Science*, Vol. 9 (4), pp. 145–167.

Wooster, W. S., Bakun, A. and McLain, D. R. 1976. The seasonal upwelling cycle along the eastern boundary of the North Atlantic. *Journal of Marine Research*, Vol. 34 (2), pp. 131–140.

Wöppelmann, G., Marcos, M., Coulomb, A., Martín-Míguez, B., Bonnetain, P., Boucher, C., Gravelle, M., Simon, B. and Tiphaneau, P. 2014. Rescue of the historical sea level record of Marseille (France) from 1885 to 1988 and its extension back to 1849–1851. *Journal of Geodesy*, Vol. 88, pp. 869-885.

Worms, J. 1983. *Loligo vulgaris*. In: *Cephalopod Life Cycles,* Vol. 1. Boyle, P. R. (ed.). Academic Press, London, pp. 143-157.

Worthington, L. V. 1976. *On the North Atlantic circulation*, No. 6. Johns Hopkins University Press, Baltimore: 110 pp.

Wylie Poag, C. and Charles de Graciansky, P. 1992. *Geologic Evolution of Atlantic Continental Rises*. Van Nostrand Reinhold Ed., New York: 378 pp.

Yebra, L., Almeida, C., Bécognée, P., Rodríguez, J. M. and Hernández-León, S. 2004. The effect of upwelling filaments and island-induced eddies on indices of feeding and metabolism in copepods. *Progress in Oceanography*, Vol. 62, pp. 151-169.

Zaafa, A., Ettahiri, O., Elkhiati, N., Blahen, M., Berraho, A., Somoue, L. and Elghrib, H. 2012a. Variability of spatial and temporal distribution of marine zooplankton communities in relation with environmental parameters in Tangier and M'Diq (Gibraltar strait) regions. *Journal of Materials and Environmental Science*, Vol. 3 (2), pp. 262-269.

Zaafa, A., Ettahiri, O., Berraho, A., Elkhiati, N., Somoue, L., Zizah, S., Ramdani, M., Blaghen, M. and Flower, R. 2012b. A comparative study of marine zooplankton communities in the Tangier and M'Diq (Gibraltar strait) regions. *Hydroécologie Appliquée*, Vol. 18, pp. 67-80.

Zariquiey, A. R. 1968. Crustáceos Decápodos Ibéricos. *Investigación Pesquera*, No. 32: 510 pp.

Zeeberg, J., Corten, A., Tjoe-Awie, P., Coca, J. and Hamady, B. 2008. Climate modulates the effects of Sardinella aurita fisheries off Northwest Africa. *Fisheries Research,* Vol. 89, pp. 65–75.

Zender, C. S., Bian, H. and Newman, D. 2003. Mineral Dust Entrainment and Deposition (DEAD) model: Description and 1990s dust climatology. *Journal of Geophysical Research D: Atmospheres*, Vol. 108, 4416. doi:4410.1029/2002JD002775.

Zender, C. S., Miller, R. L. and Tegen, I. 2004. Quantifying mineral dust mass budgets: Terminology, constraints, and current estimates. *EOS*, Vol. 85, pp. 509-512.

Zenk, W., Klein, B. and Schröder, M. 1991. Cape Verde frontal zone. *Deep-Sea Research Part A. Oceanographic Research Papers*, Vol. 38 (S1), pp. S505–S530.

Zhao, D. 2007. Seismic images under 60 hotspots: search for mantle plumes. *Gondwana Research,* Vol. 12, pp. 335–355.

Zibrowius, H. 1980. Les Scléractiniaires de la Méditerranée et de l'Atlantique nord-occidental. *Mémoires de l'Institut Océanographique de Monaco,* Vol. 11: 284 pp.

Zühlsdorff, C., Wien, K., Stuut, J. -B. W. and Henrich, R. 2007. Late Quaternary sedimentation within a submarine channel-levee system offshore Cap Timiris, Mauritania. *Marine Geology*, Vol. 240, pp. 217-234.

LIST OF ACRONYMS

AC:	Azores Current
AAIW:	Antarctic Intermediate Waters
AEMET:	Agencia Española de METeorología (Spanish Meteorological Agency)
AERONET:	AErosol RObotic NETwork
AMOC:	Atlantic Meridional Overturning Circulation
ASP:	Amnesic Shellfish Poisoning
A_T:	Total Alkalinity
ATC:	Aspartate TransCarbamylase Activity
AVHRR:	Advanced Very High Resolution Radiometer
AVISO:	Archiving, Validation and Interpretation of Satellite Oceanographic data
AZAs:	AZAspiracids
AZP:	AZaspiracid Poisoning
BATS:	Bermuda Atlantic Time-series Study
BNL:	Bottom Nepheloid Layer
CANIGO:	Canary Islands Azores Gibraltar Observation
CARBOCHANGE:	Changes in carbon uptake and emissions by oceans in a changing climate
CARBOOCEAN:	Marine carbon sources and sinks assessment
CARIACO:	CArbon Retention In a Colored Ocean
CC:	Canary Current
CCDE-IEOCD:	*Colección de Crustáceos Decápodos y Estomatópodos del Centro Oceanográfico de Cádiz del IEO* (Collection of Decapod and Stomatopod Crustaceans of the IEO Cádiz Oceanographic Centre)
CCLME:	Canary Current Large Marine Ecosystem
CCMP:	Cross-Calibrated Multi-Platform
CCN:	Cloud Condensation Nuclei
CCUS:	Canary Current Upwelling System
CDIAC:	Carbon Dioxide Information Analysis Center
CDOM:	Coloured Dissolved Organic Matter
CEC:	Canary Eddy Corridor
CECAF:	Committee for Eastern Central Atlantic Fisheries
CEPEC:	Peruvian Centre for Cetacean Research
CERSAT:	Centre de Recherche et d'Exploitation Satellitaire
CFP:	Ciguatera Fish Poisoning
CGPS:	Continuous Global Positioning System
CINECA:	Cooperative INvestigation of the central part of the Eastern Central Atlantic
CIVP:	Canary Islands Volcanic Province
CLS:	Collecte Localisation Satellites
CNES:	Centre National d'Etudes Spatiales (National Centre for Space Sciences, France)
CO_2:	Carbon dioxide
COC:	Centro Oceanográfico de Canarias (Canary Island Center of the IEO, Spain)
COMAPI:	COastal Modelling for Altimetry Product Improvement
COREWAM:	COnservation and Research of West African Aquatic Mammals
CORICA:	Corriente de contorno oriental - Canarias (eastern Canary Current)
CPUE:	Catch-Per-Unit-of-Effort
CRM:	Certified Reference Material

CSET:	Cross-Shore Ekman Transport
C_T:	Total dissolved inorganic Carbon
CTD:	conductivity-Temperature-Depth
CTXs :	CiguaToXins
CTZ:	Coastal Transition Zone
CU:	Coastal Upwelling index
CUC:	Canary Upwelling Current
CUE:	Canary Upwelling Ecosystem
CUF:	Coastal Upwelling Front
CUI:	Coastal Upwelling Index
CUJ:	Coastal Upwelling Jet
CVC:	Cape Verde Current
CVF:	Cape Verde Front
CVFZ:	Cape Verde Frontal Zone
CVIVP:	Cape Verde Islands Volcanic Province
CVOO:	Cape Verde Ocean Observatory
CZCS	Coastal Zone Color Scanner
DA:	Domoic Acid
DAC:	Dynamic Atmospheric Correction
DCM:	Deep Chlorophyll Maximum
DGOM:	Dynamic Green Ocean Model
DO:	Dissolved Oxygen
DOC:	Dissolved Organic Carbon
DOM:	Dissolved Organic Matter
DSDP:	Deep Sea Drilling Project
DSP:	Diarrhetic Shellfish Poisoning
DTXs:	DinophysisToXins
EBUE:	Eastern Boundary Upwelling Ecosystem
EBUS:	Eastern Boundary Upwelling System
ECCO2:	Estimating the Circulation and Climate of the Ocean, phase II
EEZ:	Exclusive Economic Zone
EN:	ENdangered
ENACW:	Eastern North Atlantic Central Water
EKE:	Eddy Kinetic Energy
ELISA:	Enzyme-Linked ImmunoSorbent Assay
ENACW:	Eastern North Atlantic Central Water
ESA:	European Space Agency
ESACW:	Eastern South Atlantic Central Water
ESRID:	Empirical Satellite Radiance-In situ Data
ESTOC:	European Station for Time Series in the Ocean, Canary Islands
ETS:	Electron Transfer System
FADs:	Fish Aggregating Devices
FAO:	Food and Agriculture Organization of the United Nations
FDA:	Food and Drug Administration
FES2004:	Finite Element Solution tide model 2004
FixO3:	Fixed point Open Ocean Observatory
FUST:	Flanders UNESCO Science Trust Fund

GD:	Guinea Dome
GDP:	Gross Domestic Product
GIA:	Glacial Isostatic Adjustment
GLOBEC:	Global Ocean and Ecosystem Dynamics
GLOSS:	Global Sea Level Observing System
GOT4.7:	Ocean Tide model
GPS:	Global Positioning System
HABs:	Harmful Algal Blooms
HAMSOM:	HAMburg Shelf Ocean Model
HIRLAM:	HIgh-Resolution Limited Area Model (North European weather model)
HOT:	Hawaii Ocean Time-series
HPLC:	High-Performance Liquid Chromatography
ICCAT:	International Commission for the Conservation of Atlantic Tunas
IEO:	Instituto Español de Oceanografía (Spanish Institute of Oceanography)
IFAN:	Institut Fondamental d'Afrique Noire
IGN:	Instituto Geográfico Nacional (Spanish National Geographic Institute)
IH:	Instituto Hidrográfico (Portugal)
IHM:	Instituto Hidrográfico de la Marina (Marine Hydrographic Institute, Spain)
IMEDEA:	Institut MEditerrani d'Estudis Avançats (Mediterranean Institute for Advanced Studies, Spain)
IMR:	Institute of Marine Research
IMROP:	Institut Mauritanien de Recherches Océanographiques et des Pêches
IN:	Inorganic Nutrients
INL:	Intermediate Nepheloid Layer
INMG:	Instituto Nacional de Meteorologia e Geofísica (Cabo Verde)
INRH:	Institut National de Recherche Halieutique (Morocco)
IOCAG:	Instituto de Oceanografía y CAmbio Global (Institute of Oceanography and Global Change, University of Las Palmas de Gran Canaria, Spain)
IP:	Iberian Peninsula
IPCC:	Intergovernmental Panel on Climate Change
IRSC:	Indented Rotating Sphere Carousel
ITCZ:	Inter-Tropical Convergence Zone
ITE:	Intra-Thermocline anticyclonic Eddy
IUCN:	International Union for Conservation of Nature
LADCP:	Lowered Acoustic Doppler Current Profiler
LC-MS:	Liquid Chromatography-Mass Spectrometry
LEGOS:	Laboratoire d'Etudes en Géophysique et Océanographie Spatiales
LNADW:	Lower North Atlantic Deep Water
LP:	Lanzarote Passage
LS:	Least Squares
MARINEMET:	Maritime Meteorology Pilot Project for the Northwest African Basin
MAST:	MArine Science and Technology programme
MERIS:	MEdium Resolution Imaging Spectrometer
MODIS:	MODerate resolution Imaging Spectroradiometer
Mog2D:	*Modèle 2D d'Ondes de Gravité*
MBL:	Marine Boundary Layer
MC:	Mauritanian Current

Meddy:	Mediterranean eddy
MNADW:	Middle North Atlantic Deep Water
MODIS:	MODerate resolution Imaging Spectroradiometer
MOL:	Minimum Oxygen Layer
MS:	Mass Spectrometry
MSLA:	Mean Sea Level Anomaly
MSY:	Maximum Sustainable Yield
MTX:	MaitoToXin
MW:	Mediterranean Water
NACW:	North Atlantic Central Water
NADW	North Atlantic Deep Water
NAO:	North Atlantic Oscillation
NASA:	National Aeronautics and Space Administration (USA)
NASA/OBPG:	National Aeronautics and Space Administration Ocean Biology Processing Group
NASG:	North Atlantic Subtropical Gyre
NA_T:	Normalized Total Alkalinity
NATG:	North Atlantic Tropical Gyre
NAUS:	Northwest Africa Upwelling System
NC_T:	Normalized Total dissolved inorganic Carbon
NEA:	NorthEast Atlantic
NEC:	North Equatorial Current
NECC:	North Equatorial CounterCurrent
NEP:	Net Ecosystem Production
NOAA:	National Oceanographic and Atmospheric Administration (USA)
NOAA ESRL GMD:	World Meteorological Organization (WMO), Global Atmosphere Watch (GAW) Central Calibration Laboratory (CCL) for CO_2, CH_4, N_2O, SF_6 and CO
NPP:	Net Primary Production
NWA:	NorthWest Africa, NorthWest African
NW-AUS:	NorthWest African Upwelling System
OA:	Okadaic Acid
OBIS:	Ocean Biographic Information System
OCCAM:	Ocean Circulation and Climate Advanced Modelling
ODINAFRICA:	Ocean Data and Information Network for Africa
ODP:	Ocean Drilling Program
OMZ:	Oxygen Minimum Zone
OSU:	Oregon State University
PAR:	Photosynthetically Active Radiation
pCO_2:	Partial pressure of CO_2
PdE:	Puertos del Estado (Harbour Authorities, Spain)
PEP:	Particle release region
$pH_{T,is}$:	pH in total scale at *in situ* conditions of temperature, salinity and pressure
PISCES:	Pelagic Interaction Scheme for Carbon and Ecosystem Studies
POC:	Particulate Organic Carbon
POM_{sink}:	Sinking Particulate Organic Matter
POM_{susp}:	Suspended Particulate Organic Matter
PP:	Primary Production
PSMSL:	Permanent Service for Mean Sea Level

PSP:	Paralytic Shellfish Poisoning
PTXs:	PectenoToXins
PUC:	Poleward UnderCurrent
QUIMA:	*Química Marina.* It refers to the Spanish expression of Marine Chemistry
RAPROCAN:	RAdial PROfunda de CANarias
REDMAR:	RED de MAReógrafos de Puertos del Estado (Spanish Harbours Sea Level Network)
ROMS:	Regional Ocean Modeling System
SACW:	South Atlantic Central Water
SAL:	Saharan Air Layer
SCL:	Straight Carapace Length
SCM:	Surface Chlorophyll Maximum
SD:	Standard Deviation
SeaWiFS:	Sea-viewing WIde Field-of-view Sensor
SLA:	Sea Level Anomaly
SODA:	Simple Ocean Data Assimilation
SOLAS:	Surface Ocean-Lower Atmosphere Study
SONEL:	*Système d'Observation du Niveau des Eaux Littorales*
SRFC:	Sub-regional Fisheries Commission
SST:	Sea Surface Temperature
STXs:	SaxiToXins
SVEICC:	Surveillance System for Ciguatera poisoning in the Canary Islands
T:	Cross-Shore Ekman Transport
T-UGOM:	Toulouse Unstructured Grid Ocean Model
TAC:	Total Allowable Catch
TENATSO:	Tropical Eastern North Atlantic Time-Series Observatory
TPX07.2:	Global inverse tidal model
TS:	Temperature-Salinity
TWI:	Trade Wind Inversion layer
UCAD:	Université de Dakar Cheikh Anta Diop
UHSLC:	University of Hawaii Sea Level Center
UNADW:	Upper North Atlantic Deep Water
UNCLOS:	United Nations Convention on the Law of the Sea
UNESCO:	Unite Nations Educational, Scientific and Cultural Organization
UPLC-MS:	UltraPerformance Liquid Chromatography – Mass Spectrometry
VGPM:	Vertically Generalized Production Model
VIIRS:	Visible Infrared Imaging Radiometer Suite
VINDTA:	Versatile INstrument for the Determination of Total inorganic carbon and titration Alkalinity
VOS:	Voluntary Observing Ship
WAM:	Wave modelling model
WAVEWATCH:	Wave generation model
WOCE:	World Ocean Circulation Experiment
WNACW:	Western North Atlantic Central Water
YTXs:	YessoToXins

IOC Technical Series

No.	Title	Languages
1	Manual on International Oceanographic Data Exchange. 1965	(out of stock)
2	Intergovernmental Oceanographic Commission (Five years of work). 1966	(out of stock)
3	Radio Communication Requirements of Oceanography. 1967	(out of stock)
4	Manual on International Oceanographic Data Exchange - Second revised edition. 1967	(out of stock)
5	Legal Problems Associated with Ocean Data Acquisition Systems (ODAS). 1969	(out of stock)
6	Perspectives in Oceanography, 1968	(out of stock)
7	Comprehensive Outline of the Scope of the Long-term and Expanded Programme of Oceanic Exploration and Research. 1970	(out of stock)
8	IGOSS (Integrated Global Ocean Station System) - General Plan Implementation Programme for Phase I. 1971	(out of stock)
9	Manual on International Oceanographic Data Exchange - Third Revised Edition. 1973	(out of stock)
10	Bruun Memorial Lectures, 1971	E, F, S, R
11	Bruun Memorial Lectures, 1973	(out of stock)
12	Oceanographic Products and Methods of Analysis and Prediction. 1977	E only
13	International Decade of Ocean Exploration (IDOE), 1971-1980. 1974	(out of stock)
14	A Comprehensive Plan for the Global Investigation of Pollution in the Marine Environment and Baseline Study Guidelines. 1976	E, F, S, R
15	Bruun Memorial Lectures, 1975 - Co-operative Study of the Kuroshio and Adjacent Regions. 1976	(out of stock)
16	Integrated Ocean Global Station System (IGOSS) General Plan and Implementation Programme 1977-1982. 1977	E, F, S, R
17	Oceanographic Components of the Global Atmospheric Research Programme (GARP) . 1977	(out of stock)
18	Global Ocean Pollution: An Overview. 1977	(out of stock)
19	Bruun Memorial Lectures - The Importance and Application of Satellite and Remotely Sensed Data to Oceanography. 1977	(out of stock)
20	A Focus for Ocean Research: The Intergovernmental Oceanographic Commission - History, Functions, Achievements. 1979	(out of stock)
21	Bruun Memorial Lectures, 1979: Marine Environment and Ocean Resources. 1986	E, F, S, R
22	Scientific Report of the Interealibration Exercise of the IOC-WMO-UNEP Pilot Project on Monitoring Background Levels of Selected Pollutants in Open Ocean Waters. 1982	(out of stock)
23	Operational Sea-Level Stations. 1983	E, F, S, R
24	Time-Series of Ocean Measurements. Vol.1. 1983	E, F, S, R
25	A Framework for the Implementation of the Comprehensive Plan for the Global Investigation of Pollution in the Marine Environment. 1984	(out of stock)
26	The Determination of Polychlorinated Biphenyls in Open-ocean Waters. 1984	E only
27	Ocean Observing System Development Programme. 1984	E, F, S, R
28	Bruun Memorial Lectures, 1982: Ocean Science for the Year 2000. 1984	E, F, S, R
29	Catalogue of Tide Gauges in the Pacific. 1985	E only
30	Time-Series of Ocean Measurements. Vol. 2. 1984	E only
31	Time-Series of Ocean Measurements. Vol. 3. 1986	E only
32	Summary of Radiometric Ages from the Pacific. 1987	E only
33	Time-Series of Ocean Measurements. Vol. 4. 1988	E only
34	Bruun Memorial Lectures, 1987: Recent Advances in Selected Areas of Ocean Sciences in the Regions of the Caribbean, Indian Ocean and the Western Pacific. 1988	Composite E, F, S
35	Global Sea-Level Observing System (GLOSS) Implementation Plan. 1990	E only

(continued)

36	Bruun Memorial Lectures 1989: Impact of New Technology on Marine Scientific Research. 1991	Composite E, F, S
37	Tsunami Glossary - A Glossary of Terms and Acronyms Used in the Tsunami Literature. 1991	E only
38	The Oceans and Climate: A Guide to Present Needs. 1991	E only
39	Bruun Memorial Lectures, 1991: Modelling and Prediction in Marine Science. 1992	E only
40	Oceanic Interdecadal Climate Variability. 1992	E only
41	Marine Debris: Solid Waste Management Action for the Wider Caribbean. 1994	E only
42	Calculation of New Depth Equations for Expendable Bathymerographs Using a Temperature-Error-Free Method (Application to Sippican/TSK T-7, T-6 and T-4 XBTS. 1994	E only
43	IGOSS Plan and Implementation Programme 1996-2003. 1996	E, F, S, R
44	Design and Implementation of some Harmful Algal Monitoring Systems. 1996	E only
45	Use of Standards and Reference Materials in the Measurement of Chlorinated Hydrocarbon Residues. 1996	E only
46	Equatorial Segment of the Mid-Atlantic Ridge. 1996	E only
47	Peace in the Oceans: Ocean Governance and the Agenda for Peace; the Proceedings of *Pacem in Maribus* XXIII, Costa Rica, 1995. 1997	E only
48	Neotectonics and fluid flow through seafloor sediments in the Eastern Mediterranean and Black Seas - Parts I and II. 1997	E only
49	Global Temperature Salinity Profile Programme: Overview and Future. 1998	E only
50	Global Sea-Level Observing System (GLOSS) Implementation Plan-1997. 1997	E only
51	L'état actuel de 1'exploitation des pêcheries maritimes au Cameroun et leur gestion intégrée dans la sous-région du Golfe de Guinée *(cancelled)*	F only
52	Cold water carbonate mounds and sediment transport on the Northeast Atlantic Margin. 1998	E only
53	The Baltic Floating University: Training Through Research in the Baltic, Barents and White Seas - 1997. 1998	E only
54	Geological Processes on the Northeast Atlantic Margin (8th training-through-research cruise, June-August 1998). 1999	E only
55	Bruun Memorial Lectures, 1999: Ocean Predictability. 2000	E only
56	Multidisciplinary Study of Geological Processes on the North East Atlantic and Western Mediterranean Margins (9th training-through-research cruise, June-July 1999). 2000	E only
57	Ad hoc Benthic Indicator Group - Results of Initial Planning Meeting, Paris, France, 6-9 December 1999. 2000	E only
58	Bruun Memorial Lectures, 2001: Operational Oceanography – a perspective from the private sector. 2001	E only
59	Monitoring and Management Strategies for Harmful Algal Blooms in Coastal Waters. 2001	E only
60	Interdisciplinary Approaches to Geoscience on the North East Atlantic Margin and Mid-Atlantic Ridge (10th training-through-research cruise, July-August 2000). 2001	E only
61	Forecasting Ocean Science? Pros and Cons, Potsdam Lecture, 1999. 2002	E only
62	Geological Processes in the Mediterranean and Black Seas and North East Atlantic (11th training-through-research cruise, July- September 2001). 2002	E only
63	Improved Global Bathymetry – Final Report of SCOR Working Group 107. 2002	E only
64	R. Revelle Memorial Lecture, 2006: Global Sea Levels, Past, Present and Future. 2007	E only
65	Bruun Memorial Lectures, 2003: Gas Hydrates – a potential source of energy from the oceans. 2003	E only
66	Bruun Memorial Lectures, 2003: Energy from the Sea: the potential and realities of Ocean Thermal Energy Conversion (OTEC). 2003	E only

67	Interdisciplinary Geoscience Research on the North East Atlantic Margin, Mediterranean Sea and Mid-Atlantic Ridge (12th training-through-research cruise, June-August 2002). 2003	E only
68	Interdisciplinary Studies of North Atlantic and Labrador Sea Margin Architecture and Sedimentary Processes (13th training-through-research cruise, July-September 2003). 2004	E only
69	Biodiversity and Distribution of the Megafauna / Biodiversité et distribution de la mégafaune. 2006 Vol.1 The polymetallic nodule ecosystem of the Eastern Equatorial Pacific Ocean / Ecosystème de nodules polymétalliques de l'océan Pacifique Est équatorial Vol.2 Annotated photographic Atlas of the echinoderms of the Clarion-Clipperton fracture zone / Atlas photographique annoté des échinodermes de la zone de fractures de Clarion et de Clipperton Vol.3 Options for the management and conservation of the biodiversity — The nodule ecosystem in the Clarion Clipperton fracture zone: scientific, legal and institutional aspects	E F
70	Interdisciplinary geoscience studies of the Gulf of Cadiz and Western Mediterranean Basin (14th training-through-research cruise, July-September 2004). 2006	E only
71	Indian Ocean Tsunami Warning and Mitigation System, IOTWS. Implementation Plan, 7–9 April 2009 (2nd Revision). 2009	E only
72	Deep-water Cold Seeps, Sedimentary Environments and Ecosystems of the Black and Tyrrhenian Seas and the Gulf of Cadiz (15th training-through-research cruise, June–August 2005). 2007	E only
73	Implementation Plan for the Tsunami Early Warning and Mitigation System in the North-Eastern Atlantic, the Mediterranean and Connected Seas (NEAMTWS), 2007–2011. 2007 *(electronic only)*	E only
74	Bruun Memorial Lectures, 2005: The Ecology and Oceanography of Harmful Algal Blooms – Multidisciplinary approaches to research and management. 2007	E only
75	National Ocean Policy. The Basic Texts from: Australia, Brazil, Canada, China, Colombia, Japan, Norway, Portugal, Russian Federation, United States of America. (Also Law of Sea Dossier 1). 2008	E only
76	Deep-water Depositional Systems and Cold Seeps of the Western Mediterranean, Gulf of Cadiz and Norwegian Continental margins (16th training-through-research cruise, May–July 2006). 2008	E only
77	Indian Ocean Tsunami Warning and Mitigation System (IOTWS) – 12 September 2007 Indian Ocean Tsunami Event. Post-Event Assessment of IOTWS Performance. 2008	E only
78	Tsunami and Other Coastal Hazards Warning System for the Caribbean and Adjacent Regions (CARIBE EWS) – Implementation Plan 2013–2017 (Version 2.0). 2013	E only
79	Filling Gaps in Large Marine Ecosystem Nitrogen Loadings Forecast for 64 LMEs – GEF/LME global project Promoting Ecosystem-based Approaches to Fisheries Conservation and Large Marine Ecosystems. 2008	E only
80	Models of the World's Large Marine Ecosystems. GEF/LME Global Project Promoting Ecosystem-based Approaches to Fisheries Conservation and Large Marine Ecosystems. 2008	E only
81	Indian Ocean Tsunami Warning and Mitigation System (IOTWS) – Implementation Plan for Regional Tsunami Watch Providers (RTWP). 2008	E only
82	Exercise Pacific Wave 08 – A Pacific-wide Tsunami Warning and Communication Exercise, 28–30 October 2008. 2008	E only
83.	*Cancelled*	
84.	Global Open Oceans and Deep Seabed (GOODS) Bio-geographic Classification. 2009	E only
85.	Tsunami Glossary	E, F, S
86	Pacific Tsunami Warning System (PTWS) Implementation Plan *(under preparation)*	

(continued)

87.	Operational Users Guide for the Pacific Tsunami Warning and Mitigation System (PTWS) – Second Edition. 2011	E only
88.	Exercise Indian Ocean Wave 2009 (IOWave09) – An Indian Ocean-wide Tsunami Warning and Communication Exercise – 14 October 2009. 2009	E only
89.	Ship-based Repeat Hydrography: A Strategy for a Sustained Global Programme. 2009	E only
90.	12 January 2010 Haiti Earthquake and Tsunami Event Post-Event Assessment of CARIBE EWS Performance. 2010	E only
91.	Compendium of Definitions and Terminology on Hazards, Disasters, Vulnerability and Risks in a coastal context	*Under preparation*
92.	27 February 2010 Chile Earthquake and Tsunami Event – Post-Event Assessment of PTWS Performance (Pacific Tsunami Warning System). 2010	E only
93.	Exercise CARIBE WAVE 11 / LANTEX 11—A Caribbean Tsunami Warning Exercise, 23 March 2011	
	Vol. 1 Participant Handbook / Exercice CARIBE WAVE 11 —Exercice d'alerte au tsunami dans les Caraïbes, 23 mars 2011. Manuel du participant / Ejercicio Caribe Wave 11. Un ejercicio de alerta de tsunami en el Caribe, 23 de marzo de 2011. Manual del participante. 2010	E/F/S
	Vol. 2 Report. 2011	E only
	Vol. 3 Supplement: Media Reports. 2011	E/F/S
94.	Cold seeps, coral mounds and deep-water depositional systems of the Alboran Sea, Gulf of Cadiz and Norwegian continental margin (17th training-through-research cruise, June–July 2008)	*Under preparation*
95.	International Post-Tsunami Survey for the 25 October 2010 Mentawai, Indonesia Tsunami	*Under preparation*
96.	Pacific Tsunami Warning System (PTWS) 11 March 2011 Off Pacific coast of Tohoku, Japan, Earthquake and Tsunami Event. Post-Event Assessment of PTWS Performance	*Under preparation*
97.	Exercise PACIFIC WAVE 11: A Pacific-wide Tsunami Warning and Communication Exercise, 9–10 November 2011	
	Vol. 1 Exercise Manual. 2011	E only
	Vol. 2 Report. 2013	E only
98.	Tsunami Early Warning and Mitigation System in the North-Eastern Atlantic, the Mediterranean and connected seas. First Enlarged Communication Test Exercise (ECTE1). Exercise Manual and Evaluation Report. 2011	E only
99.	Exercise INDIAN OCEAN WAVE 2011 – An Indian Ocean-wide Tsunami Warning and Communication Exercise, 12 October 2011	E only
	Vol. 1 Exercise Manual. 2011 Supplement: Bulletins from the Regional Tsunami Service Providers	
	Vol. 2 Exercise Report. 2013	
100.	Global Sea Level Observing System (GLOSS) Implementation Plan – 2012. 2012	E only
101.	Exercise Caribe Wave/Lantex 13. A Caribbean Tsunami Warning Exercise, 20 March 2013. Volume 1: Participant Handbook. 2012	E only
102.	Tsunami Early Warning and Mitigation System in the North-Eastern Atlantic, the Mediterranean and Connected Seas — Second Enlarged Communication Test Exercise (CTE2), 22 May 2012.	E only
	Vol. 1 Exercise Manual. 2012	
	Vol. 2 Evaluation Report. 2014	
103.	Exercise NEAMWAVE 12. A Tsunami Warning and Communication Exercise for the North-eastern Atlantic, the Mediterranean, and Connected Seas Region, 27–28 November 2012.	E only
	Vol. 1: Exercise Manual. 2012	
	Vol. 2: Evaluation Report. 2013	
104.	Seísmo y tsunami del 27 de agosto de 2012 en la costa del Pacífico frente a El Salvador, y seísmo del 5 de septiembre de 2012 en la costa del Pacífico frente a Costa Rica. Evaluación subsiguiente sobre el funcionamiento del Sistema de Alerta contra los Tsunamis y Atenuación de sus Efectos en el Pacífico. 2012	Español solamente (resumen en inglés y francés)
105.	Users Guide for the Pacific Tsunami Warning Center Enhanced Products for the Pacific Tsunami Warning System, August 2014. Revised Edition. 2014	E, S

106.	Exercise Pacific Wave 13. A Pacific-wide Tsunami Warning and Enhanced Products Exercise, 1–14 May 2013. Vol. 1 Exercise Manual. 2013 Vol. 2 Summary Report. 2013	E only
107.	Tsunami Public Awareness and Educations Strategy for the Caribbean and Adjacent Regions. 2013	E only
108.	Pacific Tsunami Warning and Mitigation System (PTWS) Medium-Term Strategy, 2014−2021. 2013	E only
109.	Exercise Caribe Wave/Lantex 14. A Caribbean and Northwestern Atlantic Tsunami Warning Exercise, 26 March 2014. Vol. 1 Participant Handbook. 2014	E/S
110.	Directory of atmospheric, hydrographic and biological datasets for the Canary Current Large Marine Ecosystem. 2014	E only
111.	Integrated Regional Assessments in support of ICZM in the Mediterranean and Black Sea Basins. 2014	E only
112.	*11 April 2012 West of North Sumatra Earthquake and Tsunami Event - Post-event Assessment of IOTWS Performance*	*In preparation*
113.	*Exercise Indian Ocean Wave 2014: An Indian Ocean-wide Tsunami Warning and Communication Exercise.*	*In preparation*
114.	Exercise NEAMWAVE 14. A Tsunami Warning and Communication Exercise for the North-Eastern Atlantic, the Mediterranean, and Connected Seas Region, 28–30 October 2014 Vol. 1 Manual Vol. 2 Evaluation Report – Supplement: Evaluation by Message Providers and Civil Protection Authorities	E only
115.	Oceanographic and Biological Features in the Canary Current Large Marine Ecosystem. 2015	E only
116.	Tsunami Early Warning and Mitigation System in the North-Eastern Atlantic, the Mediterranean and Connected Seas. Third Enlarged Communication Test Exercise (CTE3), 1st October 2013. Vol. 1 Exercise Manual Vol. 2 Evaluation Report	E only
117.	Exercise Pacific Wave 15. A Pacific-wide Tsunami Warning and Enhanced Products Exercise, 2–6 February 2015 Vol. 1: Exercise Manual; Vol. 2: Summary Report	E only
118.	Exercise Caribe Wave/Lantex 15. A Caribbean and Northwestern Atlantic Tsunami Warning Exercise, 25 March 2015 (SW Caribbean Scenario) Vol. 1: Participant Handbook	E only

Also in the IOC-UNESCO Technical Series:

Directory of Atmospheric, Hydrographic and Biological datasets for the Canary Current Large Marine Ecosystem

IOC-UNESCO Technical Series 110

The Canary Current Large Marine Ecosystem (CCLME) is a major upwelling region off the coast of Northwest Africa. It extends southwards from Canary Islands (Spain) and the Atlantic coast of Morocco, Western Sahara, Mauritania, Senegal, Gambia and Guinea-Bissau, but also Cape Verde and the waters of Guinea are considered adjacent areas within the zone of influence of the CCLME.

A total of 425 datasets, 27 databases and 21 time-series sites have been identified in the area. A substantial part of them were rescued from archives supported in paper copy. The current directory refers to 85 datasets, databases and time-series sites.

This catalogue and the recovered data offer an exceptional opportunity for the researchers in the CCLME to study the dynamics and trends of a multiplicity of variables, and will enable them to explore different data sources and create their own baselines and climatologies under a spatial and temporal perspective.

The *Directory of Atmospheric, Hydrographic and Biological datasets for the Canary Current Large Marine Ecosystem* will be reviewed on a systematic and routine basis and the updates to the publication will be available online at: http://www.unesco.org/new/ioc_ts110

A close collaboration has been established with different institutions in order to rescue, review and quality control the information, and to fill and to validate the fiches compiled in this directory.

The compilation of such a complex directory by the Intergovernmental Oceanographic Commission and the Instituto Español de Oceanografía would not have been possible without the financial support given by the Spanish Agency for International Development Cooperation (AECID) to the project entitled *Enhancing oceanography capacities on Western Africa countries*.

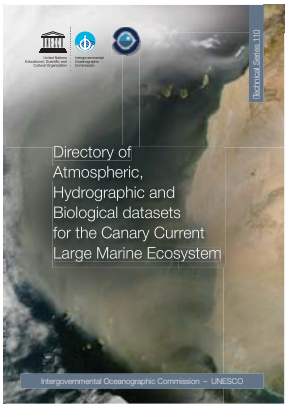

Cover photo: Saharan Air Layer outbreak moving off Africa into the North Atlantic on 2 March 2003, where vast amounts of Saharan dust can be seen as captured by the MODIS instrument aboard NASA's Terra satellite. Source: NASA

United Nations Educational, Scientific and Cultural Organization · Intergovernmental Oceanographic Commission

GOBIERNO DE ESPAÑA · Cooperación española

The Canary Current Large Marine Ecosystem (CCLME) is an eastern boundary upwelling system, in fact one of the 4 major upwelling systems in the world. The CCLME extends from the Strait of Gibraltar (around 36°N 5°W) to Bissagos Islands in the South of Guinea-Bissau (around 11°N 16°W), embracing the coasts and Economic Exclusive Zones of Morocco, Western Sahara, Mauritania, Senegal, Gambia, Guinea-Bissau and Spain (Canary Islands). Also Cape Verde and Guinea are under the area of influence of the Canary Current, and therefore are considered as part of the CCLME in this publication.

A complete characterization of the CCLME was achieved thanks to the dedication of 54 scientists from 25 institutions who have reviewed the scientific information accumulated in the CCLME during decades. In addition, they have kindly shared their own knowledge obtained after years of hard work in high level scientific research.

An active and fruitful collaboration has been established with our partner in this project, the Instituto Español de Oceanografía (IEO). Twelve of its experts have contributed as authors or co-authors of many of the articles. In their articles they have not only shared their expertise, but the know-how gained by the IEO throughout decades of international cooperation programs with African countries.

Oceanographic and biological features in the Canary Current Large Marine Ecosystem consists in 28 articles structured in the following sections: (i) the ocean geomorphology and geological materials; (ii) the hydrographic structure and the ocean circulation; (iii) the biogeochemical characteristics of the marine environment; (iv) the life in the sea; (v) and the interannual, interdecadal and long-term variability.

The main findings are highlighted in the Executive Summary together with an indication of the gaps left in the scientific knowledge in the CCLME, evoking ideas on the topics in need of a deeper scientific research and management goals in the CCLME.

Such a complex publication would not be possible without the generous financial support of a donor. The Spanish Agency for International Development Cooperation (AECID) has funded the project *Enhancing oceanography capacities on Western Africa countries.*

Oceanographic and biological features in the Canary Current Large Marine Ecosystem is also available on-line at: http://www.unesco.org/new/en/ioc/ts115

GOBIERNO DE ESPAÑA

cooperación española

United Nations Educational, Scientific and Cultural Organization

Intergovernmental Oceanographic Commission

Intergovernmental Oceanographic Commission (IOC)
United Nations Educational, Scientific and Cultural Organization (UNESCO)
7 Place de Fontenoy, 75352 Paris Cedex 07, France
Tel: +33 1 45 68 39 83/84
Fax: +33 1 45 68 58 12
http://ioc.unesco.org